Investigations of the *Z*-selective sesquiterpene cyclase; 7-epizingiberene synthase

A thesis submitted to Cardiff University

for the degree of Doctor of Philosophy by:

Chris Jones

Supervisor: Rudolf K. Allemann

2018

Declaration

This work has not been submitted in substance for any other degree or award at this or any other university or place of learning, nor is being submitted concurrently in candidature for any degree or other award.

Signed …… (candidate) Date ……

Statement 1

This thesis is being submitted in partial fulfillment of the requirements for the degree of ……..

Signed …… (candidate) Date ……

Statement 2

This thesis is the result of my own independent work/investigation, except where otherwise stated, and the thesis has not been edited by a third party beyond what is permitted by Cardiff University's Policy on the Use of Third Party Editors by Research Degree Students. Other sources are acknowledged by explicit references. The views expressed are my own.

Signed …… (candidate) Date ……

Statement 3

I hereby give consent for my thesis, if accepted, to be available online in the University's Open Access repository and for inter-library loan, and for the title and summary to be made available to outside organisations.

Signed …….. (candidate) Date ……

Statement 4: PREVIOUSLY APPROVED BAR ON ACCESS

I hereby give consent for my thesis, if accepted, to be available online in the University's Open Access repository and for inter-library loans **after expiry of a bar on access previously approved by the Academic Standards & Quality Committee.**

Signed …… (candidate) Date ……

Abstract

Sesquiterpene cyclases convert linear isoprenyl diphosphates into complex hydrocarbon structures that include multiple ring systems, chiral centres and various stereochemistry. The wild tomato plant (*Solanum habrochaites*) has shown resistance against herbivore attack that is not observed in the domesticated moneymaker tomato species. Wild tomatoes release sesquiterpenes; 7-epizingiberene and its dehydrogenated form (*R*)-curcumene to repel adult whiteflies prior to landing, whilst moneymaker tomatoes do not exhibit this ability. 7-Epizingiberene has been reported as toxic to whitefly and a phytoalexin that causes birth defects in offspring. As a result, the use of 7-epizingiberene to combat whitefly infestation gives a new possibility for crop protection, circumventing the use of potentially dangerous and environmentally damaging pesticides.

This thesis focuses on 7-epizingiberene synthase (EZS), a sesquiterpene cyclase that defies convention by using (2*Z*,6*Z*) farnesyl diphosphate as its substrate and not the universal substrate (2*E*,6*E*) farnesyl diphosphate. The project is divided into three sections. The first section involved the synthesis of (2*Z*,6*Z*) farnesyl diphosphate followed by the expression and purification of 7-epizingiberene synthase. Due to cost implications of purchasing (2*Z*,6*Z*) farnesol, multiple synthetic routes were investigated for the synthesis (2*Z*,6*Z*) farnesyl diphosphate. A Horner-Wadsworth-Emmons olefination using a Still-Gennari modified reagent gave the greatest yield of the *Z* isomer which was used for further reactions. Various cell lines and expression tags were used to optimise EZS expression and purification, whilst incubations of synthesised (2*Z*,6*Z*) farnesyl diphosphate with EZS gave catalytic products consistent with literature.

The second portion of the project was the synthesis of (2*Z*,6*Z*)-[1-^{3}H]-farnesyl diphosphate for the measurement of steady state parameters of EZS and EZS mutants. Multiple oxidations were attempted during the synthesis of radiolabelled substrate, with an oxoammonium-catalysed oxidation shown to retain the stereochemistry of the C2,C3 double bond. EZS mutants were used to investigate the metal binding motifs responsible for class I activity whilst numerous aromatic residues were subjected to single point mutation to investigate their role within the active site pocket.

The third section involved the synthesis of substrate analogues to investigate the catalytic mechanism and substrate specificity of EZS. The synthesis of deuterated and fluorinated analogues were used to investigate prospective hydride shifts and carbocation intermediates respectively. The stereochemistry required for substrate turnover was probed by the synthesis of all isomers of farnesyl diphosphate whilst oxygenated and methylated substrates were synthesised for the potential production of novel sesquiterpene products.

Acknowledgements

I would firstly like to thank my supervisor Professor Rudolf Allemann for giving me the opportunity to work on this project and his persistence to push me to achieve results, improve my practical skills and scientific knowledge. I would also like to thank Dr David Miller who has helped to supervise my project, with guidance and advice during my PhD.

There are many people from the Allemann Research group to whom I owe much gratitude. Dr Rob Mart has been an influential presence throughout the course of my PhD whose advice and assistance was greatly received and appreciated. Dr Luke Johnson has given continuous support and advice with both the chemical biology portion of this project and help with various aspects of PhD life. Since arriving to the Allemann group, Dr Alice Dunbabin has been of tremendous help and support both academically and socially. All three have taken time from their many responsibilities to help proof read and give advice on this thesis, assistance that was greatly valued.

Members of the Allemann group past and present have been of great support and help throughout the four years of study. Roger, Ryan and Sarah welcomed me to the group in my first year and quickly cemented themselves as part of my PhD life. Dr Veronica González, Dr Alan Scott, Adura, Mel, Marianna, Antonio and Dan were also of great help and support during the time that we were all working together, always happy to answer any questions or give help when needed. More recently, the arrival of Ed, Raquel, Victor, Martin and Florence have made some of the harder times of the PhD surprisingly enjoyable. Always willing to help or chat, they have become friends to which I hope I continue to know in the future. The four newest members of the Allemann group Jenny, Gwawr, Huw and Gareth also had an impact on the later stages of my project and seemed to be as invested in my thesis submission as myself. Joel Cresser-Brown has helped long days in the lab easier. His unique humour has kept spirits high and has been a great person to share an office with. I would be remised not to thank 'Big' Rob, without whom I would not have enjoyed my PhD journey half as much. From long hours in the lab, to cheeky wanders and being asked to be Godfather to his first child Walter; Rob has and always will be a great friend.

Outside of the Allemann group I would like to thank Tom Williams for all his help with characterisation of mass spectra and Rob Jenkins for assistance with NMR experiments. Gareth, Balson, Krag and Kostas have made my time in Cardiff a great experience, before and during my PhD. My family Allan, Elaine, Phil and Becky have been a constant that I could not have been without during my PhD and undergraduate degree. They have given me nonstop encouragement guiding me further than I envisaged at the start of university. I am thankful to have such a caring family that would go to any lengths to support my ambitions and help in whatever means they can. Finally I must acknowledge Chloe Barlow-Griffin. After meeting in the first year of my PhD, Chloe has stuck with me through the highs and lows of my project giving love and support that I could never expect or ask of her. I am forever indebted to her, for her understanding and cannot express my gratitude in words.

Table of Contents

Glossary of abbreviations

AaADS – *Artemisia annua* aristolochene Synthase

AaBOS – *Artemisia annua* α-bisabalol Synthase

AB – Alpine borane

ABS – α-Bisabolene Synthase

Ac – Acetate

αCBS – (-)-α-Cubebene Synthase

ADP – Adenine diphosphate

ADS – Amorphadiene Synthase

AMP – 2-amino-2-methyl-1-propanol

AS – Aristolochene Synthase

ATP – Adenine triphosphate

βME – beta mercaptoethanol

BuLi – Butyl lithium

CD – Circular dichromism

CHES – N-cyclohexyl-2-aminoethanesulfonic acid

CLB – Cell lysis buffer

CoA / HSCoA – Coenzyme A

CPM – Counts per minute

Cpn – Chaperonin

CS – Caryophyllene Synthase

CTP – Cytidyl phosphate

DCM – Dichloromethane

DCS – δ-Cadinene Synthase

DHP – 3,4-Dihydro-2*H*-pyran

DIBALH – Diisobutylaluminium hydride

DMADP – Dimethyl allyl diphosphate

DMAP – Dimethyl amino pyridine

DME – Dimethoxy ethane

DMF – Dimethyl formamide

DMS – Dimethyl sulphide

DOX – Deoxyxylulose phosphate

DTT – *Dithiothreitol*

DXPS – 1-Deoxy-ᴅ-xylulose-5-phosphate synthase

Eβ-FS – (*E*)-β-farnesene Synthase

E. coli – *Escherichia coli*

ee – Enantiomeric excess

EI – Electron ionisation

EZS – 7-Epizingiberene Synthase

FDA – Food and Drug Administration

FDP – Farnesyl diphosphate

FPLC – Fast protein liquid chromatography

GAS – Germacrene A Synthase

GB1 – Guanidine binding protein expression tag

GC-MS – Gas chromatography – Mass spectrometry

GDP – Geranyl diphosphate

GDS – Germacrene D Synthase

GGDP – Geranylgeranyl diphosphate

GRAS – Generally Regarded as Safe

h – hour

HEPES – 2[4-(2-hydroxyethyl)piperazin-1-yl]ethanesulfonic acid

His-tag – Histidine tag

HMG – 3-Hydroxy-3-methylglutaryl

HPLC – High performance liquid chromatography

HSQC – Heteronuclear Single Quantum Coherence

HWE – Horner-Wadsworth-Emmons

IC50 – Inhibitor concentration at which the response (or binding) is reduced by half

IDP – Isopentenyl diphosphate

Incorp. – Incorporation

IPI – Isopentenyl diphosphate isomerase

IPTG – Isopropyl-β-D-1-thiogalactopyranoside

IspC/D/F/H/G – Reductoisomerase

kDa - Kilo Dalton

KHMDS – Potassium hexamethyldisilazide

LB medium – Lysogeny broth medium

LDA – Lithium diisopropyl amine

LS – Lanosterol Synthase

MBP – Maltose binding protein

MEP – Methylerythritol phosphate

MES – 2-(N-morpholino)ethanesulfonic acid

min – minute/s

MOS – 2,3-monoepoxy squalene

$NADP^+$ - Nicotinamide adenine dinucleotide phosphate

NADPH – Nicotinamide adenine dinucleotide phosphate hydride

NBS – N-bromo succinimide

NCS - N-chloro succinimide

NDP – Neryl diphosphate

Ni-NTA – Nickel affinity column

NIST – National Institute of Standards and Technology

NMR – Nuclear magnetic resonance

NOESY – Nuclear Overhauser Effect Spectroscopy

OD_{600} – Optical density at 600 nm

OPP – Diphosphate moiety

pI – Isoelectric point

ppm – Parts per million

PPTS – Pyridinium *para*-toluenesulfonate

*p*TSA – *para*-Toluene sulfonic acid

Q-seph – Q-sepharose

RNA – Ribonucleic acid

RNAP - Ribonucleic acid polymerase

(*R*)-MTPA - (*R*)-(+)-α-methoxy-α-(trifluoromethyl)phenylacetyl

R-MTPA-Cl - (*R*)-(+)-α-methoxy-α-(trifluoromethyl)phenylacetyl chloride

RT – Room temperature

SaS – Santalene Synthase

Sat. – Saturated

SBS – Santalene and Bergamotene Synthase

SDS PAGE - Sodium dodecyl sulfate polyacrylamide gel

sec. – secondary

(*S*)-MTPA - (*S*)-(+)-α-methoxy-α-(trifluoromethyl)phenylacetyl

S-MTPA-Cl - (*S*)-(+)-α-methoxy-α-(trifluoromethyl)phenylacetyl chloride

Sol. – Solution

TB medium – Terrific-Broth medium

TDP – Thiamine diphosphate

Temp – Temperature

TEMPO – 4-Acetomido-2,2,6,6-tetramethyl-1-oxopiperidin-1-ium tetra fluoro borate salt

TEV – Tobacco etch virus

THF – Tetrahydrofuran

THP – Tetrahydropyran

TLC – Thin layer chromatography

TMSBr - Trimethyl silyl bromide

TMSCl – Trimethyl silyl chloride

Ts – Tosylate

TsCl – Tosyl chloride

UV-vis – Ultra violet-visible

WT – Wild type

Z-FDP – (2*Z*,6*Z*) farnesyl diphosphate

ZS – Zingiberene Synthase

Amino acid abbreviations

Alanine – A

Arginine – R

Asparagine – N

Aspartic Acid – D

Glycine – G

Histidine – H

Isoleucine – I

Leucine – L

Lysine – K

Methionine – M

Phenylalanine – F

Proline - P

Serine – S

Threonine – T

Tryptophan – W

Tyrosine – Y

Valine – V

List of Tables

List of figures

Chapter 1 – Introduction

1.1 Terpenes

The terpenome is comprised of over 50,000 structurally and stereochemically diverse natural compounds derived from the catalysis of linear isoprenyl diphosphates by terpene cyclases.[1] Terpenoids are ubiquitous throughout all kingdoms of life, possessing many different bioactivities in plants, animals, insects, bacteria, archea and fungi. Over half of known terpenoids are biosynthesised by plants with primary metabolites involved in photosynthesis, respiration and membrane structure. Secondary metabolites in plants are utilised for a range of purposes including pigmentation, protection from over exposure to light and provide crucial roles in defence. Some secondary metabolites are responsible for repelling herbivorous insects *e.g.* 7-epizingiberene (**1**) from *Solanum habrochaites* (wild tomato)[2,3] and (-)-germacrene D (**2**) from *Hemizizygia petiolata* essential oil.[4] Contrastingly, some secondary metabolites *e.g.* β-phellandrene (**3**) are synthesised by *Epipactis* (terrestrial orchids) for the attraction of *Episyrphus balteatus* (marmalade hoverfly) for pollination.[5]

In addition to uses in nature, terpene hydrocarbon skeletons can be further functionalised for uses as rubber, flavourings ((*R*)-(-)-carvone (**4**))[6], antibiotics (pentalenolactone (**5**))[7], natural contraceptives (gossypol (**6**))[8], anti-malarial (artemisinin (**7**))[9] and anti-cancer (taxol®(**8**))[10] pharmaceuticals[11] (Figure 1).

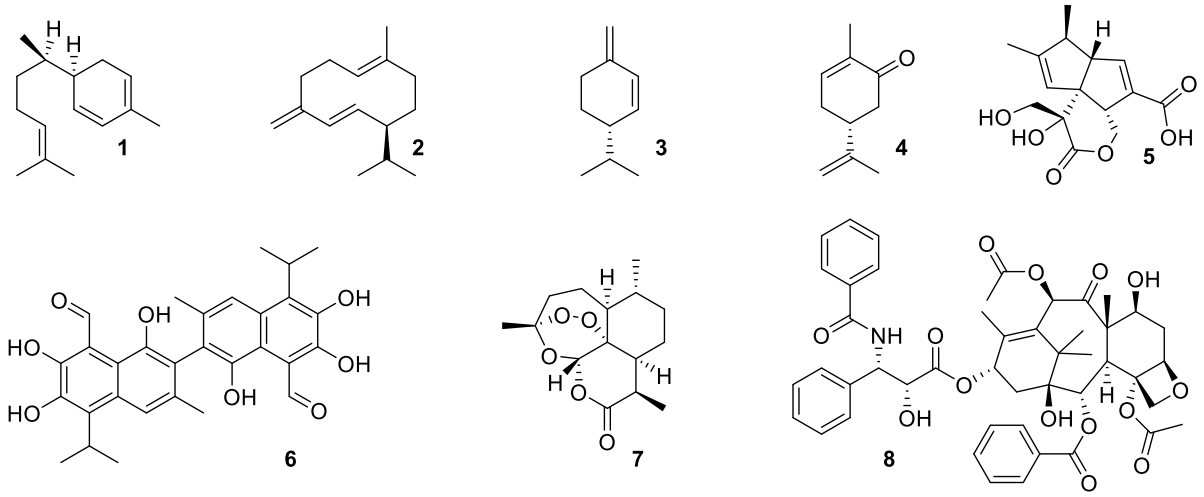

Figure 1. 7-Epizingiberene (1), (-)-germacrene D (2), β-phellandrene (3), (R)-(-)-carvone (4), pentalenolactone (5), gossypol (6), artemisinin (7) and taxol (8).

The variety and complexity of natural products within the terpenome contrasts with the fact that they are derived from two simple isoprenoid building blocks; isopentenyl diphosphate (IDP, **16**) and dimethylallyl diphosphate (DMADP, **17**).[12] Two pathways for the biosynthesis of IDP (**16**) and DMADP (**17**) are known. The mevalonate pathway (Figure 2) functions in eukaryotes, the cytosol of plants and some bacteria; and was considered the universal source of IDP and DMADP after its elucidation in the late 1950s.[13,14] The second biosynthetic pathway is known as the non-mevalonate or deoxyxylulose phosphate (DOX) or methylerythritol phosphate (MEP) pathway (Figure 3) and was recently discovered by Rohmer *et al.,*[15] and Arigoni *et al.*[16] This pathway is active *inter alia* in bacteria and the chloroplasts of green algae and higher plants.[13]

1.1.1 Mevalonate Pathway

The mevalonate pathway begins with the Claisen condensation of two acetyl-coenzyme A (**9**) molecules to give thio ester **10**.[14] The subsequent aldol reaction between **10** and **11 is** catalysed by HMG-CoA synthase to yield 3-hydroxy-3-methylglutaryl-CoA (**12**). The reduction of **12** with HMG-CoA reductase and two equivalents of NADPH gives mevalonic acid (**13**).[17] The reduction is followed by sequential phosphorylations by mevalonate kinase and adenine triphosphate to give 5-phosphomevalonic acid (**14**) and 5-diphosphomevalonic acid (**15**) respectively.[18] The ATP-mediated decarboxylation and water elimination of **15** is catalysed by diphosphomevalonate decarboxylase to give isopentenyl diphosphate (**16**).[13,19] Isomerisation of IDP (**16**) to DMADP (**17**) by isopentenyl diphosphate isomerase (IPI) proceeds *via* the reversible proton tautomerisation to the *Re* face of the IDP (**16**) double bond. This is proceeded by the stereospecific removal of the 2-*pro*-*R*-proton to give **17** in an approximate equilibrium ratio of 3:1 (DMADP(**17**):IDP(**16**)) (Figure 2).[20,21]

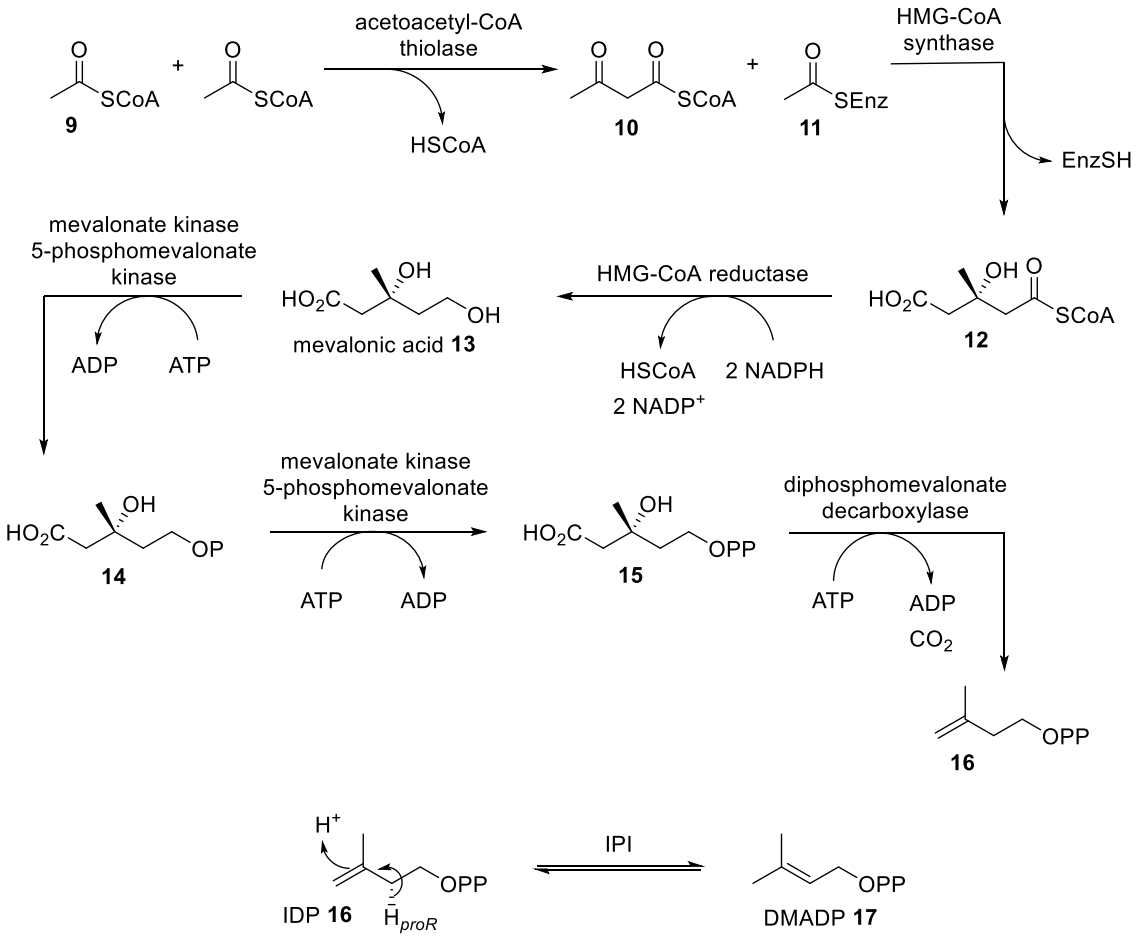

Figure 2. Mevalonate pathway (top) and IPI catalysed isomerisation of IDP (16) to DMADP (17) (bottom).

1.1.2 Non-mevalonate Pathway

The non-mevalonate pathway begins with catalytic condensation of pyruvate (**18**) and glyceraldehyde-3-phosphate (**19**) by 1-deoxy-D-xylulose-5-phosphate synthase (DXPS) and cofactor thiamine diphosphate (TPP) to give 1-deoxy-D-xylulose-5-phosphate (**20**) and carbon dioxide.[13,22] Isomerisation to the aldehyde 2-*C*-methyl-D-erythose-4-phosphate (**21**) by DXPS reductoisomerase (IspC) is followed by a NADPH reduction within the same enzyme giving 2-*C*-methyl-D-erythritol-4-phosphate (**22**).[23] A cytidyl phosphate moiety (CTP) is transferred to **22** *via* IspD catalysis to give 4-diphosphocytidyl-2-*C*-methyl-D-erythritol (**23**) followed by phosphorylation by IspF to the respective 2-phosphate (**24**).[24,25] IspF catalyses the only known natural cyclic diphosphate *via* the elimination of cytidyl monophosphate (CMP) to yield 2-*C*-methyl-D-erythritol-2,4-cyclodiphosphate (**25**). The mechanisms responsible for the final two steps of the non-mevalonate pathway are disputed. However; they are known to be catalysed by two highly oxygen sensitive iron-sulphur cluster proteins; IspG and IspH respectively.[26,27] A reductive ring opening of **25** catalysed by IspG forms 1-hydroxy-2-methyl-2-(*E*)-butenyl-4-diphosphate (**26**). IspH catalyses the two step single-electron transfer from an iron-sulfur cluster and consequent cleavage of the hydroxyl moiety to give the allylic carbanion (**27**). Protonation of the carbanion can yield either IDP (**16**) or DMADP (**17**) (Figure 3).[23,24,28]

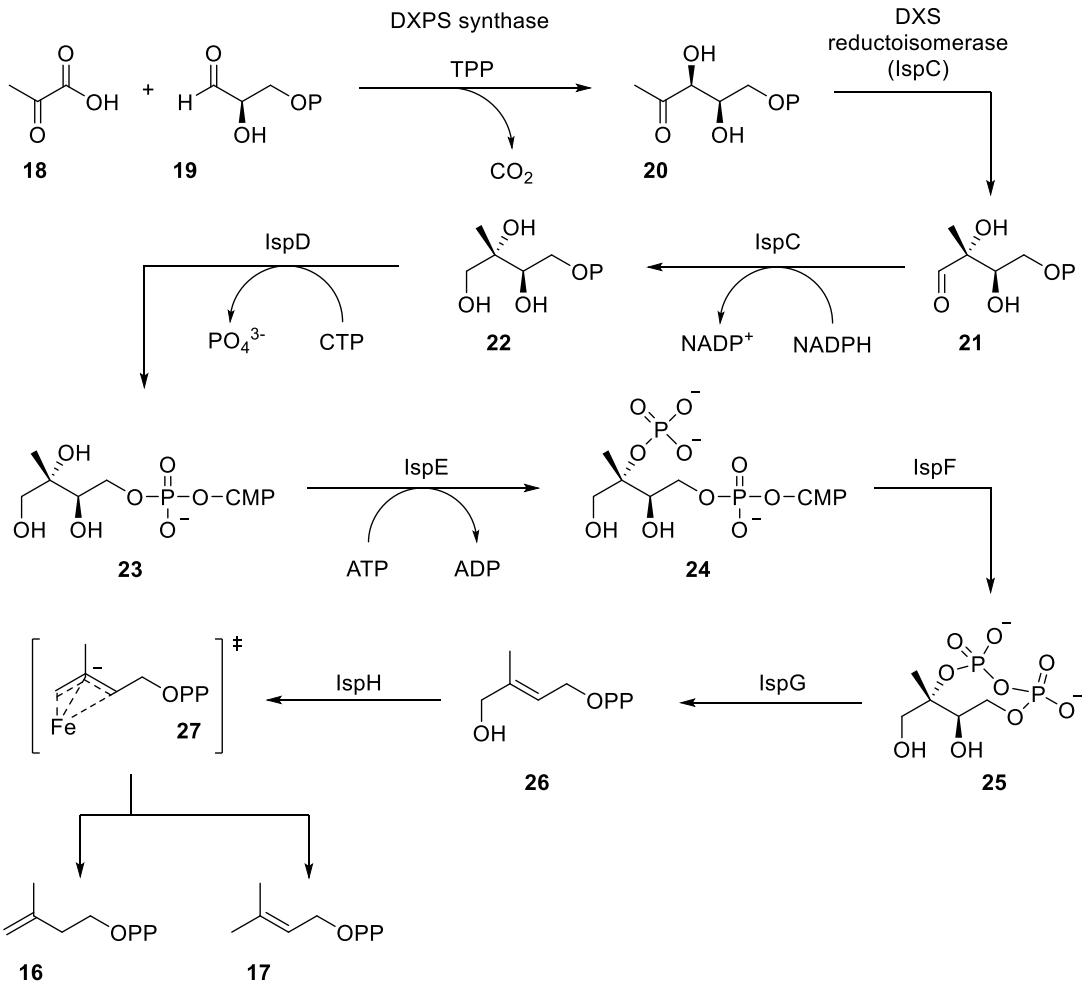

Figure 3. The non-mevalonate pathway.

1.1.3 Prenyltransferase

Activated isoprene moieties; isopentenyl diphosphate (IDP, **16**) and dimethylallyl diphosphate (DMADP, **17**) biosynthesised *via* the mevalonate or non-mevalonate pathways are substrates for prenyl transferase (not prenylating enzymes which share the same name). This class of enzymes catalyse the successive head to tail condensation reactions of IDP (**16**) and DMADP (**17**) giving larger isoprenyl diphosphates such as the monoterpene (C_{10}) parent geranyl diphosphate (GDP, **30**), the sesquiterpene (C_{15}) parent farnesyl diphosphate (FDP, **31**) and the diterpene (C_{20}) parent geranylgeranyl diphosphate (GGDP, **32**).[29,30] The biosynthesis begins with the dissociation of diphosphate from **17** resulting in the allylic cation **28**.[31] The cation then undergoes nucleophilic attack from a molecule of IDP (**16**) forming a stabilised tertiary carbocation **29**. Deprotonation occurs at a secondary α-carbon to give geranyl diphosphate (GDP, **30**).[32] Elongated isoprenyl diphosphates are consequently used as substrates for their respective terpene cyclase to begin the production of a multitude of natural products (Figure 4).[31]

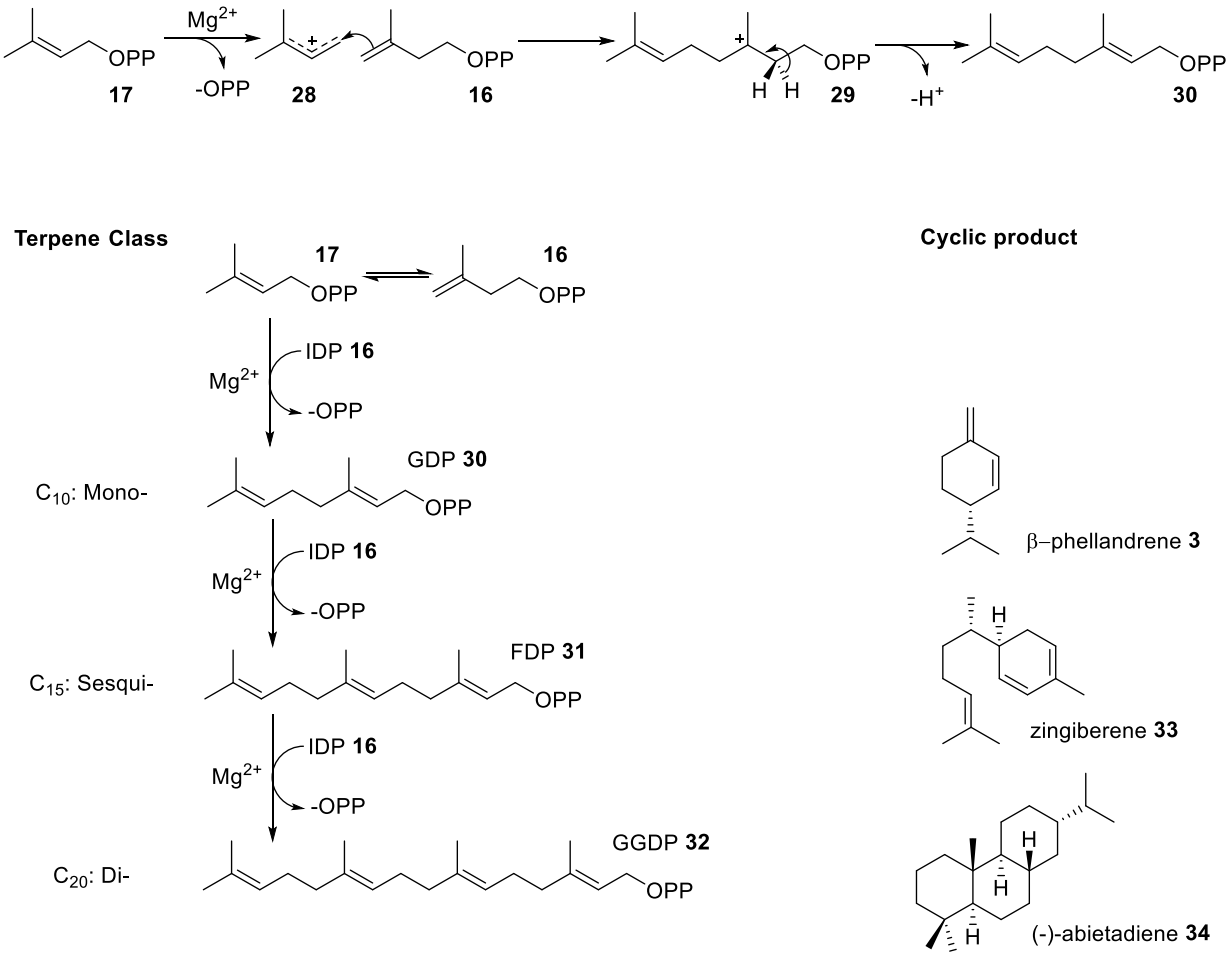

Figure 4. Biosynthesis of terpenoids (top) and nomenclature of isoprenoid substrates (bottom).

Due to the numerous chain lengths possible, Koyama and Ogura classified prenyltransferases into four groups depending on chain length and stereochemistry generated.[13] Class I prenyltransferases catalyse short chain products from GDP (C_{10}, **30**) to GGDP (C_{20}, **32**) with *E* selectivity. Class II prenyltransferases elongate FDP (C_{15}, **31**) to hexaprenyl (C_{30}) and heptaprenyl diphosphate (C_{35}) whilst class III catalyses the formation of octaprenyl (C_{40}) and decaprenyl diphosphate (C_{50}) from FDP (**31**) with *E* selectivity. Contrastingly, class IV prenyl transferases catalyse the elongation of FDP (**31**) to nonaprenyl (C_{45}) and decaprenyl diphosphate (C_{50}) but with *Z* selectivity.

Original stereochemical investigations into the mechanism of *Z*-selective enzymes were carried out on rubber biosynthesis. It was observed that chain elongation and *Z* double bond formation progressed *via* the removal of the 2-*pro*-*S*-hydrogen from IDP (**16**) in contrast to the abstraction of the 2-*pro*-*R*-hydrogen by *E* specific prenyl transferases.[33] It was postulated that the stereoselectivity

of *E* or *Z* selective prenyl transferases arose from the specific removal of the C2 *proR* or *proS* proton of IDP (**16**) (Figure 5).[34]

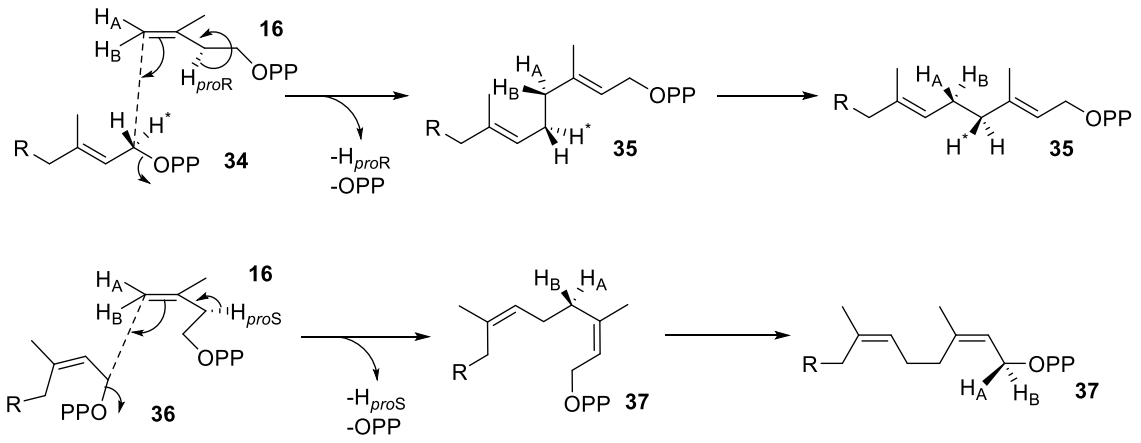

Figure 5. Proposed mechanisms of E (top) and Z (bottom) selective prenyltransferases.

In contrast, multiple investigations of *Z*-selective prenyltransferases have reported the removal of the 2-*pro-R*-hydrogen.[35–37] In recent literature, two *Z*-selective class I prenyltransferases have been discovered in *Solanum habrochaites*[30] and *S. lycopersicum*[38] for the biosynthesis of (2*Z*,6*Z*) farnesyl diphosphate (**38**) and neryl diphosphate (**39**) (Figure 6).

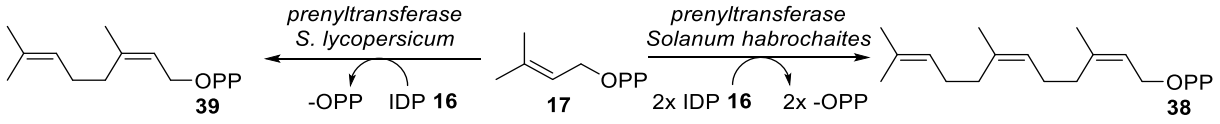

Figure 6. Biosynthesis of (2*Z*,6*Z*) FDP (38) and neryl DP (39) by catalysis of DMADP (17) and IDP (16) with Z selective prenyltransferase.

1.2 Terpene cyclases

Terpene cyclases catalyse the stereospecific conversion of linear isoprenyl diphosphate precursors (Figure 4) to a multitude of cyclic compounds.[39] As detailed in section 1.1, terpenoid products have a wide range of applications spanning the pharmaceutical industry to semiochemicals[9] for plant defence.[40,41] Terpene cyclases vary in terms of substrate and product promiscuity. Table 1 exemplifies selected terpene cyclases and the terpenoid products arising from their catalytic action:

Table 1 - Terpene cyclases with respective substrates and products (modified from publication by Pazouki *et al.*[42]

Terpene Cyclase	Species	TPS family	Substrate	Terpenoid products	Reference
Germacrene A synthase (GAS)	*Achillea milefolium*	Sesqui-	FDP (**31**)	germacrene A (**40**), β-elemene (**41**), β-selinene (**42**), α-selinene (**43**)	Pazouki *et al.*[43]
			GDP (**30**)	mycrene (**44**), (*E*)-β-ocimene (**45**), limonene (**46**), terpinolene (**47**), camphene (**48**), α-pinene (**49**)	
			NDP (**39**)	(+)-2-carene (**50**), γ-terpinene (**51**), α-terpinene (**52**), α-fenchene (**53**), α-thujene (**54**)	
Santalene synthase (SaS)	*Santalum album*	Sesqui-	FDP (**31**)	α-santalene (**55**), β-santalene (**56**), epi-β-santalene (**57**), α-exo-bergamotene (**58**), α-farnesene (**59**), β-farnesene (**60**)	Jones *et al.*[44]
			Z-FDP (**38**)	α-endo-bergamotene (**61**), α-santalene (**55**), (*Z*)-β-farnesene (**62**), epi-β-santalene (**57**), β-santalene (**56**)	
			GDP (**30**)	Linalool (**63**), geraniol (**64**), terpineol (**65**), α-pinene (**49**), camphene (**49**)	

α-Bisabolene synthase (ABS)	*Abies grandis*	Sesqui-	FDP (**31**) GDP (**30**)	(*E*)-α-bisabolene (**66**) (+)-Limonene (**46**)	Bohlmann *et al.*[45]
Lanosterol synthase (LS)	-	Tri-	2,3-monoepoxy squalene (MOS)	Lanosterol (**67**)	Huff *et al.*[46]
β-ocimene synthase	*Arabidopsis thaliana*	Mono-	FDP (**31**) GDP (**30**)	α-farnesene (**59**) (*E*)-β-ocimene (**45**)	Huang *et al.*[47]

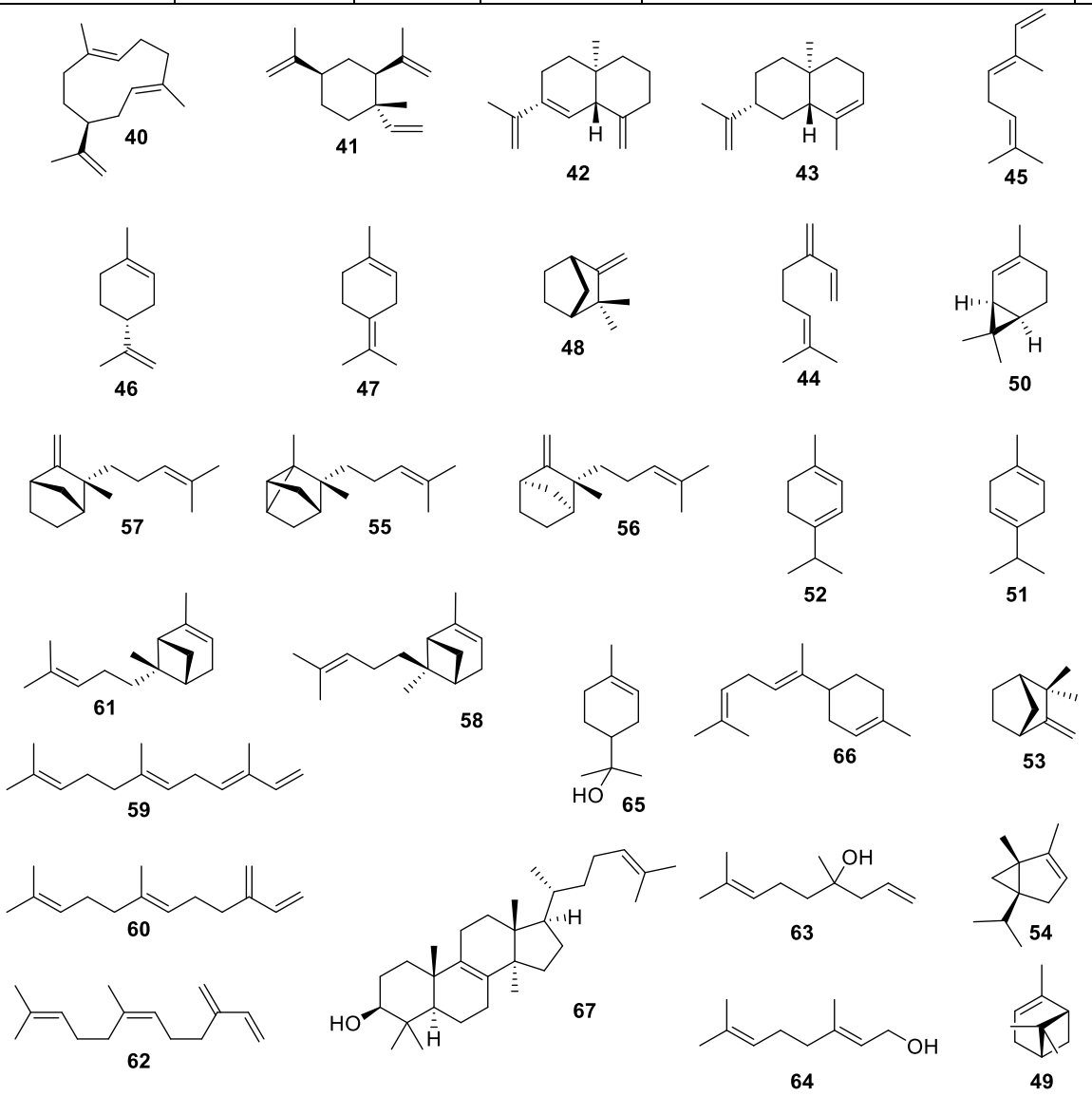

Figure 7. Structures of terpene cyclase products listed in Table 1.

Though substrates and enzymatic products may differ, the mechanisms of all terpene cyclases are initiated *via* the formation of an initial carbocation.[48] The enzyme guides the substrate through a cascade of carbocation rearrangements, cyclisations, hydride or alkyl shifts and deprotonation. The hydrophobic pocket of the active site is equipped to stabilise the formation of numerous carbocations, simulating an inert organic solvent whilst π-electrons of aromatic residues and the diphosphate co-product stabilise carbocation intermediates.[11,49] The initial cation is established *via* two different mechanisms and has led to the classification of terpene cyclases into class I and class II cyclases.

1.2.1 Class I terpene cyclases

Class I terpene cyclases catalyse the conversion of isoprenyl diphosphate substrates *via* the metal-dependent cleavage of the diphosphate moiety of the substrate to yield an initial carbocation as the first step. The structure of class I terpenoid cyclases consists of an α-helical bundle with a tertiary fold that was first observed in the crystal structure of avian FDP synthase.[50] Class I catalysis is confined to the α-helical bundle with bacterial cyclases comprised solely of this domain. In plants, multi-domain class I cyclases are also known.[51] Non-catalytic domains can be dormant whilst the β domains of some plant sesquiterpene cyclases have been shown to assist catalysis by capping the active site when the substrate in bound.[52,53] *Epi*-aristolochene[54] synthase and α-bisabolene synthase[55] are examples of terpene cyclases that are comprised of an αβ and αβγ architecture, respectively, with no activity observed in the β and γ domains (Figure 8).

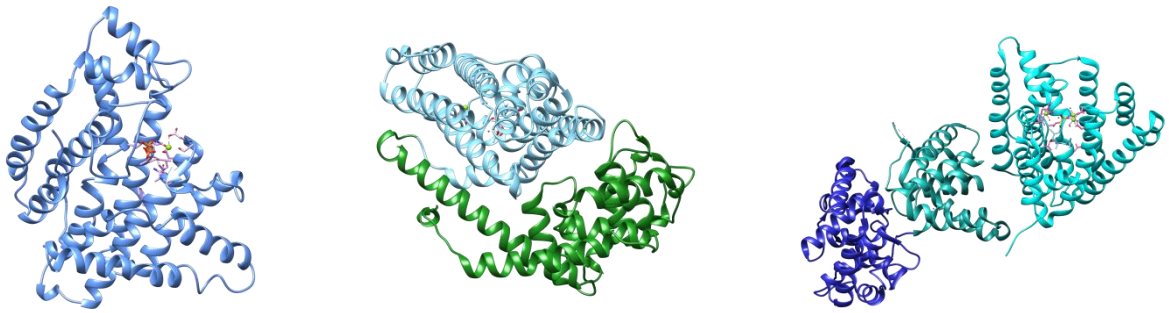

Figure 8. Cartoon representation of the X-ray crystal structures of three class I terpene cyclases. Left: avian FDP synthase (representative of the α-helical bundle in which class I activity is confined).[50] Middle: *epi*-aristolochene synthase showing the class I active α domain (blue) and the inactive β domain (green).[56] Right: α-bisabolene synthase, a three-domain plant terpene cyclase with inactive β (central) and γ (dark blue) domains.[57]

A conserved DDxxD(E) metal ion binding motif located on helix D is present across the entire class and is responsible for the coordination of two metal ions .[58] A variant second motif positioned on

helix H is referred to as the NSE/DTE motif corresponding to a (N,D)Dxx(S,T)xxxE sequence for binding a third metal ion is also conserved.[51] The NSE motif is generally found within fungi and bacteria whilst the DTE motif in commonly found in plant terpene synthases (Figure 9). The diphosphate group of the isoprenoid substrate coordinates with the metal ions enabling formation of the substrate-enzyme complex.[59]

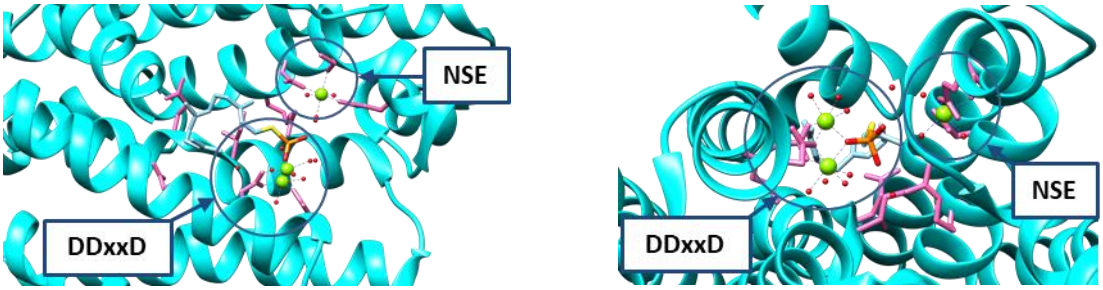

Figure 9. Cartoon representation of the class 1 catalytic alpha domain from the X-ray crystal structure of avian FDP synthase outlining the position of the DDxxD and NSE conserved motifs.[50]

In contrast, δ-cadinene synthase (DCS) from *Gossypium arboreum* has a second DDxxD region in place of the NSE/DTE motif; [60] and (*R*)-germacrene D synthase from *Solidago canadensis* where the DDxxD motif is replaced by an NDxxD sequence. Although slightly different, these motifs also chelate a trio of divalent magnesium (or manganese) ions that are required for the binding and subsequent cleavage of the diphosphate moiety.[61]

1.2.2 Class II terpene cyclases

Class II terpene cyclases are defined by protonation-initiated catalysis of isoprenyl diphosphate substrates. The structure of class II cyclases consists of two α-helical structures referred to as the β and γ domains.[62] The general catalytic acid responsible for class II catalysis arises from a central aspartate rich motif (DXDD) positioned at the interface of the β and γ domains.[63] Examples of three domain (αβγ) class II terpenoid cyclases are also known.[64,65] *Ent*-copalyl synthase contains a functional class II active site at the interface of the β and γ domains with a residual, non-functioning α domain.[66]

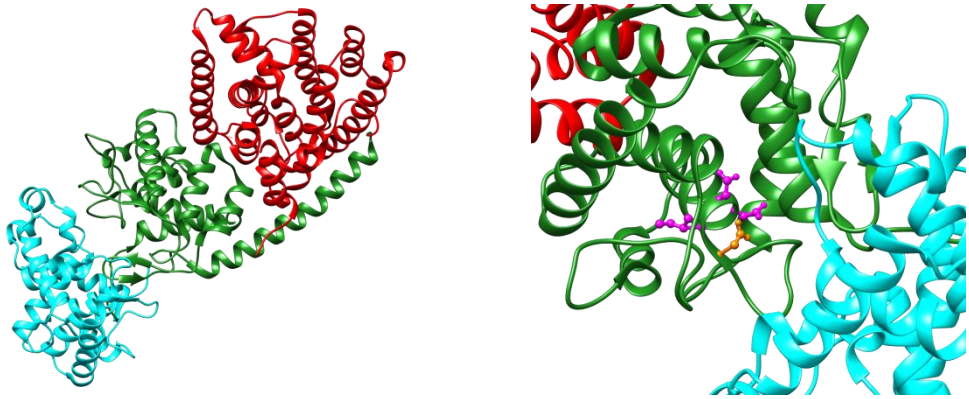

Figure 10. Left: Carton representation of the X-ray crystal structure of abietadiene synthase and Right: Class II active site highlighting the DxDD motif positioned at the interface of the β and γ domains of abietadiene synthase.[67]

The initial carbocation is formed *via* the protonation of the *distal* double bond or the protonation of an epoxide derivative of this bond, resulting in ring opening. The intramolecular cascade of carbocations ensuing from various cyclisations generally leads to the formation of multicyclic structures.[62] In the majority of cases, class II terpene cyclases catalyse reactions involving diterpene (geranylgeranyl diphosphate, **32**),[68] triterpenes[69] and derived-oxidosqualene precursors.[70] However, class II catalysed reactions have been observed in the formation of the sesquiterpene drimane (**79**) and the biosynthesis of tetra / sesterterpenoids.[71] More commonly these enzymes catalyse the formation of stereochemically and structurally complex products incorporating between one and five cyclisations and rearrangements within a single reaction.[72]

1.2.3 Bifunctional terpene cyclases

Class I and class II activities are situated in the α-domain and at the interface of the β and γ domains respectfully. Contrastingly, plant terpene cyclases containing α, β and γ domains could be monofunctional (class I or class II) or bifunctional (class I and II).[62]

An example of a bifunctional terpene cyclase is abietadiene synthase from *Abies grandis*.[64] Abietadiene synthase is responsible for the biosynthesis of (–)-abieta-8,14-diene (abietadiene) from GGDP (**32**) and is a precursor to (-)-abietic acid (**75**), utilised by grand fir trees (*Abies grandis*) in response to bark beetle attack.[73] The mechanism proceeds *via* two consecutive reactions catalysed by the class II and class I active sites.[74] Protonation of the *distal* double bond of **32** results in three consecutive ring closures and deprotonation to give (+)-copalyl diphosphate (**69**). Dissociation from the class II active site into the bulk solvent and is followed by substrate binding to the class I active site.[74] Once bound, metal dependent cleavage of the diphosphate ester *via* a concerted ring closure gives cation (**70**).[75] The ring closure is proceeded by an intramolecular proton transfer and a [1,2]

methyl migration to give cations **71** and **72** respectively.[76] Deprotonation of **72** gives abietadiene (**34**) or elimination can yield levopimaradiene (**73**) and neoabietadiene (**74**) (Figure 11).[77]

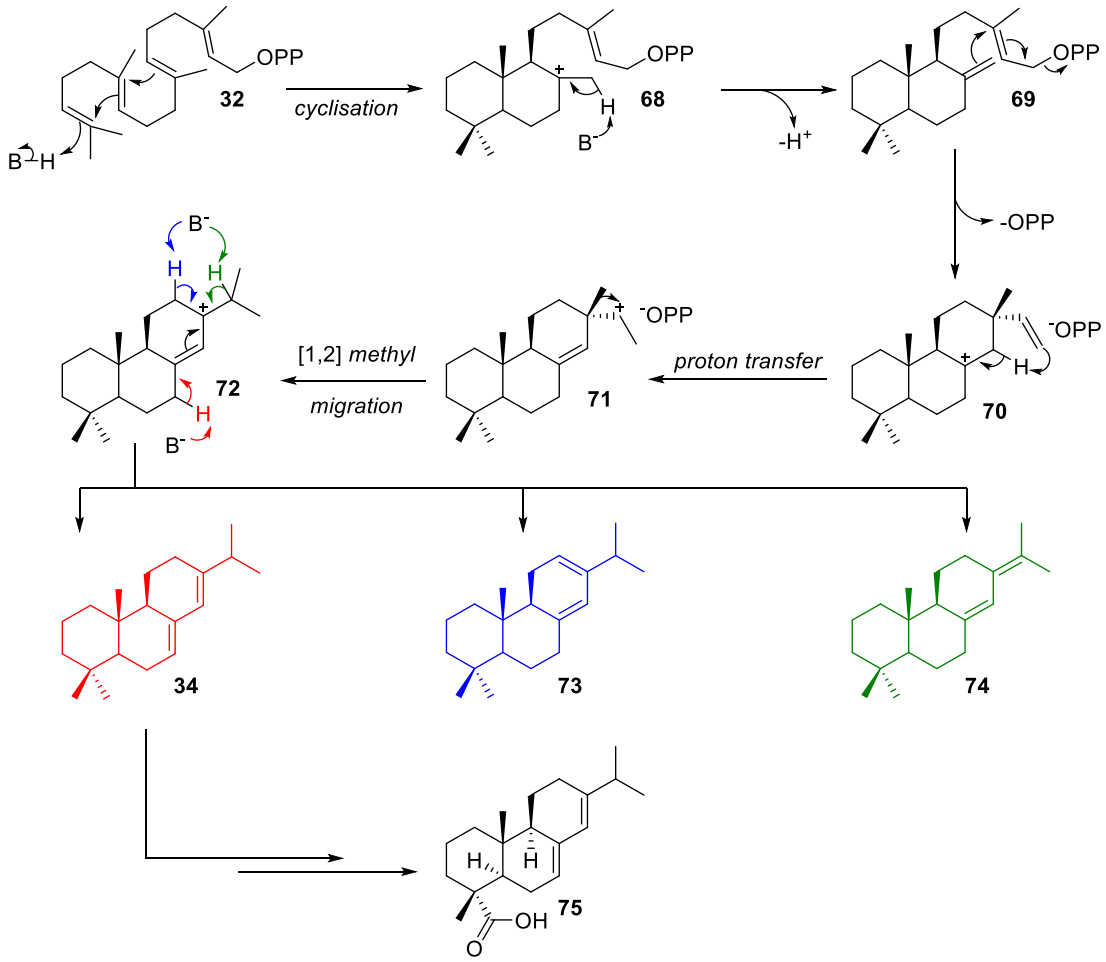

Figure 11. Catalytic mechanism of abietadiene synthase.

Singular and multidomain class I and II terpene cyclases are present throughout nature with conserved characteristics observed across multiple organisms. In addition to the classification of terpene cyclases *via* class I or II mechanisms, further categorisation of cyclases is derived according to their favoured isoprenyl substrate.

1.3 Sesquiterpene cyclases

The terpene synthase family consists of multiple sub groups each of which are designated by the isoprenyl diphosphate substrate they employ. Sesquiterpene synthases catalyse the metal dependent turnover of FDP (**31**).[78] The production of over 300 mono-, bi-, and tricyclic products are known from a multitude of plant, bacterial and fungal enzymes (Figure 12).[79] Sesquiterpene synthases generally act *via* a class I mechanism with an α-helical structure and the conserved DDxxD/E and NSE/DTE motifs incorporated at the tertiary structural fold.[62]

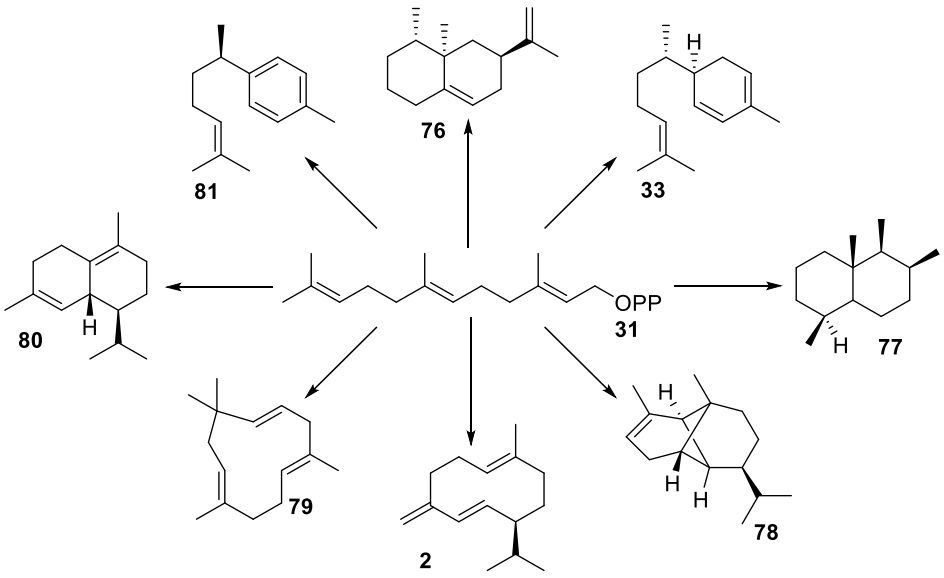

Figure 12. Examples of sesquiterpene products from terpene cyclase catalysed conversion of FDP (31); aristolochene (76), zingiberene (33), drimane (77), (-)-α-copaene (78), germacrene D (2), humulene (79), δ-cadinene (80) and curcumene (81).

1.3.1 The mechanism of initial cyclisations catalysed sesquiterpene cyclases

Sesquiterpene cyclases catalyse a number of cyclisations *i.e.* [1,6] and [1,10] ring closures. A class I mechanism used by sesquiterpene cyclases can adopt two mechanisms of diphosphate cleavage to catalyse a ring closure; a stepwise or concerted mechanism. However, the stereochemistry of (2*E*,6*E*) FDP (**31**) prohibits a [1,6] cyclisation even though sesquiterpene products containing a 6-membered ring are found in nature (Figure 13).

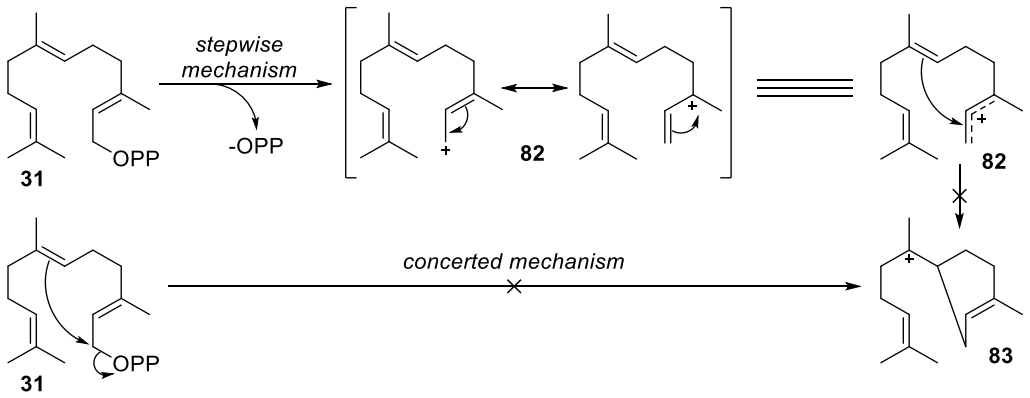

Figure 13. Prevention [1,6] cyclisation (2*E*,6*E*) FDP (31) due to a transoid configured cation (82).

1.3.2 Amorphadiene Synthase

Due to the stereochemistry of (2*E*,6*E*) FDP (**31**), enzymes such as amorphadiene synthase (ADS) catalyse a stepwise mechanism to form nerolidyl diphosphate (**84**).[80] The formation of nerolidyl diphosphate (**84**) allows for the rotation of the C2, C3 double bond to a *cisoid* conformation. The mechanism of ADS begins with the removal of the diphosphate group forming the *transoid* farnesyl carbocation (**83**). The diphosphate group attacks the C3 carbon giving nerolidyl diphosphate (**83**) allowing the free rotation of the C2, C3 bond. Ionisation of the diphosphate group is followed by a [1,6] cyclisation to afford the bisabolyl cation (**86**) with a subsequent [1,3] hydride shift yielding cation (**87**). A [1,10] ring closure and deprotonation at the prenyl tail gives amorpha-4,11-diene (**89**) (Figure 14).[80–83]

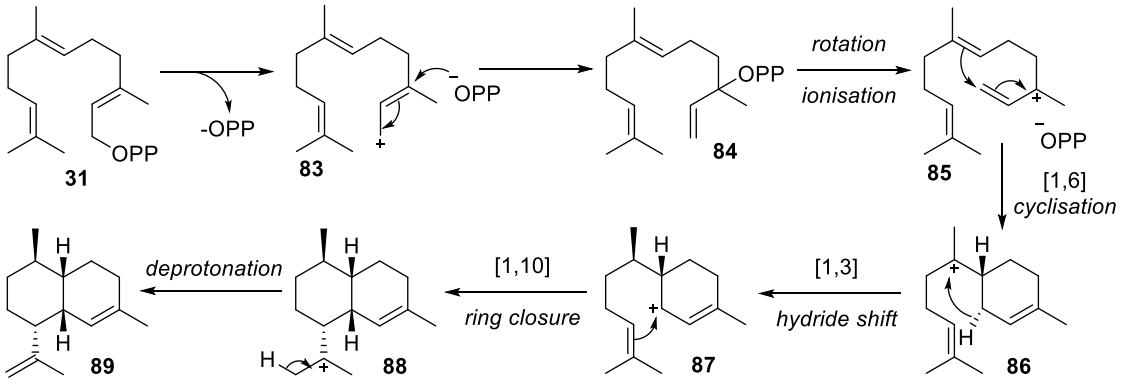

Figure 14. Catalytic mechanism of amorphadiene synthase.

1.3.3 Aristolochene Synthase

Although the formation of the nerolidyl diphosphate (**84**) intermediate is proposed in the mechanisms of numerous sesquiterpene cyclases, it is not the only mode of cyclisation.[80,84,85] Aristolochene synthase (AS) adopts a different approach to diphosphate cleavage. Figure 15 outlines the dissociation of OPP and the proposed catalytic mechanism of aristolochene synthase. Diphosphate cleavage is a result of S_N2-like attack of the C10,C11 π-bond at C1 of (2*E*,6*E*) FDP (**31**) resulting in concerted generation of the germacryl cation (**90**).[86] It is proposed that the OPP anion is positioned in an ideal proximity to C13 to act as a base and deprotonates **61** to yield germacrene A (**40**).[87] Due to the weak basic nature of the OPP anion, its conjugate acid is able to serve as a Brønsted acid when coordinated to three Mg^{2+} ions. Protonation of the C6,C7 double bond affords the eudesmane cation (**91**) which undergoes a [1,2] hydride shift and a [1,2] methyl shift to give **92** and **93** respectively. Finally, deprotonation of cation **93** gives aristolochene (**76**).[88]

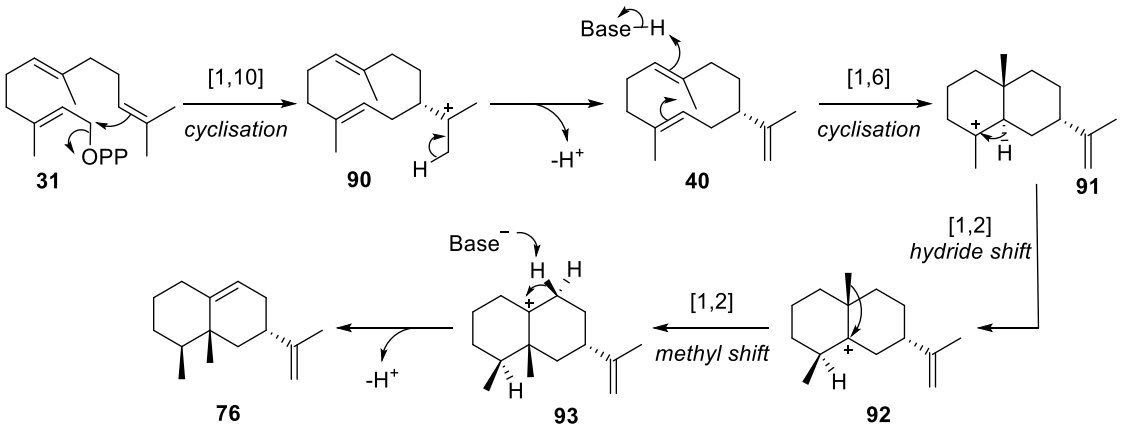

Figure 15. Catalytic mechanism of aristolochene synthase.

1.4 Methods of examining the catalytic mechanisms of sesquiterpene cyclases

Catalysis by sesquiterpene cyclases involves the intricate guidance of carbocations to a complex and stereochemically pure product. From the initial formation of the farnesyl cation (**83**), numerous cascades of carbocations, hydride and alkyl shifts, cyclisations, protonations and deprotonations are involved, influenced by the enzyme.[89] Table 1 (section 1.1) outlines examples of promiscuous terpene cyclases able to accept multiple substrates and catalyse the formation numerous products.[90] γ-Humulene synthase found in grand fir trees (*Abies grandis*) is a further example of a sesquiterpene cyclase that catalyses the turnover of FDP (**31**) to 52 products.[91] In general, sesquiterpene cyclases exhibit remarkably high fidelity by catalysing the formation of a single product. Metal binding motifs for substrate-enzyme binding (section 1.2.1) and hydrophobic/aromatic active site residues orientate the isoprenoid-tail into a favoured configuration.[92,93] This templating effect enables the distinction of similar energy pathways, stabilising carbocations and substrate configuration throughout the mechanism.[60]

Numerous experimental methods are available to study the mechanisms of terpene cyclases. Mechanistic investigations are commonly focused on potential carbocation intermediates, probing their formation *via* two approaches. Aza-analogues are used to mimic putative carbocation intermediates with an ammonium species[94] and fluorinated analogues[95] interrupt the mechanism by destabilising carbocation formation. The stereospecific incorporation of deuterium in place of hydrogen[96] enables elucidation of specific hydride shifts within the mechanism and site directed mutagenesis for the single point mutation of critical residues to probe their effect on catalytic efficiency and product formation.[97]

1.4.1 Aza-analogues

The investigation of cyclase mechanisms is made difficult by the intrinsic instability and transient nature of the carbocation intermediates that are formed. It is not possible to isolate these unstable intermediates, however, the use of quaternary nitrogen containing analogues imitates the positive species (Figure 16).[98] The sp^2 hybridised carbocation is replaced with a sp^3 hybridised nitrogen or sp^2 hybridised iminium ion. These aza-analogues are intended to mimic the stereochemical and electrostatic properties of generated intermediates as closely as is possible.[61] Due to the positive charge residing on an aza-analogue being stable, the enzyme is unable to catalyse further reactions that would occur with the corresponding carbocation. As a result, the analogues are often tightly bound to the active site acting as competitive inhibitors of the enzyme.[77] Inhibition of a terpene

cyclase by an aza-analogue therefore suggests that the corresponding carbocation is generated within the mechanism.[99]

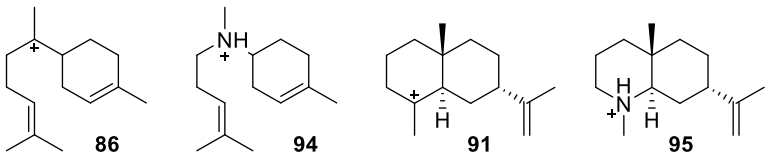

Figure 16. Examples of carbocations and their corresponding aza-analogues: bisabolyl cation (86), aza-bisabolyl cation (94), eudesmane cation (91) and aza-eudesmane cation (95).

1.4.2 Fluorinated analogues

A second method for probing carbocation formation is the incubation of fluorinated analogues with a sesquiterpene cyclase and analysis of incubation products.[100] Fluorinated substrates have been used in the mechanistic investigation of terpene cyclases as the size of fluorine relative to the substituted hydrogen does not greatly affect binding affinities.[11] Though substrate-enzyme binding is not hindered, the electronegative nature of fluorine exhibits a strong electronic influence on carbocations at the α, β and γ-positions. Inductive effects of fluorine increase the energy of the carbocation at the β and γ-positions making carbocation formation unfavourable, whilst a carbocation at the α-position is stabilised by π-donation of the fluorine lone pair or 'alpha effect' (Figure 17).[101]

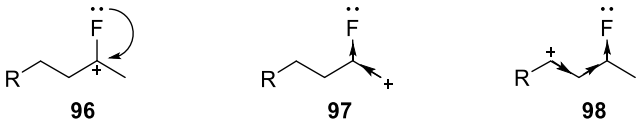

Figure 17. Electron withdrawing and donating effects of a fluorine substituent potential carbocations at the α, β and γ positions: Stabilisation of α-cation (96) *via* alpha effect (left), destabilisation of β-cation (97, middle) and γ-cation (98, right) *via* the inductive effect.

Fluorinated analogues have been utilised to investigate the mechanism of aristolochene synthase (AS) (Figure 15).[102] The [1,10] ring closure could proceed *via* two methods. The first is a stepwise ring closure by dissociation of the diphosphate group forming the farnesyl cation (**83**) and nucleophilic attack by the C10,C11 double bond to give the germacryl cation (**90**). The second method is a concerted mechanism by an intramolecular S_N2-like reaction. To investigate the whether a stepwise or concerted mechanism occurs, (2*Z*,6*E*)-2-fluorofarnesyl diphosphate (**99**) was incubated with aristolochene synthase (AS). Incubation of **99** with AS would inhibit the formation of fluoro-cation

(**100**), in contrast a concerted mechanism would give cation (**101**) and yield a fluorinated product. The incubation gave a single enzymatic product that was found to be 2-fluorogermacrene A (**102**). The formation of **102** gives evidence for a concerted mechanism and insight into the formation of the fluoro-eudesmane cation (**103**). In the catalytic mechanism of AS (Figure 15), the [1,6] cyclisation following the formation of the germacryl cation (**90**) generates the eudesmyl cation (**91**). The presence of fluorine at the C2 position reduces the nucleophilicity of the C2,C3 double bond prohibiting formation of the fluoro-eudesmyl cation (**103**) and its protonation thereby inhibiting the enzyme (Figure 18).[103,104]

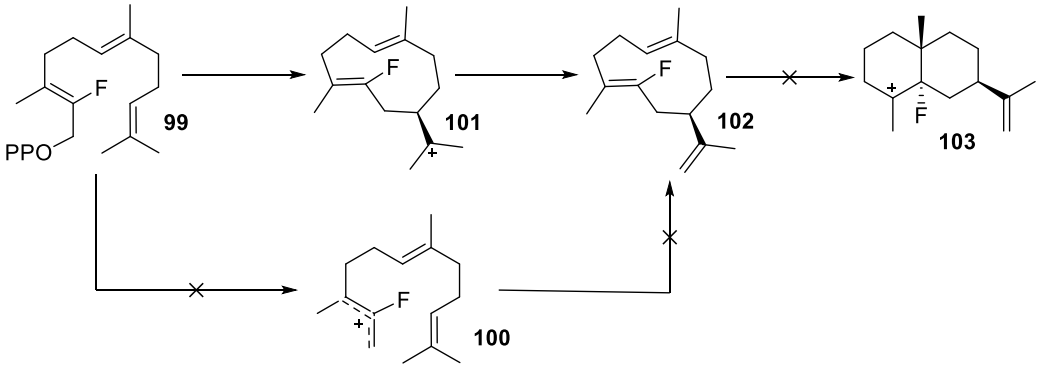

Figure 18. Possible outcomes from the incubation of (2*Z*, 6*E*)-2 fluorofarnesyl diphosphate (99) with aristolochene synthase (AS).

A second fluorinated analogue 12,13-difluorofarnesyl diphosphate (**104**) was incubated with AS to determine the nature of the initial ring closure. Incubation of **104** would inhibit the formation of the fluoro-germacryl cation (**105**) and inhibit substrate turnover whilst a stepwise mechanism may yield 12,13-difluorinated farnesenes **108** and **109** (Figure 19).[105]

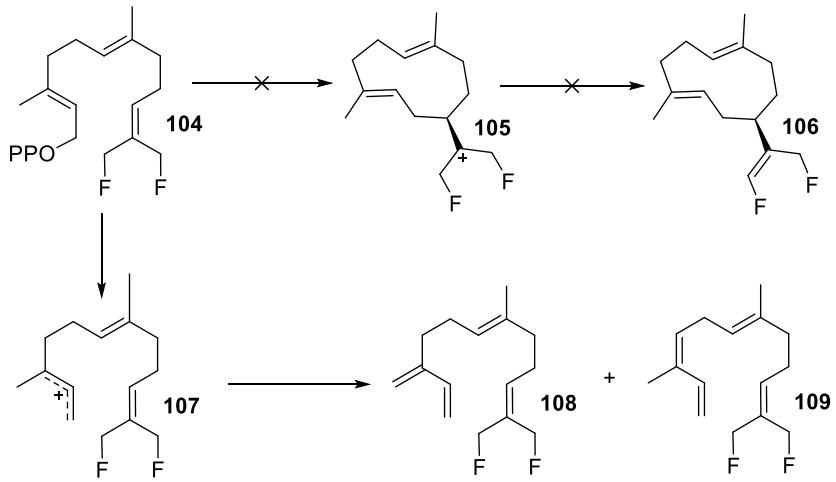

Figure 19. Possible outcomes from the incubation of (2*E*,6*E*)-12,13-difluorofarnesyl diphosphate (105) with aristolochene synthase (AS).

The incubation of **104** and AS resulted in no detectable enzymatic products. Evidence from incubations of fluorinated substrate **99** and **104** with aristolochene synthase determined that the substrate goes through a concerted [1,10]-cyclisation *via* an intramolecular S_N2 like reaction to form the germacryl cation (**90**) (Figure 15).

In contrast, the incubation of (2*E*,6*E*)-10-fluorofarnesyl diphosphate (**110**) with germacrene A synthase (GAS) resulted in 10-fluorohumulene (**114**). The presence of fluorine at the C10 position would be expected to destabilise the formation of the fluoro-germacryl cation (**115**) leading to inhibition of GAS. The formation of 10-fluorohumulene demonstrates that GAS is able to catalyse an anti-Markovnikov [1,11]-macrocyclisation from the C10, C11 double bond due to the fluorine atom invoking α-stabilisation of the cation at the C10 position (**113**) (Figure 20).[106]

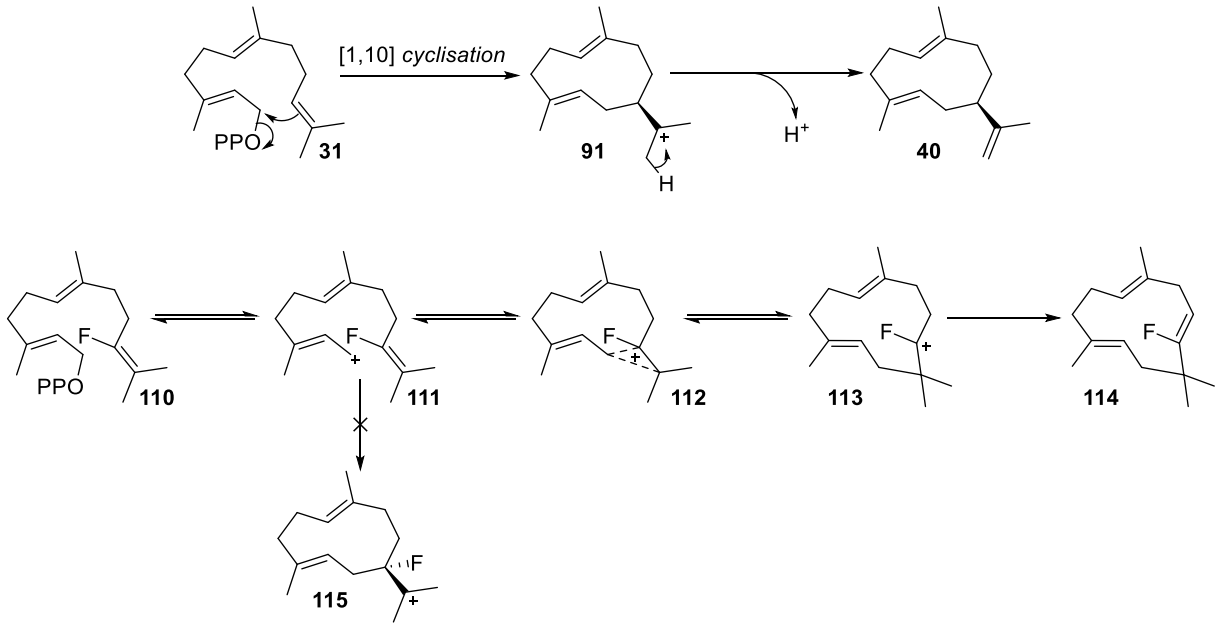

Figure 20. Catalytic mechanism of germacrene A (GAS) synthase (top) and proposed mechanism for the incubation of 110 with GAS (bottom).

1.4.3 Isotopologues

Isotopologues of (2*E*,6*E*) farnesyl diphosphate (**31**) have been critical in the elucidation of some chemical steps catalysed by terpene cyclases and for following reaction kinetics. Radiolabelled substrates have been utilised by numerous research groups for the measurement of steady state kinetics.[97,107–112] The identification of hydride shifts catalysed by terpene cyclases are investigated by the incorporation of deuterium (^{2}H) at specific positions.[113,114] Analysis of the deuterated enzymatic product when compared to the natural product would show an increase (+1 *m*/*z*) on the respective mass spectrum fragment and the loss of the corresponding proton signal on the ^{1}H NMR spectrum.[115,116]

Picaud *et al.* published an investigation of the hydride shifts that occur in the reaction catalysed by ADS (Figure 14).[117] Three deuterated analogues were synthesised for the investigation of the [1,3] hydride shift taking place immediately after the [1,6] ring closure; (2*E*,6*E*)-[1,1-$^2H_2$]-FDP (**116**), (2*E*,6*E*)-(*R*)-[1-^{2}H] -FDP (**122**) and (2*E*,6*E*)-(*S*)-[1-^{2}H]-FDP (**127**). Deuterated analogues **116**, **122** and **127** were incubated with ADS and were shown *via* gas chromatography-mass spectrometry (GC-MS) to produce deuterated amorpha-4,11-diene products. The EI$^+$ mass spectrum of amorpha-4,11-diene (**89**) has four fragment cations of interest **112**, **113**, **114** and **115** (Figure 21), which can used to analyse deuterated products by comparison of mass spectra and respective fragmentations. Incubation of substrates **116**, **122** and **127** and respective products would result in a *m*/*z* ratio increase of +1 or +2 depending on which deuteride was shifting during the mechanism (Figure 22).

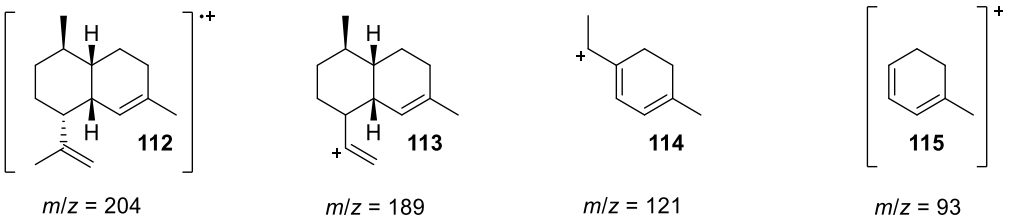

Figure 21. Ions observed in the mass spectrum of amorpha-4,11-diene (89).

The incubation of double deuterated substrate **116** showed a mass increase of +2 of fragment peaks indicative of cations **118**, **119** and **120** with a +1 increase of **121** (Figure 22). These fragmentations show deuterium movement from the C2 to C6 position giving cation **121** with an *m/z* = 94 (Figure 22). The incubation of (2*E*,6*E*)-(*R*)-[1-^{2}H]-FDP (**122**) and ADS was proposed to give deuterated amorpha-4,11-diene (**119**) at the C6 position. The respective fragmentations for cations **126** and **125** provided strong evidence for [1,3] hydride shift of the *proR* proton with no *m/*z increase of **125** whilst a +1 increase was observed with all fragmentations; **124**, **125** and **126**. To confirm the hydride shift of the *proR* proton, (2*E*,6*E*)-(*S*)-[1-^{2}H]-FDP (**127**) was incubated with ADS. The resulting mass spectrum showed fragmentations consistent with cations **129**, **130**, **131** and (Figure 22); a +1 *m/z* increase of proposed cations **122**, **123**, **124** and **125** (Figure 21). These *m/z* increases of deuterated fragments give evidence the *proS* proton does not move during the ADS mechanism, generating deuterated product **128**.[117]

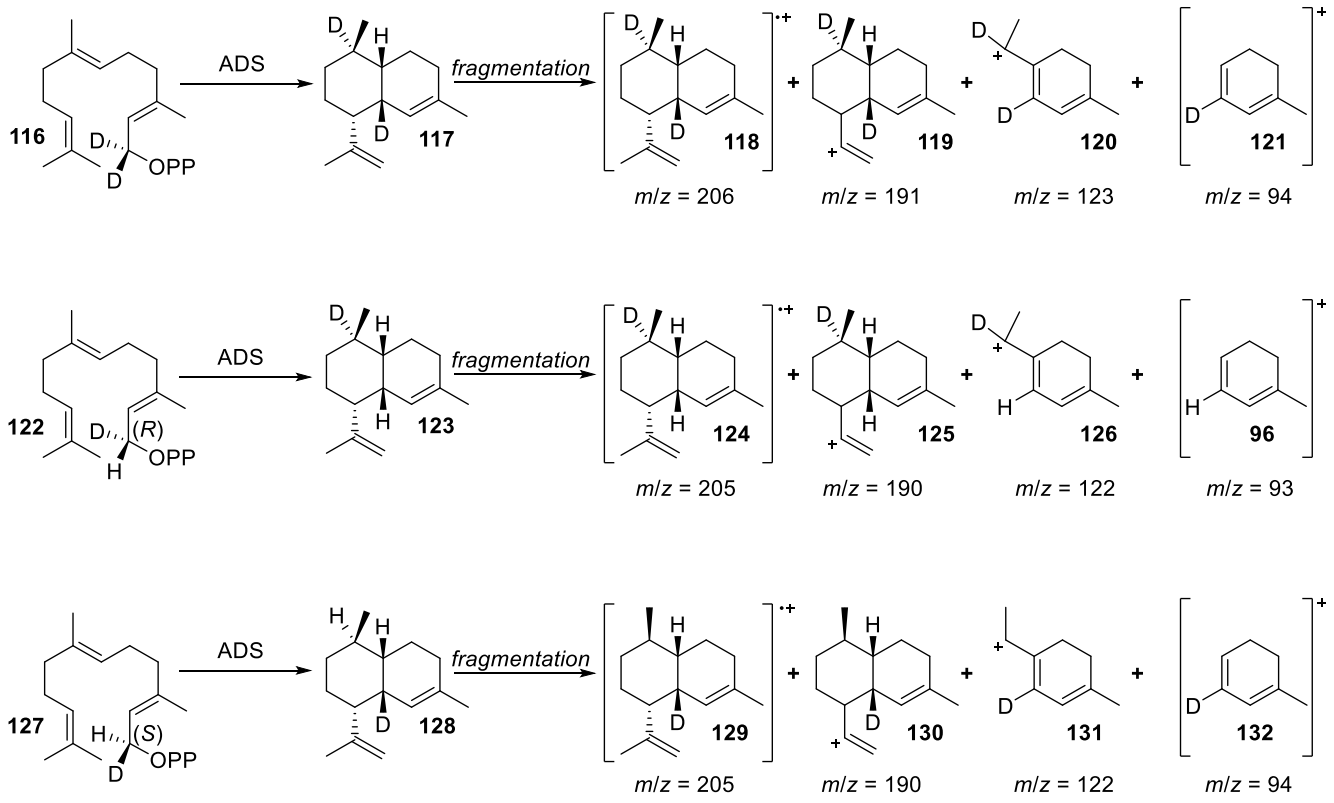

Figure 22. Pentane extractable products from the incubations of deuterated analogues 116, 122 and 127 with amorphadiene synthase and the resultant fragmentation and cation intermediates generated during GC-MS analysis.

The incubation of deuterated substrates **116**, **122** and **127** with ADS and analysis of their respective enzymatic products **117**, **123** and **129** *via* mass spectrometry shows how isotopologues are a powerful tool for the elucidation of hydride shifts.

1.4.4 Plasticity residues

Plasticity residues are specific amino acid residues within the active site of terpene cyclases that are responsible for catalytic promiscuity[54,97] It has been proposed that secondary metabolic enzymes can evolve to develop substrate promiscuity and an expanded product range[118] within the host organism. Plasticity residues can have significant functions within enzyme specificity with key mutations shown to effect product profile and reaction rates.[75,119] Terpene cyclases have been shown to have a lower catalytic efficiency than the majority of central metabolic enzymes with an average k_{cat} value approximately 30 times lower.[120] In terms of efficiency, terpene cyclases are not optimised by nature however enzymatic products have direct applications of great importance. Metabolic engineering of plasticity residues could enable proteins with improved substrate turnover relative to the natural enzyme, accessing terpenoid products that are synthetically challenging to acquire in significant quantities.

A publication by Li *et al.,*[121] reported the mutation of specific residues of *Artemisia annua* α-bisabolol synthase (AaBOS) that are responsible for product specificity. A tetra-substituted mutant AaBOS-M1 (V373N, I395V, N398I and L399T) and penta-substituted mutant AaBOS-M2 (V373N, L381A, I395V, N398I and L399T) were produced to investigate residue plasticity. Incubation of AaBOS-M1 and AaBOS-M2 with (2*E*,6*E*) FDP (**31**) yielded 29.3% and 68.8% of γ-humulene (**134**) respectively alongside α-bisabolol (**133**), (Figure 23).[121]

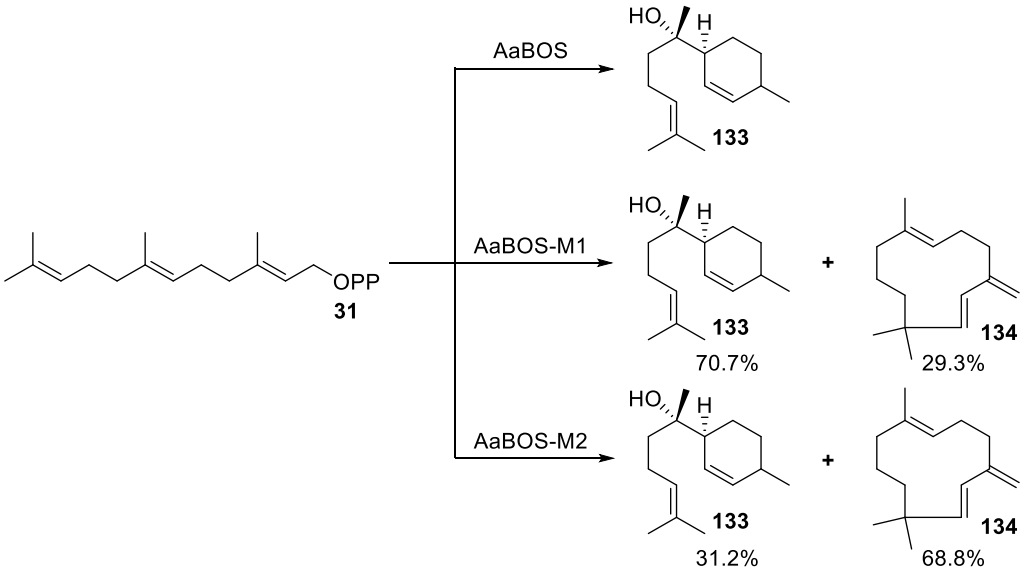

Figure 23. Product distribution of AaBOS, AaBOS-M1 and AaBOS-M2.

The L399T mutation of AaBOS-M2 resulted in a 39.5% increase of γ-humulene (**134**) formation with respect to AaBOS-M1, however single point residue mutations of AaBOS did not vary product formation giving evidence of a synergistic effect of residues.

A single point mutation T399S *A. annua* amorpha-4,11-diene synthase (AaADS), $AaADS_{T399S}$ showed a drastic increase in catalytic efficiency with respect to the wild type enzyme with k_{cat} and k_{cat}/K_M increasing by 83% and 71.7% respectively.

Table 2. Kinetic parameters of AaADS and $AaADS_{T399S}$ (modified from publication by Li *et al.*[121]).

Kinetic parameter	AaADS	$AaADS_{T399S}$
K_M (μM)	3.56	3.79
k_{cat} (s^{-1})	1.37	2.51
V_{max} ($\mu M s^{-1} mg^{-1}$)	4.12×10^{-3}	7.53×10^{-3}
k_{cat} / K_M ($\mu M s^{-1}$)	0.385	0.662

Plasticity residues can have a dramatic effect on the rate and product distribution of terpene cyclases; however the full contribution of these specific amino acids has not been studied in detail.

1.5 Non canonical sesquiterpene cyclases

Although sesquiterpene cyclases can vary in terms of product promiscuity and the presence of archaic non-functional domains, several features are conserved throughout the class of terpenoid cyclases.[122] The conserved DDxxD/E and NTE/DSE motifs, a single catalytic α domain consisting alpha helical bundle and the use of (2*E*,6*E*) farnesyl diphosphate (**31**) are universal traits adopted by the sesquiterpene cyclase family. However, individual cases of non-canonical sesquiterpene cyclases exist that contrast with these generalities.[123]

1.5.1 Geosmin Synthase

Geosmin synthase is a non-canonical sesquiterpene cyclase that uses (2*E*,6*E*) FDP (**31**) as a substrate but forms a product containing 12 carbons. Geosmin synthase from *S. coelicolor* is a class I sesquiterpene cyclase that contains two catalytically active α domains.[124,125] As previously discussed, class I terpene cyclases generally consist of a single α domain in which the class I active site resides however, multiple non-active domains may still be present as part of the protein structure. This bifunctional cyclase adopts an αα domain structure[126] with the first catalytic mechanism occurring in the α domain at the N terminus.[127]

A magnesium-dependent [1,10] cyclisation yields two products; germacradienol (**136**, 85%) and germacrene D (**2**, 15%)(red). After dissociation from the N-terminal active site, germacradienol (**136**)[128,] rebinds to the C-terminal active site, undergoing protonation-dependent cyclisation and fragmentation to give **137** and acetone. A [1,2] hydride shift, protonation and subsequent quenching of the carbocation by water gives geosmin (**139**, blue), (Figure 24).[129,130] Geosmin synthase is an uncommon example of a terpene cyclase catalysing the formation of product with less carbons than in the isoprenyl substrate.[130]

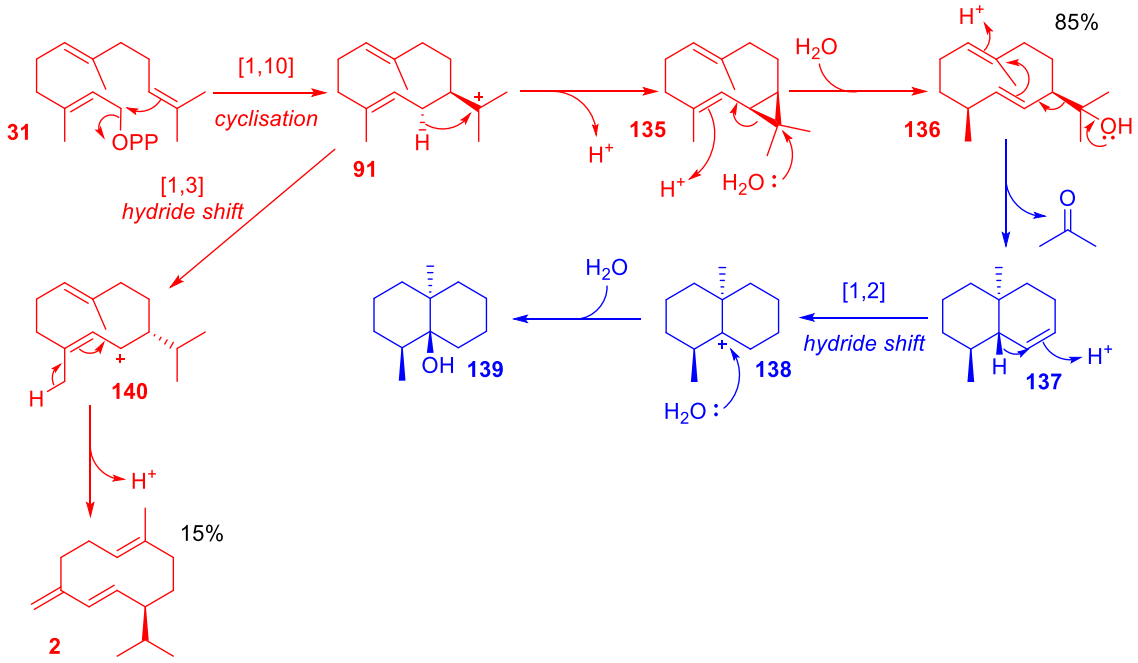

Figure 24. Catalytic mechanism of geosmin synthase.

1.5.2 Santalene and Bergamotene Synthase

Santalene and bergamotene synthase (SBS) is a three domain class I sesquiterpene cyclase isolated from the chloroplasts of the wild tomato plant, *S. habrochaites*.[131] In contrast to the majority of sesquiterpene synthases, santalene and bergamotene synthase does not utilise the 'universal' substrate (2*E*,6*E*) FDP (**31**) as a substrate instead it utilises the *cisoid* isomer (2*Z*,6*Z*) FDP (**38**) as a substrate, exhibiting product promiscuity with the formation of five different sesquiterpenes products.[3]

The proposed mechanism begins with the formation of the *cisoid* farnesyl cation (**140**) resulting from the removal of the diphosphate moiety. A [1,6] ring closure then gives bisabolyl cation isomers **141** and **145** with either a [2,7] or [3,7] cyclisation yielding the cation precursors for the bergamotene or santalene products respectively. The formation of (-)-*exo*-α-bergamotene (**58**) requires the rotation of the C6,C7 bond of cation **141** (red arrow). The rotation is followed by a [2,7] cyclisation and deprotonation to give **58** (Figure 25). A [2,7] cyclisation of **141** without rotation gives cation **143**. Deprotonation of the methylene (blue) or methyl (green) group of cation **143** gives (-)-*endo*-α-bergamotene (**61**) or (+)-*endo*-β-bergamotene (**144**) respectively (Figure 25). After the formation of cation **145**, a [3,7] cyclisation gives cationic intermediate **146** after which the mechanism can proceed in two ways. A[3,4] methyl shift and deprotonation of the resultant cation **147** gives (-)-*epi*-β-santalene (**57**). Alternatively, a [2,4] cyclisation of **146** yields (+)-α-santalene (**55**) (Figure 25).[132]

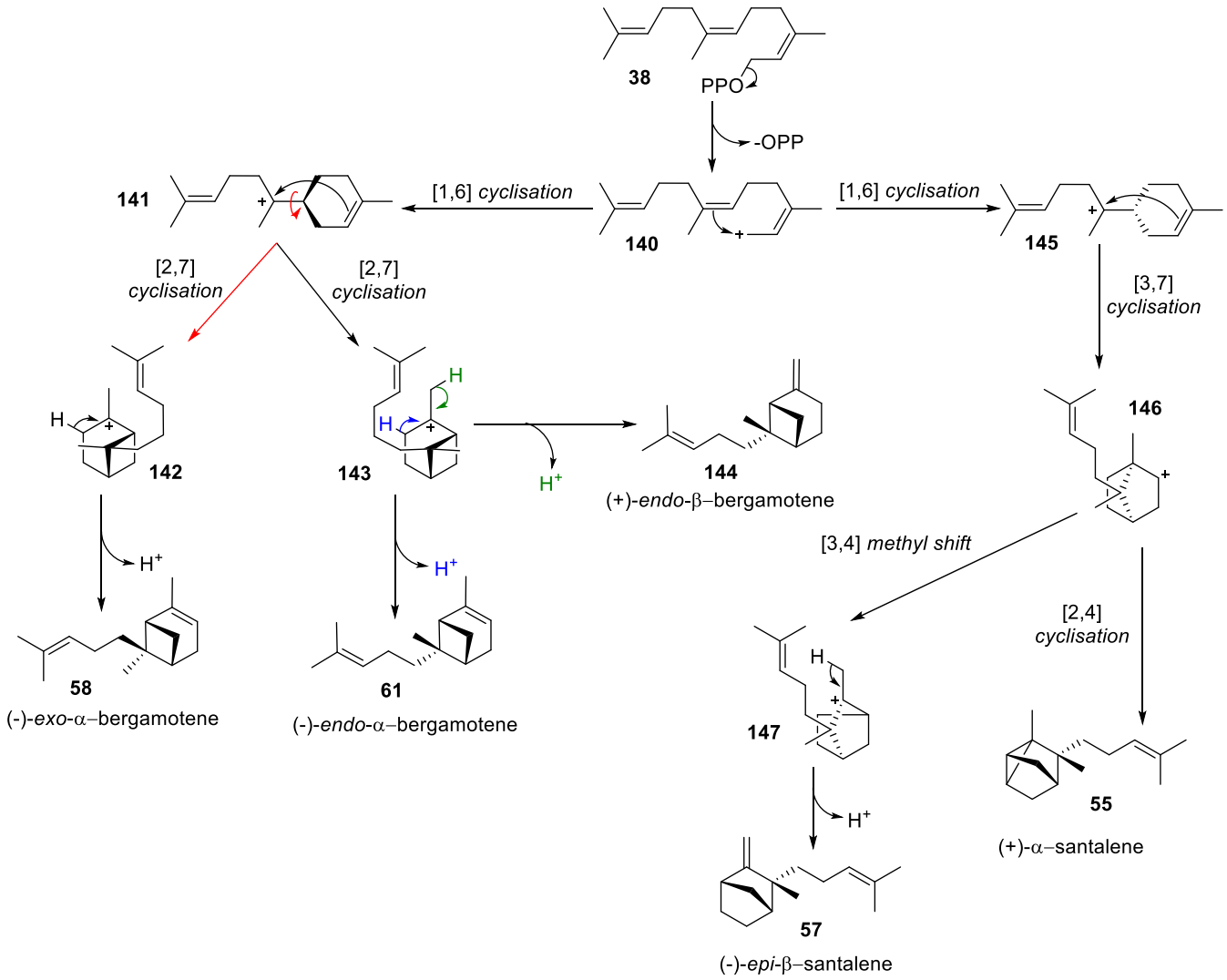

Figure 25. Catalytic mechanism of santalene and bergamotene synthase and products; (-)-*exo*-α-bergamotene (58), (-)-*endo*-α-bergamotene (61), (+)-*endo*-β-bergamotene (144), (-)-*epi*-β-santalene (57) and (+)-α-santalene (55).

Santalene and bergamotene synthase (SBS) was the first published example of a sesquiterpene synthase that does not utilise (2*E*,6*E*) FDP (**31**) as a substrate introducing a new class of terpene cyclases with *cisoid* isoprenoid substrate specificity.

1.6 Applications of sesquiterpene cyclases

With a multitude of sesquiterpene cyclases and their products characterised, an abundance of applications concerning sesquiterpene products have been developed. Terpenoid natural products have applications within the pharmaceutical,[133] fuel[134] and food industries[135] whilst others can be utilised by humans for the same purpose they are synthesised.[106] Understanding the structure, mechanism and substrate/product promiscuity of sesquiterpene cyclases could provide opportunity to quickly access structures of high complexity without the need for extensive synthetic procedures.

1.6.1 Pharmaceuticals

An example of a sesquiterpene utilised within medicine is amorpha-4,11-diene (**89**).[83] Produced from (2*E*,6*E*) FDP (**31**) through the magnesium dependent catalysis of amorphadiene synthase (ADS), **89** is a precursor of the potent anti-malarial drug artemisinin (**7**)(Figure 26).[80] Originally isolated from sweet wormwood (*Artemisia annua*), the compound's unusual highly oxygenated core is responsible for the drug's activity.[136] [82]

Gossypol (**6**) isolated from the seed stem and root of the cotton plant (*Gossypium*) is a derivative of the sesquiterpene δ-cadinene (**80**) (Figure 26). In addition to cytotoxic properties, gossypol has been proposed as a form of male contraceptive.[137] Studies funded by the Chinese government revealed that the drug was effective, well tolerated and did not result in changes in blood pressure, weight or main biochemical parameters.[138] Two undesirable side effects of gossypol were noted; hypokalemia (a reduction in blood potassium) in 10% of users and the irreversibility of the contraceptive effect in approximately 10% of users. However, research investigating the application of gossypol as a contraceptive is on-going.[8]

α-Bisabalol (**133**) is produced by α-bisabalol synthase (AaBOS) from (2*E*,6*E*) FDP (**31**) (Figure 26) and is found in chamomile (*Matricia recutita*).[139] The sesquiterpene alcohol is responsible for many beneficial effects associated with chamomile and reported to exhibit anti-inflammatory, antibacterial, anti-allergic, drug permeation and vermifugal (an agent that destroys or expels parasitic worms) properties.[140] The Food and Drug Administration (FDA) gave α-bisabolol (**133**) a Generally Regarded as Safe (GRAS) status allowing its use within commercial products.[141]

These examples are only a small number of the biologically interesting sesquiterpene products utilised within the pharmaceutical industry. Terpene cyclases give access to many structures of interest that are difficult to synthesise with high yield and correct chirality and stereochemistry through traditional synthetic organic routes. Unfortunately, though terpene cyclases can yield

complex structures, they are also a bottle neck within industrial processes as substrate turnover and product extraction can be problematic.

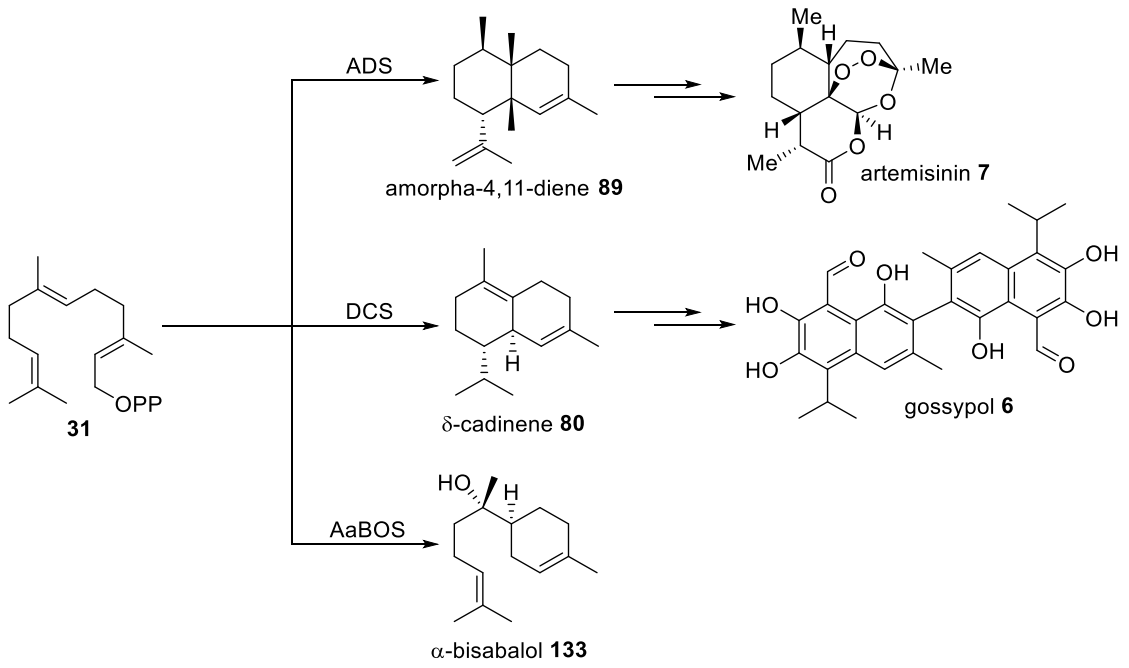

Figure 26. Sesquiterpene cyclases that yield pharmaceutically interesting products; amorphadiene synthase (ADS, top), δ-cadinene synthase (DCS, middle) and α-bisabalol synthase (AaBOS, bottom).

1.6.2 Biofuels

Dwindling fossil fuel reserves and energy security have highlighted an interest in the production of sustainable fuel sources. The use of sesquiterpene derived biofuels is an attractive alternative to currently used petroleum based fuels.[142] Low hygroscopy, high energy density and good fluidity at low temperatures advocates their use as a plausible replacement that could be assimilated into the current infrastructure.[143] Two sesquiterpene derived products; farnesane (**149**) and bisabolane (**152**) have been proposed as potential alternatives.[144]

Farnesene is the collective name for 3 stereoisomers; (2*Z*,6*E*)-α-farnesene (**148**), (2*E*,6*E*)-α-farnesene (**59**) and *E*-β-farnesene (**60**) all of which are utilised as semiochemicals by various plants, (Figure 27).[145–147] Farnesene is produced by a wide range of organisms with the hydrogenated derivative farnesane (**149**) a potential renewable fuel source. Farnesane has a cetane number of 58 (cetane number of diesel fuels must be within a 40-60 range)[148] and a -78 °C cloud temperature when compared to D2 diesels (-3 °C) gives a potential replacement for diesel and jet fuel.[149]

Bisabolene synthases are the sesquiterpene cyclases responsible for the biosynthesis of bisabolene products and are generated in various conifer species to repel attacking species.[45,150,151] Bisabolane

(**152**) is the hydrogenated derivative of three bisabolenes; α-bisobolene (**66**), β-bisabolene (**150**) and γ-bisabolene (**151**) (Figure 27). Monocyclic derived, hydrogenated sesquiterpene products such as bisabolane (**152**) are comparable with farnesane. An equivalent low cloud temperature (-78 °C) and a favourable density (bisabolane = 0.88 gmL^{-1}, farnesane = 0.77 gmL^{-1}) give premise as a diesel alternative.[152]

The application of sesquiterpene products as biofuels is not confined to the use of bisabolane (**152**) or farnesane (**149**), as many other monocyclic products are available. However, as with pharmaceutically applicable products using sesquiterpene cyclases, substrate turnover and product extraction could be slower than the required demand.

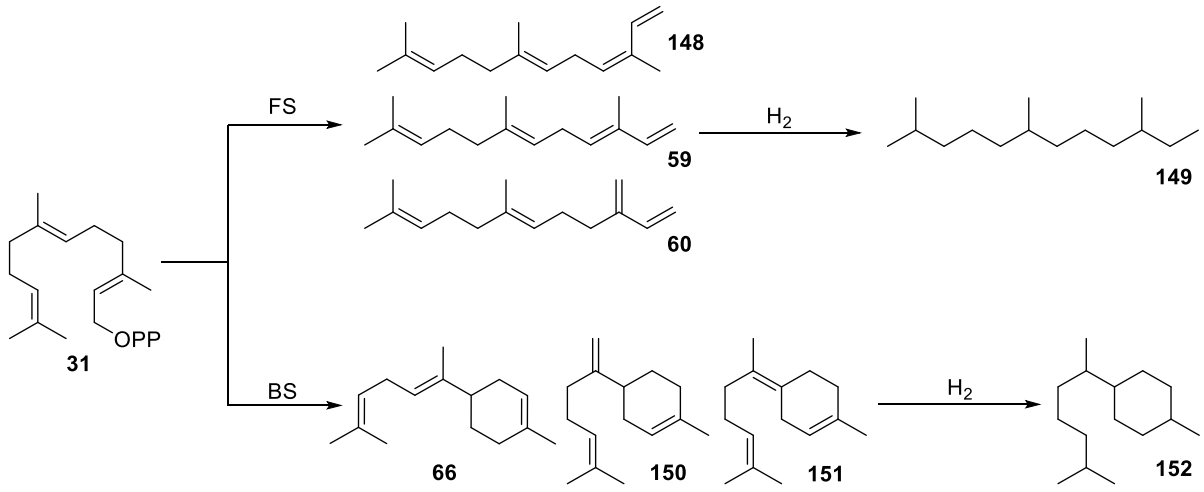

Figure 27. Sesquiterpene cyclases whose products have applications as biofuels; farnesene synthase (FS, top) and bisabolene synthase (BS, bottom).

1.6.3 Food and flavourings

Plant sesquiterpene products are often responsible for plant defence; however, some examples exhibit a second function as flavouring in food. Zingiberene (**33**) is a monocyclic sesquiterpene isolated from ginger (*Zingiber officinale*) (Figure 28). Zingiberene synthase (ZS) catalyses the cyclisation of (2*E*,6*E*) FDP (**31**) to give **33** which constitutes up to 30% of essential oils within ginger rhizomes and is responsible for the distinct flavour.[153,154]

(-)-β-Caryophyllene (**153**) is a constituent of various essential oils and can be isolated from the stems and flowers of cloves (*Syzygium aromaticum*)[155] and rosemary (*Cannabis sativa*).[156] (-)-β-caryophyllene (**153**) also contributes to the spice of black pepper.[157] The presence of four and nine membered rings is scarce in nature making (-)-β-caryophyllene (**153**) a rare structure (Figure 28).

Hernandulcin (**154**) is a derivative of α-bisabolol (**133**), the product of α-bisabolol synthase (AaBOS) (Figure 28). The compound was known to the Aztec civilisation as the 'sweet plant', later identified as *Lippia dulcis*.[158] The principle sweet component was concentrated in the leaves and flowers and judged by a human taste panel as more than 1000 times sweeter than sucrose.[159] Due to a mint aftertaste, intense sweetness and no link to tooth decay; hernandulcin (**154**) is a proposed additive for oral hygiene products.[160]

Sesquiterpenes are often the main constituents in natural flavours. Essential oils are often blends of terpenoid products with **33**, **153** and **154** being examples of sesquiterpene products responsible for intense flavours.

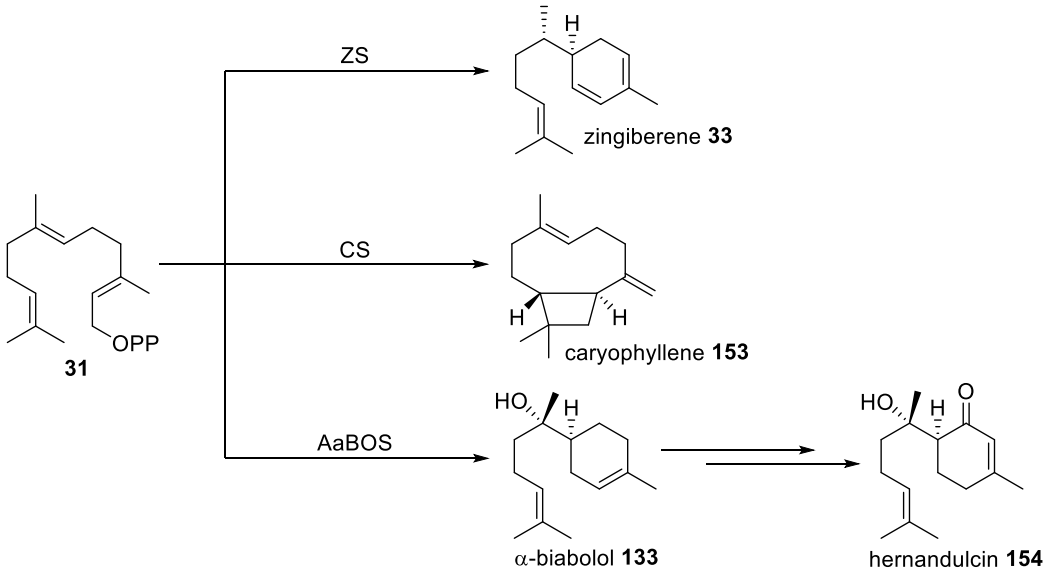

Figure 28. Sesquiterpene cyclases with products applicable as flavourings; zingiberene synthase (ZS, top), caryophyllene synthase (CS, middle) and α-bisabolol synthase (AaBOS, bottom).

1.6.4 Semiochemicals and agriculture

Semiochemicals are compounds produced by organisms which signal the change in development or behaviour of another organism without physiological activity. Within this class of chemicals are plant stress signals that are responsible for plant defence including phytopheromones that also play a role in plant development.[161] Semiochemicals are not restricted to plant-herbivore interactions with chemically mediated communication also occurring between certain ant species (*Formica subsericea*) and the majority of aphid (*aphidinae*) species.[162] It was observed by Nault *et al.* that when *Formica subsericea* were exposed to aphid alarm pheromones, they extended their antennae and opened their mandibles in preparation for attack from aphids.[163] Many plant derived

semiochemicals are sesquiterpene products with the variety of stereochemistry and chirality allowing for these compounds to act as both herbivore repellents and pollinator attractants.[164,165]

Semiochemicals have been investigated as replacements for commercial insecticides with the mode of action and subsequent impact on human and environmental health being inherently different to current chemical insecticides.[166,167] With health concerns of insecticides and potential chemical run off into water systems, the use of semiochemicals increases safety for humans and non-targeted species, with the reduction of pesticide use, increase of pest predator activity[166] and therefore increased biodiversity in agriculture ecosystems.[168]

Two sesquiterpenes of interest are (*E*)-β-farnesene (**60**) and (-)-β-caryophyllene (**153**) (Figure 29). Both sesquiterpenes have been discussed previously for their roles in biofuels and food respectively. However, the functions of **60** and **153** in nature may be applicable to agriculture. (*E*)-β-Farnesene (**60**) is an alarm pheromone for the majority of aphid species[169,170] and an attractant to the aphid predator, Asian lady beetle (*Harmonia axyridis*).[165] (-)-β-Caryophyllene (**153**) also acts as an attractant to the male Asian lady beetle[171] whilst the female showed no behavioural changes. Combination of sesquiterpenes **60** and **153** have potential in push-pull strategies utilising Asian lady beetles as a control for aphid infestation.[165] The push-pull strategy requires a combination of (*E*)-β-farnesene (**60**) and (-)-β-caryophyllene (**153**); the presence of **60** acts as a deterrent for target pests from a protected host, with a combination of **60** and **150** attracting the respective predators as a secondary defence.[172]

A second strategy in plant defence is the use of pest attractants *i.e.* the Bark beetle (*Scolytus multistriatus*) sex pheromone, (-)-α-cubebene (**155**) (Figure 29). An investigation in 1969 observed an increased attraction of male Bark beetles in response to (-)-α-cubebene (**155**) produced by virgin females tunnelling in elm logs.[173] The Bark beetle is responsible for the spread of Dutch elm disease which decimated the non-resistant population of elm trees across America and Europe.[174] The isolation of (-)-α-cubebene (**155**) gave rise to a trap and kill methodology of pest control. In contrast to using pest alarm pheromones that could result in infestations at other locations, the use of an attractant allowed for the trapping of the pests to slow the spread of disease.[175]

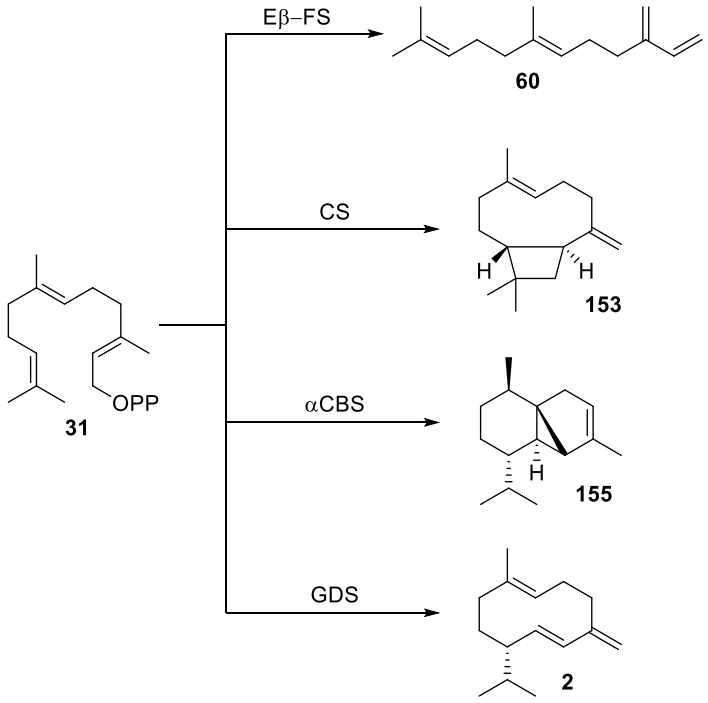

Figure 29. Sesquiterpenes with semiochemical products; (*E*)-β-farnesene (60), (-)-β-caryophyllene (153), (-)-α-cubebene (155) and (*S*)-germacrene D (2).

Germacrene D synthase (GDS) catalyses the turnover of (2*E*,6*E*) FDP (**31**) to (*S*)-germacrene D (**2**) (Figure 29), a potent arthropod repellent effective towards aphids,[176] ixodid ticks and red poultry mites.[177] Touchet *et al.* reported the synthesis and incubation of novel isoprenyl diphosphate substrates with GDS and GDS mutants, generating novel germacrene products to use in aphid behavioural assays. The incubation of (2*E*, 6*E*)-14-methylfarnesyl diphosphate (**156**) with GDS(Y406F) yielded 14 methyl germacrene D (**157**) which like the natural product, was found to be a repellent to aphids. In contrast, the incubation of (2*E,*6*E*)-14,15-dimethylfarnesyl diphosphate (**158**) with GDS(Y406F) yielded a 14,15-dimethyl germacrene D (**159**) which was found to be a potent aphid attractant (Figure 30).[178]

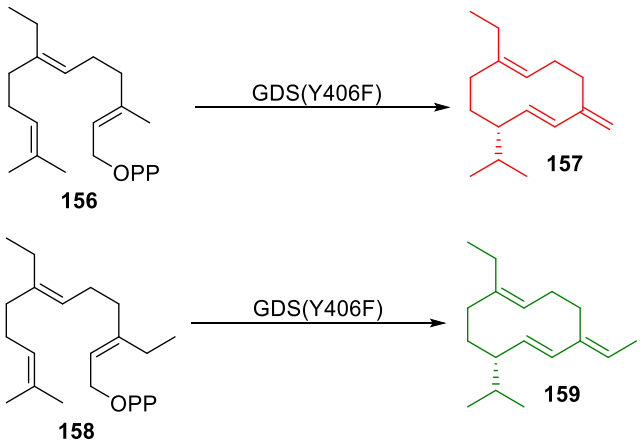

Figure 30. Novel isoprenoid substrates 141 and 143 incubated with GDS(Y406A).

This is an example of using modified isoprenoid substrates and sesquiterpene mutants to generate novel sesquiterpene products with similar and contrasting properties. Applications of sesquiterpenes cover a wide range of industries. The understanding and characterisation of sesquiterpene cyclases allows for the production of natural and novel sesquiterpene products with a plethora of applications.

1.7 Whitefly, 7-epizingiberene and 7-epizingiberene synthase

Herbivorous insects are a serious threat to agriculture through feeding on crops and their ability to transmit viruses capable of devastating the crop population in the area.[3] With food production being an essential commodity contributing substantially to the global economy, measures must be taken to minimise crop destruction.[179] Since the late 1980s, large areas spanning from Florida to South America have been plagued by geminiviruses as a result of whitefly infestation.[180] As a result, the whitefly is now thought of as a major world pest concerning various agronomic and horticultural crops including tomatoes.[181] However, various plants are capable of emitting varying amounts of volatile terpenoids (monoterpenes and sesquiterpenes) as a defence mechanism when infested with herbivores.[41] An example of this comes in the form of wild tomatoes (*Solanum habrochiates*) that unlike their cultivated counterparts (*e.g.* moneymaker) exhibit significant herbivore resistance.[2,182]

Santalene, bergamotene and 7-epizingiberene (**1**) are phytoalexins (a substance that is produced by plant tissues in response to contact with a parasite and specifically inhibits the growth of that parasite) the latter a repellent that is toxic to whitefly. Derivatives of 7-epizingiberene (**1**) may be more potent and stable repellents of whitefly and find use for increased protection of crop

populations from this devastating pest. The use of terpenes within agriculture should decrease the use of chemical pesticides which can have a devastating effect on the environment.[183]

SBS and EZS are found within the wild tomato plant (*Solanum habrochiates*) and are members of a recently discovered class of sesquiterpene synthases have been that selectively use (2*Z*,6*Z*) farnesyl diphosphate ((2*Z*,6*Z*) FDP, **38**).[3] The substrate selectivity of these enzymes is intriguing as it is unconventional for the majority of characterised sesquiterpene synthases to act in this manner.[2]

SBS and EZS are responsible for catalysing the Mg^{2+}-dependent conversion of (2*Z*,6*Z*)-FDP (**38**) to three bergamotene products **58**, **61**, **144** and two santalene products **56** and **57**[30] whilst EZS selectively and specifically yields 7-epizingiberene (**1**) (Figure 31).[2]

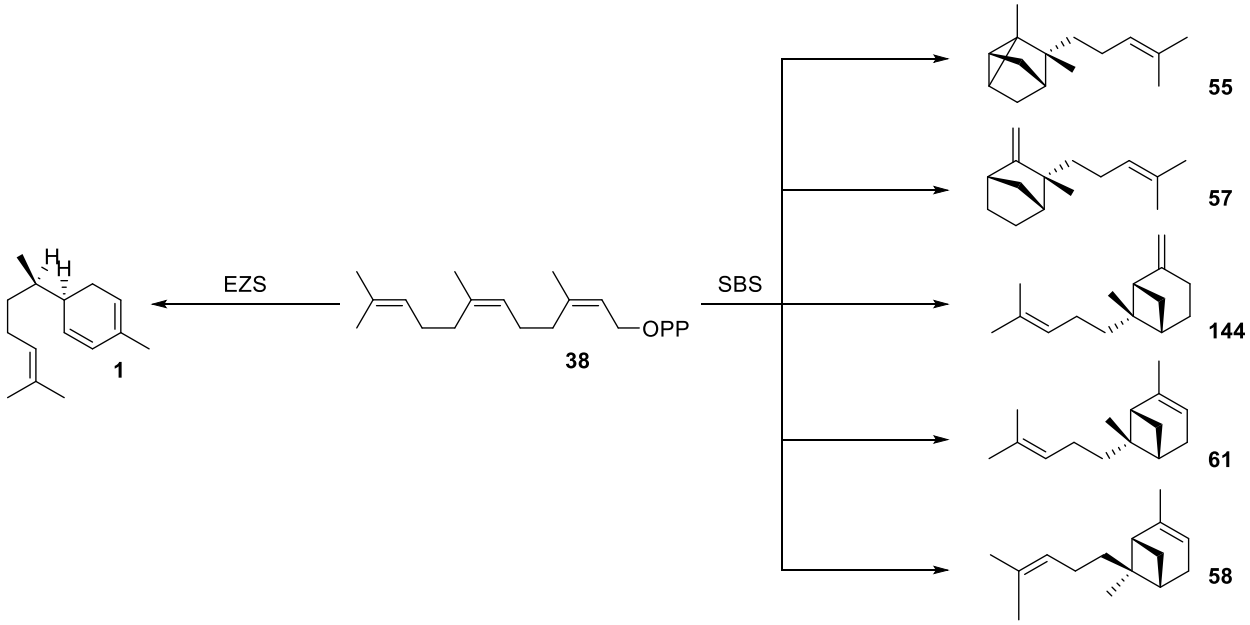

Figure 31. Products arising from EZS and SBS catalysed turnover of (2*Z*,6*Z*) FDP (38).

Generally, sesquiterpene precursors are synthesised *via* the MEV pathway however, EZS and SBS are found within the plastids suggesting that the formation of the isoprenyl precursor is produced using the DXP pathway.[184] *Z*-Prenyltransferase is responsible for the synthesis of (2*Z*,6*Z*) FDP (**38**) following the DXP pathway and is found within the plastids of the wild tomato plant alongside SBS and EZS.[184] (2*E*,6*E*) FDP (**31**) is synthesised within the cytosol (MEV pathway, Figure 2) and is therefore not available to act as a substrate for SBS and EZS.

7-Epizingiberene synthase (EZS) contains three domains and could potentially exhibit both class I and II catalytic activity. Due to structural similarities to diterpene synthases, it could be postulated that it displays class II activity.[14] However, since 7-epizingiberene synthase appears to catalyse diphosphate cleavage exclusively, activity associated with the class I active site, the β and γ domains appear catalytically silent.[3]

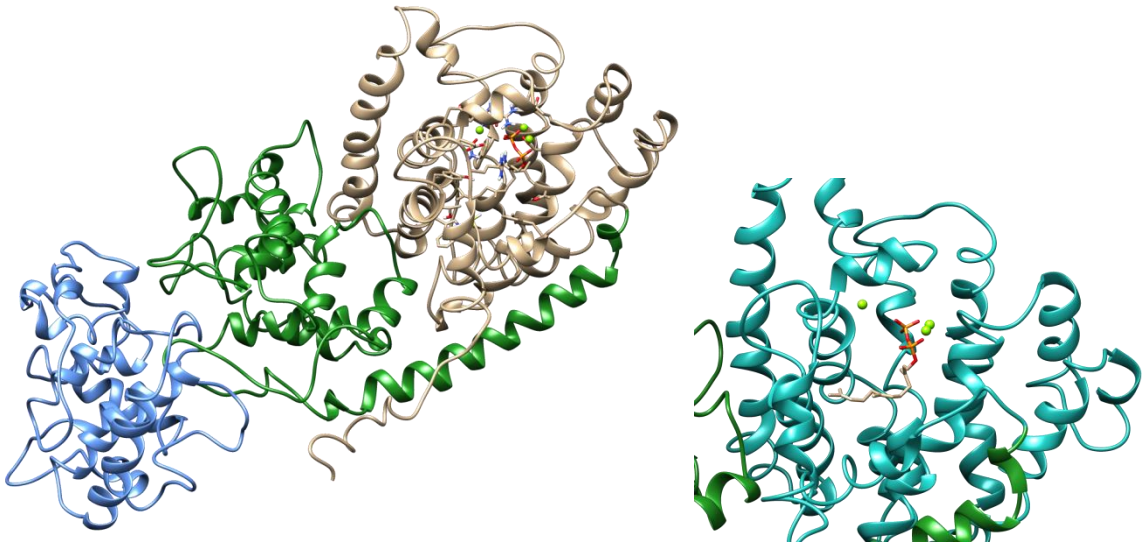

Figure 32. Cartoon representation of EZS (left) and cartoon representation of the EZS catalytic alpha domain with (2*Z*,6*Z*) FDP (38) (right).[185]

The catalytic mechanism of EZS is currently unknown. However, mechanistic predictions can be made based on knowledge of previously studied sesquiterpene synthases. Figure 33 outlines the plausible mechanistic routes that could be catalysed by EZS.

As EZS exhibits class I activity, the initial carbocation is formed *via* diphosphate cleavage. EZS could favour a concerted [1,6] ring closure to form the bisabolyl cation (**86**). Alternatively, a stepwise ring closure with diphosphate cleavage forming a farnesyl cation (**141**) followed by a [1,6] ring closure to form **86**. Numerous hydride shifts are then possible to attain the final product. A [1,3] hydride shift from C1 or C5 (shown in red and blue respectively) are possible, giving carbocations **161** and **162** followed by a deprotonation to give 7-epizingiberene (**1**). Alternatively, a [1,2] hydride shift from C6 (green) to give **160** followed by a second [1,2] hydride shift either from C1 or C5 (shown in red and blue respectively) to give **161** and **162** proceeded by deprotonation is conceivable to give 7-epizingiberene (**1**).

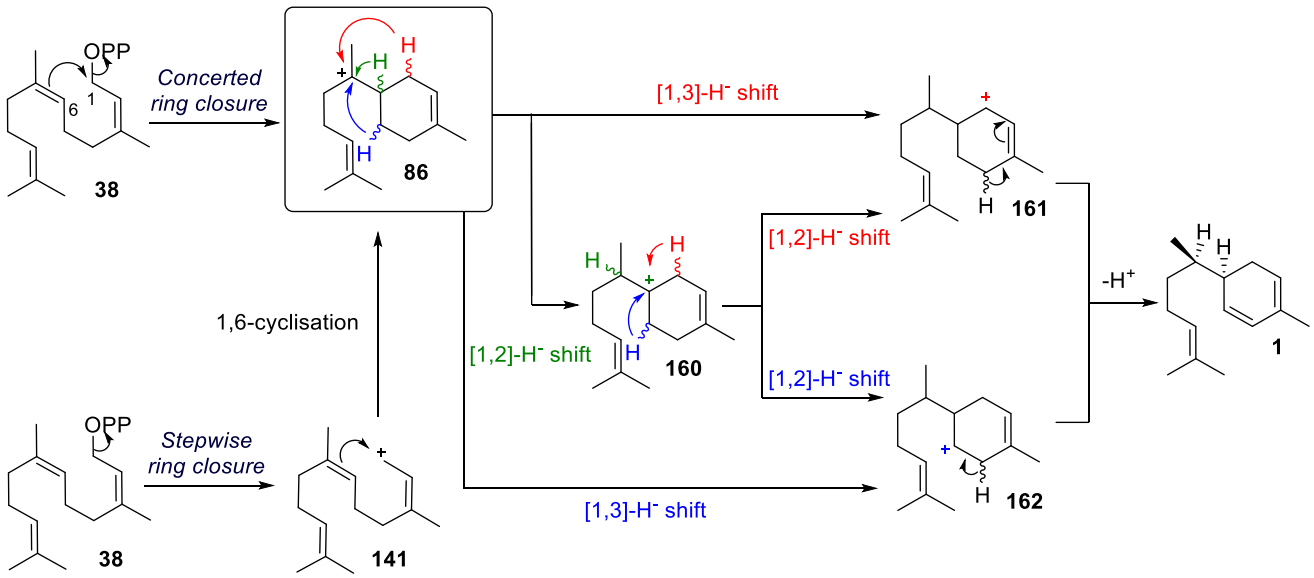

Figure 33. Plausible reaction pathways that could be catalysed by EZS.

Current publications concerning 7-epizingiberene synthase (EZS) by Bleeker *et al.*[2,3] and Sallaud *et al.*[30] have investigated gene isolation, plant cross breeding and bioassays to elicit an electroantennogram response in whitefly. Characterisation and a crystal structure have yet to be attained for EZS with K_M and k_{cat} values calculated using a GC-MS assay. All publications concerning EZS and SBS outline how both enzymes have high substrate specificity toward (2*Z*,6*Z*) farnesyl diphosphate (**38**) and not (2*E*,6*E*) farnesyl diphosphate (**31**). There have been no investigations into EZS substrate promiscuity towards stereoisomers of **31**, (2*E*,6*Z*) farnesyl diphosphate and (2*Z*,6*E*) farnesyl diphosphate (**341**).

Investigation of the mechanism, characterisation and substrate specificity of EZS may elucidate which novel substrates could yield analogues of 7-epizingiberene (**1**). A greater insight into EZS substrate specificity could yield a library of sesquiterpene products with semiochemical properties. As with germacrene D synthase site directed mutagenesis and incubation of novel substrates produced repellent and attractant semiochemicals that have applications for crop protection (Figure 30). A greater understanding of EZS may yield similar results, with metabolic engineering to incorporate EZS into cultivated tomato species previously proposed by Bleeker *et al.*[3]

1.8 Project Aims

7-Epizingiberene synthase represents a new class of sesquiterpene cyclases that defy convention by exclusively utilising the *cisoid* isomer of the previously thought 'universal' substrate FDP (**31**) and therefore warrants investigation. The initial aim of the project was the synthesis of the natural EZS substrate, (2*Z*,6*Z*)-farnesyl diphosphate (**38**) followed by expression and purification of 7-epizingiberene synthase. Following the purification of EZS; the synthesis of radiolabelled (2*Z*,6*Z*) farnesyl diphosphate, (2*Z*,6*Z*)-[1-^{3}H]-FDP (**229**), was required for the kinetic characterisation of EZS. The purpose was to discover a low cost and reproducible synthesis of **38** as the precursor (2*Z*,6*Z*) farnesol (**167**) costs £1011.00 per mg (at the time of writing), whilst the *transoid* isomer (2*E*,6*E*) farnesol (**353**) costs £99.00 for 100 g. It is not viable to purchase (2*Z*,6*Z*) farnesol (**167**) in sufficient quantity to conduct research. Site directed mutagenesis was used to investigate class I and potential class II activity of EZS as well as probing the significance of specific aromatic residues within the class I active site pocket

The second segment of the project focused on the synthesis of fluorinated substrates and isotopologues for mechanistic investigation. As discussed in sections 1.4.2 and 1.4.3, the use of these substrates can give evidence towards carbocation formation and hydride shifts that occur throughout the mechanism. Synthesis of stereoisomers of (2*Z*,6*Z*) farnesyl diphosphate (**38**) and their respective monoterpene substrates (2*E*,6*Z*) farnesyl diphosphate (**342**), (2*Z*,6*E*) farnesyl diphosphate (**341**), (2*E*,6*E*) farnesyl diphosphate (**31**), neryl diphosphate (**39**) and geranyl diphosphate (**30**) were used to give understanding to the substrate selectivity of EZS. The insight of substrate specificity allows for the synthesis of novel isoprenoid substrates for incubation with EZS. Analogues of EZS could exhibit repellent or attractant properties enabling greater herbivore resistance for cultivated tomato species.

Chapter 2 – Synthesis of (2*Z*,6*Z*) farnesyl diphosphate and the Expression and Purification of EZS and Mutants

2.1 Preface

As the common substrate of sesquiterpene cyclases, preparation procedures for (2*E*,6*E*) farnesyl diphosphate (**31**) are well documented in literature.[11,106,117,146,186,187] The precursor (2*E*,6*E*) farnesol (**353**) can be purchased directly and converted to **31** in two steps; halogenation and diphosphorylation.[188] This low cost procedure is not time consuming or labour intensive in comparison to the preparation of (2*Z*,6*Z*) farnesyl diphosphate (**38**). The equivalent precursor, (2*Z*,6*Z*) farnesol (**167**) is too expensive to purchase in the required quantities.

This chapter outlines the investigation of a high throughput, low cost synthesis of **38**. This substrate was used to test the activity of EZS and mutants which had been heterologously expressed in *E. coli*. The methods used to optimise expression and purification of EZS of sufficient purity and quantity to perform characterisation assays are also described within this chapter.

Site directed mutagenesis was used to investigate the conserved DDxxE and NSE metal binding motifs and specific active site aromatic residues. Mutants were generated by Dr Veronica González González and Mindaugas Kalvaitis with DNA sequencing of the plasmids used to confirm desired mutations. However, the expression, purification and characterisation of soluble protein had not been investigated with regards to the EZS or any respective mutants. Residues were selected using a homology model of EZS based on α-bisabolene synthase containing bound (2*Z*,6*Z*) farnesyl diphosphate (**38**) and three magnesium ions. The homology model was generated by Professor Andrea Brancale from the Cardiff University School of Pharmacy and Pharmaceutical Sciences with cartoon representations of the model used throughout this chapter.

2.2 Synthesis of (2*Z*,6*Z*) farnesyl diphosphate (38)

2.2.1 Modified Wittig approach

The preliminary steps of the proposed synthesis of EZS substrate (2*Z*,6*Z*) farnesyl diphosphate (**38**)[2] (Figure 34) were based on protocols outlined by Garneau *et al.,*[189] and Kato *et al.*[190] leading to an alkene-forming reaction used by José *et al.*,[191] to synthesise a 10:1 ratio of 2-*Z*:2-*E* isomers (**167** and **168**). (2*Z*,6*Z*) Farnesol (**167**) would then be used in the synthesis of **38**.

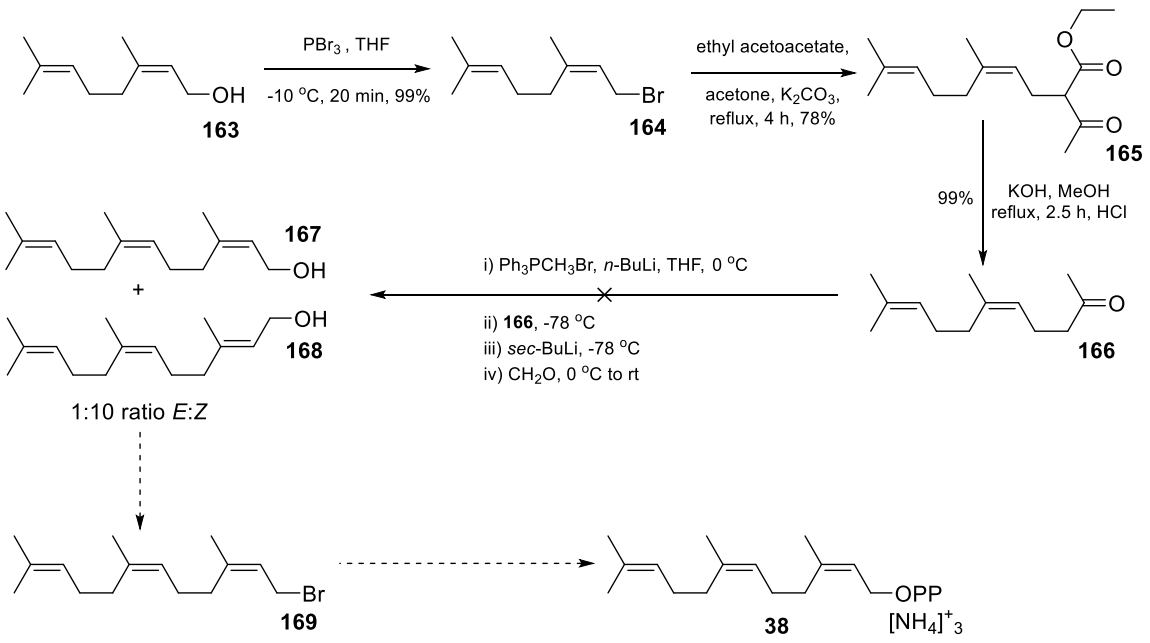

Figure 34. Proposed synthesis of (2*Z*,6*Z*) farnesyl diphosphate (38) using a modified Wittig reaction to give the *Z* C2,C3 double bond as the stereoisomer.

Nerol (**163**) was brominated using phosphorus tribromide to yield neryl bromide (**164**) in approximately quantitative yield. The carbon chain was extended by alkylating **164** with ethyl acetoacetate using potassium carbonate in dry acetone. Neryl keto ester (**165**) was decarboxylated by refluxing with potassium hydroxide in methanol to provide neryl acetone (**166**) for the key step. In the procedure outlined by José *et al.*,[191] the betaine intermediate of the Wittig reaction was deprotonated with a stronger base (*sec*-BuLi) and reacted with formaldehyde to form the hydroxymethylene unit predominantly in the *Z* configuration (10:1 *Z*:*E*) (Figure 35).

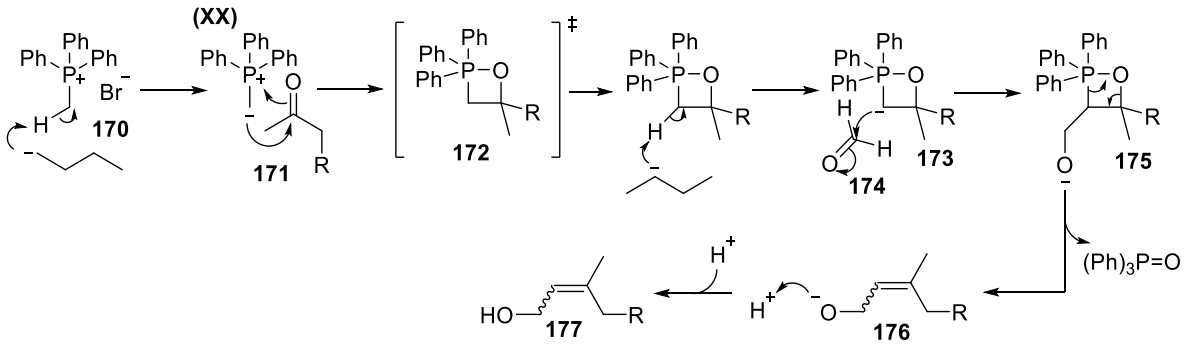

Figure 35. Proposed mechanism of the José procedure.[191]

Addition of *n*-butyl lithium to (methyl)triphenylphosphonium bromide (**170**) in dry tetrahydrofuran at 0 °C formed the ylide reagent. The reaction was stirred for 30 min, cooled to -78 °C and **171** added prior to stirring for a further 45 min at this temperature. Deprotonation of betaine intermediate **172** by addition of *sec*-butyl lithium was followed by stirring for a further 60 min. The reaction was warmed to 0 °C over 30 min and to room temperature over a further 2.5 h. Reaction products isolated *via* flash chromatography did not give ^{1}H NMR signals for alkene or methylene environments characteristic of the required product.

Numerous aspects of the reaction could lead to this failure. It was initially suspected that the betaine intermediate (**172**) was collapsing prior to the addition of *sec*-butyl lithium giving triphenyl phosphine oxide and a terminal alkene. However, analysis of ^{1}H NMR spectra of the isolated products showed no trace of a terminal alkene which would give two doublets at approximately 4.6 ppm with distinctive germinal coupling (1-3 Hz). The majority of recovered material was **166** and triphenyl phosphine. This suggests that the formation of intermediate **172** did not occur, possibly due to wet solvent or degraded *n*-butyl lithium. The reaction was repeated in turn with freshly distilled tetrahydrofuran and fresh *n*-butyl lithium but still yielded only a small quantity of an unidentified product.

The formaldehyde used for the modified Wittig procedure was prepared from cracking paraformaldehyde by distillation immediately prior to use. The ^{1}H NMR spectrum of the formaldehyde was inspected prior to use to ensure sufficient purity. Ethanal was used in place of formaldehyde to investigate whether addition of intact paraformaldehyde hindered product formation (Figure 36). Formation of the secondary alcohol would suggest that the formaldehyde was causing the reaction to fail. However, the reaction yielded the same results indicating formation of the betaine intermediate or its subsequent deprotonation were at fault.

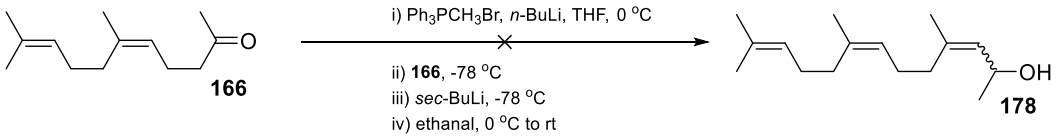

Figure 36. Modified Wittig reaction substituting formaldehyde with ethanal.

2.2.2 Wittig approach

An alternative approach to the modified Wittig reaction[191] using reagent **179** was explored (Figure 37). The use of a hydroxylated reagent would remove the requirement of formaldehyde from the reaction. Kitahara *et al.,*[192] and Syeda *et al.,*[193]published protocols outlining the a single step synthesis of allylic alcohols from aldehyde precursors using similar Wittig reagents.

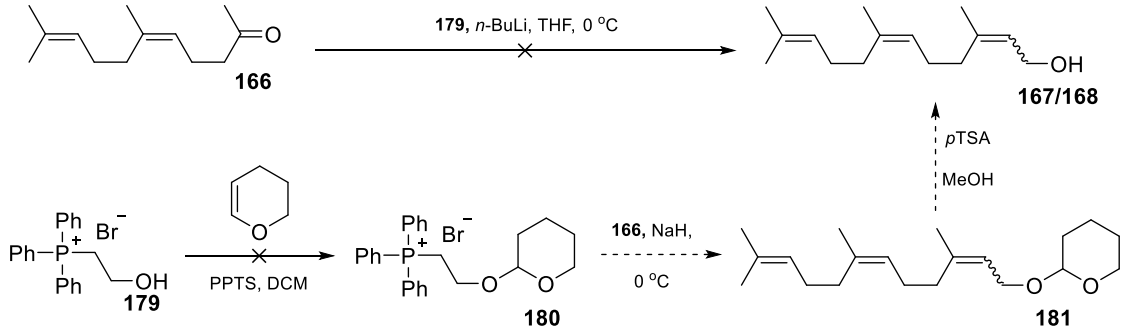

Figure 37. Proposed synthesis of (2*Z*,6*Z*) farnesol (167) using a Wittig salt to give the *Z* C2,C3 double bond.

Direct reaction of (2-hydroxyethyl)triphenylphosphonium bromide (**179**) and neryl acetone (**166**) with two equivalents of *n*-butyl lithium as a base yielded only **166**. The Wittig reaction requires ylide formation prior to the betaine intermediate. Deprotonation of the hydroxyl group on **179** could be followed by intramolecular attack of phosphorus giving triphenyl phosphine oxide and ethane as reaction products. Alternatively, intermolecular reactions between multiple deprotonated species may give dimer, trimer or polymer products. Subsequent variations shown in Table 3 gave **166** as the only isolated compound. A THP protection of **179** was attempted to stop unwanted interactions of intermediates but was unsuccessful due to the insolubility of **179** in DCM and hexane.

Table 3 - Reaction conditions attempted for the synthesis of the C2,C3 double bond using a Wittig salt.

Solvent Volume / mL	Base equivalents	Reaction time prior to **166** / min	Product
3	1	60	X
3	2	60	X
3	2.5	60	X
6	2	60	X
6	2.5	60	X
9	2	60	X
9	2.5	60	X
3	2.5	30	X
3	2.5	90	X
6	2.5	30	X
6	2.5	90	X
9	2.5	30	X
9	2.5	90	X

2.2.3 Directed Wittig approach

Multiple publications outline the use of (carbethoxymethylene)triphenylphosphorane (**188**) in *E* selective olefination reactions.[194–196] Chen *et al.,*[197] published the use of **188** in a directed Wittig reaction to achieve 100% *Z* selectivity by using a hydroxylated starting material. A synthesis (Figure 38) was proposed using a procedure outlined by Scheid *et al.,*[198] to synthesise α-hydroxylated neryl acetone (**187**) for use in a *Z* selective directed Wittig reaction. N-Bromo succinimide (NBS) bromination of *tert*-butyl acetoacetate (**182**) gave varying yields (18-100%) with the yields of repetitions being consistently low (18-25%). Reaction yields from acetylation of **183** to give **184** were consistent with literature.[197] Crude neryl bromide (**164**) was freshly prepared as outlined in Figure 34 and alkylated with **184** using potassium carbonate in dry acetone. Analysis of isolated compounds by ^{1}H NMR spectroscopy showed no peaks corresponding to the product. Due to high yields of **183** not being reproducible the pathway was not pursued further.

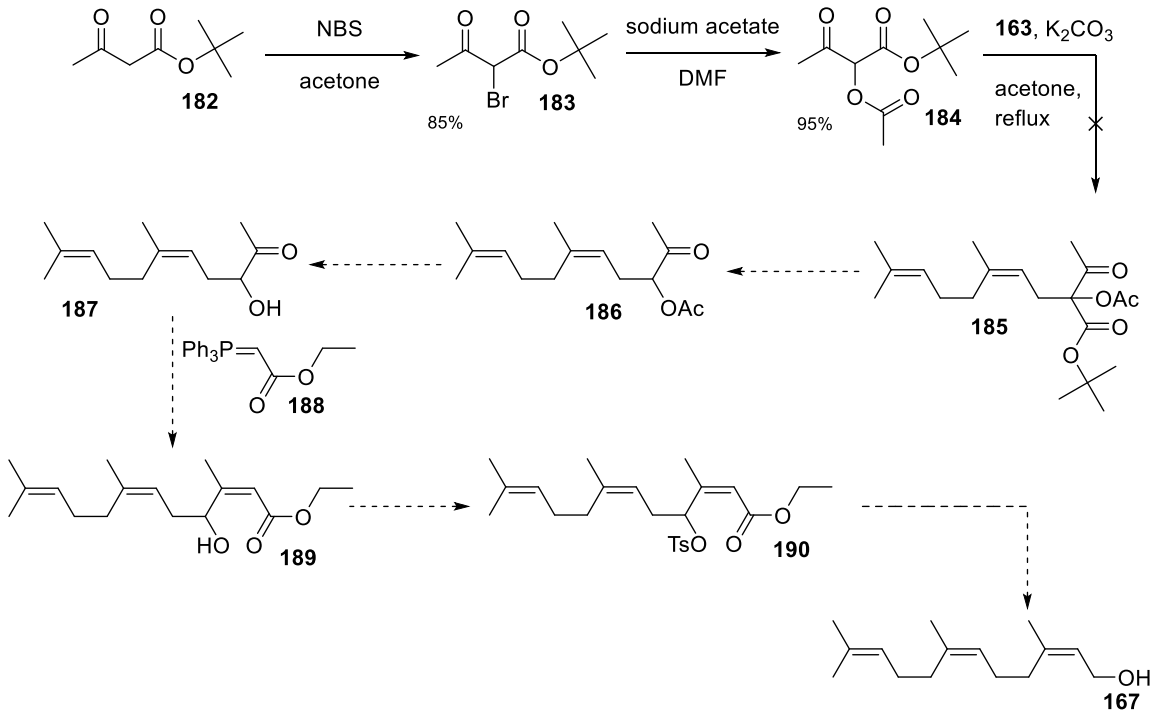

Figure 38. Proposed synthesis of (2*Z*,6*Z*) farnesol (167) using a directed Wittig reaction to give the *Z* C2,C3 double bond.

2.2.4 Anastasia approach

Installation of the C2,C3 double bond giving a 1:1 mixture of *E*:*Z* ethyl farnesoate esters was attempted *via* a procedure published by Anastasia *et al.*[199] The synthesis of **167** would follow a similar synthetic route outlined in Figure 34:

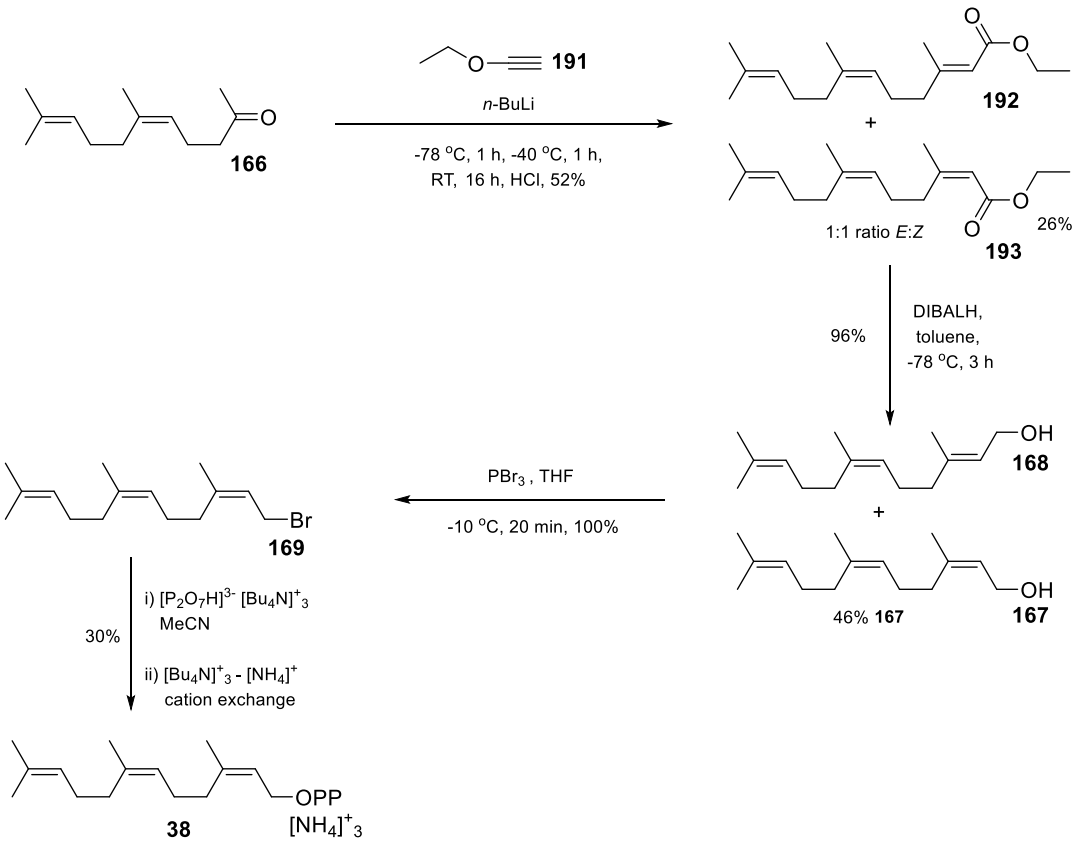

Figure 39. Synthesis of (2*Z*,6*Z*) farnesyl diphosphate (38) using an Anastasia reaction to give the *Z* C2,C3 double bond.

An experimental procedure published by Faraldos *et al.*,[200] was followed for the olefination of **166** (Figure 39). *n*-Butyl lithium was added to ethoxy acetylene (**191**) in dry THF at -78 °C. The reaction mixture was stirred for 1 h prior to the addition of **166** at -40 °C and then stirred for a further 1 h. The reaction was quenched with 1M H_2SO_4 and stirred at room temperature for 16 h. The crude product was purified *via* flash chromatography to give a 1:1 mixture of *E* and *Z* ethyl farnesoates **192** and **193**.

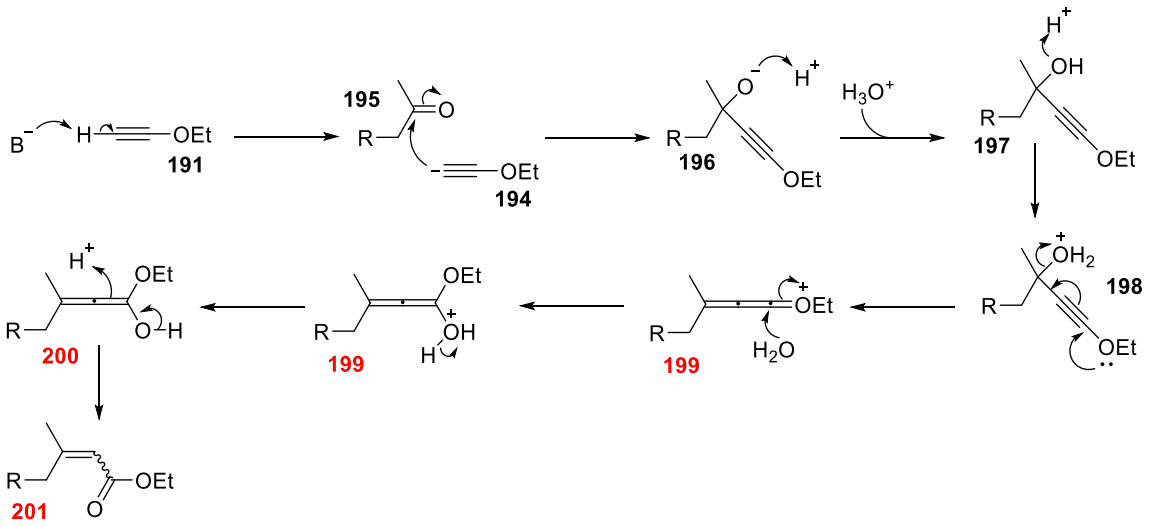

Figure 40. Proposed reaction mechanism outlined by Anastasia *et al.*[199]

The reaction mechanism proposed by Anastasia *et al.*,[199] involves the nucleophilic attack of water on intermediate **198**. The reaction is restricted to a 1:1 ratio of *E*:*Z* isomers as this interaction can occur freely from both sides (Figure 40). The reaction is difficult to monitor as product formation is not detectable until after quenching by H_2SO_4 and water.

Partial separation of the *E* and *Z* farnesoate esters was achieved *via* flash chromatography over silica (5% ethyl acetate in hexane). Improved isomer separation by flash chromatography was possible after esters **192** and **193** were reduced to alcohols **168** and **167** using diisobutyl aluminium hydride (DIBALH). Alcohol **167** was brominated using phosphorus tribromide and the crude product (**169**) diphosphorylated *via* stirring with tris-tetrabutylammonium diphosphate in anhydrous acetonitrile. The crude diphosphate was passed through a cation exchange column [Amberlyst 131 (wet H^+ form) mesh cation exchange resin pre-equilibrated with ion-exchange buffer (25 mM NH_4HCO_3, 2% isopropanol)] to give the ammonium salt as a white powder after lyophilisation. Cation exchange of the diphosphate moiety aids the removal of excess diphosphate and purification *via* high performance liquid chromatography (HPLC). Fractions containing product as viewed from the UV-vis trace from HPLC purification were lyophilized to give **38** as a white powder.

The olefination reaction was found to be the bottle-neck of the synthetic pathway. Variable yields and expensive reagents limited the through put and scale up substrate synthesis. Therefore, a different approach to **38** was investigated to circumvent the use of costly reagents allowing for the scale up of reactions.

2.2.5 Horner-Wadsworth-Emmons approach

A Horner-Wadsworth-Emmons (HWE) reaction was investigated to replace the Anastasia reaction.[199] Three HWE reagents, were used; triethyl phosphonoacetate (**202**) first published by Horner *et al.,*[201] and later defined by W. Wadsworth and W. Emmons,[202] ethyl (diphenoxyphosphoryl)acetate (**203**) proposed by Ando *et al.,*[203] and the Still-Gennari modification[204] of **202**; ethyl P, P-bis(2,2,2-trifluoroethyl)phosphonoacetate (**204**) (Figure 41).

Reagent **202** is an alternative reagent to a Wittig salt to yield *E* double bonds from the olefination of aldehydes.[201] The use of ketone **166** causes' greater steric interactions decreasing the stereo-selectivity achieved. Reagents **203** and **204** have increased *Z* stereoselectivity[203,204] though unlike **202** are not commercially available. Reagent **202** was therefore used to optimise reaction conditions prior to the use of **203** and **204** to increase the *Z* stereoselectivity.

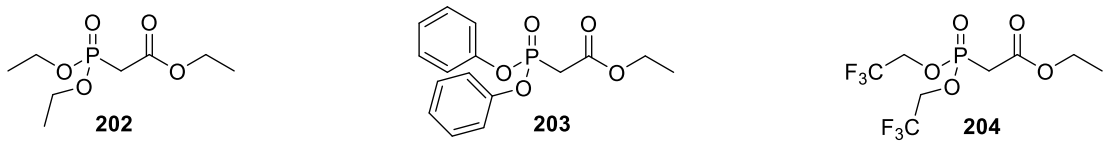

Figure 41. Horner-Wadsworth-Emmons reagents investigated for the optimisation of *Z* bond formation.

Ethyl (diphenoxyphosphoryl)acetate (**203**) was prepared *via* the procedure published by Ando *et al.,* by the condensation of diphenyl phosphite (**205**) and ethyl bromoacetate (**206**) (Figure 42).[203] The single modification to the experimental was the addition of diphenyl phosphite (**205**) and ethyl bromoacetate (**206**) *via* syringe pump to ensure the addition of reagents at a constant rate over 30 minutes in place of using a dropping funnel.

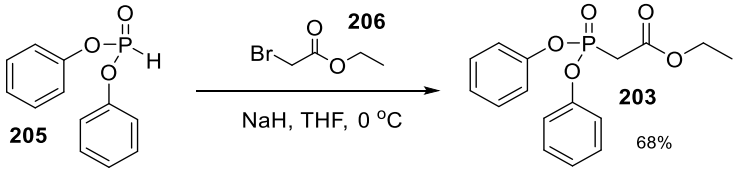

Figure 42. Synthesis of ethyl (diphenoxyphosphoryl)acetate (203).

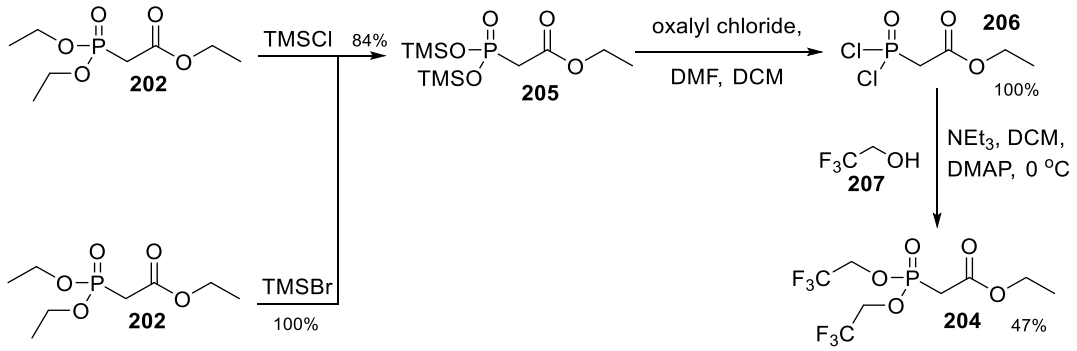

Figure 43. Synthesis of P,P-bis(2,2,2-trifluoroethyl)phosphonoacetate (204).

The Still–Gennari reagent (**204**) (Figure 43) was prepared using the protocol published by Messik *et al.*[205] Triethyl phosphonoacetate **202** and trimethylsilyl chloride (TMSCl) were sealed in a pressure tube and stirred for 7 days at 100 °C. The quantity of **205** that could be synthesised was limited by the pressure tube volume and reaction timescale. A 5 h reflux of **202** with trimethylsilyl bromide (TMSBr) eliminated the use of pressure tubes due to the higher boiling point of TMSBr compared to TMSCl (79 °C and 57 °C respectively). Procedures for the synthesis of **206** and **204** were followed directly from the publication.[205] However, purification of **204** was changed from a distillation to flash chromatography (50% ethyl acetate in hexane) with the removal of residual 2,2,2-trifluoro ethanol (**207**) under reduced pressure.

Solvent, cation and temperature effects of HWE reactions with aldehydes to achieve *E* selectivity were investigated by Thompson *et al.,*[206] and a similar investigation was carried out to increase reaction yield and *Z*:*E* ratio. Sodium hydride (NaH), lithium diisopropyl amide (LDA), potassium hexamethyldisilazide (KHMDS) and *n*-butyl lithium (*n*-BuLi) were used in attempt to increase the *Z* isomer formation when a softer counter cation was present (Li < Na < K). Thompson suggested that harder counter cations and higher reaction temperatures enable easier dissociation of the betaine intermediates. This allows the thermodynamically favourable threo intermediate (**210**) formation to give the *E* isomer over the kinetically favoured erythro configuration (**214**) resulting in the *Z* isomer (Figure 44).

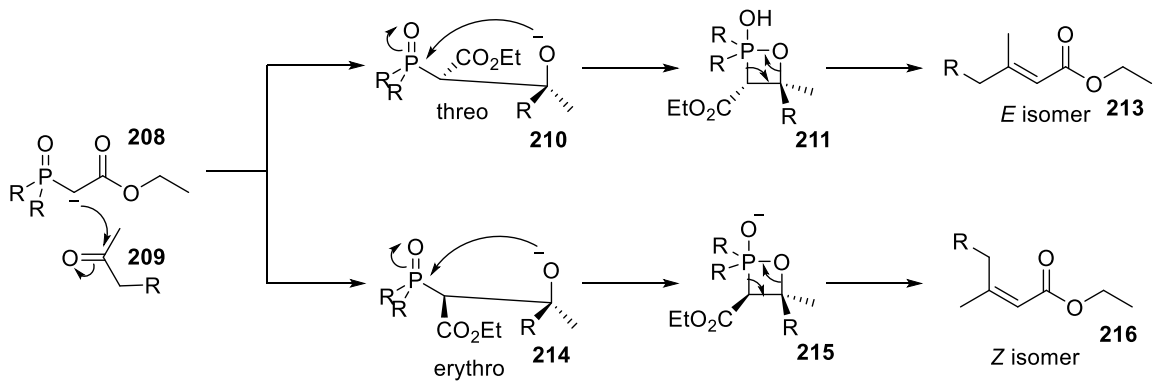

Figure 44. The formation of threo (210) and erythro (214) intermediates during a Horner-Wadsworth-Emmons reaction.

Thompson concluded that the solvation of betaine intermediate and cation chelation have greater effect on lithium-containing bases. The use of dimethoxyethane (DME) in place of THF doubled the ratio of *E:*Z when lithium containing bases were used. However, this effect was not replicated when potassium and sodium containing bases were employed.

Comparison of THF and toluene may indicate if the effect of lower polarity and dipole moment are applicable. It was found that the use of NaH in toluene at 0 °C consistently gave the highest yield and the highest proportion of *Z* isomer in the isolated product. Table 4 outlines the various conditions for reaction optimisation.

Table 4. Reaction conditions investigated for the optimal conditions for *Z* double bond formation *via* a Horner-Wadsworth-Emmons reaction.

Reagent	Solvent	Base	Temperature / °C	Ratio 192 (*E*):193 (*Z*)	Yield of 193 (*Z*)/ %
202	THF	*n*-BuLi	0	4:1	14
202	THF	KHMDS	0	4:1	11
202	THF	LDA	0	4:1	8
202	THF	NaH	0	4:1	17
202	Toluene	*n*-BuLi	0	4:1	14
202	Toluene	*n*-BuLi	-78	4:1	12
202	Toluene	NaH	0	4:1	19
202	Toluene	NaH	-78	4:1	18
203	THF	*n*-BuLi	0	2:1	21
203	THF	NaH	-78	2:1	23
203	Toluene	*n*-BuLi	-78	2:1	21
203	Toluene	NaH	0	2:1	29
204	THF	*n*-BuLi	0	1:1	33
204	THF	NaH	0	1:1	38
204	Toluene	*n*-BuLi	-78	1:1	31
204	Toluene	NaH	-78	1:1	38
204	Toluene	NaH	0	1:1	43

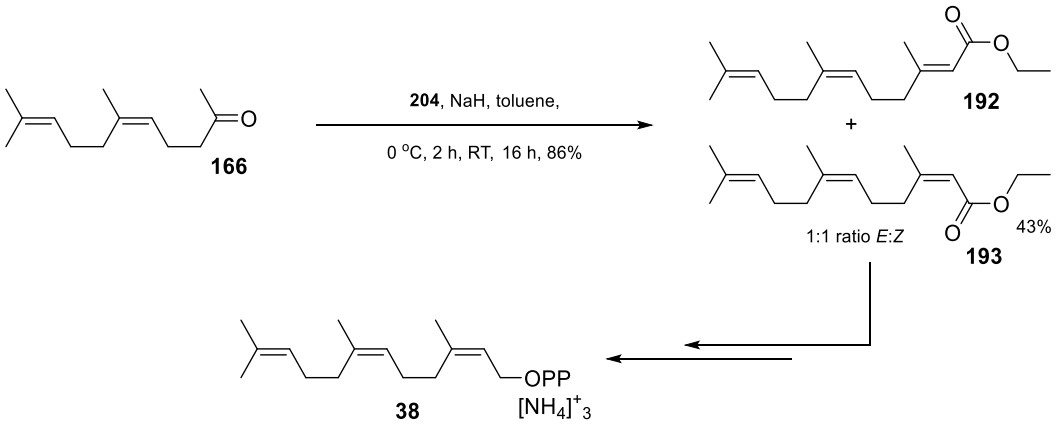

Figure 45. Synthesis of (2*Z*,6*Z*) farnesyl diphosphate (38) using a Horner-Wadsworth-Emmons reaction.

Neryl acetone (**166**) was prepared as previously described. The optimised conditions highlighted yellow in Table 4 were used for the olefination of **166** giving a 1:1 ratio of *E*:*Z* ethyl farnesoate esters **192** and **193**. The yields of this reaction were consistently high (reaction yield: 74-86%, yield of *Z* isomer: 37-43%) with the starting material readily recovered by flash chromatography. The preparation of **204** using TMSBr also allowed for a larger scale synthesis than was possible using the Anastasia olefination. The Still-Gennari modified Horner-Wadsworth-Emmons reaction was used as the primary method for installing *Z* double bonds (Figure 45).

2.3 Heterologous expression and Purification of EZS

EZS gene without 36 amino acid N-terminus signalling peptide63 inserted with a pET21a vector in conjunction with a TEV cleavage site and C-terminal His_6-tag was hetereogeneously expressed in *Escherichia coli* (*E. coli*) BL21 (DE3) cells. Transformation of this plasmid into the *E. coli* BL21 (DE3) cells was followed by overnight growth on an ampicillin containing agar plate. Bacterial colonies that had grown overnight were resistant to ampicillin and a single colony was used to innoculate lysogeny broth growth medium (LB medium) containing ampicillin and incubated in a shaker at 37 °C overnight. A sample of the overnight expression was placed into fresh LB media containing ampicillin. The culture was incubated in a shaker at 37 °C until the optical density (OD at 600 nm) of the cells reached and protein expression induced by the addition of isopropyl β-D-1-thiogalactopyranoside (IPTG). Induced cells were incubated in a shaker overnight at 20 °C and were harvested by centrifugation. The resulting pellets were used immediately or stored at -20 °C. Conditions for the optimal heterologous expression and purification of EZS were investigated and enzyme activity was tested by incubation with (2*Z*,6*Z*) FDP (**38**), with pentane extractable products analysed by GC-MS.

2.3.1 Optimising expression temperatures

The plasmid containing EZS DNA was transformed into *E. coli* BL21 (DE3) cells and protein expression tested with induction temperatures of 16 °C, 20 °C, 25 °C overnight and 37 °C for 4 h after the addition of IPTG. SDS PAGE analysis of whole cell extracts could not identify clear expression bands at the appropriate molecular weight (Appendix figure). A band above the 66.2 kDa was visible at 37 ^{o}C, corresponding to the expected molecular mass of EZS (88.5 kDa) but low expression levels meant this was inconclusive.

2.3.2 Purification of the insoluble fraction

Heterologous expression could not be conclusively identified from analysis of the SDS PAGE. Although a protein band of correct molecular mass was not observed, purification of EZS was attempted to see if protein had been expressed; using Ni-NTA methods to confirm production by SDS PAGE and to determine the most suitable conditions for expression. Cells from the incubations were re-suspended in cell lysis buffer (100 mM NaCl, 5mM βME, 20 mM TRIS base, 1% TWEEN 20, pH 7.0) and the cells lysed by sonication. The cell debris and supernatant solution were separated using a centrifuge before two methods were used in attempts to purify EZS: basic extraction of insoluble protein and Ni-NTA column. A basic extraction involves the unfolding of the proteins within inclusion bodies through raising the pH to a high level in order to solubilise them and then lowering

the pH again to refold the desired protein, ideally other proteins will precipitate and can be removed by centrifugation. The pH of the re-suspended pellet is increased to ~pH 11 to unfold the tertiary structure and stirred for half an hour prior to re-folding by decreasing the pH to pH 7-8. Harvested cells from each expression temperature were re-suspended in cell lysis buffer (100 mM NaCl, 5mM βME, 20 mM TRIS base, 1% TWEEN 20, pH 7.0) and cells lysed *via* sonication. The crude extracts obtained by centrifugation and the resultant pellets re-suspended in cell lysis buffer (CLB). A Basic extraction was performed on the insoluble fractions from the expressions (0.5 L culture) at each temperature, followed by purification by Ni-NTA column. SDS PAGE analysis showed purified protein with the mass of EZS in fractions corresponding to 5, 20 and 50 mM imidazole (Figure 46).

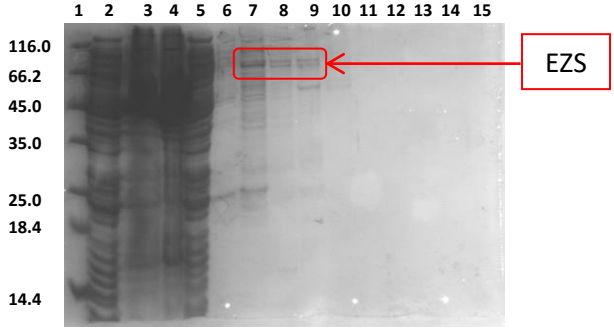

Figure 46. SDS-polyacrylamide gel showing samples from the basic extraction and Ni-NTA purification of EZS(WT) in *E. coli* BL21(DE3) expressed at 37 °C for 4 h. Lane 1) protein molecular weight ladder (x10^3 Mr), 2) insoluble fraction after basic extraction, 3) soluble fraction after basic extraction, 4) sample loaded onto Ni-NTA column, 5) flow through, 6) empty, 7) cell lysis buffer (CLB) with 5 mM imidazole, 8) CLB with 20 mM imidazole, 9) CLB with 50 mM imidazole, 10) CLB with 70 mM imidazole, 11) CLB with 100 mM imidazole, 12) CLB with 150 mM imidazole,. 13) CLB with 200 mM imidazole, 14) CLB with 300 mM imidazole and 15) CLB with 500 mM imidazole.

The activity of the purified protein from the insoluble fraction and partially purified by a Ni^{2+} affinity column was tested but no products could be identified *via* GC-MS analysis of the pentane extractable products for any of the tested expression temperatures. Within cell lysis buffer (CLB), additives are used to increase the stability of a protein in solution. Surfactant (TWEEN 20) aids the solubility of proteins by the formation of micelles whilst NaCl neutralises the net charge of the protein, both limiting protein-protein interaction and aggregation. Varying amounts of TWEEN 20 (1-5%) and NaCl (20-500 mM) were included within the cell lysis buffer (CLB) but these did not improve purification methods. The protein band with the same molecular mass was eluted at low imidazole concentrations indicating that the His tag may have hidden from effectively chelating to the Ni^{2+} resin or it was not the correct protein. Due to more or one of these issues the protein was not catalytically active.

2.3.3 Purification of the soluble fraction

Due to extraction of protein from the insoluble fraction being unsuccessful, (2*Z*,6*Z*) FDP(**38**) was incubated with a sample of the soluble fraction immediately after sonication which showed an enzymatic product peak in the pentane extracts *via* GC-MS. Purification from the soluble proportion by Ni^{2+} affinity column enabled visualisation of a band with the approximate molecular mass of EZS. Bound protein was eluted with a gradient wash of imidazole solution of increasing concentrations; 5, 20; 50, 70, 100, 150, 200, 300 and 500 mM. The EZS band was observed in fractions eluting at concentrations of 70, 100 and 150 mM imidazole when analysed by SDS PAGE (Figure 47). In all fractions containing EZS, a number of impurities were also visible on the SDS PGE. Despite impurities, the fractions containing the protein of the expected mass of EZS were combined, dialysed in cell lysis buffer to remove imidazole and a sample from the dialysed solution incubated with (2*Z*,6*Z*) FDP (**38**). GC-MS analysis of the pentane extractable extracts from the incubation of (2*Z*,6*Z*) FDP (**38**) with the dialysed protein sample showed the same peak observed from the incubation of **38** with the crude lysate. Samples from the sonicated cells of each expression temperature were visualised by SDS polyacrylamide gel. Analysis of the gel showed that the expression of EZS at 20 °C overnight was the only condition to give a visible band at the correct molecular weight in the soluble fraction (Figure 47). Therefore, a 20 °C overnight expression of EZS after induction with IPTG was used as the expression temperature.

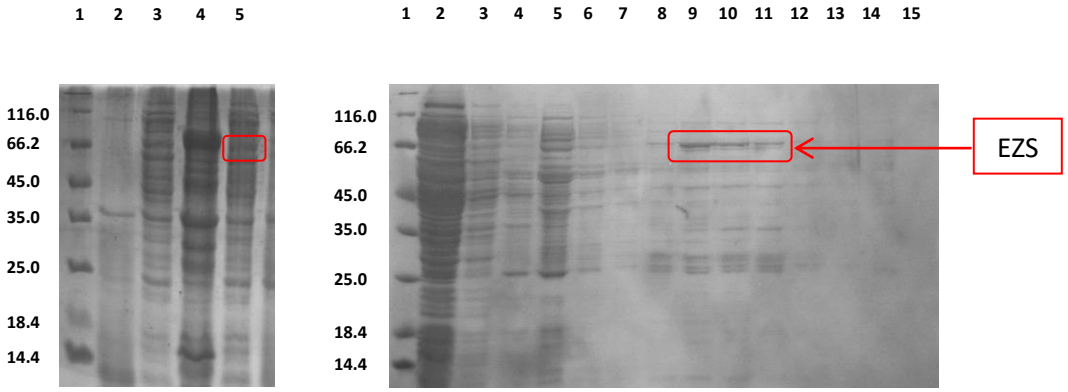

Figure 47. SDS polyacrylamide gels showing samples from sonication (left) and Ni-NTA purification of EZS from expression in *E. coli* BL21(DE3) cells expressed at 20 °C overnight. Left: Lane 1) protein molecular weight ladder (x10^3 Mr), 2) *E. coli* BL21(DE3) cells pre-induction 3) *E. coli* BL21(DE3) cells post expression, 4) insoluble fraction after sonication, 5) soluble fraction after sonication. Right: Lane 1) protein molecular weight ladder (x10^3 Mr), 2) sample loaded onto Ni-NTA column, 3) flow through, 4) CLB with 5 mM imidazole, 5-7) CLB with 20 mM imidazole, 8) CLB with 50 mM imidazole, 9) CLB with 70 mM imidazole, 10) CLB with 100 mM imidazole, 11) CLB with 150 mM imidazole, 12) CLB with 200 mM imidazole, 13) CLB with 300 mM imidazole, 14) CLB with 500 mM imidazole, 15) Ni-NTA column wash with 0.1 M NaOH.

Further purification steps were needed for full characterisation of EZS, as multiple impurities could be observed in the same fractions of the protein of the expected mass of EZS by SDS PAGE. Anion exchange fast protein liquid chromatography (FPLC) with a quaternary ammonium functionalised sepharose column (Q-seph column) was chosen as the subsequent purification step. In this

technique, protein is placed onto the column and will bind ionically to the quaternary ammonium groups of the resin. The strength of ionic bonding is determined by the negative surface charge of the protein which is eluted using an increasing gradient of NaCl in the elution buffer. Increasing the concentration of Cl^- ions in the eluent results in anion exchange and protein elution from the column. The theoretical isoelectric point (pI) (the pH at which the net charge on a protein is zero) for EZS was calculated to be approximately 6.0 using ExPasy Bioinformatics Resource Portal translate tool. Though this pH is used as the pI value, it is an approximation. The calculation considers the charges of all residues and does not take into account which residues are at the protein surface or within the bulk of the protein to which the pH of the buffer will not have an effect.

Elution fractions with 70, 100 and 150 mM imidazole (Figure 47) from the Ni^{2+} column were dialysed into a second buffer (20 mM NaCl, 5 mM βME, 20 mM TRIS base) at pH 8 rather than pH 7. This increase in pH would increase the overall negative charge of the protein resulting in stronger bonding to the Q-sepharose column and hopefully enable elution without impurities. Analysis of fractions corresponding to the peaks on the UV trace (280 nm) of the FPLC chromatogram (Figure 48) *via* SDS PAGE showed the removal of unwanted proteins from the sample; however, slight impurities were still present within the same fraction as EZS (Figure 49).

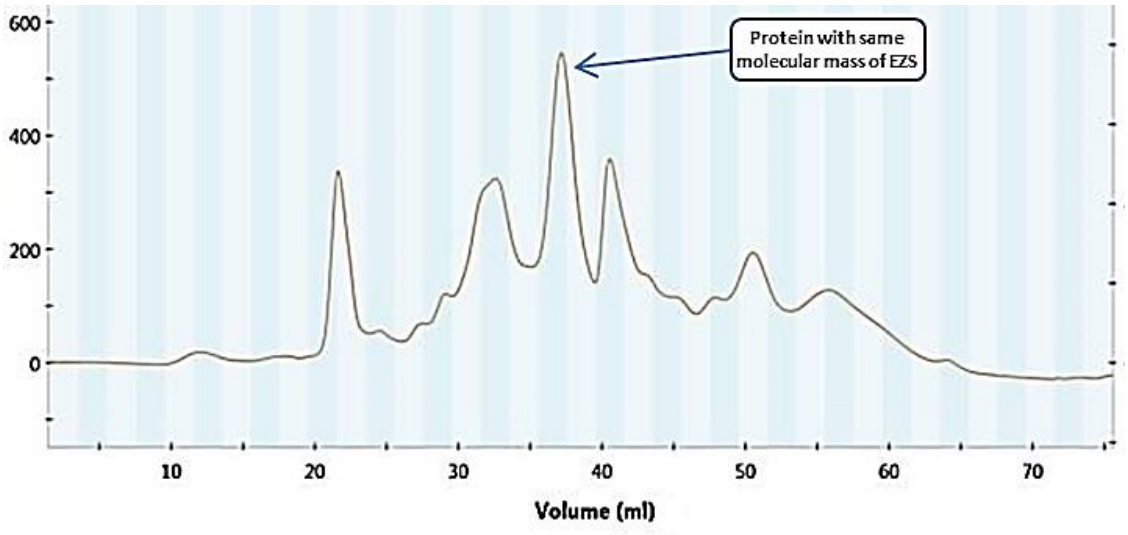

Figure 48. FPLC chromatogram of anion exchange chromatography using a Q-sepharose anion exchange column, for the purification of protein the same mass as EZS, showing the UV trace at 280 nm.

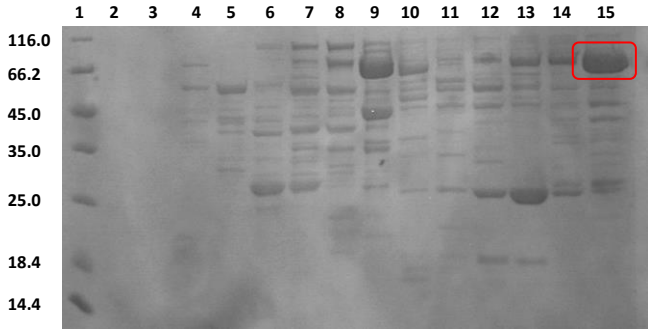

Figure 49. SDS polyacrylamide gel showing samples anion exchange FPLC (Q-sepharose column) purification. Lane 1) protein molecular weight ladder (x10^3 Mr), 2-3) waste fractions, 4-12) impurities removed during purification, 13) fraction containing EZS and large impurity with molecular mass ~25 kDa, 14-15) fraction containing EZS eluted at 140-160 mM [NaCl].

Incubation of the FPLC purified fraction with (2*Z*,6*Z*) FDP (**38**) and analysis of the pentane extractable products yielded the same product observed in the previous incubations of using crude extract and initial Ni^{2+}column purification. In an attempt to isolate pure EZS, a second Ni^{2+}-NTA affinity column was performed with the same imidazole elution gradient as previously described. The purification removed some impurities at lower imidazole (5-50 mM) concentration leaving the EZS eluted with slight impurities at higher imidazole concentrations (70-200 mM) (Figure 50).

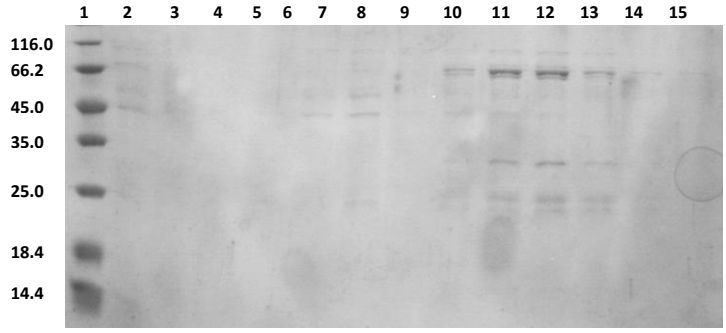

Figure 50. SDS polyacrylamide gel showing samples of Ni-NTA purification of FPLC products. Lane 1) protein molecular weight ladder (x10^3 Mr), 2) sample loaded onto Ni-NTA column, 3) flow through, 4-5) CLB with 5 mM imidazole, 6-7) CLB with 20 mM imidazole, 8-9) CLB with 50 mM imidazole, 10) CLB with 70 mM imidazole, 11) CLB with 100 mM imidazole, 12) CLB with 150 mM imidazole, 13) CLB with 200 mM imidazole, 14) CLB with 300 mM imidazole, 15) CLB with 500 mM imidazole.

Though the majority of impurities were removed and incubations of the fraction yielded the same enzymatic product upon incubation with **38** as observed in previous incubations, slight impurities were still observed (Figure 50). For characterisation of the protein, a pure sample in measurable quantities needed to be attained with a reproducible method.

2.3.4 TEV Cleavage

The impurities present with EZS displayed a similar affinity to the Ni^{2+} resin as exhibited by the His-tag of EZS (Figure 50). It was proposed that the removal of the His-tag using tobacco etch virus (TEV) protease following the purification steps outlined in section 2.3.3 could help isolate EZS. A final Ni-NTA affinity column would result in pure EZS being eluted in the flow-through whilst the cleaved His-tag and impurities remained bound to the column. TEV protease is a 25 kDa chymotrypsin-like protease with a highly sequence-specific recognition site and is often used for the removal of affinity tags from purified recombinant proteins.[207] Its high sequence specificity allows for precise cleavage of the His-tag from EZS due to the incorporation of the ENLYFQ\S cut site situated between the affinity tag and the protein.[208,209] The TEV protease used also contains a His-tag and will therefore bind to the Ni^{2+}-NTA affinity column with the cleaved His-tag and impurity upon purification.

TEV protease was placed in the dialysis tubing (14 kDa membrane) with the combined fractions of the second Ni^{2+} affinity column (Figure 50) to remove imidazole and undergo cleavage in a single step. The SDS polyacrylamide gel of the fraction from the subsequent Ni^{2+}-NTA affinity column showed pure a single band corresponding to EZS in the flow-through (Figure 51). However, fractions from the Ni^{2+} affinity column also showed EZS and the impurity within the same fraction implying that not all protein had undergone cleavage. Fractions containing pure and impure EZS were incubated with **38** to establish whether removal of the His-tag from the protein affected activity. GC-MS analysis of the pentane extractable products showed both samples were active. The TEV cleavage step was repeated at 5 °C and 25 °C overnight with separate batches of protein. Complete cleavage of the His-tag was never achieved; however a reproducible and effective purification technique for EZS was achieved.

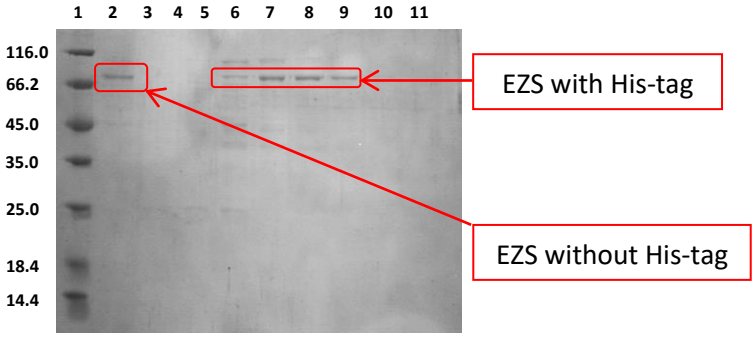

Figure 51. SDS polyacrylamide gel showing samples of Ni-NTA purification of EZS His-tag cleavage experiment using TEV protease. Lane 1) protein molecular weight ladder (x10^3 Mr), 2) sample loaded onto Ni-NTA column, 3) flow through, 4) CLB with 5 mM imidazole, 5) CLB with 20 mM imidazole, 6) CLB with 50 mM imidazole, 7) CLB with 70 mM imidazole, 8) CLB with 100 mM imidazole, 8) CLB with 150 mM imidazole, 9) CLB with 200 mM imidazole, 10) CLB with 300 mM imidazole, 11) CLB with 500 mM imidazole.

Although EZS was purified successfully, the quantities generated were insufficient for use in incubations and characterisation assays, with a concentration 3 μM (3 mL of buffer) determined by Bradford assay.[210] Due to this, further avenues were explored to increase the expression levels of EZS.

2.4 Improving expression yields with expression tags

Purification of EZS showed low expression of soluble protein which gave insufficient purity for downstream analysis (Figure 51). To increase the production of soluble protein, the use of expression tags were investigated. Expression tags are used to improve the production of recombinant proteins by improving the folding and solubility. Though the mechanism of action is not well understood, two explanations are available: the fusion of a stable structure to an insoluble protein will increase stability and improve folding, or the ''molten globule hypothesis'' which states the presence of a fusion tag may act as a nucleus for folding.[211,212]

2.4.1 Maltose Binding Protein

Maltose-binding protein (MBP) has an approximate molecular mass of 42 kDa and is commonly used as an expression tag. MBP is used with recombinant proteins with a dual purpose of increasing solubility and aiding purification by use as an affinity tag.[213214] Previous expression and purification of EZS yielded poor expression of soluble protein and difficulty during purification. A MBP-EZS fusion protein would ideally increase EZS solubility whilst giving a different method of purification that would circumvent the issue of non-specific binding observed with purification *via* Ni^{2+}-NTA affinity column (Figure 47).

The MBP-EZS fusion protein was designed and constructed by Dr Robert Mart using a golden gate assembly method. A plasmid harbouring the MBP-EZS gene was incorporated into *E. coli* BL21(DE3) competent cells and expressed using the protocol previously outlined (section 2.3.3). Harvested cells were re-suspended in cell lysis buffer (CLB), lysed by sonication and the resultant insoluble and soluble fractions analysed by SDS PAGE to inspect the expression of the construct. A combined approximate mass of EZS (88 kDa) and MBP (42 kDa)[215] would give a band at 130 kDa; above the 116.2 kDa marker of the protein ladder. The SDS PAGE of soluble and insoluble fractions after sonication showed a band with the same molecular mass as the EZS-MBP construct in the soluble fraction which is not present within the insoluble fraction.

A Ni^{2+}-NTA affinity column was used as a primary method of purification of the soluble fraction and bound protein washed with cell lysis buffer before being washed with a gradient of imidazole solutions of increasing concentration: 5, 20, 100, 200 and 500 mM. The SDS PAGE showed that the band with the same molecular mass as MBP-EZS did not bind to the Ni^{2+}affinity column (Figure 52).

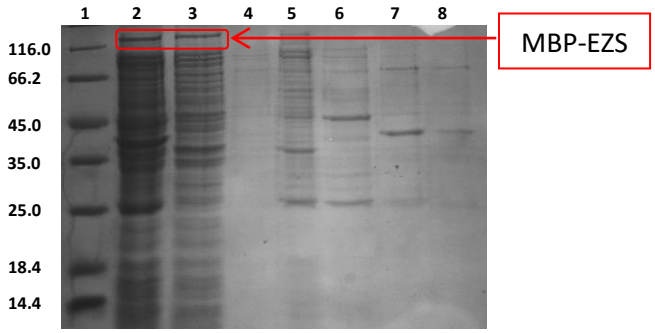

Figure 52. SDS polyacrylamide gel showing samples of Ni-NTA purification of soluble fraction after sonication of cells containing the MBP-EZS construct protein. Lane 1) protein molecular weight ladder (x10^3 Mr), 2) sample loaded onto Ni-NTA column, 3) flow through, 4) CLB with 5 mM imidazole, 5) CLB with 20 mM imidazole, 6) CLB with 100 mM imidazole, 7) CLB with 200 mM imidazole an 5) CLB with 500 mM imidazole.

An incubation of a sample from the soluble fraction with (2*Z*,6*Z*) FDP (**38**) was conducted to determine the activity of the protein of correct molecular mass before attempting purification. Although a band of correct molecular mass for EZS could not be observed in the soluble fractions of previous purifications by SDS PAGE (Figure 47), substrate turnover was still observed *via* GC-MS analysis of the pentane extractable products from the incubation of **38** and the crude lysate. Unfortunately, no enzymatic products were visible from the analysis of the pentane extract from the incubation compound **38** with a sample of the soluble fraction (crude lysate) from the purification of MBP-EZS and the construct was not investigated further.

2.4.2 Guanidine Binding Protein

Guanidine binding protein expression tag (GB1) is used to aid the solubilisation of insoluble recombinant protein by co-expression.[216] The GB1 domain is derived from guanine nucleotide-binding protein and consists of 56 residues with an approximate weight of 8 kDa. Due to its small size, GB1 is often used as a fusion tag for the expression of proteins for protein NMR samples and has been reported to significantly improve the over expression of recombinant proteins in *E. coli*.[217]

The GB1-EZS construct was designed and prepared by Dr Robert Mart *via* golden gate assembly. The fusion protein was transformed into *E. coli* BL21(DE3) competent cells and protein expression induced by the addition of IPTG. Two different expression conditions were performed; 37 °C for 4 h and 20 °C overnight and cells harvested by centrifugation post expression. Samples of harvested cells were run on an SDS PAGE and did not show a band with the same molecular mass as GB1-EZS.

However, overexpression bands were also not observed with previously investigated expressions. The harvested cells from both expressions were re-suspended in cell lysis buffer and the cells lysed by sonication. Cell debris in the sonicated suspensions was separated from the lysate by centrifugation and the resultant insoluble and soluble fractions of both expressions were analysed by SDS PAGE. Analysis showed large quantities of a protein with the same molecular mass GB1-EZS in the insoluble fractions of both expressions. However, slight bands for a protein of correct molecular mass were observed in the soluble fractions from the expression at 20 °C overnight. A basic extraction of the insoluble fractions were attempted to extract protein, resulting in a band with the same molecular mass of the GB1-EZS construct in the supernatant when analysed by SDS PAGE (Figure 53).

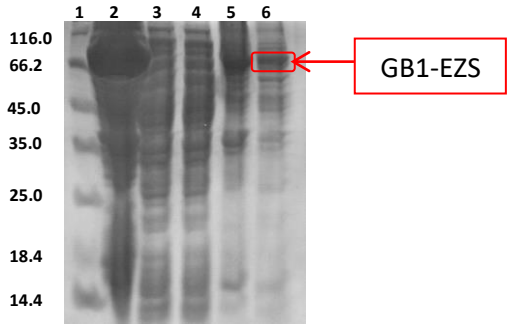

Figure 53. SDS polyacrylamide gels showing samples from sonication and basic extraction of the GB1-EZS construct. Lane 1) protein molecular weight ladder (x10^3 Mr), 2) *E. coli* BL21(DE3) cells post expression, 3) soluble fraction after sonication, 4) insoluble fraction after sonication, 5) insoluble fraction after basic extraction, 6) soluble fraction after basic extraction.

Incubations of the samples from the soluble fraction (20 °C overnight expression) and the lysate after the basic extractions of the insoluble fraction (37 °C for 4 hours and 20 °C overnight) showed no enzymatic products in the pentane extractable products *via* GC-MS. The purpose of the construct was to enhance the expression of soluble protein that in turn would aid purification. The GB1-EZS construct did significantly increase expression however, the minimal protein that could be extracted from the cells was not active and therefore new avenues for protein expression were investigated.

2.5 Investigating Different Cell Lines to Increase Expression of EZS

2.5.1 *E. coli* ArcticExpress RP

At conventional expression temperatures (20 – 40 °C) high expression can decrease the cells' ability to correctly fold recombinant protein giving insoluble protein and inclusion bodies. However, colder expression temperatures can increase the yield of soluble protein.[218] *E. coli* chaperonins GroEL and GroES are co-expressed by the cell to assist with the stabilisation and refolding of un- or partially folded proteins. However, these chaperonins have been shown to lose 70% of their activity at colder expression temperatures (12 °C) when compared to the optimal 30 °C incubation temperature.[219]

The ArcticExpress RP expression strain was designed to co-express the cold adapted chaperonins Cpn10 and Cpn60 from the psychrophilic bacterium sourced from Antarctic sea water, *Oleispira antarctica*.[218] Cpn10 and Cpn60 chaperonins have 74% and 54% amino acid similarity to GroEL and GroES respectively. Both chaperonins exhibit high protein refolding activities in *vitro* at lower temperatures (4-12 °C), 16 fold greater than at 30 °C. Co-expression of these chaperonins within ArcticExpress cells has been shown to improve protein folding at lower temperatures to potentially give greater yields of soluble, active recombinant protein.[220]

The plasmid containing EZS gene was incorporated into ArcticExpress RP cells, protein expression induced by the addition of IPTG and EZS expressed overnight at 10 °C for 24 h. Cells from the expression were harvested by centrifugation and re-suspended in cell lysis buffer (CLB). Re-suspended cells were lysed by sonication, cell debris separated from the lysate by centrifugation and samples from soluble and insoluble fractions analysed by SDS PAGE. Analysis showed a large expression band with the same molecular mass as EZS present within the insoluble fraction (Figure 54). A slight band of the same molecular mass was also visible within the soluble fraction however, the yield of the soluble protein looked comparable to that observed with protein expression in *E. coli* BL21(DE3) (Figure 47). A sample from the soluble fraction was incubated with **38** and the pentane extractable products analysed by GC-MS showing the same product observed in previous incubations (section 2.3.3).

A basic extraction was attempted on the insoluble fraction to investigate whether insoluble protein could be purified. Samples of the insoluble and soluble fractions before basic extraction were analysed by SDS PAGE and showed a band with the same molecular mass as EZS remained within the insoluble fraction (Figure 54). To ensure no active protein had been extracted and not been observed, a sample from the soluble fraction was incubated with **38** however no enzymatic products were observed in the pentane extracts when analysed by GC-MS.

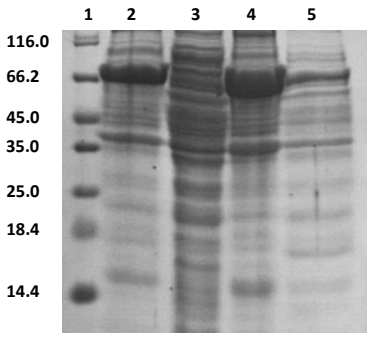

Figure 54. SDS polyacrylamide gels showing samples from sonication and basic extraction of the EZS(WT) expressed in *E. coli* ArcticExpress RP for 24 h at 10 °C. Lane 1) protein molecular weight ladder (x10^3 Mr), 2) insoluble fraction after sonication, 3) soluble fraction after sonication, 4) insoluble fraction after basic extraction, 5) soluble fraction after basic extraction.

2.5.2 *E. coli* C41 (DE3) pLysS

C41(DE3) pLysS competent cells are derived from BL21(DE3) strain containing a mutation that decreases the activity of the T7 RNA polymerase (RNAP). This reduced level of T7 RNAP activity prevents cell death that can be associated with the over expression of recombinant toxic proteins. C41(DE3) pLysS also contain a chloramphenicol resistant plasmid which expresses small quantities of T7 lysozyme that is an inhibitor of T7 RNA polymerase and also suppresses the basal expression of T7 RNA polymerase prior to induction.[221–223]

A greater density of cells is required for higher yields of protein due to the limitation of the T7 RNA polymerase within each cell. When using Luria-Bertani (LB) medium,[224] the cells were incubated at 37 °C prior to induction at an OD_{600} of 0.8-1.0 in contrast to previous cell lines in which protein expression was induced at an OD_{600} of 0.6. Terrific-Broth (TB) medium is an enriched medium developed to improve yields of *E. coli* and growth was used as the primary growth medium; with protein expression induced at an OD_{600} of 0.6. The high cell density required for the overproduction of proteins can lead to acidic conditions to which phosphate buffer present within TB media regulates physiological pH for cell growth.[225]

A plasmid containing EZS gene was incorporated into *E. coli* C41 (DE3) pLysS competent cells and cultures grown in TB media. An investigation of how expression is affected by cell stress was conducted by temperature shock. Three incubations were conducted; the first incubation was cooled to 10 °C directly before induction of protein expression by the addition of IPTG (cold shock), the second was placed in a 42 °C water bath for 40 seconds before induction (heat shock) and the third induced directly (no shock). Induced cells were then incubated overnight at 20 °C. The cells from each expression were harvested by centrifugation and the cells re-suspended in cell lysis

buffer. The suspended cells were lysed by sonication, cell debris removed *via* centrifuge and a sample of the soluble fraction incubated with (2*Z*,6*Z*) FDP (**38**). GC-MS analysis of the pentane extractable products showed no products from heat shocked incubation and two different products from the cold shock and no shock incubations respectively.

A Ni^{2+}-NTA affinity column was used for the purification of the soluble fraction from the cold shock incubation. Bound protein was eluted as previously stated (section 2.3.3) and analysis of the SDS PAGE showed pure protein with a band at the same molecular mass as EZS in the 70 and 100 mM fractions and the same band with impurities eluted at 20 and 50 mM imidazole concentrations. Samples from each elution were incubated with **38** to assess whether active protein was present. The pentane extractable products of the incubations were analysed *via* GC-MS and showed no enzymatic products for the pure protein eluted at 70 and 100 mM imidazole concentrations. Incubation of the impure fractions (eluents at 20 and 50 mM imidazole) showed an enzymatic product with a molecular ion peak *m/z* = 204. However, the mass spectrum of the product peak was not the same as the enzymatic product previously observed.

Harvested cells from the no shock incubation were re-suspended in cell lysis buffer, lysed by sonication, cell debris separated from the lysate using a centrifuge and samples from the insoluble and soluble fractions analysed *via* SDS PAGE. As previously observed with the cold shock incubation, a band with the same molecular mass as EZS was not present in the insoluble fraction and could not be seen in the soluble fraction due to the presence of multiple impurities. Incubation of a sample from the soluble fraction with (2*Z*,6*Z*) FDP (**38**) and analysis of the pentane extractable product *via* GC-MS. The mass spectrum of the enzymatic product observed on the total ion chromatogram showed a molecular ion peak *m/z* = 204 that was not the same product from the incubation of purified protein and **38** from the cold shock expression.

Purification of the soluble fraction using a Ni^{2+}-NTA affinity column gave a band with the same molecular mass as EZS in fractions 70 – 300 mM imidazole when samples from the eluent fraction were analysed by SDS page. The fractions in which the band was observed were combined, dialysed into cell lysis buffer to remove imidazole, concentrated and a sample incubated with **38**. Pentane extractable products were analysed *via* GC-MS and showed a single enzymatic product. A sample of the purified protein was analysed by SDS PAGE. In comparison to previous expressions, analysis of the SDS PAGE showed minor impurities with a greater ratio of a protein with the same molecular mass as EZS to other proteins in the same fraction.

A second Ni^{2+}-NTA affinity column with the same gradient of imidazole elution was used to remove impurities observed by SDS PAGE after the previous purification step. Analysis of the fractions from the second Ni^{2+}-NTA affinity column showed a protein with the same molecular mass as EZS was eluted at by 70 mM imidazole solution. The fraction was dialysed to remove imidazole and a sample of the fraction incubated with **38**. GC-MS analysis of the pentane extractable products from the incubation showed the same enzymatic product previously observed from the incubation of the sample from the first Ni^{2+}-NTA affinity column with **38**. This showed that the expression of EZS using *E. coli* C41 (DE3) pLysS competent cells with no shock treatment gave improved quantities of active enzyme, compared to previous methods. However; after two Ni-NTA columns, one impurity remained in the soluble fraction and therefore a new method protocol was investigated to ensure the protein with the same molecular mass as EZS was responsible for the generation of enzymatic product.

Purification of protein with the correct molecular mass for EZS from the soluble fraction for characterisation was achieved *via* a three step process. The first purification step was a Ni^{2+}-NTA affinity column of the soluble fraction after sonication, with a step wise elution of 5, 20, 300 and 500 mM imidazole solution, with protein elution observed by SDS PAGE analysis in the 300 and 500 mM fractions (Figure 55). The appropriate fractions from the Ni^{2+}-NTA affinity column were combined and purified by anion exchange (Q-sepharose column) FPLC. SDS PAGE analysis of the eluted proteins showed a band with the same molecular mass as EZS and a single impurity at an approximate molecular mass of 18.4 kDa (Figure 56). The protein partially purified by FPLC was isolated and buffer exchanged (100 mM NaCl, 5 mM βME, 20 mM TRIS base and pH 8.0) using a spin column with a 50 kDa membrane yielding a single band of the correct mass on the SDS PAGE (Figure 56). Incubation of the purified protein with (2*Z*,6*Z*) FDP (**38**) and analysis of the pentane extractable products by GC-MS gave the same enzymatic product observed from the incubation of the protein partially purified from the no shock expression. This protocol was adopted as the primary method for the purification as it yielded pure active protein and removed the need for time consuming dialysis steps.

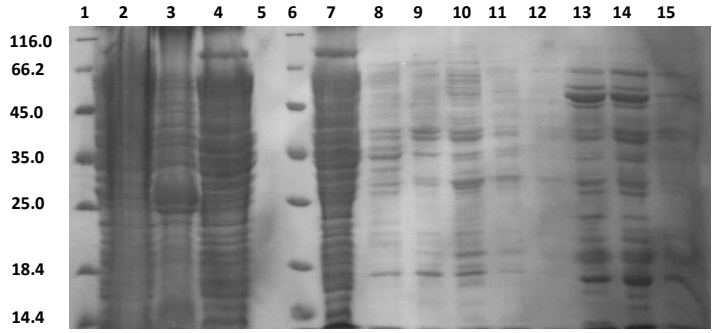

Figure 55.SDS polyacrylamide gels showing samples from sonication and Ni-NTA purification of EZS from expression in *E. coli* C41(DE3) pLysS cells expressed at 20 °C overnight. Left: Lane 1) protein molecular weight ladder (x10^3 Mr), 2) *E. coli* C41(DE3) pLysS cells post expression, 3) insoluble fraction after sonication, 4) soluble fraction after sonication, 5) empty, 6) protein molecular weight ladder (x10^3 Mr), 7) sample loaded onto Ni-NTA column, 8-9) CLB with 5 mM imidazole, 10-12) CLB with 20 mM imidazole, 13-14) CLB with 300 mM imidazole, 15) CLB with 500 mM imidazole.

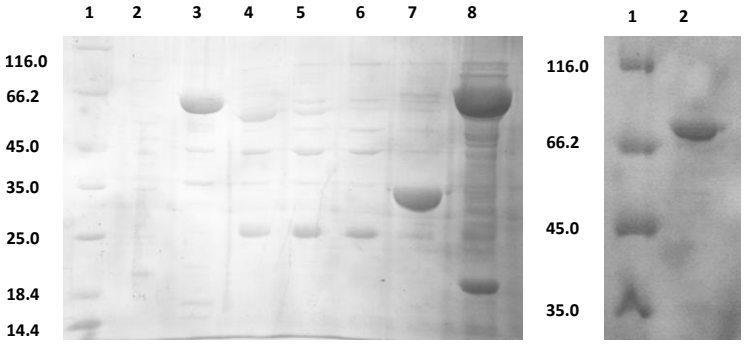

Figure 56. SDS polyacrylamide gels showing samples anion exchange FPLC (Q-sepharose column) purification (left) and sample after spin column with 50 kDa membrane cut off (right). Left: Lane 1) protein molecular weight ladder (x10^3 Mr), 2-7) impurities removed during purification, 8) fraction containing EZS and impurity with molecular mass ~18.4 kDa eluted at 140-160 mM [NaCl]. Right: Lane 1) protein molecular weight ladder (x10^3 Mr), 2) EZS sample after purification / buffer exchange using spin column with 50 kDa membrane cut off.

Circular dichromism (CD) spectroscopy was used to analyse the secondary structure of EZS. The structures of sesquiterpene cyclases comprise α-helical bundles with which a distinct CD spectrum containing two minima at 208 nm and 222 nm. Previous protocols for EZS purification by the Allemann group involved basic extraction yielding inactive or unstable protein. It was proposed that the harsh refolding conditions employed to extract protein from the insoluble fractions was responsible for the loss of activity by misfolding (section 2.3.2). Purification of EZS in the soluble fraction had not been attempted and therefore it was not known whether the structure of the soluble protein was purely α-helical or misfolded.

The CD spectrum of EZS (Figure 57) showed the characteristic minima for an α-helical secondary structure. This spectrum was then used as a reference for future work concerning single point mutations EZS gene to ensure that single amino acid substitutions had not caused structural changes.

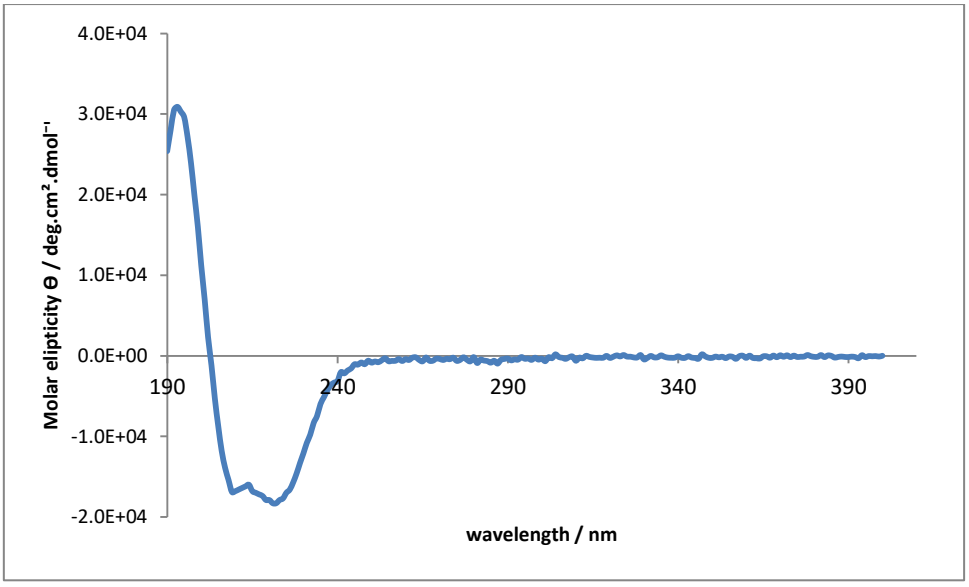

Figure 57. Circular dichromism spectrum of EZS. The sample was prepared by taking concentrated EZS sample (Figure 56), in 20 mM Tris base buffer pH 8.0 and diluting in 10 mM potassium phosphate buffer pH 8.0 to achieve the final EZS concentration of 10 µM. Prior to each individual CD scan, a blank containing potassium phosphate buffer was performed. Molar residue ellipticity was calculated using equation 1.1 (8.1.12), and data plotted. The path length of quartz cuvette was 1 mm and total volume was 300 µL.

2.6 Incubation of (2*Z*,6*Z*) farnesyl diphosphate (38) and EZS

Analysis of the pentane extractable products from (2*Z*,6*Z*) farnesyl diphosphate (**38**) incubation with pure EZS *via* GC-MS yielded two enzymatic products (Figure 58). A major peak at 15.3 min and a minor peak at 14.9 min corresponding to 7-epizingiberene (**1**) and curcumene (**81**) respectively are in agreement with literature. The mass spectra of the compound eluted at 15.3 min (Figure 60), showed a molecular ion peak with *m*/*z* = 204 indicative of a sesquiterpene product and the mass spectrum of 14.8 min (Figure 61), showed a molecular ion peak with *m*/*z* = 202 corresponding to an oxidised product.

Farnesenes were synthesised from (2*Z*,6*Z*) farnesol (**167**) to confirm enzymatic products were not resulting from the cleavage of the diphosphate group and subsequent deprotonation which would also give a *m*/*z* = 204. The farnesene standard was run using the same method on GC-MS and was observed to give a retention time of 23.4 min and a mass spectrum that was distinctive from enzymatic products (Figure 62). However, this mass spectrum matched the product from the cold shock incubation showing that the cold shock protocol resulted in the production of a farnesene product by EZS incubation with (2*Z*,6*Z*) FDP (**38**).

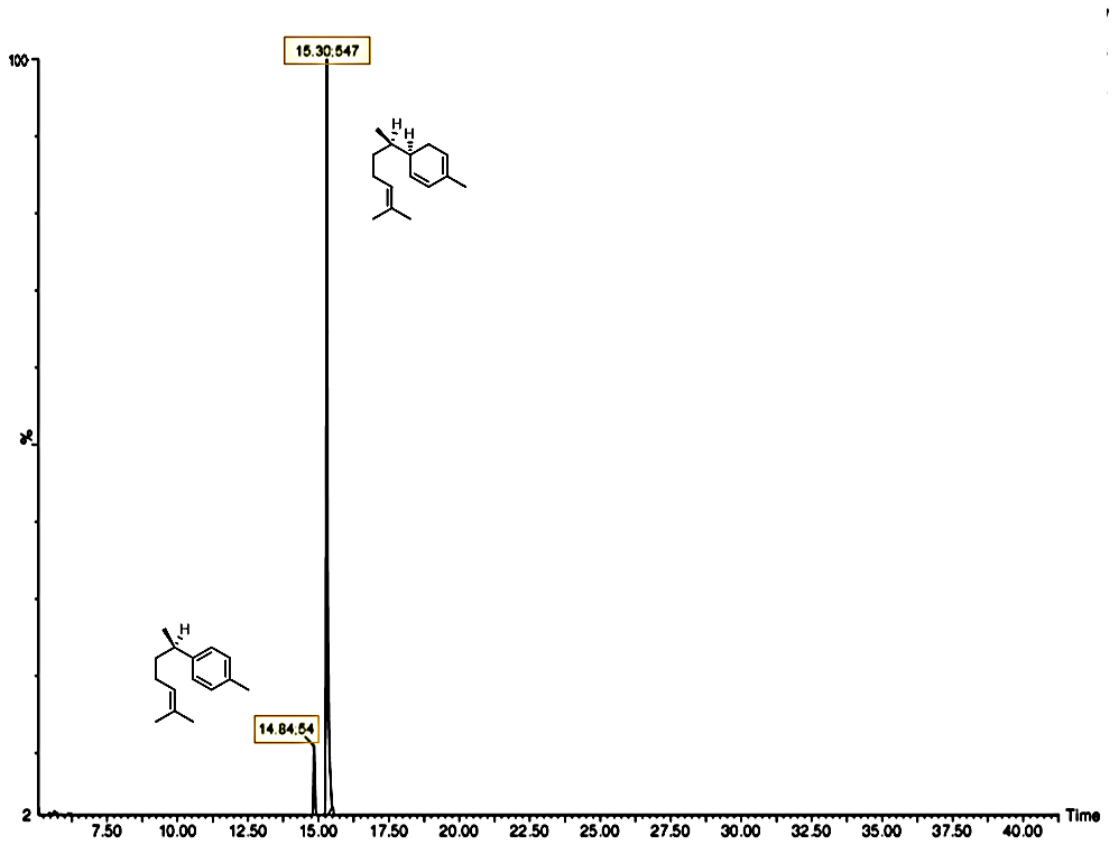

Figure 58. Total ion chromatogram of the pentane extractable products arising from incubation of 38 with EZS.

Figure 59 outlines the possible molecular ion fragments that may be responsible for the major species observed in the EI^+ mass spectrum (Figure 60).

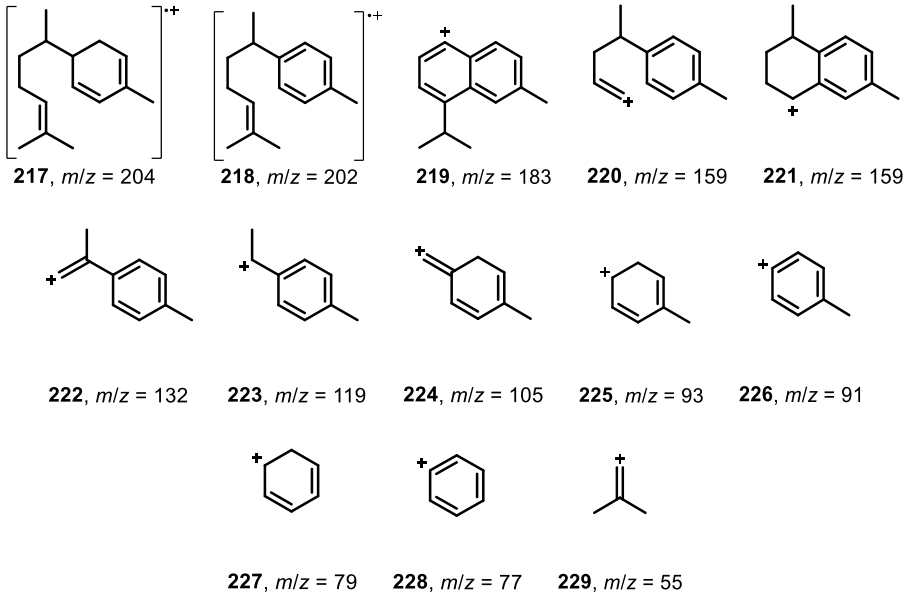

Figure 59. Possible fragments of 217 and *m/z* values.

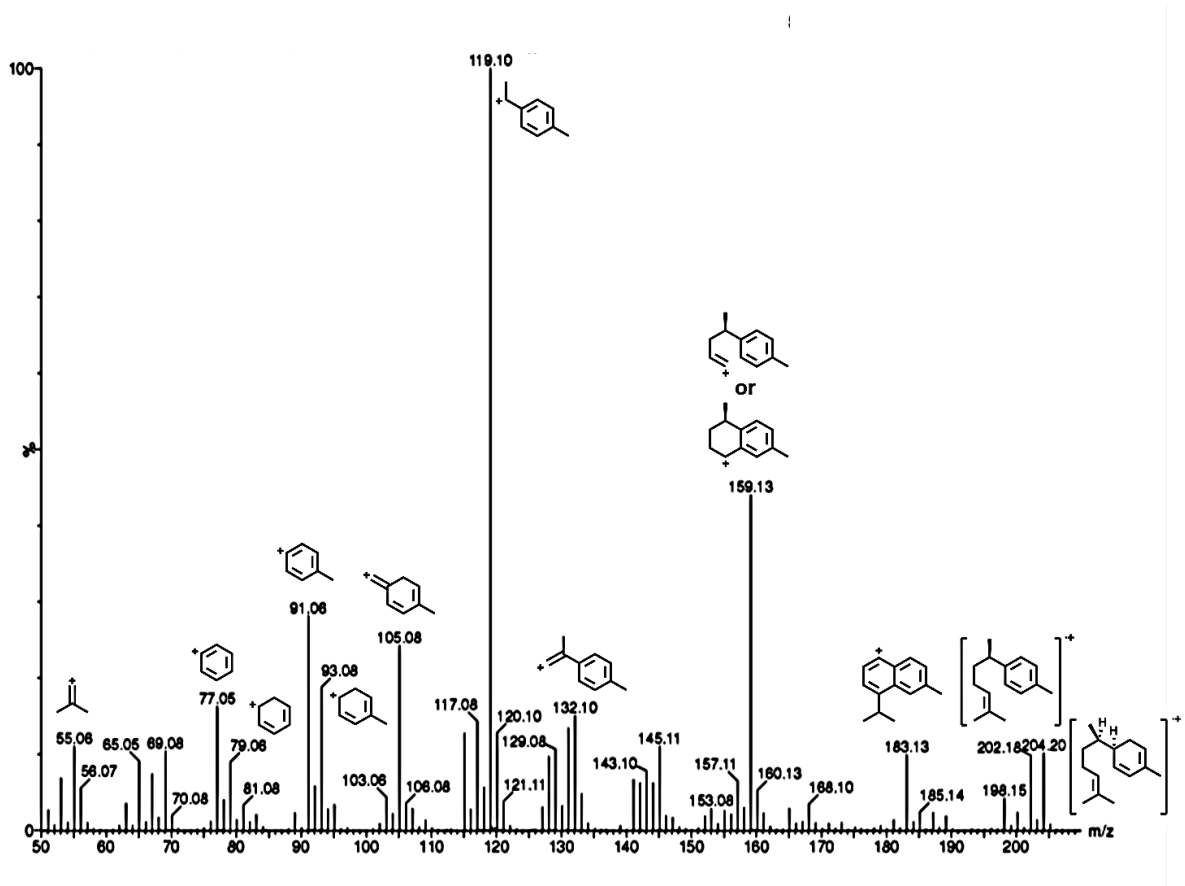

Figure 60. Mass spectrum of the compound eluting at 15.3 min on the total ion chromatogram in Figure 58.

Extending the reaction time resulted in a negligible increase in curcumene (**81**) and atmospheric exposure did not result in further oxidation (Figure 58). It was noted that when air was removed from the incubation with additional pentane filling the incubation vial, the curcumene product was significantly reduced without the need to degas buffers or undertake incubations under inert conditions.

The mass spectrum of **81** (Figure 61), shows a fragmentation pattern containing all fragment peaks observed in the respective mass spectrum of 7-epizingiberene (**1**) excluding the *m/z* = 204 peak.

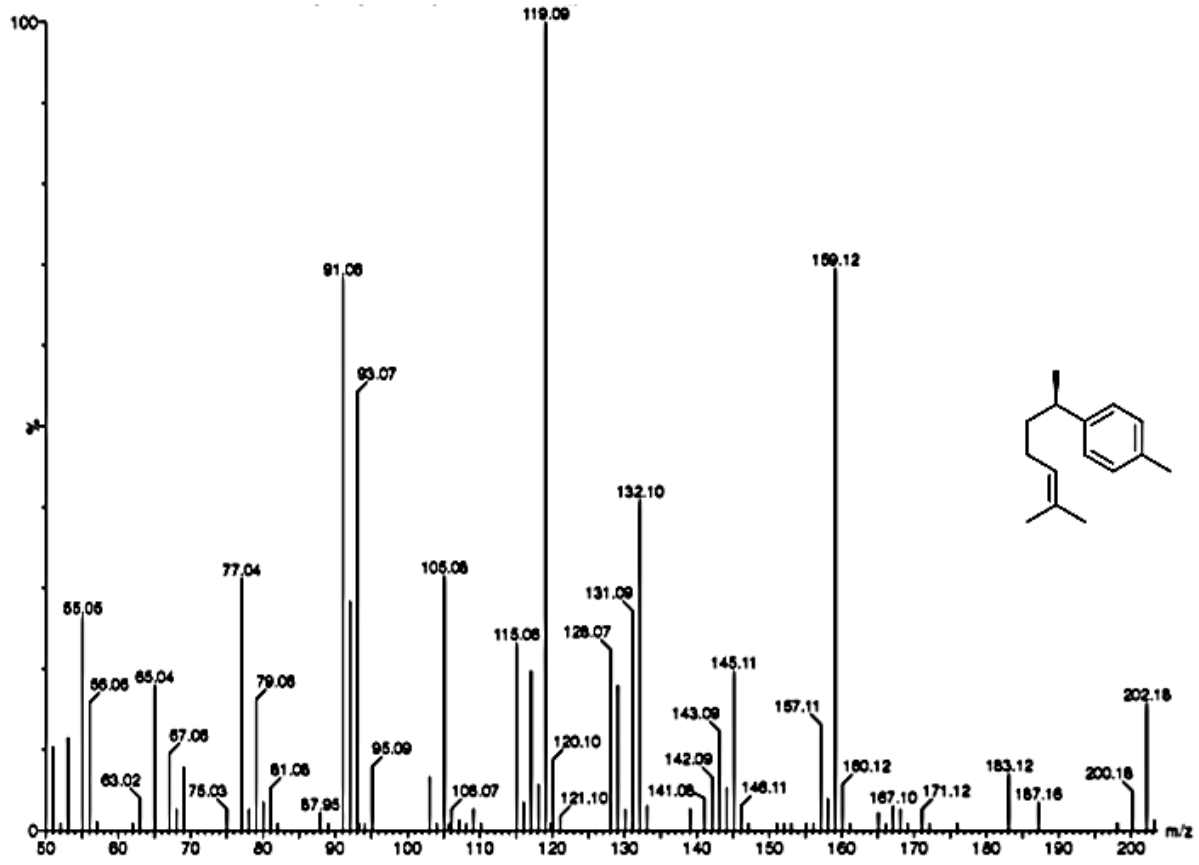

Figure 61. Mass spectrum of the compound eluting at 14.8 min on the total ion chromatogram in Figure 58.

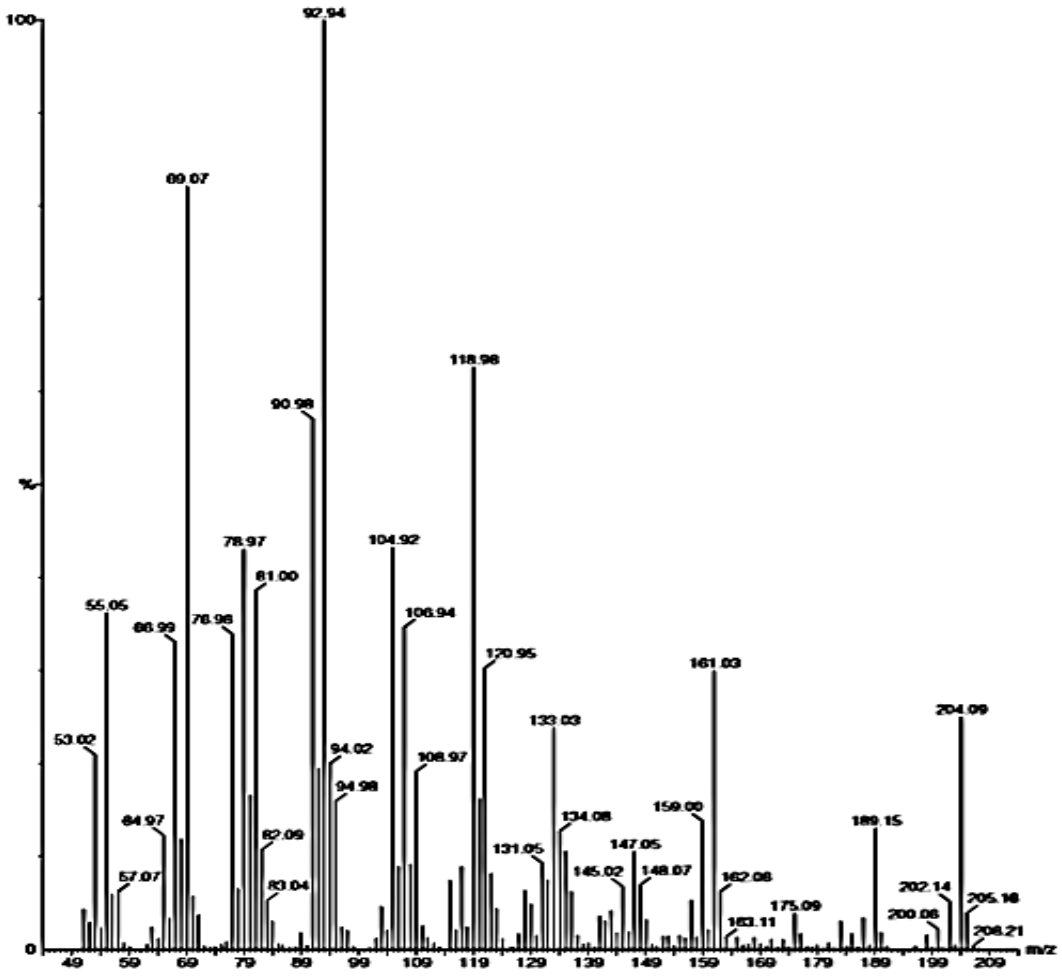

Figure 62. Mass spectrum of farnesene product generated from (2*Z*,6*Z*) farnesol (167).

2.7 Site Directed mutagenesis

2.7.1 Metal binding motifs

Alterations to the conserved residues in these active site motifs should also reveal their importance in catalysis, possibly modifying K_M and k_{cat} values. Several active site residues were changed using site directed mutagenesis to alanine (A) to remove the negative charge of residues thought to be responsible for the chelation of magnesium ions in the active site. The removal of the charge should affect the binding of respective magnesium ions and cease or severely limit enzymatic activity.

Four metal binding motif mutants were generated. The aspartate (D) and glutamate (E) residues of the **D**DXX**E** motif were altered to generate EZS(D495A) and EZS(E499A) whilst the asparagine (N) and glutamate (E) residues of the **N**S**E** motif were altered to generate EZS(N640A) and EZS(E648A). Cartoon representations of targeted residues prior to mutation with orientation to (2*Z*,6*Z*) FDP (38) and magnesium ions are shown in Figure 63 (D495 and E499) and Figure 64 (N640 and E648).

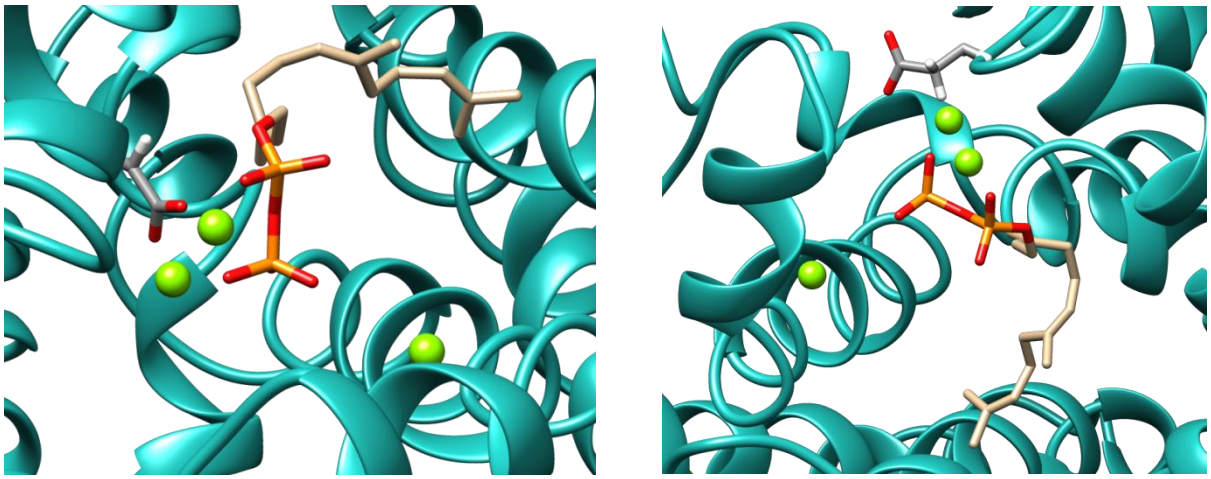

Figure 63. Cartoon representations of EZS homology model based on α-bisabolene synthase. Residues D495 (left) and E499 (right) of the conserved *D*DxxE motif are highlighted showing their orientation to bound magnesium ions and (2*Z*,6*Z*) FDP (38).[185]

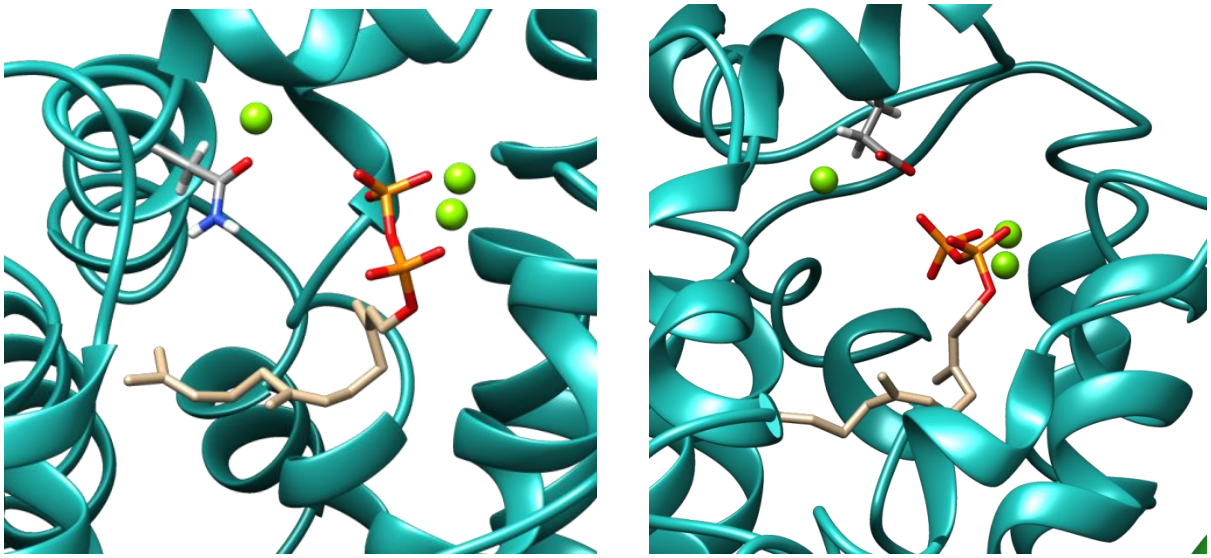

Figure 64. Cartoon representations of EZS homology model based on α-bisabolene synthase. Residues D495 (left) and E499 (right) of the conserved *DD*xx*E* motif are highlighted showing their orientation to bound magnesium ions and (2*Z*,6*Z*) FDP (38).[185]

The method of mutant expression and purification was duplicated from the protocol used to produce active EZS (section 2.5.2). Incubation of (2*Z*,6*Z*) FDP (**38**) with each mutant and analysis of the pentane extractable products *via* GC-MS showed no enzymatic products were produced by EZS(D495A), EZS(E499A) and EZS(N640A). The incubation EZS(E648A) with **38** did gave an enzymatic product which was found to be 7-epizingiberene (**1**) *via* GC-MS analysis of the pentane extractable products.

2.7.2 Aromatic active site residues

Active site aromatic residues are crucial for the stabilisation of unstable carbocation intermediates by electron donation from the delocalised π-system.[226] In addition to the stabilising effect, aromatic residues are large; therefore steric interactions may influence substrate binding and folding into reaction ready conformations. Mutation of these residues to alanine (A) could have two effects on enzyme activity; destabilisation of carbocation intermediates and increased substrate promiscuity resulting from less steric bulk allowing for greater mobility of substrate within the active site.[227]

As the crystal structure of EZS is not known, a homology model based on α-bisabolene synthase was generated to identify potential active site aromatic residues that are in close proximity to the bound substrate. These residues were targeted for alteration to alanine to generate four EZS mutants; EZS(F598A), EZS(F705A), EZS(Y483A) and EZS(Y716A).

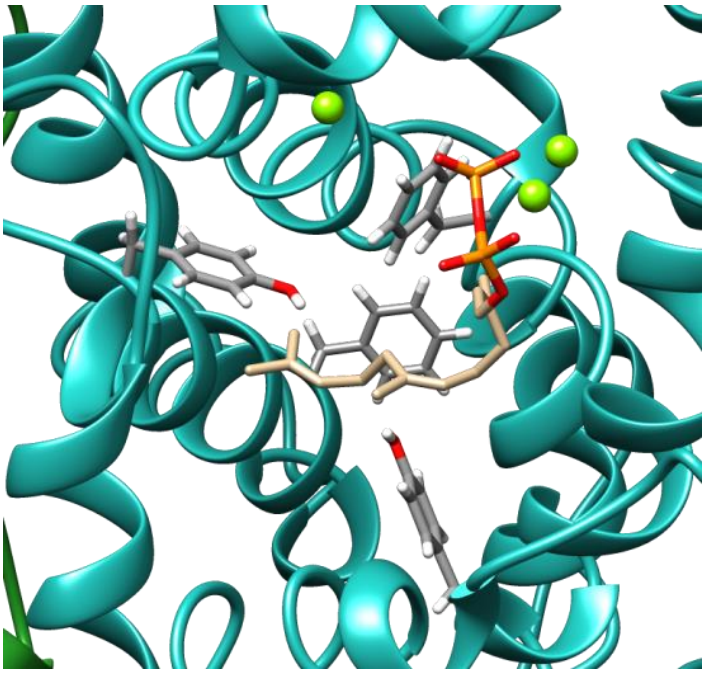

Figure 65. Cartoon representations of EZS homology model based on α-bisabolene. Putative aromatic active site residues F598, F705, Y483 and Y716 are highlighted showing their orientation to bound magnesium ions and (2*Z*,6*Z*) FDP (38).[185]

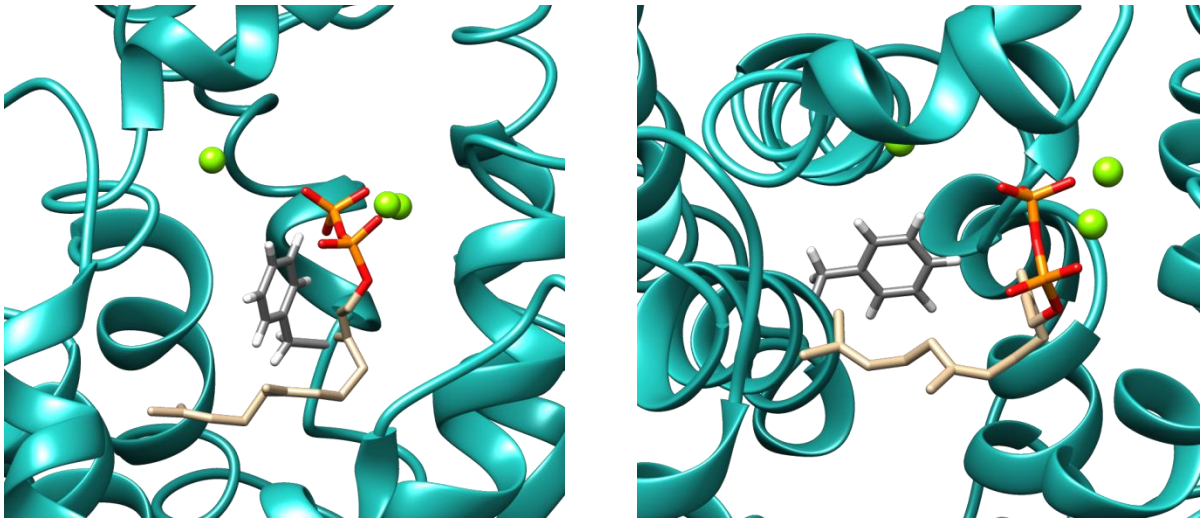

Figure 66. Cartoon representations of EZS homology model based on α-bisabolene synthase. Putative aromatic residues F598 (left) and F705 (right) are highlighted showing their orientation to bound magnesium ions and (2*Z*,6*Z*) FDP (38).[185]

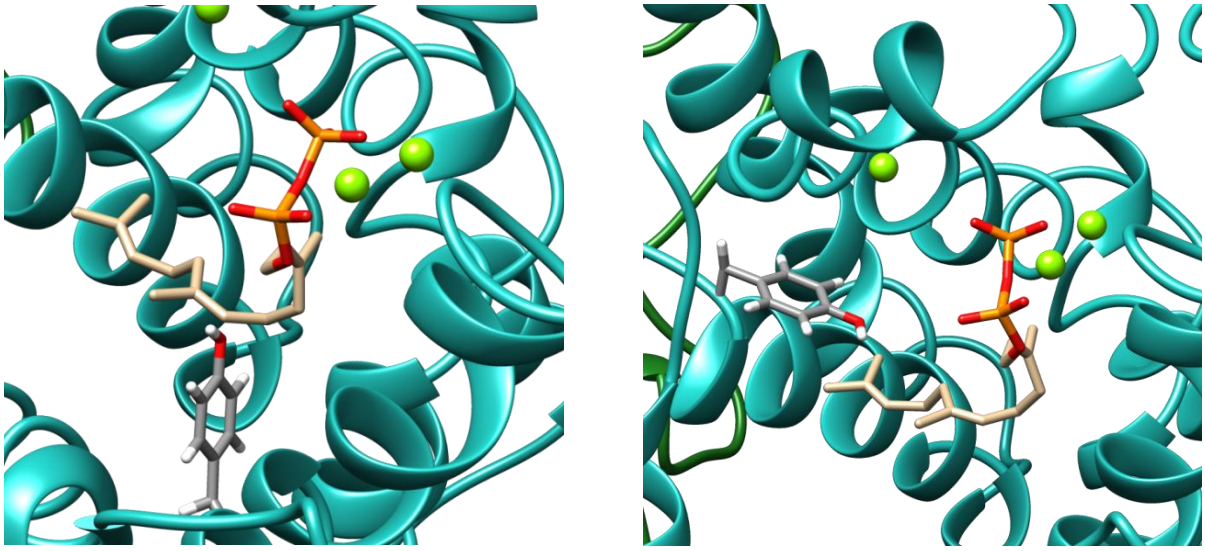

Figure 67. Cartoon representations of EZS homology model based on α-bisabolene synthase. Putative aromatic residues Y483 (left) and Y716 (right) are highlighted showing their orientation to bound magnesium ions and (2*Z*,6*Z*) FDP (38).[185]

EZS aromatic active site mutants EZS(F598A), EZS(F705A), EZS(Y483A) and EZS(Y716A) were incubated with (2*Z*,6*Z*) FDP (**38**) and the pentane extractable products analysed *via* GC-MS. Mutants EZS(F598A), EZS(F705A) and EZS(Y716A) showed no enzymatic products giving evidence that the residue is important during catalysis as CD spectroscopy (section 2.7.3) showed mutants were folded correctly. Alternatively the mutation from a large to a small residue caused steric changes to the active site inhibiting activity. Contrastingly, EZS(Y483A) yielded 7-epizingiberene (**1**) as an enzymatic product giving evidence that the residue may not contribute directly to the mechanism.

2.7.3 CD spectroscopy of EZS mutants

CD spectra of all EZS mutants generated were measured to assess whether each single amino acid substitution had altered the global secondary structure of the protein significantly. Of the 8 mutants generated, two were active; EZS(E648A) and EZS(Y483A) the CD spectra of which can be are shown in Figure 69 and Figure 70 respectively. Both spectra show minima at 208 and 222 nm that are characteristic of an α-helical secondary structure. This distinctive trace confirms that the alterations to the protein did not alter the secondary structure. The CD spectra of other mutants were also measured; EZS(D495A) and EZS(E499A) (Figure 68), EZS(N640A) (Figure 69), EZS(F598A) (Figure 70) and EZS(F705A) (Figure 71) showing the same characteristic minima for an α-helical structure indicating that none of the alterations performed significantly altered the overall protein fold.

The CD spectra of EZS(Y716A) (Figure 71) showed a slight decrease in molar ellipticity between 240-320 nm. Though the difference in amplitudes may imply a partial misfolding, the CD spectra contained the distinctive two minima at 208 nm and 222 nm for an α-helical secondary structure. As

no other minima representative of β-sheets (218 nM) or random coils (195 nm) were observed, the discrepancies were not thought to arise from structural change but experimental variability.

Samples were prepared by taking a sample (Figure 56, section 2.5.2) in 20 mM Tris base buffer pH 8.0 and diluting in 10 mM potassium phosphate buffer pH 8.0 to achieve the final EZS concentration of 10 µM. Prior to each individual CD scan, a blank containing potassium phosphate buffer was performed. Molar residue ellipticity was calculated using equation 1.1 (8.1.12) and data plotted. The path length of quartz cuvette was 1 mm and total volume was 300 µL

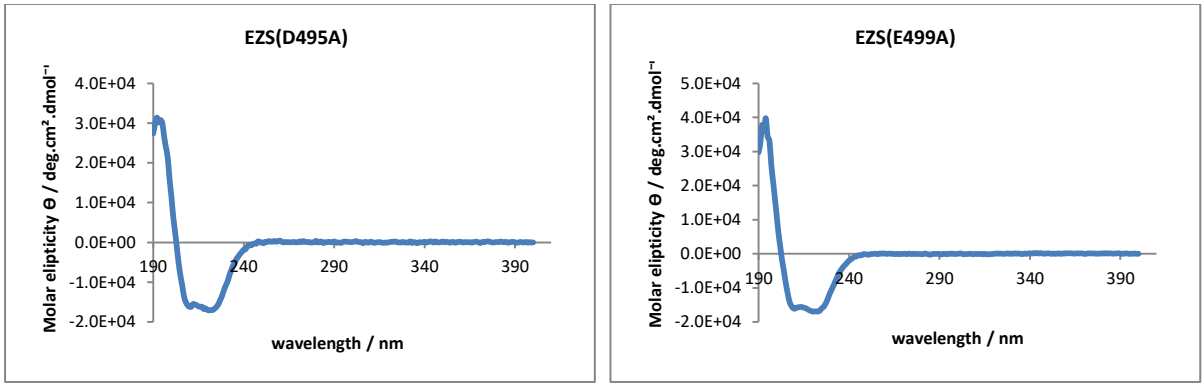

Figure 68. Circular dichromism spectra of EZS(D495A) (left) and EZS(E499A) (right).

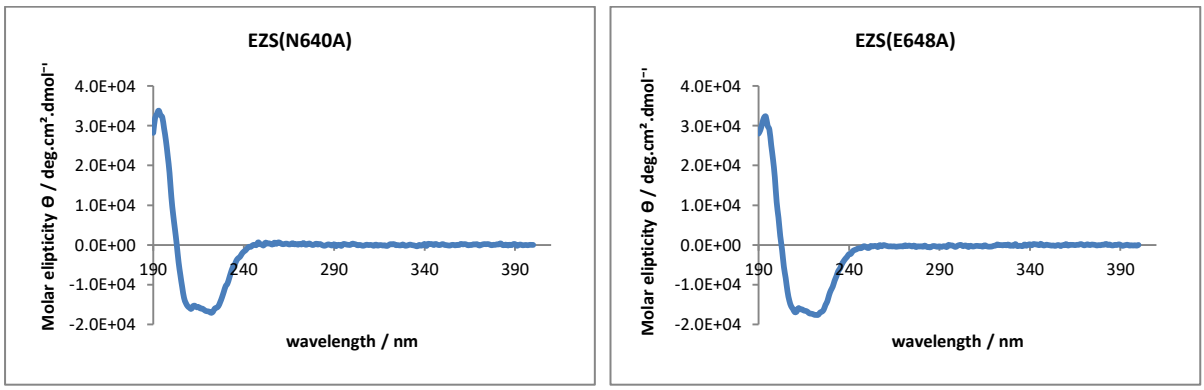

Figure 69. Circular dichromism spectra of EZS(N640A) (left) and EZS(E642A) (right).

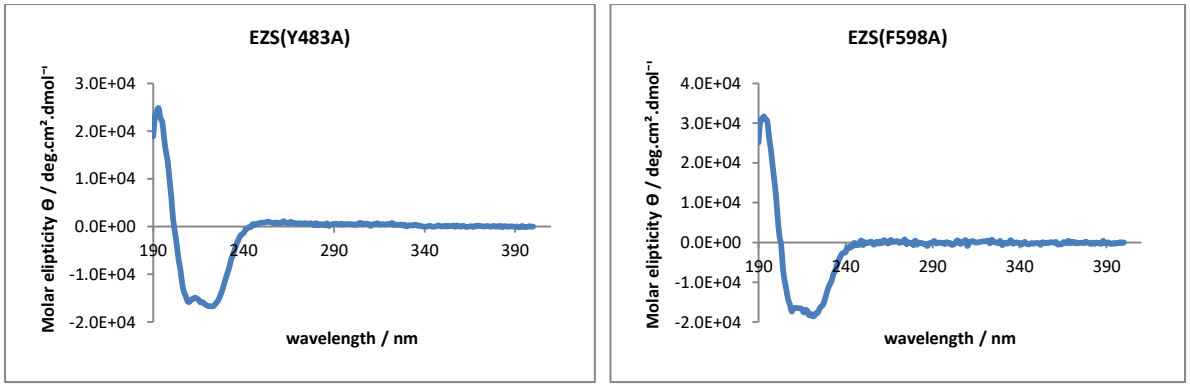

Figure 70. Circular dichromism spectra of EZS(Y483A) (left) and EZS(F598A) (right).

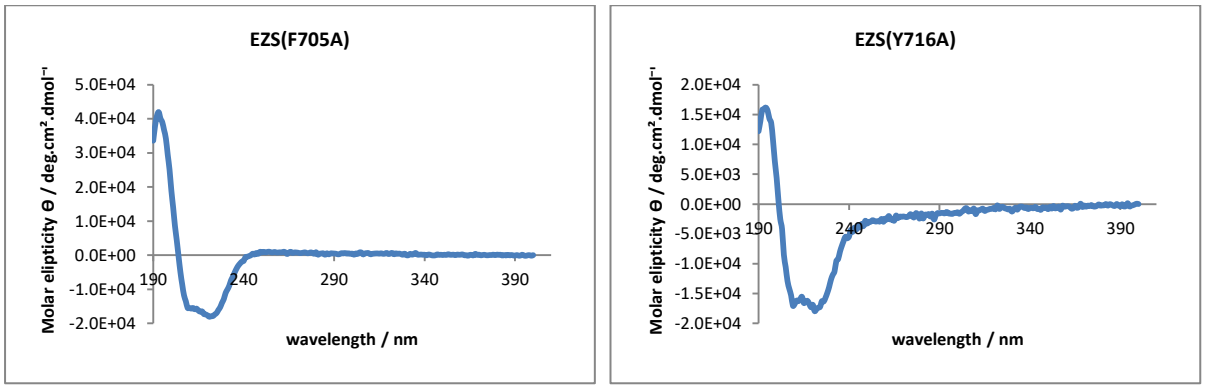

Figure 71. Circular dichromism spectra of EZS(F705A) (left) and EZS(Y716A) (right).

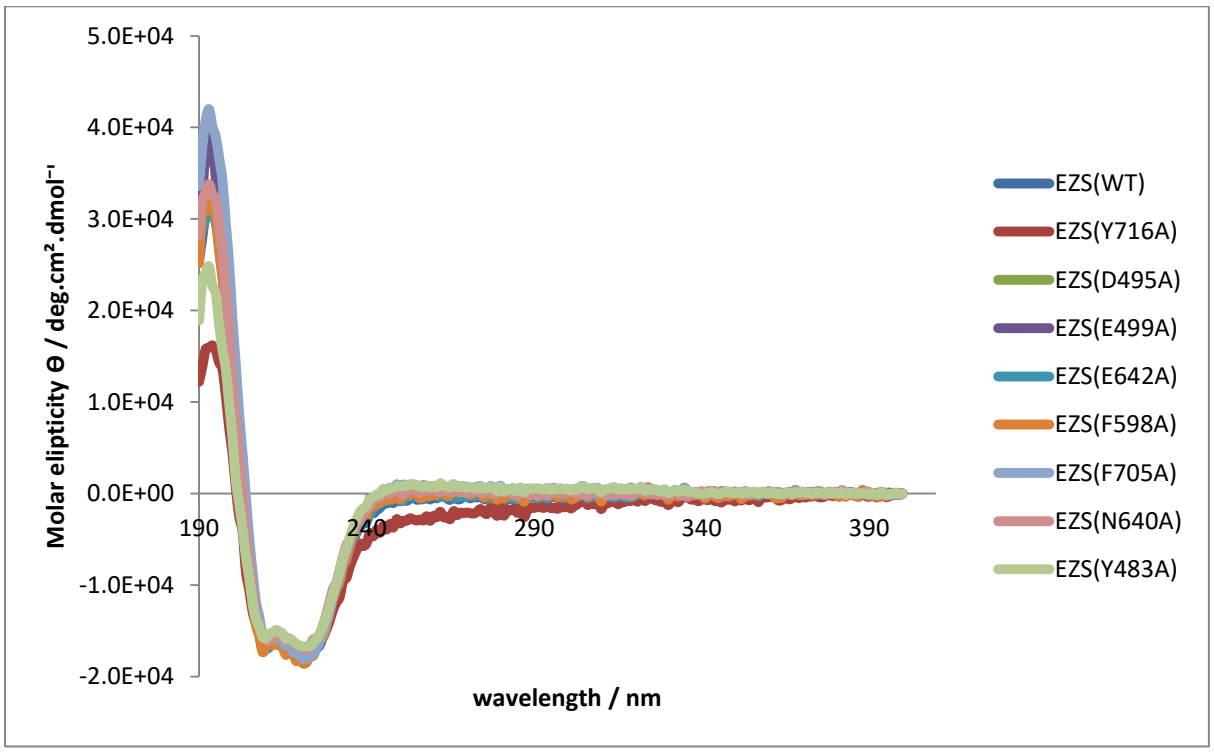

Figure 72. Overlaid circular dichromism spectra of EZS(WT) and EZS mutants.

The CD spectra of the individual EZS mutants and wild type enzyme were overlaid to confirm that the single point mutations did not affect protein structure (Figure 72). Two mutant proteins exhibited activity upon incubation with **38** however, the remaining six did not. As the overall protein structure remained constant across all mutants, the loss of activity was directly related to the alteration of key active site residues.

2.8 Summary

Outlined in this chapter were the numerous synthetic routes investigated for the preparation of (2*Z*,6*Z*) farnesyl diphosphate (**38**). Though published literature had shown a procedure for the synthesis of (2*Z*,6*Z*) farnesol (**167**) directly from neryl acetone (**166**) using a modified Wittig reaction, this synthesis could not be replicated and therefore, different procedures were investigated. Two synthetic routes yielded **38**; the Anastasia approach and the Horner-Wadsworth-Emmons synthesis utilising a Still-Gennari modification. Both protocols gave a 1:1 ratio of (2*Z*,6*Z*) farnesol (**167**) and (2*E*,6*Z*) farnesol (**168**) with modification of reaction conditions not increasing the ratio of the *Z* isomer in relation to the *E* isomer. The Horner-Wadsworth-Emmons synthesis achieved a 41% yield of **167** over the olefination and reduction steps whilst the Anastasia synthesis gave a 24% yield of **167**. The Horner-Wadsworth-Emmons synthesis was chosen as the method for synthesising **38** over the Anastasia protocol due to higher yield, lower cost of reagents and easier reaction scale up.

EZS was overexpressed in *E. coli* BL21 (DE3) and ArcticExpress RP cells. Investigation of the soluble fraction showed that active EZS was present though attempts at purification were unsuccessful due to low expression of soluble protein. Although the use of expression tags MBP and GB1 did not increase the expression of soluble protein, large expression bands were observed *via* SDS PAGE for the GB1-EZS fusion protein though purification of protein proved problematic.

The use of *E. coli* C41 (DE3) pLysS cells for the expression of EZS yielded larger expression of soluble protein than observed comparative EZS expressions using *E. coli* BL21 (DE3) and ArcticExpress RP cells. The greater expression of EZS allowed for a 3 step purification yielding protein of sufficient purity and quantity to confirm the isolated protein was solely responsible for substrate turnover and characterisation assays.

Out of the eight mutants incubated with (2*Z*,6*Z*) farnesyl diphosphate (**38**), two EZS mutants; EZS(E648A) and EZS(Y483A) gave enzymatic product. Mutation of selected metal binding residues showed that the aspartate (A) and glutamate (E) residues of **D**Dxx**E** and the asparagine (N) residue of **N**SE were crucial for enzyme activity. In contrast the glutamate residue of NS**E** was not crucial for catalysis with enzymatic product observed in the pentane extracts of EZS(E648A) incubation with **38**. The mutation of aromatic active site residues in mutants; EZS(F598A), EZS(F705A) and EZS(Y716A) resulted in the loss of enzyme activity, giving evidence that they contribute to the catalytic mechanism. Analysis of the mutants overall fold using circular dichromism spectroscopy showed that all mutants had the same secondary structure as the wild type and therefore loss of activity did not result from misfolding (Figure 72).

Chapter 3 – Characterisation of EZS and Investigation of active site residues

3.1 Preface

This chapter will outline the synthesis of radiolabelled (2*Z*,6*Z*) farnesyl diphosphate; (2*Z*,6*Z*)-[1-^{3}H]-farnesyl diphosphate (**229**) for the kinetic characterisation of 7-epizingiberene synthase (EZS) and mutants. Characterisation of sesquiterpene cyclases by the Allemann group has required (2*E*,6*E*)-[1-^{3}H]-farnesyl diphosphate for steady state kinetic assays. (2*E*,6*E*)-[1-^{3}H]-farnesyl diphosphate is commercially available but the radiolabelled substrate for EZS is not commercially available and required synthesis.

Prior to steady state kinetic characterisation of EZS, incubation conditions concerning time, pH and buffer concentrations required optimisation. Steady state kinetic parameters K_M, k_{cat} and V_{max} were calculated for EZS, EZS(E648A) and EZS(Y483A) to determine the effect of the single point mutations on catalytic efficiency.

3.2 Radioactive isotopologue

3.2.1 Synthesis of (2*Z*,6*Z*)–[1-^{3}H]–farnesyl diphosphate (229)

Numerous publications have outlined pathways for the incorporation of tritium at the C1 position of farnesyl diphosphate and analogous substrates. The chosen alcohol is typically oxidised to the corresponding aldehyde and subsequently reduced with sodium borotritide ($NaBT_4$) to yield the desired radiolabelled product.

Numerous oxidations published in the literature for (2*E*,6*E*) farnesyl diphosphate (**31**) were attempted to yield (2*Z*,6*Z*) farnesal (**217**).[228, 229, 113] Manganese (IV) oxide has been previously used within the Allemann group for this purpose. However, oxidation of (2*Z*,6*Z*) farnesol (**167**) resulted in a 1:1 mixture of (2*Z*,6*Z*) farnesal (**217**) and (2*E*,6*Z*) farnesal (**220**). The reaction was repeated numerous times and variations to determine the cause of isomeric scrambling. Table 5 shows variation in MnO_2 equivalents, time, temperature and solvent attempted for the oxidation.

Table 5. Variations of time, temperature, solvent, reagent molar equivalence isomeric scrambling of the C2,C3 bond during the oxidation of (2*Z*,6*Z*) farnesol (167) to (2*Z*,6*Z*) farnesal (217).

Time / h	MnO_2 equiv.	Solvent	Temp / °C	Scrambling (Y/N)
16	5	Hexane	25	Y
16	10	Hexane	25	Y
16	20	Hexane	25	Y
16	30	Hexane	25	Y
48	30	Hexane	25	Y
16	30	Hexane	68	Y
16	30	Hexane	0	Y
48	30	Hexane	0	Y
4	30	DCM	25	Y
16	30	DCM	25	Y
48	30	DCM	25	Y

The oxidation was initially performed for 16 hours with 5 equivalents of MnO_2. The reaction had not gone to completion after this time period and it was initially proposed that the poor condition of old reagent was the cause. Fresh manganese (IV) oxide was used under the same conditions; however the reaction still did not go to completion. The reaction was repeated with 30 equivalents of MnO_2 and a longer reaction time of 48 hours however, the reaction did not proceed to completion. DCM was used in place of hexane and the reaction went to completion after 48 hours with 30 equivalents of MnO_2. Though starting material was now fully consumed, each variation attempted exhibited

scrambling of the stereochemistry C2,C3 double bond when analysed *via* ^{1}H NMR spectroscopy. Two doublets characteristic of an aldehyde environment were observed at 9.90 and 9.85 ppm integrating to one proton. Two doublets integrating to one proton were also observed at 5.82 and 5.78 ppm corresponding to the alkene proton at the C2 position (Figure 73). The presence of two aldehyde and alkene (C2 position) proton environments on the ^{1}H NMR spectrum gives evidence that the oxidation procedures were causing isomeric scrambling of the C2,C3 double bond.

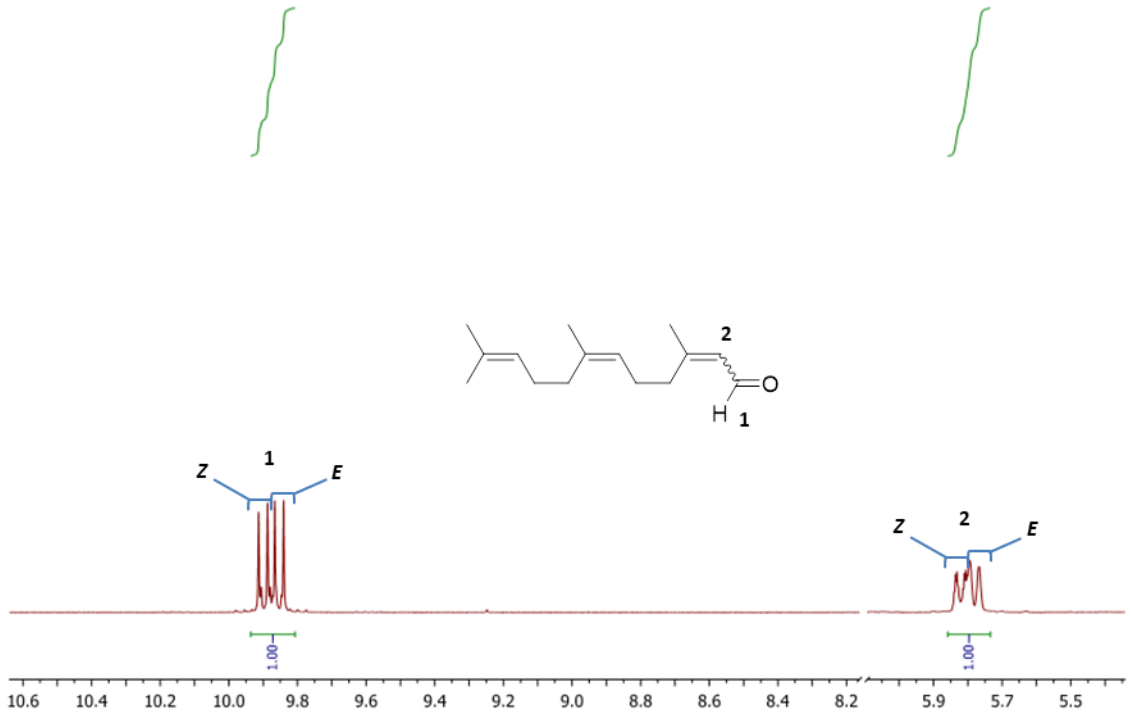

Figure 73. A ^{1}H NMR spectrum of a mixture of aldehydes (2*Z*,6*Z*)-3,7,11-trimethyldodeca-2,6,10-trienal (217) and (2*E*,6*Z*)-3,7,11-trimethyldodeca-2,6,10-trienal (220).

Yamamoto *et al.*[228] published that *E*/*Z* isomerisation of the C2, C3 double bond occurred in the presence of MnO_2 at room temperature however, isomerisation did not occur when reacted with MnO_2 at 0 °C in hexane. Reaction conditions were duplicated with (2*Z*,6*Z*) farnesol (**167**) and isomerisation still occurred. Consequently, an alternative method of oxidation was sought. A Swern oxidation[230] and a Dess-Martin oxidation[231] were investigated as possible oxidation methods.

Both methods resulted in the *E*/*Z* isomerisation of the C2/C3 double bond. It was proposed that residual base or acid in the reaction mixtures; NEt_3 in the Swern oxidation or acetic acid in the Dess-Martin reaction were responsible. The presence of base or acid could aid tautomerisation of the aldehyde to an enolate (**221**) or enol (**219**) allowing the free rotation of the C2/C3 sigma bond. Subsequent tautomerisation to the aldehyde would yield a mixture of *E* and *Z* isomers (Figure 74).

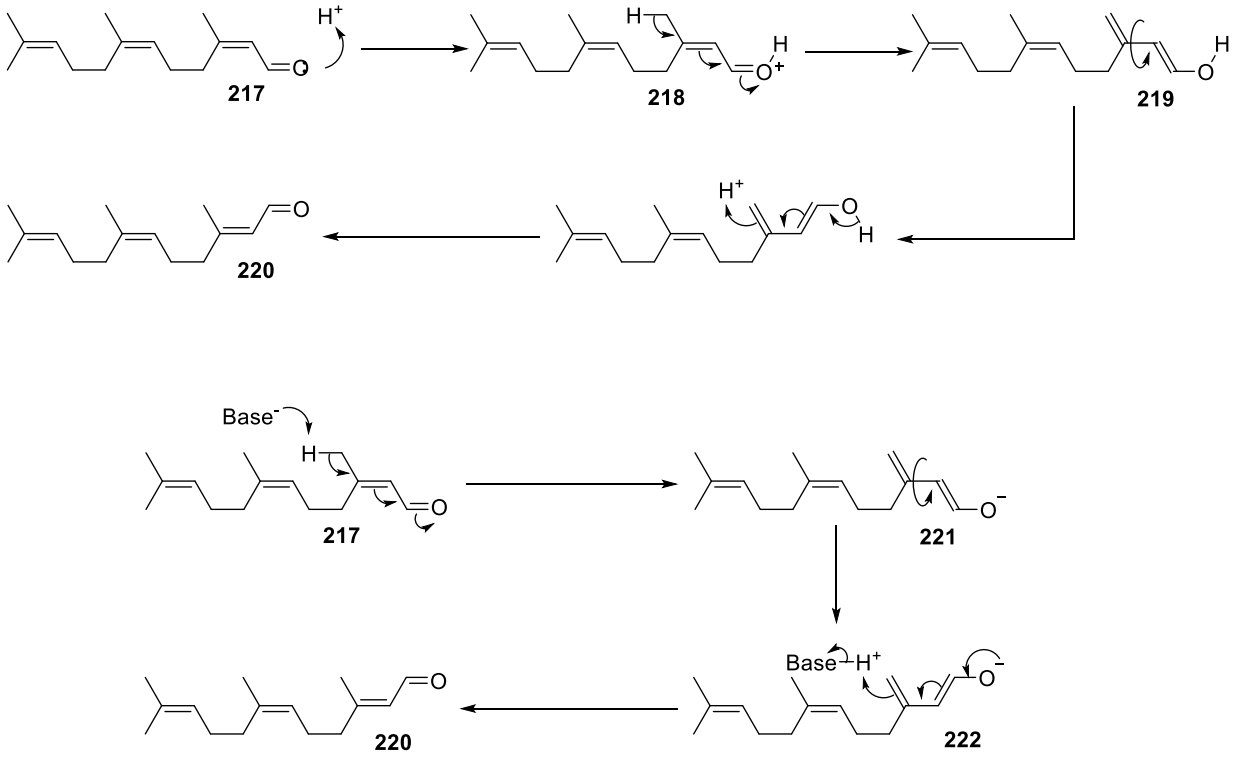

Figure 74. Plausible mechanisms for the acid catalysed isomerisation (top) and base catalysed isomerisation (bottom) of (2*Z*,6*Z*) farnesal (217) to (2*E*,6*Z*) farnesal (220).

An alternative oxidation procedure was found in a publication by Bobbitt *et*, al.[232] The use of an oxoammonium oxidation reagent, 4-acetamido-2,2,6,6-tetramethyl-1-oxopiperidin-1-ium tetra fluoroborate salt (TEMPO salt) (**226**) in DCM was shown to achieve fast and high yielding oxidation reactions with an allylic alcohol substrate. **226** was prepared from the corresponding free radical by oxidation with sodium hypochlorite and subsequent reaction with fluoroboric acid (Figure 75).

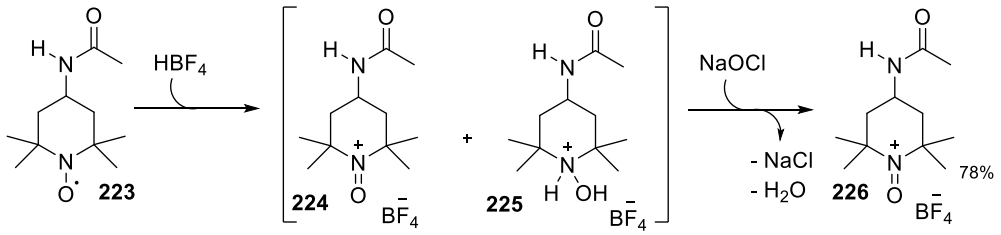

Figure 75. Synthesis of 4-acetamido-2,2,6,6-tetramethyl-1-oxopiperidin-1-ium tetra fluoroborate salt (226).

Oxidation of (2*Z*,6*Z*) farnesol (**167**) with TEMPO salt (**226**) resulted in a single aldehyde product and was passed through a silica plug to remove excess oxidation reagent. Dess Martin and Swern oxidation products both required purification *via* column chromatography as multiple reaction products were observed. Nuclear Overhauser Effect Spectroscopy (NOESY) was used to confirm the *Z*

isomer showing close spatial arrangement of the aldehyde proton and methylene environment. The use of the TEMPO salt gave a quick method of oxidation with aldehyde **217** of sufficient purity to be used without further purification isolated after passing the crude reaction mixture through a short silica plug.

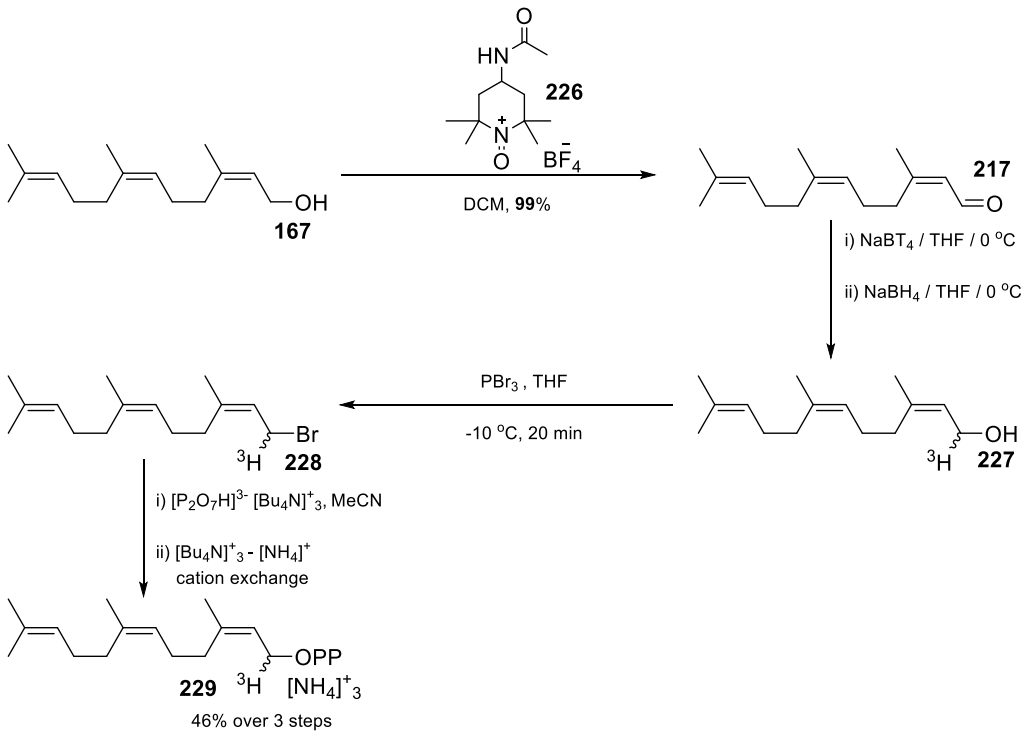

Figure 76. Synthesis of (2*Z*,6*Z*)-[1-^{3}H]-farnesyl diphosphate (229).

The next step of the synthesis was the incorporation of tritium by reducing aldehyde **217** with sodium borotritide, the radiolabelled equivalent of sodium borohydride. Sodium borohydride reactions typically use protic solvents such as methanol or ethanol which result in the evolution of $H_{2(g)}$. To restrict the emission of gaseous radioactive waste, anhydrous tetrahydrofuran was used as the reaction solvent. Micromolar quantities of sodium borotritide ($NaBT_4$) were required for radiolabelling and unreacted farnesal (**217**) was subsequently reduced with excess unlabelled sodium borohydride to drive the reaction to completion. Bromination, diphosphorylation and ion exchange proceeded *via* established protocol outlined in chapter 2. Radioactive diphosphate was not purified *via* HPLC with excess pyrophosphate removed using a SNAP Ultra C18 Biotage column. Use of the enclosed column for purification reduced the risk of radioactive contamination (Figure 76). Lyophilisation of the fractions gave purified (2*Z*,6*Z*)-[1-^{3}H]-farnesyl diphosphate (**229**). A sample of **229** was dissolved in water and dispersed in Ecoscint A scintillation cocktail and the radioactivity of **229** analysed using a liquid scintillation counter and found to have a specific activity of 2.8 mCi

$mmol^{-1}$ (equation 1.4, 8.1.13). The liquid scintillation counter quantified radioactivity in counts per minute (CPM) which was converted to activity using equation 1.2 (8.1.13).

All reactions and radioactivity were monitored *via* TLC analysis. The silica, to which the product was bound, was removed from the plate emulsified in Ecoscint A scintillation cocktail and radioactivity analysed using a liquid scintillation counter. This method was particularly useful in the reduction of **217** as a secondary spot was visible *via* TLC. However, when the compound bound silica was suspended in Ecoscint A scintillation cocktail and measured using a liquid scintillation counter, analysis showed no radioactivity was present.

3.3 Kinetic characterisation of EZS

3.3.1 Incubation optimisation

The steady state kinetic parameters for the reaction of EZS catalysing the turnover of (2*Z*,6*Z*) FDP (**38**) to 7-epizingiberene synthase were determined using a radiolabelled-substrate assay. A concentration range of (2*Z*,6*Z*)-[1-^{3}H]-FDP (**229**) was incubated with a known concentration of EZS for a defined time period. Organic incubation products were extracted with hexane and eluted through a short silica column with hexane. Any aqueous soluble residual material would not be extracted into organic layer with only enzymatically derived hydrocarbon products passing through the silica. Organic extracts were emulsified with Ecoscint O scintillation cocktail and analysed using a liquid scintillation counter. The results (CPM) were converted to a rate using equation 1.2 (8.1.13) and fitted to a Michaelis-Menten curve to determine V_{max}, K_M and k_{cat}.

Incubation conditions were optimised prior to the measurement of steady state parameters. The catalysis buffer for the incubation of (2*Z*,6*Z*)-[1-^{3}H]-FDP (**229**) with [EZS] was taken from the protocol published by Bleeker *et al.*[3] The buffer comprised of 25 mM HEPES ((2[4-(2-hydroxyethyl)piperazin-1-yl]ethanesulfonic acid), 10 mM $MgCl_2$ and 5 mM DTT (dithiothreitol) at pH 7.2 was used as a starting reference for the optimisation of [EZS], [$MgCl_2$], pH and incubation length.

For the optimisation of EZS concentration, an [EZS] range 2–200 nM was incubated with **229** in catalysis buffer (25 mM HEPES, 10 mM $MgCl_2$, 5 mM DTT, pH 7.2) for 10 minutes at 30 °C. The hexane extracted products were emulsified in Ecoscint O scintillation cocktail and analysed using a liquid scintillation counter. The reaction rate increased linearly with [EZS] and plateaued to a maximum between [EZS] of 50–200 nM. The plateau at higher concentrations suggests enzyme aggregation thereby altering the concentration of active enzyme, which is required for the calculation of steady state parameters. However, the reaction rate at concentrations in the linear range (2–50 nM) is directly proportional to [EZS] therefore the concentration remains constant. A [EZS] of 30 nM was chosen as it resides central within the linear range with adequate activity for steady state kinetic experiments (Figure 77).

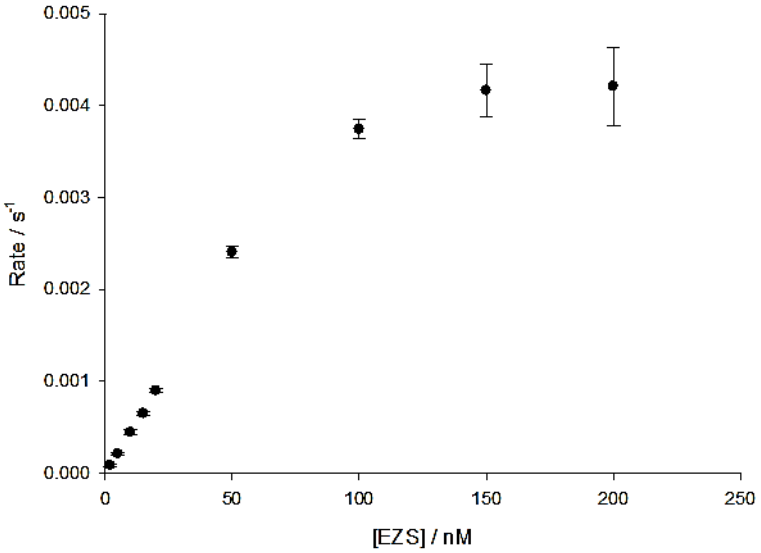

Figure 77. Plot of reaction rate for EZS catalysed production of radiolabelled products from (2*Z*,6*Z*)-[1-^{3}H]-FDP (229) against various [EZS]. Reaction conditions: buffer (25 mM HEPES, 10 mM $MgCl_2$, 5 mM DTT, pH 7.2), 10 minutes, 30 °C.

The concentration of Mg^{2+} was optimised using the same reaction conditions previously stated (section 3.3.1). A [Mg^{2+}] range of 2–20 mM was used in the incubation of **229** with EZS (30 nM) for 10 minutes at 30 °C. The plot of rate vs. [Mg^{2+}] showed an increase in reaction rate to a maximum at 15 mM with an increase in [Mg^{2+}] concentration to 20 and 25 mM resulted in a diminished reaction rate. A [Mg^{2+}] of 15 mM was therefore chosen as the optimal [Mg^{2+}] concentration as it yielded the fastest rate (Figure 78).

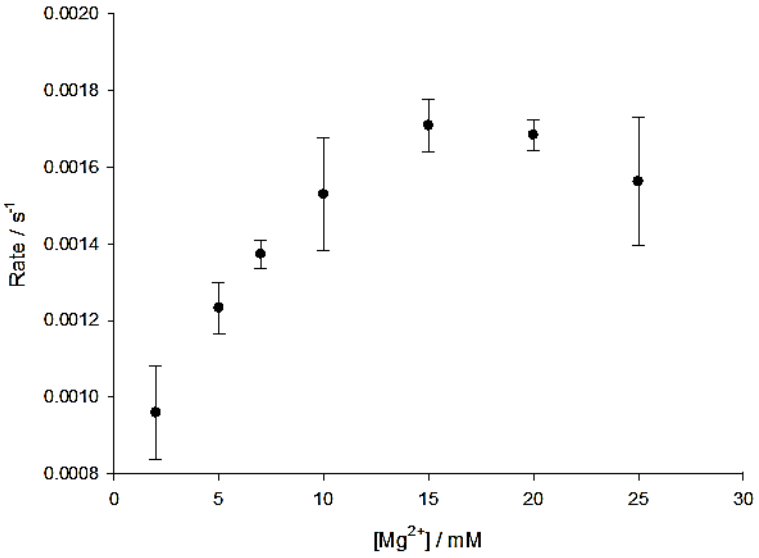

Figure 78. Plot of reaction rate for EZS catalysed production of radiolabelled products from (2*Z*,6*Z*)-[1-^{3}H]-FDP (229) against various [Mg^{2+}]. Reaction conditions: 30 nM [EZS], buffer (25 mM HEPES, 10 mM $MgCl_2$, 5 mM DTT, pH 7.2), 10 minutes, 30 °C.

In order to determine the optimal reaction time, incubations of EZS (30 nM) and (2*Z*,6*Z*)-[1-^{3}H]-farnesyl diphosphate (**229**) in catalysis buffer (25 mM HEPES, 15 mM $MgCl_2$, 5 mM DTT, pH 7.2) at 30 °C for variable time lengths. A time range from 5–20 minutes was examined with the results showing a linear positive correlation between rate and time. A reaction time of 10 minutes was chosen as the ideal reaction length as sufficient counts were detected for analysis after this time (Figure 79).

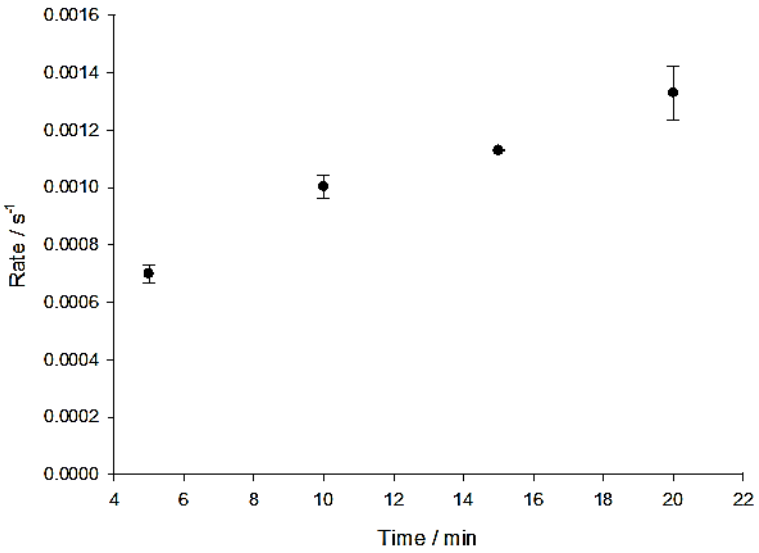

Figure 79. Plot of reaction rate for EZS catalysed production of radiolabelled products from (2*Z*,6*Z*)-[1-^{3}H]-FDP (229) against various end-point times for the stopped assay. Reaction conditions: 30 nM [EZS], buffer (25 mM HEPES, 15 mM $MgCl_2$, 5 mM DTT, pH 7.2), 30 °C.

For the determination of the optimal reaction pH, EZS (30 nM) was incubated of with (2*Z*,6*Z*)-[1-^{3}H]-farnesyl diphosphate (**229**) in catalysis buffer (25 mM HEPES, 15 mM $MgCl_2$, 5 mM DTT) for 10 minutes at 30 °C, over a pH range of 5-10.5.

Optimisation of pH was approached using different buffers to span a pH range. The range pH 6–10 was investigated using three buffers; MES (2–(N-morpholino)ethanesulfonic acid) for pH 6–6.5, HEPES for pH 7–8.5 and CHES (N-cyclohexyl-2-aminoethanesulfonic acid) for pH 9–10 (Figure 80).

To assess whether these different buffers affected the reaction outcome, a second experiment using MTEN buffer (50 mM MES, 25 mM TRIS Base, 25 mM ethanolamine, 100 mM NaCl) was performed. This allowed incubation across a pH range of 5 – 9 to be analysed with no change in buffer (Figure 80).

The third investigation was over a larger pH range 5– 10.5 using MES (pH 5-6.5), HEPES (pH 7-8.5) and AMP (2-amino-2-methyl-1-propanol, pH 10.5) (Figure 81)

Figures 8 and 9 show that changes in buffer did not alter the overall outcome. pH 8.0 was chosen as optimal for carrying out future incubations as the curve reaches a maximum at pH 8.5 either side of which the rate of EZS decreases.

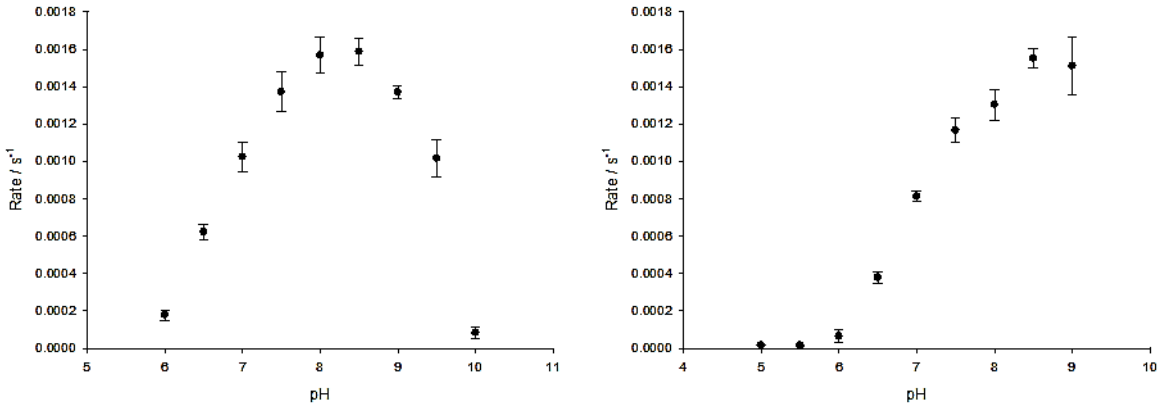

Figure 80. Plot of reaction rate for EZS catalysed production of radiolabelled products from (2*Z*,6*Z*)-[1-^{3}H]-FDP (229) against various pH; pH 6-10 (left) and pH 5-9 (right). Reaction conditions: 30 nM [EZS], buffer (25 mM HEPES, 15 mM $MgCl_2$, 5 mM DTT) for 10 minutes at 30 °C.

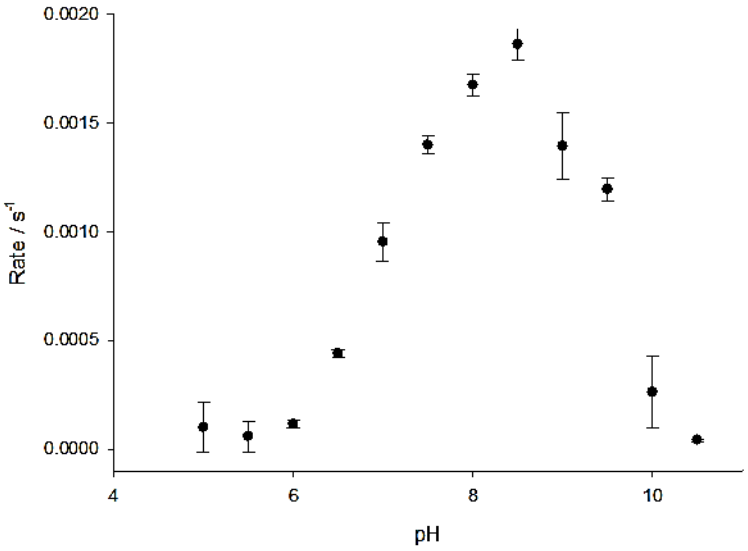

Figure 81. Plot of reaction rate for EZS catalysed production of radiolabelled products from (2*Z*,6*Z*)-[1-^{3}H]-FDP (229) against various pH. Reaction conditions: 30 nM [EZS], buffer (25 mM HEPES, 15 mM $MgCl_2$, 5 mM DTT) for 10 minutes at 30 °C.

3.3.2 Steady state kinetic parameters of EZS catalysed reaction

Measurement of the steady state kinetic parameters proceeded using the optimised conditions; [EZS] = 30 nM in catalysis buffer (25 mM HEPES, 15 mM $MgCl_2$, 5 mM DTT, pH 8) for 10 minutes at 30 °C. A K_M value of 7.12 ± 2.86 µM and a k_{cat} of 0.29 ± 0.10 s^{-1} were reported by Bleeker *et al.* Measurements were therefore carried out varying the concentration of (2*Z*, 6*Z*)-[1-^{3}H]-FDP (**229**) from 0.2 to 70 µM. Values of 6.23 ± 0.6 µM and 0.047 ± 0.001 s^{-1} were found for K_M and k_{cat} respectively (Figure 82). A change in methodology from GC-MS (used by Bleeker *et. al.*[3]) to radiolabelled assays (utilised in this investigation), have been reported to give different values for steady state kinetic parameters. Though comparable values using both methods have been reported for bacterial terpene cyclases,[233,234] kinetic assays utilising radiolabelled FDP are preferable. This is because radiolabelled assays are able to detect product at much lower substrate concentrations and a larger range of data can be obtained, GC-MS can be insensitive to the levels of product formed at sub-K_M concentrations for terpene cyclase catalysed reactions.

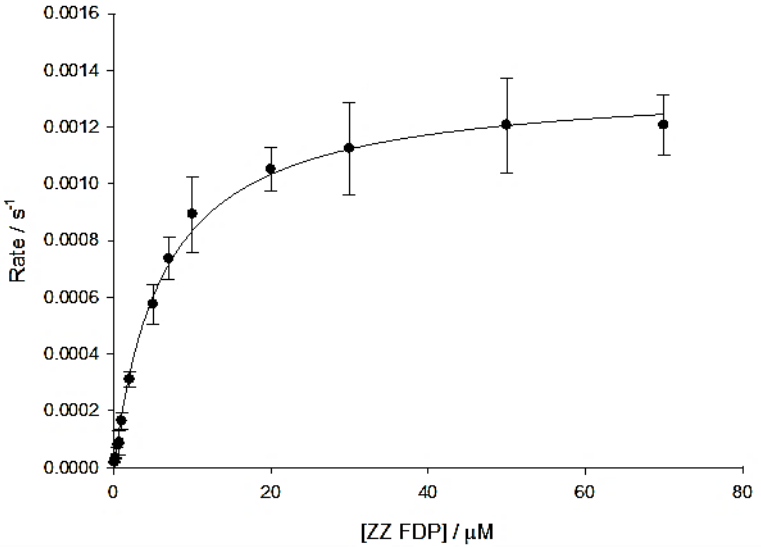

Figure 82. A representative graph for the calculation of steady state kinetic parameters of EZS.

Comparisons of the steady state kinetic parameters of EZS with other sesquiterpene cyclases shows that the K_M and k_{cat} values determined in this work are fairly typical of this group of enzyme catalysed reactions. The K_M of (2*Z*,6*Z*) FDP (**38**) with EZS when compared to (2*E*,6*E*) FDP (**31**) with other sesquiterpene cyclases is the same order of magnitude (with the exception of aristolochene synthase). It can also be noted that EZS appears to have a lower affinity towards (2*Z*,6*Z*) FDP (**38**) than other sesquiterpene cyclases to (2*E*,6*E*) FDP (**31**). The K_M of (2*Z*,6*Z*) FDP (**38**) with EZS is double that of the other cyclases with the exception of γ-humulene synthase (Table 5). The k_{cat} value however, is very similar to that of aristolochene synthase and germacrene A synthase, showing a comparably high substrate turnover. With the exception of aristolochene synthase, the catalytic efficiency of EZS appears to be similar to that of other terpene cyclases.

Table 6. Comparison of steady state kinetic measurements for the turnover of [1-^{3}H]-substrates with terpene cyclases.

Terpene cyclase	Substrate	k_{cat} / s^{-1}	K_M / µM	k_{cat}/K_M / s^{-1} µM (x10^{-3})
EZS(WT)	**38**	0.047 ± 0.001	6.2 ± 0.6	7.6 ± 0.8
δ-Cadinene Synthase	**31**	0.01 ± 0.001	3.2 ± 0.5	3.1 ± 0.6
PR-Aristolochene Synthase	**31**	0.043 ± 0.002	0.6 ± 0.1	71.6 ± 12.4
Amorphadiene Synthase	**31**	0.01603 ± 0.0006	2.25 ± 0.3	7.1 ± 1.0
Germacrene A synthase	**31**	0.043 ± 0.02	3.4 ± 0.3	12.6 ± 6.0
R-Germacrene D synthase	**31**	0.02	3.0 ± 0.3	6.7 ± 0.3
S-Germacrene D synthase	**31**	0.03	2.9 ± 0.3	10.3 ± 0.3
γ-humulene synthase	**31**	0.024	4.7	5.1

The synthesis of (2*Z*,6*Z*)–[1-^{3}H]–farnesyl diphosphate (**229**) allowed for the characterisation and comparison of EZS(WT) with other sesquiterpene cyclases. The steady state kinetics parameters were found to be comparable to the values published by Bleeker *et al.*[3] However, the use of a radiolabelled substrate in place of a GC-MS methodology gave a significant decrease in k_{cat}.

3.3.3 Steady state kinetic parameters of EZS(E648A) catalysed reaction

Incubation of (2*Z*, 6*Z*) FDP (**38**) with the four metal binding motif mutants; EZS(D495A), EZS(E499A), EZS(N640A) and EZS(E648A) and analysis of the pentane extractable products *via* GC-MS showed only mutant EZS(E648A) was active (section 2.7.1). Steady state kinetics of EZS(E648A) catalysed turnover of (2*Z*,6*Z*)–[1-^{3}H]–farnesyl diphosphate (**229**) were performed using under the same reaction conditions as for the wild type enzyme (section 3.3.2) and fitted to a Michaelis-Menten curve (Figure 83).

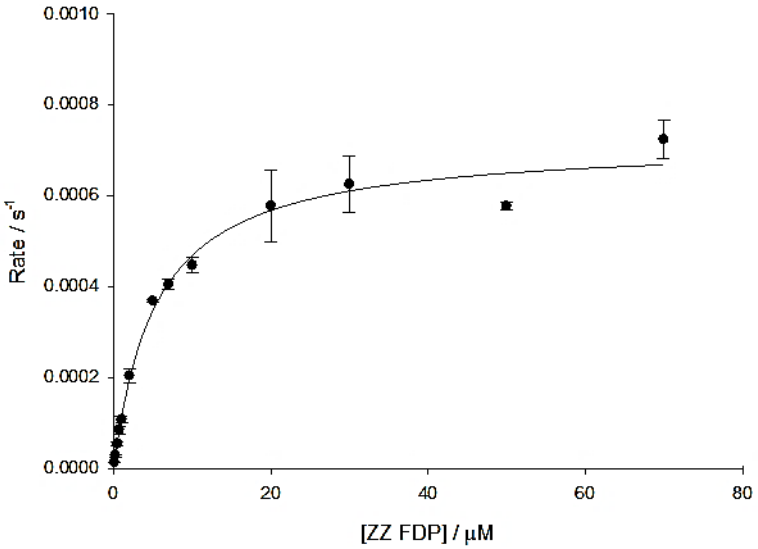

Figure 83. A representative graph for the calculation of steady state kinetic parameters of EZS(E648A).

The K_M and k_{cat} were found to be 5.32 ± 0.5 µM and 0.023 ± 0.001 s^{-1} respectively with a k_{cat}/K_M = 4.3 x10^{-3} ± 0.0004 s^{-1} µM. These values indicated a higher binding affinity and slower substrate turnover resulting in a lower catalytic efficiency when compared to the wild type parameters determined earlier (K_M = 6.2 ± 0.6 µM, k_{cat} = 0.047 ± 0.001 s^{-1}, k_{cat}/K_M = 7.6 x10^{-3} ± 0.0008 s^{-1} µM). In contrast to the asparagine residue, the glutamate residue of the NSE motif appeared to not be crucial for catalysis. The mutation glutamate to alanine (EZS(E648A)) was directly responsible for the decrease in enzymatic efficiency when compared to the wild type. However, the mutant was still capable of

catalysis. This result gives evidence that the single point mutation of glutamate residue E648 to alanine increased the substrate binding of EZS despite the NSE motif being responsible for the coordination of a magnesium ion for diphosphate binding.

3.3.4 Steady state kinetic parameters of EZS(Y483A) catalysed reaction

EZS aromatic active site mutants EZS(F598A), EZS(F705A), EZS(Y483A) and EZS(Y716A) were incubated with (2*Z*, 6*Z*) FDP (**38**) and the pentane extractable products analysed *via* GC-MS showing only mutant EZS(Y483A) was active (section 2.7.2). Steady state kinetics of EZS(Y483A) catalysed turnover of (2*Z*,6*Z*)–[1-^{3}H]–farnesyl diphosphate (**229**) were performed using under the same reaction conditions as for the wild type enzyme (section 3.3.2) and fitted to a Michaelis-Menten curve (Figure 84).

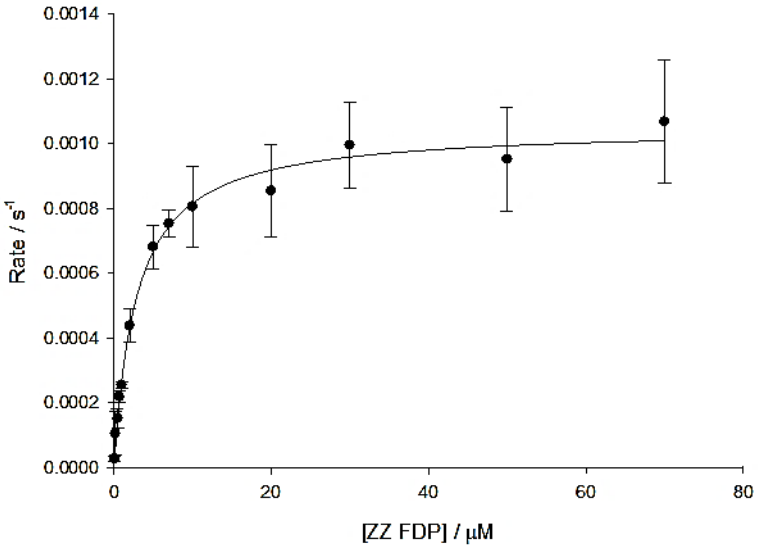

Figure 84. A representative graph for the calculation of steady state kinetic parameters of EZS(Y483A).

The K_M and k_{cat} were found to be 2.87 ± 0.4 μM and 0.037 ± 0.001 s^{-1} respectively with a k_{cat}/K_M = 12.9 x10^{-3} ± 0.0018 μM. As observed with EZS(E648A), the mutation resulted in a higher binding affinity and slower substrate turnover to that of EZS(WT). The Y483A single point mutation resulted in the highest binding affinity whilst not decreasing substrate turnover to the extent of the E648A mutation. The EZS(Y483A) mutant therefore exhibited largest catalytic efficiency of the three enzymes tested (Table 7).

Table 7. Comparison of steady state kinetic measurements for the turnover of (2*Z*,6*Z*)-[1-^{3}H]-FDP (229) EZS(WT), EZS(E648A) and EZS(Y483A).

EZS(XX)	k_{cat} / s^{-1}	K_M / µM	k_{cat}/K_M / s^{-1} µM (x10^{-3})
WT	0.047 ± 0.001	6.2 ± 0.6	7.6 ± 0.8
E648A	0.023 ± 0.001	5.3 ± 0.5	4.3 ± 0.4
Y483A	0.037 ± 0.001	2.9 ± 0.4	12.9 ± 1.8

Interestingly, the Y483A mutation appeared to have a greater effect on binding affinity than the E648A single amino acid substitution. These values indicated that the tyrosine (Y) residue within the active site has a greater influence on substrate binding than the glutamate (E) of the NS**E** metal binding motif. In concurrence with an increased affinity for the substrate, the mutation of the tyrosine (Y) residue to alanine (A) resulted in an increase in substrate turnover compared to the EZS(E648A) mutant. The increase in k_{cat} indicates that the glutamate residue may aid product release from the active site. The product release is the rate limiting step due to an organic hydrocarbon product being released into an aqueous buffer.

The E648A mutation lowered the catalytic efficiency of the enzyme in comparison to the wild type. However, other single point mutations of the metal binding motifs; D495A, E499A and N640A gave no enzymatic product when the respective mutant was incubated with (2*Z*,6*Z*) FDP (**38**). These results show that although the E648 residue influences catalytic efficiency, it is not crucial for activity.

3.5 Summary

During the synthesis of **229** the stereochemical integrity of the C2,C3 double bond of (2*Z*, 6*Z*) farnesal (**217**) proved problematic due to acid or base catalysed isomerisation of the product α,β unsaturated aldehyde. Numerous attempts at replicating oxidations published for (2*E*,6*E*) farnesol (**353**) did not yield a single product and were often time consuming with low yield. A TEMPO catalysed reaction was found to be an ideal alternative to previous protocols. The short reaction time and simple isolation from the reaction mixture allowed the reaction product to be used without more extensive purification.

Optimisation of incubation conditions revealed ideal conditions for EZS productivity to be: [EZS] = 30 nM, $[Mg^{2+}]$ = 15 mM, and pH 8.0. The relationship of time and reaction rate was found to be linear within a range of 5-20 min; therefore an incubation time of 10 min was chosen to ensure sufficient product formation within a reasonable productive timeframe. Kinetic parameters determined from steady state kinetic assays show comparable catalytic efficiency to that of previously characterised sesquiterpene cyclases.

Two EZS mutants; EZS(E648A) and EZS(Y483A) were active and characterised. The values determined from steady state kinetics showed a greater binding affinity and slower substrate turnover when compared to the wild type. Mutation of selected metal binding residue motif showed that the glutamate residue of NS**E** was not critical for enzyme activity. However, its mutation resulted in a loss of catalytic efficiency. Analysis of the data from the steady state kinetic experiments showed decreased substrate turnover and an increased binding affinity when compared with the wild type. EZS(Y483A) was found to have an effect on substrate binding affinity with the K_M of **38** with EZS(Y483A) lower and the catalytic efficiency increased when compared to the wild type.

Chapter 4 –Examination of the catalytic mechanism of 7-Epizingiberine Synthase

4.1 Preface

This chapter outlines the synthesis of numerous analogues used as probes to investigate the catalytic mechanism of 7-epizingiberene synthase (Figure 85). Analogues synthesised include fluorinated analogues **230** and **231** to examine cation stability and deuterated analogues **232**, **233** and **234** to examine the stereo- and regiospecificity of hydride shift rearrangements of intermediate carbocations.

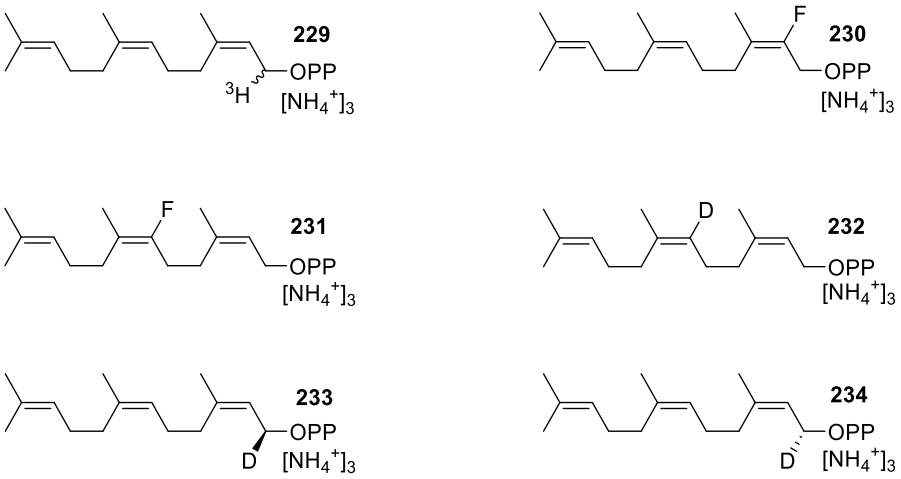

Figure 85. (2*Z*,6*Z*) FDP analogues discussed within this chapter.

Kinetic assays were performed in triplicate and non-linear regression was used to generate K_M and k_{cat} parameters to fit Michaelis-Menten curves to experimental data. Analogues that did not yield enzymatic products were tested as inhibitors and non-linear regression was similarly used to generate parameters to fit Michaelis-Menten curves to experimental data to establish K_M, $K_{M(app)}$ and K_i values. Lineweaver-Burk plots were used to infer the mode of inhibition.

All incubations were performed in tandem with an incubation containing substrate and incubation buffer, but no enzyme. This was used to identify which products arose *via* enzymatic involvement and not as a result of Mg^{2+} induced cleavage or other side products of substrate degradation. The GC-MS method remained constant; an injection temperature of 100 °C was followed by a temperature gradient of 80 °C (1 min hold) to 180 °C (4 °C increase min^{-1}, 2 min hold).

4.2 Fluorinated Substrate analogues

4.2.1 Synthesis of (2*E*,6*Z*)-2-fluorofarnesyl diphosphate (230)

Fluorine-containing substrates are valuable tools for investigating the catalytic mechanisms of sesquiterpene synthases.[106,109] The atomic radii of fluorine (41 pm) and hydrogen (53 pm)[235] are approximate to one another, minimising unfavourable steric interactions in the active site. However, fluorine causes significant perturbations in the electronic structure of the substrate-enzyme complex and particularly affects the stability of carbocation intermediates. Fluorine can stabilise geminal carbocation formation (**236**) *via* the alpha effect, but its electronegative nature will raise the energy of the carbocation in the alpha position (**237**) and inhibit its formation (Figure 86). If positioned on an alkene, the presence of the fluorine significantly reduces the π-bond electron density and therefore the nucleophilicity and basicity of the bond in turn.

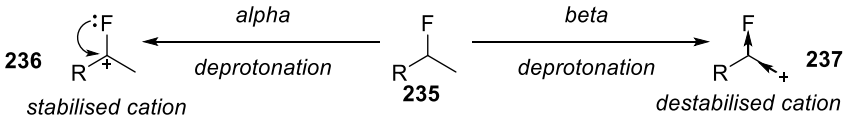

Figure 86. Effect of fluorine on carbocation stability.

The catalytic mechanism of EZS is currently not known. It is possible that the mechanism could proceed either *via* a concerted or by stepwise ring closure. Incorporation of fluorine at the C2 position of **38** would inhibit a stepwise mechanism by increasing the energy of the farnesyl cation (**141**) *via* electron withdrawal. Contrastingly; a concerted mechanism would cyclise **38** to give carbocation (**239**) and possibly result in a fluorinated product (**240**) (Figure 87).

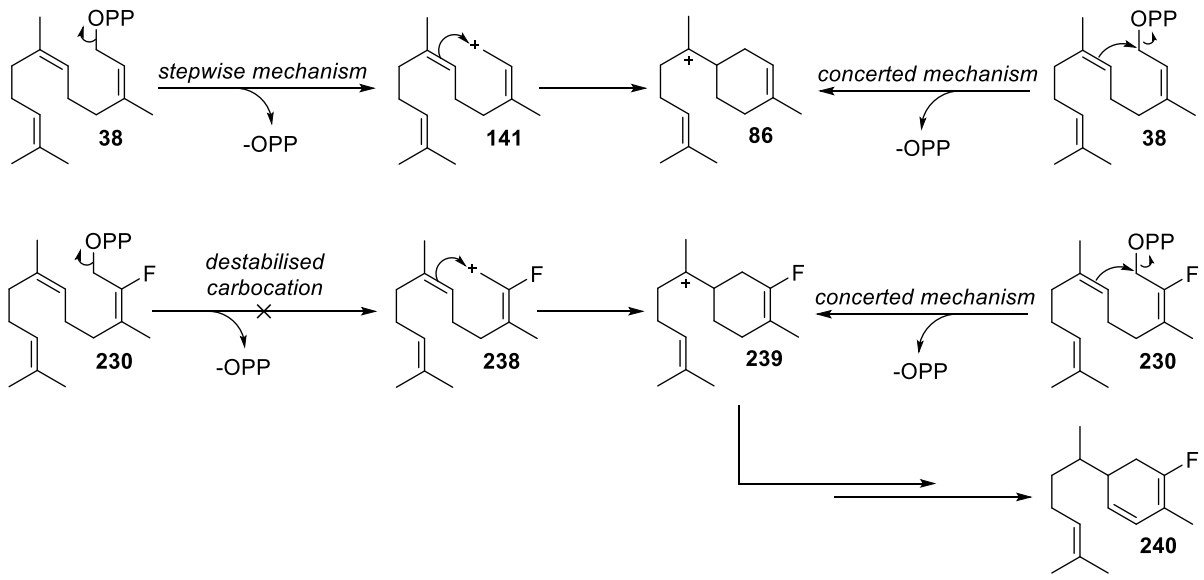

Figure 87. Possible stepwise and concerted mechanisms that may be catalysed by EZS and the expected effect of 2-fluoro substitution on formation of 7-epizingiberine.

The synthesis of **230** was achieved by chain extension of nerol (**163**) to yield neryl acetone (**166**). The commercially available Horner-Wadsworth-Emmons reagent triethyl-2-fluoro-2-phosphonoacetate (**241**) was employed to incorporate fluorine at the C2 position (Figure 88).

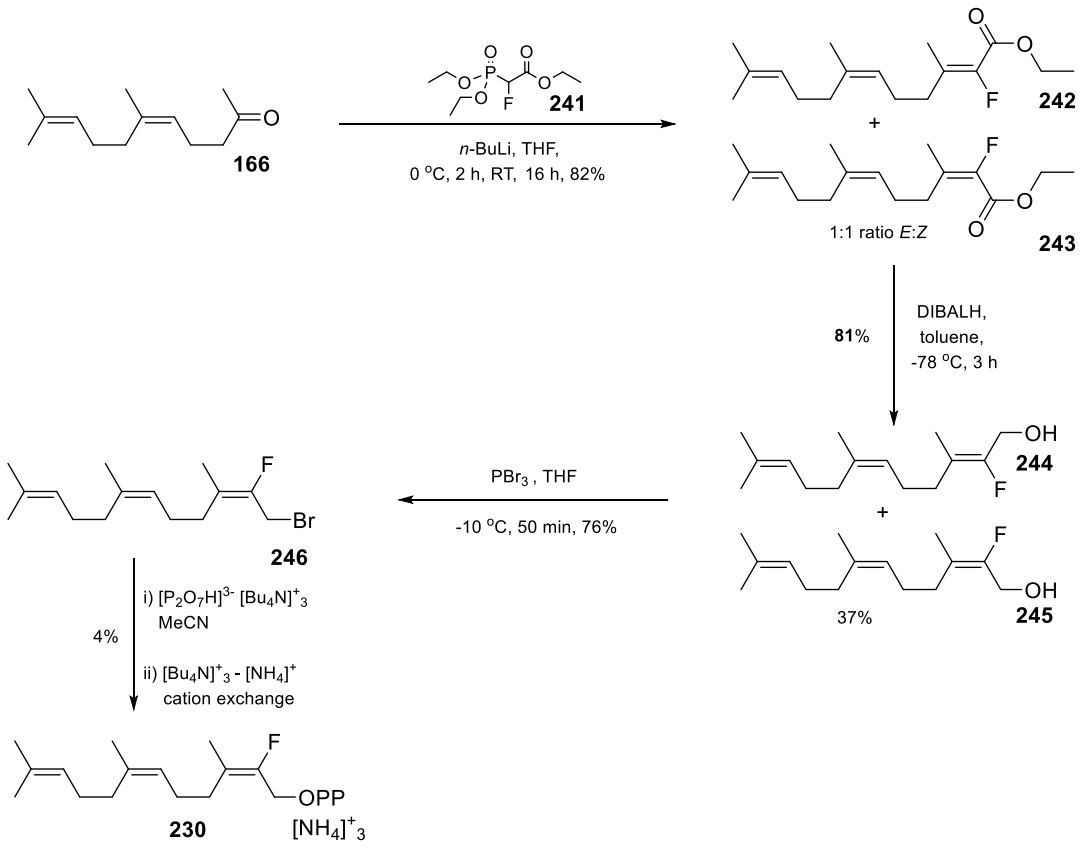

Figure 88. Synthesis of (2*E*,6*Z*)-2-fluorofarnesyl diphosphate (230).

Olefination of **166** using **241** resulted in a tetra-substituted double bond with no stereocontrol. A 1:1 ratio of *E*:*Z* isomers was obtained with the various conditions previously investigated (Table 4, 2.2.5). Reduction to alcohols **244** and **245** was followed by silica gel chromatography to isolate **245** for bromination and conversion to a diphosphate as previously described. The presence of fluorine necessitated increasing the bromination reaction time from 15 to 50 minutes. Even this extended reaction time was insufficient to consume all the starting material, but the appearance of multiple side products *via* thin layer chromatography (TLC) coincided with a decrease in overall yield when further increasing the reaction time. After work up, bromide **246** was the sole product observed by ^{1}H and Heteronuclear Single Quantum Coherence (HSQC) NMR spectroscopy.

4.2.2 Incubation of (2*E*,6*Z*)-2-fluorofarnesyl diphosphate (230) and EZS

Formation of an enzymatic product from an incubation of **230** and EZS would suggest a concerted ring closure to form the bisabolyl cation (**86**) (Figure 87). However, GC-MS analysis of the pentane extractable products of **230** and EZS incubation showed no enzymatic products were formed from the incubation, even after extended time, suggesting a stepwise mechanism inhibited by the presence of fluorine inhibiting the formation of the farnesyl cation (**141**). Competitive assays with (2*Z*,6*Z*)-[1-^{3}H]-farnesyl diphosphate (**229**) and varying concentrations of **230** were performed to establish substrate binding and mode of inhibition.

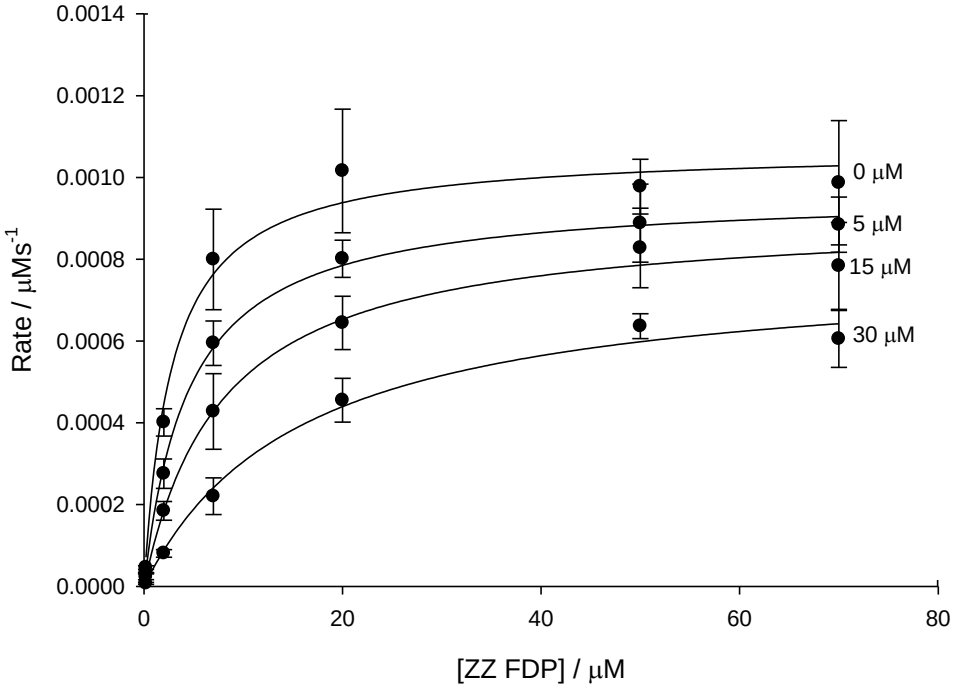

Figure 89. Michaelis-Menten plots for incubations of (2*Z*,6*Z*)-[1-^{3}H]-FDP (229) with EZS and inhibitor (2*E*,6*Z*)-2-fluorofarnesyl diphosphate (230); 0 μM, 5 μM, 15 μM and 30 μM.

Michaelis-Menten (Figure 89) and Lineweaver-Burk (Figure 90) plots show data trends characteristic of a competitive inhibitor. The data plots of the Lineweaver-Burk plot (Figure 90) for a competitive inhibitor intercept the same point of the y-axis. In this example, the linear plots intercept each other at a value < x = 0 and might not be considered as a competitive inhibitor. However, data points on a Lineweaver Burk plot visualising uncompetitive inhibitors do not intercept each other whilst the data points concerning non-competitive inhibition intercept at the x-axis. Consequently, (2*E*,6*Z*)-2-fluorofarnesyl diphosphate (**230**) is characterised as a competitive inhibitor with the discrepancy of the intercept attributed to experimental error. The K_i calculated from the $K_{M(app)}$ vs. [**230**] plot (Figure 90) was 5.37 ± 1.19 μM. This concentration is comparable to the K_M of (2*Z*,6*Z*) FDP (**38**) at 6.2 ± 0.6 μM (Figure 82, chapter 3), showing fluorine had minimal effects on binding and caused an increase in the energy of the fluorofarnesyl cation (**238**) resulting in EZS inhibition.

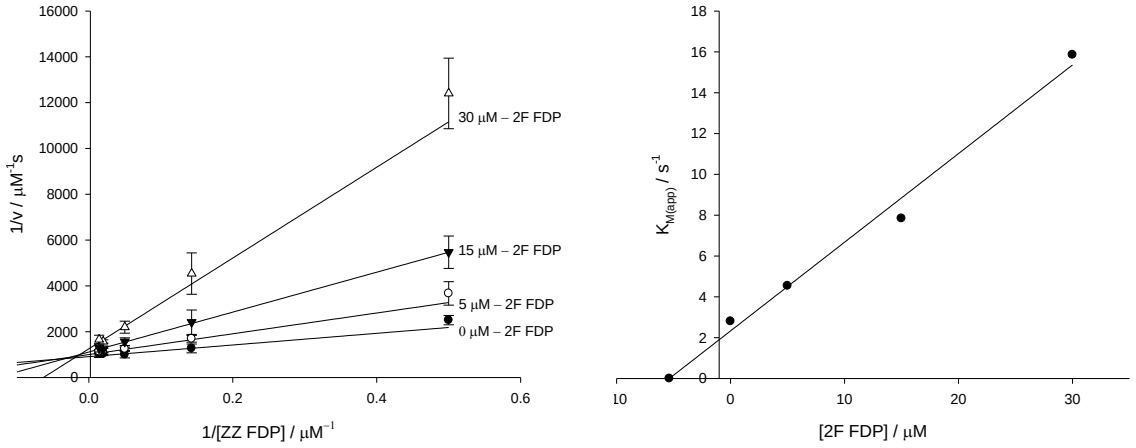

Figure 90. Lineweaver-Burk Plot (left) and $K_{M(app)}$ vs. concentration plot (right) for 230.

A stepwise [1,6] ring closure to produce the bisabolyl cation (**86**) (Figure 91) then requires carbocation rearrangements *via* various plausible hydride shifts, or combinations thereof, before deprotonation to yield 7-epizingiberene.

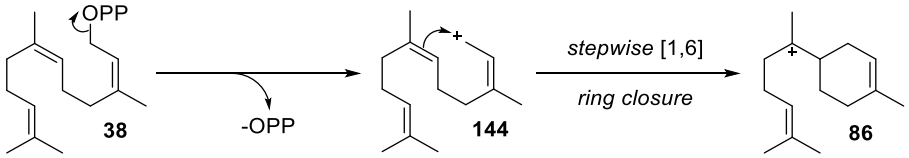

Figure 91. 230 inhibition of EZS implies formation of bisabolyl cation (86) *via* a stepwise, rather than concerted reaction.

4.2.3 Synthesis of (2*Z*,6*E*)-6-fluorofarnesyl diphosphate (231)

Incubation of (2*E*,6*E*)-10-fluorofarnesyl diphosphate (**110**) with germacrene A synthase resulted in an unusual 1,11-macrocylisation and the formation of a fluorinated hydrocarbon (Figure 20, section 1.4.2). Similarly, incubation of **231** with EZS should prohibit the formation of cation **248** and inhibit the enzyme (Figure 92). However, an anti-Markovnikov 1,7-macrocyclisation to yield a fluorinated hydrocarbon (**250**) might be possible (Figure 93).

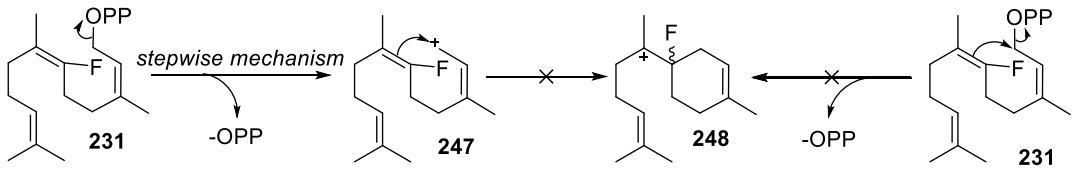

Figure 92. 231 inhibition of EZS by destabilisation of an on-path carbocation.

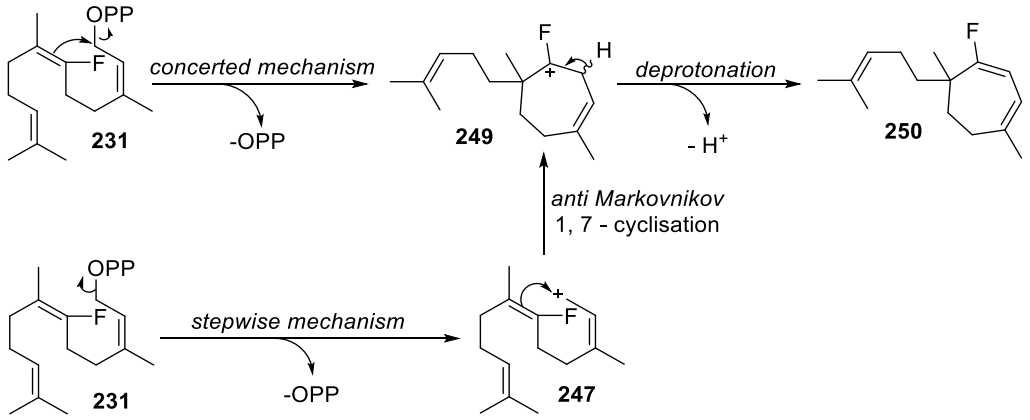

Figure 93. Potential outcome of a 1,7-cyclisation.

(2*Z*,6*E*)–6-fluorofarnesyl diphosphate (**231**) was prepared through an extended version of the synthesis of previous analogues (Figure 94). Fluorine was installed at the C6 position *via* a Horner-Wadsworth-Emmons reaction using commercially available 6-methylheptan-2-one (**251**) and **241**.

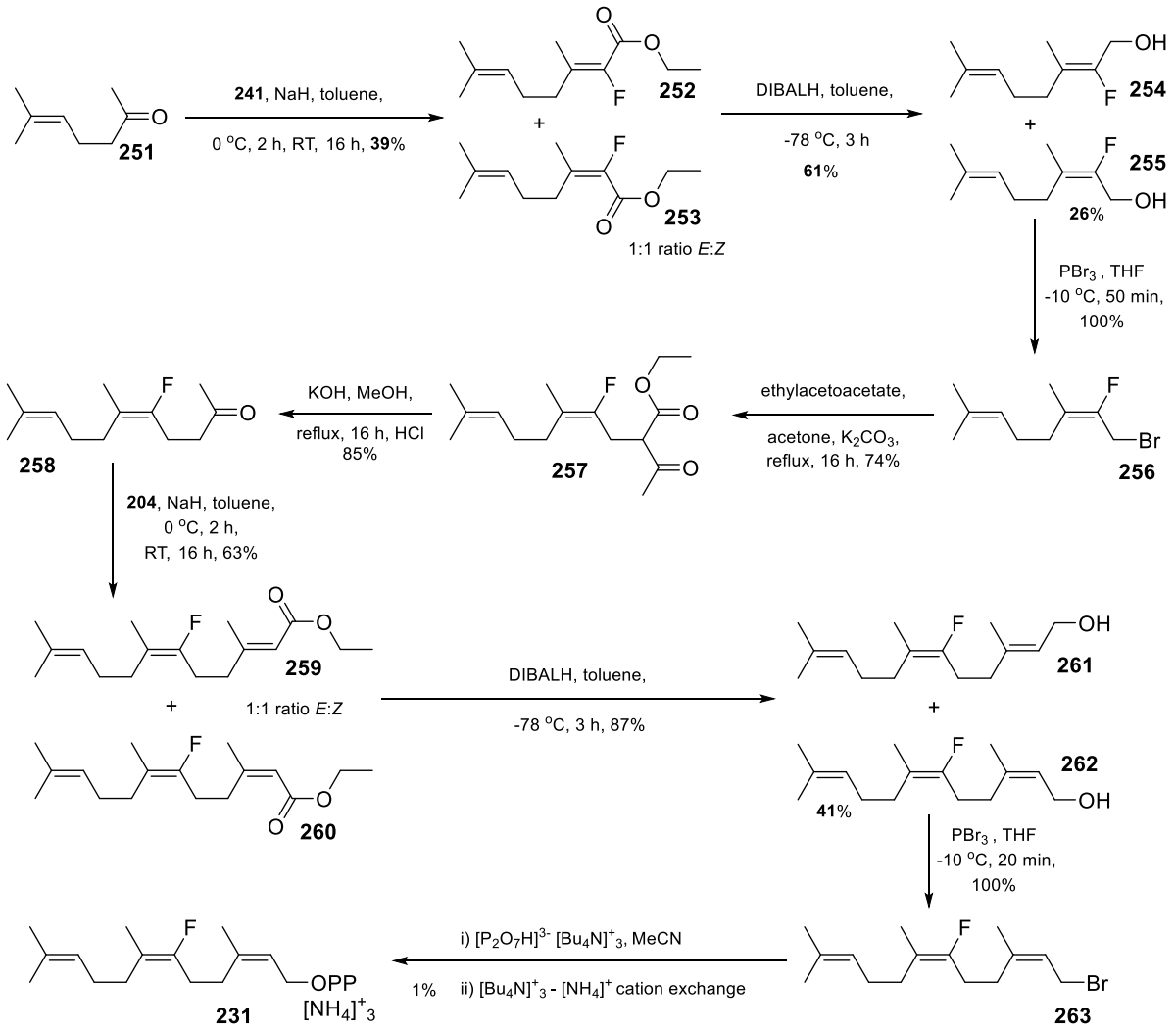

Figure 94. Synthesis of (2*Z*,6*E*)–6-fluorofarnesyl diphosphate (231).

The initial Horner-Wadsworth-Emmons reaction and subsequent bromination of fluorinated nerol (**255**) gave comparable yields of product to the analogous synthesis of **230** (Figure 88). Carefully maintaining the temperature of the bromination reaction at -10 °C limited the formation of side products. The presence of fluorine did not affect the reactivity of the substrate throughout the remainder of the synthesis**,** with the *Z*-C2,C3 double bond installed by previously optimised conditions (Table 4, 2.2.5)

4.2.4 Incubation of (2*Z*,6*E*)-6-fluorofarnesyl diphosphate (231) and EZS

Analysis of pentane extractable products from the incubation of (2*Z*,6*E*)-6-fluorofarnesyl diphosphate (**231**) and EZS by GC-MS analysis showed no enzymatic products suggesting that the presence of fluorine inhibits the formation of the bisabolyl cation. Competitive kinetics experiments were again used to establish if FDP analogue **231** was binding within the active site and the mode of inhibition.

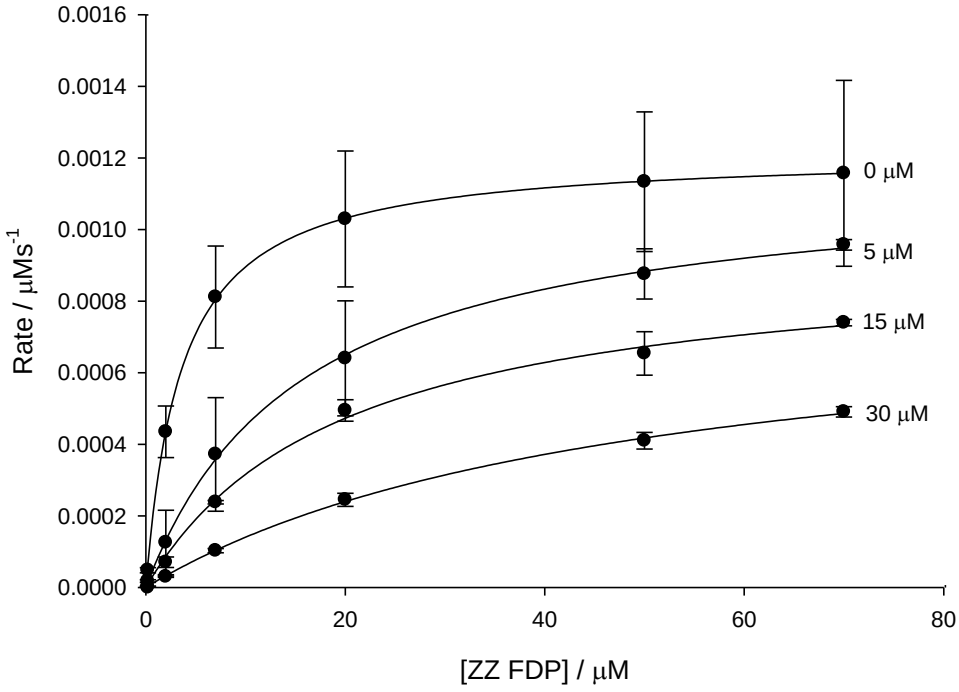

Figure 95. Michaelis-Menten plots for incubations of (2*Z*,6*Z*)-[1-^{3}H]-FDP with EZS and inhibitor (2*Z*,6*E*)-6-fluorofarnesyl diphosphate (231); 0 μM, 5 μM, 15 μM and 30 μM.

Analysis of the data using Michaelis-Menten (Figure 95) and Lineweaver-Burk (Figure 96) plots show (2*Z*,6*E*)-2-fluorofarnesyl diphosphate (**230**) acts as a competitive inhibitor for EZS with linear plots of inhibition data intercepting the y-axis at the same point. The K_i of **231** was found by plotting $K_{M(app)}$ against [**231**] to be 3.04 ± 0.39 μM (Figure 96) showing an affinity of similar magnitude to EZS as (2*Z*,6*Z*)-FDP (**38**)(Figure 82).

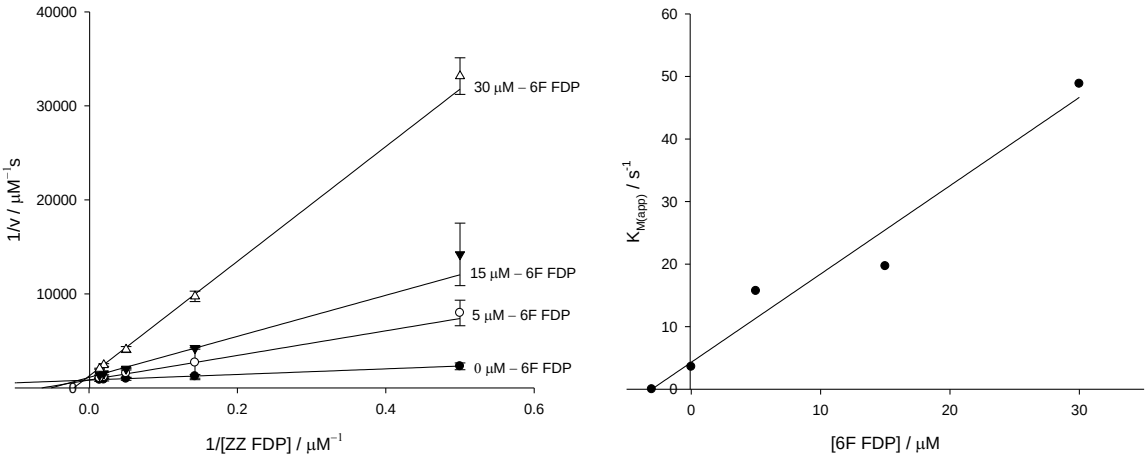

Figure 96. Lineweaver-Burk Plot (left) and $K_{M(app)}$ vs. concentration plot (right) for inhibition of EZS by 231.

4.3 Deuterated Analogues

4.3.1 Synthesis of (2*Z*,6*Z*)-[6-^{2}H]-farnesyl diphosphate (232)

Numerous hydride shifts are possible *en route* from the bisabolyl cation (**86**) to 7-epizingiberene. Heavy isotopes have been used on many occasions to track hydride movements *via* mass spectrometry and ^{1}H NMR analysis.[115,116,236] The incubation of (2*Z*,6*Z*)-[6-^{2}H]-farnesyl diphosphate (**232**) with EZS and analysis of enzymatic products would give insight into which hydride shifts occur. Hydride shifts in the catalytic mechanism of EZS could occur from the C1, C5 and C6 positions to stabilise the bisabolyl cation. Two [1,3] hydride shifts from C1 or C5 to C7 would quench the charge at the tertiary centre. Contrastingly, two consecutive [1,2] hydride shifts initially from the C6 to C7 position followed by a second [1,2] hydride shift from either the C1 or C5 positions to the carbocation at the C6 position. The residing charges are then quenched *via* deprotonation. The incubation of (2*Z*,6*Z*)-[6-^{2}H]-farnesyl diphosphate (**232**) with EZS would yield one of two deuterated products; **266** or **270** (Figure 97) depending on which combination of hydride shifts occur during the catalytic mechanism. Determination of the correct hydride shifts could then be elucidated *via* analysis using GC-MS or ^{1}H NMR spectroscopy.

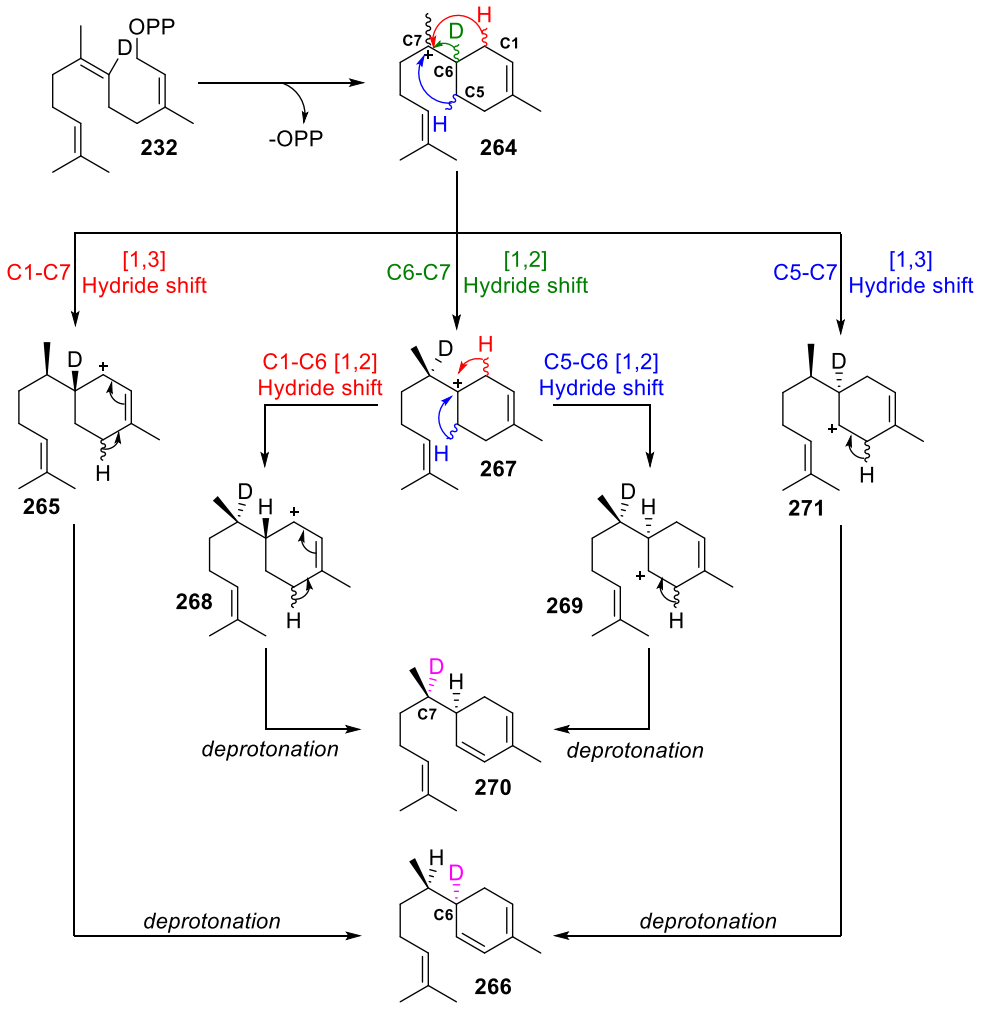

Figure 97. Two enzymatic products 235 and 239 that could occur from the incubation of 233 with EZS involving hydride shifts from the C1, C5 or C6 positions.

Incorporation of deuterium at the C6 position was pursued in two ways (Figure 99). The first technique employed an Anastasia reaction[199] which was quenched with deuterated sulfuric acid and deuterium oxide according to a procedure published by Faraldos *et al.*[200] The reaction gave 100% deuterium incorporation. However, the reagents were costly, limiting the scales of subsequent reactions resulting in inadequate quantities of material later in the synthesis (Figure 39, 2.2.4). Therefore a second, scalable approach with cheaper reagents was sought to allow for a higher throughput of material.

A second approach involved using a deuterated Still-Gennari/Horner-Wadsworth-Emmons reagent to incorporate the isotopic label. Deuteration of the reagent was attempted *via* a protocol outlined by Christianson *et al.*[237] Reagent **204** and potassium carbonate were stirred for 48 hours in deuterium oxide and deuterated product extracted with ethyl acetate. However, even after repeating this procedure three times on the same material, only 80% isotopic labelling was achieved.

However, refluxing a mixture of **204** and potassium carbonate in deuterium oxide then extracting the reaction mixture with dichloromethane yielded 100% isotopically labelled reagent **204** (Figure 98). ^{1}H and ^{2}H NMR spectroscopy was used to confirm labelling. The methylene of the starting material (P(C*H*$_2$)C=O) was no longer visible of the ^{1}H NMR spectrum whilst a doublet at. δ 2.90 was visible of the ^{2}H NMR spectrum showing incorporation.

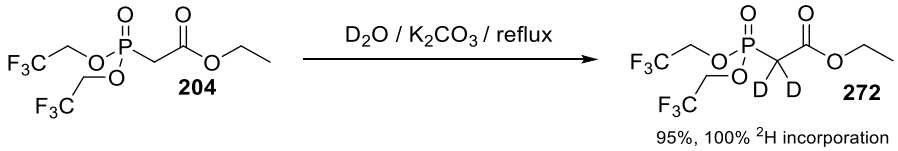

Figure 98. Isotopic labelling of 204.

Ketone **251** which was used in both Anastasia and Horner-Wadsworth-Emmons olefination reactions, with the synthesis proceeding *via* steps described previously for other (2*Z*,6*Z*) FDP (**38**) analogues with modifications at the C6 position **231** (Figure 94).

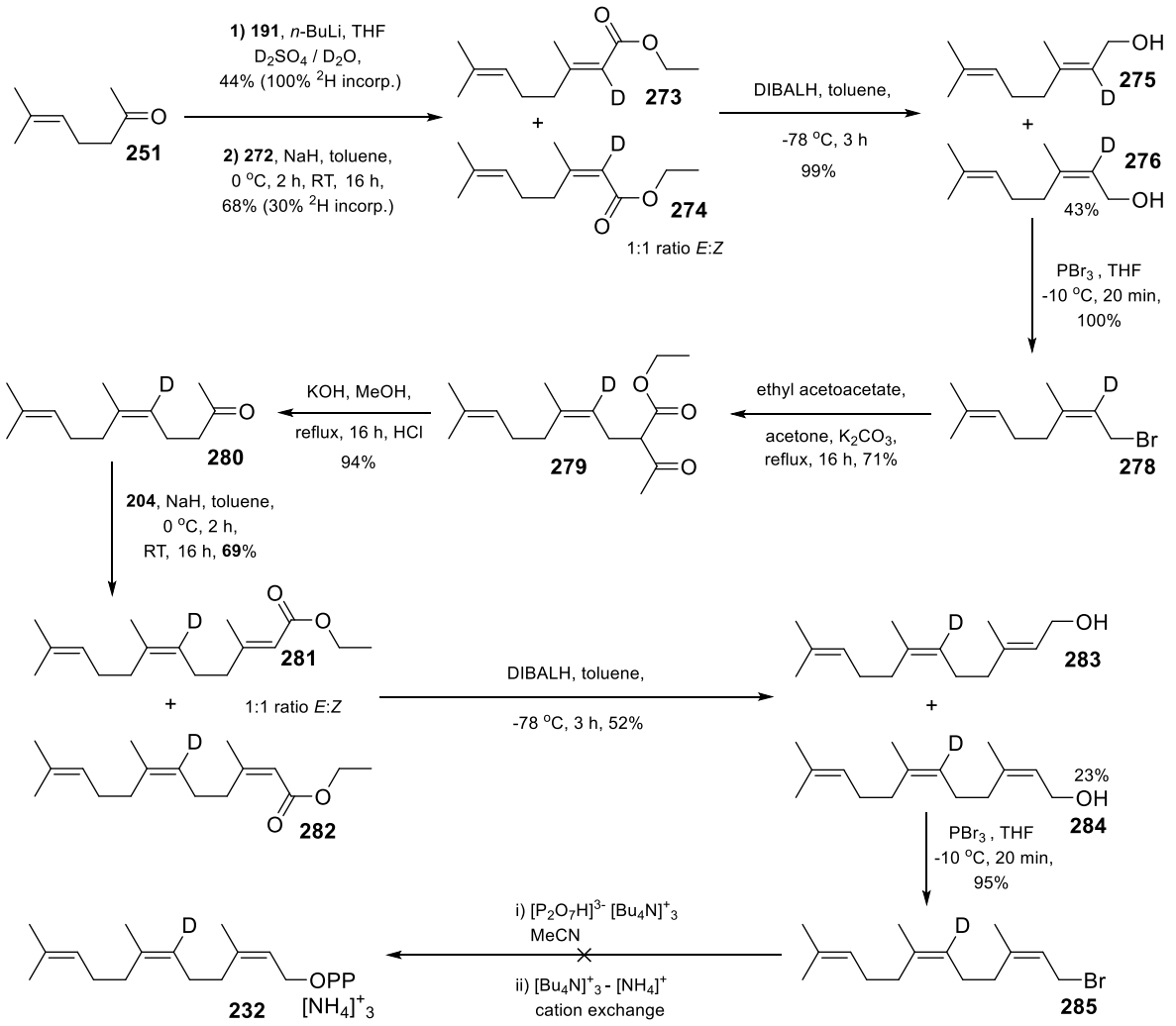

Figure 99. Synthesis of (2*Z*,6*Z*)- [6-^{2}H]-farnesyl diphosphate (232).

Deuterated precursor **274** was synthesised under optimised *Z*-selective olefination conditions (Table 4, 2.5.2). A 1:1 *E*:*Z* ratio was observed however, the reaction products showed only a 30% incorporation of deuterium as judged by ^{1}H NMR and ^{2}H NMR spectroscopy. Incorporation of deuterium was observed *via* ^{2}H NMR spectroscopy with a singlet visible at δ = 5.53 ppm and a singlet integrating to 0.7 H representative a proton environment at δ = 5.53 ppm on the ^{1}H NMR spectrum. The reaction was repeated with fresh reagent to ensure experimental error was not to blame for the low deuterium incorporation. It was speculated that proton deuterium exchange may have occurred during quenching and work up of the reaction. The reaction was therefore repeated and quenched with deuterium oxide in place of water, however no improvement in deuterium incorporation was observed.

Proton-deuteron exchange *via* deprotonation of the alkene proton with *n*-butyl lithium and subsequent quenching with deuterium oxide did not achieved a greater incorporation than observed after the Horner-Wadsworth-Emmons olefination. The synthetic pathway was continued using the

30% labelled product (Figure 99). Incorporated deuterium was readily observed *via* ^{2}H NMR spectroscopy and respective proton peaks were seen at the same ppm shift in ^{1}H NMR spectra of **284**. Unfortunately, after bromination, diphosphorylation and purification steps diphosphate **232** could not be recovered after lyophilisation.

4.3.2 Synthesis of (2*Z*,6*Z*)-(*S*)-[1-^{2}H]-farnesyl diphosphate (233)

Following cyclisation, the catalytic mechanism of 7-epizingiberine synthesis by EZS requires hydride shifts from either the C1 or the C5 positions. Hydride shifts from an allylic position have been shown by Tantillo *et al.* to be energetically favourable *via* computational methods.[238] Therefore investigations of hydride shifts using isotopic labelling focussed on the C1 position. Two pathways are feasible: a [1, 3] hydride shift from the C1 to C7 position, or two consecutive [1, 2] hydride shifts firstly from the C6 to C7 position and then the C1 to C6 position. It is currently unknown which hydride; the *proR* or *proS* at the C1 position migrates. Stereoselective deuterium labelling and incubation with EZS was used to generate deuterated 7-epizingiberene products. GC-MS and analysis of the fragmentation pattern arising from the enzymatic products were used to investigate these rearrangements by comparing fragment masses with possible rearrangement pathways starting with **233** (Figure 100).

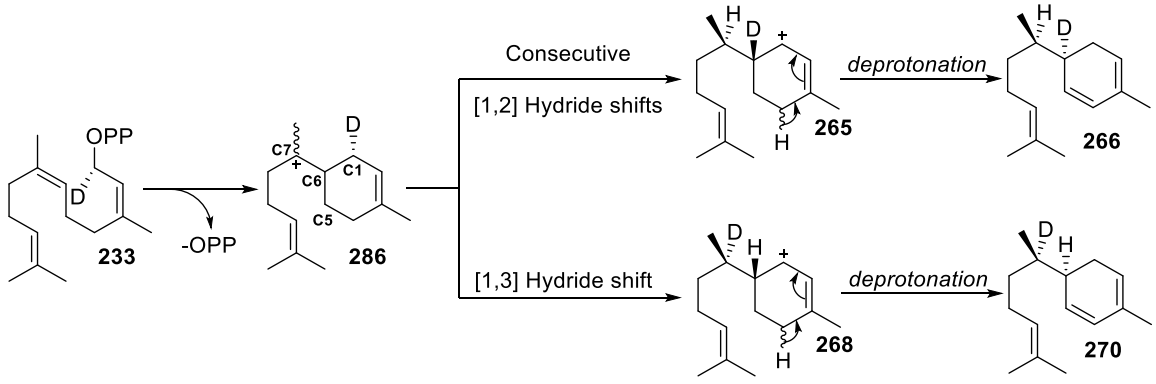

Figure 100. Possible hydride shifts from EZS catalysed reaction of 233.

Attempts to synthesise **289** by direct reduction of ethyl farnesoates **193** with lithium aluminium deuteride ($LiAlD_4$) yielded the desired product. However, due to the poor condition of the reducing agent the reaction could not be driven to completion and fresh reagent could no longer be purchased. A reduction outlined by Yamakawa *et, al.*[239] showed reduction of esters using an in *situ* transmetalation reduction using lithium chloride and sodium borohydride. Various attempts at this

reduction using lithium chloride and sodium borohydride showed no reduction of **192** to **168** and was not investigated further. Instead, a sequential oxidation-reduction strategy was followed. Oxidation of (2*Z*,6*Z*) farnesol (**167**) with TEMPO furnished aldehyde **217** which was reduced with sodium borodeuteride ($NaBD_4$) to incorporate a first isotopic label (Figure 101).

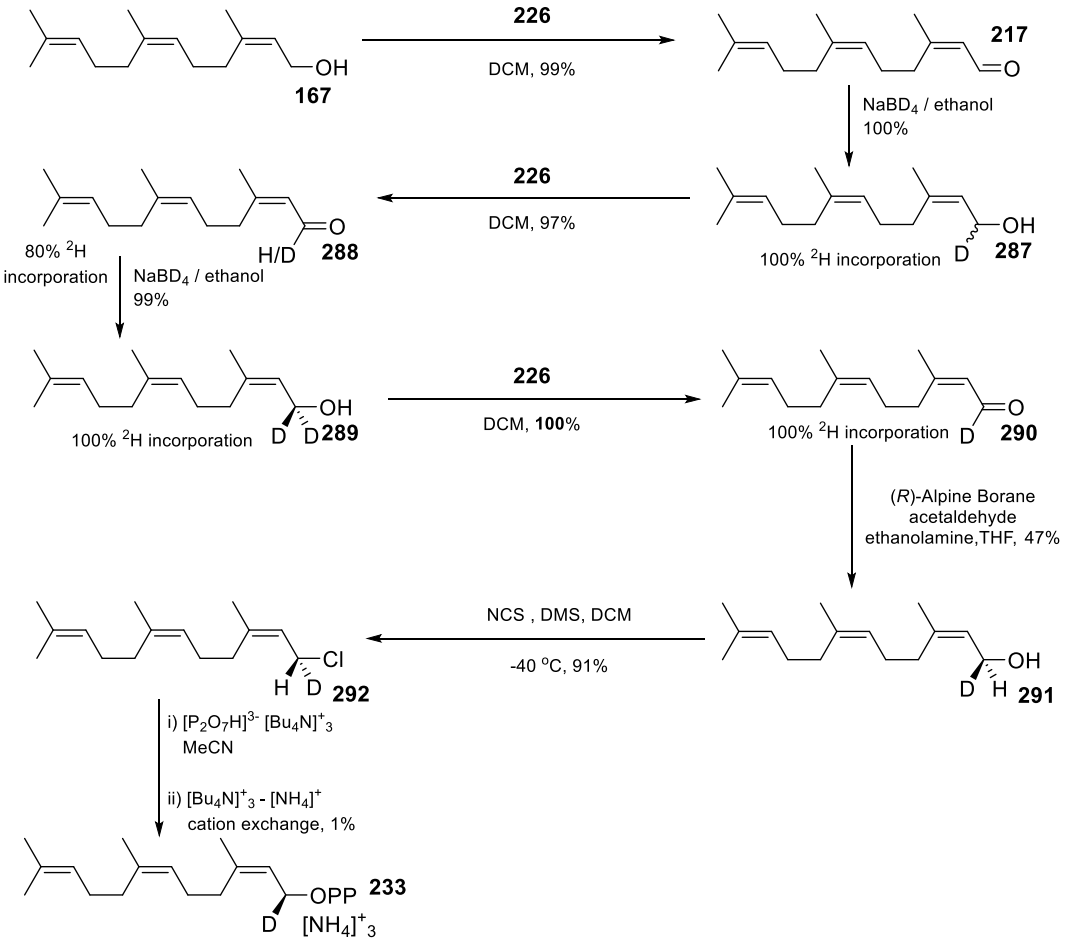

Figure 101. Synthesis of (2*Z*,6*Z*)-(*S*)-[1-^{2}H]-farnesyl diphosphate (233).

An oxidation reaction using TEMPO salt reagent **226** resulted in a single aldehyde product which was found to be of sufficient purity and correct stereochemistry when analysed *via* ^{1}H and NOESY NMR spectroscopy. Contrary to the synthesis of **229** (Figure 76), $NaBD_4$ reductions were carried out in ethanol rather than THF with reaction times of protic solvent reductions being considerably shorter than those in THF. Unlike some other methods detailed in the literature,[112] the TEMPO salt oxidation did not completely prefer H^+ over D^+ when oxidising of **287**, with aldehyde **288** showing only 80% deuterium incorporation (Figure 102).

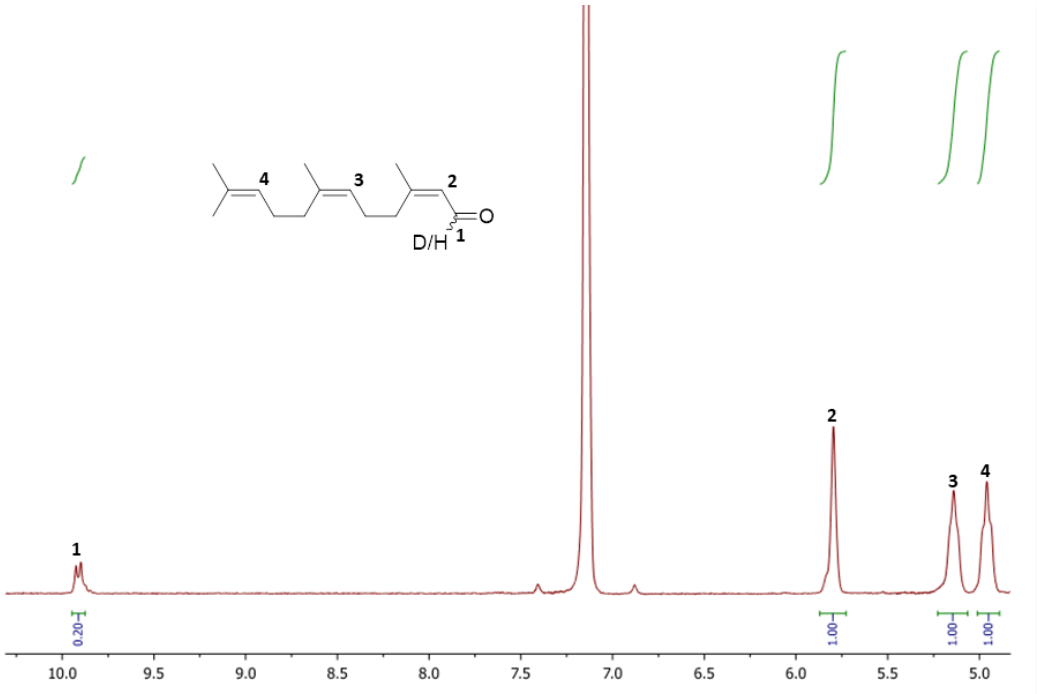

Figure 102. ^{1}H NMR spectrum of aldehyde (257) with 80% deuterium incorporation.

However, reduction of **288** with sodium borodeuteride followed by re-oxidation afforded aldehyde **290** with which the characteristic aldehyde environment was not observed in the ^{1}H NMR spectrum. Deuterium incorporation into aldehydes was confirmed using ^{2}H NMR spectroscopy and mass spectrometry for the purified alcohols **287** and **289.**

Deuterated (2*Z*,6*Z*) farnesal (**290**) was then reacted with an alpine borane chiral reducing agent to yield the desired enantiomer. Reduction of aldehyde **290** with (*R*)-Alpine borane (**294**) delivers the hydride to the *Re* face of the aldehyde yielding the (*S*) enantiomer as the product. Stereochemical control arises from the coordination of the borane to the carbonyl oxygen atom. This coordination aligns the reacting partners for a hydride shift from the tertiary centre opposite to give α-pinene (**49**) and a boro-ester product **292**. Excess Alpine borane reagent was quenched with acetaldehyde and the boron-oxygen coordination complex was cleaved *via* the addition of ethanolamine to give the desired enantiomer **291** (Figure 103).

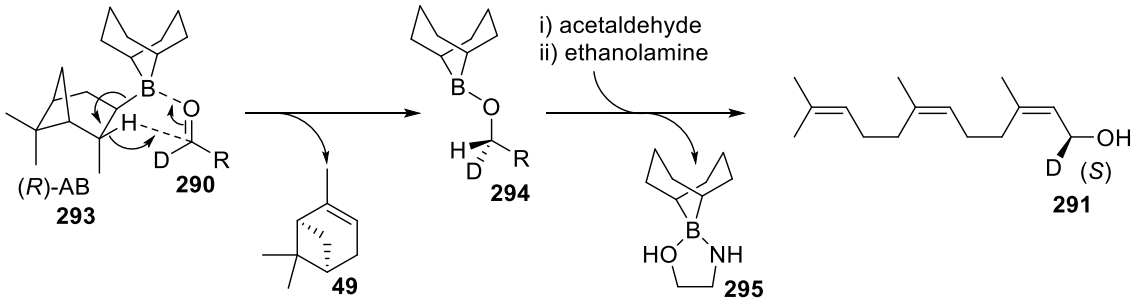

Figure 103. Reduction of 290 with (*R*)-alpine borane (293) at the *Re* face to give 291.

Direct analysis of the enantiomeric excess *via* ^{1}H NMR spectroscopy is not possible without the use of a chiral solvent, nor would chiral HPLC be able to distinguish between deuterium and hydrogen. Enantiomeric analysis was therefore investigated using Mosher's ester derivatives followed by ^{1}H NMR spectroscopic analysis. (2*Z*,6*Z*)-(*S*)-[1-^{2}H]-farnesol (**291**) was reacted in turn with (*S*)-(+)-α-methoxy-α-(trifluoromethyl)phenylacetyl chloride (*S*-MTPA-Cl) and (*R*)-(+)-α-methoxy-α-(trifluoromethyl)phenylacetyl chloride (*R*-MTPA-Cl) yielding a pair of diastereoisomers **297** and **288** respectively (Figure 104).

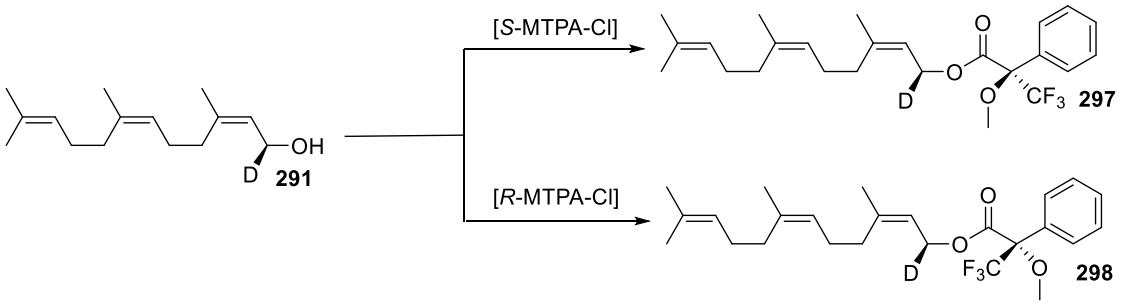

Figure 104. Synthesis of Mosher's esters 297 and 298.

Mosher's esters are commonly used for identifying enantiomers at secondary carbon centres. In solution the trifluoro group of MTPA adopts a rigid linear conformation between the carbonyl and enantiomeric proton (Figure 105). This conformation aligns the phenyl and methoxy groups of MTPA with the R^1 and R^2 groups at the enantiomeric centre respectively. The close spatial arrangement of the methoxy group influences the ^{1}H NMR resonance for R^2 causing its chemical shift to move downfield. In contrast, the phenyl group causes shielding of R^1 and its chemical shift will shift in the opposite direction. Synthesis of the Mosher's ester with the contrasting MTPA enantiomer (Figure 106) will result in the opposite effects on the ^{1}H NMR spectroscopic resonances with the R^1 peak shifting down field and the R^2 peak shifting upfield.[240,241]

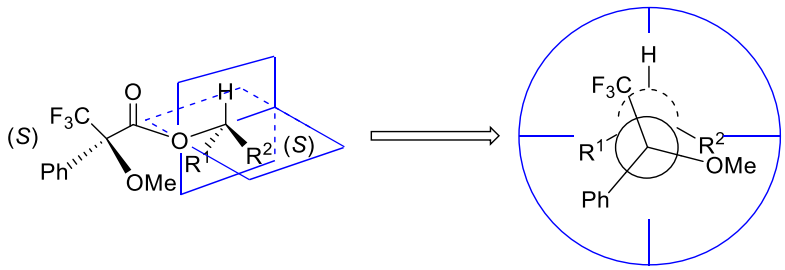

Figure 105. Lowest energy conformation of a Mosher's Ester (*S*)-MTPA.

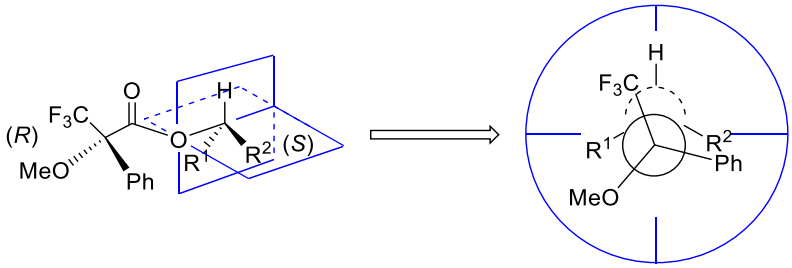

Figure 106. Lowest energy conformation of a Mosher Ester (*R*)-MTPA.

Analysis of *R* and *S* isotopically labelled primary alcohol was slightly more complicated due to the similarity of the deuterium and proton substituents at its chiral centre. As the deuterium and proton are very similar in size, there is no strong preference for either to adopt an eclipsed conformation with the trifluoromethyl group (Figure 105 and Figure 106); only the carbon chain is prohibited from adopting this conformation by its steric bulk. Figure 107 shows the two possible conformations of **297** achievable through rotation around the carbon oxygen sigma bond. The proton rotates between alignment with the trifluoromethyl and phenyl groups whilst not being affected by the deshielding methoxy group on the opposing face. Figure 108 shows the lowest energy conformation of **298** and outlines the opposite effect with the proton environment able to rotate between alignment with the trifluoromethyl and methoxy groups. Interaction of the C1 proton with the methoxy group on **298** results in de-shielding of the proton environment. This interaction causes downfield shift of the respective peak on the ^{1}H NMR spectrum. When compared to the analogous peak of **297** a downfield shift of the **298** proton is observed on the ^{1}H NMR spectrum. Contrary to secondary alcohols, the ^{1}H NMR signals for R will not be affected by the synthesis of the Mosher's ester. The rotation to align H or D with the trifluoromethyl group allows R group to interact with both phenyl and methoxy groups (Figure 107 and Figure 108), therefore shielding and de-shielding effects would be equilibrated and no net changes in chemical shift are be observed.[242]

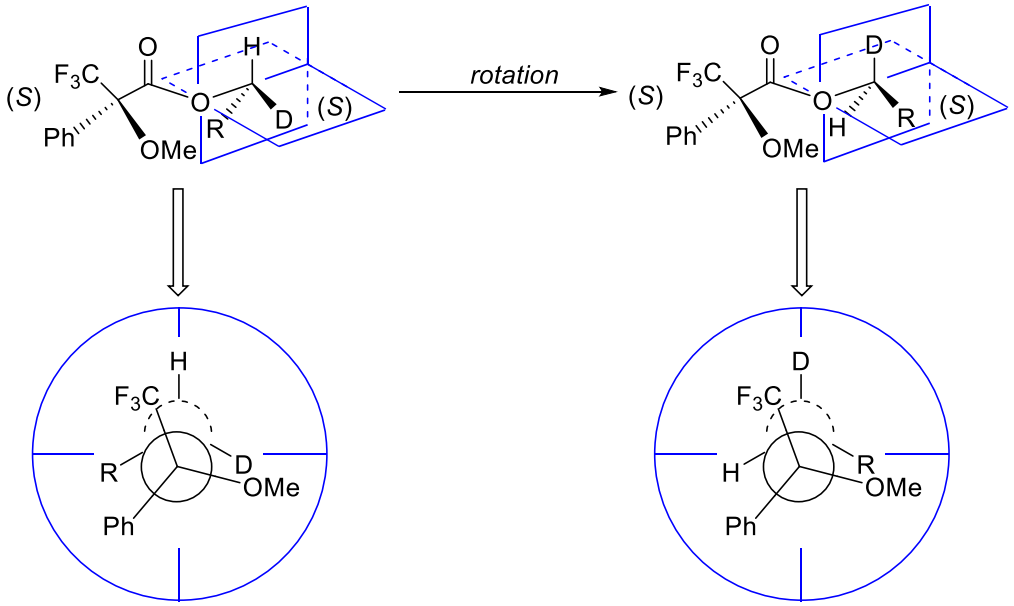

Figure 107. Lowest energy conformations of 297.

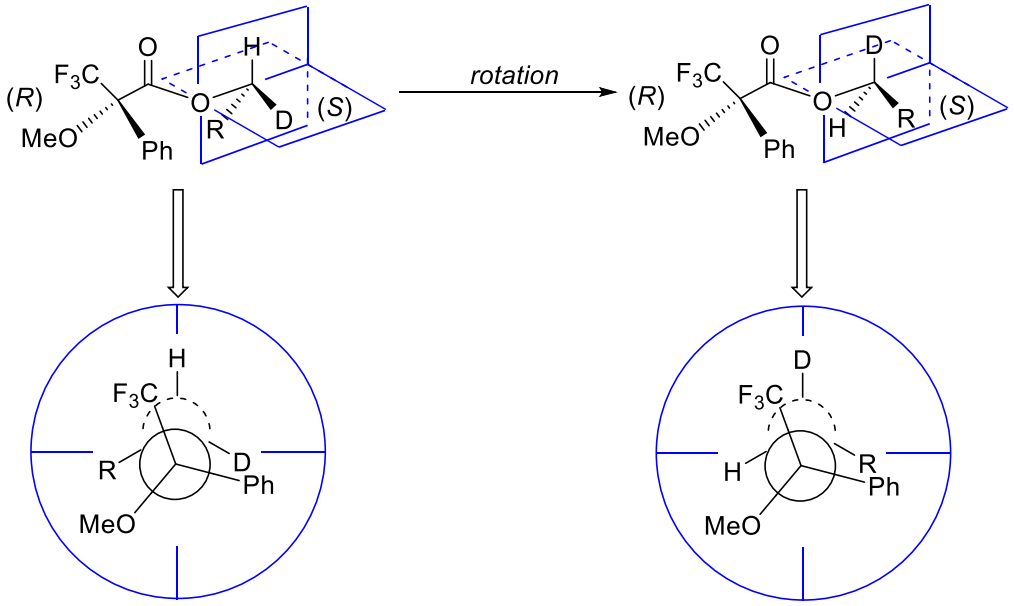

Figure 108. Lowest energy conformations of 298.

^{1}H NMR spectroscopic analysis of **297** and **298** showed the proton environment at the C1 position of **298** was shifted downfield to 4.82 ppm compared to that of **297** at 4.77 ppm (Figure 109). It was also observed that the chemical shift of the alkene proton of R remained the same in both spectra as

predicted. Chemical shifts of **297** and **298** were concordant with literature values of (S)-[1-^{2}H]-farnesyl-(S)-α-methoxy-α-(trifluoromethyl)phenyl-acetate (2*E*,6*E* isomer).[243]

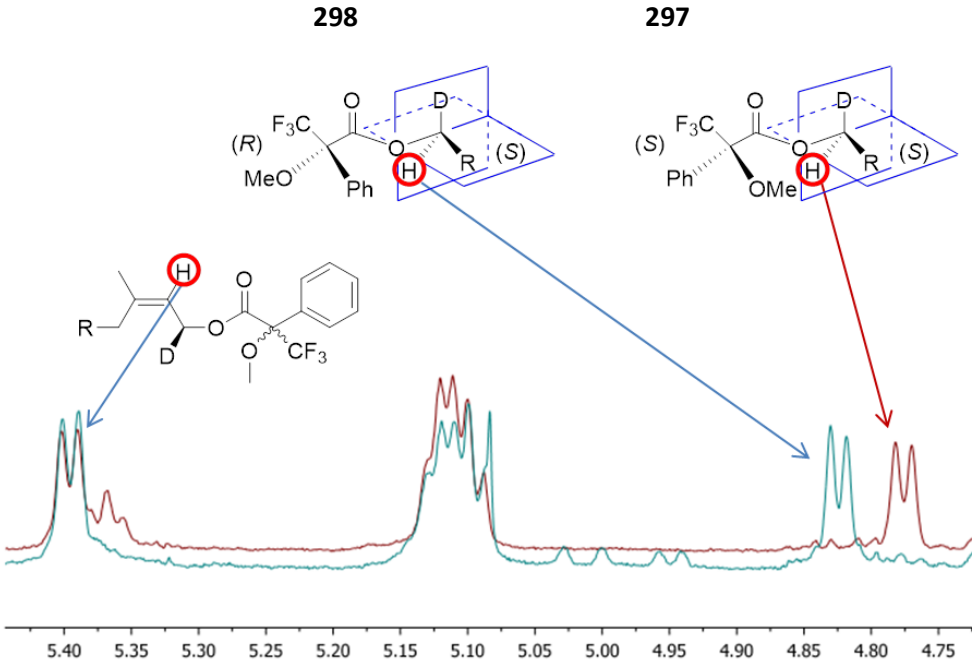

Figure 109. Overlaid ^{1}H NMR spectra of (2*Z*,6*Z*)-(*S*)-[1-^{2}H]farnesyl-(*R*)-α-methoxy-α-(trifluoromethyl)phenyl-acetate (298)(blue) and (2*Z*,6*Z*)-(*S*)-[1-^{2}H]farnesyl-(*S*)-α-methoxy-α-(trifluoromethyl)phenyl-acetate (297)(red).

Determination of enantiomeric excess (*ee*) was attempted *via* decoupling experiments using ^{1}H NMR spectroscopy. Decoupling by irradiation of the C2 alkene peak (circled red in Figure 110) at δ = 5.4 ppm of **297** and **297** gave two singlets for the proton environment at the C1 position (circled blue in Figure 110) at δ = 4.77 and 4.82 ppm respectively, with no other decoupled environments observed. The presence of one singlet environment on each spectrum indicates a single enantiomer is present (Figure 110). A racemic mixture would result in two doublets on a ^{1}H NMR spectrum arising from two distinct proton environments. Upon irradiation, both environments would decouple to form two singlets. As only one peak in each spectrum experienced decoupling, a single enantiomer is present. However due to the small quantity of each ester synthesised, the product peaks of **297** and **298** are in close proximity to the baseline. For the calculation of *ee*, precise integration of each peak is required. Due to slight impurities in the same region as the peaks of interest disrupting the baseline, an exact enantiomeric excess could not be determined. However, due to the presence of one singlet environment on each spectrum after the irradiation at δ = 5.4 ppm, **291** was deemed to be of sufficient quality to use.

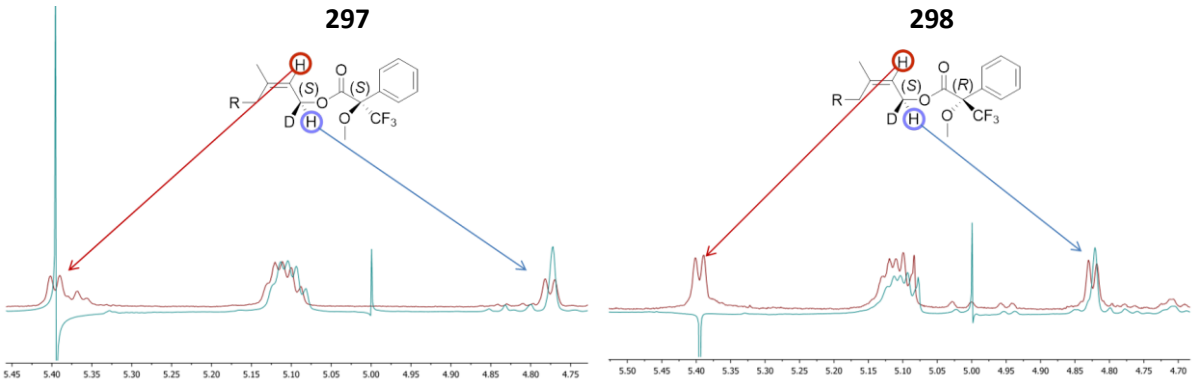

Figure 110. ^{1}H NMR Decoupling experiment for 297 (left) and 298 (right); irradiation at δ = 5.4 ppm resulting in the collapse of the respective doublets to singlets at δ = 4.77 (297, left) and 4.82 ppm (298, right).

With the required enantiomer confirmed, diphosphorylation of **291** proceeded *via* chlorination as described previously rather than phosphorus tribromide bromination as chlorination by this method cleanly inverts the stereocentre,[244,245] in this example yielding the *R* enantiomer. Diphosphorylation inverts the centre for a second time giving retention of stereochemistry over the two steps.

4.3.3 Synthesis of (2*Z*,6*Z*)-(*R*)-[1-^{2}H]-farnesyl diphosphate (234)

A hydride shift from the (*R*) proton at the C1 position is a possibility in the catalytic mechanism of EZS. As with the (*S*) enantiomer **233**, two deuterated products may be synthesised from the incubation of **234** and EZS with consecutive [1,2] hydride shifts giving **266** and a [1,3] hydride shift yielding **270** (Figure 111).

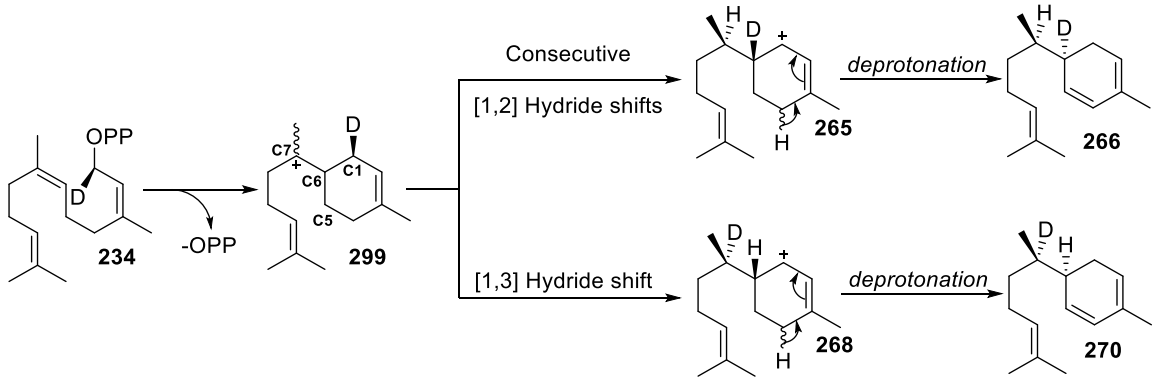

Figure 111. Possible hydride shifts from EZS catalysed reaction of 234.

The synthesis of (2*Z*,6*Z*)-(*R*)-[1-^{2}H]-farnesyl diphosphate (**234**) was analogous to that of **233** (Figure 101) but used (*S*)-alpine borane (**302**) as the reducing agent to yield the desired enantiomer (Figure 112).

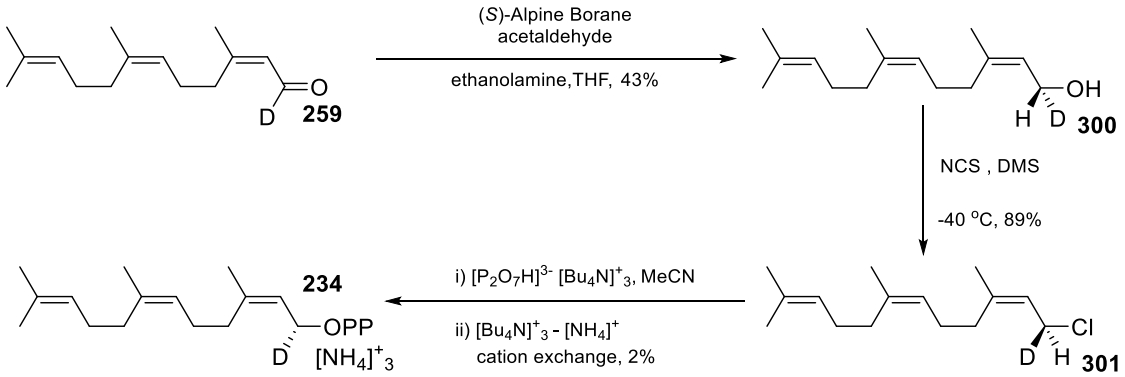

Figure 112. Synthesis of (2*Z*,6*Z*)-(*R*)-[1-^{2}H]-farnesyl diphosphate (234).

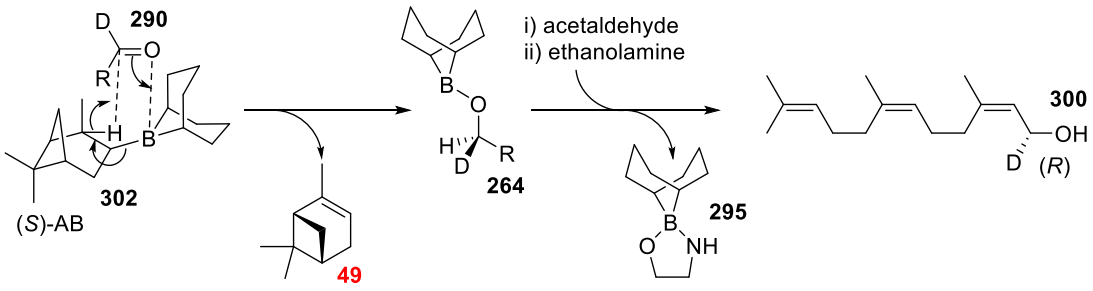

Figure 113. Reduction of 290 with (*S*)-alpine borane (302) at the *Si* face to give 300.

Mosher's ester analysis of alcohol **300** as described above was used to confirm the required enantiomer had been synthesised. The ^{1}H NMR spectrum showed a characteristic downfield shift of the C1 proton from the S-MTPA derived ester **303** (red, δ = 4.83 ppm) when compared to the R-MTPA derived ester **304** (blue, δ = 4.77 ppm) (Figure 114). ^{1}H NMR decoupling experiments were utilised to confirm the presence of a single enantiomer. Upon irradiation of the alkene peak at δ = 5.40 ppm the respective doublets of the C1 proton environments collapsed to singlets (Figure 115). Though slight impurities inhibited the calculation of *ee,* no surrounding proton environments were affected by irradiation and **300** was deemed of sufficient purity to use. **300** was chlorinated and diphosphorylated as previously described in order to prepare the diphosphate with retention of configuration.

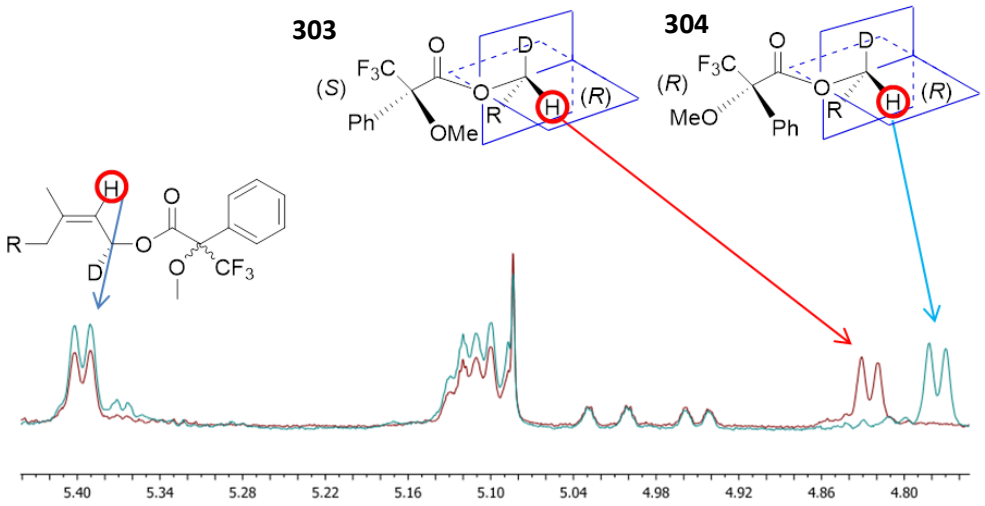

Figure 114. Overlaid ^{1}H NMR spectra of (2*Z*,6*Z*)-(*R*)-[1-^{2}H]farnesyl-(S)-α-methoxy-α-(trifluoromethyl)phenyl-acetate (303)(red) and (2*Z*,6*Z*)-(*R*)-[1-^{2}H]farnesyl-(*R*)-α-methoxy-α-(trifluoromethyl)phenyl-acetate (304)(blue).

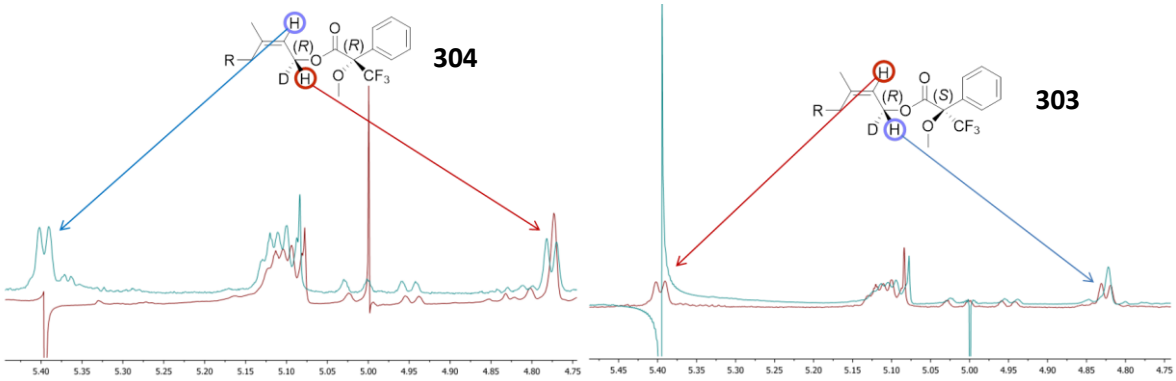

Figure 115. ^{1}H NMR Decoupling experiment for 304 (left) and 303 (right); irradiation at δ = 5.4 ppm resulting in the collapse of the respective doublets to singlets at δ = 4.77 (304, left) and 4.83 ppm (303, right).

4.3.4 Incubation of 233 and 234 with EZS

The catalytic mechanism of EZS can proceed *via* two possible pathways from the C1 position; a [1,3] hydride shift or two consecutive [1,2] hydride shifts. Nor is it known which of the *proR* or *proS* hydrides migrate (Figure 116).

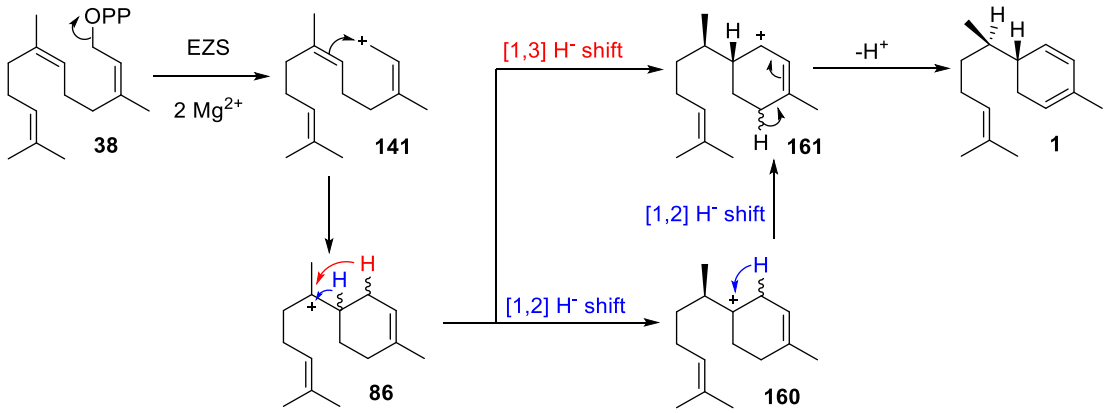

Figure 116. Possible hydride shifts occurring from the C1 position during the catalytic mechanism of EZS

4.3.5 Incubation of (2*Z*,6*Z*)-(*R*)-[1-^{2}H]-farnesyl diphosphate (234) and EZS

The incubation of (2*Z*,6*Z*)-(*R*)-[1-^{2}H]-farnesyl diphosphate (**234**) with EZS could give rise to three different deuterated products depending on the catalytic mechanism followed (Figure 117). Analysis of the pentane extractable products *via* GC-MS yielded a single enzymatic product (Figure 118).

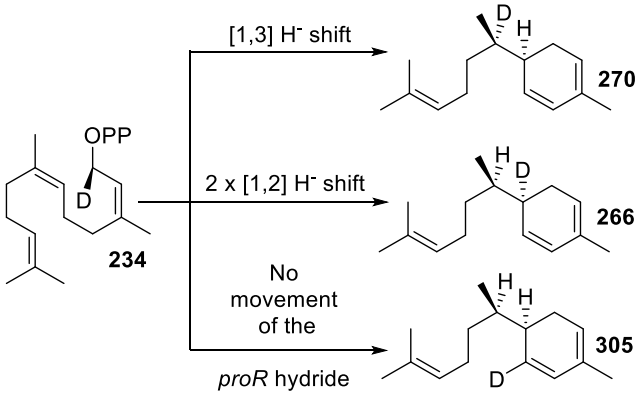

Figure 117. Possible pentane extractable products arising from incubation of EZS and 234.

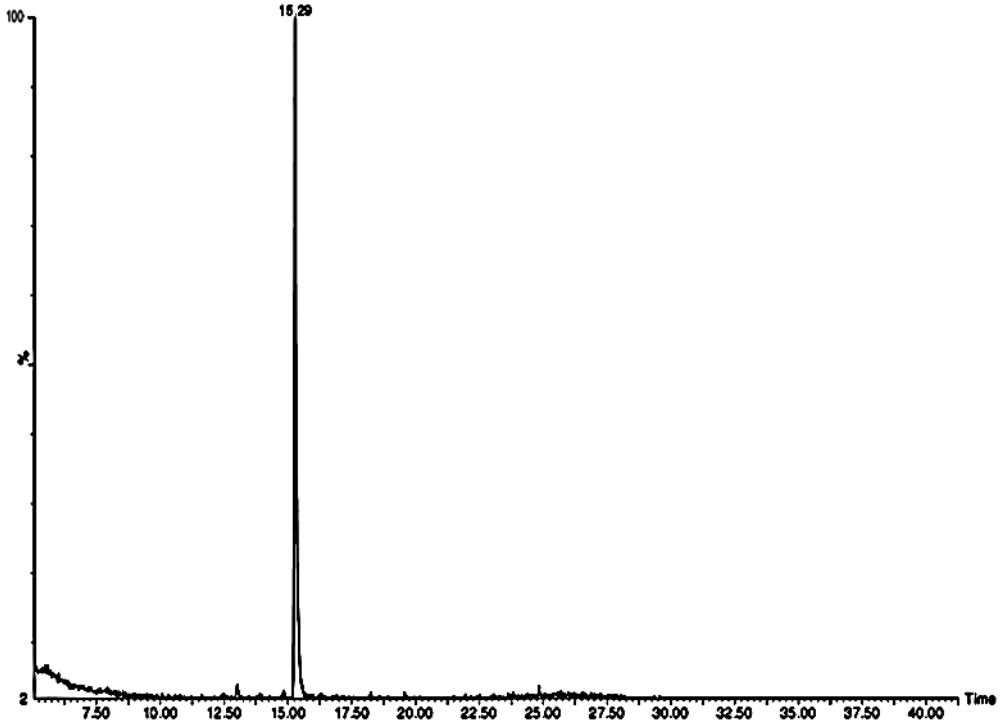

Figure 118. Total ion chromatogram of the pentane extractable products arising from incubation of 234 with EZS.

The mass spectrum of this product was analysed and plausible fragments corresponding to the *m/z* values were assigned (Figure 119). Due to the various hydride shifts that are plausible during the catalytic mechanism of EZS (Figure 117), multiple deuterated products could be responsible for the peak on the gas chromatogram (Figure 118). The compound responsible for the peak at 15.29 minutes (Figure 118) showed deuterium incorporation on the mass spectrum (Figure 119). An *m/z* increase of +1 is observed in numerous peaks of the mass spectrum when compared with the mass spectrum of 7-epizingiberene (**1**) (Figure 60, 2.6) indicating isotope labelling.

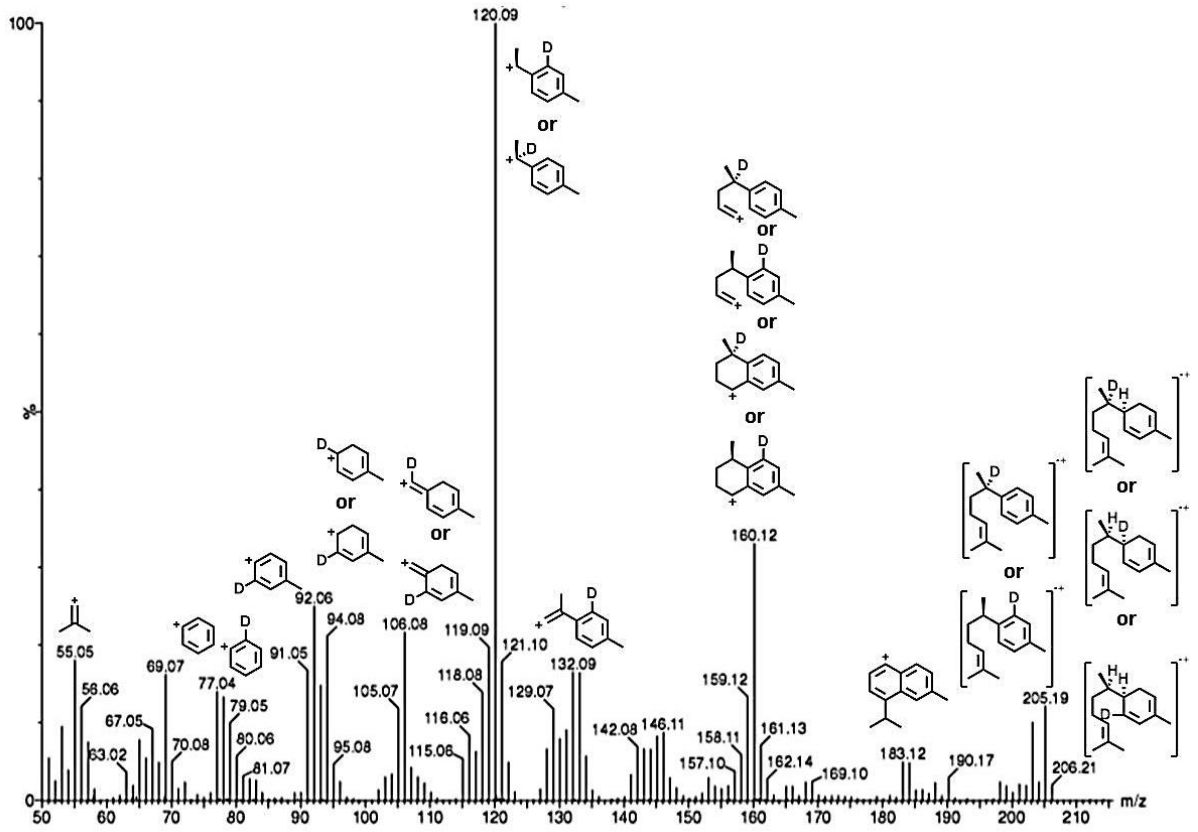

Figure 119. Mass spectrum of the compound eluting at 15.29 min on the total ion chromatogram.

The mass spectrum (Figure 119) gives some insight into the destination of the C1 *proR* proton of (2*Z*,6*Z*) farnesyl diphosphate (**38**) in the EZS catalysed conversion of **134**. Peaks at *m/z* = 205 and 203 correspond to ionised deuterated 7-epizingiberene (**306, 309 or 311**) and curcumene respectively whilst a peak at *m/z* = 120 is also present indicating the deuteride undergoes a [1,3] shift (**308**) or remains in the same position (**313**) during the catalytic mechanism. Aromatisation of the ring would result in the loss of deuterium if a [1,2] shift had occurred from the C1 to the C6 position (**223**) within the catalytic mechanism giving a peak at *m/z* = 119, ruling out this scenario (Figure 120).

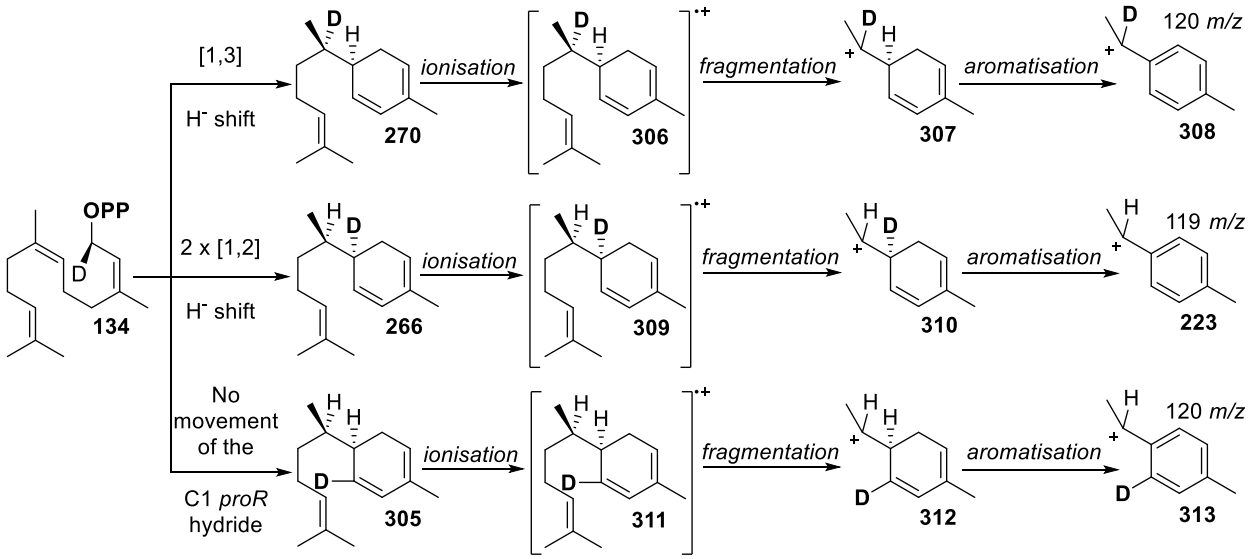

Figure 120. Fragmentations of product that give ions with *m/z* = 119 and 120.

Two cations are plausible for the species with *m/z* = 106. A [1,3] shift giving deuterated product **270**, ionisation and fragmentation would give cation **316** whilst no movement giving rise to **305** with ionisation and fragmentation to give cation **321**. The *m/z* = 106 peak can only occur *via* no deuterium movement or a [1,3] hydride shift during the catalytic mechanism. Again this data disfavours consecutive [1,2] hydride shifts as ionisation, fragmentation and terminal alkene formation would remove the deuterium to give a major fragment **224** at *m/z* = 105 (Figure 121).

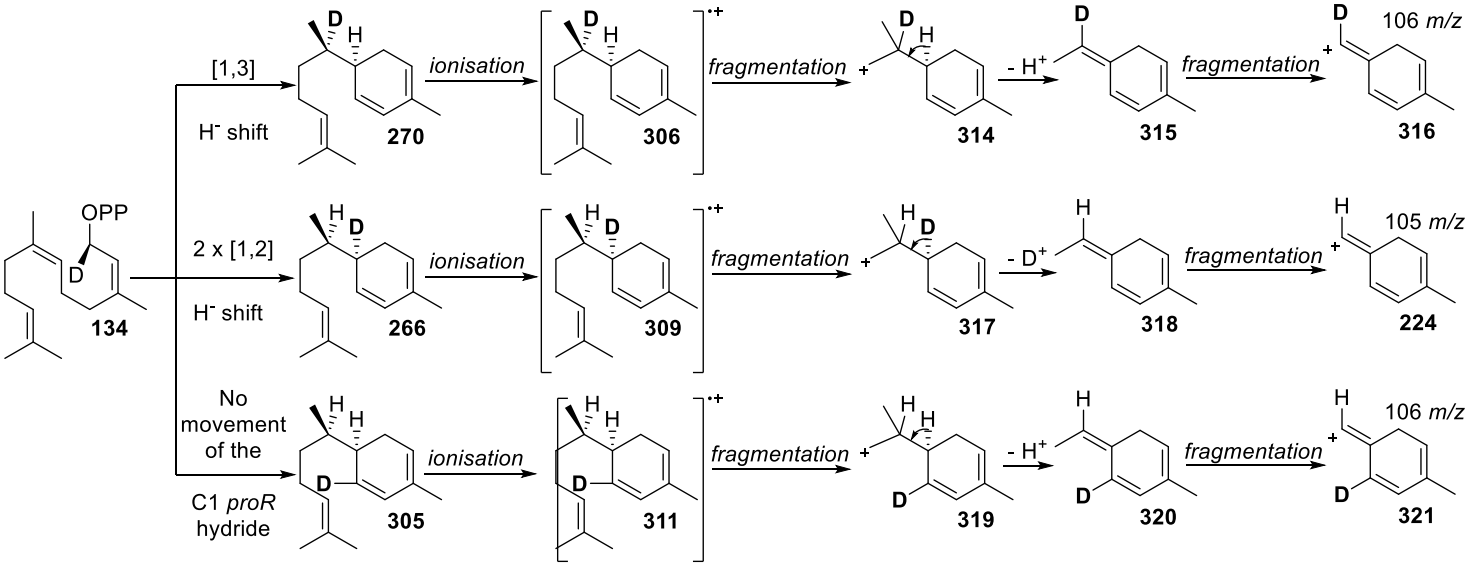

Figure 121. Fragmentations of possible products that give *m/z* = 105 and 106.

A peak at *m/z* = 94 could correspond to possible two cations. Consecutive [1,2] hydride shifts or no movement of the *R* deuteron could give the *m/z* value observed for cations **322** and **323** respectively after product ionisation and fragmentation. A [1,3] shift and ionisation of the deuterated product **270** would give **306** and consequent fragmentation would yield cation **225** with a *m/z* = 93 (Figure 122). This data again disfavours consecutive [1,2] shifts, but additionally suggests the *R* deuteron does not migrate.

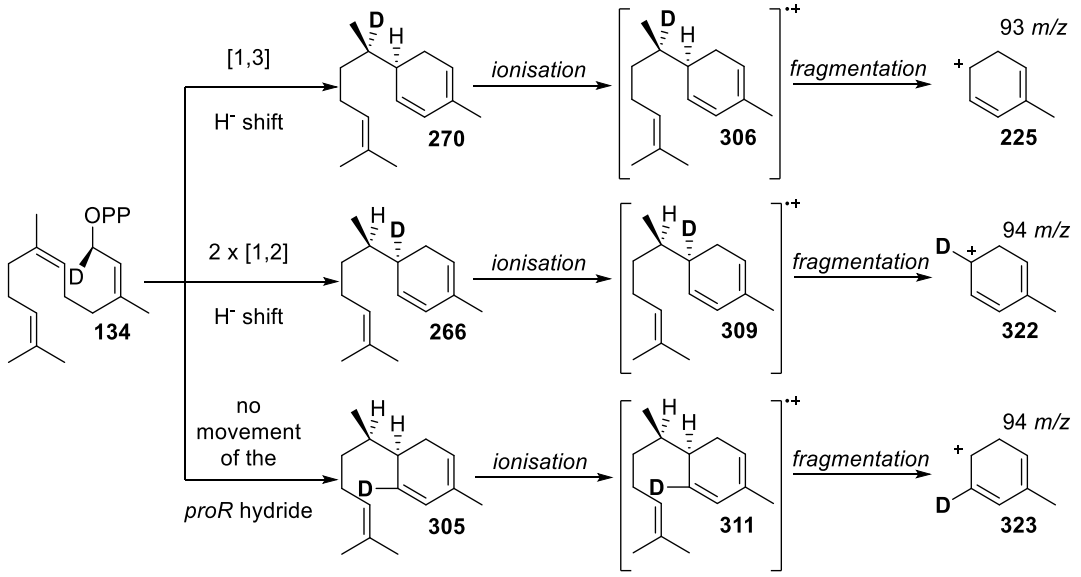

Figure 122. Fragmentations of product that give *m/z* = 93 and 94.

Lower *m/z* regions of the mass spectrum are more complicated and do not clearly implicate any of the possibilities. Fragmentation and aromatisation can affect the ratio *m/z* = 92:91 (Figure 123) and *m/z* = 78:77 (Figure 124). With no definitive way of knowing which fragments occur and at what ratios, relying on the interpretation of these peak ratios alone would not allow for the elucidation of the catalytic mechanism. However, the evidence gained from these fragmentation patterns and peaks discussed in Figure 120 and Figure 121 give insight into the role of *proR* proton at the C1 position

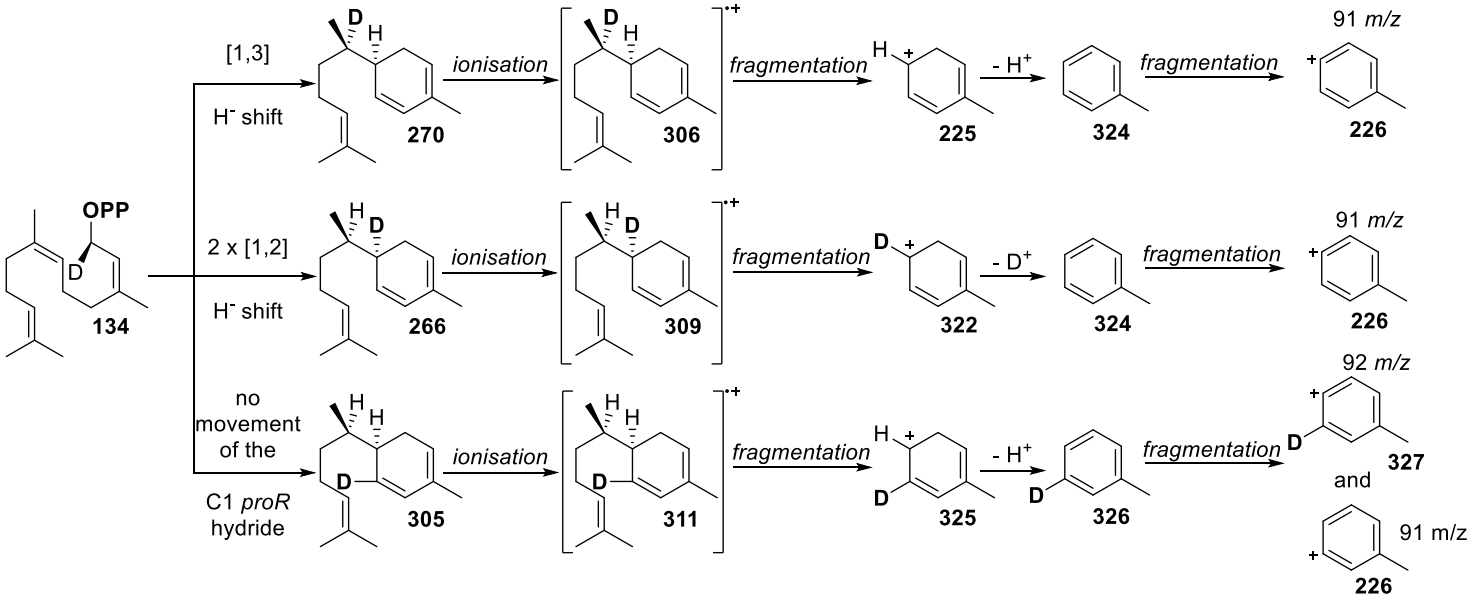

Figure 123. Fragmentations of product that give m/z = 92 and 91.

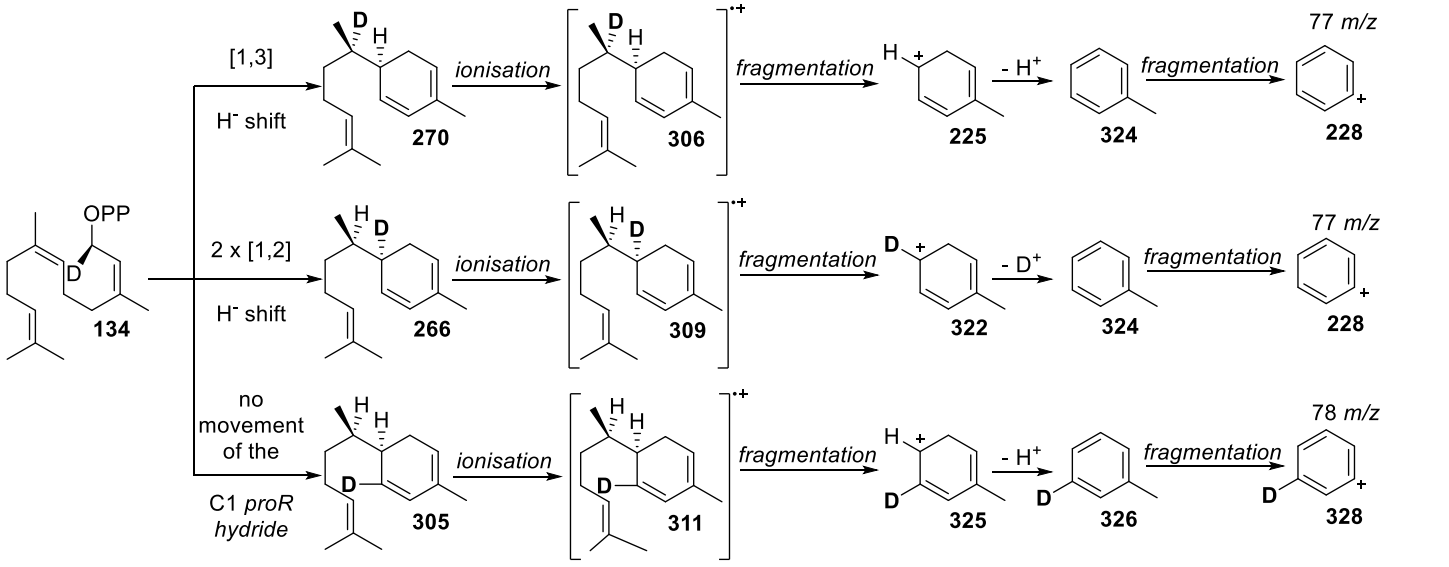

Figure 124. Fragmentations of product that give m/z = 78 and 77.

Overall, the data strongly suggest that the *R* proton at the C1 position does not migrate during 7-epizingiberene synthesis by EZS. The consequent fragmentation pattern is therefore as a result of the formation of deuterated 7-epizingiberene (**305**) (Figure 125).

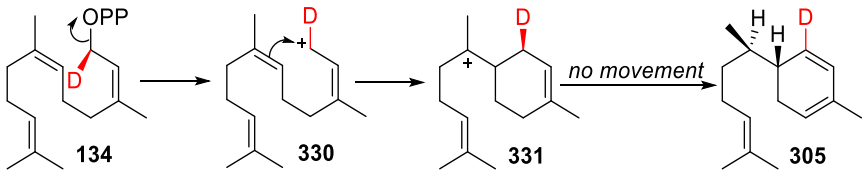

Figure 125. Role of *proR* proton at C1 position.

4.3.6 Incubation of (2*Z*,6*Z*)-(*S*)-[1-^{2}H]-farnesyl diphosphate (233)

The pentane extractable products arising from the incubation of (2*Z*,6*Z*)-(*S*)-[1-^{2}H]-farnesyl diphosphate (**233**) and EZS (Figure 126) were analysed *via* GC-MS. A single enzymatic product was observed at 15.27 min. However, several non-enzymatic products were also observed and identified as impurities from the substrate (2*Z*,6*Z*)-(*S*)-[1-^{2}H]-farnesyl diphosphate (**233**) (Figure 127).

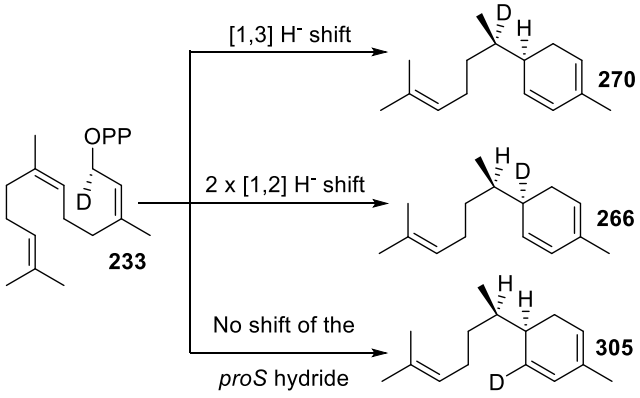

Figure 126. Possible incubation products of 134 and EZS.

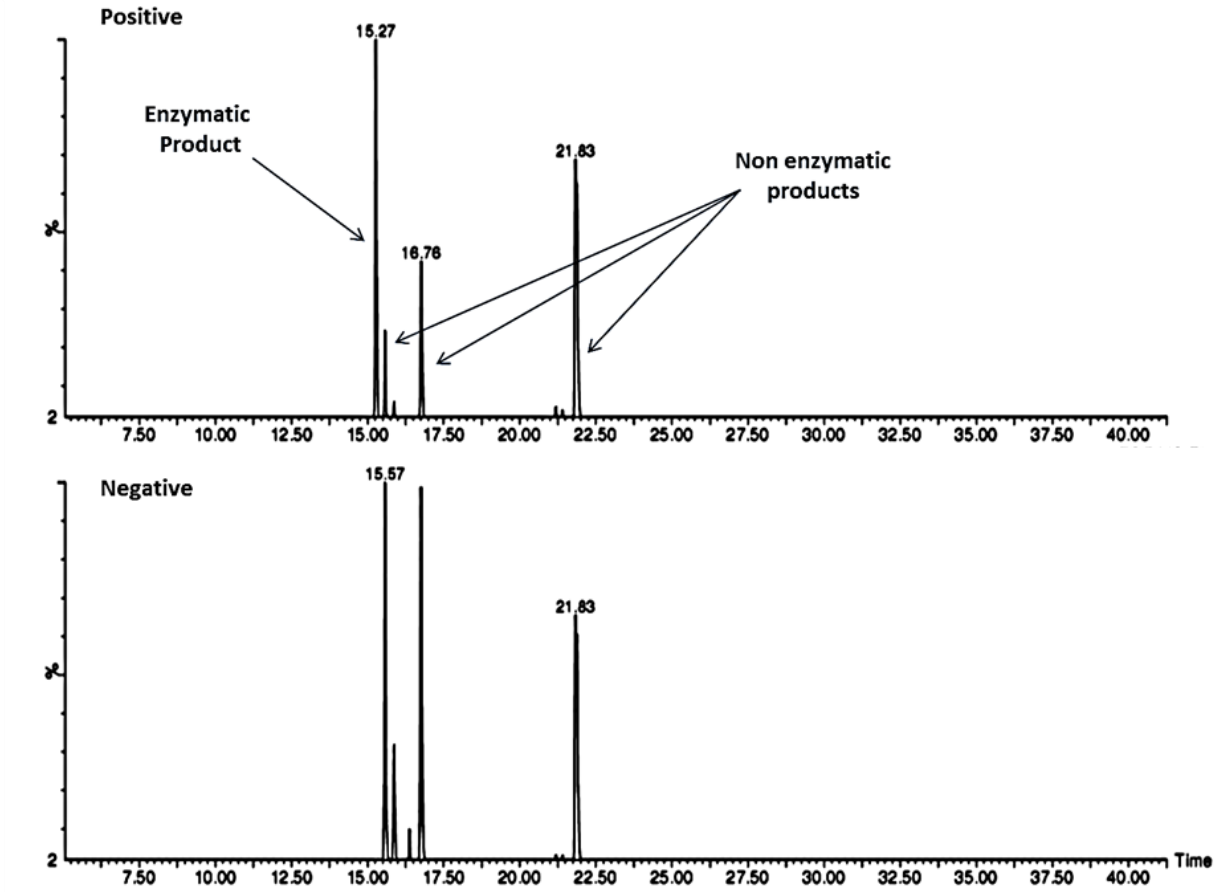

Figure 127. Total ion chromatograms of the pentane extractable products from; the incubation 233 and EZS (top), the incubation 233 with no EZS (bottom. Enzymatic product eluted at 15.27 minutes (top).

The mass spectrum of the compound eluted at 15.3 min shows a fragmentation pattern consistent with 7-epizingiberene (Figure 60, 2.6). Consistent with incubation products of **234** and EZS, peaks; 205 and 203 imply deuterated 7-epizingiberene (**306, 309 or 311**) and curcumene respectively. Peaks at *m/z* = 160 and 120 are again plausible if the deuteride is undergoing a [1,3] shift or remaining in the same position.

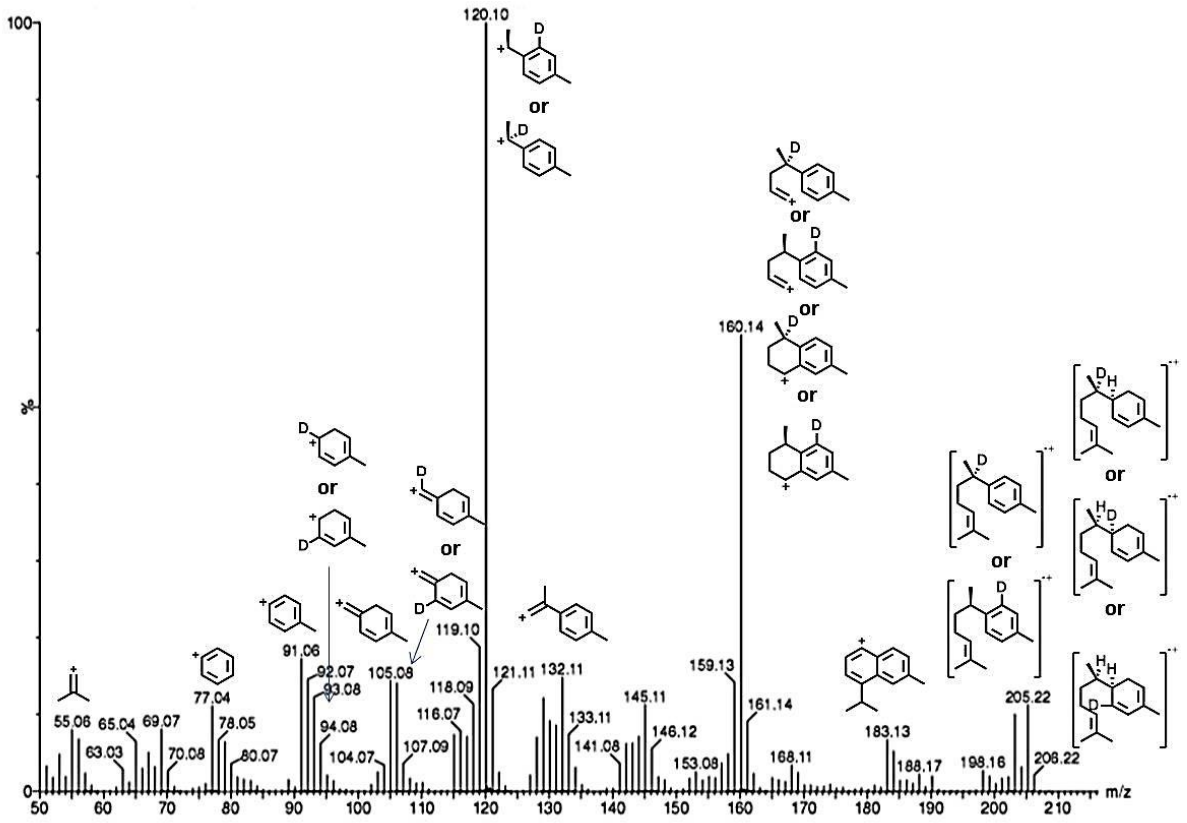

Figure 128. Mass spectrum of the compound eluted at 15.27 minutes on the total ion chromatogram.

A subtle difference in the peak intensity of *m/z* = 132 between the spectra shows that a non deuterated cation fragment is present. The relative intensity of the *m/z* = 133 to the 132 peak is significantly reduced in for the *S*-deuterium substrate (Figure 128) compared to the *R*-deuterium substrate (Figure 119). Two catalytic mechanisms could yield fragments **335** and **340**; a [1,3] shift placing deuterium at the C7 position or consecutive [1,2] shifts to place deuterium at the C6 position. Both positions would result in the loss of deuterium *via* alkene formation and aromatisation respectively after fragmentation of the parent molecular ions **306** ([1,3] hydride shift) and **305** (consecutive [1,2] hydride shifts). Contrastingly, no movement would yield a fragmentation peak at *m/z* = 133 (Figure 129) corresponding to cation **340**.

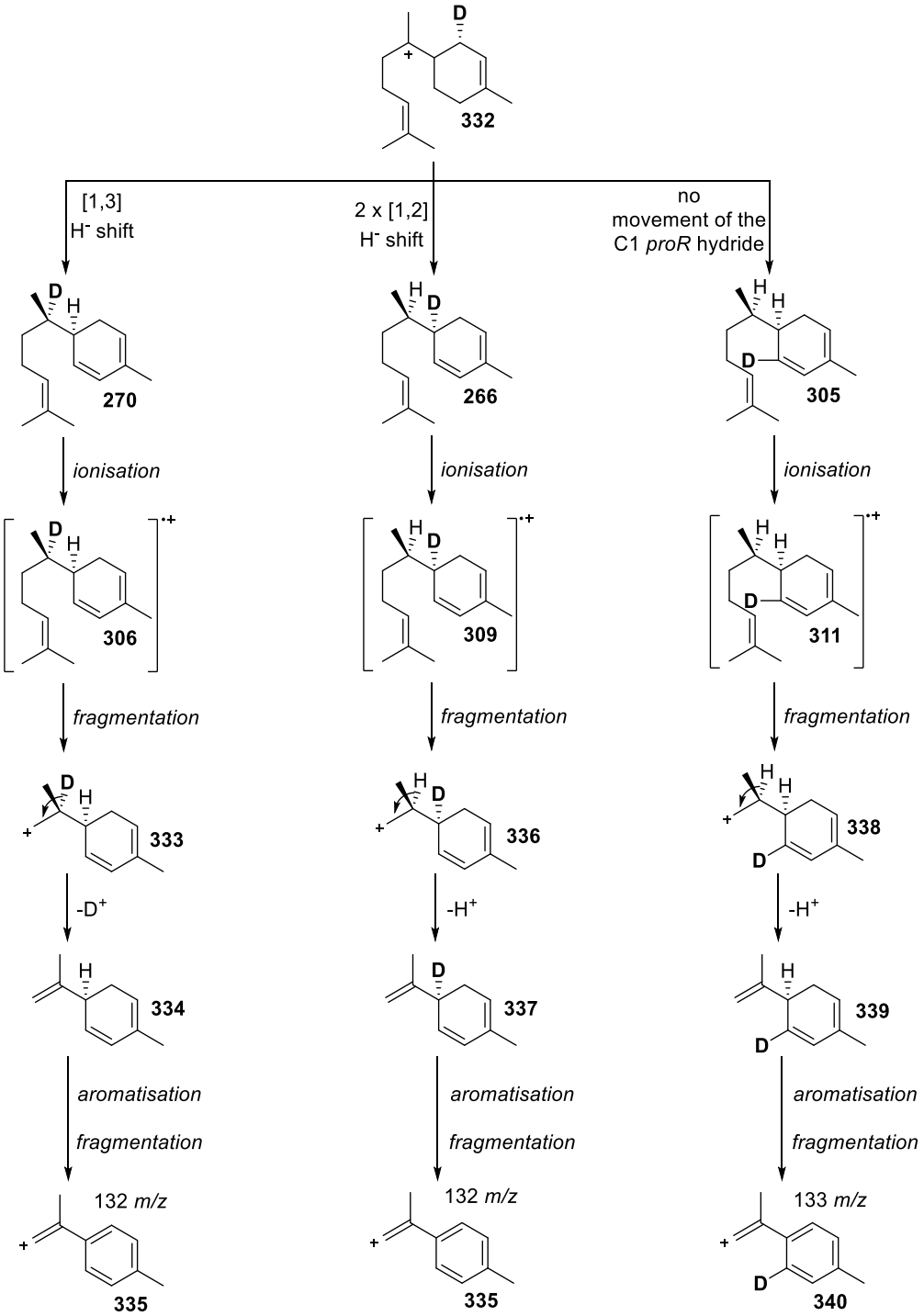

Figure 129. Fragmentations of product to give *m/z* = 132 and 133.

A peak at *m/z* = 106 corresponds to a deuterated fragments **316** and **321**, that can only form if a [1,3] shift or no shift of the *S* C1 proton is occurring respectively. However, an *m/z* = 105 peak of equal intensity to the *m/z* = 106 peak is also observed on the mass spectrum 7-epizingiberene (Figure 60. 2.6). The *m/z* = 105 fragment cation **224** is only plausible *via* two consecutive [1,2] shifts, where fragmentation and deprotonation will remove the deuterium (Figure 121). The equal intensity of these two peaks (Figure 130) suggests multiple catalytic mechanisms may be at work.

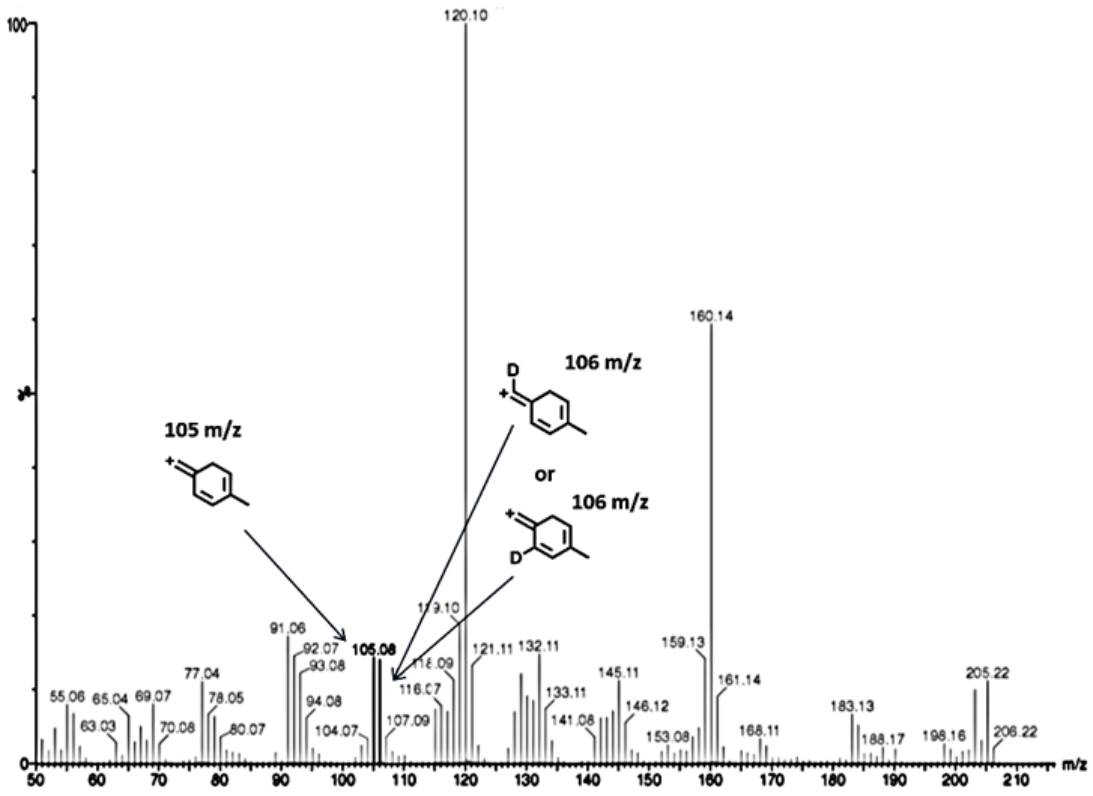

Figure 130. Highlighted *m/z* = 105 and 106 fragmentation peaks.

As outlined earlier (Figure 122), the *m/z* = 94 peak indicates the presence of deuterium on the ring which would occur from no deuterium movement (cation **323**) or consecutive [1,2] hydride shifts (cation **322**). The greater intensity of the *m/z* = 93 fragment peak (cation **225**) in conjunction with the *m/z* = 94 fragment peak suggest that the catalytic mechanism may proceed *via* both and [1,3] and consecutive [1,2] shifts as a single mechanism would show only one fragment.

Prevalent peaks corresponding to *m/z* = 91 (cation **226**, Figure 123) and *m/z* = 77 (cation **228**, Figure 124) fragment cations suggest that deuterium is not positioned on the ring. The mass spectrum of the product from (2*Z*,6*Z*)-(*R*)-[1-^{2}H]-farnesyl diphosphate (**234**) incubation with EZS gave dominant peaks at *m/z* = 92 (cation **328,** Figure 123) and 78 (cation **329**, Figure 124), (Figure 119), strongly suggesting that the *R* deuteron at the C1 position was not involved within the catalytic mechanism. If the *S* deuteron was not utilised as part of the catalytic mechanism, it would remain on the ring as observed for the *R* deuteron of (2*Z*,6*Z*)-(*R*)-[1-^{2}H]-farnesyl diphosphate (**234**). In this scenario the same fragmentation peaks at *m/z* = 92 and 78 would be visible at the same intensity as in Figure 119. However, these fragmentation peaks are not observed in the mass spectrum taken from the incubation product of EZS and (2*Z*,6*Z*)-(*S*)-[1-^{2}H]-farnesyl diphosphate (**233**) (Figure 128). Although a

definitive pathway of the *S* deuteron cannot be elucidated, the absence of these peaks suggests that it may be utilised throughout the catalytic mechanism of EZS.

This reasoning is not conclusive. In order to properly ascertain the role of the *proS* proton at the C1 position ^{1}H NMR experiments of the incubation products (2*Z*,6*Z*)-(*R*)-[1-^{2}H]-farnesyl diphosphate (**234**) and (2*Z*,6*Z*)-(*S*)-[1-^{2}H]-farnesyl diphosphate (**233**) with EZS must be compared to a fully characterised ^{1}H NMR spectrum of 7-epizingiberene (**1**). This would show the position of the deuterium on labelled product in relation to non-labelled 7-epinzingiberene (**1**) and allow the proposal of a suitable mechanism. From the evidence presented, it is plausible to suggest that the *proS* proton at the C1 position is utilised within the catalytic mechanism of EZS though not *via* which mechanism.

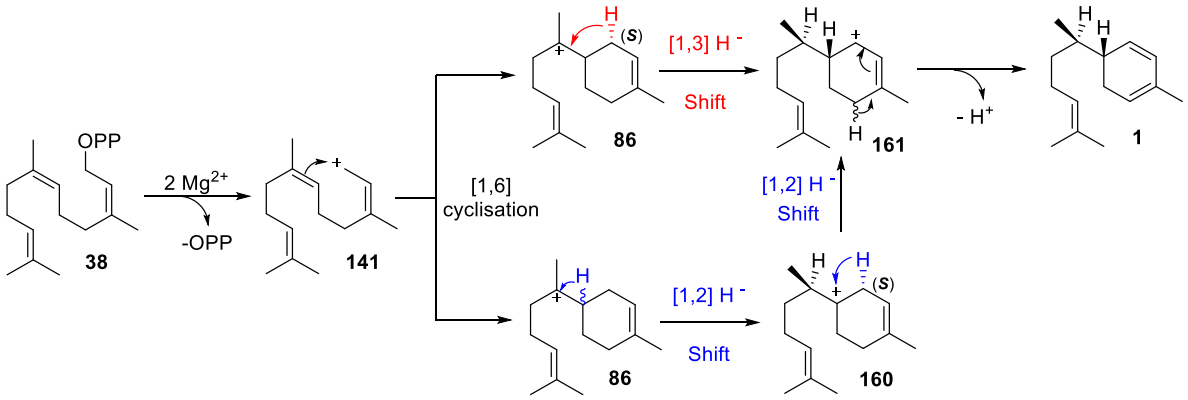

Figure 131. Possible roles of the *proS* proton at the C1 position during the catalytic mechanism of EZS.

4.4 Summary

This chapter outlined the synthesis of substrates designed to investigate the catalytic mechanism of 7-epizingiberene synthase. GC-MS analysis of the pentane extractable products from the incubation of substrates and EZS gave insights into carbocation intermediates and hydride shifts occurring during the catalytic mechanism.

The inhibition of EZS by (2*E*,6*Z*)-2-fluoro-FDP (**230**) gives evidence for a stepwise ring closure. The presence of fluorine at the C2 position resulted in the inhibition of EZS due to the electronegative nature of fluorine increasing the energy of the potential farnesyl cation (**238**, Figure 87). The increase in carbocation energy prevented the formation of the farnesyl cation (**238**), inhibition of the catalytic mechanism and evidence of a stepwise catalytic mechanism (Figure 91). (2*Z*,6*E*)-6-fluoro-FDP (**231**) was shown to be a competitive inhibitor of EZS *via* preventing the formation of the bisabolyl cation (**248**, Figure 92). The use of fluorinated analogues enabled clarification of two carbocation intermediates generated during the catalytic mechanism of EZS and elucidation of a stepwise mechanism (Figure 87)

The exact nature of the hydride shifts could not be inferred from analysis of the pentane extractable products arising from incubations of **233** and **234** with EZS. The mass spectrum of **234** and EZS product gives strong evidence that the *R* proton at the C1 position does not undergo hydride shifts. Insight into the role of the C1(*S*) proton from analysis of the pentane extractable products of **233** with EZS was not definitive, suggesting both [1,3] and consecutive [1,2] hydride shifts may be occurring.

233 and **234** were synthesised for the investigation of a mechanism that utilises a single pathway. Therefore, a mechanism could not be determined by incubation of **233** and **234** with EZS alone. It was proposed that resonance of the C2,C3 double bond could stabilise the carbocation formation caused by hydride shifts from the C1 position. The respective hydride shifts from the C5 position were thought to be less favourable as stabilisation *via* resonance is not possible. However, as no definitive shifts were concluded *via* the incubation of C1 deuterated analogues **233** and **234** with EZS, hydride shifts from the C5 position are plausible. The elucidation of hydride shifts occurring during the catalytic mechanism of EZS requires the synthesis of deuterated analogues at the (2*Z*,6*Z*)-(*S*)-[5-^{2}H]-farnesyl (**426**) diphosphate, (2*Z*,6*Z*)-(*R*)-[5-^{2}H]-farnesyl (**427**) diphosphate and (2*Z*,6*Z*)-[6-^{2}H]-farnesyl diphosphate (**232**). Analysis of the enzymatic products from the incubation of the deuterated analogues with EZS *via* GC-MS and ^{1}H NMR spectroscopy would enable the determination of hydride shifts.

Chapter 5 – Synthesis and Incubation of Substrates to Probe EZS Substrate Specificity

5.1 Preface

Literature regarding 7-epizingiberene synthase have stated that EZS will not except the 'universal substrate' (2*E*,6*E*) FDP (**31**) as a substrate showing high substrate specificity towards the *cisoid* isomer (2*Z*,6*Z*) FDP (**38**). This chapter outlines the synthesis of three stereoisomers of **38**; (2*E*,6*Z*) FDP (**342**), (2*E*,6*E*) FDP (**31**) and (2*Z*,6*E*) FDP (**341**). The substrate specificity of EZS was investigated by incubation of the respective compounds with EZS and analysis of the pentane extractable products *via* GC-MS.

The monoterpene substrate equivalents of **38** and **31** have also been synthesised. Sesquiterpene cyclases have been observed to utilise monoterpene substrates to generate terpenoid products.[42] Analysis of pentane extracts from the incubation of substrates **30** and **39** with EZS showed EZS accepted the monoterpene analogues as substrates; however, a large decrease in binding efficiency was observed when compared to the sesquiterpene substrates.

Figure 132 shows the analogues that were synthesised and incubated with EZS that will be discussed within this chapter:

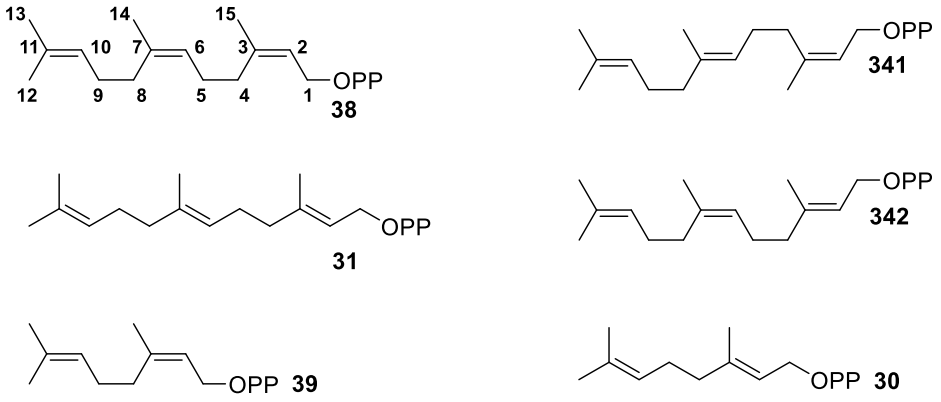

Figure 132. Sesquiterpenoid and monoterpenoid substrates used for the investigation of the substrate stereoselectivity of EZS.

As described in chapter 4, kinetic parameters for each compound were also measured to determine their potency and mode of action as inhibitors. Inhibition assays using neryl diphosphate (**39**) and geranyl diphosphate (**30**) were used to confirm substrate enzyme binding was occurring and approximate K_i values calculated from an IC50 plot.

5.2 (2*E*,6*Z*) farnesyl diphosphate (342)

5.2.1 Synthesis of (2*E*,6*Z*) farnesyl diphosphate (342)

The synthesis of (2*E*,6*Z*) farnesyl diphosphate (**342**) and subsequent incubation with EZS would show if the C2,C3 double bond stereochemistry is important for substrate turnover. Incubation of EZS with (2*E*,6*Z*) farnesyl diphosphate (**342**) could give further evidence of a stepwise or concerted ring closing mechanism as was inferred from analysis of (2*E*,6*Z*)-2-fluorofarnesyl diphosphate (**230**) as an inhibitor of EZS (Figure 87, 4.2.1). The bond orientation of the C2,C3 double bond is not aligned for an intramolecular S_N2-like reaction adopted by a concerted mechanism. A stepwise mechanism could permit the rotation of the C2,C3 double bond *via cis*-nerolidyl diphosphate (**344**) (Figure 133). A [1,6] cyclisation affording the bisabolyl cation (**86**), hydride shifts and deprotonation would then give 7-epizingiberene (**1**).

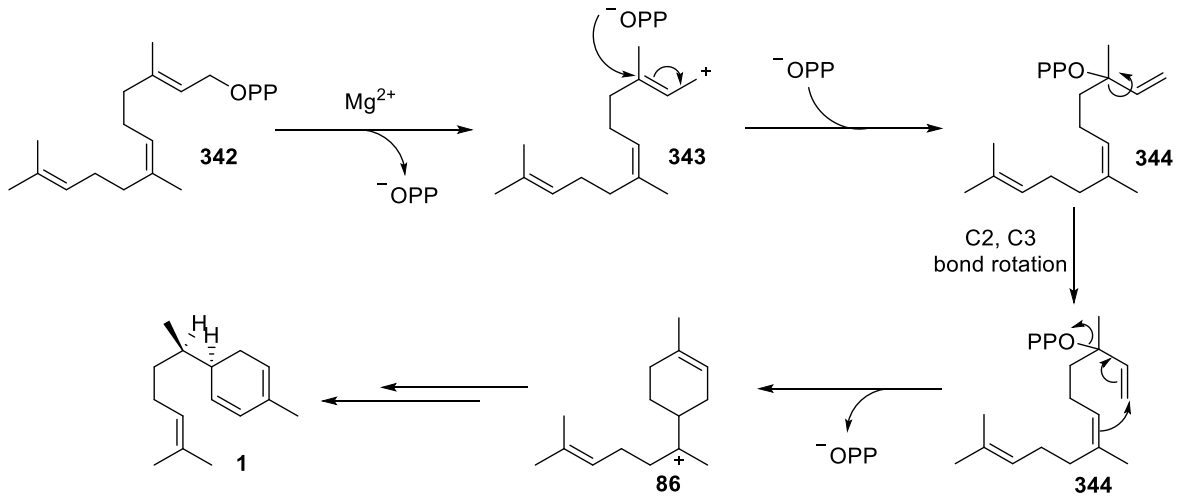

Figure 133. Potential outcome of the incubation of 342 with EZS *via* the *cis* nerolidyl diphosphate (344) intermediate.

The rotation of the C2,C3 double bond is not uncommon in sesquiterpene cyclase catalysis with the allylic transposition essential for a 1,6 cyclase like amorphadiene synthase (ADS) (Figure 14, 1.3.2).[246,117]

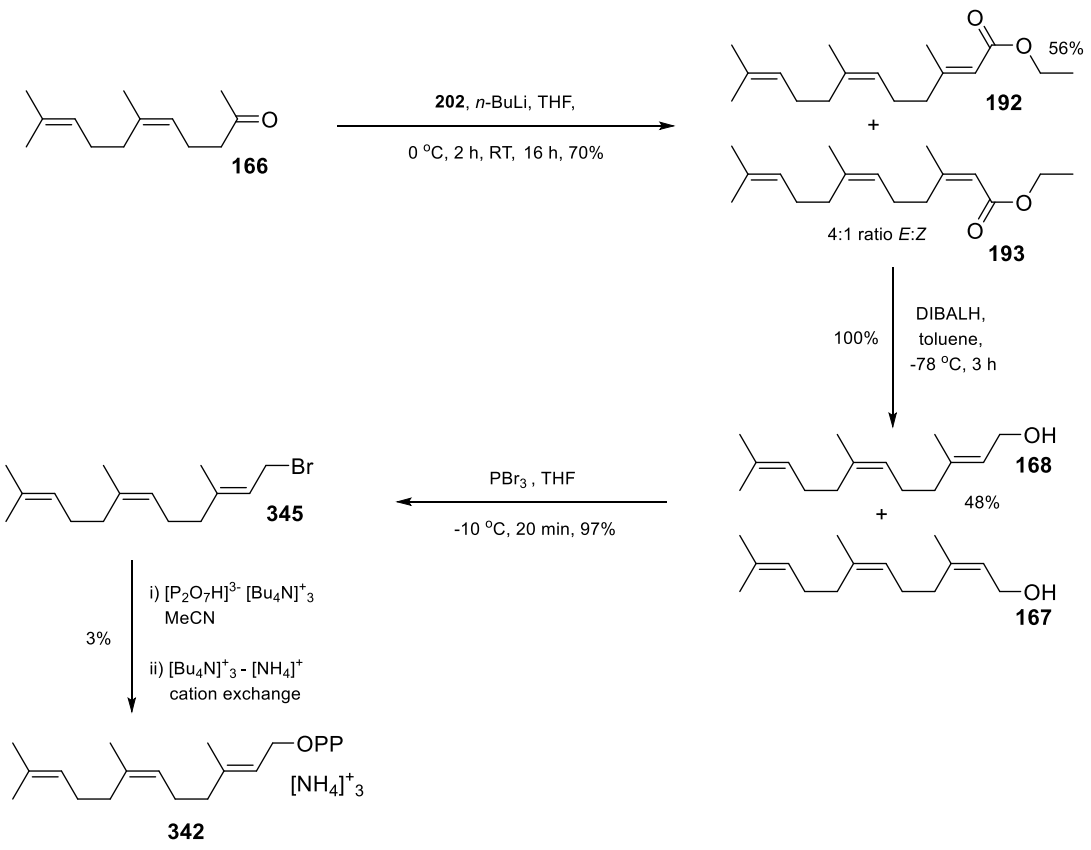

Figure 134. Synthesis of (2*E*,6*Z*) farnesyl diphosphate (342).

The synthesis of (2*E*,6*Z*) farnesyl diphosphate (**342**) is shown in Figure 134. Neryl acetone (**166**) was synthesised as previously described (Figure 34, 2.2.5). The synthesis of **342** was slightly modified to that of **38** (Figure 45, 2.2.1) where the olefination reaction conditions were altered for greater *E* selectivity of the C2,C3 double bond (Table 4, 2.2.5).

5.2.2 Incubation of (2*E*,6*Z*) farnesyl diphosphate (342) and EZS

GC-MS analysis of the pentane extractable products from the incubation of (2*E*,6*Z*) farnesyl diphosphate (**342**) with EZS showed no detectable enzymatic products even after extended reaction times. Kinetic parameters for **342** were measured to determine the potency and mode of action as an inhibitor. Increasing concentrations of **342**; 5 μM, 15 μM and 30 μM were used to understand the mode enzyme inhibition.

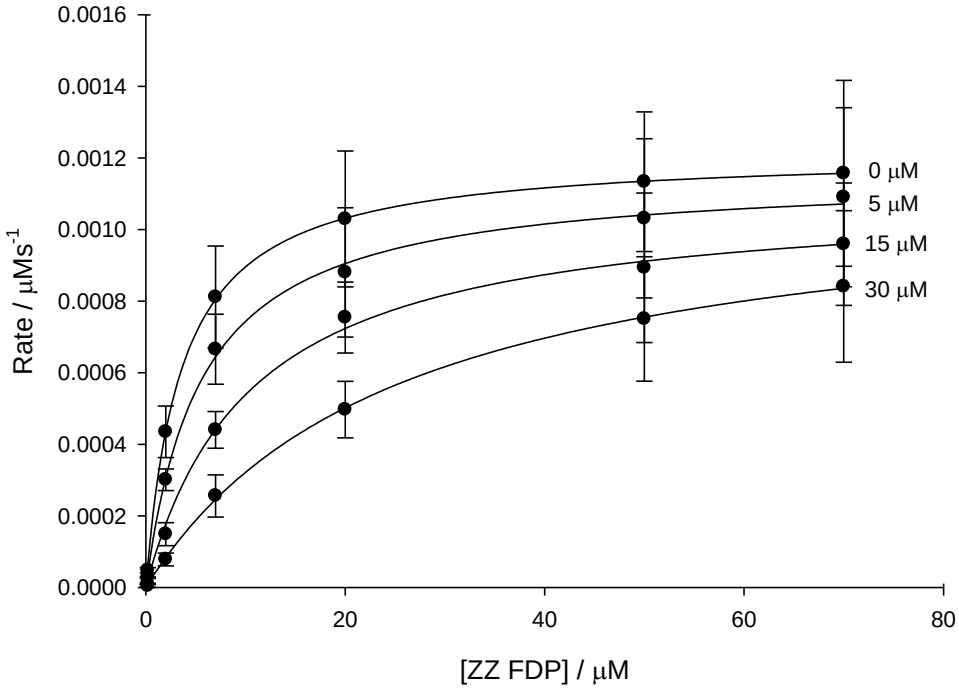

Figure 135. Michaelis-Menten plots for incubations of (2*Z*,6*Z*)-[1-^{3}H]-FDP (229) with EZS and inhibitor (2*E*,6*Z*) farnesyl diphosphate (342); 0 μM, 5 μM, 15 μM and 30 μM.

The overlaid curves of the Michaelis-Menten kinetics (Figure 135) show that inhibition of EZS occurs with increasing concentrations of (2*E*,6*Z*) farnesyl diphosphate (**342**) with observable changes to the rate with the increasing addition of **342**. The Lineweaver-Burk double-reciprocal plot shows the lines of different inhibitor concentration intercepting at one point on the y-axis (Figure 136). Interception at this point indicates **342** acts as a competitive inhibitor of EZS. Plotting $K_{M(app)}$ vs. inhibitor concentration allowed measurement of K_i = 2.86 ± 1.56 μM for (2*E*,6*Z*) FDP (**342**) (Figure 136).

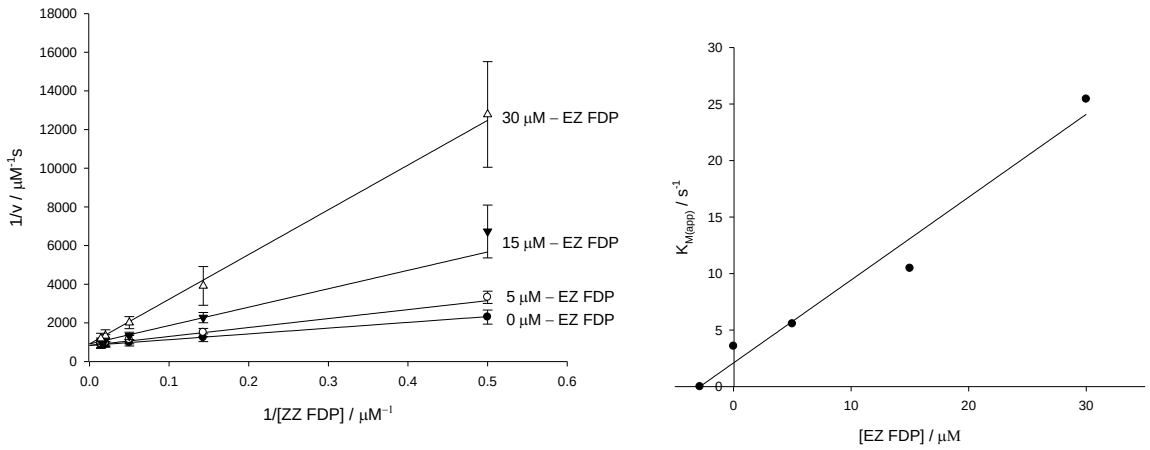

Figure 136. Lineweaver-Burke Plot (left) and $K_{M(app)}$ vs. concentration plot (right) for 342 inhibition assays.

The comparable K_M and K_i values of (2*Z*,6*Z*) FDP (**38**)(K_M = 6.24 ± 0.641 μM) and (2*E*,6*Z*) FDP (**342**) (K_i = 2.86 μM) shows EZS has a high affinity for **342**. The *trans* stereochemistry of the C2,C3 double bond does not appear to affect the binding efficiency of the enzyme-substrate complex however, *Z* conformation seems crucial for substrate activity. In contrast to studies previously conducted by the Allemann group on terpene cyclases such as ADS,[80] EZS appears unable to generate a nerolidyl diphosphate intermediate (**344**) for rotation of the C2,C3 bond to permit a [1,6] cyclisation (Figure 137).

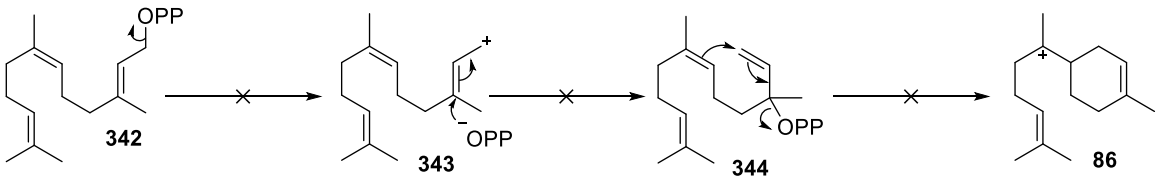

Figure 137. The unsuccessful turnover of (2*E*,6*Z*) farnesyl diphosphate (342) when incubated with EZS.

5.3 (2*Z*,6*E*) farnesyl diphosphate (341)

5.3.1 Synthesis of (2*Z*,6*E*) farnesyl diphosphate (341)

The C2, C3 double bond of (2*Z*,6*E*) farnesyl diphosphate (**341**) has *Z* stereochemistry and therefore ideally orientated for a [1,6] cyclisation. Figure 138 outlines potential mechanistic pathways if **341** was accepted as a substrate. Alternatively (2*Z*,6*E*) farnesyl diphosphate (**341**) may inhibit the enzyme suggesting that stereochemistry of the C6,C7 double bond and orientation of the prenyl tail influences substrate turnover.

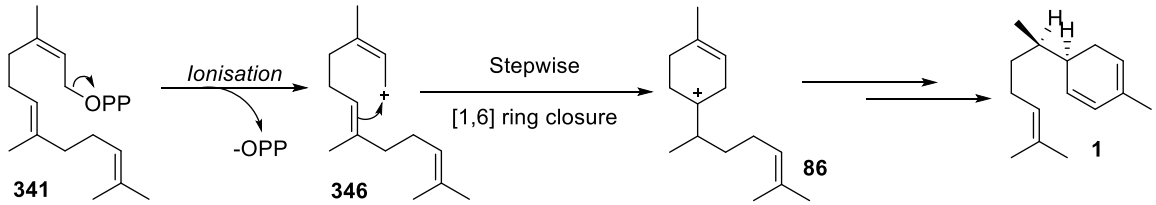

Figure 138. Potential catalytic mechanism of EZS when incubated with (2*Z*,6*E*) farnesyl diphosphate (341).

The synthesis of (2*Z*,6*E*) farnesyl diphosphate (**341**) was conducted following the procedure outlined in Figure 139. Substituting nerol (**163**) for geraniol (**64**) resulted in the C6,C7 *E* double bond of **341**. The instillation of the C2,C3 *Z* double bond was achieved *via* a Horner-Wadsworth-Emmons reaction using the optimised conditions in (Table 4, 2.2.5) for the synthesis of **38** (Figure 45, 2.2.5).

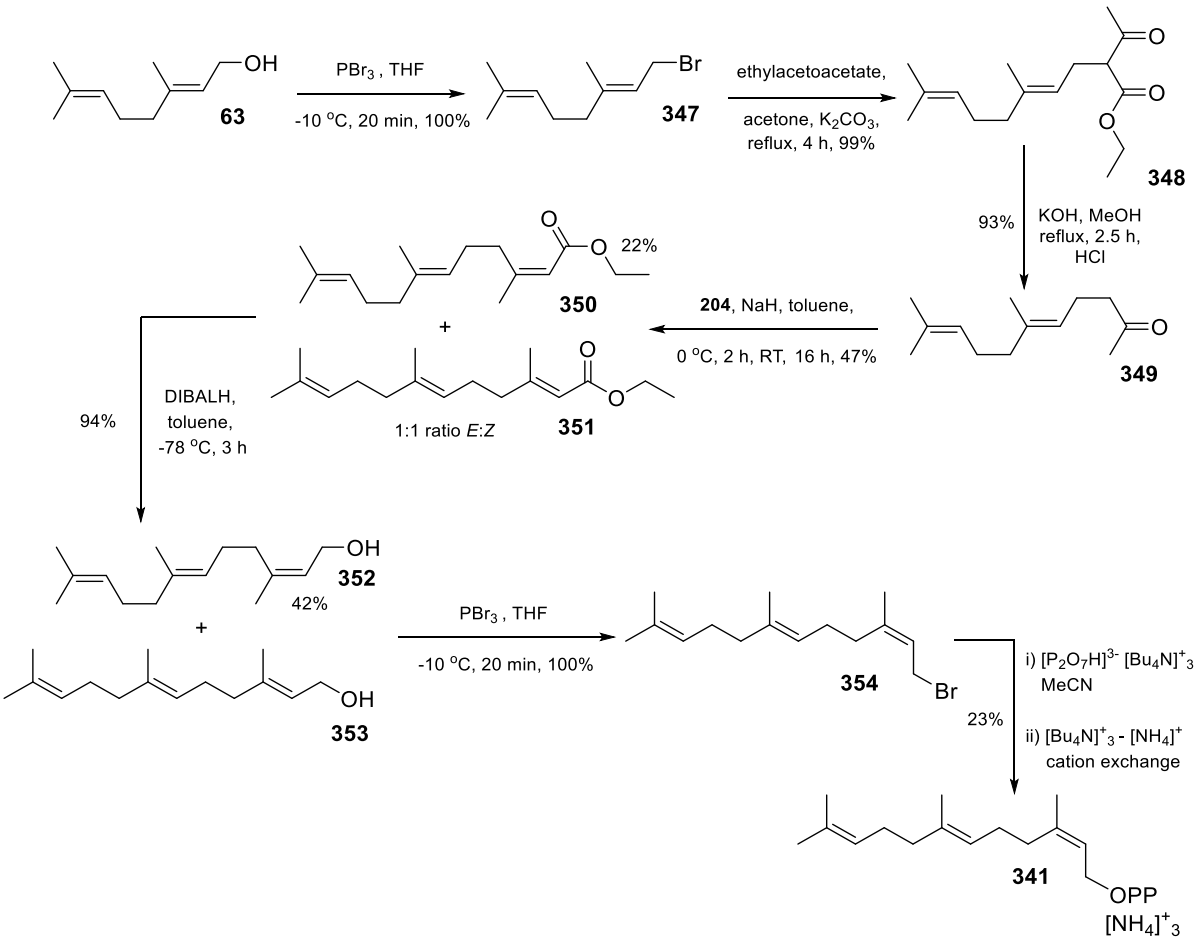

Figure 139. Synthesis of (2*Z*,6*E*) farnesyl diphosphate (341).

5.3.2 Incubation of (2*Z*,6*E*) farnesyl diphosphate (341) and EZS

GC-MS analysis of the pentane extractable products from the incubation of **341** with EZS showed no detectable enzymatic products were generated. Inhibition of EZS by **341** gives insight to the orientation of C6,C7 double required for the formation of product. Kinetic parameters for **341** were measured to determine the potency and mode of action as an inhibitor. Increasing concentrations of **341**; 5 μM, 15 μM and 30 μM were used to understand the mode enzyme inhibition.

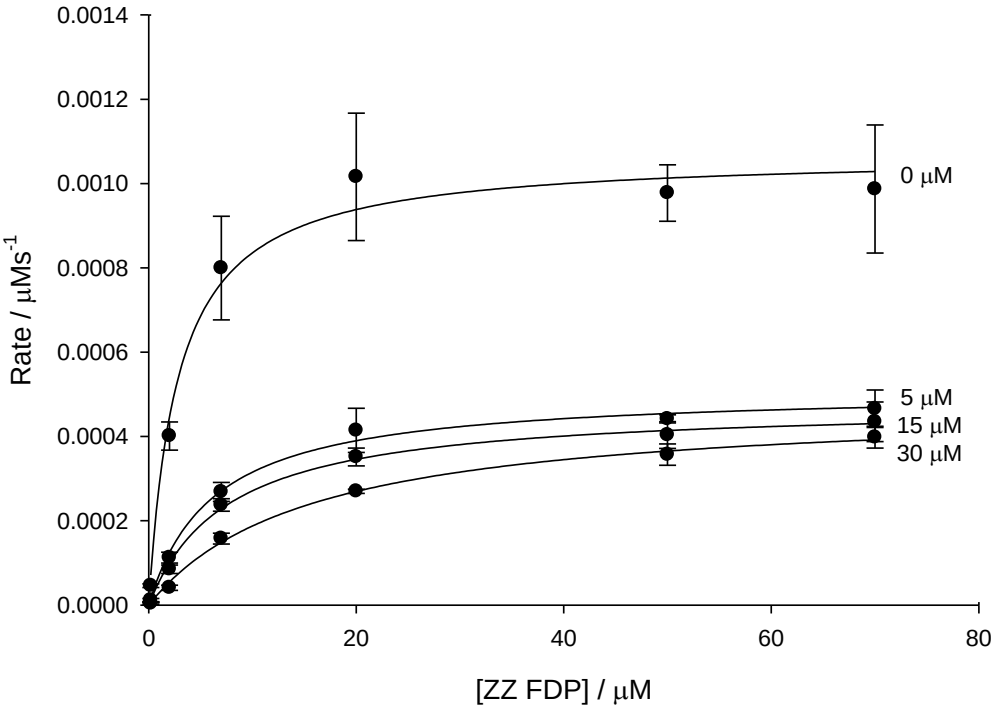

Figure 140. Michaelis-Menten plots for incubations of (2*Z*,6*Z*)-[1-^{3}H]-FDP (229) with EZS and inhibitor(2*Z*,6*E*) farnesyl diphosphate (341); 0 μM, 5 μM, 15 μM and 30 μM.

The Michaelis-Menten plots show a clear indication of inhibition with both V_{max} and $K_{M(app)}$ changing with addition of higher inhibitor concentrations (Figure 140). The mode of inhibition is not clear from this plot as the apparent variation of V_{max} could indicate uncompetitive or non-competitive modes of inhibition. However, the values of V_{max} are all of similar orders of magnitude and replotting the data as a Lineweaver-Burk double reciprocal plot (Figure 141) shows data trends characteristic of a competitive inhibitor with discrepancies of plotted data possibly caused by experimental error during the assay. A plot of $K_{M(app)}$ against (2*Z*,6*E*) FDP (**341**) concentration gave an inhibitor K_i of 7.64 ± 0.83 μM (Figure 141). This value is within the same magnitude as K_M and K_i of (2*Z*,6*Z*) FDP (**38**)(K_M = 6.24 ± 0.641 μM) and (2*E*,6*Z*) FDP (**342**) (K_i = 2.86 ± 1.56 μM). The comparative K_i value of **341** to **342** and the K_M of **38** gives evidence that the stereochemistry of the C6,C7 double bond does not retract from the formation of the enzyme-substrate complex.

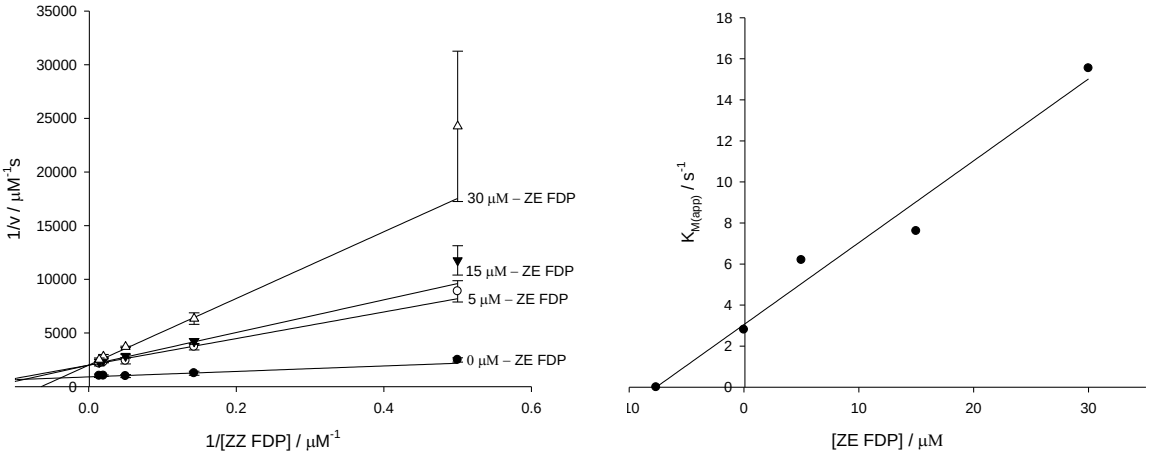

Figure 141. Lineweaver-Burke Plot (left) and $K_{M(app)}$ vs. concentration plot (right) for 341.

The *Z* conformation of the C2,C3 double bond makes a 1,6 cyclisation plausible. However, inhibition of EZS when incubated with **341** gives evidence that the stereochemistry of the C6,C7 double bond is crucial for product formation (Figure 142).

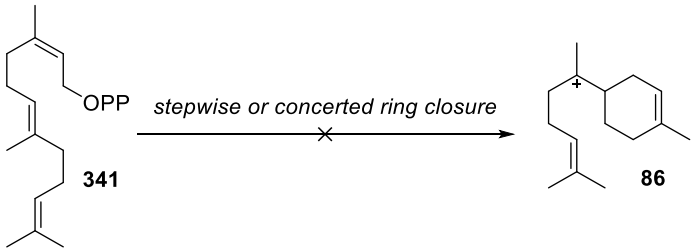

Figure 142. The unsuccessful turnover of (2*Z*,6*E*) farnesyl diphosphate (341) when incubated with EZS.

5.4 (2*E*,6*E*) farnesyl diphosphate (31)

5.4.1 Synthesis of (2*E*,6*E*) farnesyl diphosphate (31)

The investigation by Bleeker *et al.,*[3] showed the incubation of EZS with (2*E*,6*E*) farnesyl diphosphate (**31**) resulted in no enzymatic products.[3] **31** is the natural substrate of sesquiterpene cyclases with EZS, santalene and bergamotene synthase (SBS) being the known exceptions.[131, 3] The preparation of **31** was required to corroborate results with published data.

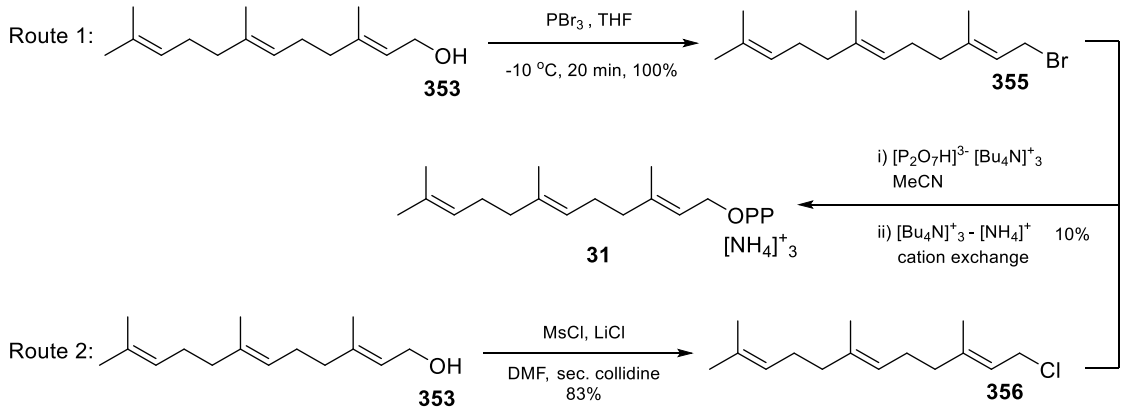

Figure 143. Synthesis of (2*E*,6*E*) farnesyl diphosphate (31) *via* halide intermediates 355 or 356.

Synthesis of **31** proceeded *via* three different methods. Routes 1 and 2 investigated different halogenation protocols prior to the diphosphorylation reaction and purification previously discussed. Route 1 proceeded *via* a phosphorus tribromide bromination which achieved crude bromide **355** with 100% yield and route 2 proceeded through a chlorination outlined by Collington *et al.,*[247] and Davisson *et al.*[188] Mesyl chloride and *sec*. collidine were added to a mixture of **353** in DMF at 0 °C and stirred for 30 minutes. Lithium chloride was added to the reaction mixture and stirred for a further two hours and the reaction quenched with water giving the crude chloride **356** with 83% yield. The halogenations were both effective however, route 1 was favourable due to the shorter reaction time and higher percentage yield.

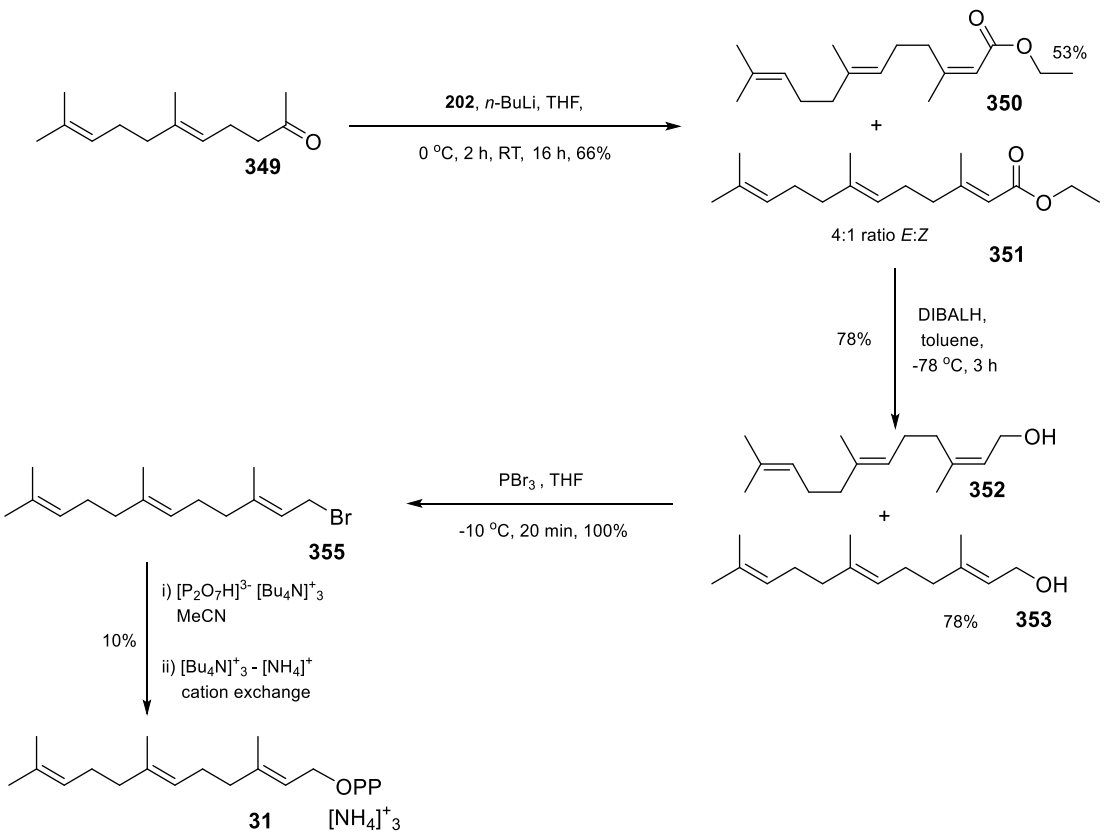

Figure 144. Synthesis of (2*E*,6*E*) farnesyl diphosphate (31).

Route 3 was based on the synthesis of **38** (Figure 45, 2.2.5) and is outlined in Figure 144 and was investigated to utilise side product from the synthesis of (2*Z*,6*E*) farnesyl diphosphate (**341**) (Figure 139). Modifications to the synthesis of **31** were the reaction conditions used for the olefination of **38**. As outlined in (Table 4, 2.2.5), the use of **204** and *n*-butyl lithium with tetrahydrofuran gave the greatest yield and ratio of *E*:*Z* isomers. Farnesoate esters **350** and **351** were partially separated for analysis prior to being pooled and reduced to the corresponding alcohols **352** and **353** which were separated *via* flash chromatography prior to bromination.

5.4.2 Incubation of (2*E*,6*E*) farnesyl diphosphate (31) and EZS

The incubation of (2*E*,6*E*) farnesyl diphosphate (**31**) with EZS and subsequent GC-MS analysis of the pentane extractable products showed no enzymatic products. This result is in agreement with literature as **31** was proposed to not be a substrate of EZS.[3] The substrate's affinity to the enzyme or subsequent mode of inhibition was not investigated within the literature. Therefore, kinetic parameters for **31** were measured to determine the potency and mode of action as an inhibitor. Increasing concentrations of **31**; 5 μM, 15 μM and 30 μM were used to understand the mode enzyme inhibition.

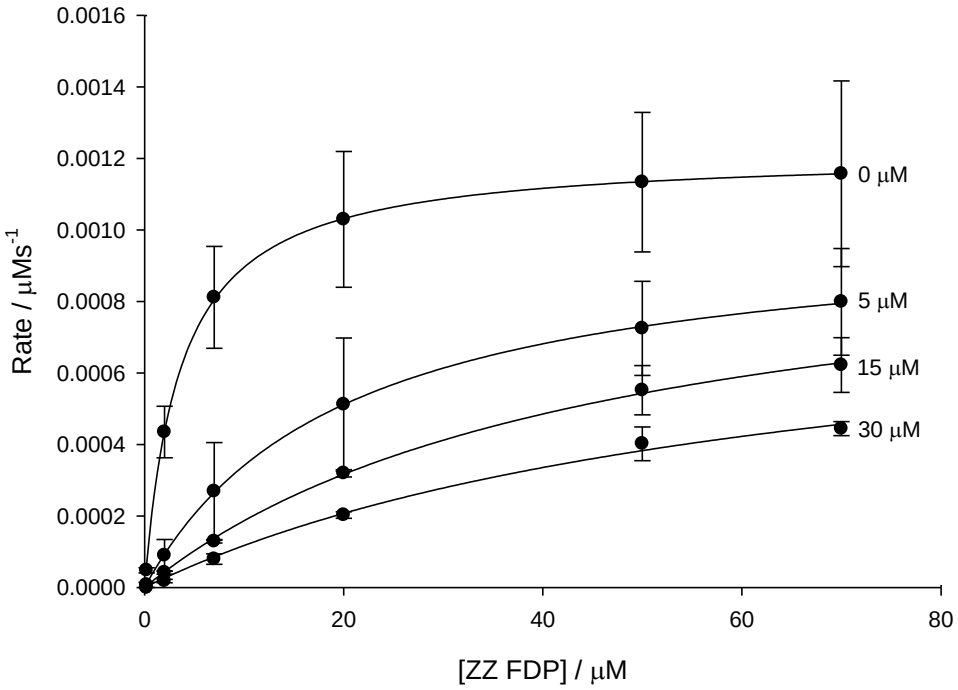

Figure 145. Michaelis-Menten plots for incubations of (2*Z*,6*Z*)-[1-^{3}H]-FDP (229) with EZS and inhibitor (2*E*,6*E*) farnesyl diphosphate (31); 0 μM, 5 μM, 15 μM and 30 μM.

Assays of previously discussed substrates **341** and **342** have shown that *Z* stereochemistry of the substrates double bonds are required for product formation. It has also been shown that other stereoisomers of (2*Z*,6*Z*) FDP (**38**); **341** and **342** act as competitive inhibitors. The Michaelis-Menten plots (Figure 145) of the increasing inhibitor concentrations used and the respective Lineweaver-Burke plot show that (2*E*,6*E*) FDP (**31**) acts as a competitive inhibitor. The plot of $K_{M(app)}$ against **31** concentration (Figure 146) gives a K_i of 4.17 ± 0.29 μM, consistent with values found for stereoisomers **341** and **342**.

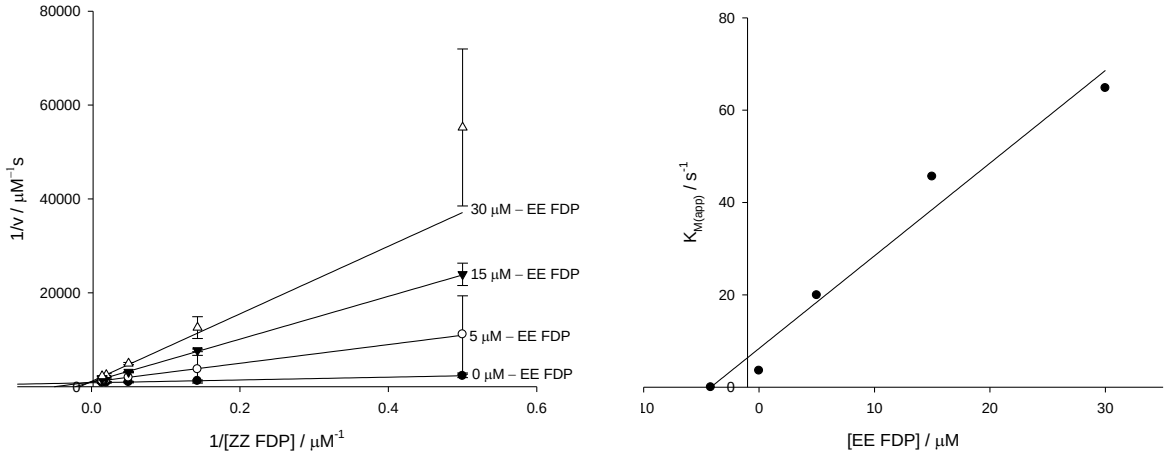

Figure 146. Lineweaver-Burke Plot (left) and $K_{M(app)}$ vs. concentration plot (right) for 31 inhibition assay.

An enzymatic product was not observed from the pentane extractable products from the incubation of (2*E*,6*E*) farnesyl diphosphate (**31**) with EZS. This gives evidence that EZS is not able to invert the stereochemistry of the C2, C3 double bond and undergo a [1,6] cyclisation giving the bisabolyl cation (**86**) (Figure 147). Kinetic assays of **31** and the subsequent fitting of data to a Michaelis-Menten curve and Lineweaver Burke plot shows **31** inhibits the catalytic mechanism of EZS. The Lineweaver Burke plot shows the data points for each concentration of **31** intercepts at the same point at the y-axis, characteristic of a competitive inhibitor with a plot of [**31**] vs. $K_{M(app)}$ giving K_i values at similar concentrations observed for other stereoisomers.

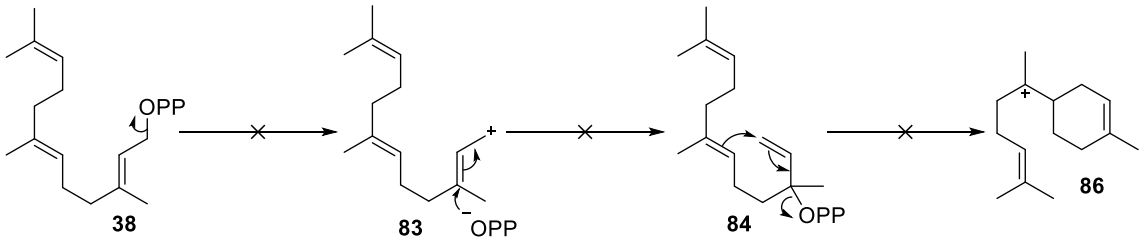

Figure 147. The unsuccessful turnover of (2*E*,6*E*) farnesyl diphosphate (31) when incubated with EZS.

5.5 Neryl diphosphate (39) and geranyl diphosphate (30)

5.5.1 Synthesis of neryl diphosphate (39) and geranyl diphosphate (30)

Sesquiterpene cyclases have been reported to accept monoterpene diphosphates neryl diphosphate (**39**) and geranyl diphosphate (**31**)[48] as substrates. The C2,C3 double bond of **39** positions the diphosphate in the correct conformation for a [1,6] cyclisation to give the α-terpinyl cation (**357**). Various hydride shifts, cyclisations and deprotonations can give rise to numerous monoterpene products including terpenines such as α-terpenine (**52**),[43] bicyclic products e.g. α-pinene (**49**) and phellandrenes such as α-phellandrene (**358**) (Figure 148).[44]

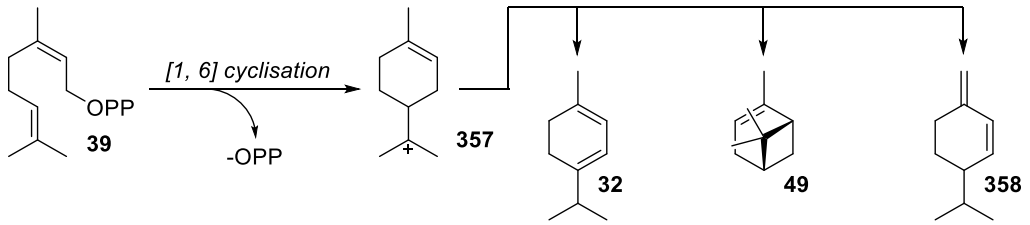

Figure 148. Potential catalytic products of EZS incubation with neryl diphosphate (39).

Neryl diphosphate (**39**) and geranyl diphosphate (**30**) were synthesised *via* the reaction pathways outlined in Figure 149 and Figure 150 respectively. PBr_3 bromination of the alcohol precursors **166** and **63** was preferred over other methods investigated (Figure 147). The crude bromides were used without purification, diphosphorylated and purified in the manner previously outlined for the synthesis of **38** (Figure 45, 2.2.5).

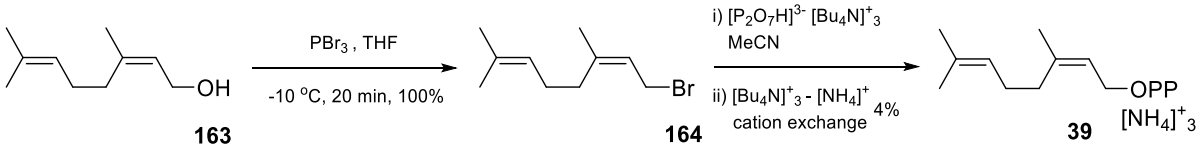

Figure 149. Synthesis of neryl diphosphate (39).

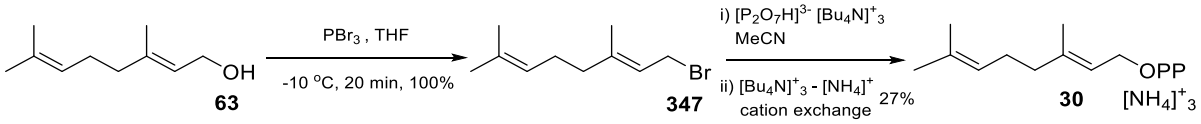

Figure 150. Synthesis of geranyl diphosphate (30).

5.5.2 Incubation of neryl diphosphate (39) and EZS

The incubation of neryl diphosphate (**39**) with EZS and analysis of the pentane extractable products *via* GC-MS showed a single peak in the total ion chromatogram of **39** incubations with EZS and without EZS (Figure 151). The mass-spectrum of the compound responsible for each peak was cross referenced with the National Institute of Standards and Technology (NIST) library and found to be limonene. The *Z* stereochemistry of the C2,C3 double bond of **39** positions the analogue for a [1,6] cyclisation upon the loss of the diphosphate moiety. The presence of Mg^{2+} ions within the incubation buffer can assist the cleavage of diphosphate yielding the neryl cation. Cyclisation and deprotonation can give limonene without enzymatic catalysis.

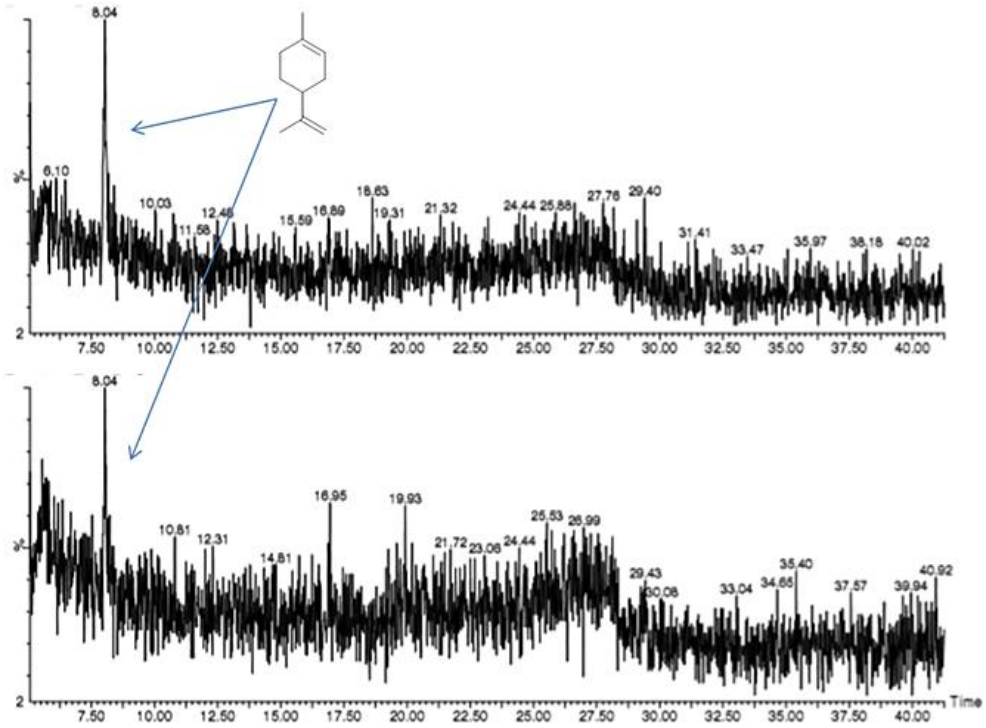

Figure 151. Total ion chromatograms of pentane extractable products from neryl diphosphate (39) incubations: neryl diphosphate (39) and EZS incubation (upper) and neryl diphosphate (39) with no EZS incubation (lower).

Analysis of the pentane extracts from the incubation *via* GC-MS showed no enzymatic products were present. An inhibition assay increasing the concentration of neryl diphosphate (**39**) whilst keeping the concentration of (2*Z*,6*Z*)-[1-^{3}H]-FDP (**229**) constant was performed. The assay was used to assess if neryl diphosphate (**39**) was binding to EZS or cyclising prior to the formation of the enzyme-substrate complex due to Mg^{2+} ions within the incubation buffer.

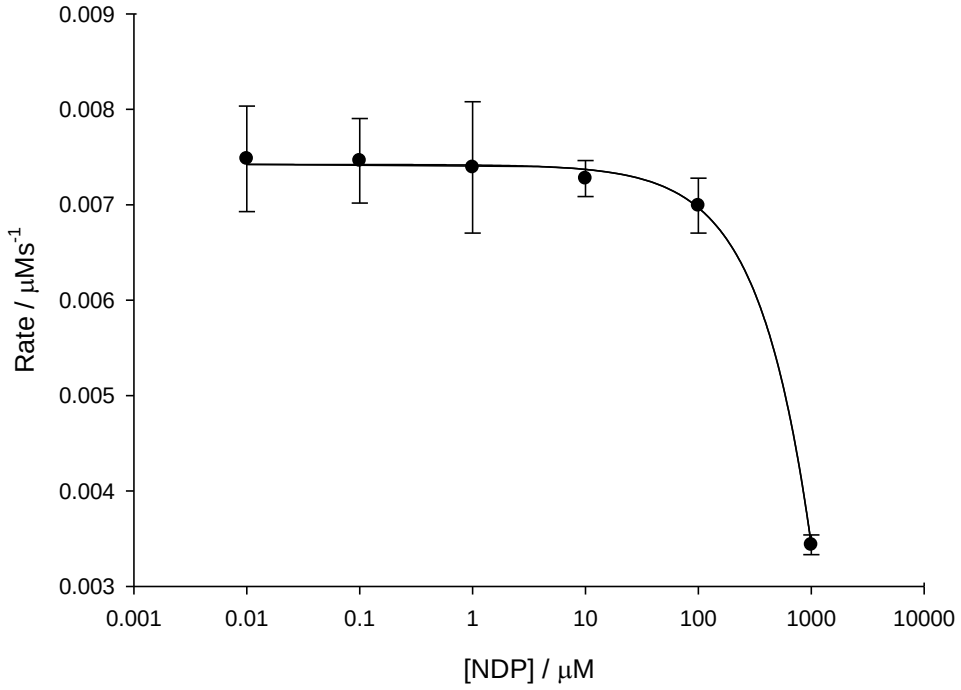

Figure 152. 39 IC50 plot for the incubation of (2*Z*,6*Z*)-[1-^{3}H]-FDP (229)with EZS and inhibitor neryl diphosphate (39); 0.01 µM - 1000 µM range.

The IC50 plot shows an approximate K_i of neryl diphosphate (**39**) as 474 ± 24 µM (Figure 152). In comparison to previous inhibitors incubated with EZS, the enzyme exhibited low affinity towards **39**. As previously discussed, the ability of **39** to cyclise due to Mg^{2+} ions within the buffer may be a major reason for the low binding efficiency. The substrate may not be able to form the enzyme-substrate complex as cyclisation had already occurred. The shorter chain length of **39** in comparison to the natural substrate (2*Z*,6*Z*) farnesyl diphosphate (**38**) may also play a role in binding. It has been observed that the stereochemistry of the C2,C3 and C6,C7 double bonds are critical for product formation. However, the differing stereochemistry has not greatly affected the binding efficiency of the substrate to the enzyme. Binding of the diphosphate moiety to the DDxxE motif of EZS aids the removal of diphosphate. However, the large approximated K_i value from the incubation of **39** with EZS gives evidence that the prenyl tail contributes to substrate anchorage within the active site.

5.5.3 Incubation of geranyl diphosphate (30) and EZS

GC-MS analysis of the pentane extractable products from the incubation of **30** with EZS showed no enzymatic products. In contrast to **39**, geranyl diphosphate (**30**) has not been known to cyclise due to Mg^{2+} ions within catalysis buffer. The *E* stereochemistry of the C2,C3 double bond does not orientate the molecule into a favourable conformation for a [1,6] cyclisation. An inhibition assay increasing the concentration of geranyl diphosphate (**30**) and constant [**229**] was performed determine if **30** was binding with EZS and if applicable, an approximate K_i value.

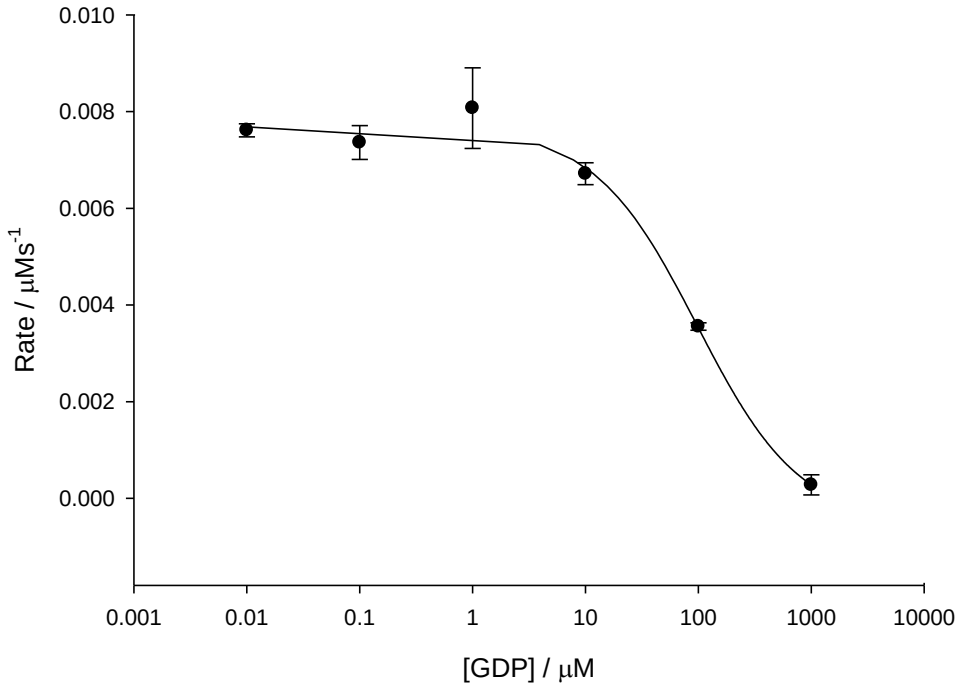

Figure 153. 30 IC50 plot for the incubation of (2*Z*,6*Z*)-[1-^{3}H]-FDP (229) with EZS and inhibitor geranyl diphosphate (30); 0.01 μM - 1000 μM range.

The IC50 plot shows that **30** does bind to EZS and inhibits the enzyme with an approximate K_i of 97.3 ± 24.6 μM (Figure 153). Though significantly tighter binding to EZS than observed with **39**, this value is an order of magnitude greater than seen with farnesyl substrates. The large approximated K_i value in comparison to farnesyl substrates gives further evidence to the importance of the prenyl chain to binding as part of the enzyme-substrate complex. The farnesyl substrate equivalent, (2*E*,6*E*) FDP (**31**), exhibited a K_i of 4.17 μM giving evidence further that the prenyl tail contributes towards substrate binding.

5.6 Summary

This chapter has focussed on the synthesis of FDP isomers and the analysis of enzymatic products from substrate incubations with EZS. Substrate specificity of EZS towards (2*Z*,6*Z*) FDP (**38**) and inhibition of enzymatic activity when incubated with analogues **342**, **341** and **31** show the necessity for any novel substrate to contain all *Z* double bonds.

Though the stereochemistry **342**, **341** and 31 did not yield enzymatic product when incubated with EZS; the enzyme still exhibited a strong affinity to the FDP analogues which were shown to act as competitive inhibitors with K_i values similar to the K_M of (2*Z*,6*Z*) FDP (**38**). The inhibition of the catalytic mechanism by the various analogues shows that the stereochemistry of the C2,C3 and C6,C7 double bonds are vital for product formation.

EZS is unable to isomerise the stereochemistry of the C2,C3 double *via* the nerolidyl diphosphate intermediate (**344**) as observed in the catalytic mechanisms other sesquiterpene cyclases.[104] The C6,C7 bond also has a role on product formation and appears to inhibit substrate turnover. This may result from orientation of the substrate in the active site preventing the [1,6] cyclisation occurring.

Neryl diphosphate (**39**) and geranyl diphosphate (**30**) incubations with EZS did not yield enzymatic products. Approximate K_i values calculated from the IC50 curves for NDP (**39**) (Figure 152) and GDP (**30**) (Figure 153) showed a low affinity of EZS to both analogues. This low affinity gives some evidence that the prenyl tail has a role in binding within the enzyme-substrate complex with removal of the prenyl group decreasing the binding efficiency of EZS towards the substrate. A comparison of K_i values can be observed in Table 8.

Table 8. Inhibition constants (K_i) of sesquiterpenoid and monoterpenoid substrates with EZS.

Analogue	K_i / µM
(2*E*, 6*Z*) farnesyl diphosphate (**342**)	2.86 ± 1.56
(2*Z*, 6*E*) farnesyl diphosphate (**341**)	7.64 ± 0.83
(2*E*, 6*E*) farnesyl diphosphate (**31**)	4.17 ± 0.29
Neryl diphosphate (**38**)	*474 ± 24
Geranyl diphosphate (**30**)	*97.3 ± 24.6

*approximate value from IC50 curve

Chapter 6 – Synthesis of Novel Substrates and Incubation with EZS

6.1 Preface

This chapter outlines the synthesis of novel oxygen containing and methylated (2*Z*,6Z) FDP (**38**) analogues to be incubated with EZS with the aim of producing new sesquiterpenoids (Figure 154).

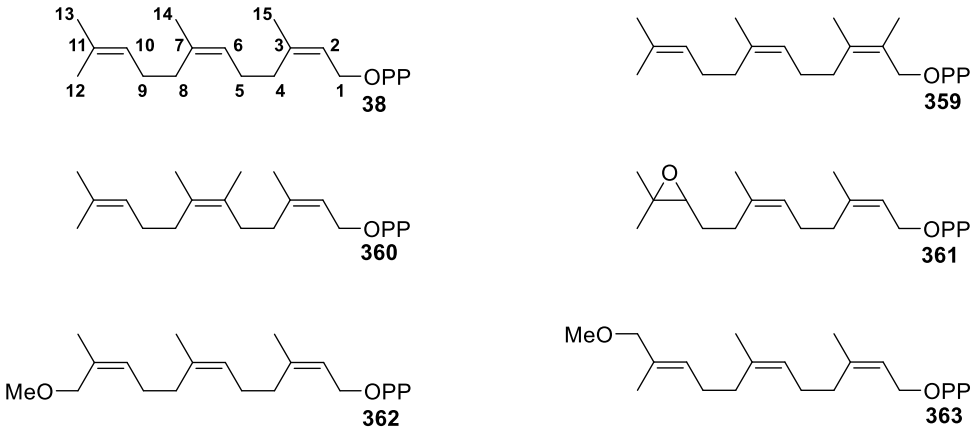

Figure 154. Novel sesquiterpene analogues of (2*Z*,6*Z*) FDP (38) discussed in this chapter.

The analogues were incubated with EZS as described in previous chapters. Products of successful incubations of analogues with EZS were analysed *via* GC-MS and compared to entries in the National Institute of Standards and Technology (NIST) library. The fragmentation patterns of novel products were compared with library data to give insight into plausible products based on existing sesquiterpene backbones. If no enzymatic product was observed, an inhibition assay and IC50 plot was used to establish that the analogue was binding to the enzyme and an approximate $K_{i.}$

6.2 Methylated substrates

6.2.1 Synthesis of (2*Z*,6*Z*)-2-methylfarnesyl diphosphate (359)

The incubation of (2*E*,6*E*)-14,15-dimethylfarnesyl diphosphate (**158**) with germacrene D synthase (GDS) resulted in an attractant semiochemical (Figure 30, 1.6.4) with properties in direct contrast to the repellent germacrene D (Figure 29, 1.6.9). (2*Z*,6*Z*)-2-Methylfarnesyl diphosphate (**359**) was synthesised with this result in mind, with the potential to form methylated zingiberene product **366** upon incubation with EZS. Methyl groups would lower the energy of neighbouring carbocation **364** (Figure 155) through electron donation. However, substrate binding may be hindered by adverse steric interactions resulting in inhibition of EZS rather than the formation of enzymatic product.

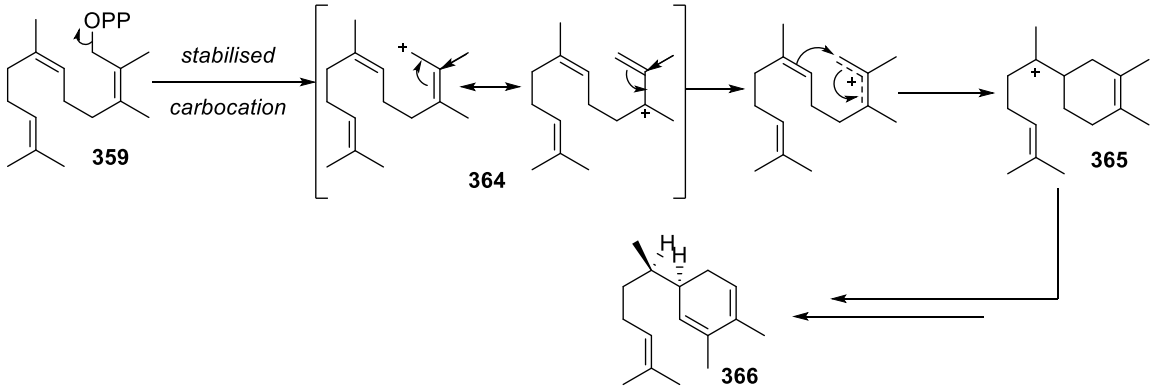

Figure 155. Potential outcome of the incubation of EZS and 359 showing the electron donation of the methyl substituent towards neighbouring carbocations.

A methylated Horner-Wadsworth-Emmons reagent (**368**) was synthesised to introduce a methyl substituent at the C2 position. An Arbuzov reaction[248] yielded phosphonoacetate ester (**368**) which was trimethyl silylated, chlorinated then reacted with 2,2,2-trifluoroethanol (**207**) to yield a methylated Still-Gennari variant[204,205] reagent **371** (Figure 156).

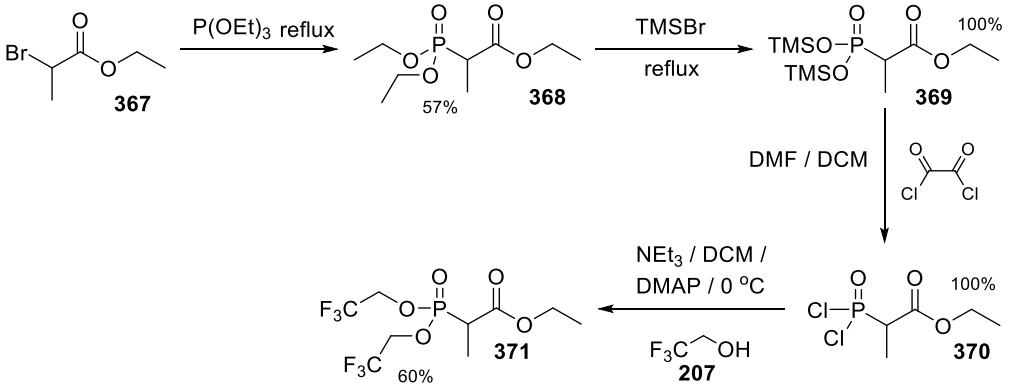

Figure 156. Synthesis of methylated Still-Gennari/Horner-Wadsworth-Emmons reagent 371.

Reagent **371** was used for the olefination of neryl acetone (**166**), which was prepared as previously described (Figure 34, 2.2.1). The synthetic procedure progressed by the DIBALH reduction of the resultant methylated ethyl farnesoates esters **372** and **373** to their respective alcohols **374** and **375**. PBr_3 bromination and subsequent diphosphorylation yielded (2*Z*,6*Z*)-2-methylfarnesyl diphosphate (**359**) (Figure 157).

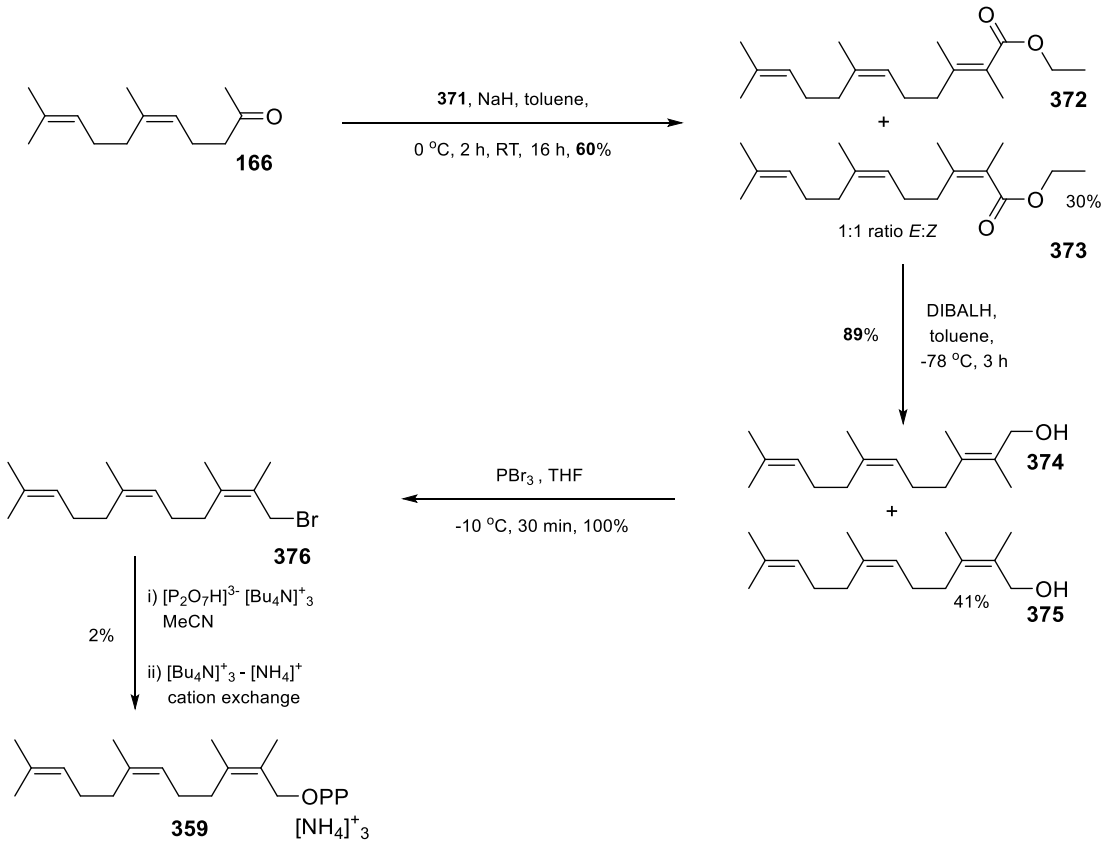

Figure 157. Synthesis of (2*Z*,6*Z*)-2-methylfarnesyl diphosphate (359).

Reagent **371** and commercially available **368** were used in respective olefinations of **166**. The Still-Gennari modification showed no improvement in stereocontrol, with both reagents yielding a 1:1 ratio of *E*:*Z* methylated farnesoates esters **372** and **373**. Unlike fluorinated analogues, bromination of **375** with phosphorus tribromide was not hindered by the presence of a methyl group.

6.2.2 Incubation of (2*Z*,6*Z*)-2-methylfarnesyl diphosphate (359) with EZS

Incubation of (2*Z*,6*Z*)-2-methylfarnesyl diphosphate (**359**) and EZS yielded six pentane extractable products (Figure 158). Three products (peaks at 18.14, 19.33 and 24.11 minutes) were shown not to be enzymatic products by comparison with a control experiment containing **359** in solution with no enzyme (Figure 159). Despite no impurities being visible in the ^{1}H NMR spectrum or UV trace of HPLC of **359**; the total ion chromatogram of pentane extractable products of the starting material showed the same impurities observed in the **359**/EZS incubation (Figure 160). However, three peaks corresponding to enzymatic products from the incubation of **359** and EZS were eluted at 15.38, 18.17 and 18.44 minutes. On the mass-spectra, all products had a molecular parent ion consistent with methylated products at *m/z* = 218. The generation of multiple sesquiterpenoid products resulting from (2*Z*,6*Z*)-2-methyl-FDP (**359**) incubation suggests EZS possesses a degree of promiscuity that has not previously been observed.

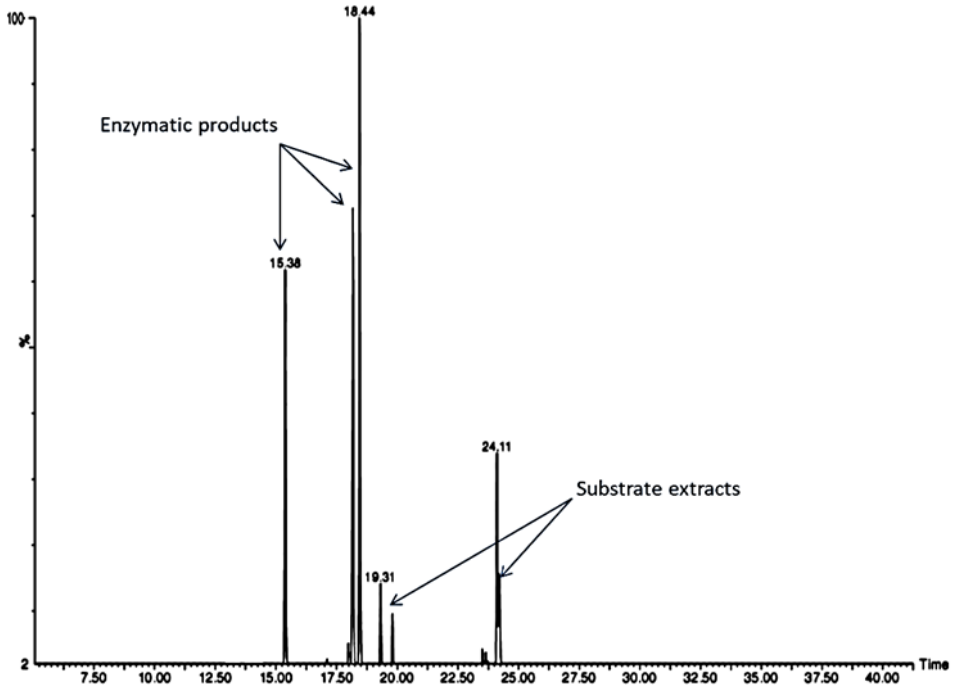

Figure 158. Total ion chromatogram of the pentane extractable products from incubation of 359 with EZS.

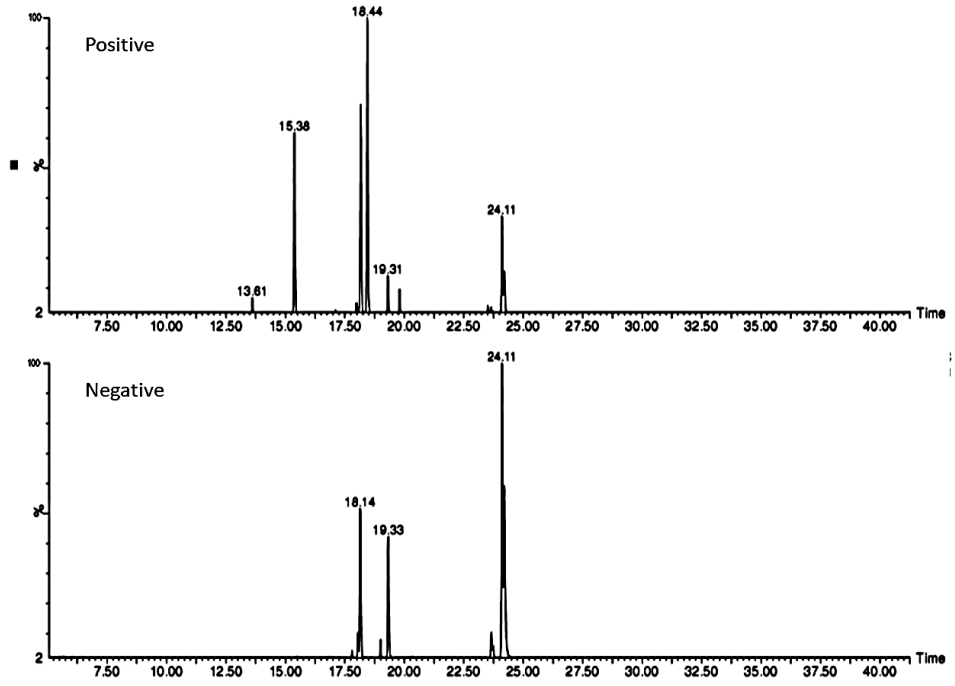

Figure 159. Total ion chromatogram of the pentane extractable products from; incubation of 359 with EZS (positive, top) and 359 without EZS (negative, bottom).

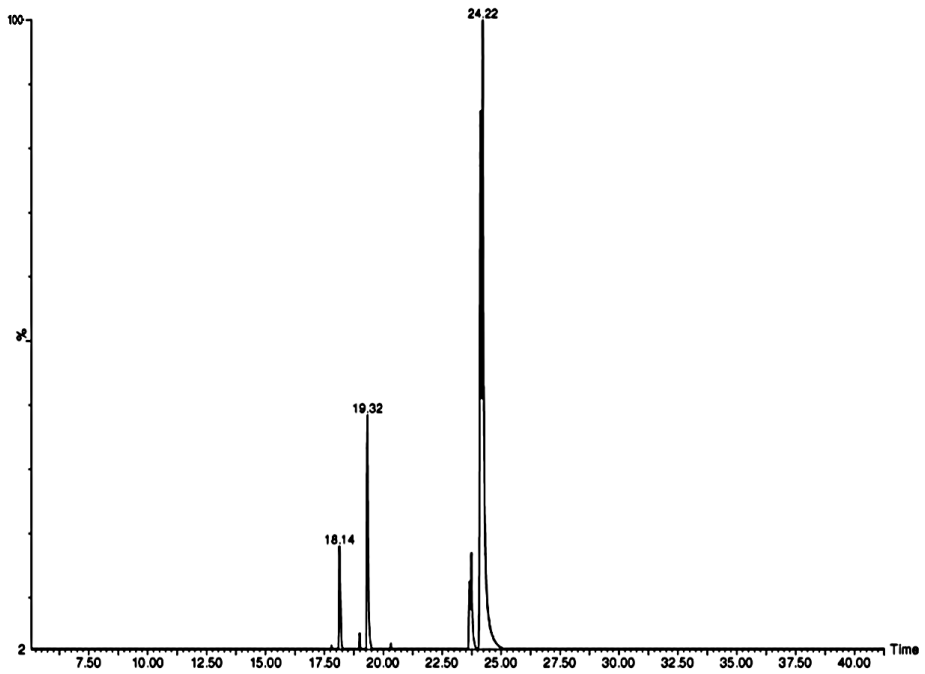

Figure 160. Total ion chromatogram of the pentane extractable extracts of substrate 359.

The peak at 15.38 minutes was determined to be 2-methylfarnesene comparison to the mass spectrum of farnesene products synthesised from (2*Z*,6*Z*)-2-methylfarnesol (**375**). The peak at 18.17 minutes had a mass spectrum splitting pattern consistent with a zingiberene product (Figure 163). When compared to the mass spectrum of 7-epizingiberene, (Figure 60, 2.6), all major fragments were present with *m/z* values increased by 14, indicating a methylated product (Figure 162). As observed from the incubation and kinetics assays using (2*E*,6*Z*)-2-fluoro-FDP (**230**) (Figure 89, 4.2.2) the mechanism of EZS is likely to proceed *via* the farnesyl cation (**364**). The incorporation of a methyl group at the C2 position would stabilise cation formation through inductive effects. It is plausible that a [1,6] ring closure and required hydride shifts could proceed following the removal of the diphosphate group as the substrate has the same stereochemistry as (2*Z*,6*Z*) FDP (**38**) (Figure 161).

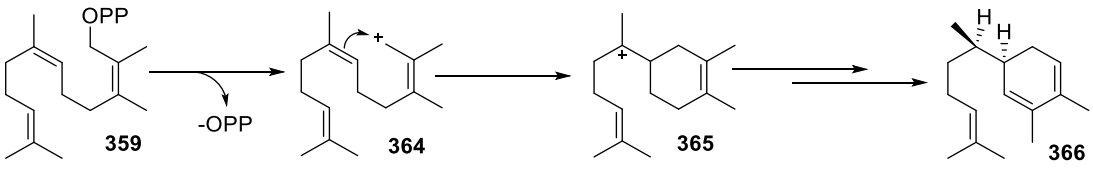

Figure 161. Potential outcome of 359 incubation with EZS.

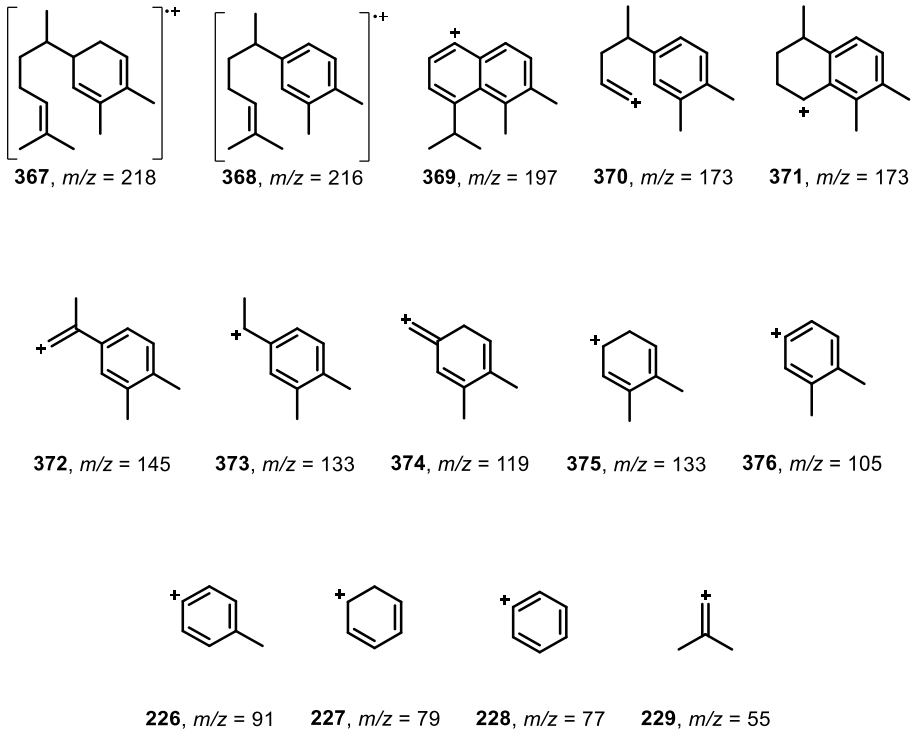

Figure 162. Possible fragmentations of 371 and the respective *m/z* values; *m/z* values of fragmentations in the upper and middle rows and increase by 14 due to methyl substituent.

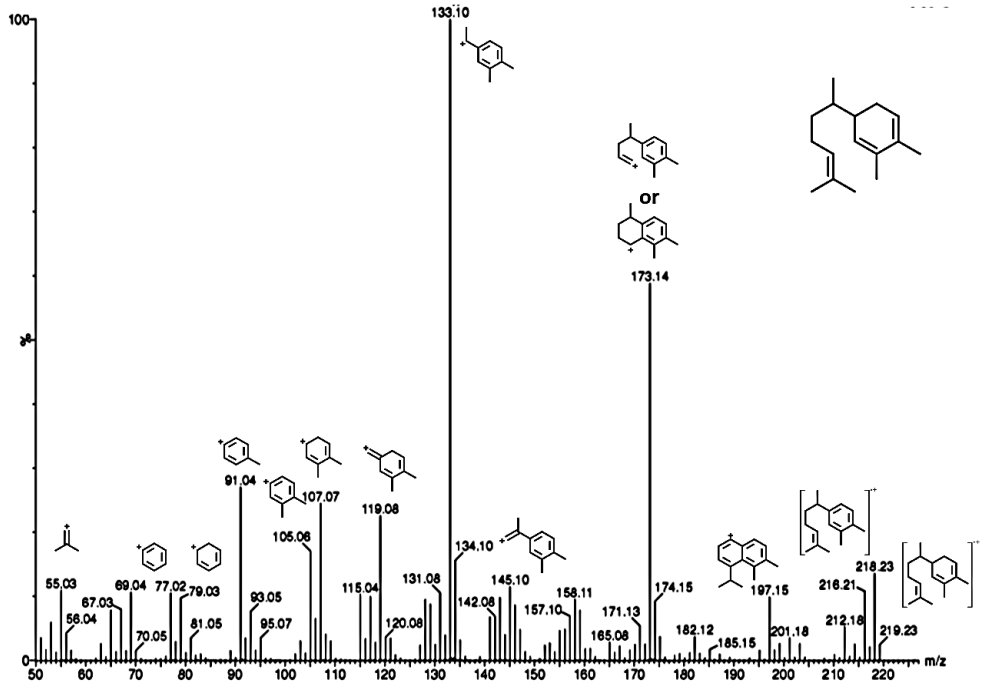

Figure 163. Mass spectrum and possible fragmentations of the enzymatic product eluted at 18.2 minutes.

It is impossible to predict whether 2-methyl-7-epizingiberene (**366**) may act as either a repellent, attractant or have no semiochemical properties towards whitefly. However, a comparison of incubations results of (2*Z*,6*Z*)-2-methylfarnesyl diphosphate (**359**) with EZS and (2*E*,6*Z*) farnesyl diphosphate (**342**) with EZS (Figure 135, 5.2.2) suggests that the inhibition caused by **342** may not

due to steric hindrance. The methyl group at the C2 position of **359** gives further evidence that EZS inhibition by **342** is a result of the C1, C2 double bond stereochemistry preventing a [1,6] cyclisation from occurring (Figure 137, 5.2.2).

The final enzymatic product at retention time 18.44 minutes did not have the characteristic splitting pattern observed for zingiberene products on the mass spectrum (Figure 164). 2-Methylfarnesene and (2*Z*,6*Z*)-2-methylfarnesol (**375**) were synthesised but analysis *via* GC-MS did not match the product. Comparison of the product fragmentation pattern was cross referenced with the NIST library however; due to the novel nature of the substrate, no insight to the product structure was gained.

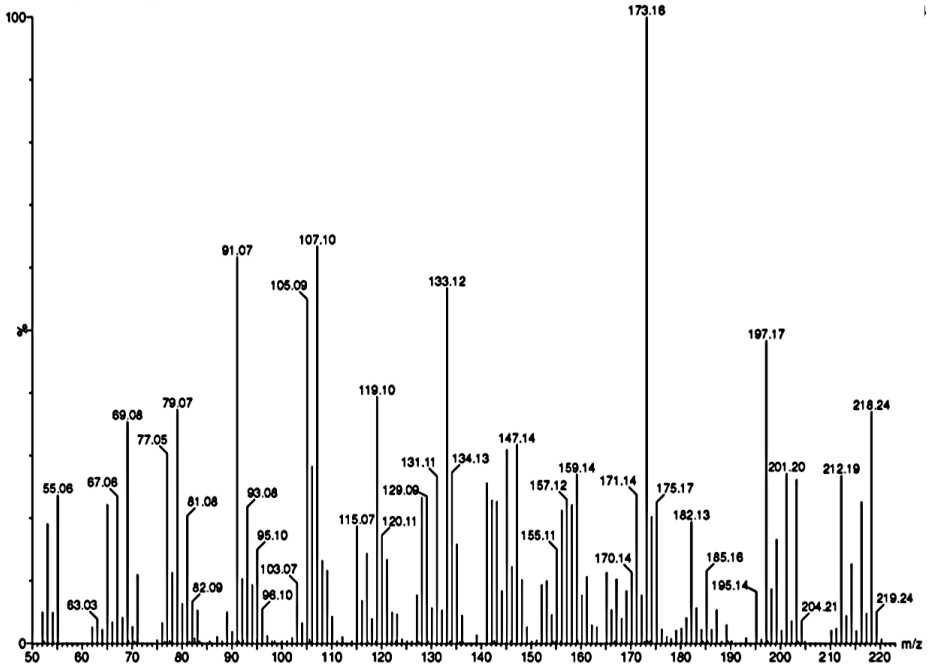

Figure 164. Mass spectrum of unknown enzymatic product that eluted at 18.4 minutes.

6.2.3 Synthesis of (2*Z*,6*Z*)-6-methylfarnesyl diphosphate (360)

Incorporation of a methyl group at the C6 position could lower the energy of the bisabolyl-like cation intermediate (**378**) and may lead to methylated products **380** or **381** (Figure 165).

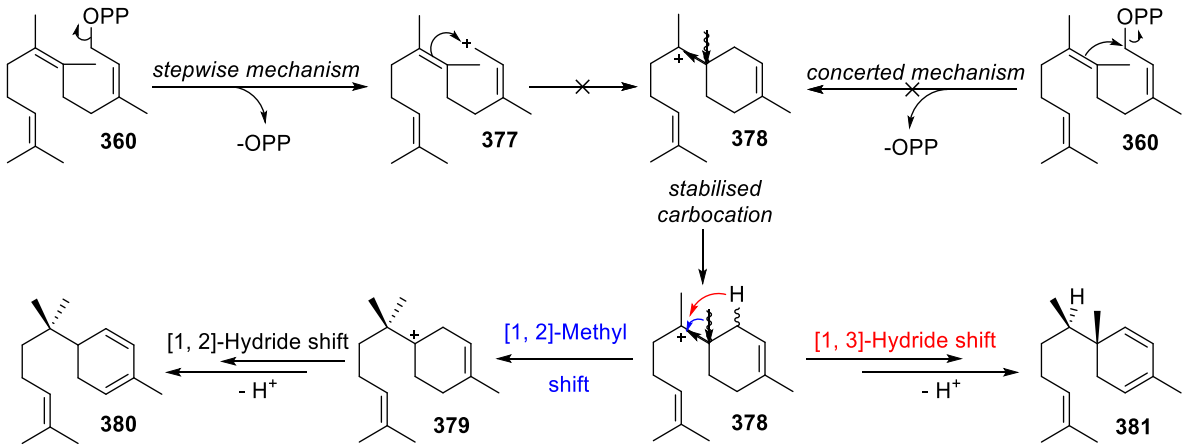

Figure 165. Potential outcome and methylated enzymatic products from the incubation of 360 with EZS.

Echoing the synthesis of (2*Z*,6*E*)-6-fluorofarnesyl diphosphate (**231**) (Figure 94, 4.2.3) the synthesis of (2*Z*,6*Z*)-6-methylfarnesyl diphosphate (**360**) was achieved from commercially available **368**, no modification of reagent **368** was deemed necessary (Figure 166).

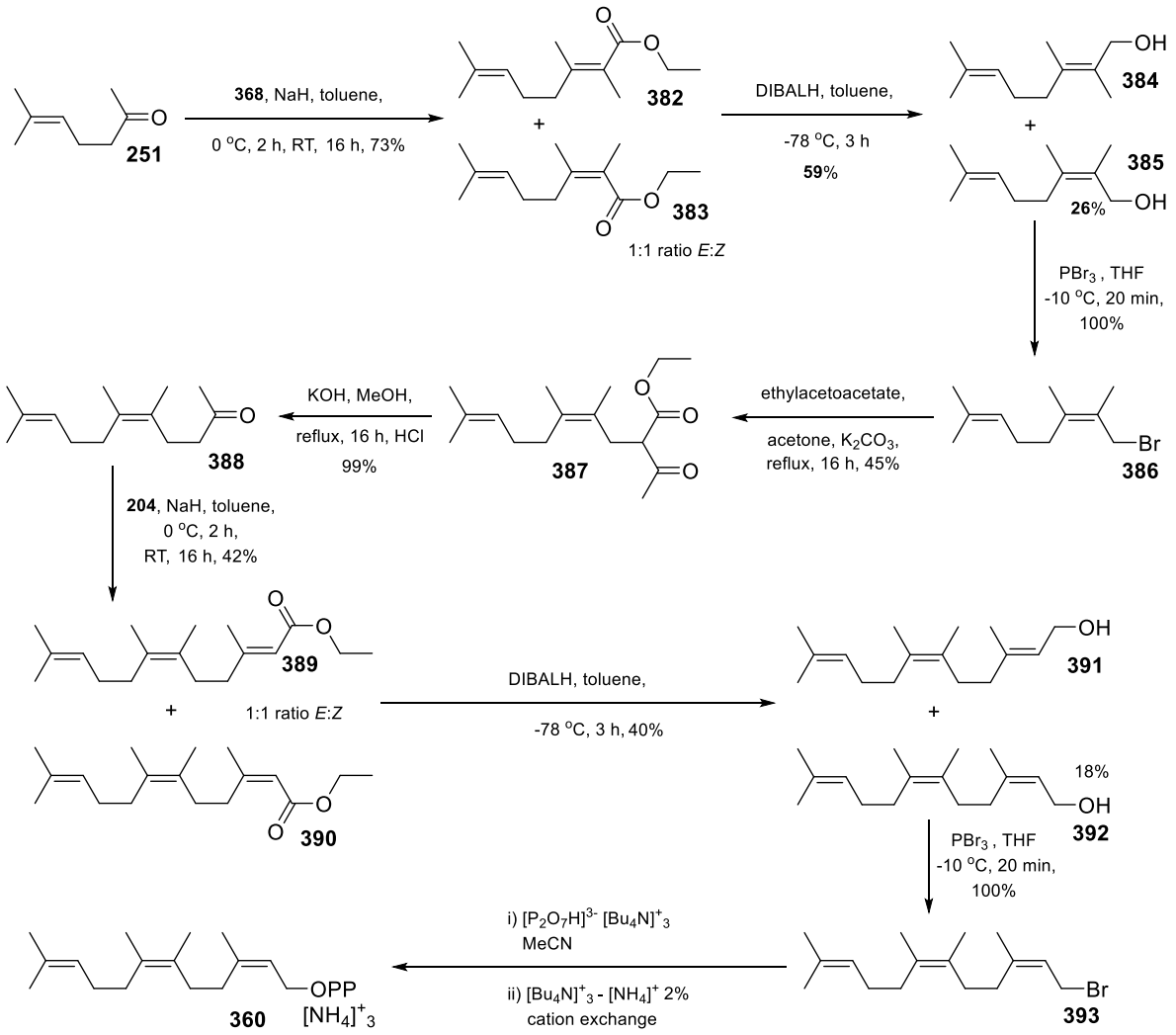

Figure 166. Synthesis of (2*Z*,6*Z*)-6-methylfarnesyl diphosphate (360).

Chain extension of bromide **386** to give ketoester **387** appeared to result in the formation of rotamers. The two species were only observed *via* ^{1}H NMR spectroscopy with two overlapping quartets at 2.64 and 2.61 ppm and overlapping triplets at 1.27 and 1.26 ppm signifying the two ethyl groups (Figure 167). The rotamers were not observed *via* ^{13}C NMR and could not be separated. The synthetic route proceeded *via* decarboxylation of the rotamer mixture to give ketone **388** as a single product. Subsequent synthetic steps were continued using the established protocol for the synthesis of (2*Z*,6*Z*) FDP (**38**) (Figure 45, 2.2.5).

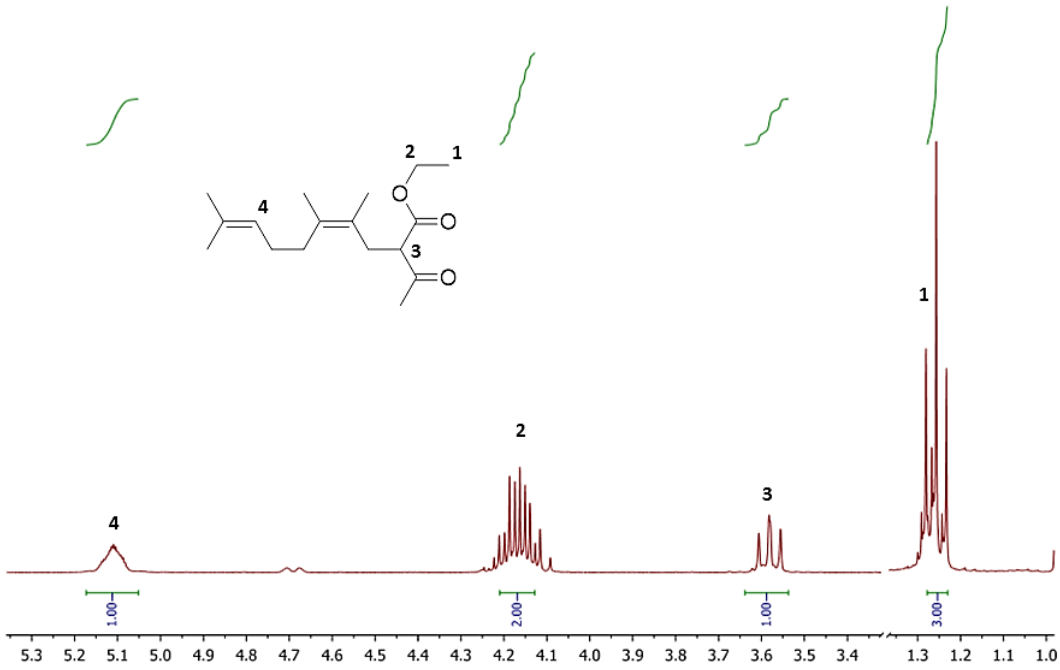

Figure 167. Cropped ^{1}H NMR spectrum of rotamer intermediate 387 showing overlapping quartet and triplet peaks resulting from restricted rotation caused by the methyl substituent.

6.2.4 Incubation of (2*Z*,6*Z*)-6 methylfarnesyl diphosphate (360) and EZS

It was proposed that the incubation of (2*Z*,6*Z*)-6-methylfarnesyl diphosphate (**360**) and EZS may yield enzymatic products. Electron donation from methyl group at the C6 position could lower the energy of the bisabolyl-like cation (**378**) resulting in catalytic turnover of **360** by EZS. GC-MS analysis of the pentane extractable products showed no enzymatic products. An inhibition assay was therefore performed to assess binding and an approximate K_i of **360**.

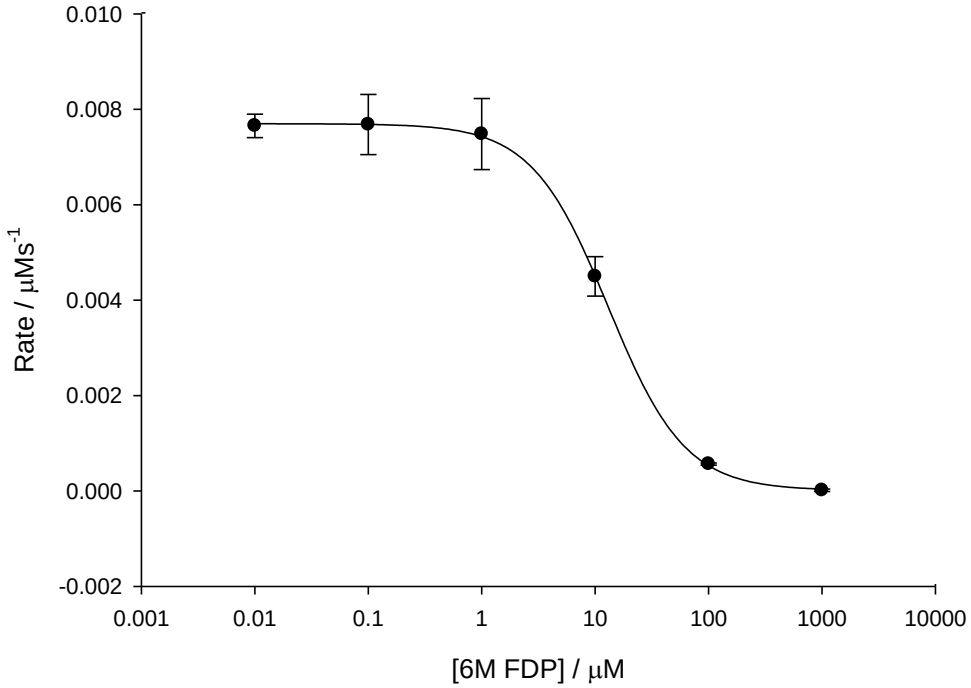

Figure 168. 360 IC50 plot for the incubation of (2*Z*,6*Z*)-[1-^{3}H]-FDP (229) with EZS and inhibitor (2*Z*,6*Z*)-6-methylfarnesyl diphosphate (360); 0.01 μM - 1000 μM range.

The IC50 curve of the **360** inhibition assay gave an approximate K_i of 13.1 ± 1.7 μM (Figure 168), a value which is of the same magnitude observed for other farnesyl substrates (Table 8, 5.6). The presence of the methyl group at the C6 position therefore does not appear to greatly affect formation of an enzyme-substrate complex. Because the stereochemistry of **360** matches the natural substrate **38** the double bond must be correctly aligned, therefore the methyl group disrupts product formation. The methyl group may either effect the orientation of the substrate within the active site or directly inhibit the mechanism by impeding hydride shifts or cation formation. In contrast to the large K_i values observed of NDP (**39**) and GDP (**30**) 474 ± 24 μM and 97.3 ± 24.6 μM respectively, the presence of the additional prenyl unit appears to allow effective binding of the substrate to the active site.

6.3 Oxygenated analogues

6.3.1 Synthesis of (2*Z*,6*Z*)–10,11-epoxyfarnesyl diphosphate (361)

Oxygenated analogues have been reported as substrates for various sesquiterpene synthases including ADS, where incubation of oxygenated FDP analogues gave rise to oxygen-containing enzymatic products.[9] Small changes to FDP substrates have been shown to have large effects on the properties of the natural product as discussed previously. Installation of an epoxide across the C10,C11 bond to form **361** may result in the oxygenated zingiberene product **394** after EZS incubation (Figure 169).

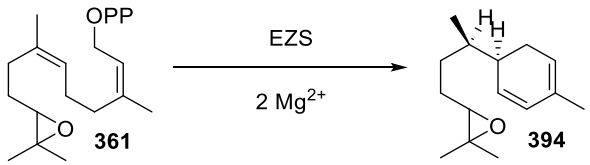

Figure 169. Possible enzymatic product from the incubation of 361 with EZS.

Synthesis of **361** began from (2*Z*,6*Z*) farnesol (**167**) which was synthesised *via* the procedure previously outlined (Figure 45, 2.2.5). Tetrahydropyran (THP) protection of alcohol **167** was followed by selective bromohydrin (**396**) formation at the distal double bond using *N*–bromosuccinimide in tetrahydrofuran/water. Intramolecular S_N2-like epoxide ring closure with potassium carbonate in methanol yielded **397**.[249] Deprotection of the alcohol was followed by bromination with phosphorus tribromide and diphosphorylation gave **361** (Figure 170).

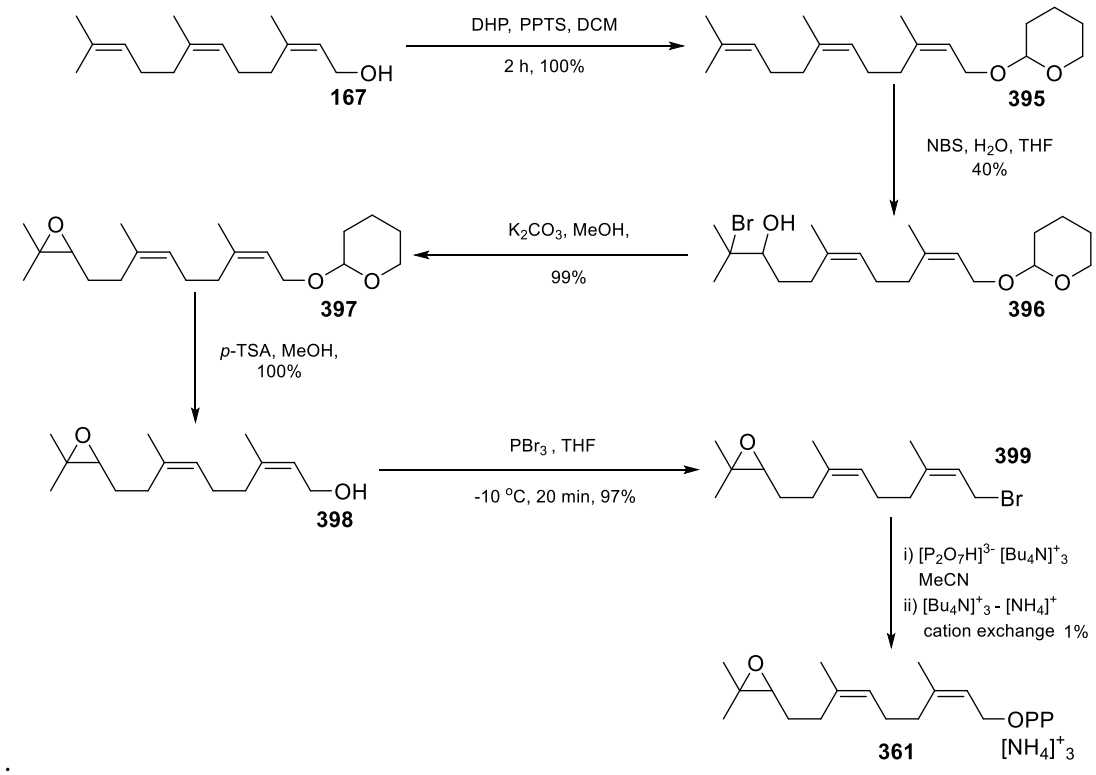

Figure 170. Synthesis of (2*Z*,6*Z*)-10,11-epoxyfarnesyl diphosphate (361).

6.3.2 Incubation of (2*Z*,6*Z*)-10,11-epoxyfarnesyl diphosphate (361) and EZS

Analysis of the pentane extractable products from the incubation of (2*Z*,6*Z*)-10,11-epoxyfarnesyl diphosphate (**361**) and EZS *via* GC-MS identified no enzymatic products. Unfortunately, a very limited quantity of **361** was available and it was not possible to run inhibition assays, limiting the conclusion that can be drawn from this experiment.

6.3.3 Synthesis of (2*Z*,6*Z*,10*Z*)-12-methoxyfarnesyl diphosphate (362)

Analogues containing modifications to the distal prenyl group have proven to be accepted as substrates by other sesquiterpene synthases.[106] Introduction of a 12-methoxy group to **38** may yield enzymatic product **400** upon the incubation of **362** with EZS (Figure 171). In addition, the methoxy group introduces stereochemistry across the C10,C11 double bond which may influence substrate specificity.

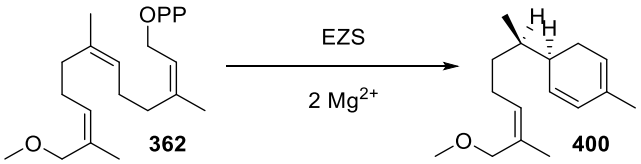

Figure 171. Possible enzymatic product from the incubation of 362 with EZS.

The synthesis of **362** began from epoxide **397**. Formation of aldehyde **401** was achieved with sodium periodate and periodic acid as outlined by Corey *et al,*[250] (Figure 172). **401** was subjected to a Horner-Wadsworth-Emmons reaction with a Still-Gennari modification,[204] followed by reduction to alcohol **403** using DIBALH and methylation using sodium hydride and methyl iodide. Subsequent alcohol deprotection, bromination and diphosphorylation were carried out as previously outlined (Figure 39, 2.2.4).

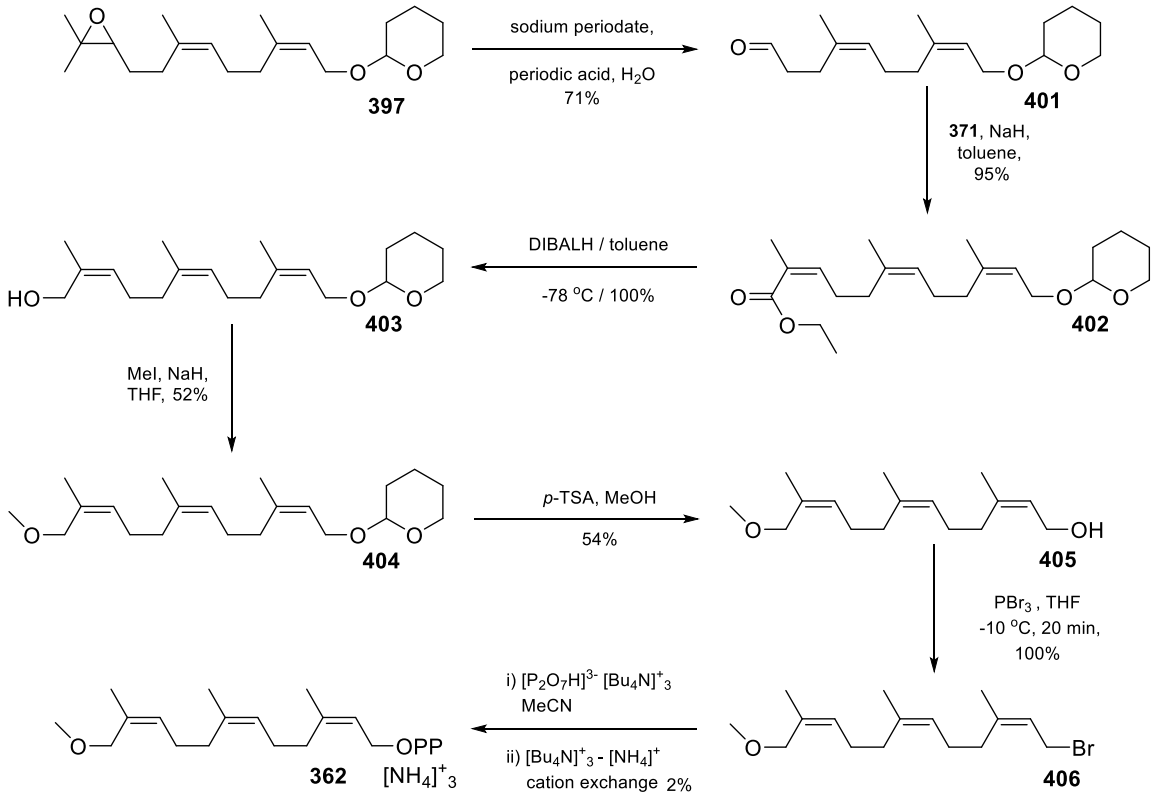

Figure 172. Synthesis of (2*Z*,6*Z*,10*Z*)-12 methoxyfarnesyl diphosphate (362).

In contrast to olefination reactions using ketone substrates, reaction of aldehyde **401** under the *Z* selective modified conditions (Table 4, 2.2.5) proceeded to completion with negligible quantities of the *E* isomer observed *via* TLC or ^{1}H NMR spectroscopic analysis. Methylation of alcohol **403** then followed. However, despite using excess methylation reagent, (up to 30 equivalents) the reaction did not go to completion even with extended reaction times. Deprotection of **404** to give alcohol **405**

was carried out following a literature protocol.[251] It was observed that if the reaction duration was extended, side products formed, decreasing the yield of desired product. The reaction was therefore monitored by TLC and upon consumption of starting material the reaction was quenched immediately, preventing side product formation.

6.3.4 Incubation of (2*Z*,6*Z*,10*Z*)-12 methoxyfarnesyl diphosphate (362) and EZS

GC-MS analysis of the pentane extractable incubation products of **362** with EZS showed one major enzymatic product at 21.6 minutes (Figure 173). The molecular ion peak *m/z* = 234 is consistent with a methoxy functionalised sesquiterpenoid product (Figure 175). Product formation from the incubation of **362** with EZS shows that analogues of (2*Z*,6*Z*) FDP (**38**) with modification at the C12 position of the prenyl tail are potential targets for future substrates of EZS.

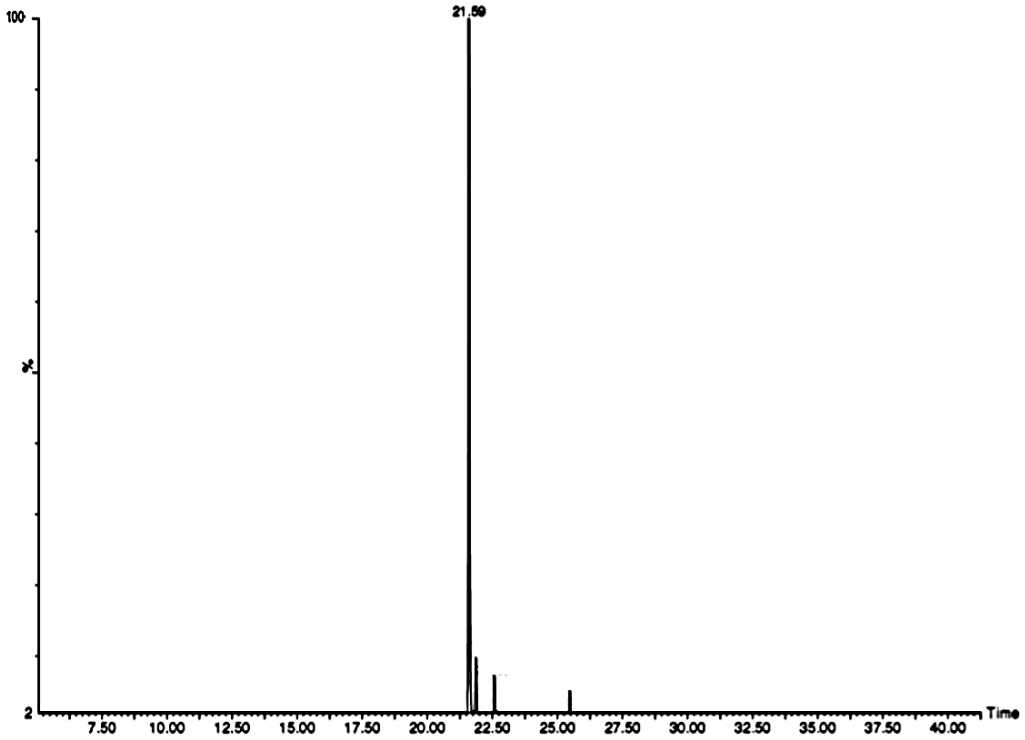

Figure 173. Total ion chromatogram of the pentane extractable products from the incubation of 362 and EZS.

The mass spectrum of another enzymatic product peak at 21.58 minutes suggested a cyclised methoxy sesquiterpenoid (Figure 175). Previous work within the Allemann Group (Dr Melodi Demiray) observed that the incubation of (2*E*,6*E*,10*E*)-12-methoxyfarnesyl diphosphate yielded two enzymatic products, 12-methoxy-β-sesquiphellandrene (**407**) and 12-methoxy-zingiberene (**408**),

upon incubation with amorphadiene synthase (ADS) (Figure 174). Both cyclised products showed fragmentations similar to that observed in the EZS generated product.

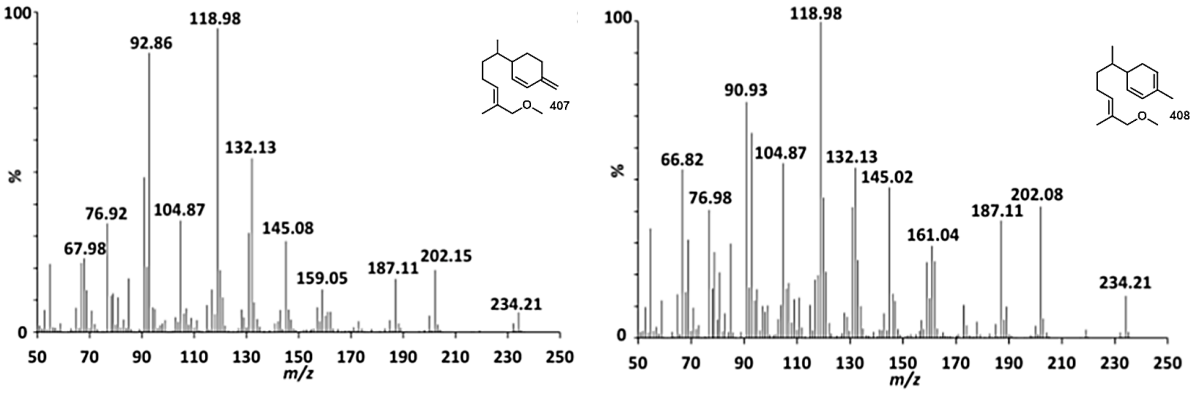

Figure 174. Mass spectra of ADS generated products; 12-methoxy-β-sesquiphellandrene (407, left) and 12-methoxy-zingiberene (408, right).

Multiple fragments on the mass spectrum of the 21.6 peak support a methoxy-substituted cyclised product (Figure 175). Fragments at *m/z* = 203 and 202 give evidence to the removal of the methoxy group and deprotonation respectively. A dominant peak at *m/z* = 119 and fragmentations at *m/z* = 105, 91 and 77 indicate a cyclised product as previously observed in the mass spectra of 7-epizingiberene (**1**)(Figure 60, 2.6) and curcumene (**81**) (Figure 61, 2.6). The intensity of these fragments (Figure 174) offer further evidence of a [1,6] ring closure and a 12-methoxy-7-epizingiberene (**400**) product. Figure 176 outlines the formation of a plausible methoxy zingiberene product resulting from the incubation of **362** and EZS. In order to rule out hydrolysis of **362**, (2*Z*,6*Z*,10*Z*)-12-methoxyfarnesol (**405**) was analysed *via* GC-MS. The retention time of the gas chromatogram and the fragmentation patterns of the mass spectrum were different to that of the product.

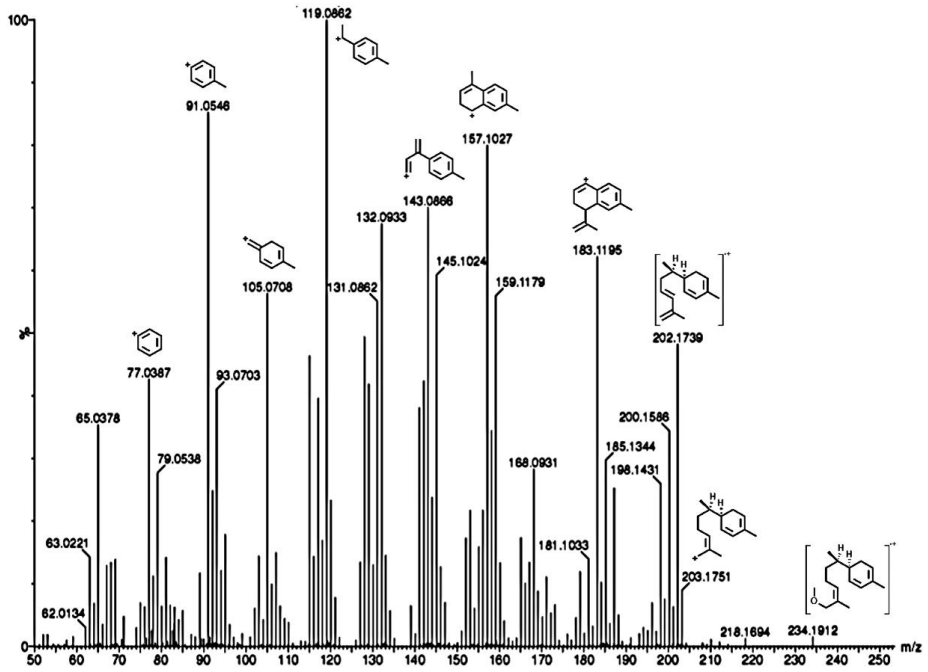

Figure 175. Mass spectrum of EZS generated compound eluted at 21.6 minutes and proposed fragment assignments.

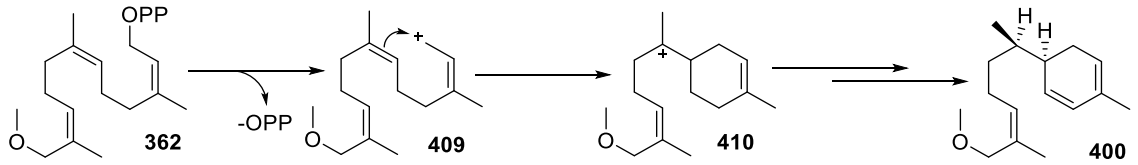

Figure 176. Possible catalytic mechanism of EZS upon incubation with 362.

6.3.5 Synthesis of (2*Z*,6*Z*,10*E*)-13-methoxyfarnesyl diphosphate (363)

With **362** shown to be a substrate for EZS, the corresponding (2*Z*,6*Z*,10*E*)-13-methoxyfarnesyl diphosphate (**363**) was a key analogue to probe the substrate scope and stereochemical preferences at the distal prenyl unit. The incubation of **363** with EZS may yield **411** (Figure 177) implying novel analogues of 7-epizingiberene (1) could be generated *via* the functionalisation of the both the C12 and C13 positions of the substrate prenyl tail.

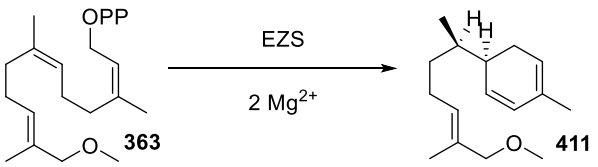

Figure 177. Possible enzymatic product of 363 incubation with EZS.

Preparation of **363** was proposed *via* a selenium dioxide (SeO_2) oxidation of neryl acetone (**166**) to install a hydroxyl group at the C12 position. Methylation and a Horner-Wadsworth-Emmons reaction to install the C2, C3 double bond of **363** would be followed by a DIBALH reduction, bromination and diphosphorylation (Figure 178).

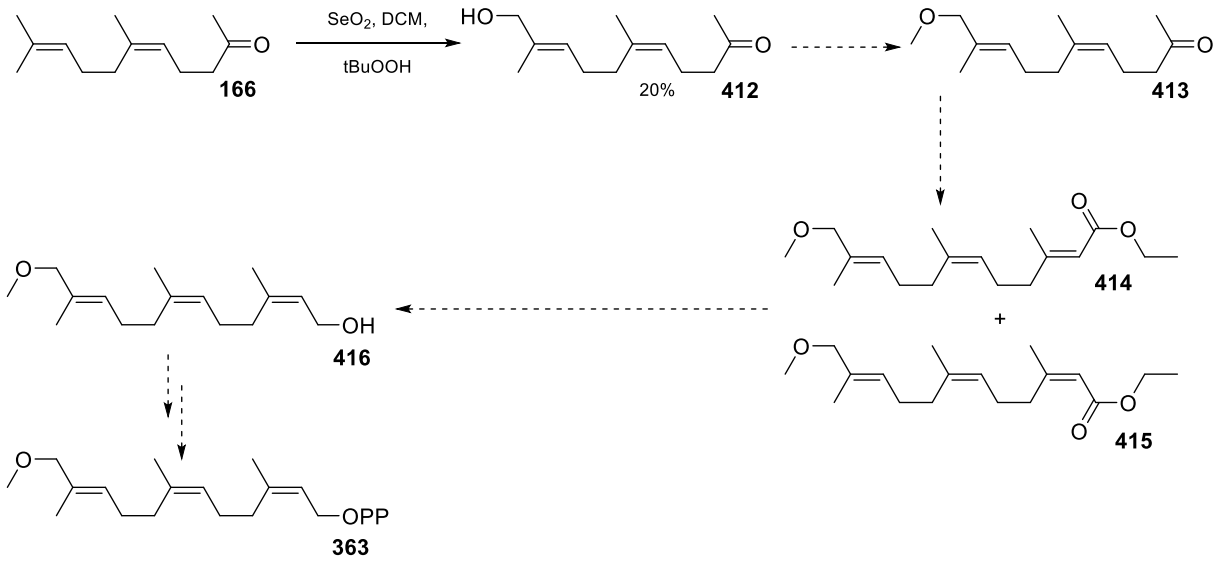

Figure 178. Initial synthesis of (2*Z*,6*Z*,10*E*)-13-methoxyfarnesyl diphosphate (363) utilising a selenium oxide oxidation.

Analysis of the ^{1}H NMR spectrum of the selenium dioxide oxidation reactions showed three reaction products: the expected product **412**, a product hydroxylated at the C8 position, and an aldehyde environment that was evident by a characteristic ^{1}H NMR peak at 9.9 ppm. It was proposed that the

by-products arose from the oxidation of neryl acetone (**166**) at the C7 position and oxidation of hydroxylated neryl acetone (**412**) by excess selenium dioxide in the reaction mixture. Oxygenated products could not be separated *via* flash chromatography and olefination was not attempted.

A modified route was therefore followed (Figure 179). Aldehyde **401** was synthesised in the same manner as previously discussed *via* the THP protection of (2*Z*,6*Z*) farnesol (**167**) (Figure 172), followed by with a Horner-Wadsworth-Emmons reaction to install the *E* C10,C11 double bond and then continued in the same manner outlined for the synthesis of **362** (Figure 172).

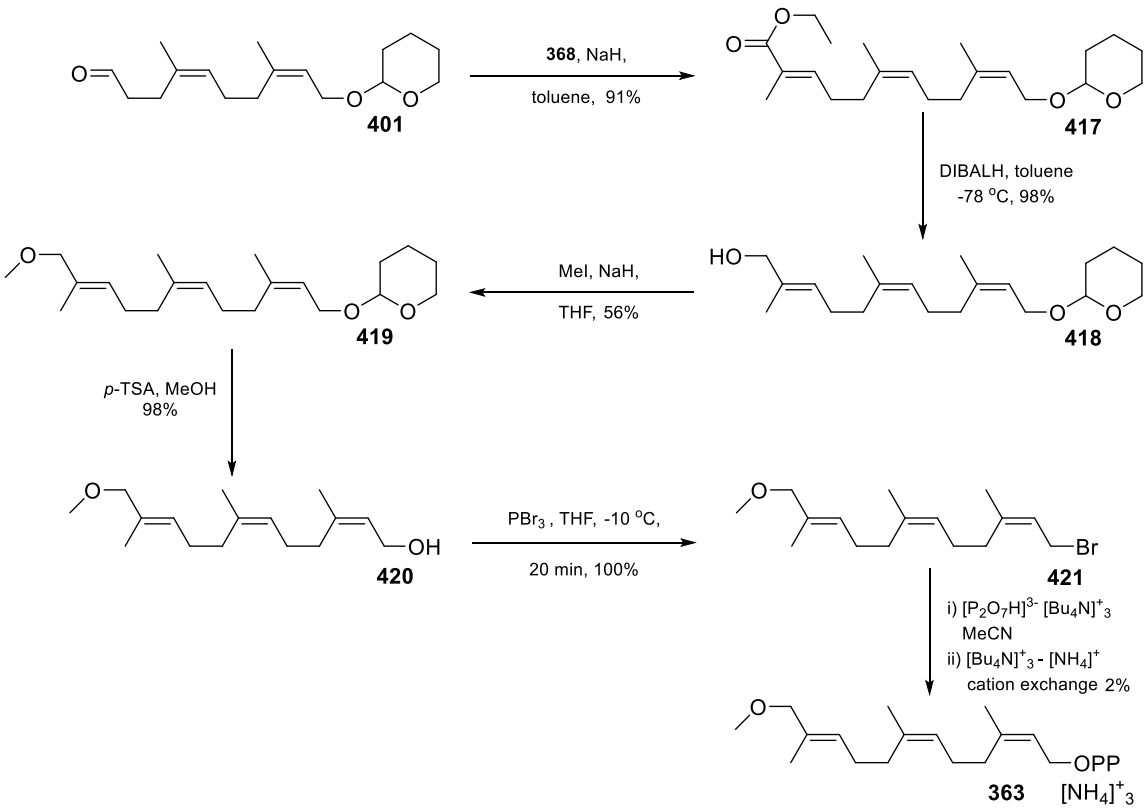

Figure 179. Synthesis of (2*Z*,6*Z*,10*E*)-13-methoxyfarnesyl diphosphate (363).

The key step within the synthesis of **363** was the Horner-Wadsworth-Emmons reaction to give *E* stereochemistry across the C10, C11 double bond for which conditions optimised in the synthesis of **38** (Table 4, 2.2.5) were used. Negligible quantities of **402** were removed *via* flash chromatography.

6.3.6 Incubation of (2*Z*,6*Z*,10*E*)-13-methoxyfarnesyl diphosphate (363) and EZS

GC-MS analysis of the pentane extractable products of **363** and EZS incubation yielded no enzymatic products. An inhibition assay was used to indicate whether **363** was bound to the active site and to approximate a value for K_i.

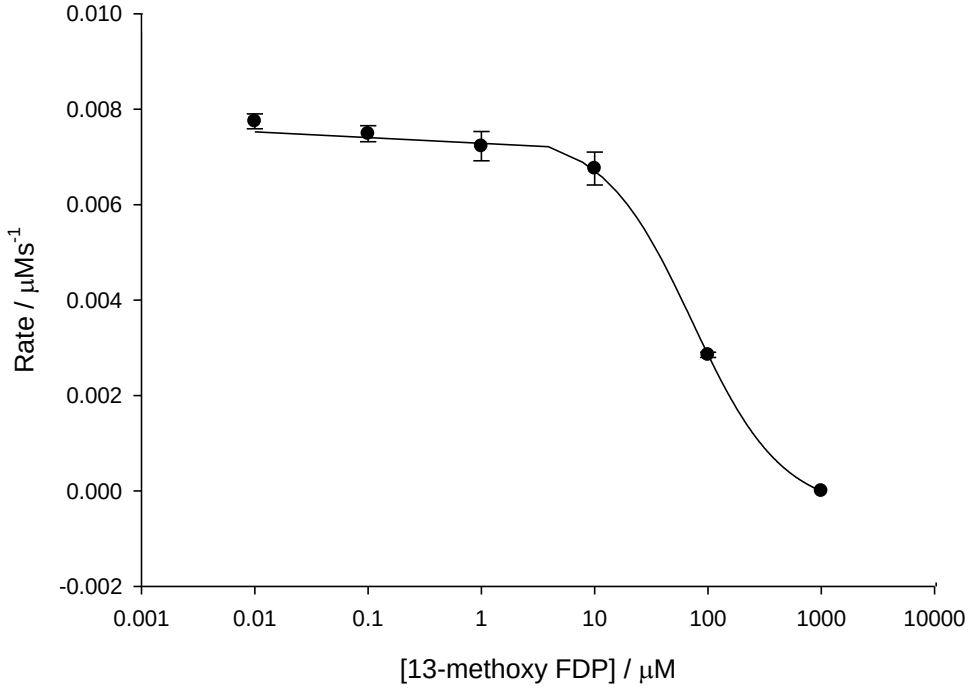

Figure 180. IC50 plot for the incubation of (2*Z*,6*Z*)-[1-^{3}H]-FDP (229) with EZS and inhibitor (2*Z*,6*Z*,10*E*)-13-methoxyfarnesyl diphosphate (363); 0.01 μM - 1000 μM range.

The IC50 curve showed that **363** and EZS bind to form an enzyme-substrate complex with a K_i of 72.7 ± 6.8 μM (Figure 180), comparable to that of geranyl diphosphate (**30**), suggesting the methoxy group of **363** may cause unfavourable steric or electronic interactions with residues in the active site.

6.4 Summary

Numerous methylated and oxygenated novel substrates were synthesised and incubated with EZS. Previous publications outlined the substrate specificity of EZS to only accept (2*Z*,6*Z*) FDP (**38**) reporting that (2*E*,6*Z*) FDP (**342**) and GDP (**30**) were not substrates, though further investigation of potential substrates was not performed. This work found evidence of EZS substrate promiscuity, with enzymatic products observed from the incubation of methylated and methoxygenated substrates **359** and **362**.

Three enzymatic products were detected *via* GC-MS of the pentane extracts of (2*Z*,6*Z*)-2-methyl FDP (**359**) incubation with EZS. One of the products was identified as methylfarnesene, produced through the removal of the diphosphate group and subsequent deprotonation and another product remains unidentified. The mass spectrum of the third product gave evidence for a cyclised zingiberene analogue, with preliminary analysis suggesting the product could be 2-methyl-7-epizingiberene. This result shows the potential of EZS to produce novel sesquiterpene products. Continuity of this investigation involves preparative scale incubations of **359** with EZS to determine enzymatic products *via* NMR spectroscopy.

(2*Z*,6*Z*)-6-methyl FDP (**360**) proved to be an inhibitor of EZS with an approximate K_i similar to that calculated for (2*E*,6*Z*) FDP (**342**), (2*Z*,6*E*) FDP (**341**) and (2*E*,6*E*) FDP (**31**). Inhibition of EZS by **360** could be due to substrate binding effects or hindering hydride shifts during the catalytic mechanism. A [1,2] hydride shift from the C6 position, Figure 131 (4.3.6), would not be possible for this substrate whilst a [1,3] hydride shift may also be disrupted resulting from the orientation of the methyl group within the active site obstructing hydride movement.

Incubations of EZS and (2*Z*,6*Z*)-10,11-epoxyfarnesyl diphosphate (**361**) showed no enzymatic products, but (2*Z*,6*Z*,10*Z*)-12-methoxyfarnesyl diphosphate (**362**) incubation with EZS resulted in one major enzymatic product. The mass spectrum of the product analysed by GC-MS showed a fragmentation pattern consistent with a cyclised methoxygenated product. A sample of (2*Z*,6*Z*,10*Z*)-12-methoxyfarnesol (**405**) was analysed by the same method and was shown to have both different retention time and fragmentation pattern to that to that of the product. Whilst a preparative scale incubation of **405** and EZS is required to unambiguously assign its structure by ^{1}H NMR spectroscopy, a comparison of fragmentation patterns to similar products previously isolated within the Allemann group supports the formation of a methoxyzingiberene product. However, 12-methoxyfarnesene cannot be ruled out without synthesis and comparison of its fragmentation pattern with that of the enzymatic product. In contrast to **361**, isomeric (2*Z*,6*Z*,10*E*)-13-methoxy FDP (**363**) was shown to be an inhibitor of EZS. An inhibition assay using **363** gave an approximate K_i an

order of magnitude larger than that observed for stereoisomer substrates **342**, **341** and **31**. However, the K_i of (2*Z*,6*Z*,10*E*)-13-methoxyfarnesyl diphosphate (**363**) appears to be lower than monoterpene substrates neryl diphosphate (**39**) and geranyl diphosphate (**30**) indicating that the prenyl tail plays a role in the substrate enzyme binding.

Chapter 7 – Conclusions and Future Work

7.1 Conclusion

This project describes investigations of the *Z*-selective sesquiterpene cyclase; 7-epizingiberene synthase. These investigations were performed to elucidate the catalytic mechanism, stereochemical substrate specificity and promiscuity of EZS. This was achieved by the synthesis and incubation of (2*Z*,*6Z*) FDP(**167**) and numerous isotopologues, stereoisomers, fluorinated, oxygenated and methylated analogues with EZS.

Substrates synthesised during this project are outlined in (Figure 181). Analogues highlighted green (**38**, **229**, **233**, **234**, **259** and **362**) yielded enzymatic products upon incubation with EZS. Analogues highlighted red (**341**, **342**, **31**, **230** and **231**) were not accepted as substrates and their mode of inhibition investigated. Analogues highlighted purple (**39**, **30**, **360** and **363**) did not yield enzymatic product when incubated with EZS and were shown to bind to the enzyme though the mode of inhibition was not investigated. The analogue highlighted black (**361**) was not a substrate of EZS though determination of binding or mode of inhibition was not investigated.

A synthesis of (2*Z*,6*Z*) farnesyl diphosphate (**38**) using a Still-Gennari[204] modified Horner-Wadsworth-Emmons reaction[202] as the key olefination reaction for the installation of the C2,C3 double bond gave an overall yield of 9% over seven steps. The olefination conditions investigated during this synthetic route were duplicated or modified in order to synthesise all other substrates excluding neryl diphosphate (**39**) and geranyl diphosphate (**30**). The reproducible method enabled the synthesis of multiple substrates to which analogues **359** and **362** yielded enzymatic products upon incubation with EZS.

The synthesis of (2*Z*,6*Z*)–[1-^{3}H]–farnesyl diphosphate (**229**)(Figure 76, 3.2.1) allowed for the measurement of steady state parameters of EZS and EZS mutants that exhibited activity upon incubation with **38**. Mutants of EZS were generated to investigate the metal binding motifs, DDxxE and NSE, responsible for class I activity whilst numerous aromatic residues were subjected to single point mutation to investigate their role within the active site pocket. Analysis of the data from the steady state kinetic experiments concerning EZS(E648A) showed decreased substrate turnover and an increased binding affinity when compared with the wild type. EZS(Y483A) was found to have an effect on substrate binding affinity with a lower K_M of **38** with EZS(Y483A) and an increase in catalytic efficiency when compared to the wild type.

Inhibition studies were also performed with EZS and substrates that did not yield enzymatic products upon incubation with EZS. Fluorinated substrates and stereo isomer analogues of (2*Z*,6*Z*) FDP (**38**) were investigated and found to be competitive inhibitors of EZS. Other analogues that were accepted as substrates were examined using radiolabelled assays and an IC50 plot each, with each

analogue exhibiting substrate binding and enzyme inhibition. (2*Z*,6*Z*)-10,11-Epoxyfarnesyl diphosphate (**361**) was not used within inhibition assays due to the quantity of substrate. The inhibitory nature of stereoisomers of **38** has shown that the *Z* stereochemistry of the C2,C3 and C6,C7 double bonds are crucial for substrate turnover. Analysis of data from inhibition assays performed with monoterpene analogues neryl diphosphate (**39**) and geranyl diphosphate (**30**) showed that the removal of the prenyl tail significantly reduces substrate binding to the active site. Analogues **39** and **30** exhibited K_M values 1 and 2 orders of magnitude greater than their sesquiterpene equivalents **38** and **31**. These results give insight that the prenyl tail is significant for substrate binding to the active site.

Fluorinated analogues **230** and **231** were shown to be competitive inhibitors of EZS giving evidence of a stepwise ring closure during the catalytic mechanism. Inhibition of EZS when incubated with **230** and **231** suggests the formation of the farnesyl (**141**) and bisabolyl (**86**) cations respectively. Deuterated analogues (2*Z*,6*Z*)-(*S*)-[1-^{2}H]-farnesyl diphosphate (**233**) and (2*Z*,6*Z*)-(*R*)-[1-^{2}H]-farnesyl diphosphate (**234**) provided insight to the roles of the *proR* and *proS* protons at the C1 position. Analysis of the pentane extractable products from the incubations of substrates **233** and **234** with EZS suggests that the *proR* proton is not involved within the catalytic mechanism whilst the *proS* proton participates in a manner that was not fully elucidated.

This project has furthered the understanding of the *Z*-selective sesquiterpene cyclase; 7-epizingiberene. It was previously thought that EZS would only accept (2*Z*,6*Z*) farnesyl diphosphate (**38**) as a substrate, however this work has shown the protein has greater substrate promiscuity than previously acknowledged. Methylated analogue **359** and methoxygenated analogue **362** both yielded enzymatic products when incubated with EZS whilst analogues **360**, **361** and **363** did not give enzymatic products, with **361** and **363** shown to inhibit EZS.

This work gives precedence that EZS is able to accept substrates with modifications to the hydrocarbon skeleton. This provides a potential avenue for the synthesis of non-canonical substrates which upon incubation with EZS could generate analogues of 7-epizingiberene which may have agricultural importance.

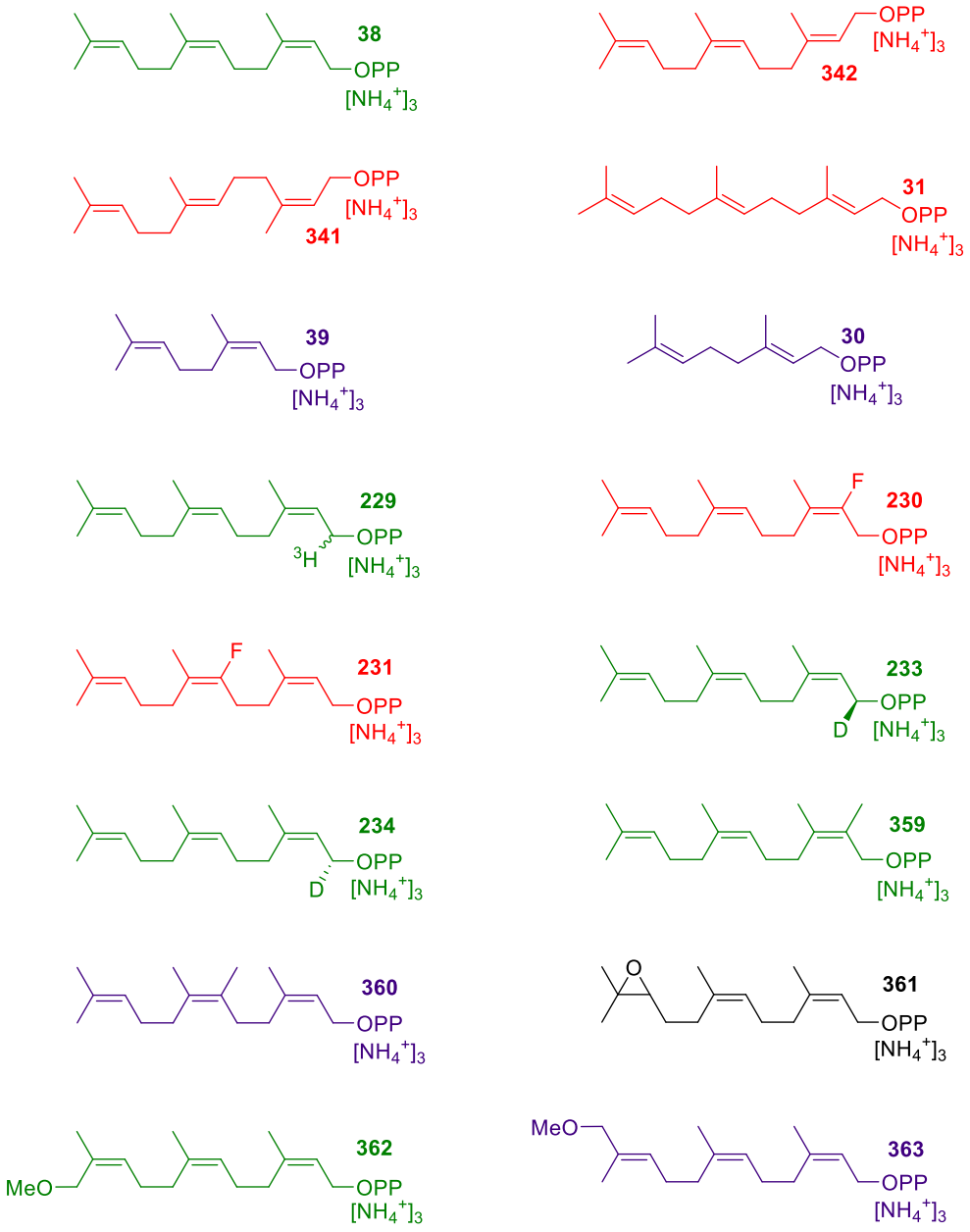

Figure 181. Synthesised analogues: Analogues which EZS accepted as substrates (green). Analogues which acted as inhibitors of EZS and mode of inhibition investigated (red). Analogues that acted as EZS inhibitors (purple). Analogue which did not yield enzymatic product when incubated with EZS (black).

7.2 Future Work

7.2.1 Inhibition studies

Future work following the completion of this project could involve the synthesis of **361** and the investigation of substrates that do not yield enzymatic product upon incubation with EZS to determine their modes of inhibition.

7.2.2 Preparative scale incubations

(2*Z*,6*Z*) Farnesyl diphosphate (**38**), (2*Z*,6*Z*)-2-methylfarnesyl diphosphate (**359**), (2*Z*,6*Z*,10*Z*)-12-methoxy farnesyl diphosphate (**362**), (2*Z*,6*Z*)-(*S*)-[1-^{2}H]-farnesyl diphosphate (**233**) and (2*Z*,6*Z*)-(*R*)-[1-^{2}H]-farnesyl diphosphate (**234**) yielded enzymatic product upon incubation with EZS. Preparative scale incubations of each analogue with EZS and extraction of pentane extractable products should yield enough product for ^{1}H NMR analysis. A ^{1}H NMR spectrum of **38** and peak assignment would help elucidate the catalytic mechanism of EZS when compared to the ^{1}H NMR spectra of the enzymatic products from the incubations of deuterated analogues **233** and **234** with EZS. (2*Z*,6*Z*)-2-methyl-FDP (**359**) and (2*Z*,6*Z*,10*Z*)-12-methoxy FDP (**362**) both yielded enzymatic products that were proposed to be analogous compounds of 7-epizingiberene. Preparative scale incubation of **362** and analysis of the extracted products by ^{1}H NMR spectroscopy would aid characterisation of the methoxylated product. Equivalently, a preparative scale incubation of **359** would enable the separation of the three enzymatic products by preparative scale thin layer chromatography. The analysis of each product by ^{1}H NMR spectroscopy would assist the characterisation of the methylated enzymatic products.

7.2.3 Proposed synthesis (2*Z*,6*Z*) farnesol (167)

Various procedures were investigated to synthesise (2*Z*,6*Z*) farnesol (167). Two olefination procedures were successful; an Anastasia reaction[199] and a Still-Gennari[204] modified Horner-Wadsworth-Emmons reaction.[202] Both reactions yielded (2*Z*,6*Z*) farnesol (**167**) and (2*E*,6*Z*) farnesol (**168**) in a 1:1 ratio. A synthesis using a directed Wittig reaction published by Chen *et, al.,*[197] giving 100% *Z* stereochemistry was also attempted using α-hydroxylated neryl acetone (**187**) in place of hydroxyl acetone (**422**). The synthesis of **187** to be the reactant in the directed Wittig reaction was not achieved and therefore the *Z* selective reaction was not performed. A synthesis of (2*Z*,6*Z*) farnesol (**167**) is outlined in Figure 182 using the published olefination reaction[197] as the initial step.

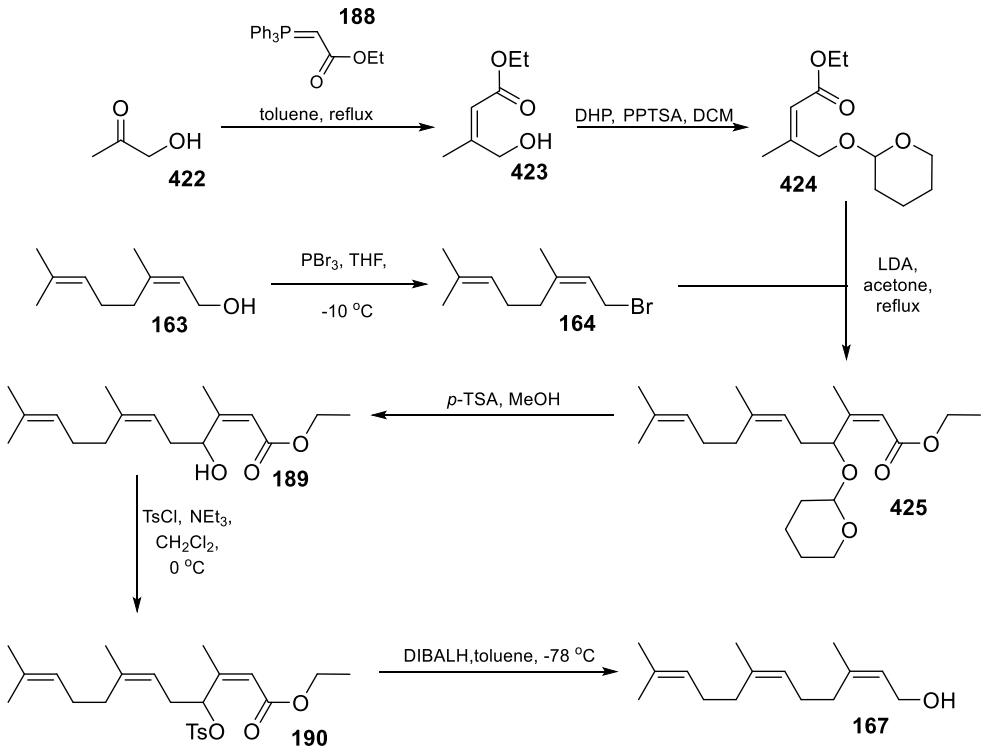

Figure 182. Proposed synthesis of (2*Z*,6*Z*) farnesol (167).

7.2.4 Synthesis of deuterated isotopologues

Numerous hydride shifts are plausible within the EZS catalytic mechanism (Figure 183). This project focussed on the hydride shifts occurring from the C1 position; however isotopologues that would investigate hydride shifts from C5 and C6 positions could be synthesised in future.

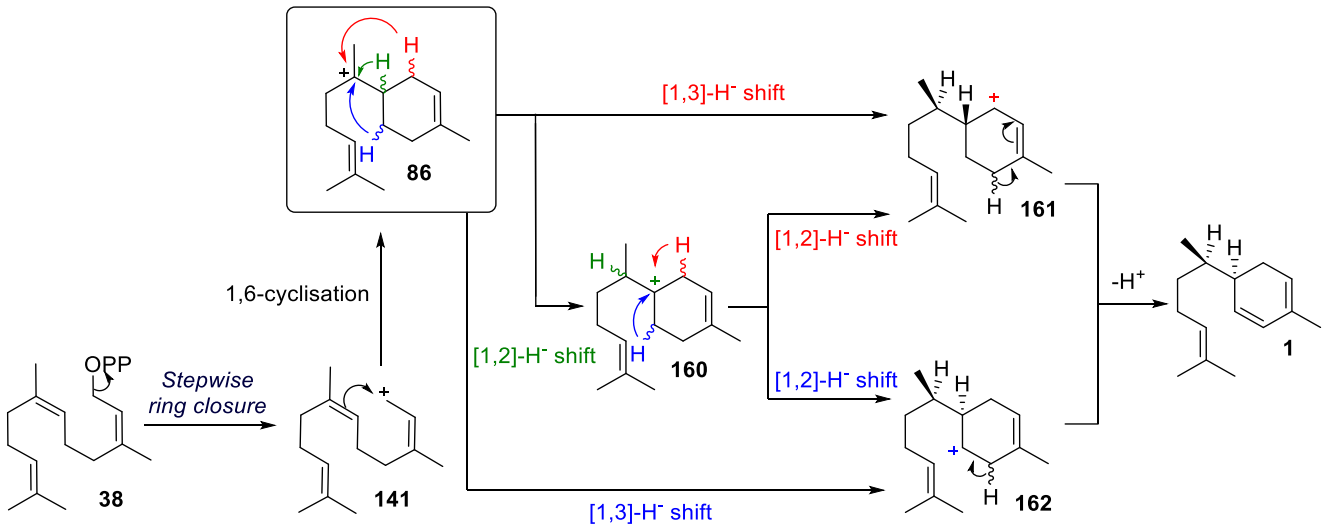

Figure 183. Plausible hydride shifts that require further investigation.

The synthesis of three deuterated isotopologues and analysis of the enzymatic products resulting from their incubation with EZS would give further insight into the catalytic mechanism. The synthesis of (2*Z*,6*Z*)-[6-^{2}H]-farnesyl diphosphate (**232**) was outlined in Figure 99 (4.3.1) though isolation of the final diphosphate was not achieved and could not be repeated within the time constraints of the project. The synthesis of deuterated analogues (2*Z*,6*Z*)-(*S*)-[5-^{2}H]-farnesyl diphosphate (**426**) and (2*Z*,6*Z*)-(*R*)-[5-^{2}H]-farnesyl diphosphate (**427**) would also give information on the hydride shifts that may occur during the catalytic mechanism of EZS (Figure 184).

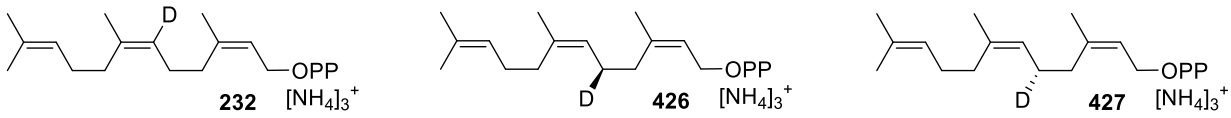

Figure 184. Prospective future deuterated analogues 232, 426 and 427.

The synthesis of **426** outlined in Figure 185 which echoes the synthesis of (2*Z*,6*Z*) FDP (**167**) (Figure 45) and (2*Z*,6*Z*)-(*S*)-[1-^{2}H]-farnesyl diphosphate (**233**) (Figure 101). The preparation of deuterated neral (**430**) from nerol (**163**) is followed by a reduction using (*R*)-Alpine Borane (**293**) to yield the *S*-deuterated enantiomer **432** and chlorination to yield **433**. The formation of the β-keto ester (**434**) is the step that requires investigation as the reaction may result in the inversion, retention or scrambling of chirality at the deuterated position. The synthetic pathway then proceeds *via* the same procedure as outlined in Figure 45 (2.2.5) to give (2*Z*,6*Z*)-(*S*)-[5-^{2}H]-farnesyl diphosphate (**426**).

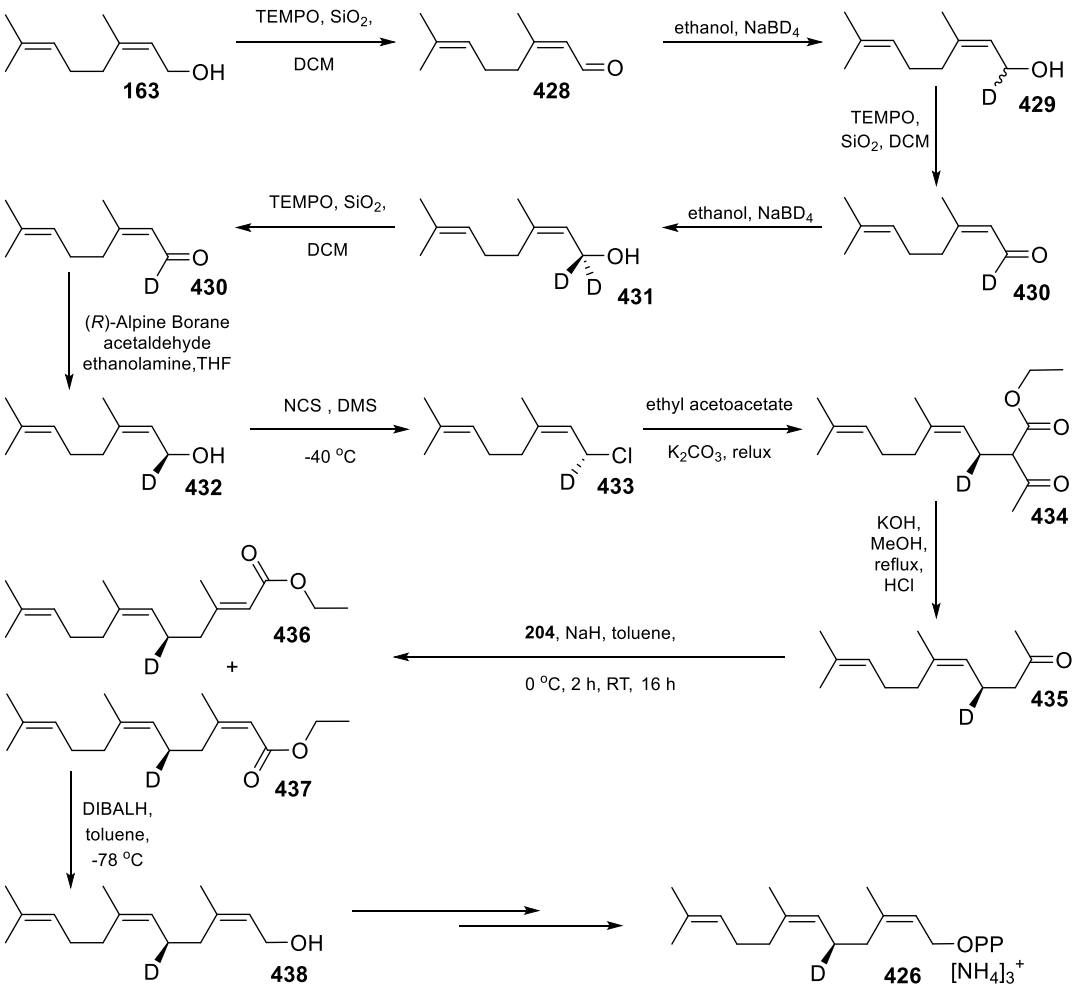

Figure 185. Proposed synthesis of (2*Z*,6*Z*)-(*S*)-[5-^{2}H]-farnesyl diphosphate (426).

The synthesis of (2*Z*,6*Z*)-(*R*)-[5-^{2}H]-farnesyl diphosphate (**427**) would follow the same procedure outlined in Figure 185 however, deuterated aldehyde **430** would be reduced using (*S*)-Alpine Borane (**302**) instead of (*R*)-Alpine Borane (**293**) to give the desired enantiomer.

7.2.5 Synthesis of novel FDP analogues

Future work following the completion of this project could involve the synthesis of methylated analogues **439** and **440** (Figure 187). This project showed that EZS is able to accept (2*Z*,6*Z*)-2-methylfarnesyl diphosphate (**359**) and (2*Z*,6*Z*,10*Z*)-12-methoxyfarnesyl diphosphate (**362**) as substrates. These results give precedent that other analogous (2*Z*,6*Z*) FDP substrates incubated with EZS may yield 7-epizingiberene derivatives.

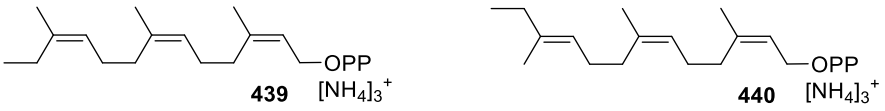

Figure 186. Prospective methylated analogues 439 and 440.

The synthesis of (2*Z*,6*Z*,10*Z*)-12-methylfarnesyl diphosphate (**439**) is outlined in Figure 187. The synthesis starts from alcohol **403** (Figure 172, 6.3.3). The methyl group of **443** is incorporated after oxidation of **403** to aldehyde **441**, a Wittig reaction to give **442** and hydrogenation of the terminal double bond.

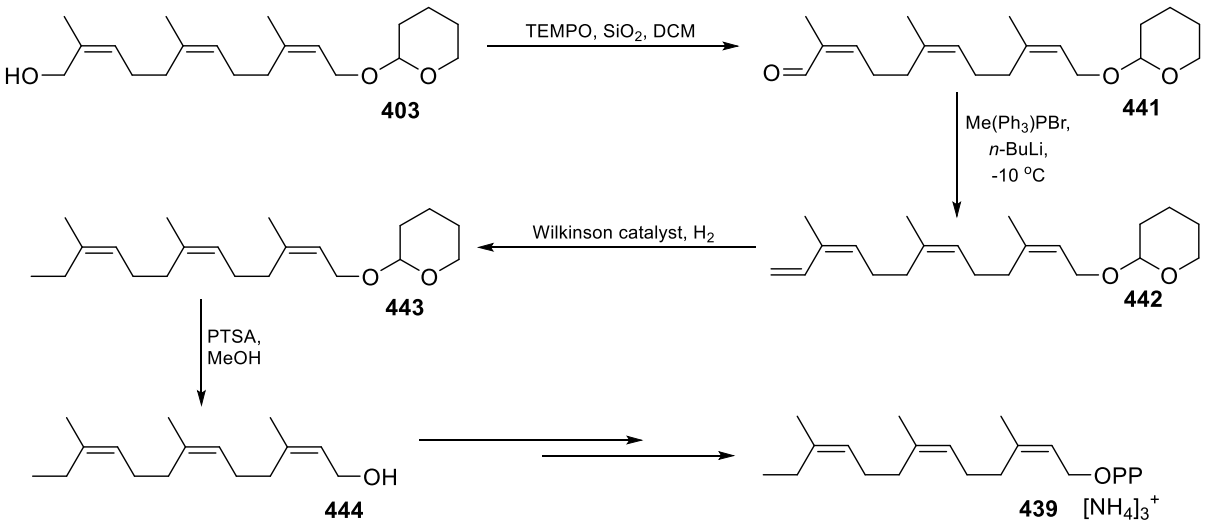

Figure 187. Proposed synthesis of (2*Z*,6*Z*,10*Z*)-12-methylfarnesyl diphosphate (439).

Chapter 8 – Materials and Methods

8.1 Biological Materials and Methods

8.1.1 Bacterial strains and preparation

Numerous chemically competent cell lines of *E.coli* were used during the course of this research; XL1-Blue cloning strain was used for the cloning of plasmid DNA and for the transformation and expression of protein; BL21(DE3), BL21 (DE3) – RP, ArcticExpress (DE3) and C41 (DE3) pLysS expression strains were used for the test and preparative expressions of 7-EZS (WT) prior to C41 (DE3) pLysS being used for all expressions of 7-EZS (WT) and mutants.

8.1.2 Competent Cells

Calcium chloride Buffer I

Calcium chloride (1.11 g, 100 mM) was dissolved in deionised water (100 mL). The solution was sterilised in an autoclave (121 °C, 20 minutes)

Calcium chloride Buffer II

Calcium chloride (1.11 g, 100 mM) was dissolved in deionised water (50 mL) and glycerol (15 mL, 15% v/v) was added. The solution was made up to final volume using deionised water prior to sterilisation in an autoclave (121 °C, 20 minutes)

Preparation of competent cells

For the preparation of C41 (DE3) pLysS chemically competent cells an agar stab courtesy of Prof. Martin J. Warren from the School of Biosciences at the University of Kent. Agar stab was perforated with a sterile metal loop and sample spread onto an agar plate containing chloramphenicol (0.1 mM) and incubated at 37 °C overnight. A single colony was placed into LB media (100 mL) with 50 µL chloramphenicol solution (25 mg/mL in ethanol) and grown overnight at 37 °C. Overnight culture (1 mL) was used to inoculate LB media (100 mL) containing 50 µL chloramphenicol solution (25 mg/mL in ethanol) and grown at 37 °C to an optical density of 0.9 at 600 nm (OD_{600}). The cells were harvested by centrifugation (4000 rpm / 10 minutes / 4°C) and the supernatant discarded. The pellet was gently re-suspended in calcium chloride buffer I (40 mL) and centrifuged (4000 rpm / 10 minutes / 4°C). Supernatant was discarded and the pellet gently re-suspended in calcium chloride buffer II (10 mL) and divided into 50 µL aliquots, flash frozen in liquid N_2 and stored at -80 °C.

For the preparation ofBL21 (DE3) chemically competent cells; a 50 µL aliquot was incubated in LB media (100 mL) and grown overnight at 37 °C. Overnight culture (1 mL) was used to inoculate LB media (100 mL) and the same procedure was followed.

8.1.3 Super-competent cells

Rubidium chloride buffer I

Rubidium chloride (100 mM), potassium acetate (30 mM), calcium chloride (10 mM), manganese chloride (50 mM) were dissolved in deionised water and glycerol (15%) was added. The pH of the solution was adjusted to 5.8, the final volume made up using deionised water and sterilised by filtration through a sterile 0.2 µM syringe filter under aseptic conditions.

Rubidium chloride buffer II

Rubidium chloride (10 mM), 3-(*N*-morpholino)propanesulfonic acid (MOPS, 10 mM), calcium chloride (75 mM) were dissolved in deionised water and glycerol (15%) was added. The pH of the solution was adjusted to 6.5, the final volume made up using deionised water and sterilised by filtration through a sterile 0.2 µM syringe filter under aseptic conditions.

Preparation of super-competent cells

Agar stab was perforated with a sterile metal loop and sample spread onto an agar plate containing chloramphenicol (0.1 mM) and incubated at 37 °C overnight. A single colony was placed into LB media (100 mL) with 50 µL chloramphenicol solution (25mg/mL in ethanol) and grown overnight at 37 °C. Overnight culture (1 mL) was used to inoculate LB media (100 mL) containing 50 µL chloramphenicol solution (25 mg/mL in ethanol) and grown at 37 °C to an optical density of 0.9 at 600 nm (OD_{600}). The cells were harvested by centrifugation (4000 rpm / 10 minutes / 4°C) and the supernatant discarded. The pellet was gently re-suspended in rubidium chloride buffer I (40 mL) and centrifuged (4000 rpm / 10 minutes / 4°C). Supernatant was discarded and the pellet gently re-suspended in rubidium chloride buffer II (10 mL) and divided into 50 µL aliquots, flash frozen in liquid N_2 and stored at -80 °C.

8.1.4 Growth media and antibiotic solutions

Luria-Bertani (LB) medium

Sodium chloride (10 gL^{-1}), yeast extract (5 gL^{-1}) and tryptone (10 gL^{-1}) were dissolved in deionised water and the resulting solution was sterilised in an autoclave (121 °C, 20 minutes) and cooled to room temperature prior to use. Required antibiotics were added at time of use under sterile conditions.

Terrific-Broth (TB) medium

Tryptone (12 g L^{-1}), yeast extract (24 g L^{-1}) and glycerol (4 mL L^{-1}) were dissolved in deionised water (800 mL), the resulting solution adjusted to 900 mL with deionised water and sterilised in an autoclave (121 °C, 20 minutes) and cooled to room temperature prior to use. Required antibiotics and phosphate buffer (0.17 M KH_2PO_4 and 0.72 M K_2HPO_4, 100 mL L^{-1}).

Phosphate buffer

Potassium phosphate monobasic (0.17 M, 23.14 g L^{-1}) and potassium phosphate dibasic (0.72 M, 125.4 g L^{-1}) were dissolved in deionised water (1 L) and sterilised in an autoclave (121 °C, 20 minutes).

LB agar plates

Yeast extract (5 g L^{-1}), sodium chloride (10 g L^{-1}), tryptone (10 g L^{-1}) and agar (15 g L^{-1}) were dissolved in deionised water and sterilised in an autoclave (121 °C, 20 minutes). The required antibiotic was added to the cooled agar (~40 °C) and the resultant mixture poured into plates under aseptic condition. The plates were cooled prior to storage at 4 °C.

Ampicillin

Ampicillin was dissolved in deionised water to give a 100 mgmL^{-1} solution which water filter sterilised through a 0.2 µM syringe filter under aseptic conditions and stored at 4 °C.

Chloramphenicol

Chloramphenicol was dissolved in ethanol to give a 25 mgmL^{-1} and stored at 4 °C.

Kanamycin

Kanamycin was dissolved in deionised water to give a 50 mgmL^{-1} solution which water filter sterilised through a 0.2 µM syringe filter under aseptic conditions and stored at 4 °C.

8.1.5 SDS-Page

SDS resolving buffer

A solution of Tris-Base (27.23 g, 1.5 M) in deionised water (100 mL) was adjusted to pH 8.8 and the final volume made to 150 mL.

SDS stacking buffer

A solution of Tris-Base (6.06 g, 0.5 M) in deionised water (80 mL) was adjusted to pH 6.8 and the final volume made to 100 mL.

Electrode running buffer (x10)

SDS (10 g, 10% w/v), Glycine (150.14 g, 2 M) and Tris-base (30.3 g, 0.25 M) were dissolved in deionised water (1L). Electrode buffer was diluted 10 fold with deionised water prior to use.

SDS sample Buffer

Bromophenol blue (0.2 mL of 0.6% w/v solution), glycerol (2.5 mL), SDS (2 mL of 10% w/v solution), SDS stacking buffer (1.25 mL), deionised water (3.55 mL) and β-mercaptoethanol were mixed into solution and stirred at room temperature.

Resolving gel (12%)

Resolving buffer (2.5 mL), 10% (w/v) SDS (0.1 mL), deionised water (3.4 mL) and 30% acrylamide / bis-acrylamide (4.0 mL) were mixed together. Immediately prior to use; 10% ammonium persulfate solution (APS, 50 µL, 100 $mgmL^{-1}$ in dH_2O) and N,N,N',N'-tetramethylenediamine (TEMED, 15 µL) were added to the solution a gently mixed to initiate polymerisation.

Stacking gel (4%)

Stacking buffer (2.5 mL), 10% (w/v) SDS (0.1 mL), deionised water (5.7 mL) and 30% acrylamide / bis-acrylamide (1.7 mL) were mixed together. Immediately prior to use; 10% ammonium persulfate solution (APS, 50 µL, 100 $mgmL^{-1}$ in dH_2O) and N,N,N',N'-tetramethylenediamine (TEMED, 20 µL) were added to the solution a gently mixed to initiate polymerisation.

SDS gel stain

Coomasie brilliant bluR-250 (60 mg) was dissolved in ethanol (10 mL). The resultant solution was made up to 1L with deionised water and acidified with concentrated hydrochloric acid (~2 mL).

SDS-Page protocol

Resolving and stacking gel solution were prepared as outlined above. The resolving gel was first poured, overlain with isopropanol and allowed to polymerise. Isopropanol was removed and stacking gel poured and allowed to polymerise after the addition of a comb to create loading wells. Fraction samples (10 µL) were incubated in SDS sample buffer (10 µL) for 5 minutes at 90 °C and loaded onto the gel. Electrode running buffer was added and the gel run for 1 hour at 150 V.

SDS-Page visualisation

After gel had run, it was removed from the plates, submerged in water placed in a microwave for 2 minutes. Water was replaced and the gel placed in the microwave for a further 2 minutes. Water was replaced with SDS gel stain, microwaved for 2 minutes and placed on a shaker to cool whilst stirring. SDS gel stain was decanted and the gel placed in water and microwaved for 2 minutes a further two times at which point all bands were visible and SDS gel stain was removed.

8.1.6 DNA purification

Miniprep of DNA

A single colony from an agar plate was used to inoculate LB medium (10 mL, containing appropriate antibiotic) and incubated overnight at 37 °C whilst shaking. Cells were harvested *via* centrifugation (4000 rpm, 10 minutes, 4 °C). Extraction and purification of DNA using a QIAprep spin miniprep kit (QIAGEN, Crawley, UK) *via* the manufacturers protocol was used in conjunction with EconoSpin All-in-1 mini spin columns (Epoch Biolabs, Inc, TX, USA).

Agarose gel DNA purification

A DNA sample from the agarose gel was removed and 3 volumes of QG buffer to 1 volume gel (100 mg gel ~ 100 µL) were added. The mixture was incubated at 50 °C and vortexed periodically to aid solvation of the gel. Isopropanol (1 gel volume) was added to the sample, mixed by inversion and bound to a QIAquick column *via* centrifugation (1 minute). Buffer QG (500 µL) was added to the column and centrifuged for 1 minute. Buffer PE (750 µL) was added to the column and left to stand for 3 minutes prior to centrifugation for 1 minute. DNA was eluted into a clean eppendorf by the addition of autoclaved water (50 µL), left to stand for 1 minute and centrifuged for 1 minute.

8.1.7 Transformation of Competent Cells

The appropriate plasmid and competent cells were thawed at 0 °C. DNA solution (1-1.5 µL) was added to competent cells and gently mixed. The DNA / cell mixture was incubated at 0 °C for 30 minutes and heat for 45 seconds at 42 °C. The mixture was incubated at 0 °C for 2 minutes prior to the addition of LB medium (1 ml, containing no antibiotic) and incubated for 1 hour under shaking at 37 °C. Cells were harvested by centrifugation (13000 rpm, 1 minute, Eppendorf centrifuge 5415R) and the majority of supernatant discarded. Cells were resuspended in remaining LB medium (~50 µL), plated on agar plates containing appropriate antibiotic and incubated at 37 °C overnight.

8.1.8 Expression of EZS

General method of protein expression: A single transformed colony was used to inoculate 100 mL of growth medium (LB / TB) with appropriate antibiotic and the culture was shaken overnight at 37 °C. Overnight growth (10 mL) was placed into 500 mL growth medium (LB / TB) and the appropriate antibiotics added. The inoculated broth was shaken at 37 °C until the optical density of cells (OD at 600 nm) reached 0.6 – 0.7 at which point isopropyl β-D-1-thiogalactopyranoside (IPTG, 60 mg) was added to induce protein expression. The medium was incubated at the required temperature an time as deduced by test expressions and cells harvested *via* centrifugation (4000 rpm, 15 minutes, 4 °C) and the respective cell pellet stored at -20 °C.

8.1.9 Purification methods

Cell lysis buffer 1

2-Mercaptoethanol (350 µL, 5 mM), TRIS Base (2.4 g / 20 mM), TWEEN 20 (91 µL, 1%) and sodium chloride (5.84 g, 100 mM) were dissolved in dH_2O (900 mL) and the pH of solution adjusted to pH 7.5 by the addition of hydrochloric acid (6 M). The mixture was then diluted to a volume of 1L with dH_2O.

Cell lysis buffer 2

2-Mercaptoethanol (350 µL, 5 mM), sodium chloride (5.84 g, 100 mM) and TRIS Base (2.4 g / 20 mM) were dissolved in dH_2O (900 mL) and the pH of solution adjusted to pH 7.5 by the addition of hydrochloric acid (6 M). The mixture was then diluted to a volume of 1L with dH_2O.

Cell lysis buffer 3

Into dH_2O (900 mL) was added sodium chloride (29.2 g, 500 mM), TRIS Base (2.4 g / 20 mM) and 2-mercaptoethanol (350 µL, 5 mM). Hydrochloric acid (6 M) was added to the solution to adjust the pH to pH 8 and the mixture diluted with dH_2O to a total volume of 1 L.

Cell lysis buffer 4

Sodium chloride (1.17 g, 100 mM), 2-mercaptoethanol (350 µL, 5 mM) and TRIS Base (2.4 g / 20 mM) were dissolved in dH_2O (900 mL) and the pH of solution adjusted to pH 8 by the addition of hydrochloric acid (6 M). The mixture was then diluted to a volume of 1L with dH_2O.

Sonication protocol

Pellet was defrosted on ice and cell lysis buffer (~100 mL), lysozyme (~30 mg) and phenylmethanesulfonyl fluoride (PMSF, ~10 mg) were added with suspension achieved *via* stirring at 5 °C. Suspended cells were placed in and ice/salt bath and sonicated: time; 5 minutes pulse ON; 5 seconds pulse OFF; 15 seconds. Lysed cell debris was harvested *via* centrifugation (18500 rpm, 40 min, 4 °C).

Basic extraction protocol

Insoluble fraction from sonication was suspended in cell lysis buffer (~60 mL) at 5 °C. Sodium hydroxide (6 M) was added dropwise to the suspended cells to increase the pH to pH 11 and stirred at 5 °C for 30 minutes. 2-mercaptoethanol (50 µL) was added to the suspension and the pH of the solution adjusted to pH 8 by the dropwise addition of hydrochloric acid (1 / 6 M) and stirred at 5 °C for 30 minutes. Cell debris was harvested *via* centrifugation (18500 rpm, 40 min, 4 °C).

Ni^{2+}-NTA affinity column protocol

Ni^{2+}affinity resin was equilibrated into appropriate buffer prior to the addition of supernatant containing extracted protein which was passed through the column 3 times. Numerous elution methods using increasing concentration of imidazole solutions were attempted to better elute impurities:

1. Buffer (1 x CV), 5 mM (1 x CV), 20 mM (1 x CV), 50 mM (1 x CV), 70 mM (1 x CV), 100 mM (1 x CV), 150 mM (1 x CV), 200 mM (1 x CV), 300 mM (1 x CV) and 500 mM (1 x CV)
2. Buffer (2 x CV), 5 mM (2 x CV), 20 mM (2 x CV), 50 mM (1 x CV), 70 mM (1 x CV), 100 mM (1 x CV), 150 mM (1 x CV), 200 mM (1 x CV), 300 mM (1 x CV) and 500 mM (1 x CV)
3. Buffer (2 x CV), 5 mM (4 x CV), 20 mM (4 x CV), 50 mM (1 x CV), 70 mM (1 x CV), 100 mM (1 x CV), 150 mM (1 x CV), 200 mM (1 x CV), 300 mM (1 x CV) and 500 mM (1 x CV)
4. Buffer (1 x CV), 5 mM (1 x CV), 20 mM (1 x CV), 300 mM (1 x CV) and 500 mM (1 x CV)
5. Buffer (4 x CV), 5 mM (6 x CV), 20 mM (6 x CV), 300 mM (2 x CV) and 500 mM (1 x CV)

CV = column volume

Ni^{2+}-NTA affinity column Imidazole buffer 1

Imidazole (68.1 g, 1 M), 2-mercaptoethanol (350 µL, 5 mM), TRIS Base (2.4 g / 20 mM), TWEEN 20 (91 µL, 1%) and sodium chloride (5.84 g, 100 mM) were dissolved in dH_2O (900 mL) and the pH of solution adjusted to pH 7.5 by the addition of hydrochloric acid (6 M). The mixture was then diluted to a volume of 1L with dH_2O.

Ni^{2+}-NTA affinity column Imidazole buffer 2

2-Mercaptoethanol (350 µL, 5 mM), imidazole (68.1 g, 1 M), sodium chloride (5.84 g, 100 mM) and TRIS Base (2.4 g / 20 mM) were dissolved in dH_2O (900 mL) and the pH of solution adjusted to pH 7.5 by the addition of hydrochloric acid (6 M). The mixture was then diluted to a volume of 1L with dH_2O.

Ni^{2+}-NTA affinity column Imidazole buffer 3

Into dH_2O (900 mL) was added sodium chloride (29.2 g, 500 mM), TRIS Base (2.4 g / 20 mM), 2-mercaptoethanol (350 µL, 5 mM) and imidazole (68.1 g, 1 M). Hydrochloric acid (6 M) was added to the solution to adjust the pH to pH 8 and the mixture diluted with dH_2O to a total volume of 1 L.

Ni^{2+}-NTA affinity column Imidazole buffer 4

Sodium chloride (1.17 g, 100 mM), 2-mercaptoethanol (350 µL, 5 mM), imidazole (68.1 g, 1 M) and TRIS Base (2.4 g / 20 mM) were dissolved in dH_2O (900 mL) and the pH of solution adjusted to pH 8 by the addition of hydrochloric acid (6 M). The mixture was then diluted to a volume of 1L with dH_2O.

Ni^{2+}-NTA affinity column Imidazole buffer 5

Imidazole (68.1 g, 1 M), 2-mercaptoethanol (350 µL, 5 mM), TRIS Base (2.4 g / 20 mM), TWEEN 20 (91 µL, 1%) and sodium chloride (1.17 g, 20 mM) were dissolved in dH_2O (900 mL) and the pH of solution adjusted to pH 7.5 by the addition of hydrochloric acid (6 M). The mixture was then diluted to a volume of 1L with dH_2O.

Dialysis protocol

Solution requiring dialysis was placed in dialysis tubing with 14 kDa membrane. Dialysis tubing was then placed into desired buffer (3 L) and stirred slowly at 5 °C. Dialysis was also achieved in four hours *via* the same protocol by replacing dialysis buffer (3 L) after 2 hours.

Spin Column buffer exchange / purification

Protein in solution was placed into a spin column with a molecular cut off of 50 kDa and concentrated to 1 mL. The concentrated mixture was diluted to 5 mL with pre-kinetics buffer and concentrated to 1 mL. The process was repeated a further 5 times.

FPLC Q-sepharose low salt buffer

Into dH_2O (900 mL) was added Tris Base (2.4 g, 20 mM), 2-mercaptoethanol (350 µL, 5 mM) and sodium chloride (1.17 g, 20 mM). The pH of the solution was adjusted to pH 8.0 prior to the dilution of the mixture to 1L. Buffer was filtered under *vaccuo* and degassed immediately prior to use.

FPLC Q-sepharose high salt buffer

Into dH_2O (900 mL) was added Tris Base (2.4 g, 20 mM), 2-mercaptoethanol (350 µL, 5 mM) and sodium chloride (58.4 g, 1 M). The pH of the solution was adjusted to pH 8.0 prior to the dilution of the mixture to 1L. Buffer was filtered under *vaccuo* and degassed immediately prior to use.

Anion exchange chromatography

Protein samples from Ni-NTA affinity column were dialysed into to FPLC Q-sepharose low salt buffer. The resulting solution was injected and eluted through a resource Q-sepharose column with a gradient flow of FPLC Q-sepharose high salt buffer (70 mL, 0-50% gradient) at a flow rate of 3 $mLmin^{1}$ followed by an isocratic flow of FPLC Q-sepharose high salt buffer (18.1 mL, 100%) at 3 $mLmin^{-1}$. UV absorbance was monitored at 280 nm.[252]

8.1.10 Bradford Assay

The Bradford assay was used to determine the concentration of product in solution after purification.

Bradford Reagent

Brilliant Blue G250 (10 mg) was dissolved in ethanol (2 mL) and H_3PO_4 added (80%, 10 mL). dH_2O was use to bring the final volume of solution to 100 mL where upon was stored in the dark at 4 °C.

Bradford Assay Protocol

A solution of bovine serum albumin (BSA, 1 $mgmL^{-1}$) in dH_2O was used to prepare a range solutions of varying concentrations; 0 – 100 μgmL^{-1} in 200 µL of deionised water. Bradford reagent (800 µL) was added to a solution and left to stand for 2 minutes after which the absorbance was measured from 400 – 600 nm using a SHAMADZU BioSpec-mini UV spectrophotometer. The ratio of absorbance's at 590 nm and 450 nm was calculated and plotted to give a standard curve. The procedure was repeated using samples of purified protein and the ratio of absorbance compared to the BSA standard curve to give the concentration of each sample.

8.1.11 Incubation and GC-MS analysis of enzymatic products

Incubation Buffer

Magnesium chloride (71.5 mg, 15 mM), 4-(2-hydroxyethyl)-1-piperazineethanesulfonic acid (HEPES, 298 mg, 25 mM) and dithiothreitol (88.6 mg, 5mM) was dissolved in dH_2O (40 mL). The pH was adjusted to pH 8.0 by the addition sodium hydroxide (1 M) and diluted to 50 mL with distilled water.

Incubation Protocol

Incubation buffer (200 µL), EZS (40 µL) and (2*Z*, 6*Z*) FDP (**38**, 10 µL, 20 mM)were placed in a GC-MS vial. Incubation mixture was overlain with pentane (1 mL) and incubated on a bench top shaker overnight. Incubation mixture and pentane were votexed for 5 seconds and the aqueous layer removed prior to the analysis of the pentane layer *via* GC-MS.

GC-MS method

Sample is injected at 80 °C and oven temperature held constant for 1 minute. A temperature gradient of 4 °C / min then follows for 15 minutes increasing the oven temperature from 80 to 180 °C.

8.1.12 Circular dichromism spectroscopy

Purified protein was buffer exchanged into K_XPO_4 (pH 8.0) buffer using a spin column (50 kDa molecular weight cut off). Protein stock was diluted with K_XPO_4 (pH 8.0) buffer to achieve a (10 µM) and circular dichromism experiments performed on an Applied PhotoPhysics Chirascan spectrometer. Spectra of protein (10 µM) K_XPO_4 (pH 8.0) buffer were measured between 190 nm and 600 nm in a 10 mm quartz cuvettes under N_2. Each protein was scanned in triplicate and the average of the three scans used for data plotting and analysis.

Calculation of mean residue molar ellipticity

Data points obtained from the CD spectrum were converted to mean residue ellipticity (MRE) using equation 1.1:

$$[\Theta]_{\mathrm{MRE}} = \frac{[\Theta]}{n.c.l}$$

Θ = molar ellipticity in millidegrees

n = number of peptide bonds in the protein

c = molar concentration of protein in the sample

l = path length in cm

8.1.13 Steady State Kinetics

EZS-pre kinetics buffer

Sodium chloride (5.84 g, 100 mM), TRIS Base (2.4 g, 20 mM) and 2-mercaptoethanol (350 µL, 5 mM) were dissolved in dH_2O (900 mL). Hydrochloric acid (1 M, 6 M and *conc*) was added to adjust the pH of the solution to pH 8.0 prior to dilution of the mixture to 1L with dH_2O.

Kinetics catalysis buffer A

Magnesium chloride (28.6 mg, 30 mM), TRIS base (30.1 mg, 25 mM) and dithiothreitol (15.4 mg, 10 mM) were dissolved in dH_2O (5 mL). The pH was altered to pH 8.0 and the solution diluted to 10 mL with deionised water.

Kinetics catalysis Buffer B

TRIS base (30.1 mg, 25 mM) was dissolved in dH_2O (5 mL). The pH was altered to pH 8.0 and the solution diluted to 10 mL with deionised water.

Steady State kinetics Protocol

Buffer A (125 µL), buffer B (60-105 µL) and (2*Z*, 6*Z*)-[1-^{3}H]-farnesyl diphosphate (0.1 - 70 µM) were placed in an eppendorf and cooled to 0 °C. Volume buffer B varied for the concentration change of (2*Z*, 6*Z*)-[1-^{3}H]-farnesyl diphosphate with a total volume of 235 µL. EZS (500 nM stock, 15 µL) was added to the solution at 0 °C and overlain with hexane (1 mL). Eppendorf was placed in a bench top shaker and incubated (10 min, 350 rpm, 30 °C). Incubations were immediately placed on ice and ethylenediaminetetraacetic acid (EDTA, 100 µL, 0.1 M) added. The reaction was vortexed for 5 seconds, the hexane overlay removed and passed through silica into scintillation cocktail (PerkinElmer OPTI-FLUOR® O, 15 mL). Extraction of enzymatic product was repeated with Hexane (900 µL x 2) and the extracts passed through silica. Hexane (1 mL) was passed through the silica pad into scintillation cocktail and the hexane / cocktail mixture vortexed for 5 seconds. Radioactive mixture was analysed using a TRI-CARB 2900TR Liquid Scintillation Analyzer.

Conversion of counts per minute (CPM) to rate

Equation 1.2

$$Rate = \frac{CPM}{(time\ x\ activity)}$$

CPM = Counts per minute

Time = Incubation time (seconds)

Equation 1.3

$$Activity = \frac{CPM\ of\ radioactive\ stock}{volume\ of\ radioactive\ stock}$$

Calculation of specific activity

Equation 1.4

$$Specific\ activity = \frac{moles}{radioactivity}$$

Michaelis-Menten equation

Equation 1.5

$$v = \frac{\delta[P]}{\delta t} = \frac{V_{max}\,[S]}{K_m + [S]}$$

v = rate of reaction

[P] = product concentration

V_{max} = maximum rate of reaction system

[S] = substrate concentration

K_M = Michaelis-Menten constant

Calculation of k_{cat}

Equation 1.6

$$V_{\max} = [\mathrm{E}_{Total}]\ x\ k_{\mathrm{cat}}$$

V_{max} = maximum rate of reaction (the point at which all active sites are saturated)

$[E_{Total}]$ = total concentration of enzyme

K_{cat} = substrate turnover number

8.1.14 Inhibition Studies

Inhibition assay – Steady state kinetics protocol

Buffer A (125 µL), buffer B (60-105 µL), (2*Z*, 6*Z*)-[1-^{3}H]-farnesyl diphosphate (0.2 – 70 µM) and inhibitor (5-30 µM)were placed in an eppendorf and cooled to 0 °C. Volume of buffer B was varied for the concentration changes of (2*Z*,6*Z*)-[1-^{3}H]-farnesyl diphosphate and inhibitor so the total volume of (2*Z*,6*Z*)-[1-^{3}H]-farnesyl diphosphate, inhibitor and buffers was 235 µL. EZS (30 nM) was added to the solution at 0 °C and overlain with hexane (1 mL). Eppendorf was placed in a bench top shaker and incubated (10 min, 350 rpm, 30 °C). Incubations were immediately placed on ice and ethylenediaminetetraacetic acid (EDTA, 100 µL, 0.1 M) added. The reaction was vortexed for 5

seconds, the hexane overlay removed and passed through silica into scintillation cocktail (PerkinElmer OPTI-FLUOR® O, 15 mL). Extraction of enzymatic product was repeated with hexane (900 µL x 2) and the extracts passed through silica. Hexane (1 mL) was passed through the silica pad into scintillation cocktail and the hexane / cocktail mixture vortexed for 5 seconds. Radioactive mixture was analysed using a TRI-CARB 2900TR Liquid Scintillation Analyzer.

Inhibition assay – inhibitor binding assay protocol

Buffer A (125 µL), buffer B (60-105 µL), (2*Z*, 6*Z*)-[1-^{3}H]-farnesyl diphosphate (8 µM) and inhibitor (0.01-1000 µM) were placed in an eppendorf and cooled to 0 °C. Volume of buffer B was varied for the concentration changes of the inhibitor so the total volume of (2*Z*,6*Z*)-[1-^{3}H]-farnesyl diphosphate, inhibitor and buffers was 235 µL. EZS (30 nM) was added to the solution at 0 °C and overlain with hexane (1 mL). Eppendorf was placed in a bench top shaker and incubated (10 min, 350 rpm, 30 °C). Incubations were immediately placed on ice and ethylenediaminetetraacetic acid (EDTA, 100 µL, 0.1 M) added. The reaction was vortexed for 5 seconds, the hexane overlay removed and passed through silica into scintillation cocktail (PerkinElmer OPTI-FLUOR® O, 15 mL). Extraction of enzymatic product was repeated with hexane (900 µL x 2) and the extracts passed through silica. Hexane (1 mL) was passed through the silica pad into scintillation cocktail and the hexane / cocktail mixture vortexed for 5 seconds. Radioactive mixture was analysed using a TRI-CARB 2900TR Liquid Scintillation Analyzer.

Lineweaver-Burk Plot

A Lineweaver-Burk plot (double reciprocal plot) was used as method for visualising enzyme kinetics for the determination of the mode of inhibition. Plots were derived from fitting experimental data to the following equation 1.7:

$$\frac{1}{v} = \frac{K_m + [S]}{V_{max}\,[S]} = \frac{K_m}{V_{max}}\,\frac{1}{[S]} + \frac{1}{V_{max}}$$

Graphical calculation of k_i

A plot of $K_{M(app)}$ vs. inhibitor concentration [I] was used to calculate the inhibition constant k_i. Experimental data was used for data points and linear regression utilised to visualise the x-intercept representing k_i. Equation 1.8:

$$K_{\mathrm{i}} = \frac{[\mathrm{I}]}{\left(\frac{K_{\mathrm{M(app)}}}{K_M}\right) - 1}$$

K_i = inhibition constant

[I] = inhibitor concentration

$K_{M(app)}$ = apparent value of K_M at different inhibitor concentrations

Standard errors of the weighted mean

A weighted average was calculates to estimate to true value of K_M and k_{cat} as each set of measurements for the same experiment was carried out separately and independently. The weighted average mean (X_{wav}) was calculated using the following equation 1.9:

$$X_{\mathrm{wav}} = \frac{\sum W_{\mathrm{i}}\, X_{\mathrm{i}}}{\sum W_{\mathrm{i}}}$$

X_{WAV} = weighted average mean

W_i= reciprocal square of each measurements uncertainty

X_i = each value in the sample

Calculation of W_i

The reciprocal squares of each measurements of individual uncertainty were calculated using the following equation 1.10:

$$W_{\mathrm{i}} = \frac{1}{\sigma_{\mathrm{i}}{}^2}$$

σ = uncertainty of measurement

Standard error of the weighted mean

Equation 1.10

$$\sigma_{\mathrm{wav}} = \frac{1}{\sqrt{\sum W_{\mathrm{i}}}}$$

σ_{WAV} = standard error of the weighted mean

Propagation of error

The following equation was used to calculate the propagation of errors when appropriate (If $Z = X/Y$).

Equation 1.11:

$$\left(\frac{\Delta Z}{Z}\right) = \sqrt{\left(\frac{\Delta X}{X}\right)^2 + \left(\frac{\Delta Y}{Y}\right)^2}$$

X and *Y* = experimentally measured values

ΔX and *ΔY* = error of experimentally measured values

Z = calculate value

Δ*Z* = propagated error

8.2 Organic Synthesis Experimental

All chemicals were purchased from Sigma-Aldrich, Alfa-Aesar, Fisher Scientific or Fluorochem and used without further purification unless otherwise stated.

Anhydrous tetrahydrofuran (THF), diethyl ether (Et_2O), toluene, and acetonitrile were obtained from an MBraun SPS800 solvent purification system. ^{1}H NMR, ^{2}H NMR, ^{13}C NMR, ^{31}P NMR and ^{19}F NMR spectra were measured on a Bruker Avance III 600, Bruker Avance 500, Bruker Avance III HD 400 and a Bruker Fourier 300 NMR spectrometer. The spectra are reported as chemical shifts in parts per million, downfield from tetramethylsilane (^{1}H and ^{13}C), trichlorofluoromethane (^{19}F) and phosphoric acid (^{31}P), multiplicity (s-singlet, d-doublet, t-triplet, q-quartet, quin-quintet, m-multiplet, dd-doublet of doublet and dq-doublet of quartet), integral, multiplicity, coupling and assignment, respectively. Assignments are made to the limitations of COSY, DEPT 90/135, NOESY and gradient HSQC spectra.

Mass spectra were measured on a Waters GCT Premier time of flight mass spectrometer and a Waters LCT time of flight mass spectrometer. The methods used are the same as described in Section 8.1.11. Thin layer chromatography (TLC) was performed on pre-coated aluminium plates of silica G/UV254. TLC visualisations were performed with 4.2% ammonium molybdate and 0.2% ceric sulfate in 5% H_2SO_4 (Hanessian's stain), 0.1% berberine hydrochloride in EtOH or UV light.

Ion-exchange chromatography was performed using ion-exchange resin (Amberlyst 131 wet, H^+ form) pre-equilibrated with ion-exchange buffer (25 mM NH_4HCO_3 containing 2% isopropanol, 2 CV). Reverse phase HPLC was performed on a system comprising of a Dionex P680 pump and a Dionex UVD170U detector unit. The column used was a 150 x 21.2 mm Phenomenex Luna C-18 column. Crude diphosphates were eluted under isocratic conditions with 10% B for 20 min, a linear gradient to 60% B over 25 min, then a linear gradient to 100% B over 5 min and finally with 100% B for 10 min; solvent B: acetonitrile; solvent A: 25 mM ammonium bicarbonate in water, flow rate 5.0 cm^3min^{-1}, detection at 220 nm.

8.2.1 Synthesis of (2*Z*,6*Z*) farnesyl diphosphate (38)

Preparation of (Z)-1-bromo-3,4-dimethylocata-2,6-diene (164):

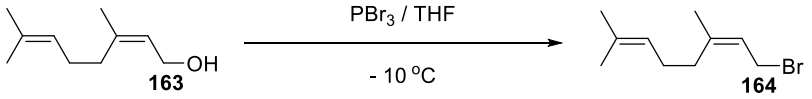

A stirred solution of nerol (10 g, 64.8 mmol, 1 eq.) in anhydrous tetrahydrofuran (25 mL) was cooled to -10 °C and phosphorous tribromide (3.04 mL, 32.4 mmol, 0.5 eq.) was added dropwise. The resulting solution was stirred at -10 °C for 15 minutes and then concentrated under reduced pressure. The resulting residue was dissolved in diethyl ether-hexane (1:1, 30 mL) and washed with saturated sodium hydrogen carbonate solution (3 x 15 mL), water (3 x 15 mL) and brine (15 mL). The organic fraction was dried over sodium sulfate, filtered and the solvent removed under reduced pressure. The product was further dried under vacuum for 1 hour to yield bromide **164** as a pale yellow oil (14 g, 99%) which was used without further purification.

^{1}H NMR (300 MHz, $CDCl_3$) δ 5.55 (1H, t, *J* = 8.5 Hz, C*H*CH_2Br), 5.18 – 5.09 (1H, m, CC*H*CH_2), 4.02 (2H, d, *J* = 8.5 Hz, C*H*$_2$Br), 2.16 (4H, m, CHC*H*$_2$C*H*$_2$C), 1.77 (3H, s, CH_2C(C*H*$_3$)CH), 1.70 (3H, s, C*H*$_3$CCH), 1.63 (3H, s, C*H*$_3$CCH).

Preparation of ethyl (Z)-2-acetyl-5,9-dimethyldeca-4,8-dienoate (165):

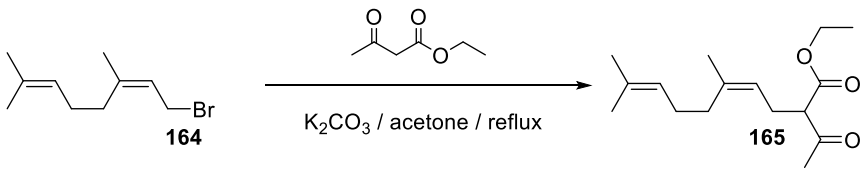

Crude bromide **164** (14 g, 64.8 mmol, 1 eq.) was dissolved in anhydrous acetone (30 mL) and ethyl acetoacetate (16.9 g, 16.5 mL, 129.6 mmol, 2 eq.) and anhydrous potassium carbonate (18.0 g, 129.6 mmol, 2 eq.) were added. The resulting suspension was refluxed at 60 °C for 4 hours. The solution was then concentrated under reduced pressure and residue was dissolved in diethyl ether (20 mL) and washed with water (3 x 15 mL) and brine (15 mL) before being dried over sodium sulfate and the solvent removed under reduced pressure. The residue was purified by flash chromatography on silica gel (20% ethyl acetate in hexane) to yield **165** as a clear oil (13.46 g, 78%).

^{1}H NMR (300 MHz, $CDCl_3$) δ 5.09 – 5.03 (2H, m, 2 x (CH_3)CC*H*), 4.20 (2H, q, *J* = 7.1 Hz, CH_3C*H*$_2$O), 3.43 (1H, t, *J* = 7.5 Hz, COC*H*CO), 2.55 (2H, t, *J* = 7.4 Hz, CCHC*H*$_2$CH), 2.22 (3H, s, COC*H*$_3$), 2.17-1.94 (4H, m,

2 x allylic C*H*$_2$), 1.69(6H, s, 2 x C*H*$_3$), 1.62 (3H, s, C*H*$_3$), 1.28 (3H, t, *J* = 7.1 Hz,C*H*$_3$CH$_2$O). **^{13}C NMR** (75 MHz, $CDCl_3$) δ 169.6 (CH_3*C*(O)CH), 147.1 (CH_3CH_2O*C*(O)), 138.6 & 131.9 (2 x (CH_3)*C*CH), 123.9 & 120.3 (2 x CH_3C*C*H), 61.3 (CH_3*C*H_2O), 60.0 (C(O)*C*HC(O)), 31.8 (allylic *C*H_2), 29.00 (*C*H_3C(O)), 26.5 (CCH*C*H_2CH), 26.3 (allylic *C*H_2), 25.6 & 23.3 (2 x *C*H_3), 17.5 (*C*H_3), 14.0 (OCH_2*C*H_3). **LRMS** (EI$^+$): 248.18 (5% [M – H_2O]), 175.15 (7%), 159.12 (10%), 136.13 (50%), 121.10 (65%), 119.09 (75%), 109.10 (78%), 93.07 (100%), 79.06 (45%), 67.05 (32%). **HRMS** (EI$^+$): calculated for $C_{16}H_{24}O_2$ [M-H_2O]$^+$; 248.1776, found 248.1776.

Preparation of (Z)-6,10-dimethylundeca-5,9-dien-2-one (166):

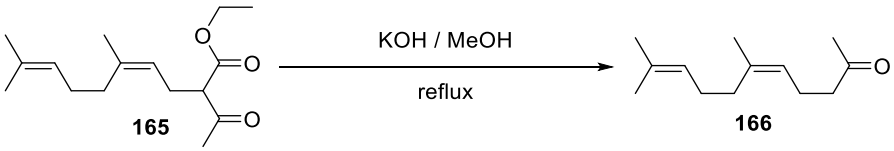

Potassium hydroxide (8.5 g, 151.6 mmol, 1 eq.) was added to a solution of **165** (13.46 g, 50.5 mmol, 1eq.) in methanol (20 mL) and refluxed at 65 °C for 2 hours. The reaction mixture was then cooled, and then acidified with dilute hydrochloric acid (1 M, 10 mL). The mixture was extracted with diethyl ether (3 x 15 mL) and the organic layers combined and washed with saturated sodium hydrogen carbonate solution (3 x 10 mL), water (3 x 10 mL) and brine (10 mL). The organic portion was dried over anhydrous sodium sulfate, filtered and concentrated under reduced pressure. Purification *via* flash chromatography on silica gel (10% ethyl acetate in hexane) provided ketone **166** as a clear oil (9.8 g, 99%).

^{1}H NMR (300 MHz, $CDCl_3$) δ 5.15 – 5.03 (2H, m, 2 x (CH_3)CC*H*), 2.45 (2H, t, *J* = 7.3 Hz, C*H*$_2$C(O)), 2.26 (2H, dd, *J* = 14.6, 7.2 Hz, C*H*$_2$CH$_2$C(O)), 2.14 (3H, s, CH$_2$C(O)C*H*$_3$), 210 – 1.95 (4H, m, 2 x allylic C*H*$_2$), 1.69 (6H, s, 2 x C*H*$_3$), 1.61 (3H, s, (C*H*$_3$)CCH). **^{13}C NMR** (75 MHz, $CDCl_3$) δ 209.00 (CH_3*C*(O)), 142.7 & 136.5 (2 x (CH_3)*C*CH), 124.0 &123.3 (2 x (CH_3)C*C*H), 43.9 (CH_2*C*H_2C(O)), 31.7 & 26.4 (2 x allylic *C*H_2), 29.8 (*C*H_3C(O)), 25.6 & 23.2 (2 x (*C*H_3)CCH), 22.1 (CH_2*C*H_2CO), 17.8 (*C*H_3). **LRMS** (EI$^+$): 194.17 (7% [M]), 176.15 (95%), 151.11 (35%), 133.10 (80%), 121.10 (85%), 105.06 (100%), 93.06 (95%), 79.05 (82%), 69.06 (92%). **HRMS** (EI$^+$): calculated for $C_{13}H_{22}O$ [M]$^+$; 194.1671, found 194.1677.

Preparation of ethyl (2Z,6Z)-3,7,11-trimethyldodeca-2,6,10-trienoate (193):

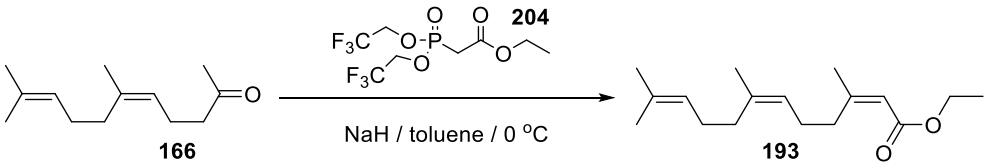

A stirred suspension of sodium hydride (161 mg, 6.70 mmol, 1.3 eq.) in anhydrous toluene (40 mL) was cooled to 0 °C and ethyl 2-(bis(2,2,2-trifluoroethoxy)phosphoryl)acetate **204** (2.05 g, 6.17 mmol, 1.2 eq.) was added dropwise. The reaction mixture was stirred at room temperature for 1 hour and cooled to 0 °C. Neryl acetone **166** (1 g, 5.14 mmol, 1 eq.) was added dropwise and the reaction mixture stirred at room temperature for 16 hours. The reaction was quenched with water (20 mL) and products extracted with diethyl ether (3 x 20 mL). Organic extracts were washed with water (3 x 20 mL) and brine (3 x 20 mL), dried over sodium sulphate, filtered and concentrated under reduced pressure. Purification *via* flash chromatography (2% ethyl acetate in hexane) gave **193** as a clear oil (571 mg, 43%).

^{1}H NMR (300 MHz, $CDCl_3$) δ 5.58 (1H, s, CC*H*C(O)OEt), 5.13 – 5.00 (2H, m, 2 x (CH_3)CC*H*), 4.06 (2H, q, *J* = 7.1 Hz, OCH_2CH_3), 2.62 – 2.52 (2H, m, $CH_2(CH_3)$CCHC(O)), 2.15 – 2.04 (2H, m, $CH_2CH_2(CH_3)$CCHC(O)), 2.00 – 1.89 (4H, m, 2 x allylic CH_2), 1.81 (3H, d, *J* = 1.3 Hz, $CH_2(CH_3)$CCHC(O)), 1.61 (6H, s, 2 x CH_3), 1.54 (3H, s, CH_3), 1.20 (3H, t, *J* = 7.1 Hz, OCH_2CH_3). **^{13}C NMR** (75 MHz, $CDCl_3$) δ 166.3 (CH*C*(O)O), 160.1 ((CH_3)*C*CHC(O)O), 135.8 & 131.5 (2 x (CH_3)*C*CH), 124.4 & 124.3 (2 x (CH_3)C*C*H), 116.2 (C*C*HC(O)O), 59.4 (OCH_2CH_3), 33.7 ($CH_2(CH_3)$CCHC(O)), 31.9 & 26.63 (2 x CH_2), 26.60 ($CH_2CH_2(CH_3)$CCHC(O)) 25.7 & 25.4 & 23.4 17.6 (4 x CH_3), 14.1 (OCH_2CH_3). **LRMS** (EI^+): 264.21 (5% [M]), 218.17 (55%), 197.10 (55%), 183.11 (45%), 159.08 (42%), 143.08 (40%), 128.07 (85%), 93.07 (100%), 82.04 (60%), 69.07 (25%). **HRMS** (EI^+): calculated for $C_{17}H_{28}O_2$ $[M]^+$; 264.2089, found 264.2089.

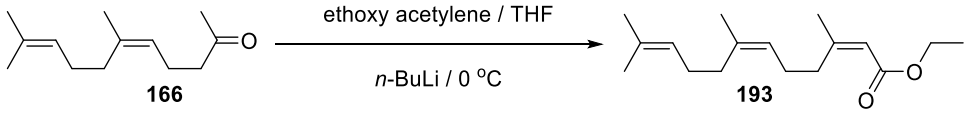

To a stirred solution of ethoxy acetylene (250 mg, 1.8 mmol, 2.5 eq.) and anhydrous THF (20 mL) was cooled to -78 °C and *n*-butyl lithium (720 µL, 1.79 mmol, 2.5 eq.) was added dropwise. The reaction mixture was stirred for 1 hour at -78 °C and warmed to -40 °C prior to the addition of neryl acetone (**166**)(160 mg, 0.7 mmol, 1 eq.) and was stirred for 1 hour. The reaction mixture was allowed to warm to room temperature and was stirred for 16 hours. The reaction was quenched with water (10

mL) and the products extracted with diethyl ether (3 x 10 mL). Organic extracts were washed with water (3 x 10 mL), brine (20 mL), dried over sodium sulphate and concentrated under *vaccuo.* Purification *via* flash chromatography (2% ethyl acetate in hexane) provided ester **193** as a clear oil (49 mg, 26%).

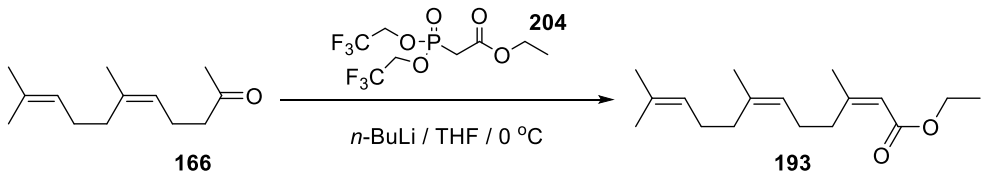

A stirred solution of ethyl 2-(bis(2,2,2-trifluoroethoxy)phosphoryl)acetate **204** (4.37 g, 13.2 mmol, 1.5 eq.) in anhydrous tetrahydrofuran (30 mL) was cooled to 0 °C and *n*-butyl lithium (5.3 mL, 13.2 mmol, 1.5 eq., 2.5M in hexanes) was added dropwise. The resulting solution was stirred at room temperature for 1 hour, cooled to 0 °C and neryl acetone **166** (1.71 g, 8.8 mmol, 1 eq.) added dropwise. The reaction mixture was stirred for 16 hours at room temperature. The reaction was quenched with water (10 mL) and the product was extracted with diethyl ether (3 x 20 mL). The combined organic phases were washed with water (3 x 10 mL) and brine (2 x 10 mL), then dried over sodium sulphate, filtered and the solvent removed under reduced pressure. Purification *via* flash chromatography on silica gel (2% ethyl acetate in hexane) provided ester **193** as a clear oil (763 mg, 33%).

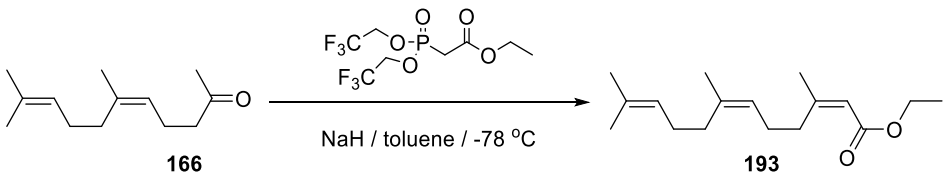

A stirred suspension of sodium hydride (161 mg, 6.70 mmol, 1.3 eq.) in anhydrous toluene (40 mL) was cooled to 0 °C and **204** (2.05 g, 6.17 mmol, 1.2 eq.) was added dropwise. The reaction mixture was stirred at room temperature for 1 hour and cooled to -78°C. **166** (1 g, 5.14 mmol, 1 eq.) was added dropwise and the reaction mixture stirred at room temperature for 16 hours. The reaction was quenched with water (20 mL) and products extracted with diethyl ether (3 x 20 mL). Organic extracts were washed with water (3 x 20 mL) and brine (3 x 20 mL), dried over sodium sulphate, filtered and concentrated under reduced pressure. Purification via flash chromatography (2% ethyl acetate in hexane) gave **193** as a clear oil (517 mg, 38%).

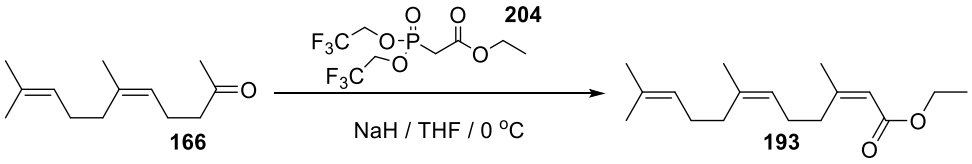

A stirred suspension of sodium hydride (185 mg, 7.72 mmol, 3 eq.) in anhydrous tetrahydrofuran (**20** mL) was cooled to 0 °C and **204** (930 mg, 2.80 mmol, 1.1 eq.) was added dropwise. The reaction mixture was stirred at room temperature for 1 hour and cooled to 0 °C. **166** (500 mg, 2.57 mmol, 1 eq.) was added dropwise and the reaction mixture stirred at room temperature for 16 hours. The reaction was quenched with water (**10** mL) and products extracted with diethyl ether (3 x 10 mL). Organic extracts were washed with water (3 x 10 mL) and brine (3 x 10 mL), dried over sodium sulphate, filtered and concentrated under reduced pressure. Purification *via* flash chromatography (10% ethyl acetate in hexane) gave **193** as a clear oil (260 mg, 38%).

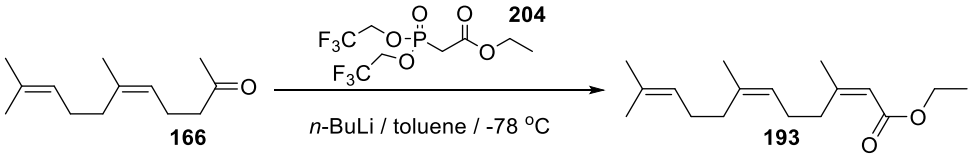

A stirred suspension of **204** (930 mg, 2.80 mmol, 1.1 eq.) in anhydrous toluene (**20** mL) was cooled to 0 °C and *n*-BuLi (1.1 mL, 2.80 mmol, 1.1 eq, 2.5 M in hexane.) was added dropwise. The reaction mixture was stirred at room temperature for 1 hour and cooled to -78 °C. **166** (500 mg, 2.57 mmol, 1 eq.) was added dropwise and the reaction mixture stirred at room temperature for 16 hours. The reaction was quenched with water (**10** mL) and products extracted with diethyl ether (3 x 10 mL). Organic extracts were washed with water (3 x 10 mL) and brine (3 x 10 mL), dried over sodium sulphate, filtered and concentrated under reduced pressure. Purification *via* flash chromatography (10% ethyl acetate in hexane) gave **193** as a clear oil (227 mg, 31%).

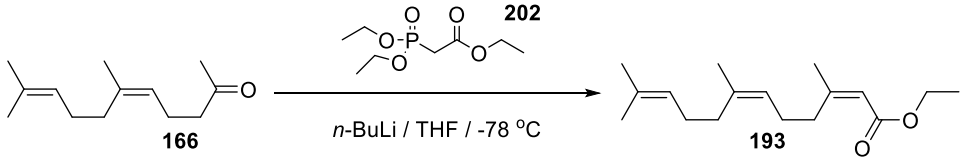

A stirred solution of ethyl 2-(diethoxyphosphoryl)acetate **202** (865 mg, 3.9 mmol, 1.5 eq.) in anhydrous tetrahydrofuran (20 mL) was cooled to 0 °C and *n*-butyl lithium (1.54 mL, 3.9 mmol, 1.5 eq., 2.5M in hexanes) was added dropwise. The resulting solution was stirred at room temperature

for 1 hour, cooled to -78 °C and **166** (500 mg, 2.6 mmol, 1 eq.) added dropwise. The reaction mixture was stirred for 16 hours at room temperature. The reaction was quenched with water (10 mL) and the product was extracted with diethyl ether (3 x 20 mL). The combined organic phases were washed with water (3 x 10 mL) and brine (2 x 10 mL), then dried over sodium sulphate, filtered and the solvent removed under reduced pressure. Purification *via* flash chromatography on silica gel (2% ethyl acetate in hexane) provided ester **193** as a clear oil (82 mg, 12 %).

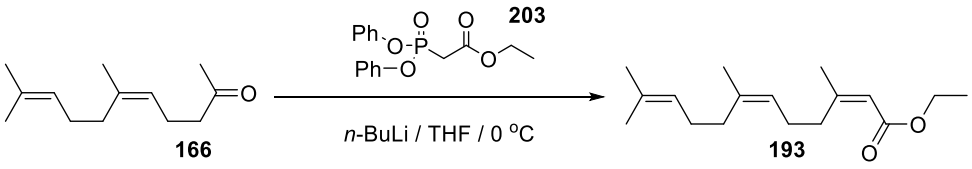

A stirred solution of ethyl 2-(diphenoxyphosphoryl)acetate **203** (1.85 g, 5.77 mmol, 1.5 eq.) in anhydrous tetrahydrofuran (40 mL) was cooled to 0 °C and *n*-butyl lithium (2.3 mL, 5.77 mmol, 1.5 eq., 2.5M in hexanes) was added dropwise. The resulting solution was stirred at room temperature for 1 hour, cooled to 0 °C and **166** (750 mg, 38.5 mmol, 1 eq.) added dropwise. The reaction mixture was stirred for 16 hours at room temperature. The reaction was quenched with water (10 mL) and the product was extracted with diethyl ether (3 x 20 mL). The combined organic phases were washed with water (3 x 20 mL) and brine (3 x 20 mL), then dried over sodium sulphate, filtered and the solvent removed under reduced pressure. Purification *via* flash chromatography on silica gel (2% ethyl acetate in hexane) provided ester **193** as a clear oil (214 mg, 21 %).

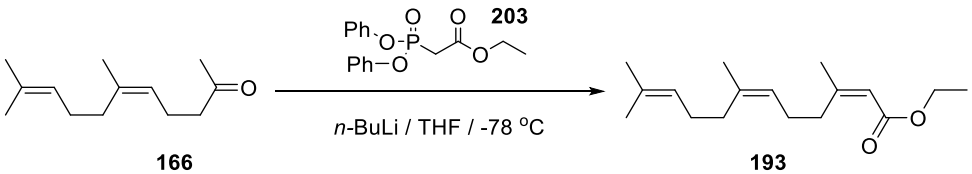

A stirred solution of **203** (1.85 g, 5.8 mmol, 1.5 eq.) in anhydrous tetrahydrofuran (50 mL) was cooled to 0 °C and *n*-butyl lithium (2.3 mL, 5.8 mmol, 1.5 eq., 2.5M in hexanes) was added dropwise. The resulting solution was stirred at room temperature for 1 hour, cooled to -78 °C and **166** (750 mg, 3.85 mmol, 1 eq.) added dropwise. The reaction mixture was stirred for 16 hours at room temperature. The reaction was quenched with water (20 mL) and the product was extracted with diethyl ether (40 mL). The combined organic phases were washed with water (3 x 10 mL) and brine (3 x 10 mL), then dried over sodium sulphate, filtered and the solvent removed under reduced

pressure. Purification *via* flash chromatography on silica gel (2% ethyl acetate in hexane) provided ester **193** as a clear oil (217 mg, 21%).

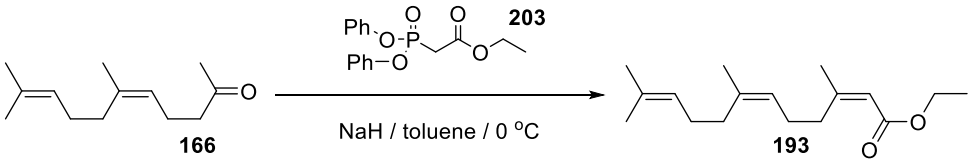

A stirred suspension of sodium hydride (990 mg, 24.8 mmol, 1.7 eq.) in anhydrous toluene (30 mL) was cooled to 0 °C and **203** (7.0 g, 21.9 mmol, 1.5 eq.) was added dropwise. The reaction mixture was stirred at room temperature for 1 hour and cooled to 0 °C. **166** (2.83 g, 14.6 mmol, 1 eq.) was added dropwise and the reaction mixture stirred at room temperature for 16 hours. The reaction was quenched with water (20 mL) and products extracted with diethyl ether (3 x 20 mL). Organic extracts were washed with water (3 x 20 mL) and brine (20 mL), dried over sodium sulphate, filtered and concentrated under reduced pressure. Purification *via* flash chromatography (2% ethyl acetate in hexane) gave **193** as a clear oil (386 mg, 29%).

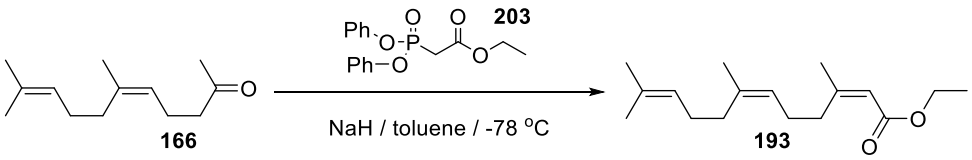

A stirred suspension of sodium hydride (990 mg, 24.8 mmol, 1.7 eq.) in anhydrous toluene (30 mL) was cooled to 0 °C and **203** (7.0 g, 21.9 mmol, 1.5 eq.) was added dropwise. The reaction mixture was stirred at room temperature for 1 hour and cooled to -78 °C. **166** (2.83 g, 14.6 mmol, 1 eq.) was added dropwise and the reaction mixture stirred at room temperature for 16 hours. The reaction was quenched with water (20 mL) and products extracted with diethyl ether (3 x 20 mL). Organic extracts were washed with water (3 x 20 mL) and brine (20 mL), dried over sodium sulphate, filtered and concentrated under reduced pressure. Purification *via* flash chromatography (2% ethyl acetate in hexane) gave **193** as a clear oil (309 mg, 23%).

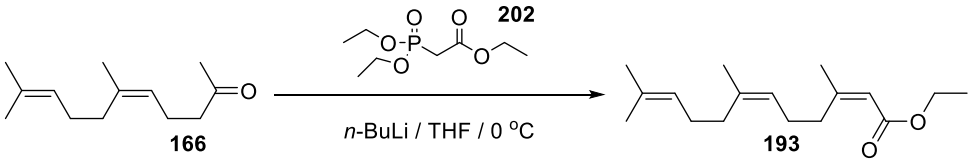

A stirred solution of **202** (630 mg, 2.57 mmol, 1 eq.) in anhydrous tetrahydrofuran (20 mL) was cooled to 0 °C and *n*-butyl lithium (1.1 mL, 2.83 mmol, 1.1 eq., 2.5M in hexanes) was added dropwise. The resulting solution was stirred at room temperature for 1 hour, cooled to 0 °C and **166** (500 mg, 2.57 mmol, 1 eq.) added dropwise. The reaction mixture was stirred for 16 hours at room temperature. The reaction was quenched with water (5 mL) and the product was extracted with diethyl ether (3 x 10 mL). The combined organic phases were washed with water (3 x 10 mL) and brine (10 mL), then dried over sodium sulphate, filtered and the solvent removed under reduced pressure. Purification *via* flash chromatography on silica gel (2% ethyl acetate in hexane) provided ester **193** as a clear oil (93 mg, 14%).

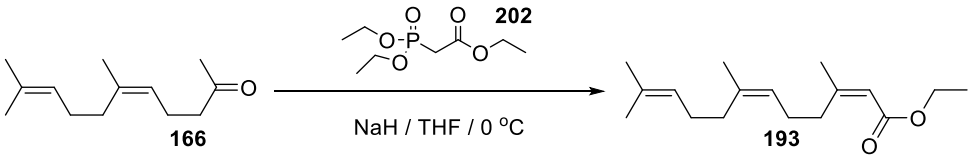

A stirred suspension of sodium hydride (185 mg, 7.72 mmol, 3 eq.) in anhydrous tetrahydrofuran (**20** mL) was cooled to 0 °C and **202** (630 mg, 2.80 mmol, 1.1 eq.) was added dropwise. The reaction mixture was stirred at room temperature for 1 hour and cooled to 0 °C. **166** (500 mg, 2.57 mmol, 1 eq.) was added dropwise and the reaction mixture stirred at room temperature for 16 hours. The reaction was quenched with water (**10** mL) and products extracted with diethyl ether (3 x 10 mL). Organic extracts were washed with water (3 x 10 mL) and brine (3 x 10 mL), dried over sodium sulphate, filtered and concentrated under reduced pressure. Purification *via* flash chromatography (10% ethyl acetate in hexane) gave **193** as a clear oil (116 mg, 17%).

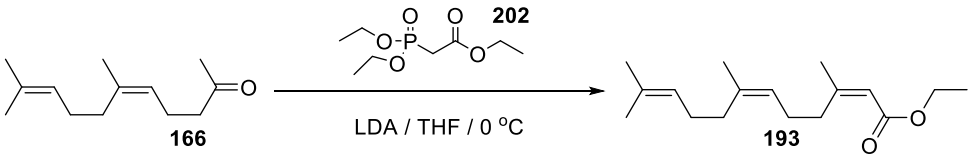

A stirred solution of **202** (630 mg, 2.80 mmol, 1.1 eq.) in anhydrous tetrahydrofuran (20 mL) was cooled to 0 °C and lithium diisopropylamide (827 mg, 7.72 mmol, 3 eq.) was added dropwise. The

resulting solution was stirred at room temperature for 1 hour, cooled to 0 °C and **166** (500 mg, 2.57 mmol, 1 eq.) added dropwise. The reaction mixture was stirred for 16 hours at room temperature. The reaction was quenched with water (10 mL) and the product was extracted with diethyl ether (3 x 10 mL). The combined organic phases were washed with water (3 x 10 mL) and brine (3 x 10 mL), then dried over sodium sulphate, filtered and the solvent removed under reduced pressure. Purification *via* flash chromatography on silica gel (2% ethyl acetate in hexane) provided ester **193** as a clear oil (56 mg, 8%).

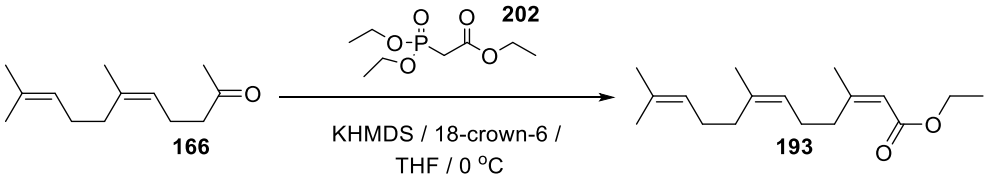

A stirred suspension of Potassium bis(trimethylsilyl)amide (7.7 mL mg, 7.72 mmol, 3 eq.) and 18-crown-6 (2.04 g, 7.72 mmol, 3 eq.) in toluene (20 mL) was cooled to 0 °C and **202** (630 mg, 2.83 mmol, 1.1 eq.) was added dropwise. The reaction mixture was stirred at room temperature for 1 hour and cooled to 0 °C. **166** (500 mg, 2.57 mmol, 1 eq.) was added dropwise and the reaction mixture stirred at room temperature for 16 hours. The reaction was quenched with water (10 mL) and products extracted with diethyl ether (3 x 10 mL). Organic extracts were washed with water (3 x 10 mL) and brine (3 x 10 mL), dried over sodium sulphate, filtered and concentrated under reduced pressure. Purification *via* flash chromatography (2% ethyl acetate in hexane) gave **193** as a clear oil (75 mg, 11%).

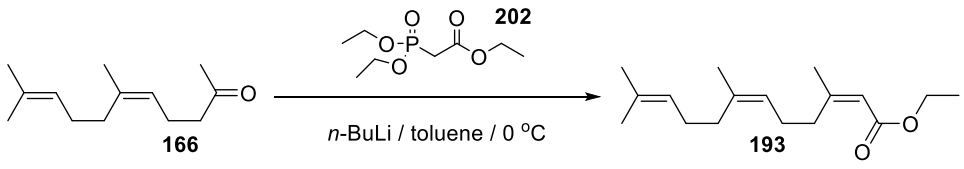

A stirred solution of ethyl 2-(diethoxyphosphoryl)acetate **202** (865 mg, 3.9 mmol, 1.5 eq.) in anhydrous toluene (20 mL) was cooled to 0 °C and *n*-butyl lithium (1.54 mL, 3.9 mmol, 1.5 eq., 2.5M in hexanes) was added dropwise. The resulting solution was stirred at room temperature for 1 hour, cooled to 0 °C and **166** (500 mg, 2.6 mmol, 1 eq.) added dropwise. The reaction mixture was stirred for 16 hours at room temperature. The reaction was quenched with water (10 mL) and the product was extracted with diethyl ether (3 x 20 mL). The combined organic phases were washed with water

(3 x 10 mL) and brine (2 x 10 mL), then dried over sodium sulphate, filtered and the solvent removed under reduced pressure. Purification *via* flash chromatography on silica gel (2% ethyl acetate in hexane) provided ester **193** as a clear oil (84 mg, 14%).

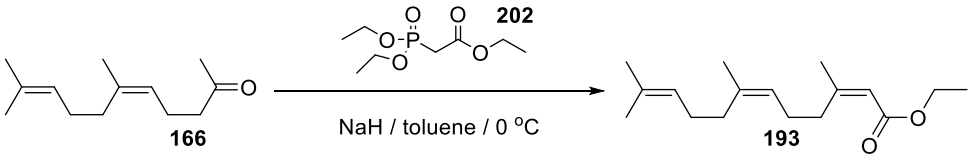

A stirred suspension of sodium hydride (185 mg, 7.72 mmol, 3 eq.) in anhydrous toluene (**20** mL) was cooled to 0 °C and **202** (630 mg, 2.80 mmol, 1.1 eq.) was added dropwise. The reaction mixture was stirred at room temperature for 1 hour and cooled to 0 °C. **166** (500 mg, 2.57 mmol, 1 eq.) was added dropwise and the reaction mixture stirred at room temperature for 16 hours. The reaction was quenched with water (**10** mL) and products extracted with diethyl ether (3 x 10 mL). Organic extracts were washed with water (3 x 10 mL) and brine (3 x 10 mL), dried over sodium sulphate, filtered and concentrated under reduced pressure. Purification *via* flash chromatography (10% ethyl acetate in hexane) gave **193** as a clear oil (130 mg, 19%).

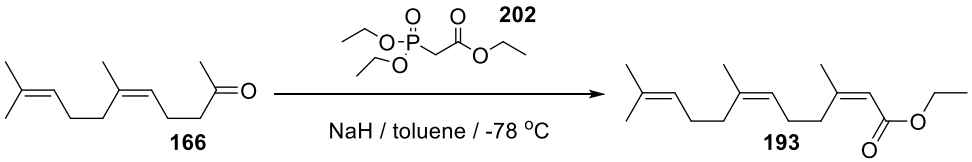

A stirred suspension of sodium hydride (185 mg, 7.72 mmol, 3 eq.) in anhydrous toluene (**20** mL) was cooled to 0 °C and **202** (630 mg, 2.80 mmol, 1.1 eq.) was added dropwise. The reaction mixture was stirred at room temperature for 1 hour and cooled to -78 °C. **166** (500 mg, 2.57 mmol, 1 eq.) was added dropwise and the reaction mixture stirred at room temperature for 16 hours. The reaction was quenched with water (**10** mL) and products extracted with diethyl ether (3 x 10 mL). Organic extracts were washed with water (3 x 10 mL) and brine (3 x 10 mL), dried over sodium sulphate, filtered and concentrated under reduced pressure. Purification *via* flash chromatography (10% ethyl acetate in hexane) gave **193** as a clear oil (123 mg, 18%).

Preparation of (2Z, 6Z)-3,7,11-trimethyldodeca-2,6,10-trien-1-ol (167):

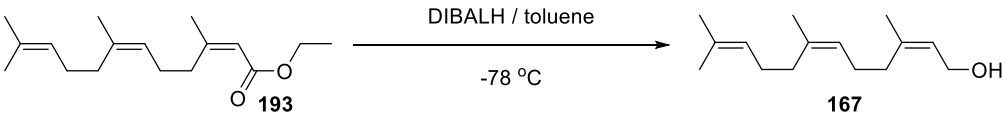

Diisobutylaluminimiun hydride (6.9 mL, 6.93 mmol, 3 eq.) was added to a stirred solution of **193** (604 mg, 2.28 mmol, 1 eq.) in anhydrous toluene (20 mL) at -78 °C. The reaction was stirred for 3 hours at -78 °C and quenched with saturated potassium sodium tartrate solution (20 mL). Reaction products were extracted with dichloromethane (3 x 30 mL). Combined organic extracts were washed with water (3 x 20 mL), brine (2 x 20 mL), dried over sodium sulphate and concentrated under reduced pressure. Purification *via* flash chromatography on silica gel (5% ethyl acetate in hexane) to yield **167** as a clear oil (0.487 g, 96%).

^{1}H NMR (300 MHz, $CDCl_3$) δ 5.38 (1H, t, *J* = 7.2 Hz CC*H*CH_2O), 5.07 – 5.01 (2H, m, 2 x (CH_3)CC*H*), 4.02 (2H, d, *J* = 7.2 Hz, CHC*H*$_2$OH), 2.07 – 2.00 (4H, m, 2 x allylic C*H*$_2$), 1.99 – 1.90 (4H, m, 2 x allylic C*H*$_2$), 1.68 (3H, s, C*H*$_3$), 1.62 (6H, s, 2 x C*H*$_3$), 1.54 (3H, s, C*H*$_3$). **^{13}C NMR** (125 MHz, $CDCl_3$) δ 140.0 ((CH_3)*C*CHCH_2O), 136.2 & 131.7 (2 x (CH_3)*C*CH), 124.5 (C*C*HCH_2O), 124.4 & 124.2 (2 x (CH_3)C*C*H), 59.0 (CH*C*H_2O), 32.2 & 31.9 & 26.6 & 26.3 (4 x allylic *C*H_2), 25.7 (*C*H_3), 23.5 & 23.3 ((2 x (*C*H_3)CCH), 17.7 (*C*H_3). **LRMS** (EI^+): 204.19 (75% [M – H_2O]), 189.17 (40%), 161.13 (90%), 133.10 (35%), 119.08 (100%), 105.07 (55%), 93.07 (80%), 69.07 (17%). **HRMS** (EI^+): calculated for [$C_{15}H_{24}$][M –H_2O]; 204.1878, found 204.1879.

Table 9. 2D proton NMR correlations revealing spatial arrangement in 167

167: NOESY ^{1}H - ^{1}H interactions	
From / ppm	To / ppm
5.38	4.02
5.38	1.68
5.05	2.04
5.05	1.93
5.05	1.58
4.02	2.04

Preparation of (2Z,6Z)-1-bromo-3,7,11-trimethyldodeca-2,6,10-triene (169):

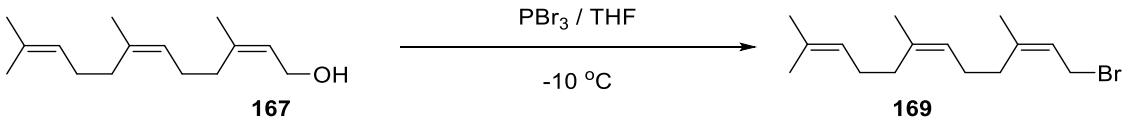

167 **169**

Phosphorus tribromide (15 µL, 0.158 mmol, 1 eq.) was added dropwise to a stirred solution of (2*Z*,6*Z)* farnesol (**167**)(70 mg, 0.315 mmol, 2 eq.) in anhydrous tetrahydrofuran (3 mL) at -10 °C. The solution was stirred for 15 minutes and concentrated under vaccuo. The residue was dissolved in diethyl ether (5 mL) and washed with sodium hydrogen carbonate (3 x 10 mL), water (3 x 10 mL) and brine (10 mL), dried over sodium sulfate, filtered and concentrated under reduced pressure. The product was dried under vacuum for a further 2 hours to yield bromide as a pale yellow oil (90 mg, 100%) which was used without further purification.

^{1}H NMR (300 MHz, $CDCl_3$) δ 5.47 (1H, t, *J* = 8.6 Hz, C*H*CH_2Br), 5.08 – 4.97 (2H, m, 2 x CC*H*CH_2), 3.94 (2H, d, *J* = 8.6 Hz, C*H*$_2$Br), 2.11 – 2.03 (4H, m, 2 x allylic C*H*$_2$), 2.01 – 1.96 (4H, m, 2 x allylic C*H*$_2$) 1.71 (3H, s, C*H*$_3$), 1.62 (6H, s, 2 x C*H*$_3$), 1.55 (3H, s, C*H*$_3$).

Preparation of (2Z,6Z)-3,7,11-trimethyldodeca-2,6,10-trien-1-yl diphosphate (38):

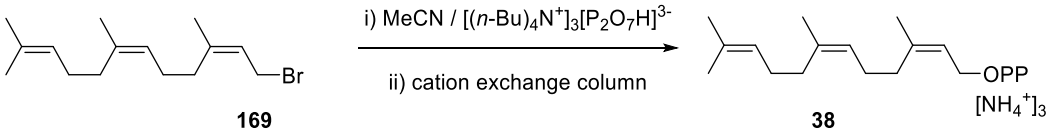

169 **38**

A stirred solution of (2*Z*,6*Z*) farnesyl bromide (**169**)(90 mg, 0.315 mmol, 1 eq.) in anhydrous acetonitrile (5 mL) was added tris tetrabutyl ammonium pyrophosphate (569 g,0.473 mmol, 1.5 eq.) and stirred at room temperature overnight. The reaction mixture was concentrated under reduced pressure and the resultant residue dissolved in buffer solution (25 mM NH_4HCO_3, 2% iPrOH) (5 mL) and the tris tetrabutylammonium salt counter ions were exchanged for ammonium by ion exchange column containing Amberlyst 131 (wet H^+ form) mesh cation exchange resin pre-equilibrated with ion-exchange buffer (25 mM NH_4HCO_3, 2% isopropanol). The appropriate fractions were collected and lyophilized to yield (2*Z*,6*Z*) farnesyl diphosphate (**38**) as a white powder. The powder was dissolved in buffer solution (25 mM NH_4HCO_3, 2% iPrOH) (5 mL) and purified using HPLC (Solvent A: acetonitrile, solvent B: 2% iPrOH). The appropriate fractions were collected and lyophilized to give (2*Z*, 6*Z*) farnesyl diphosphate (**38**) as a white powder (107 mg, 30%).

^{1}H NMR (400 MHz, D_2O) δ 5.32 (1H, t, *J* = 7.2 Hz, C*H*CH_2O), 5.12 – 5.01 (2H, m, 2 x CC*H*CH_2), 4.30 (2H, t, *J* = 6.9 Hz, CH_2O), 2.03 – 1.99 (4H, m, 2 x allylic CH_2), 1.97 – 1.92 (4H, m, 2 x allylic CH_2) 1.61 (3H, s, (CH_3)CCHCH_2O), 1.54 (6H, s, (CH_3)$_2$CCH), 1.48 (3H, s, CH_2CH_2(CH_3)CCH).**^{13}C NMR** (150 MHz, $CDCl_3$) δ 142.4 ((CH_3)*C*CHCH_2O), 137.2 & 133.7 ((CH_3)*C*CHCH_2), 124.9 (C*C*HCH_2O), 121.01 & 120.95 (C*C*HCH_2), 62.2 (CH*C*H_2O), 31.5 (CH_2CH_2C(CH_3)), 31.1 (*C*H_2CH_2C(CH_3)), 25.9 ((CH_3)$_2$CH_2*C*H_2C), 25.8 ((CH_3)$_2$*C*H_2CH_2C), 24.9 ((*C*H_3)CCH_2CHO), 22.6 & 22.4 ((*C*H_3)$_2$CCH), 16.9 (CH_2CH_2(*C*H_3)CCH).**^{31}P NMR** (162 MHz, $CDCl_3$) δ -7.11 (d, *J* = 21.6 Hz, CH_2O*P*(O)$_2$OP(O)$_3$), -10.46 (d, *J* = 21.6 Hz, CH_2OP(O)$_2$O*P*(O)$_3$). **HRMS** (ES^-): calculated for [$C_{15}H_{27}O_7P_2$][M]; 381.1232, found 381.1229.

8.2.2 Synthesis of (2*E*,6*Z*) farnesyl diphosphate (342)

Preparation of ethyl (2E,6Z)-3,7,11-trimethyldodeca-2,6,10-trienoate (192):

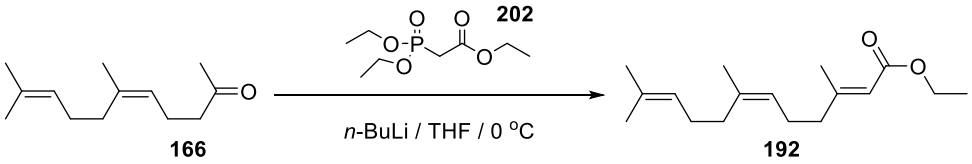

A stirred solution of **202** (630 mg, 2.57 mmol, 1 eq.) in anhydrous tetrahydrofuran (20 mL) was cooled to 0 °C and *n*-butyl lithium (1.1 mL, 2.83 mmol, 1.1 eq., 2.5M in hexane) was added dropwise. The resulting solution was stirred at room temperature for 1 hour, cooled to 0 °C and **166** (500 mg, 2.57 mmol, 1 eq.) added dropwise. The reaction mixture was stirred for 16 hours at room temperature. The reaction was quenched with water (5 mL) and the product was extracted with diethyl ether (3 x 10 mL). The combined organic phases were washed with water (3 x 10 mL) and brine (3 x 10 mL), then dried over sodium sulphate, filtered and the solvent removed under reduced pressure. Purification *via* flash chromatography on silica gel (2% ethyl acetate in hexane) provided ester **192** as a clear oil (372 mg, 56%).

^{1}H NMR (300 MHz, $CDCl_3$) δ 5.60 (1H, s, CC*H*C(O)OEt), 5.15 – 4.97 (2H, m, 2 x (CH_3)CC*H*), 4.08 (2H, q, *J* = 7.1 Hz, OCH_2CH_3), 2.09 (3H, d, *J* = 1.2 Hz, CH_2(CH_3)CCHC(O)), 2.10 – 2.06 (4H, m, 2 x allylic CH_2), 2.00 – 1.89 (4H, m, 2 x allylic CH_2), 1.62 (6H, s, 2 x CH_3), 1.54 (3H, s, CH_3), 1.22 (3H, t, *J* = 7.1 Hz, OCH_2CH_3). **^{13}C NMR** (75 MHz, $CDCl_3$) δ 166.9 (CH*C*(O)O), 159.8 ((CH_3)*C*CHC(O)O), 136.2 & 131.5 (2 x (CH_3)*C*CH), 124.2 & 123.7 (2 x (CH_3)CC*H*), 115.6 (C*C*HC(O)O), 59.5 (O*C*H_2CH_3), 41.2 (*C*H_2(CH_3)CCHC(O)), 32.0 & 26.5 (2 x *C*H_2), 25.9 (*C*H_2CH_2(CH_3)CCHC(O)), 25.7 & 23.3 & 18.8 & 17.6 (4 x *C*H_3), 14.3 (OCH_2*C*H_3). **LRMS** (ES^+): 265.22 (87% [M + H]), 243.08 (50%), 225.03 (90%), 208.04 (70%), 193.12 (30%), 180.05 (65%), 171.10 (40%), 147.12 (25%). **HRMS** (ES^+): calculated for [$C_{17}H_{29}O_2$] [M + H]; 265.2168, found 265.2159.

Preparation of (2E, 6Z)-3,7,11-trimethyldodeca-2,6,10-trien-1-ol (168):

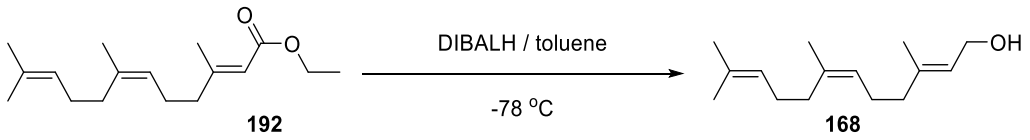

192 168

A stirred solution of **192** (372 mg,1.4 mmol, 1 eq.) in anhydrous toluene (30 mL) was cooled to -78 °C and diisobutylaluminium hydride (4.2 mL, 4.22 mmol, 3 eq.) was added dropwise. The reaction was stirred at -78 °C for 4 hours and warmed to 0 °C. Reaction was quenched with Rochelle salts (10 mL) and products extracted with dichloromethane (4 x 20 mL). Organic extracts were washed with water (3 x 20 mL) and brine (2 x 20 mL), dried over sodium sulphate, filtered and concentrated under reduced pressure. Purification of **168** *via* flash chromatography on silica gel (10% ethyl acetate in hexane) to yield **168** as a clear oil (303 mg, 97%).

^{1}H NMR (500 MHz, $CDCl_3$) δ 5.35 (1H, t, *J* = 6.9, CC*H*CH_2O), 5.07 – 5.02 (2H, m, 2 x (CH_3)CC*H*), 4.09 (2H, d, *J* = 6.9 Hz, CHC*H*$_2$OH), 2.09 – 1.89 (8H, m, 4 x allylic C*H*$_2$), 1.62 (3H, s, C*H*$_3$), 1.62 (3H, s, C*H*$_3$), 1.61 (3H, s, C*H*$_3$), 1.54 3H, s, C*H*$_3$). **^{13}C NMR** (126 MHz, $CDCl_3$) δ 139.8 ((CH_3)*C*CHCH$_2$O), 135.6 & 131.6 ((2 x CH_3)*C*CH), 124.6 (C*C*HCH$_2$O), 124.3 & 123.3 (2 x (CH_3)C*C*H), 59.4 (CH*C*H$_2$O), 39.8 & 32.0 & 26.6 & 26.2 (4 x allylic *C*H$_2$), 25.7 & 23.4 & 17.7 & 16.3 (4 x *C*H$_3$). **LRMS** (ES^+): 205.20 (100% [M – H_2O]), 143.10 (10%), 123.96 (7%) **HRMS** (ES^+): calculated for [$C_{15}H_{25}$] [M – H_2O]; 205.1956, found 205.1964.

Table 10. 2D proton NMR correlations revealing spatial arrangement in 168

168: NOESY ^{1}H - ^{1}H interactions	
From / ppm	To / ppm
5.35	4.09
5.35	2.01
5.04	2.01
5.04	1.62
4.09	1.62

Preparation of (2E,6Z)-1-bromo-3,7,11-trimethyldodeca-2,6,10-triene (345):

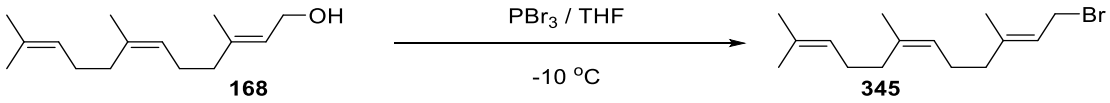

168 **345**

To a stirred solution of (2*E*,6*Z*) farnesol (**168**) (303 mg, 1.36 mmol, 2 eq.) in anhydrous tetrahydrofuran (20 mL) was added phosphorus tribromide (64 µL, 0.68 mmol, 1 eq.) dropwise at -10 °C. The reaction mixture was stirred at -10°C for 30 minutes and concentrated under *vaccuo*. The concentrate was dissolved in diethyl ether (20 mL). The organic extracts were washed with saturated sodium bicarbonate solution (3 x 10 mL), water (3 x 10 mL) and brine (2 x 10 mL). Organic layers were dried over sodium sulphate, filtered and concentrated under reduced pressure to give bromide (**345**) as a pale yellow oil (377 mg, 97%) which was used without further purification.

^{1}H NMR (500 MHz, $CDCl_3$) δ 5.39 (1H, t, *J* = 8.4, CC*H*CH_2Br), 5.07 – 5.02 (2H, m, 2 x (CH_3)CC*H*), 4.09 (2H, d, *J* = 8.4 Hz, CHC*H*$_2$Br), 2.11 – 1.88 (8H, m, 4 x allylic C*H*$_2$), 1.62 (3H, s, C*H*$_3$), 1.61 (3H, s, C*H*$_3$), 1.61 (3H, s, C*H*$_3$), 1.54 (3H, s, C*H*$_3$).

Preparation of (2E, 6Z)-3,7,11-trimethyldodeca-2,6,10-trien-1-yl diphosphate (342):

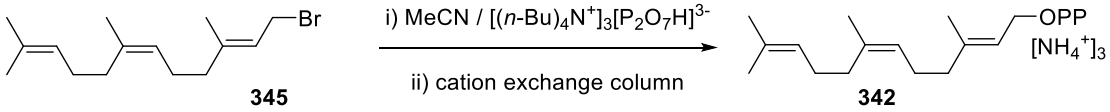

345 **342**

A mixture of (2*E*,6*Z*) farnesyl bromide (**345**) (377 mg, 1.32 mmol, 1 eq.) and tris tetrabutyl ammonium pyrophosphate (2.39 g,2.64 mmol, 2 eq.) in anhydrous acetonitrile (10 mL) was stirred at room temperature for 16 hours. The reaction mixture was concentrated under reduced pressure and the resultant residue dissolved in buffer solution (25 mM NH_4HCO_3, 2% iPrOH) (10 mL) and the tris tetrabutylammonium salt counter ions were exchanged for ammonium by ion exchange column containing Amberlyst 131 (wet H^+ form) mesh cation exchange resin pre-equilibrated with ion-exchange buffer (25 mM NH_4HCO_3, 2% isopropanol). The appropriate fractions were collected and lyophilized to yield (2*E*,6*Z*) farnesyl diphosphate as a white powder. The powder was dissolved in buffer solution (10 mL)(25 mM NH_4HCO_3, 2% iPrOH) (5 mL) and purified using HPLC (Solvent A: acetonitrile, solvent B: 2% iPrOH). The appropriate fractions were collected and lyophilized to give (2*E*,6*Z*) farnesyl diphosphate as a white powder (20 mg, 3%).

^{1}H NMR (400 MHz, D_2O) δ 5.34 (1H, t, *J* = 7.2 Hz, C*H*CH_2O), 5.13 – 5.05 (2H, m, 2 x CC*H*CH_2), 4.31 (2H, t, *J* = 6.8 Hz, CH_2O), 2.05 – 1.99 (4H, m, 2 x allylic CH_2), 1.96 – 1.91 (4H, m, 2 x allylic CH_2) 1.61 (3H, s, (CH_3)CCHCH_2O), 1.54 (6H, s, (CH_3)$_2$CCH), 1.49 (3H, s, CH_2CH_2(CH_3)CCH). **^{31}P NMR** (162 MHz, $CDCl_3$) δ -7.33 (d, *J* = 23.2 Hz, $CH_2OP(O)_2OP(O)_3$), -10.51 (d, *J* = 23.2 Hz, $CH_2OP(O)_2OP(O)_3$). **HRMS** (ES^-): calculated for [$C_{15}H_{27}O_7P_2$][M]; 381.1232, found 381.1233.

8.2.3 Synthesis of (2*Z*,6*E*) farnesyl diphosphate (341)

Preparation of (E)-1-bromo-3,7-dimethylocta-2,6-diene (347):

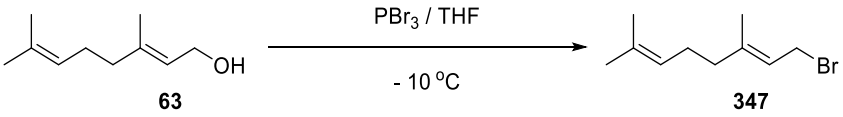

63 **347**

Geraniol (**63**) (8 g, 51.9 mmol, 2 eq.) in anhydrous tetrahydrofuran (30 mL) was cooled to -10 °C and phosphorus tribromide (7.02 g, 25.9 mmol, 1 eq.) added dropwise. Reaction mixture was stirred at -10 °C for 20 minutes and quenched with sat. sodium bicarbonate (20 mL). Reaction product was extracted with diethyl ether (3 x 15 mL). Organic extracts were washed with water (3 x 10 mL), brine (3 x 10 mL), dried over sodium sulphate, filtered and concentrated under reduced pressure to give **347** (11.3 g, 100%) as a pale yellow oil which was used without further purification.

^{1}H NMR (300 MHz, $CDCl_3$) δ 5.54 (1H, t, *J* = 8.5, CC*H*CH_2Br), 5.12 – 5.04 (1H, m, (CH_3)CC*H*), 4.04 (2H, d, *J* = 8.5 Hz, CHCH_2Br), 2.17 – 2.03 (4H, m, 2 x allylic CH_2), 1.74 (3H, s, CH_3), 1.69 (3H, s, CH_3), 1.61 (3H, s, CH_3).

Preparation of ethyl (E)-2-acetyl-5,9-dimethyldeca-4,8-dienoate (348):

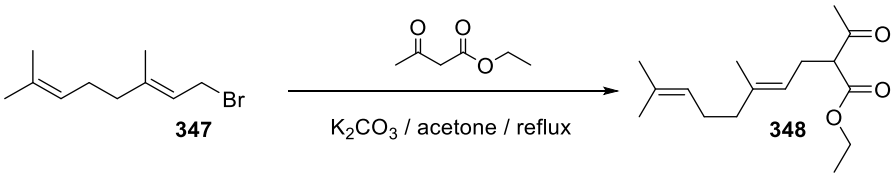

347 **348**

Crude bromide **347** (11.26 g, 51.9 mmol, 1 eq.) and ethyl acetoacetate (13.49 g, 103.7 mmol, 2 eq.) were dissolved in anhydrous acetone (50 mL). Potassium carbonate (17.9 g, 129.7 mmol, 2.5 eq.) was added the suspension was refluxed for 4 hours at 60 °C. The reaction mixture was concentrated under reduced pressure and reaction products dissolved in diethyl ether (30 mL). Ethereal layer was

washed with water (3 x 20 mL) and brine (20 mL), dried over sodium sulphate and concentrated under *vaccuo*. Reaction product was purified by flash chromatography on silica gel (20% ethyl acetate in hexane) to give **348** as a clear oil (13.8 g, 99%).

^{1}H NMR (300 MHz, $CDCl_3$) δ 5.08 – 5.01 (2H, m, 2 x (CH_3)CC*H*), 4.19 (2H, q, *J*= 7.1 Hz, CH_3CH_2O), 3.45 (1H, t, *J*= 7.5 Hz, COC*H*CO), 2.56 (2H, t, *J*= 7.4 Hz, CCHCH_2CH), 2.23 (3H, s, COCH_3), 2.10 – 1.92 (4H, m, 2 x allylic CH_2), 1.67 (3H, s, CH_3), 1.63 (3H, s, CH_3), 1.59 (3H, s, CH_3), 1.27 (3H, t, *J*= 7.1 Hz,CH_3CH$_2$O). **^{13}C NMR** (75 MHz, $CDCl_3$) δ 203.3 (CH_3CH_2OC(O)), 169.6 (CH_3*C*OCH), 138.4 & 131.6 (2 x (CH_3)*C*CH), 124.0 & 119.6 (2 x CH_3C*C*H), 61.4 (CH_3CH_2O), 59.8 (C(O)*C*HC(O)), 39.7 (allylic *C*H_2), 29.2 (*C*H_3C(O)), 26.9 (CCH*C*H_2CH), 26.5 (allylic *C*H_2), 25.7 & 17.7 & 16.1 (3 x *C*H_3), 14.1 (OCH$_2$*C*H_3). **LRMS** (ES^-): 265.18 (100% [M - H]), 243.12 (25%), 213.00 (55%), 203.06 (10%), 187.06 (65%), 171.07 (10%), 141.02 (35%), 116.91 (30%). **HRMS** (ES^+): calculated for [$C_{16}H_{25}O_3$] [M – H^+]; 265.1804, found 265.1797.

Preparation of (E)-6,10-dimethylundeca-5,9-dien-2-one (349):

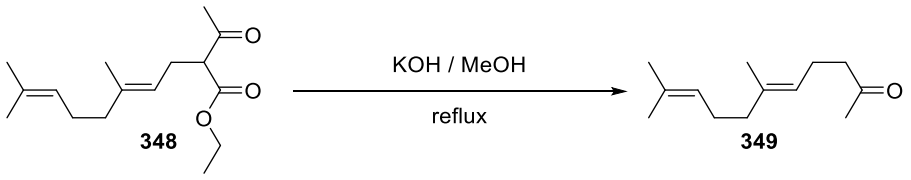

To a solution of **348** (13.8 g, 51.9 mmol, 1 eq.) in methanol (50 mL) was added potassium hydroxide (8.73 g, 155.6 mmol, 3 eq.) and the reaction mixture was refluxed at 65 °C for 2 hours. The reaction mixture was cooled to room temperature and acidified with dilute hydrochloric acid (1 M, 10 mL). Organic products were extracted with diethyl ether (30 mL) and combined ethereal layers were washed with water (3 x 20 mL) and brine (30 mL). Organic layers were dried over anhydrous sodium sulphate, filtered and concentrated under reduced pressure. Purification *via* flash chromatography on silica gel (10% ethyl acetate in hexane) gave **349** as a clear oil (9.37 g, 93%).

^{1}H NMR (300 MHz, $CDCl_3$) δ 5.04 – 4.96 (2H, m, 2 x (CH_3)CC*H*), 2.39 (2H, t, *J* = 7.3 Hz, CH_2C(O)), 2.19 (2H, dd, *J* = 14.6, 7.2 Hz, CH_2CH$_2$C(O)), 2.07 (3H, s, CH$_2$C(O)CH_3), 2.02 – 1.86 (4H, m,2 x allylic CH_2), 1.60 (3H, s, (CH_3)CCH), 1.54 (3H, s, (CH_3)CCH), 1.52 (3H, s, (CH_3)CCH). **^{13}C NMR** (75 MHz, $CDCl_3$) δ 209.1 (CH_3*C*(O)), 136.4 & 131.5 (2 x (CH_3)*C*CH), 124.2 & 122.5 (2 x (CH_3)C*C*H), 43.8 (CH_2CH_2C(O)), 39.6 & 26.6 & 22.5 (3 x allylic *C*H_2), 30.0 (*C*H_3C(O)) 25.7 (*C*H_3), 17.7 & 16.0 (2 x *C*H_3). **LRMS** (ES^+): 195.17 (60% [M + H]), 177.16 (100%), 137.13 (5%), 123.97 (4%), 121.09 (4%), 109.10 (4%). **HRMS** (ES^+): calculated for [$C_{13}H_{23}O$] [M + H]; 195.1749, found 195.1745.

Preparation of ethyl (2Z,6E)-3,7,11-trimethyldodeca-2,6,10-trienoate (350):

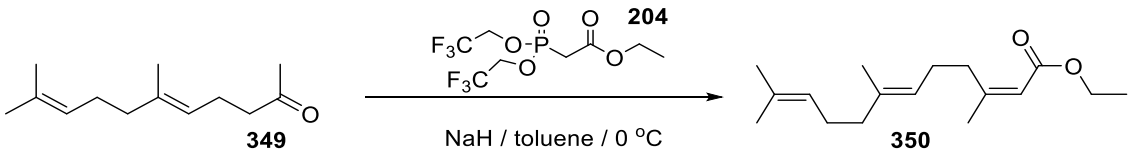

A stirred suspension of sodium hydride (161 mg, 6.74 mmol, 1.5 eq.) in anhydrous toluene (30 mL) was cooled to 0 °C and ethyl 2-(bis(2,2,2-trifluoroethoxy)phosphoryl)acetate (2.24, 6.74 mmol, 1.5 eq.) was added dropwise. The reaction mixture was stirred at room temperature for 1 hour and cooled to 0 °C. Geranyl acetone (872 mg, 4.49 mmol, 1 eq.) was added dropwise and the reaction mixture stirred at room temperature for 16 hours. The reaction was quenched with water (10 mL) and products extracted with diethyl ether (30 mL). Organic extracts were washed with water (3 x 10 mL) and brine (20 mL), dried over sodium sulphate, filtered and concentrated under reduced pressure. Purification *via* flash chromatography (5% ethyl acetate in hexane) gave **350** as a clear oil (205 mg, 22%).

^{1}H NMR (500 MHz, $CDCl_3$) δ 5.66 (1H, s, CC*H*C(O)OEt), 5.12 – 5.05 (2H, m, 2 x (CH_3)CC*H*), 4.14 (2H, q, *J* = 7.1 Hz, O$CH_2$$CH_3$), 2.67 – 2.62 (2H, m, $CH_2$$(CH_3)$CCHC(O)), 2.21 – 2.15 (2H, m, $CH_2$$CH_2$$(CH_3)$CCHC(O)), 2.09 – 2.02 (4H, m, 2 x allylic CH_2), 1.89 (3H, d, *J* = 1.3 Hz, $CH_2$$(CH_3)$CCHC(O)), 1.68 (6H, s, 2 x CH_3), 1.60 (3H, s, CH_3), 1.27 (3H, t, *J* = 7.1 Hz, OCH_2CH_3). **^{13}C NMR** (75 MHz, $CDCl_3$) δ 166.4 (CH*C*(O)O), 160.3 ((CH_3)*C*CHC(O)O), 135.8 & 131.5 (2 x (CH_3)*C*CH), 124.3 & 124.2 (2 x (CH_3)CC*H*), 116.2 (*C*CHC(O)O), 59.5 (O*C*H_2CH_3), 33.4 (*C*$H_2$$(CH_3)$CCHC(O)) 26.7 (allylic *C*H_2), 25.9 (*C*$H_2CH_2$$(CH_3)$CCHC(O)), 25.7 (allylic *C*H_2), 25.4 & 18.8 & 17.7 & 16.0 (4 x *C*H_3), 14.35 (OCH_2*C*H_3). **LRMS** (ES^+): 265.22 (100% [M + H]), 243.08 (10%), 219.17 (5%), 215.05 (2%), 191.18 (5%), 183.13 (5%). **HRMS** (ES^+): calculated for [$C_{17}H_{29}O_2$] [M + H]; 265.2168, found 265.2162.

Preparation of (2Z, 6E)-3,7,11-trimethyldodeca-2,6,10-trien-1-ol (352):

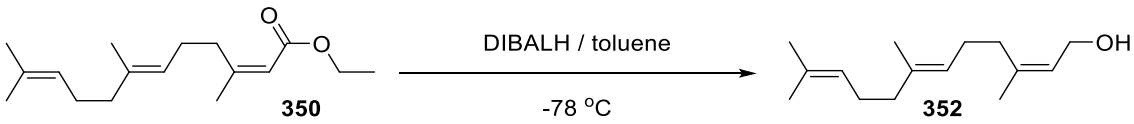

350 (205 mg, 0.78 mmol, 1 eq.) in anhydrous toluene (10 mL) was cooled to -78 °C and diisobutyl aluminium hydride added dropwise. The reaction was stirred until complete consumption of starting material was observed via TLC (20% ethyl acetate in hexane). Reaction was warmed to 0 °C, quenched with Rochelle salts (5 mL) and stirred at room temperature for 16 hours. Organic products

were extracted with dichloromethane (3 x 10 mL) and combined organic layers washed with water (3 x 10 mL) and brine (3 x 10 mL). Organic extracts were dried over sodium sulphate, filtered and concentrated under reduced pressure. Purification *via* flash chromatography over silica (5% ethyl acetate in hexane) gave **352** as a clear oil (162 mg, 94%).

^{1}H NMR (500 MHz, $CDCl_3$) δ 5.37 (1H, t, *J* = 7.1 Hz CC*H*CH_2O), 5.06 – 5.00 (2H, m, 2 x (CH_3)CC*H*), 4.04 (2H, t, *J* = 7.1 Hz, CHC*H*$_2$OH), 2.07 – 1.96 (6H, m, 3 x allylic C*H*$_2$), 1.94 – 1.88 (2H, m, allylic C*H*$_2$), 1.69 (3H, s, C*H*$_3$), 1.61 (3H, s, C*H*$_3$), 1.53 (6H, s, 2 x C*H*$_3$). **^{13}C NMR** (126 MHz, $CDCl_3$) δ 140.1 ((CH_3)*C*CHCH_2O), 136.0 & 131.5 (2 x (CH_3)*C*CH), 124.4 (*C*CHCH_2O), 124.2 & 123.6 (2 x (CH_3)C*C*H), 59.1 (CH*C*H_2O), 39.7 & 32.0 & 26.7 & 26.5 (4 x allylic *C*H_2), 25.7 (*C*H_3), 23.5 (*C*H_3), 17.7 & 16.0 (2 x (*C*H_3)CCH). **LRMS** (EI$^+$): 222.20 (2% [M]), 204.17 (100%), 189.16 (65%), 161.13 (70%), 133.10 (40%), 119.08 (75%), 107.08 (40%), 93.06 (95%), 69.07 (30%) **HRMS** (EI$^+$): calculated for [$C_{15}H_{26}O$] [M]; 222.1984, found 222.1982.

Table 11. 2D proton NMR correlations revealing spatial arrangement in 352

352: NOESY ^{1}H - ^{1}H interactions	
From / ppm	To / ppm
5.37	4.04
5.37	1.69
5.03	2.02
5.03	1.90
5.03	1.69
5.03	1.61
5.03	1.53
4.04	2.02

Preparation of (2Z,6E)-1-bromo-3,7,11-trimethyldodeca-2,6,10-triene (354):

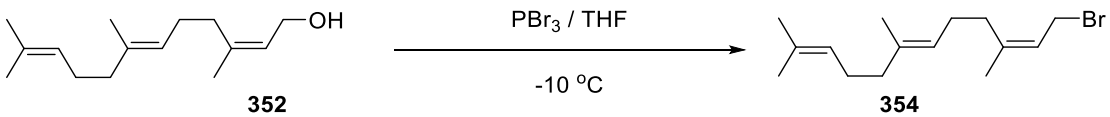

352 **354**

Phosphorus tribromide (200 µL, 0.26, 1 eq.) was added to a stirred solution of **352** (114 mg, 0.51 mmol, 2 eq.) in anhydrous tetrahydrofuran (10 mL) at -10 °C. The reaction proceeded for 15 minutes at which point complete consumption of starting material was observed *via* TLC (20% ethyl acetate

in hexane). Volatile solvents were removed under reduced pressure and the residue dissolved in diethyl ether (10 mL). Organic extracts were washed with sat. sodium bicarbonate sol. (3 x 5 mL), water (3 x 5 mL) and brine (2 x 5 mL). Ethereal extracts were dried over sodium sulphate, filtered and concentrated under *vaccuo* to give **354** as a crude yellow oil (146 mg, 100%) which was used without further purification.

^{1}H NMR (500 MHz, $CDCl_3$) δ 5.47 (1H, t, *J* = 8.3 Hz, CC*H*CH_2Br), 5.09 – 5.00 (2H, m, 2 x (CH_3)CC*H*), 3.94 (2H, d, *J* = 8.3 Hz, CHC*H*$_2$Br), 2.12 – 2.04 (4H, m, 2 x allylic C*H*$_2$), 2.01 – 1.91 (4H, m, 2 x allylic C*H*$_2$), 1.71 (3H, s, C*H*$_3$), 1.62 (3H, s, C*H*$_3$), 1.55 (3H, s, C*H*$_3$), 1.54 (3H, s, C*H*$_3$).

Preparation of (2Z,6E)-3,7,11-trimethyldodeca-2,6,10-trien-1-yl diphosphate (341):

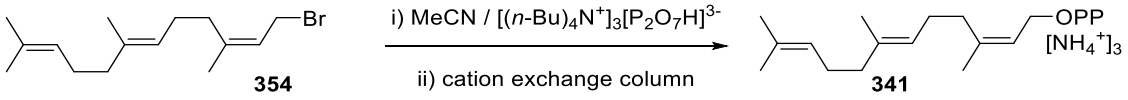

Tris tetra butyl ammonium pyrophosphate (694 mg, 0.76 mmol, 1.5 eq.) in anhydrous acetonitrile (5 mL) was added to crude bromide **354** (146 mg, 0.51 mmol, 1 eq.) under argon. The reaction was stirred for 16 hours at room temperature and volatile solvents removed under reduced pressure to give crude diphosphate as a brown oil. Crude diphosphate was dissolved in buffer solution (25 mM NH_4HCO_3, 2% iPrOH) (3 mL) and the tris tetrabutylammonium salt counter ions were exchanged for ammonium by ion exchange column containing Amberlyst 131 (wet H^+ form) mesh cation exchange resin pre-equilibrated with ion-exchange buffer (25 mM NH_4HCO_3, 2% isopropanol). The appropriate fractions were collected and lyophilized to yield (2*Z*,6*E*) farnesyl diphosphate (**341**) as a white powder. The powder was dissolved in buffer solution (25 mM NH_4HCO_3, 2% iPrOH) (5 mL) and purified using HPLC (Solvent A: acetonitrile, solvent B: 2% iPrOH). The appropriate fractions were collected and lyophilized to give (2*Z*,6*E*) farnesyl diphosphate as a white powder. (52 mg, 23%).

^{1}H NMR (400 MHz, D_2O) δ 5.32 (1H, t, *J* = 7.2 Hz, C*H*CH_2O), 5.17 – 5.07 (2H, m, 2 x (CH_3)CC*H*), 4.30 (2H, t, *J* = 6.9 Hz, C*H*$_2$O), 2.16 – 2.03 (4H, m, 2 x allylic C*H*$_2$), 2.03 – 1.92 (4H, m, 2 x allylic C*H*$_2$), 1.54 (6H, s, (C*H*$_3$)$_2$CCH), 1.48 (3H, s, CH_2CH_2(C*H*$_3$)CCH). **^{31}P NMR** (162 MHz, $CDCl_3$) δ -7.11 (d, *J* = 23.6 Hz), -10.46 (d, *J* = 20.2 Hz). **HRMS** (ES^-): calculated for [$C_{15}H_{27}O_7P_2$][M]; 381.1232, found 381.1237.

8.2.4 Synthesis of (2*E*,6*E*) farnesyl diphosphate (31)

Preparation of ethyl (6E)-3,7,11-tromethyldodeca-2,6,10-trienoate (351):

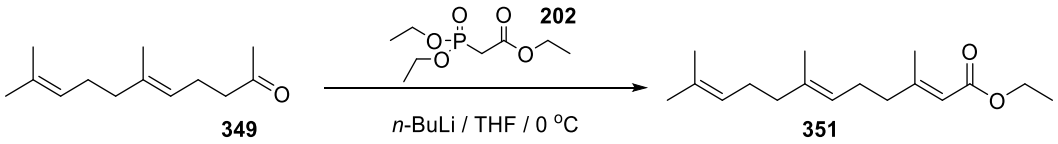

349 351

n-Butyl lithium (5.3 mL, 13.17 mmol, 1.5 eq., 2.5 M in hexane) was added to dropwise to a stirred solution of triethyl phosphonoacetate (**202**) (4.37 g, 13.17 mmol, 1.5 eq.) in anhydrous tetrahydrofuran (50 mL) at 0 °C. The reaction was stirred at room temperature for 1 hour and cooled to 0 °C prior to the dropwise addition of **349** (1.71 g, 8.78 mmol, 1 eq.). Reaction was stirred for 16 hours at room temperature and quenched with water (20 mL). Organic products were extracted with diethyl ether (3 x 20 mL) and washed with water (3 x 20 mL), brine (3 x 20 mL) and dried over sodium sulphate. Organic layers were filtered and concentrated under reduced pressure. Purification *via* flash chromatography (10% ethyl acetate in hexane) gave a mixture of esters **350** and **351** as a clear oil (1.54 g, 66%). Flash chromatography (5% ethyl acetate in hexanes) partially separated esters **350** and **351** for analysis.

^{1}H NMR (500 MHz, $CDCl_3$) δ 5.64 (1H, s, CC*H*C(O)OEt), 5.16 – 5.02 (2H, m, 2 x $(CH_3)CCH$), 4.14 (2H, q, *J* = 7.1 Hz, OCH_2CH_3), 2.16 (3H, d *J* = 1.1 Hz, $CH_2(CH_3)CCHC(O)$), 2.21 – 2.11 (4H, m, 2 x allylic CH_2), 2.07 – 1.94 (4H, m, 2 x allylic CH_2), 1.68 (3H, s, CH_3), 1.60 (6H, s, 2 x CH_3), 1.27 (3H, t, *J* = 7.1 Hz, OCH_2CH_3). **^{13}C NMR** (75 MHz, $CDCl_3$) δ 166.95 (CH*C*(O)O), 159.92 ($(CH_3)CCHC(O)O$), 136.14 & 131.37 (2 x $(CH_3)CCH$), 123.51 & 122.89 (2 x $(CH_3)CCH$), 115.59 (C*C*HC(O)O), 59.49 (OCH_2CH_3), 40.98 & 39.68 & 26.65 & 25.94 (4 x allylic CH_2), 25.73 & 18.83 & 17.71 & 15.99 (4 x CH_3), 14.35 (OCH_2CH_3). **LRMS** (ES^+): 265.22 (100% [M + H]), 243.08 (20%), 219.17 (15%), 215.05 (12%), 191.18 (25%), 183.13 (15%). **HRMS** (ES^+): calculated for $[C_{17}H_{29}O_2]$ [M + H]; 265.2168, found 265.2173.

Preparation of (2E, 6E)-3,7,11-trimethyldodeca-2,6,10-trien-1-ol (353):

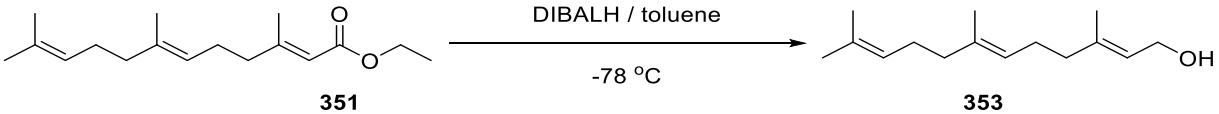

351 353

Esters **350** and **351** (1.53 g, 5.79 mmol, 1 eq.) in anhydrous toluene (30 mL) was cooled to -78 °C. DIBALH (17.4 mL, 17.38 mmol, 3 eq.) was added dropwise and the reaction stirred until complete

consumption of starting material was observed *via* TLC (20% ethyl acetate in hexanes). The reaction was warmed to 0 °C, quenched with Rochelle salts (20 mL) and stirred for 16 hours at room temperature. Organic products were extracted with DCM (3 x 20 mL) and washed with water (3 x 20 mL) and brine (3 x 20 mL). Organic layers were dried over sodium sulphate, filtered and concentrated under *vaccuo*. Purification *via* flash chromatography (5% ethyl acetate in hexanes) gave **353** as a clear oil (0.998 g, 78%).

^{1}H NMR (300 MHz, $CDCl_3$) δ 5.43 (1H, t, *J* = 6.9 Hz CC*H*CH_2O), 5.19 – 5.05 (2H, m, 2 x $(CH_3)CCH$), 4.16 (2H, t, *J* = 6.9 Hz, $CHCH_2OH$), 2.19 – 1.96 (8H, m, 4 x allylic CH_2), 1.69 (6H, s, 2 x CH_3), 1.61 (6H, s, 2 x CH_3). **^{13}C NMR** (75 MHz, $CDCl_3$) δ 139.8 ($(CH_3)CCHCH_2O$), 135.4 & 131.4 (2 x $(CH_3)CCH$), 124.3 ($CCHCH_2O$), 123.8 & 123.3 (2 x $(CH_3)CCH$), 59.4 ($CHCH_2O$), 39.7 & 39.6 & 26.7 & 26.3 (4 x allylic CH_2), 25.7 (CH_3), 17.7 (CH_3), 16.30 & 16.0 (2 x CH_3)CCH). **LRMS** (ES^+): 222.20 (2% [M]), 204.19 (40%), 189.17 (15%), 161.13 (30%), 133.10 (22%), 119.09 (55%), 107.09 (50%), 93.07 (100%), 79.06 (55%), 69.07 (65%). **HRMS** (EI^+): calculated for $[C_{15}H_{26}O]$ [M]; 222.1984, found 222.1994.

Table 12. 2D proton NMR correlations revealing spatial arrangement in 353

353: NOESY ^{1}H - ^{1}H interactions	
From / ppm	To / ppm
5.43	4.16
5.43	1.65
5.12	2.06
5.12	1.65
4.16	1.65

Preparation of (2E,6E)-1-bromo-3,7,11-trimethyldodeca-2,6,10-triene (355):

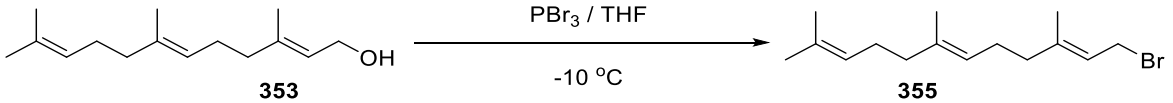

353 **355**

Phosphorus tribromide (26 µL, 0.27 mmol, 1 eq.) was added dropwise to a stirred solution of **353** (120 mg, 0.54 mmol, 2 eq.) in anhydrous THF (10 mL) at -10 °C. Reaction was quenched with sat. sodium bicarbonate sol. (5 mL) upon completion observed *via* TLC (20% ethyl acetate in hexanes). Reaction products were extracted with diethyl ether (3 x 10 mL) and ethereal layers were washed with water (3 x 10 mL) and brine (3 x 10 mL). Products were dried over sodium sulphate, filtered and

concentrated under reduced pressure to give **355** as a crude yellow oil (153 mg, 100%) which was used without further purification.

^{1}H NMR (300 MHz, $CDCl_3$) δ 5.47 (1H, t, *J* = 8.4 Hz, CC*H*CH_2Br), 5.06 – 4.98 (2H, m, 2 x (CH_3)CC*H*), 3.96 (2H, d, *J* = 8.4 Hz, CHC*H*$_2$Br), 2.09 – 1.87 (8H, m, 4 x allylic C*H*$_2$), 1.67 (3H, s, C*H*$_3$), 1.62 (3H, s, C*H*$_3$), 1.53 (3H, s, C*H*$_3$).

Preparation of (2E,6E)-1-chloro-3,7,11-trimethyldodeca-2,6,10-triene (356):

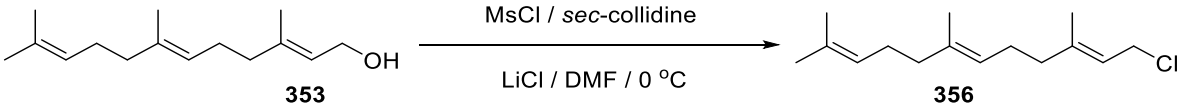

353 **356**

(2*E*,6*E*) Farnesol (**353**) (200 mg, 0.9 mmol, 1 eq.) in anhydrous dimethylformamide (20 mL) was cooled to 0 °C and mesyl chloride (207 mg, 1.8 mmol, 2 eq.) and *sec*-collidine (654 mg, 5.4 mmol, 6 eq.) added. The mixture was stirred at 0 °C for 30 min and lithium chloride (165 mg, 3.6 mmol, 4 eq.) in anhydrous DMF (5 mL) was added dropwise. The reaction mixture was stirred for 2 hours at 0 °C and quenched with dH_2O (10 mL). The quenched reaction mixture was diluted with hexane (10 mL) and the aqueous layer washed with hexane (3 x 10 mL). Combined organic layers were washed with *sat.* copper sulphate solution (3 x 10 mL), *sat.* sodium bicarbonate solution (3 x 10 mL) and brine (20 mL). Organic layers were dried over anhydrous magnesium sulphate, filtered and solvent removed under reduced pressure to give chloride **356** as a pale yellow oil (180 mg, 83%).

^{1}H NMR (500 MHz, $CDCl_3$) δ 5.36 (1H, m, CC*H*CH_2Cl), 5.06 – 4.99 (2H, m, 2 x (CH_3)CC*H*), 3.99 (2H, d, *J* = 7.9 Hz, CHC*H*$_2$Cl), 2.07 – 2.04 (4H, m, 2 x allylic C*H*$_2$), 2.03 – 1.96 (4H, m, 2 x allylic C*H*$_2$), 1.70 (3H, s, C*H*$_3$), 1.62 (6H, s, 2 x C*H*$_3$), 1.54 (3H, s, C*H*$_3$).

Preparation of (2E,6E)-3,7,11-trimethyldodeca-2,6,10-trien-1-yl diphosphate (31):

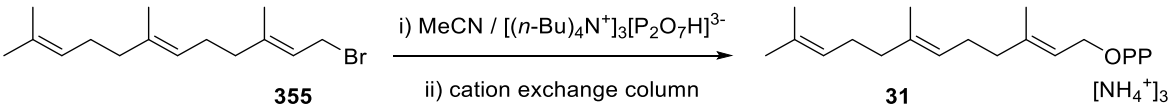

355 **31**

Tris tetra butyl ammonium pyrophosphate (974 mg, 1.08 mmol, 2 eq.) in anhydrous acetonitrile was added to crude bromide **355** (154 mg, 0.54 mmol, 1 eq.) under argon. The reaction was stirred for 16 hours at room temperature and volatile solvents removed under reduced pressure to give crude diphosphate as a brown oil. Crude diphosphate was dissolved in buffer solution (25 mM NH_4HCO_3, 2% iPrOH) (10 mL) and the tris tetrabutylammonium salt counter ions were exchanged for

ammonium by ion exchange column containing Amberlyst 131 (wet H^+ form) mesh cation exchange resin pre-equilibrated with ion-exchange buffer (25 mM NH_4HCO_3, 2% isopropanol). The appropriate fractions were collected and lyophilized to yield (2*E*,6*E*) farnesyl diphosphate as a white powder. The powder was dissolved in buffer solution (25 mM NH_4HCO_3, 2% iPrOH) (10 mL) and purified using HPLC (Solvent A: acetonitrile, solvent B: 2% iPrOH). The appropriate fractions were collected and lyophilized to give (2*E*,6*E*) farnesyl diphosphate as a white powder (23 mg, 10%).

^{1}H NMR (500 MHz, D_2O) δ 5.43 – 5.33 (1H, m, CC*H*CH_2O), 5.17 – 5.07 (2H, m, 2 x (CH_3)CC*H*), 4.44 – 4.37 (2H, m, CHCH_2O), 2.16 – 2.03 (4H, m, 2 x allylic CH_2), 2.03 – 1.92 (4H, m, 2 x allylic CH_2), 1.65 (3H, s, CH_3), 1.61 (3H, s, CH_3), 1.55 (6H, s, 2 x CH_3). **^{31}P NMR** (202 MHz, D_2O) δ -8.71 (d, *J* = 24.5 Hz), -10.60 (d, *J* = 20.2 Hz). **HRMS** (ES^-): calculated for $[C_{15}H_{27}O_7P_2]$[M]; 381.1232, found 381.1235.

8.2.5 Synthesis of neryl diphosphate (39)

Preparation of (Z)-2-acetyl-5,9-dimethyldeca-4,8-dien-1-yl diphosphate (39):

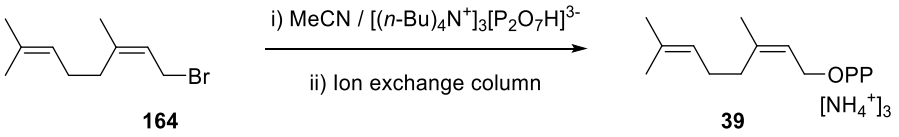

164 **39**

A mixture of neryl bromide (**164**) (169 mg, 0.78 mmol, 1 eq.) and tris tetrabutyl ammonium pyrophosphate (1.05 g, 1.17 mmol, 1.5 eq.) in anhydrous acetonitrile (4 mL) was stirred at room temperature for 16 hours. The reaction mixture was concentrated under reduced pressure and the resultant residue dissolved in buffer solution (25 mM NH_4HCO_3, 2% iPrOH) (5 mL) and the tris tetrabutylammonium salt counter ions were exchanged for ammonium by ion exchange column containing Amberlyst 131 (wet H^+ form) mesh cation exchange resin pre-equilibrated with ion-exchange buffer (25 mM NH_4HCO_3, 2% isopropanol). The appropriate fractions were collected and lyophilized to yield neryl diphosphate as a white powder. The powder was dissolved in buffer solution (25 mM NH_4HCO_3, 2% iPrOH) (5 mL) and purified using HPLC (Solvent A: acetonitrile, solvent B: 2% iPrOH). The appropriate fractions were collected and lyophilized to give neryl diphosphate as a white powder (12 mg, 4%).

^{1}H NMR (500 MHz, D_2O) δ 5.38 (1H, t, *J* = 6.6 Hz, CC*H*CH_2O), 5.14 (1H, t, *J* = 7.0 Hz, (CH_3)CC*H*), 4.91 – 4.86 (2H, m, CCHCH_2O), 2.13 – 1.98 (4H, m, 2 x allylic CH_2), 1.67 (3H, s, CH_3), 1.63 (3H, s, CH_3), 1.55

(3H, s, CH_3). **^{31}P NMR** (202 MHz, D_2O) δ -7.45 (d, *J* = 19.4 Hz), -11.13 (d, *J* = 17.2 Hz). **HRMS** (ES^-): calculated for $[C_{10}H_{19}O_7P_2][M]$; 313.0606, found 313.0608.

8.2.6 Synthesis of geranyl diphosphate (30)

Preparation (E)-2-acetyl-5,9-dimethyldeca-4,8-dien-1-yl diphosphate (30):

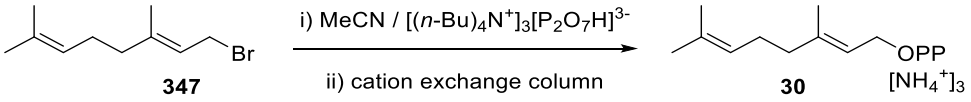

347 **30**

Tris tetra butyl ammonium pyrophosphate (1.16 g, 1.29 mmol, 2 eq.) in anhydrous acetonitrile (10 mL) was added to crude bromide **347** (140 mg, 0.65 mmol, 1 eq.) under argon. The reaction was stirred for 16 hours at room temperature and volatile solvents removed under reduced pressure to give crude diphosphate as a brown oil. Crude diphosphate was dissolved in buffer solution (25 mM NH_4HCO_3, 2% iPrOH) (10 mL) and the tris tetrabutylammonium salt counter ions were exchanged for ammonium by ion exchange column containing Amberlyst 131 (wet H^+ form) mesh cation exchange resin pre-equilibrated with ion-exchange buffer (25 mM NH_4HCO_3, 2% isopropanol). The appropriate fractions were collected and lyophilized to yield geranyl diphosphate as a white powder. The powder was dissolved in buffer solution (25 mM NH_4HCO_3, 2% iPrOH) (5 mL) and purified using HPLC (Solvent A: acetonitrile, solvent B: 2% iPrOH). The appropriate fractions were collected and lyophilized to give geranyl diphosphate as a white powder (27 mg, 11%).

^{1}H NMR (500 MHz, D_2O) δ 5.39 (1H, t, *J* = 6.5 Hz, CC*H*CH_2O), 5.14 (1H, t, *J* = 7.0 Hz, (CH_3)CC*H*), 4.40 (2H, t, *J* = 6.5 Hz, CCHCH_2O), 2.11 – 1.99 (4H, m, 2 x allylic CH_2), 1.64 (3H, s, CH_3), 1.61 (3H, s, CH_3), 1.55 (3H, s, CH_3). **^{31}P NMR** (202 MHz, D_2O) δ -7.32 (d, *J* = 19.4 Hz), -10.40 (d, *J* = 17.2 Hz). **HRMS** (ES^-): calculated for $[C_{10}H_{19}O_7P_2][M]$; 313.0606, found 313.0602.

8.2.7 Synthesis of (2*E*,6*Z*)-2-fluorofarnesyl diphosphate (230)

Preparation of ethyl (6Z)-2-fluoro-3,7,11-trimethyldodeca-2,6,10-trienoate (243):

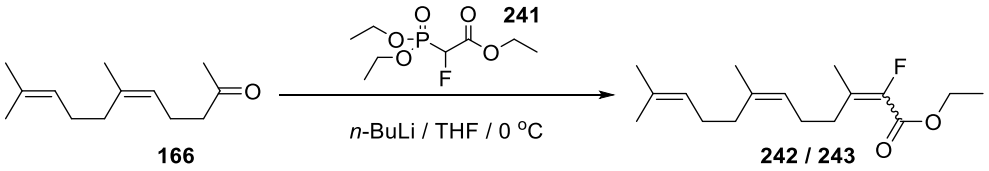

2-Fluoro triethyl phosphono acetate (**241**)(2.67 g, 11.0 mmol, 1.1 eq.) in anhydrous THF (40 mL) was cooled to 0 °C and *n*-butyl lithium (4.4 mL, 11.0 mmol, 1.1 eq., 2.5 M in hexane) added dropwise. The reaction was stirred at room temperature for 1 hour and cooled to 0 °C. Neryl acetone (**166**) (1.95 g, 10.0 mmol, 1 eq.) was added dropwise and the reaction mixture stirred at room temperature for 16 hours. Reaction was quenched with water (20 mL) and reaction products extracted with diethyl ether (3 x 20 mL). Combined ethereal layers were washed with water (3 x 20 mL), brine (3 x 20 mL), dried over sodium sulphate and filtered. Product was concentrated under reduced pressure and purified *via* flash chromatography (10% ethyl acetate in hexane) gave a mixture of fluorinated esters **242** and **243** as a clear oil (2.31 g, 82%). Flash chromatography (5% ethyl acetate in hexanes) partially separated esters **242** and **243** for analysis.

^{1}H NMR (300 MHz, $CDCl_3$) δ 5.11 – 4.99 (2H, m, 2 x $(CH_3)CCH$), 4.20 (2H, q, *J* = 7.1 Hz, OCH_2CH_3), 2.47 (2H, ddd, *J* = 8.1, 5.1, 1.8 Hz, $CH_2(CH_3)CCFC(O)$), 2.23 – 2.14 (2H, m, $CH_2CH_2(CH_3)CCHC(O)$), 2.00 – 1.88 (4H, m, 2 x allylic CH_2), 1.79 (3H, d, *J* = 4.3 Hz, $CH_2(CH_3)CCHC(O)$), 1.62 (6H, s, 2 x CH_3), 1.54 (3H, s, CH_3), 1.27 (3H, t, *J* = 7.1 Hz, OCH_2CH_3). **^{13}C NMR** (75 MHz, $CDCl_3$) δ 161.3 (CHC(O)O), 153.2 (d, *J* = 224.2 Hz, $(CH_3)CC(F)$), 142.0 (d, *J* = 18.1 Hz, $(CH_3)CC(F)$), 136.5 &, 131.7 (2 x $(CH_3)CCH$), 124.2 & 123.9 (2 x $(CH_3)CCH$), 61.0 (OCH_2CH_3), 32.7 (d, *J* = 7.0 Hz, $CH_2CH_2(CH_3)CC(F)$), 31.9 & 31.4 (2 x CH_2), 26.6 (d, *J* = 2.9 Hz, $CH_2(CH_3)CC(F)$), 25.7 & 23.4 & 17.6 (3 x CH_3), 16.8 (d, *J* = 4.6 Hz, $(CH_3)CC(F)$), 14.2 (OCH_2CH_3). **^{19}F NMR** (376 MHz, $CDCl_3$) δ -126.95. **LRMS** (EI^+): 282.20 (25% [M]), 262.19 (20%), 218.99 (60%), 173.13 (55%), 137.13 (75%), 109.10 (85%), 81.17 (100%)**. HRMS** (EI^+): calculated for $[C_{17}H_{27}O_2F][M]$; 282.1995, found 282.1994.

Preparation of (2E,6Z)-2-fluoro-3,7,11-trimethyldodeca-2,6,10-trien-1-ol (245):

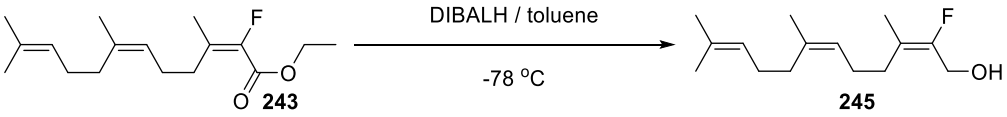

Fluorinated ethyl farnesoates **242** and **243** (2.31 g, 8.2 mmol, 1 eq.) in anhydrous toluene (20 mL) were cooled to -78 °C. DIBALH (41 mL, 40.9 mmol, 5 eq.) was added dropwise and stirred until reaction completion was observed *via* TLC (20% ethyl acetate in hexane). Reaction was quenched with Rochelle salts (10 mL) at 0 °C and the resultant mixture stirred at room temperature for 16 hours. Reaction products were extracted using DCM (3 x 10 mL). Combined organic layers were washed with water (3 x 10 mL), brine (3 x 10 mL), dried over sodium sulphate, filtered and concentrated under reduced pressure. Purification *via* flash chromatography (5% ethyl acetate in hexane) gave **245** as a colourless oil (727 mg, 37%).

^{1}H NMR (300 MHz, $CDCl_3$) δ 5.15 – 5.06 (2H, m, 2 x $(CH_3)CCH$), 4.21 (2H, d, *J* = 23.0 Hz, $CFCH_2OH$), 2.16 – 1.96 (8H, m, 4 x allylic CH_2), 1.71 (6H, s, 2 x CH_3), 1.70 (3H, s, CH_3), 1.62 (3H, s, CH_3). **^{13}C NMR** (126 MHz, $CDCl_3$) δ 153.6 (d, *J* = 244.0 Hz, $(CH_3)CC(F)CH_2OH$), 136.8 ($(CH_3)CCH$), 131.8 ($(CH_3)CCH$), 124.1 & 123.9 ($(CH_3)CCH$), 115.8 (d, *J* = 14.0 Hz, $(CH_3)CC(F)CH_2OH$), 57.8 (d, *J* = 31.6 Hz, $C(F)CH_2OH$), 32.0 (d, *J* = 4.9 Hz, $CH_2(CH_3)CC(F)CH_2OH$), 26.6 & 26.0 (2 x allylic CH_2), 26.2 (d, *J* = 3.0 Hz, $CH_2CH_2(CH_3)CC(F)CH_2OH$), 25.7 & 23.3 & 17.7 (3 x CH_3), 13.6 (d, *J* = 8.8 Hz, $(CH_3)CC(F)CH_2OH$). **^{19}F NMR** (376 MHz, $CDCl_3$) δ -119.40. **LRMS** (EI^+): 222.18 (25% $[M - H_2O]$), 202.17 (30%), 187.15 (35%), 137.08 (40%), 105.07 (35%), 91.05 (60%), 81.07 (40%), 69.07 (100%). **HRMS** (EI^+): calculated for $[C_{15}H_{23}F][M - H_2O]$; 222.1784, found 222.1787.

Table 13. 2D proton NMR correlations revealing spatial arrangement in 245

245: NOESY ^{1}H - ^{1}H interactions	
From / ppm	To / ppm
5.09	2.06
5.09	1.70
5.09	1.62
4.21	2.06

Preparation of (2E,6Z)-1-bromo-2-fluoro-3,7,11-trimethyldodeca-2,6,10-triene (246):

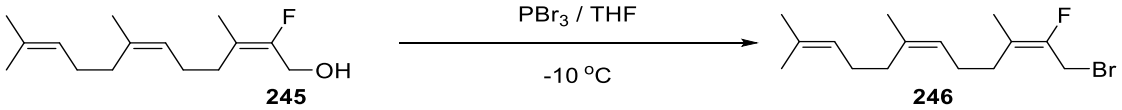

245 (360 mg, 1.5 mmol, 2 eq.) in anhydrous THF (20 mL) was cooled to -10 °C and PBr_3 (710 µL, 0.75 mmol, 1 eq.) added dropwise. The reaction proceeded for 50 minutes at -10 °C and was quenched with *sat*. sodium bicarbonate solution (10 mL). Reaction products were extracted with diethyl ether (3 x 10 mL) and combined ethereal layers washed with water (3 x 10 mL), brine (3 x 10 mL) and dried over sodium sulphate. Organic product was filtered and concentrated under *vaccuo* to give **246** as a pale yellow oil (343 mg, 76%) which was used without further purification.

^{1}H NMR (500 MHz, $CDCl_3$) δ 5.09 – 5.02 (2H, m, 2 x $(CH_3)CCH$), 4.00 (2H, d, *J* = 23.0 Hz, $CFCH_2Br$), 2.08 – 1.91 (8H, m, 4 x allylic CH_2), 1.69 (3H, s, CH_3), 1.63 (6H, s, 2 x CH_3), 1.54 (3H, s, CH_3). **^{19}F NMR** (376 MHz, $CDCl_3$) δ -121.56.

Preparation of (2E,6Z)-2-fluoro-3,7,11-trimethyldodeca-2,6,10-trien-1-yl diphosphate (230):

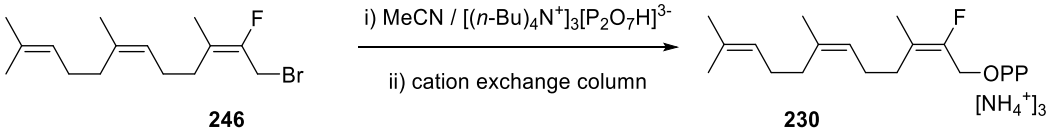

A mixture of crude bromide (**246**) (343 mg, 1.13 mmol, 1 eq.) and tris tetrabutyl ammonium pyrophosphate (1.53 g, 1.70 mmol, 1.5 eq.) in anhydrous acetonitrile (10 mL) was stirred at room temperature for 16 hours. The reaction mixture was concentrated under reduced pressure and the resultant residue dissolved in buffer solution (25 mM NH_4HCO_3, 2% iPrOH) (10 mL) and the tris tetrabutylammonium salt counter ions were exchanged for ammonium by ion exchange column containing Amberlyst 131 (wet H^+ form) mesh cation exchange resin pre-equilibrated with ion-exchange buffer (25 mM NH_4HCO_3, 2% isopropanol). The appropriate fractions were collected and lyophilized to yield diphosphate **230** as a white powder. The powder was dissolved in buffer solution (25 mM NH_4HCO_3, 2% iPrOH) (8 mL) and purified using HPLC (Solvent A: acetonitrile, solvent B: 2% iPrOH). The appropriate fractions were collected and lyophilized to give diphosphate **230** as a white powder. (22 mg, 4%).

^{1}H NMR (500 MHz, $CDCl_3$) δ 5.09 – 5.02 (2H, m, 2 x $(CH_3)CCH$), 4.41 (2H, m, $CFCH_2O$), 2.08 – 1.91 (8H, m, 4 x allylic CH_2), 1.69 (3H, s, CH_3), 1.63 (6H, s, 2 x CH_3), 1.54 (3H, s, CH_3). **^{19}F NMR** (376 MHz, $CDCl_3$) δ -121.56. **^{31}P NMR** (162 MHz, $CDCl_3$) δ -6.85 (d, *J* = 21.2 Hz, $CH_2OP(O)_2OP(O)_3$), -10.22 (d, *J* = 21.2 Hz, $CH_2OP(O)_2OP(O)_3$). **HRMS** (ES^-): calculated for $[C_{15}H_{26}FO_7P_2][M]$; 399.1138, found 399.1143.

8.2.8 Synthesis of (2*Z*,6*E*)-6-fluorofarnesyl diphosphate (231)

Preparation of ethyl (E)-2-fluoro-3,7-dimethylocta-2,6-dienoate(253)

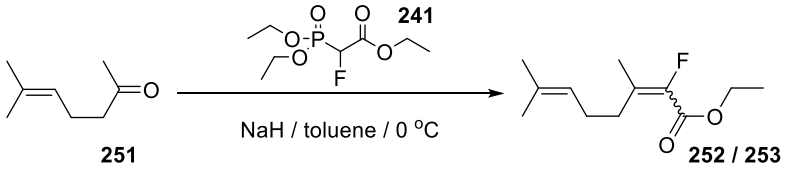

2-Fluoro triethyl phosphonoacetate (25.0 g, 103.2 mmol, 1.2 eq.) was added to a stirred suspension of sodium hydride (4.47 g, 111.8 mmol, 1.3 eq.) in anhydrous toluene (150 mL) at 0 °C. The suspension was stirred for 1 hour at room temperature and cooled to 0 °C prior to the addition of **251** (10.85 g, 86.0 mmol, 1 eq.). The reaction mixture was stirred at room temperature for 16 hours, quenched with water (30 mL) and organic products extracted with diethyl ether (3 x 30 mL). Ethereal layers were washed with water (3 x 30 mL) and brine (3 x 30 mL), dried over sodium sulphate, filtered and concentrated under reduced pressure. Purification *via* flash chromatography (10% ethyl acetate in hexane) gave a mixture of fluorinated esters **252** and **253** as a clear oil (7.22 g, 39%). Flash chromatography (5% ethyl acetate in hexanes) partially separated esters **252** and **253** for analysis.

^{1}H NMR (300 MHz, $CDCl_3$) δ 5.09 – 5.00 (1H, m, $(CH_3)CCH$), 4.20 (2H , q, *J* = 7.1 Hz, OCH_2CH_3), 2.51 – 2.44 (2H, m, $CH_2(CH_3)CC(CH_3)C(O)$), 2.24 – 2.14 (2H, s, allylic CH_2), 1.79 (3H, d, *J* = 4.3 Hz, CH_3), 1.54 (6H, s, 2 x CH_3), 1.27 (3H, t, *J* = 7.1 Hz, OCH_2CH_3). **^{13}C NMR** (75 MHz, $CDCl_3$) δ 161.1 (d, *J* = 31.3 Hz, $(CH_3)CC(F)C(O)$), 152.9 (d, *J* = 241.3 Hz, $(CH_3)CC(F)$), 142.2 (d, *J* = 23.4 Hz, $(CH_3)CC(F)$), 132.8 ($(CH_3)CCH$), 123.2 ($(CH_3)CCH$), 60.9 (OCH_2CH_3), 32.5 (d, *J* = 6.9 Hz, $CH_2CH_2(CH_3)CC(F)$), 32.0 (d, *J* = 4.3 Hz, $CH_2(CH_3)CC(F)$), 25.7 (CH_3), 17.6 (CH_3), 16.7 (CH_3), 14.2 (OCH_2CH_3). **^{19}F NMR** (471 MHz, $CDCl_3$) δ -126.81. **LRMS** (EI^+): 214.14 (5% [M]), 194.13 (55%), 146.07 (40%), 118.04 (55%), 105.07 (35%), 91.05 (25%), 77.04 (18%), 69.07 (100%). **HRMS** (EI^+): calculated for $[C_{12}H_{19}O_2F][M]$; 214.1369, found 214.1369.

Preparation of (E)-2-fluoro-3,7-dimethylocta-2,6-dien-1-ol (255):

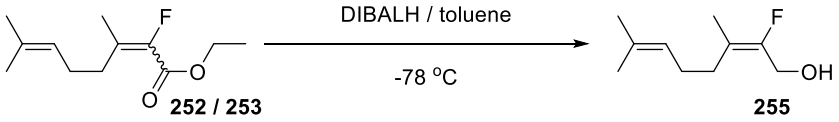

DIBALH (103 mL, 103 mmol, 5 eq., 1 M in hexane) was added to a mixture of **252** and **253** (7.22 g, 34.3, 1 eq.) in anhydrous toluene (50 mL) at -78 °C. Reaction was quenched with Rochelle salt (20 mL) at 0 °C when complete consumption of starting material was observed *via* TLC (20% ethyl acetate in hexane). The suspension was stirred for 16 hours at room temperature and organic products extracted with DCM (3 x 20 mL). Combined organic extracts were washed with water (3 x 20 mL), brine (3 x 20 mL), dried over sodium sulphate, filtered and concentrated under *vaccuo*. Fluorinated alcohol **255** was purified by flash chromatography (5% ethyl acetate in hexane) to give **255** as a clear oil (1.53 g, 26%).

^{1}H NMR (300 MHz, $CDCl_3$) δ 5.15 – 5.02 (1H, m, $(CH_3)CC\mathit{H}$), 4.20 (2H , d, *J* = 20.9 Hz, $CC(F)C\mathit{H}_2OH$), 2.08 (4H, m, 2 x allylic $C\mathit{H}_2$), 1.70 (6H, s, 2 x $C\mathit{H}_3$), 1.60 (3H, s, $C\mathit{H}_3$). **^{13}C NMR** (75 MHz, $CDCl_3$) δ 153.6 (d, *J* = 243.7 Hz, $(CH_3)C\mathit{C}(F)CH_2OH$), 133.1 ($(CH_3)\mathit{C}CH$), 123.3 ($(CH_3)C\mathit{C}H$), 115.7 (d, *J* = 13.9 Hz, $(CH_3)\mathit{C}C(F)CH_2OH$), 57.8 (d, *J* = 31.7 Hz, $C(F)\mathit{C}H_2OH$), 31.8 (d, *J* = 4.8 Hz, $\mathit{C}H_2(CH_3)CC(F)CH_2OH$), 26.4 (d, *J* = 3.0 Hz, allylic $\mathit{C}H_2$), 25.7 ($\mathit{C}H_3$), 17.66 ($\mathit{C}H_3$), 13.5 (d, *J* = 8.9 Hz, $(\mathit{C}H_3)CC(F)CH_2OH$). **^{19}F NMR** (471 MHz, $CDCl_3$) δ -119.18. **LRMS** (EI^+): 154.12 (40% [M – H_2O]), 139.09 (35%), 111.06 (100%), 109.04 (50%), 97.04 (20%), 91.05 (30%), 77.04 (18%), 69.07 (22%). **HRMS** (EI^+): calculated for [$C_{10}H_{15}F$][M – H_2O]; 154.1158, found 154.1157.

Table 14. 2D proton NMR correlations revealing spatial arrangement in 255

255: NOESY ^{1}H - ^{1}H interactions	
From / ppm	To / ppm
5.09	2.08
5.09	1.70
5.09	1.60
4.20	2.08

Preparation of (E)-1-bromo-2-fluoro-3,7-dimethylocta-2,6-diene (256):

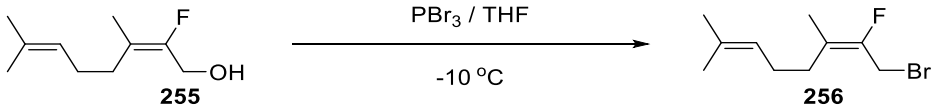

255 (1.53 g, 8.85 mmol, 2 eq.) in anhydrous THF (20 mL) was cooled to -10 °C and PBr_3 (0.41 mL, 4.43 mmol, 1 eq.) added dropwise. Reaction was quenched with sat. sodium bicarbonate sol. (10 mL) after 50 minutes. Reaction products were extracted with diethyl ether (3 x 10 mL) and combined organic extracts were washed with water (3 x 10 mL) and brine (2 x 10 mL). Organic extracts were dried over sodium sulphate, filtered and concentrated under reduced pressure to give **256** as a pale yellow oil (2.09 g, 100%) which was used without further purification.

^{1}H NMR (500 MHz, $CDCl_3$) δ 5.06 – 5.00 (1H, m, $(CH_3)CCH$), 4.00 (2H , d, *J* = 23.0 Hz, $CC(F)CH_2Br$), 2.10 – 1.95 (4H, m, 2 x allylic CH_2), 1.64 (3H, s, CH_3), 1.63 (3H, s, CH_3), 1.54 (3H, s, CH_3). **^{19}F NMR** (471 MHz, $CDCl_3$) δ -114.49 (s).

Preparation of ethyl (E)-2-acetyl-4-fluoro-5,9-dimethyldeca-4,8-dienoate (257):

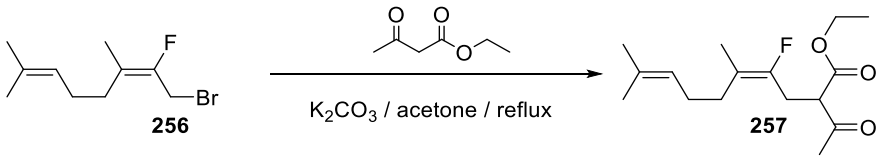

Ethyl acetoacetate (2.31 g, 17.78 mmol, 2 eq.) and potassium carbonate (2.46 g, 17.8 mmol, 2 eq.) were added to **256** (2.09 g, 8.89 mmol, 1 eq.) in dry acetone and refluxed at 60 °C. Volatile solvents were removed under reduced pressure and organic products take into diethyl ether. Organic extracts were washed with water (3 x 20 mL), brine (3 x 20 mL) dried over sodium sulphate and filtered. Products were concentrated under *vaccuo* and purified by flash chromatography (20% ethyl acetate in hexane) to give **257** as a colourless oil (2.06 g, 74%).

^{1}H NMR (300 MHz, $CDCl_3$) δ 5.08 (1H, t, *J* = 6.9 Hz, $(CH_3)CCH$), 4.20 (2H, q, *J* = 7.1 Hz, CH_3CH_2O), 3.76 (1H, t, *J*= 7.1 Hz, $COCHCO$), 2.81 (2H, dd, *J* = 21.6, 7.2 Hz, $CCFCH_2CH$), 2.27 (3H, s, $COCH_3$), 2.11 – 1.91 (4H, m, 2 x allylic CH_2), 1.69 (3H, s, CH_3), 1.62 (3H, s, CH_3), 1.61 (3H, s, CH_3), 1.28 (3H, t, *J*= 7.1 Hz,CH_3CH_2O). **^{13}C NMR** (75 MHz, $CDCl_3$) δ 202.2 ($CH_3C(O)CH$), 169.0 ($CH_3CH_2OC(O)$), 151.2 (d, *J* = 241.5 Hz, $CH_3CC(F)CH_2$), 132.3 ($(CH_3)CCH$), 123.5 ($(CH_3)CCH$), 114.0 (d, *J* = 14.3 Hz, $(CH_3)CC(F)CH_2$), 61.6 (CH_3CH_2O), 56.5 ($C(O)CHC(O)$), 31.8 (d, *J* = 5.3 Hz, $CH_2(CH_3)CC(F)CH_2$), 29.6 ($CH_3C(O)$), 27.0 (d, *J* =

28.8 Hz, $(CH_3)CC(F)CH_2$), 26.4 (d, *J* = 3.1 Hz, $(CH_3)CCHCH_2$), 25.7 (CH_3), 17.7 (CH_3), 13.4 (OCH_2CH_3), 13.3 (CH_3). **^{19}F NMR** (471 MHz, $CDCl_3$) δ -112.92. **LRMS** (EI^+): 284.18 (5% [M]), 264.17 (10%), 242.17 (7%), 215.11 (5%), 195.10 (100%), 127.06 (35%), 109.06 (30%), 69.07 (55%). **HRMS** (EI^+): calculated for $[C_{16}H_{25}O_3F][M]$; 284.1788, found 284.1786.

Preparation of (E)-5-fluoro-6,10-dimethylundeca-5,9-dien-2-one (258):

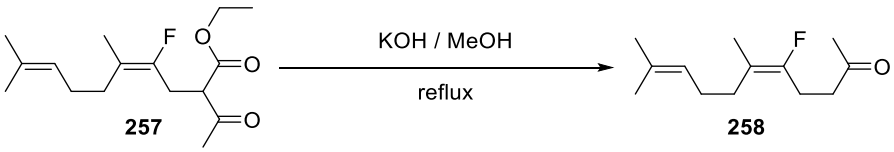

257 **258**

A mixture of potassium hydroxide (1.18 g, 21.10, 3 eq.) and **257** (2.0 g, 7.03 mmol, 1 eq.) in methanol (40 mL) was refluxed at 65 °C for 3 hours. The reaction mixture was cooled to room temperature and acidified with 1M HCl (10 mL). Organic products were extracted with diethyl ether (3 x 15 mL) and washed with water (3 x 10 mL) and brine (3 x 10 mL). Washed organic layers were dried over sodium sulphate, filtered and concentrated under reduced pressure. Purification *via* flash chromatography gave **258** as a pale yellow oil (1.27 g, 85%).

^{1}H NMR (300 MHz, $CDCl_3$) δ 5.08 (1H, t, *J* = 5.3 Hz, $(CH_3)CCH$), 2.69 – 2.60 (2H, m, $CH_2C(O)$), 2.58 – 2.42 (2H, m, $CH_2CH_2C(O)$), 2.17 (3H, s, $CH_2C(O)CH_3$), 2.01 (4H, dt, *J* = 12.9, 5.9 Hz, 2 x allylic CH_2), 1.69 (3H, s, CH_3), 1.62 (3H, s, CH_3), 1.61 (3H, s, CH_3). **^{13}C NMR** (75 MHz, $CDCl_3$) δ 207.7 ($CH_3C(O)$), 153.5 (d, *J* = 242.1 Hz, $(CH_3)CCF$), 132.2 ($(CH_3)CCH$), 123.6 ($(CH_3)CCH$), 111.9 (d, *J* = 14.9 Hz, $(CH_3)CCF$), 40.5 ($CH_2CH_2C(O)$), 31.9 (d, *J* = 5.7 Hz, $CH_2(CH_3)CCF$), 30.0 ($CH_3C(O)$), 26.4 (allylic CH_2), 25.7 (CH_3), 22.6 (d, *J* = 29.6 Hz, $((CH_3)CCFCH_2)$, 17.7 (CH_3), 13.3 (d, *J* = 9.6 Hz, $(CH_3)CCF$). **^{19}F NMR** (471 MHz, $CDCl_3$) δ -112.97. **LRMS** (EI^+): 212.16 (2% [M]), 192.15 (35%), 174.14 (25%), 159.12 (70%), 143.09 (100%), 123.08 (25%), 109.06 (50%), 95.08 (55%), 79.05 (25%), 69.07 (95%). **HRMS** (EI^+): calculated for $[C_{13}H_{21}OF][M]$; 212.1576, found 212.1579.

Preparation of ethyl (2Z,6E)-6-fluoro-3,7,11-trimethyldodeca-2,6,10-trienoate (260):

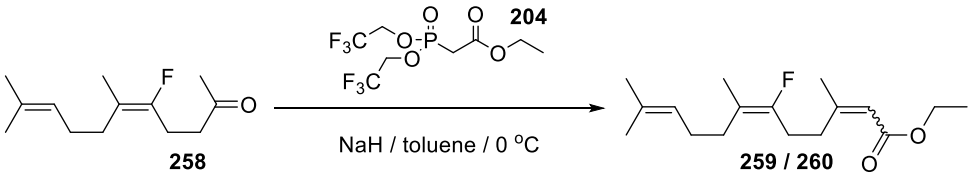

A suspension of sodium hydride (378 mg, 9.41 mmol, 2.2 eq.) in anhydrous toluene (30 mL) was cooled to 0 °C. **204** (2.85 mg, 8.56 mmol, 2 eq.) was added to the stirred suspension and the reaction stirred at room temperature for 1 hour. The reaction mixture was cooled to 0 °C and **258** (909 mg, 4.28 mmol, 1 eq.) added and reaction stirred at room temperature for 16 hours. Reaction was quenched with water (10 mL) and reaction products extracted with diethyl ether (3 x 20 mL). Combined organic extracts were washed with water (3 x 20 mL) and brine (3 x 20 mL). Extracts were dried over sodium sulphate, filtered and concentrated under reduced pressure. Purification *via* flash chromatography (10% ethyl acetate in hexane) gave a mixture of fluorinated esters **259** and **260** as a clear oil (762 mg, 63%). Flash chromatography (5% ethyl acetate in hexanes) partially separated esters **259** and **260** for analysis.

^{1}H NMR (300 MHz, $CDCl_3$) δ 5.61 (1H, s, CC*H*C(O)OEt), 5.07 – 4.95 (1H, m, $(CH_3)CCH$), 4.07 (2H, q, *J* = 7.1 Hz, OCH_2CH_3), 2.69 (2H, t, *J* = 7.6 Hz, $CH_2(CH_3)CCHC(O)$), 2.35 (2H, dt, *J* = 23.5, 7.5 Hz, $(CH_3)CC(F)CH_2$), 2.06 – 1.85 (4H, m, 2 x allylic CH_2), 1.82 (3H, s, CH_3), 1.61 (3H, s, CH_3), 1.55 (3H, d, *J* = 2.3 Hz, $(CH_3)CC(F)CH_2$),1.53 (3H, s, CH_3), 1.20 (3H, t, *J* = 7.1 Hz, OCH_2CH_3). **^{13}C NMR** (75 MHz, $CDCl_3$) δ 166.1 (CHC(O)O), 159.1 ($(CH_3)CCHC(O)O$), 154.2 (d, *J* = 243.8 Hz, $(CH_3)CCF$), 132.0 ($(CH_3)CCH$), 123.8 ($(CH_3)CCH$) 116.8 (CCHC(O)O), 111.9 (d, *J* = 15.0 Hz, $(CH_3)CCF$), 59.6 (OCH_2CH_3), 31.9 (d, *J* = 5.6 Hz, $CH_2(CH_3)CCF$), 30.9 ($CH_2(CH_3)CCHC(O)$), 27.3 (d, *J* = 29.7 Hz, $(CH_3)CCFCH_2$), 26.7 (d, *J* = 3.1 Hz, allylic CH_2), 25.73 & 25.69 & 17.6 & 14.3 (4 x CH_3), 13.3 (d, *J* = 9.7 Hz, OCH_2CH_3). **^{19}F NMR** (471 MHz, $CDCl_3$) δ -111.33. **LRMS** (EI^+): 262.19 (7% [M]), 216.15 (50%), 197.10 (55%), 159.09 (47%), 145.08 (70%), 128.07 (85%), 119.09 (100%), 105.07 (62%), 91.06 (85%), 69.07 (70%). **HRMS** (EI^+): calculated for $[C_{17}H_{27}O_2F][M]$; 282.1995, found 282.1991.

Preparation of (2Z,6E)-6-fluoro-3,7,11-trimethyldodeca-2,6,10-trien-1-ol (262):

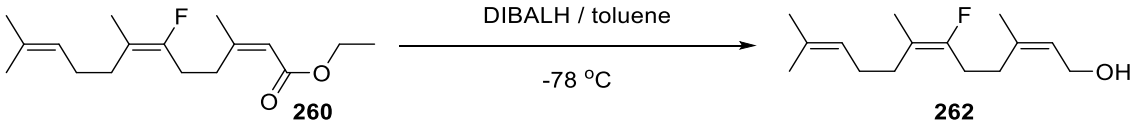

260 **262**

DIBALH (8.1 mL, 8.10 mmol, 3 eq.) was added dropwise to a stirred solution of **259** and **260** (762 mg, 2.70 mmol, 1 eq.) in anhydrous toluene (20 mL) at -78 °C. Reaction was quenched with Rochelle salts (10 mL) at 0°C after complete consumption of starting material was observed *via* TLC (20% ethyl acetate in hexane). The resulting mixture was stirred at room temperature for 16 hours. Reaction products were extracted with DCM (3 x 10 mL) and combined organic layers were washed with water (3 x 10 mL) and brine (3 x 10 mL). Organic layers were dried over sodium sulphate, filtered and concentrated under reduced pressure. Purification *via* flash chromatography (5% ethyl acetate in hexane) gave **262** as a colourless oil (266 mg, 41%).

^{1}H NMR (500 MHz, $CDCl_3$) δ 5.40 (1H, t, *J* = 7.2 Hz CC*H*CH_2O), 5.03 – 4.98 (1H, m, (CH_3)CC*H*), 4.03 (2H, d, *J* = 7.2, CHC*H*$_2$OH), 2.29 – 2.16 (4H, m, 2 x allylic C*H*$_2$), 1.98 (2H, dd, *J* = 15.0, 7.4 Hz, (CH_3)CCFC*H*$_2$), 1.87 – 1.82 (2H, m, allylic C*H*$_2$), 1.68 (3H, s, C*H*$_3$), 1.62 (3H, s, C*H*$_3$), 1.55 (3H, d, *J* = 3.3 Hz, (C*H*$_3$)CCF), 1.53 (3H, s, C*H*$_3$). **^{13}C NMR** (75 MHz, $CDCl_3$) δ 154.2 (d, *J* = 243.0 Hz, (CH_3)C*C*F), 138.6 & 132.2 ((2 x (CH_3)*C*CH), 125.3 (C*C*HCH_2O), 123.6 ((CH_3)C*C*H), 112.0 (d, *J* = 15.3 Hz, (CH_3)*C*CF), 59.0 (CH*C*H$_2$O), 32.0 (d, *J* = 5.8 Hz, *C*H$_2$$(CH_3)$CCF), 29.2 (allylic *C*H$_2$), 27.2 (d, *J* = 29.7 Hz, (CH_3)CCF*C*H$_2$), 26.7 (d, *J* = 2.9 Hz, allylic *C*H$_2$), 25.7 & 23.4 & 17.6 (3 x *C*H$_3$), 13.2 (d, *J* = 9.8 Hz, (*C*H$_3$)CCF). **^{19}F NMR** (471 MHz, $CDCl_3$) δ -111.63. **LRMS** (EI$^+$): 212.16 (3% [M – H_2O]), 203.18 (8%), 202.17 (100%), 200.16 (60%), 198.14 (35%), 187.15 (70%), 185.13 (55%), 183.12 (65%), 181.10 (22%), 179.10 (7%), 173.13 (8%). **HRMS** (EI$^+$): calculated for [$C_{15}H_{23}F$][M – H_2O]; 222.1784, found 222.1784.

Table 15. 2D proton NMR correlations revealing spatial arrangement in 262

262: NOESY ^{1}H - ^{1}H interactions	
From / ppm	To / ppm
5.40	4.03
5.40	1.68
5.00	2.23
5.00	1.62
4.02	1.84

Preparation of (2Z,6E)-1-bromo-6-fluoro-3,7,11-trimethyldodeca-2,6,10-triene (263):

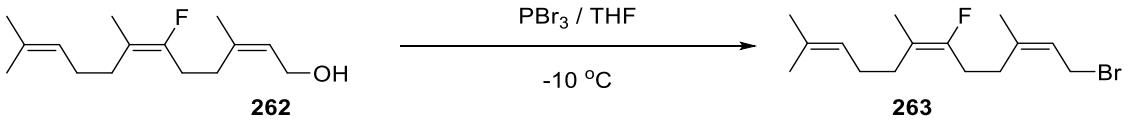

262 **263**

PBr_3 (55 µL, 0.58 mmol, 1 eq.) was added to a stirred solution of **262** (280 mg, 1.16 mmol, 2 eq.) in anhydrous tetrahydrofuran (30 mL) at -10 °C. Complete consumption of the reaction was observed *via* TLC (20% ethyl acetate in hexane) and was quenched with sat. sodium bicarbonate sol. (20 mL) at 0 °C. Reaction products were extracted with diethyl ether (3 x 20 mL) and combined organic layers washed with water (3 x 10 mL) and brine (3 x 10 mL). Organic layers were dried over sodium sulphate, filtered and concentrated under reduced pressure to give **263** as a pale yellow oil (353 mg, 100%) which was used without further purification.

^{1}H NMR (400 MHz, $CDCl_3$) δ 5.50 (1H, t, *J* = 8.5 Hz CC*H*CH_2O), 5.07 – 4.96 (1H, m, (CH_3)CC*H*), 3.92 (2H, d, *J* = 8.5, CHC*H*$_2$Br), 2.31 – 2.16 (4H, m, 2 x allylic C*H*$_2$), 2.02 – 1.80 (4H, m, 2 x allylic C*H*$_2$), 1.71 (3H, s, C*H*$_3$), 1.62 (3H, s, C*H*$_3$), 1.54 (6H, s, 2 x C*H*$_3$). **^{19}F NMR** (376 MHz, $CDCl_3$) δ -111.80.

Preparation of (2Z,6E)-6 fluoro-3,7,11-trimethyldodeca-2,6,10-trien-1-yl diphosphate (231):

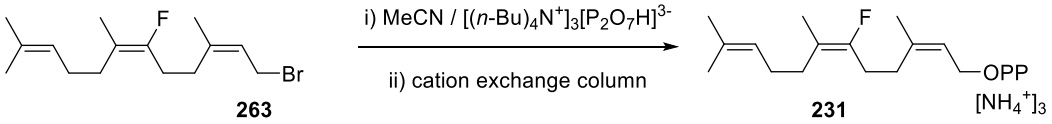

Tris tetra butyl ammonium pyrophosphate (2.1 g, 2.33 mmol, 2 mmol) in anhydrous acetonitrile (10 mL) was added to crude bromide **263** (353 mg, 1.16 mmol, 1 eq.) under argon. The reaction was stirred for 16 hours at room temperature and volatile solvents removed under reduced pressure to give crude diphosphate as a brown oil. Crude diphosphate was dissolved in buffer solution (25 mM NH_4HCO_3, 2% iPrOH) (10 mL) and the tris tetrabutylammonium salt counter ions were exchanged for ammonium by ion exchange column containing Amberlyst 131 (wet H^+ form) mesh cation exchange resin pre-equilibrated with ion-exchange buffer (25 mM NH_4HCO_3, 2% isopropanol). The appropriate fractions were collected and lyophilized to yield diphosphate as a white powder. The powder was dissolved in buffer solution (25 mM NH_4HCO_3, 2% iPrOH) (10 mL) and purified using HPLC (Solvent A: acetonitrile, solvent B: 2% iPrOH). The appropriate fractions were collected and lyophilized to give **231** as a white powder. (5 mg, 1%).

^{1}H NMR (500 MHz, D_2O) δ 5.46 – 5.35 (1H, m, CC*H*CH_2O), 5.16 – 5.05 (1H, m, (CH_3)CC*H*), 4.39 – 4.23 (2H, m, CHC*H*$_2$O), 2.38 – 2.12 (4H, m, 2 x allylic C*H*$_2$), 2.09 – 1.95 (2H, m, (CH_3)CCFC*H*$_2$), 1.70 (3H, s, C*H*$_3$), 1.62 (3H, s, C*H*$_3$), 1.55 (6H, s, 2 x C*H*$_3$). **^{31}P NMR** (202 MHz, D_2O) δ -9.01 (d, *J* = 13.4 Hz), -10.33 (d, *J* = 16.9 Hz). **^{19}F NMR** (471 MHz, D_2O) δ -111.91 (s). **HRMS** (ES^-): calculated for $[C_{15}H_{26}FO_7P_2][M]$; 399.1138, found 399.1137.

8.2.9 Synthesis of (2*Z*,6*Z*)-2-methylfarnesyl diphosphate (359)

Preparation of ethyl (2Z,6Z)-2,3,7,11-tetramethyldodeca-2,6,10-trienoate (373):

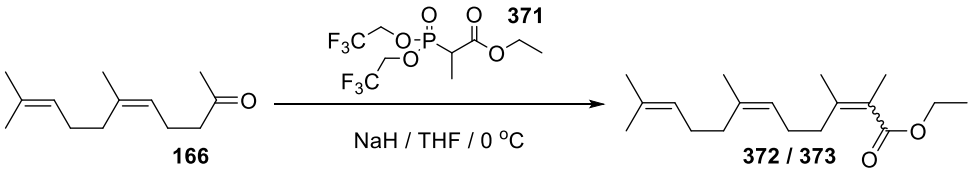

A stirred suspension of sodium hydride (296 mg, 12.35 mmol, 1.6 eq.) in anhydrous toluene (40 mL) was cooled to 0 °C and **371** (4 g, 11.58 mmol, 1.5 eq.) was added dropwise. The reaction mixture was stirred at room temperature for 1 hour and cooled to 0 °C. Neryl acetone (**166**) (1.5 g, 7.7 mmol, 1 eq.) was added dropwise and the reaction mixture stirred at room temperature for 16 hours. The reaction was quenched with water (20 mL) and products extracted with diethyl ether (3 x 20 mL). Organic extracts were washed with water (20 mL) and brine (20 mL), dried over sodium sulphate, filtered and concentrated under reduced pressure. Purification *via* flash chromatography (10% ethyl acetate in hexane) gave a mixture of **372** and **373** as a clear oil (612 mg, 60%). Flash chromatography (5% ethyl acetate in hexanes) partially separated esters **372** and **373** for analysis.

^{1}H NMR (300 MHz, $CDCl_3$) δ 5.19 – 5.11 (2H, m, 2 x $(CH_3)CCH$), 4.19 (2H, q, *J* = 7.1 Hz, OCH_2CH_3), 2.41 – 2.30 (2H, m, $CH_2(CH_3)CC(CH_3)C(O)$), 2.21 – 2.09 (2H, m, $CH_2CH_2(CH_3)CC(CH_3)C(O)$), 2.02 – 1.96 (4H, m, 2 x allylic CH_2), 1.88 (3H, d, *J* = 1.2 Hz, $CH_2(CH_3)CC(CH_3)C(O)$), 1.85 (1H, s, $(CH_3)CC(CH_3)C(O)$), 1.79 (3H, s, CH_3), 1.62 (3H, s, CH_3), 1.30 (3H, t, *J* = 7.1 Hz, OCH_2CH_3). **^{13}C NMR** (75 MHz, $CDCl_3$) δ 170.0 ($C(CH_3)C(O)O$), 169.8 ($(CH_3)CC(CH_3)C(O)O$), 146.1 ($(CH_3)CC(CH_3)C(O)$), 145.6 ($(CH_3)CC(CH_3)C(O)$), 136.0 & 131.7 (2 x $(CH_3)CCH$), 124.7 &, 124.2 (2 x $(CH_3)CCH$), 60.0 (OCH_2CH_3), 36.7 ($CH_2(CH_3)CC(CH_3)C(O)$), 36.5 ($CH_2CH_2(CH_3)CC(CH_3)C(O)$), 31.9 & 26.9 (2 x CH_2), 20.3 (CH_2), 17.7 (CH_2), 15.9 (CH_2), 15.3 (CH_2), 14.3 (OCH_2CH_3). **LRMS** (EI^+): 278.23 (15% [M]), 232.17 (100%), 217.16 (30%), 173.10 (30%), 142.09 (30%), 109.09 (35%), 96.06 (70%), 81.07 (25%). **HRMS** (EI^+): calculated for [$C_{18}H_{30}O_2$]; 278.2246, found 278.2253.

Preparation of (2Z,6Z)-2,3,7,11-tetramethyldodeca-2,6,10-trien-1-ol (375):

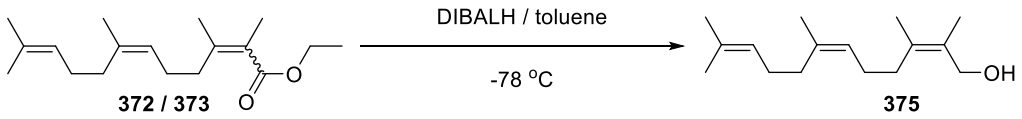

372 and **373** (596 mg, 2.14 mmol, 1 eq.) in anhydrous toluene (20 mL) was cooled to -78 °C and DIBALH (8.56 mL, 8.56 mmol, 4 eq., 1 M in hexane) added dropwise. The reaction was monitored by TLC (20% ethyl acetate in hexane) and was quenched with Rochelle salts (20 mL) at 0 °C. The resulting mixture was stirred for 16 hours at room temperature and extracted with DCM (3 x 10 mL). Combined organic extracts were washed with water (3 x 10 mL) and brine (3 x 10 mL), dried over sodium sulphate, filtered and concentrated under reduced pressure. Purification *via* flash chromatography (5% ethyl acetate in hexane) gave **375** as a colourless oil (207 mg, 41%).

^{1}H NMR (500 MHz, $CDCl_3$) δ 5.07 – 5.02 (2H, m, 2 x $(CH_3)CCH$), 4.01 (2H, d, *J* = 0.5 Hz, $(CC(CH_3)CH_2OH)$, , 2.09 – 2.04 (2H, m, allylic CH_2), 2.02 – 1.89 (6H, m, 3 x allylic CH_2), 1.68 (3H, s, CH_3), 1.62 (9H, s, 3 x CH_3), 1.54 (3H, s, CH_3). **^{13}C NMR** (75 MHz, $CDCl_3$) δ 136.2 ($CC(CH_3)CH_2O$), 132.9 ($(CH_3)CC(CH_3)CH_2O$), 131.7 & 128.5 (2 x $(CH_3)CCH$), 124.8 & 124.2 (2 x $(CH_3)CCH$), 63.6 (CH_2O), 34.3 & 31.9 & 26.9 & 26.7 (4 x allylic CH_2), 25.8 & 23.4 & 18.8 (3 x CH_3), 17.7 (CH_3), 16.9 (CH_3). **LRMS** (ES^+): 219.21 (100% [M – H_2O]), 215.05 (18%), 163.15 (15%), 149.13 (12%), 123.96 (15%). **HRMS** (ES^+): calculated for $[C_{16}H_{27}]^+$ [M – H_2O]; 219.2113, found 219.2120.

Table 16. 2D proton NMR correlations revealing spatial arrangement in 375

375: NOESY ^{1}H - ^{1}H interactions	
From / ppm	To / ppm
5.03	1.94
5.03	1.62
4.01	2.07
1.68	1.62

Preparation of (2Z,6Z)-1-bromo-2,3,7,11-tetramethyldodeca-2,6,10-triene (376):

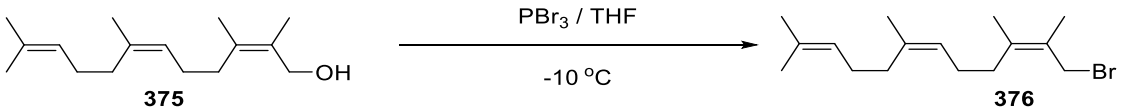

375 **376**

A solution of **375** (206 mg, 0.87 mmol, 2 eq.) in anhydrous THF (20 mL) was cooled to -10 °C and phosphorus tribromide (41 µL, 0.44, 1 eq.) added dropwise. Reaction was quenched with *sat*. sodium bicarbonate sol. (10 mL) at 0 °C when complete consumption of starting material was observed *via* TLC (20% ethyl acetate in hexane). Reaction product was extracted with diethyl ether (3 X 10 mL) and washed with water (3 x 10 mL) and brine (3 x 10 mL). Washed organic layers were dried over sodium sulphate, filtered and concentrated under reduced pressure to give **376** as a pale yellow oil (260 mg, 100%) which was taken forward without further purification.

^{1}H NMR (300 MHz, $CDCl_3$) δ 5.10 – 4.98 (2H, m, 2 x $(CH_3)CCH$), 4.00 (2H, s, $(CC(CH_3)CH_2Br$), 2.09 – 1.91 (8H, m, 4 x allylic CH_2), 1.62 (6H, s, 2 x CH_3), 1.54 (9H, s, 3 x CH_3).

Preparation of (2Z, 6Z)-2,3,7,11-tetramethyldodeca-2,6,10-trien-1-yl diphosphate (359):

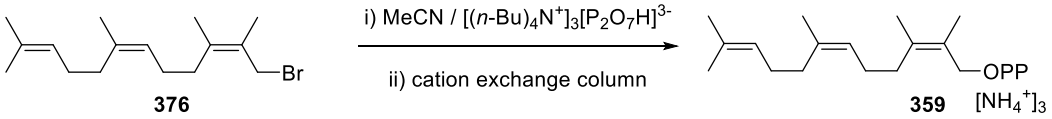

376 **359**

A mixture of crude bromide **376** (260 g, 0.87 mmol, 1 eq.) and tris tetrabutyl ammonium pyrophosphate (1.57 g, 1.74 mmol, 2 eq.) in anhydrous acetonitrile (10 mL) was stirred at room temperature for 16 hours. The reaction mixture was concentrated under reduced pressure and the resultant residue dissolved in buffer solution (25 mM NH_4HCO_3, 2% iPrOH) (15 mL) and the tris tetrabutylammonium salt counter ions were exchanged for ammonium by ion exchange column containing Amberlyst 131 (wet H^+ form) mesh cation exchange resin pre-equilibrated with ion-exchange buffer (25 mM NH_4HCO_3, 2% isopropanol). The appropriate fractions were collected and lyophilized to yield diphosphate **359** as a white powder. The powder was dissolved in buffer solution (25 mM NH_4HCO_3, 2% iPrOH) (10 mL) and purified using HPLC (Solvent A: acetonitrile, solvent B: 2% iPrOH). The appropriate fractions were collected and lyophilized to give diphosphate **359** as a white powder (7 mg, 2%).

^{1}H NMR (500 MHz, D_2O) δ 5.17 – 5.13 (2H, m, 2 x $(CH_3)CCH$), 4.38 (2H, d, *J* = 4.8 Hz, $(CC(CH_3)CH_2O$), 2.09 – 2.04 (2H, m, allylic CH_2), 2.02 – 1.89 (6H, m, 3 x allylic CH_2), 1.65 (3H, s, CH_3), 1.64 (3H, s, CH_3),

1.61 (6H, s, 2 x CH_3), 1.56 (3H, s, CH_3). **^{31}P NMR** (202 MHz, D_2O) δ -9.41 (d, *J* = 13.8 Hz), -10.62 (d, *J* = 17.2 Hz). **HRMS** (ES^-): calculated for [$C_{16}H_{29}O_7P_2$][M]; 395.1389, found 395.1385.

8.2.10 Synthesis of (2*Z*,6*Z*)-6-methylfarnesyl diphosphate (360)

Preparation of ethyl (Z)-2,3,7-trimethylocta-2,6-dienoate (383):

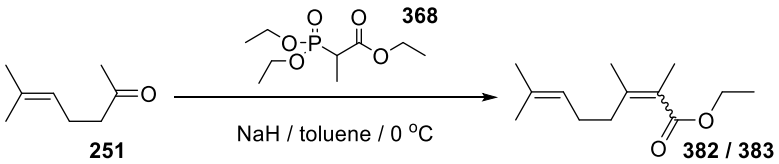

368 (24.1 g, 101.1 mmol, 1.5 eq.) was added to a stirred solution of sodium hydride (2.43 g, 101.1 mmol, 1.5 eq.) in anhydrous toluene (100 mL) at 0 °C. The reaction was stirred for 1 hour at room temperature, cooled to 0 °C and **251** (8.55 g, 64.1 mmol, 1 eq.) was added. The reaction was stirred at room temperature for 16 hours and quenched with water (30 mL). Organic products were extracted with diethyl ether (3 x 20 mL), washed with water (30 mL), brine (30 mL), dried over sodium sulphate, filtered and concentrated under *vaccuo.* Purification *via* flash chromatography (10% ethyl acetate in hexane) gave a mixture of **382** and **383** as a clear oil (10.4 g, 73%). Flash chromatography (5% ethyl acetate in hexanes) partially separated esters **382** and **383** for analysis.

^{1}H NMR (300 MHz, $CDCl_3$) δ 5.19 – 5.07 (1H, m, $(CH_3)CCH$), 4.19 (2H , q, *J* = 7.1 Hz, OCH_2CH_3), 2.42 – 2.30 (2H, m, $CH_2(CH_3)CC(CH_3)C(O)$), 2.19 – 2.14 (2H, m, allylic CH_2), 1.87 (3H, s, CH_3), 1.85 (3H, s, CH_3), 1.80 (3H, s, CH_3), 1.62 (3H, s, CH_3), 1.31 (3H, t, *J* = 7.1 Hz, OCH_2CH_3). **^{13}C NMR** (75 MHz, $CDCl_3$) δ 169.9 ($(CH_3)CC(CH_3)C(O)$), 146.1 ($(CH_3)CC(CH_3)C(O)$), 145.6 ($(CH_3)CC(CH_3)C(O)$), 131.8 ($(CH_3)CCH$), 124.0 ($(CH_3)CCH$), 60.0 (OCH_2CH_3), 36.5 ($CH_2(CH_3)CC(CH_3)C(O)$), 29.7 ($CH_2CH_2(CH_3)CC(CH_3)C(O)$), 20.9 ($CH_3$), 17.6 ($CH_3$), 15.9 ($CH_3$), 15.3 ($CH_3$), 14.3 ($OCH_2CH_3$). **LRMS** ($ES^+$): 211.17 (97% [M]), 209.15 (100%), 195.10 (55%), 181.12 (72%), 165.12 (50%), 153.12 (50%), 137.12 (48%), 125.96 (55%), 113.06 (25%) **HRMS** (ES^+): calculated for [$C_{13}H_{23}O_2$] [M]; 211.1698, found 211.1698.

Preparation of (Z)-2,3,7-trimethylocta-2,6-dien-1-ol (385):

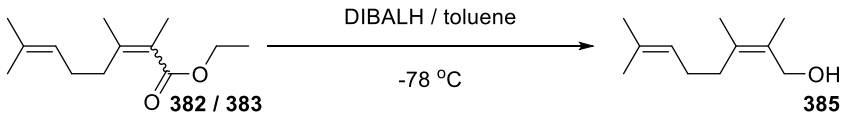

DIBALH (143 mL, 142.8 mmol, 3 eq., 1 M in hexane) was added to a mixture of **382** and **383** (10 g, 47.6, 3 eq.) in anhydrous toluene (50 mL) at -78 °C. Reaction was quenched with Rochelle salt (30 mL) at 0 °C when complete consumption of starting material was observed *via* TLC (20% ethyl acetate in hexane). The suspension was stirred for 16 hours at room temperature and organic products extracted with DCM (3 x 20 mL). Combined organic extracts were washed with water (3 x 20mL), brine (3 x 20 mL), dried over sodium sulphate, filtered and concentrated under *vaccuo*. methylated alcohols **384** and **385** was purified by flash chromatography (5% ethyl acetate in hexane) to give **385** as a clear oil (2.06 g, 26%).

^{1}H NMR (300 MHz, $CDCl_3$) δ 5.04 (1H, t, *J* = 7.1 Hz, $(CH_3)CC\mathit{H}$), 4.00 (2H , d, *J* = 0.6 Hz, $CC(CH_3)$ $C\mathit{H}_2OH$), 2.11 – 1.92 (4H, m, 2 x allylic $C\mathit{H}_2$), 1.68 (3H, d, *J* = 0.6 Hz, $CC(C\mathit{H}_3)$ CH_2OH), 1.62 (6H, s, 2 x $C\mathit{H}_3$), 1.52 (6H, s, 2 x $C\mathit{H}_3$). **^{13}C NMR** (75 MHz, $CDCl_3$) δ 132.9 ($(CH_3)\mathit{C}C$), 132.5 ($(CH_3)\mathit{C}C$), 128.5 ($(CH_3)C\mathit{C}(CH_3)$ CH_2OH), 124.1 ($(CH_3)C\mathit{C}H$), 63.5 ($C(CH_3)$ $\mathit{C}H_2OH$), 34.1 & 27.1 (2 x allylic $\mathit{C}H_2$), 25.7 & 18.8 (2 x $(\mathit{C}H_3)CCH$), 17.6 ($\mathit{C}H_3$), 16.8 ($C(\mathit{C}H_3)$ CH_2OH). **LRMS** (EI^+): 150.14 (65% [M – H_2O]), 135.12 (70%), 133.10 (80%), 107.08 (100%), 91.05 (55%), 79.06 (20%). **HRMS** (EI^+): calculated for $[C_{11}H_{18}]^+$ [M – H_2O]; 150.1409, found 150.1403.

Table 17. 2D proton NMR correlations revealing spatial arrangement in 385

385: NOESY ^{1}H - ^{1}H interactions	
From / ppm	To / ppm
5.04	2.02
5.04	1.5
4.00	2.02
1.68	1.52

Preparation of (Z)-1-bromo-2,3,7-trimethylocta-2,6-diene (386):

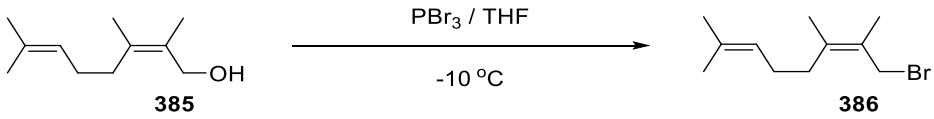

385 **386**

Phosphorus tribromide (0.57 mL, 6.03 mmol, 1 eq.) was added dropwise to a stirred solution of **385** (2.03 g, 12.06 mmol, 2 eq.) in anhydrous tetrahydrofuran (20 mL) at -10 °C. The solution was stirred for 15 minutes and concentrated under vaccuo. The residue was dissolved in diethyl ether (20 mL) and washed with sodium hydrogen carbonate (3 x 10 mL), water (3 x 10 mL) and brine (10 mL), dried over sodium sulfate, filtered and concentrated under reduced pressure to yield bromide as a pale yellow oil (2.78 g, 100%) which was used without further purification.

^{1}H NMR (300 MHz, $CDCl_3$) δ 5.22 – 5.10 (1H, m, $(CH_3)CC\mathit{H}$), 4.09 (2H, s, $CC(CH_3)$ $C\mathit{H}_2Br$), 2.21 – 2.02 (4H, m, 2 x allylic $C\mathit{H}_2$), 1.79 (3H, s, $C\mathit{H}_3$), 1.78 (3H, s, $C\mathit{H}_3$), 1.72 (3H, s, $C\mathit{H}_3$), 1.71 (3H, s, $C\mathit{H}_3$), 1.63 (3H, s, $C\mathit{H}_3$).

Preparation of ethyl (Z)-2-acetyl-4,5,9-trimethyldeca-4,8-dienoate (387):

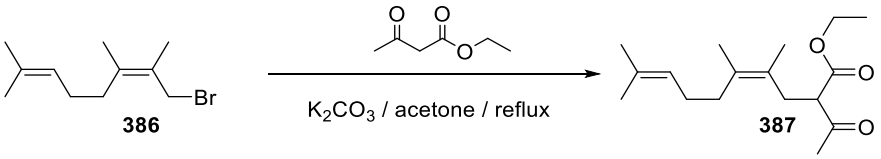

386 **387**

Crude bromide **386** (2.78 g, 12.03 mmol, 1 eq.) and ethyl acetoacetate (3.13 g, 24.05 mmol, 2 eq.) were dissolved in anhydrous acetone (30 mL). Potassium carbonate (3.32 g, 24.05 mmol, 2 eq.) was added the suspension was refluxed for 4 hours at 60 °C. The reaction mixture was concentrated under reduced pressure and reaction products dissolved in diethyl ether (30 mL). Ethereal layer was washed with water (3 x 20 mL) and brine (2 x 20 mL), dried over sodium sulphate and concentrated under *vaccuo*. Reaction product was purified by flash chromatography on silica gel (20% ethyl acetate in hexane) to give **387** as a clear oil (1.52 g, 45%).

^{1}H NMR (300 MHz, $CDCl_3$) δ 5.15 – 5.08 (1H, m, $(CH_3)CC\mathit{H}$), 4.17 (1H, q, *J*= 7.1 Hz, $CH_3C\mathit{H}_2O$), 4.16 (1H, q, *J*= 7.1 Hz, $CH_3C\mathit{H}_2O$), 3.62 – 3.55 (1H, m, $COC\mathit{H}CO$)., 2.64 (1H, qd, *J* = 14.1 Hz, 0.7 Hz, $CC(CH_3)C\mathit{H}_2CH$), 2.61 (1H, qd, *J* = 14.1 Hz, 0.7 Hz, $CC(CH_3)C\mathit{H}_2CH$), 2.22 (3H, s, $COC\mathit{H}_3$), 2.13 – 1.95 (4H, m, 2 x allylic $C\mathit{H}_2$), 1.69 (s, 3H), 1.63 (3H, d, *J* = 0.7 Hz, $C\mathit{H}_3$), 1.61 (3H, s, $C\mathit{H}_3$), 1.27 (1H, t, *J* = 7.1 Hz, $C\mathit{H}_3CH_2O$). 1.26 (1H, t, *J* = 7.1 Hz, $C\mathit{H}_3CH_2O$). 1.26 (1H, t, *J* = 7.1 Hz, $C\mathit{H}_3CH_2O$). **^{13}C NMR** (75 MHz,

$CDCl_3$) δ 203.4 (CH_3C(O)CH), 170.0 (CH_3CH_2OC(O)), 131.8 ((CH_3)CCH), 131.7 ((CH_3)CC(CH_3)), 124.2 (CH_3CCH), 123.8 ((CH_3)CC(CH_3)), 61.3 (CH_3CH_2O), 58.6 (C(O)CHC(O)), 34.4 (allylic CH_2), 32.5 (CC(CH_3)CH_2), 29.2 (CH_3C(O)), 27.0 (allylic CH_2), 25.7 (CH_3), 18.6 (CH_3), 18.1 (CH_3), 17.6 (CH_3), 14.1 (OCH_2CH_3). **LRMS** (ES^-): 279.20 (50% [M]), 259.04 (15%), 213.03 (100%), 197.91 (5%), 185.00 (5%), 162.84 (7%), 141.01 (15%), 120.90 (17%), 118.9 (30%). **HRMS** (ES^-): calculated for [$C_{17}H_{27}O_3$][M]; 279.1960, found 279.1961.

Preparation of (Z)-5,6,10-trimethylundeca-5,9-dien-2-one (388):

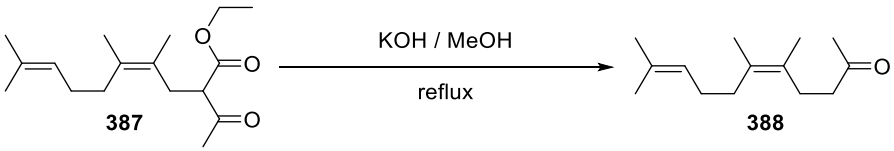

A mixture of potassium hydroxide (830 mg, 14.77 mmol, 3 eq.) and **387** (1.38 g, 4.92 mmol, 1 eq.) in methanol (30 mL) was refluxed at 70 °C for 3 hours. The reaction mixture was cooled to room temperature and acidified with 1M HCl. Organic products were extracted with diethyl ether (3 x 20 mL) and washed with water (3 x 20 mL) and brine (3 x 10 mL). Washed organic layers were dried over sodium sulphate, filtered and concentrated under reduced pressure. Purification *via* flash chromatography gave **388** as a pale yellow oil (1.01 g, 99%).

^{1}H NMR (300 MHz, $CDCl_3$) δ 5.15 – 5.06 (1H, m, (CH_3)CC*H*), 2.51 – 2.42 (2H, m, CH_2C(O)), 2.34 – 2.23 (2H, m, CH_2CH$_2$C(O)), 2.15 (3H, s, CH_2C(O)CH_3), 2.07 – 1.95 (4H, m, 2 x allylic CH_2), 1.69 (3H, s, CH_3), 1.64 (3H, s, CH_3), 1.62 (3H, s, CH_3), 1.61 (3H, s, CH_3). **^{13}C NMR** (75 MHz, $CDCl_3$) δ 209.3 (CH_3C(O)), 131.6 ((CH_3)CCH), 129.3 ((CH_3)CC(CH_3)), 126.6 ((CH_3)CC(CH_3)), 124.4 ((CH_3)CCH), 42.9 (CH_2CH_2C(O)), 34.3 (CH_2CH_2C(O)), 29.9 (CH_3C(O)), 28.3 & 27.1 (2 x allylic CH_2), 25.8 & 18.5 & 18.2 & 17.6 (4 x CH_3). **LRMS** (ES^+): 209.19 (50% [M + H]), 191.18 (100%), 151.14 (5%), 135.11 (5%). **HRMS** (ES^+): calculated for [$C_{14}H_{25}O$][M + H]; 209.1905, found 209.1907.

Preparation of ethyl (2Z,6Z)-3,6,7,11-tetramethyldodeca-2,6,10-trienoate (390):

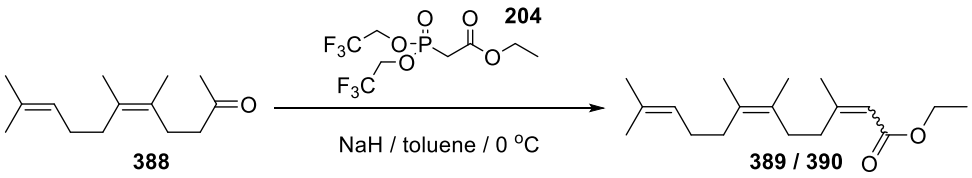

A stirred suspension of sodium hydride (230 mg, 5.7 mmol, 1.6 eq.) in anhydrous toluene (30 mL) was cooled to 0 °C and **204** (1.75 g, 5.34 mmol, 1.5 eq.) was added dropwise. The reaction mixture was stirred at room temperature for 1 hour and cooled to 0 °C. Methyl neryl acetone(**388**) (743 mg, 3.56 mmol, 1 eq.) was added dropwise and the reaction mixture stirred at room temperature for 16 hours. The reaction was quenched with water (20 mL) and products extracted with diethyl ether (3 x 10 mL). Organic extracts were washed with water (3 x 20 mL) and brine (20 mL), dried over sodium sulphate, filtered and concentrated under reduced pressure. Purification *via* flash chromatography (10% ethyl acetate in hexane) gave a mixture of **389** and **390** as a clear oil (772 mg, 42%). Flash chromatography (5% ethyl acetate in hexanes) partially separated esters **389** and **390** for analysis.

^{1}H NMR (300 MHz, $CDCl_3$) δ 5.57 (1H, s, CC*H*C(O)OEt), 5.10 – 5.02 (1H, m, $(CH_3)CCH$), 4.06 (2H, q, *J* = 7.1 Hz, OCH_2CH_3), 2.57 (2H, dd, *J* = 9.5, 6.9 Hz, $CH_2(CH_3)CCHC(O)$), 2.10 (2H, dd, *J* = 9.3, 7.0 Hz, $CH_2CH_2(CH_3)CCHC(O)$), 1.99 – 1.91 (4H, m, 2 x allylic CH_2), 1.83 (3H, d, *J* = 1.3 Hz, $CH_2(CH_3)CCHC(O)$), 1.63 (3H, s, CH_3), 1.61 (3H, s, CH_3), 1.57 (3H, s, CH_3), 1.53 (3H, s, CH_3), 1.20 (3H, t, *J* = 7.1 Hz, OCH_2CH_3). **^{13}C NMR** (75 MHz, $CDCl_3$) δ 166.3 (CH*C*(O)O), 160.4 ($(CH_3)CCHC(O)O$), 131.6 & 128.8 & 127.8 ($(CH_3)CC$), 124.6 ($(CH_3)CCH$), 115.9 (C*C*HC(O)O), 59.4 (OCH_2CH_3), 34.3 (allylic CH_2), 32.9 ($CH_2(CH_3)CCHC(O)$), 32.7 ($CH_2CH_2(CH_3)CCHC(O)$), 27.2 (allylic CH_2), 25.8 & 25.5 & 18.5 & 18.3 & 17.6 (5 x CH_3), 14.4 (OCH_2CH_3). **LRMS** (ES^+): 279.23 (100% [M + H]), 265.06 (45%), 243.08 (55%), 233.19 (6%), 205.19 (7%), 200.01 (3%), 151.15 (3%). **HRMS** (ES^+): calculated for $[C_{18}H_{31}O_2]$[M + H]; 279.2324, found 279.2323.

Preparation of (2Z,6Z)-3,6,7,11-tetramethyldodeca-2,6,10-trien-1-ol (392):

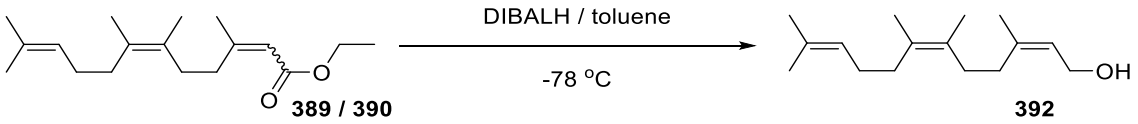

389 / 390 392

Esters **389** and **390** (753 mg, 2.7 mmol, 1 eq.) in anhydrous toluene (20 mL) was cooled to -78 °C. DIBALH (13.5 mL, 13.5 mmol, 5 eq., 1 M in hexane) was added dropwise and the reaction stirred until complete consumption of starting material was observed *via* TLC (20% ethyl acetate in hexanes). The reaction was warmed to 0 °C, quenched with Rochelle salts (5 mL) and stirred for 16 hours at room temperature. Organic products were extracted with DCM (3 x 10 mL) and washed with water (3 x 10 mL) and brine (3 x 10 mL). Organic layers were dried over sodium sulphate, filtered and concentrated under *vaccuo*. Purification *via* flash chromatography (5% ethyl acetate in hexanes) gave **192** as a clear oil (189 mg, 18%).

^{1}H NMR (300 MHz, $CDCl_3$) δ 5.45 (1H, t, *J* = 7.2 Hz, $(CH_3)CC\mathit{H}CH_2OH$), 5.17 – 5.12 (1H, m, $(CH_3)CC\mathit{H}$), 4.10 (2H, d, *J* = 7.1 Hz, $(CCHC\mathit{H}_2OH)$, 2.12 (4H, s, 2 x allylic $C\mathit{H}_2$), 2.03 (4H, d, *J* = 2.6 Hz, 2 x allylic $C\mathit{H}_2$), 1.79 (3H, s, $C\mathit{H}_3$), 1.70 (3H, s, $C\mathit{H}_3$), 1.67 (3H, s, $C\mathit{H}_3$), 1.65 (3H, s, $C\mathit{H}_3$), 1.62 (3H, s, $C\mathit{H}_3$). **^{13}C NMR** (75 MHz, $CDCl_3$) δ 140.5 ($(CH_3)\mathit{C}C(CH_3)CH_2O$), 131.6 & 129.1 & 128.0 (3 x$(CH_3)\mathit{C}C$), 124.4 & 124.2 (2 x $(CH_3)C\mathit{C}H$), 59.0 ($CH\mathit{C}H_2O$), 34.4 & 33.1 & 31.1 & 27.2 (4 x allylic $\mathit{C}H_2$), 25.8 & 23.7 & 18.7 (3 x $\mathit{C}H_3$), 18.4 ($\mathit{C}H_3$), 17.7 ($\mathit{C}H_3$). **LRMS** (EI^+): 218.20 (70% [M – H_2O]), 203.18 (50%), 175.15 (75%), 162.14 (12%), 149.13 (35%), 135.12 (60%), 121.10 (35%), 107.09 (100%), 93.07 (37%), 79.05 (7%), 69.07 (9%). **HRMS** (EI^+): calculated for [$C_{16}H_{26}$][M – H_2O]; 218.2035, found 218.2035.

Table 18. 2D proton NMR correlations revealing spatial arrangement in 392

392: NOESY ^{1}H - ^{1}H interactions	
From / ppm	To / ppm
5.45	4.10
5.45	1.79
5.15	2.03
5.15	1.67
4.10	2.12
1.79	1.70

Preparation of (2Z,6Z)-1-bromo-3,6,7,11-tetramethyldodeca-2,6,10-triene (393):

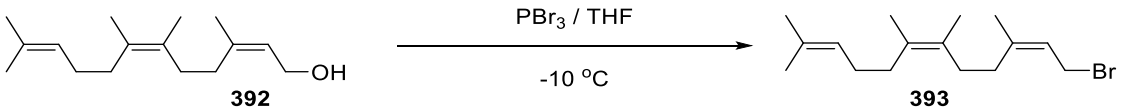

392 **393**

Phosphorus tribromide (34 µL, 0.36, 1 eq.) was added to a stirred solution of **392** (172 mg, 0.73 mmol, 2 eq.) in anhydrous tetrahydrofuran (10 mL) at -10 °C. The reaction proceeded for 15 minutes at which point complete consumption of starting material was observed *via* TLC (20% ethyl acetate in hexane). Volatile solvents were removed under reduced pressure and the residue dissolved in diethyl ether (3 x 10 mL). Organic extracts were washed with sat. sodium bicarbonate sol. (3 x 10 mL), water (3 x 10 mL) and brine (2 x 10 mL). Ethereal extracts were dried over sodium sulphate, filtered and concentrated under *vaccuo* to give **393** as a crude yellow oil (218 mg, 100%) which was used without further purification.

^{1}H NMR (300 MHz, $CDCl_3$) δ 5.33 (1H, t, *J* = 7.6 Hz, $(CH_3)CC\mathit{H}CH_2Br$), 5.21 – 5.05 (1H, m, $(CH_3)CC\mathit{H}$), 4.02 (2H, d, *J* = 7.6 Hz, $(CCHC\mathit{H}_2Cl)$, 2.23 – 1.99 (8H, m, 4 x allylic $C\mathit{H}_2$), 1.71 (3H, s, $C\mathit{H}_3$), 1.69 (3H, s, $C\mathit{H}_3$), 1.66 (3H, s, $C\mathit{H}_3$), 1.64 (6H, s, 2 x $C\mathit{H}_3$).

Preparation of (2Z, 6Z)-6 methyl-3,7,11-trimethyldodeca-2,6,10-trien-1-yl diphosphate (360):

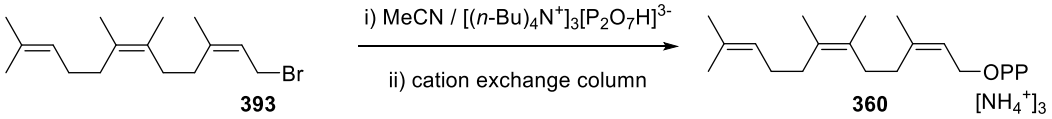

393 **360**

A mixture of **393** (218 mg, 0.73 mmol, 1 eq.) and tris tetrabutyl ammonium pyrophosphate (1.31 g, 1.46 mmol, 2 eq.) in anhydrous acetonitrile (10 mL) was stirred at room temperature for 16 hours. The reaction mixture was concentrated under reduced pressure and the resultant residue dissolved in buffer solution (25 mM NH_4HCO_3, 2% iPrOH) (10 mL) and the tris tetrabutylammonium salt counter ions were exchanged for ammonium by ion exchange column containing Amberlyst 131 (wet H^+ form) mesh cation exchange resin pre-equilibrated with ion-exchange buffer (25 mM NH_4HCO_3, 2% isopropanol). The appropriate fractions were collected and lyophilized to yield diphosphate **360** as a white powder. The powder was dissolved in buffer solution (25 mM NH_4HCO_3, 2% iPrOH) (7 mL) and purified using HPLC (Solvent A: acetonitrile, solvent B: 2% iPrOH). The appropriate fractions were collected and lyophilized to give **360** as a white powder (6 mg, 2%).

^{1}H NMR (500 MHz, D_2O) δ 5.47 – 5.39 (1H, m, $(CH_3)CCHCH_2O$), 5.16 – 5.08 (1H, m, $(CH_3)CCH$), 4.42 – 4.36 (2H, m, $CCHCH_2O$), 2.17 – 2.07 (4H, m, 2 x allylic CH_2), 2.02 (4H, m, 2 x allylic CH_2), 1.67 (3H, s, CH_3), 1.61 (3H, s, CH_3), 1.58 (6H, s, 2 x CH_3), 1.55 (3H, s, CH_3). **^{31}P NMR** (202 MHz, D_2O) δ -9.51 (d, *J* = 11.0 Hz), -10.69 (d, *J* = 18.3 Hz). **HRMS** (ES^-): calculated for $[C_{16}H_{29}O_7P_2][M]$; 395.1389, found 395.1390.

8.2.11 Synthesis of (2*Z*,6*Z*)-[6-^{2}H]-farnesyl diphosphate (232)

Preparation of ethyl 2-deutero-3,7-dimethylocta-2,6-dienoate (274):

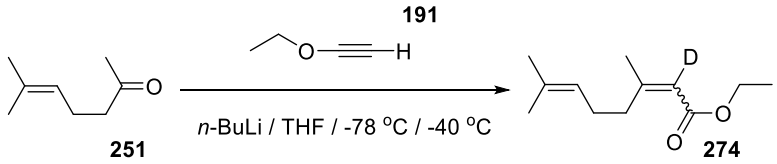

251 (1.8 g, 14.3 mmol, 1 eq.) in anhydrous THF (30 mL) was cooled to -78 °C and *n*-butyl lithium (14.3 mL, 2.5 M, 35.7 mmol, 2.5 eq.) added dropwise. The reaction mixture was warmed to -40 °C and ethoxy acetylene (**191**)(2.5 g, 35.7 mmol, 2.5 eq.) added dropwise. The reaction mixture was slowly warmed to room temperature and stirred for 16 hours. The reaction was mixture was cooled to 0 °C and quenched with D_2SO_4 / D_2O (10 mL). Reaction products were extracted with diethyl ether (3 x 10 mL), washed with D_2O (3 x 10 mL), brine (3 x 10 mL), dried over sodium sulphate and filtered. Organic products were concentrated under reduced pressure and purified by silica column (10% ethyl acetate in hexane) gave a mixture of **273** and **274** as a clear oil (1.25 g, 44%).

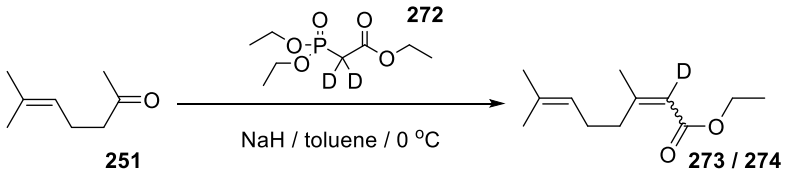

Sodium hydride (1.07 g, 26.8 mmol, 1.2 eq.) in anhydrous toluene (50 mL) was cooled to 0 °C and **272** (7.74 g, 24.6 mmol, 1.1 eq.) was added dropwise. The reaction was stirred for 1 hour at room temperature, cooled to 0 °C and **251** (2.8 g, 22.3 mmol, 1 eq.) was added. The reaction was stirred at room temperature for 16 hours and quenched with D_2O (20 mL). Organic products were extracted with diethyl ether (3 x 20 mL), washed with D_2O (3 x 20 mL), brine (20 mL), dried over sodium sulphate, filtered and concentrated under *vaccuo.* Purification *via* flash chromatography (10% ethyl

acetate in hexane) gave a mixture of **273** and **274** as a clear oil (2.98 g, 68%, 30% ^{2}H incorporation). Flash chromatography (5% ethyl acetate in hexanes) partially separated esters **27** and **274** for analysis.

^{1}H NMR (300 MHz, $CDCl_3$) δ 5.53 (0.7H, s, $(CH_3)CCH/D$), 5.08 – 4.92 (1H, m, $(CH_3)CCH$), 4.01 (2H , q, *J* = 7.1 Hz, OCH_2CH_3), 2.56 – 2.45 (2H, m, $CH_2(CH_3)CC(CH_3)C(O)$), 2.09 – 1.97 (2H, m, allylic CH_2), 1.76 (3H, s, CH_3), 1.56 (3H, s, CH_3), 1.50 (3H, s, CH_3), 1.15 (3H, t, *J* = 7.1 Hz, OCH_2CH_3).**^{2}H NMR** (77 MHz) δ 5.67 ($1^{2}H$, s, $(CH_3)CCD$).**^{13}C NMR** (75 MHz, $CDCl_3$) δ 169.7 ($(CH_3)CC(D)C(O)$), 146.0 ($(CH_3)CC(D)C(O)$), 145.6 ($(CH_3)CC(D)C(O)$), 131.8 ($(CH_3)CCH$), 124.0 ($(CH_3)CCH$), 60.0 (OCH_2CH_3), 36.5 ($CH_2(CH_3)CC(D)C(O)$), 29.7 ($CH_2CH_2(CH_3)CC(D)C(O)$), 21.0 (CH_3), 17.6 (CH_3), 15.9 (CH_3), 15.3 (CH_3), 14.3 (OCH_2CH_3).

Preparation of (Z)-2-deutero-3,7-dimethylocta-2,6-dien-1-ol (276):

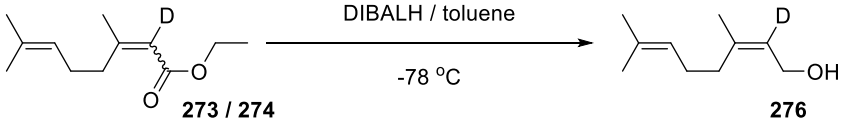

Esters **273** and **274** (1.25 g, 5.81 mmol, 1 eq.) in anhydrous toluene (20 mL) was cooled to -78 °C and DIBALH (29 mL, 1 M, 29.01 mmol, 5 eq.) was added dropwise. Reaction mixture was stirred at room temperature for 16 hours and cooled to 0 °C prior to being quenched by the addition of sat. Rochelle salts (30 mL). Reaction products were extracted with DCM (3 x 20 mL) and combined organic extracts washed with water (3 x 20 mL) and brine (3 x 20 mL). Washed organic extracts were dried over anhydrous sodium sulphate, filtered and concentrated under *vaccuo*. Purification *via* flash chromatography (5% ethyl acetate in hexanes) gave **276** as colourless oil (767 mg, 43%).

^{1}H NMR (500 MHz, $CDCl_3$) δ 5.08 – 4.99 (1.7H, m, $(CH_3)CCH$ & $(CH_3)CCD$), 4.02 (2H, s, $(CH_3)CH/DCH_2OH$), 2.06 – 1.97 (4H, m, 2 x allylic CH_2), 1.68 (3H, s, CH_3), 1.62 (3H, s, CH_3), 1.54 (3H, s, CH_3).**^{13}C NMR** (126 MHz, $CDCl_3$) δ 140.0 ($(CH_3)CC$), 132.5 ($(CH_3)CC$), 124.3 – 123.9 ($(CH_3)CCDCH_2OH$), 123.8 ($(CH_3)CC$), 58.9 ($C(CH_3)$ CH_2OH), 31.9 & 26.5 (2 x allylic CH_2), 25.7 & 23.4 (2 x $(CH_3)CCH$), 17.7 (CH_3).**^{2}H NMR** (61 MHz) δ 5.14 ($1^{2}H$, s, $(CH_3)CCD$).

Table 19. 2D proton NMR correlations revealing spatial arrangement in 276

276: NOESY ^{1}H - ^{1}H interactions	
From / ppm	To / ppm
5.04	4.02
5.04	2.02
5.04	1.68
4.02	2.02

Preparation of (Z)-1-bromo-2-deutero-3,7-dimethylocta-2,6-diene (278):

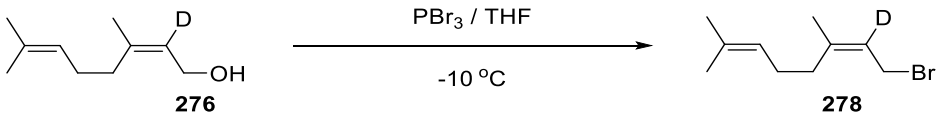

276 **278**

Phosphorus tribromide (0.6 mL, 0.65 mmol, 1 eq.) was added dropwise to a stirred solution of **276** (201 mg, 1.3 mmol, 2 eq.) in anhydrous THF (10 mL) at -10 °C. The reaction mixture was stirred at -10 °C until complete consumption of starting material was observed *via* TLC (20% ethyl acetate in hexanes), warmed to 0 °C and quenched with *sat.* sodium bicarbonate solution (5 mL). Reaction product was extracted with diethyl ether (3 x 5 mL), washed with water (3 x5 mL), brine (3 x5 mL) and dried over sodium sulphate. Dried organic extracts were filtered and concentrated under reduced pressure to give **278** a pale yellow oil (282 mg, 100%) which was taken forward without further purification.

^{1}H NMR (300 MHz, $CDCl_3$) δ 5.08 – 5.01 (1H, m, $(CH_3)CC\mathit{H}$), 3.94 (2H, s, CC(D) $C\mathit{H}_2Br$), 2.11 – 2.00 (4H, m, 2 x allylic $C\mathit{H}_2$), 1.71 (3H, s, $C\mathit{H}_3$), 1.62 (3H, s, $C\mathit{H}_3$), 1.55 (3H, s, $C\mathit{H}_3$). **^{2}H NMR** (77 MHz) δ 5.51 (1^{2}H, s, $(CH_3)CC\mathit{D}$).

Preparation of ethyl (Z)-2-acetyl-4-deutero-5,9-dimethyldeca-4,8-dienoate (279):

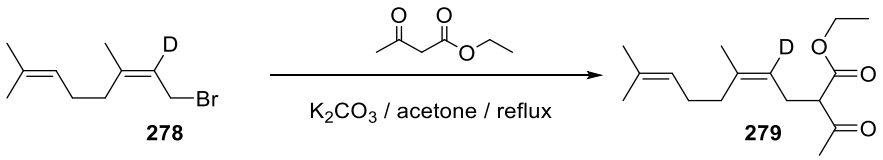

278 **279**

Crude bromide **278** (282 mg, 1.3 mmol, 1 eq.), potassium carbonate (360 mg, 2.6 mmol, 2 eq.) and ethyl acetoacetate (337 mg, 2.6 mmol, 2 eq.) in anhydrous acetone (20 mL) was heated under reflux

at 60 °C for 3 hours. The reaction was quenched with water (10 mL) and reaction products extracted with diethyl ether (3 x 10 mL). Combined organic extracts were washed with water (3 x 10 mL), brine (3 x 10 mL), dried over anhydrous sodium sulphate and filtered. Filtered organic extracts were concentrated under reduced pressure and purified *via* flash chromatography (20% ethyl acetate in hexanes) to give **279** as a clear yellow oil (282 mg, 71%).

^{1}H NMR (300 MHz, $CDCl_3$) δ 5.16 – 4.98 (1.7H, m, $(CH_3)CCH/D$), 4.19 (2H, q, *J* = 7.1 Hz, CH_3CH_2O), 3.42 (1H, t, *J* = 7.6 Hz, COC*H*CO), 2.55 (2H, t, *J* = 6.9 Hz, CCH/DCH_2CH), 2.23 (3H, s, $COCH_3$), 2.11 – 2.00 (4H, m, 2 x allylic CH_2), 1.69 (3H, s, CH_3), 1.68 (3H, s, CH_3), 1.61 (3H, s, CH_3), 1.27 (3H, t, *J* = 7.1 Hz,CH_3CH_2O). **^{13}C NMR** (75 MHz, $CDCl_3$) δ 203.18 ($CH_3CH_2OC(O)$), 169.61 (CH_3COCH), 138.37 & 131.89 ($(CH_3)CCH$ & $(CH_3)CCD$), 123.99 (CH_3CCH), 120.39 – 119.49 (CH_3CCD). 61.33 (CH_3CH_2O), 60.02 (C(O)CHC(O)), 31.88 (allylic CH_2), 29.12 ($CH_3C(O)$), 26.54 ($CCDCH_2CH$), 26.41 (allylic CH_2), 25.73 & 23.37 (2 x CH_3), 17.67 (CH_3), 14.12 (OCH_2CH_3). **^{2}H NMR** (77 MHz) δ 5.02 (1^2H, s, $(CH_3)CCD$).

Preparation of (Z)-5-deutero-6,10-dimethylundeca-5,9-dien-2-one (280):

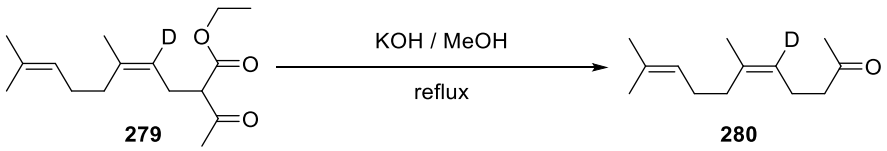

279 **280**

Keto ester **279** (245 mg, 0.92 mmol, 1 eq.) was dissolved in methanol (20 mL) and potassium hydroxide (154 mg, 2.75 mmol, 3 eq.) added. The reaction mixture was heated under reflux at 80 °C for 3 hours and quenched with water (10 mL). Quenched reaction mixture was acidified by the addition of 1 M hydrochloric acid (5 mL) and products extracted with diethyl ether (3 x 10 mL). Combined organic extracts were washed with water (3 x 10 mL), brine (3 x 10 mL), dried over anhydrous sodium sulphate and filtered. Organic extracts were concentrated under *vaccuo* and purified *via* flash chromatography (20% ethyl acetate in hexanes) to give **280** as a colourless oil (168 mg, 94%).

^{1}H NMR (300 MHz, $CDCl_3$) δ 5.15 – 5.03 (1.7H, m, $(CH_3)CCH$ & $(CH_3)CCH/D$), 2.46 (2H, t, *J* = 7.4 Hz, $CH_2C(O)$), 2.31 – 2.21 (2H, m, $CH_2CH_2C(O)$), 2.15 (3H, s, $CH_2C(O)CH_3$), 2.07 – 1.99 (4H, m, 2 x allylic CH_2), 1.69 (6H, s, 2 x CH_3), 1.62 (3H, s, CH_3). **^{13}C NMR** (75 MHz, $CDCl_3$) δ 209.1 ($CH_3C(O)$), 136.4 & 131.7 (2 x $(CH_3)CCH$), 124.2 ($(CH_3)CCH$), 122.5 – 120.5 (m, $(CH_3)CCH/D$), 44.0 ($CH_2CH_2C(O)$), 31.8 & 26.5 (2 x allylic CH_2), 30.0 ($CH_3C(O)$), 25.8 & 23.3 (2 x $(CH_3)CCH$), 22.2 (CH_2CH_2CO), 17.7 (CH_3). **^{2}H NMR** (61 MHz) δ 5.17 (1^2H, s, $(CH_3)CCD$).

Preparation of ethyl (2Z,6Z)-6-deutero-3,7,11-trimethyldodeca-2,6,10-trienoate (282):

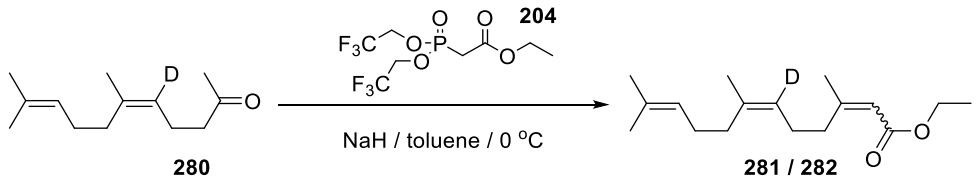

Sodium hydride (333 mg, 8.43 mmol, 2.2 eq.) in anhydrous toluene (20 mL) was cooled to 0 °C. **204** (2.52 g, 7.58 mmol, 2 eq.) was added dropwise to the stirred suspension and the reaction mixture stirred at room temperature for 1 hour. The reaction mixture was cooled to 0 °C and **280** (740 mg, 3.79 mmol, 1 eq.) added dropwise and stirred for 16 hours at room temperature. The reaction was quenched with water (10 mL) and organic products extracted with diethyl ether (3 x 10 mL) and combined organic extracts washed with water (3 x 10 mL) and brine (2 x 10 mL). Washed organic extracts were dried over anhydrous sodium sulphate, filtered and concentrated under reduced pressure. Purification *via* flash chromatography (10% ethyl acetate in hexane) gave a mixture of **281** and **282** as a clear oil (693 mg, 69%). Flash chromatography (5% ethyl acetate in hexanes) partially separated esters **281** and **282** for analysis.

^{1}H NMR (300 MHz, $CDCl_3$) δ 5.67 (1H, s, CC*H*C(O)OEt), 5.23 – 5.04 (1.7H, m, $(CH_3)CCH$ & $(CH_3)CCH/D$), 4.15 (2H, q, *J* = 7.1 Hz, OCH_2CH_3), 2.65 (2H, t, *J* = 7.8 Hz, $CH_2(CH_3)CCHC(O)$), 2.19 – 2.15 (2H, m, $CH_2CH_2(CH_3)CCHC(O)$), 2.09 – 2.04 (4H, m, 2 x allylic CH_2), 1.90 (3H, s, CH_3), 1.70 (3H, s, CH_3), 1.62 (3H, s, CH_3), 1.29 (3H, t, *J* = 7.1 Hz, OCH_2CH_3). **^{13}C NMR** (75 MHz, $CDCl_3$) δ 166.3 (CH*C*(O)O), 160.1 ($(CH_3)CCHC(O)O$), 136.2 & 131.5 (2 x $(CH_3)CCH$), 124.5 – 124.3 (m, $(CH_3)CCD$), 124.2 ($(CH_3)CCH$), 116.2 (C*C*HC(O)O), 59.5 (OCH_2CH_3), 33.7 ($CH_2(CH_3)CCHC(O)$), 31.9 & 26.6 (2 x CH_2), 26.5 ($CH_2CH_2(CH_3)CCHC(O)$), 25.8 & 25.4 & 23.4 & 17.7 (4 x CH_3), 14.4 (OCH_2CH_3). **^{2}H NMR** (77 MHz) δ 5.69 (1^2H, s, $(CH_3)CCD$).

Preparation of (2Z,6Z)-6-deutero-3,7,11-trimethyldodeca-2,6,10-trien-1-ol (284):

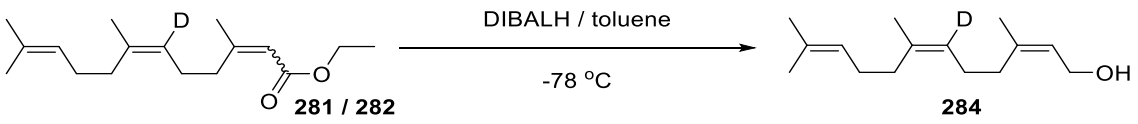

Esters **281** and **282** (884 mg, 3.33 mmol, 1 eq.) in anhydrous toluene (20 mL) was cooled to -78 °C and DIBALH (16.7 mL, 16.7 mmol, 5 eq., 1 M in hexane) added dropwise. The reaction mixture was stirred at -78 °C until complete consumption of starting material was observed *via* TLC (20% ethyl

acetate in hexanes), quenched with Rochelle salts (10 mL) and stirred for 16 hours at room temperature. Organic products were extracted with DCM (3 x 10 mL) and combined organic products washed with water (3 x 10 mL), brine (2 x 10 mL) and dried over anhydrous sodium sulphate. Dried organic extracts were filtered, concentrated under reduced pressure and purified *via* flash chromatography (5% ethyl acetate in hexanes) to give **284** as a colourless oil (172 mg, 23%).

^{1}H NMR (300 MHz, $CDCl_3$) δ 5.38 (1H, t, *J* = 7.1 Hz CC*H*CH_2O), 5.11 – 4.98 (1.7H, m, (CH_3)CC*H* & (CH_3)CC*H/D*), 4.02 (2H, t, *J* = 7.1 Hz, CHCH_2OH), 2.10 – 1.87 (8H, m, 4 x allylic CH_2), 1.68 (3H, s, CH_3), 1.62 (6H, s, 2 x CH_3), 1.54 (3H, s, CH_3). **^{13}C NMR** (75 MHz, $CDCl_3$) δ 139.9 ((CH_3)*C*CHCH_2O), 136.1 & 131.7 (2 x (CH_3)*C*CH), 124.8 – 124.4 ((CH_3)C*C*D), 124.5 (C*C*HCH_2O) 124.2 ((CH_3)C*C*H), 59.0 (CH*C*H_2O), 32.2 & 31.9 & 26.6 & 26.2 (4 x allylic *C*H_2), 25.7 (*C*H_3), 23.4 & 23.2 ((2 x (*C*H_3)CCH), 17.6 (*C*H_3). **^{2}H NMR** (61 MHz) δ 5.13 (1^{2}H, s, (CH_3)CC*D*).

Table 20. 2D proton NMR correlations revealing spatial arrangement in 284

284: NOESY ^{1}H - ^{1}H interactions	
From / ppm	To / ppm
5.38	4.02
5.38	1.68
5.05	2.04
5.05	1.68
5.05	1.62
4.02	2.04

Preparation of (2Z,6Z)-1-bromo-6-deutero-3,7,11-trimethyldodeca-2,6,10-triene (285):

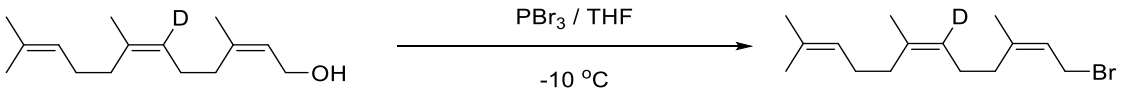

284 **285**

Alcohol **284** (172 mg, 0.77 mmol, 2 eq.) was dissolved in anhydrous tetrahydrofuran (10 mL) and cooled to -10 °C. Phosphorus tribromide (36 µL, 0.38 mmol, 1 eq.) was added dropwise and the reaction mixture stirred at -10 °C until complete consumption of starting material was observed *via* TLC (20% ethyl acetate in hexanes). The reaction was quenched with *sat.* sodium bicarbonate solution (5 mL) and organic products extracted with diethyl ether (3 x 10 mL). Combined organic extracts were washed with water (3 x 10 mL), brine (10 mL), dried over anhydrous sodium sulphate

and filtered. Filtered organic extracts were concentrated under reduced pressure to give **285** as a pale yellow oil (209 mg, 95%) which was used without further purification.

^{1}H NMR (300 MHz, $CDCl_3$) δ 5.36 (1H, t, *J* = 7.1 Hz CC*H*CH_2Br), 5.09 – 4.95 (1.7H, m, (CH_3)CC*H* & (CH_3)CC*H/D*), 3.87 (2H, t, *J* = 7.1 Hz, CHCH_2Br), 2.10 – 1.87 (8H, m, 4 x allylic CH_2), 1.68 (3H, s, CH_3), 1.62 (6H, s, 2 x CH_3), 1.54 (3H, s, CH_3).**^{2}H NMR** (61 MHz) δ 5.15 (1^2H, s, (CH_3)CC*D*).

8.2.12 Synthesis of (2*Z*,6*Z*)-(*S*)-[1-^{2}H]-farnesyl diphosphate (233)

Preparation of (2Z,6Z)-3,7,11-trimethyldodeca-2,6,10-trienal (217):

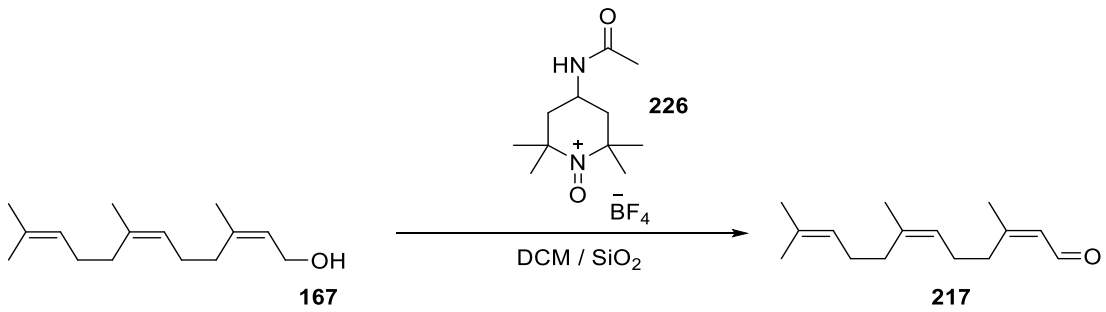

167 **217**

(2*Z*,6*Z*) farnesol **167** (526 mg, 2.37 mmol, 1 eq.) was added to a stirred suspension of 4-acetamido-2,2,6,6-tetramethyl-1-oxopiperidin-1-ium tetra fluoroborate salt, (TEMPO salt, **226**) (781 mg, 2.60 mmol, 1.1 eq.) and silica (20 mg, 0.33 mmol, 0.14 eq.) in dichloromethane (10 mL). The reaction was stirred at room temperature until complete consumption of starting material was observed *via* TLC (20% ethyl acetate in hexanes). Reaction mixture was filtered through a silica plug with dichloromethane. Eluent was concentrated under *vaccuo* to give **217** as a pale yellow oil (516 mg, 99%) which was used without further purification.

^{1}H NMR (300 MHz, $CDCl_3$) δ 9.98 (1H, d, *J* = 7.9 Hz, CHC(O)*H*), 5.87 (1H, d, *J* = 7.9 Hz, C*H*CH(O)), 5.22 (1H, t, *J* = 5.7 Hz, (CH_3)CC*H*), 5.04 (1H, t, *J* = 6.5 Hz, (CH_3)CC*H*), 2.20 (2H, t, *J* = 7.3 Hz, allylic CH_2), 2.15 – 2.07 (2H, m, allylic CH_2), 2.07 – 1.98 (4H, m, 2 x allylic CH_2), 1.73 (3H, s, CH_3), 1.69 (3H, s, CH_3), 1.61 (3H, s, CH_3), 1.47 (3H, s, CH_3).

Table 21. 2D proton NMR correlations revealing spatial arrangement in 217

217: NOESY ^{1}H - ^{1}H interactions	
From / ppm	To / ppm
9.98	2.20
9.98	5.22
5.22	1.73
5.04	2.11
5.04	2.01
5.04	1.69

Preparation of (2Z,6Z)-1-deutero-3,7,11-trimethyldodeca-2,6,10-trien-1-ol (287):

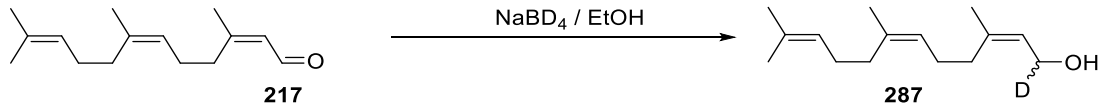

217 **287**

Crude aldehyde **217** (521 mg, 2.36 mmol, 1 eq.) was added to a stirred solution of sodium borodeuteride (300 mg, 7.10 mmol, 3 eq.) in ethanol (20 mL). The reaction mixture was stirred at room temperature until complete consumption of starting material was observed *via* TLC (20% ethyl acetate in hexane). Reaction mixture was quenched with hydrochloric acid (1 M, 5 mL) and organic products extracted with diethyl ether (3 x 10 mL). Combined organic extracts were washed with water (3 x 10 mL) and brine (2 x 10 mL), dried over anhydrous sodium sulphate and filtered. Filtered organic extracts were concentrated under reduced pressure and purified *via* silica chromatography (20% ethyl acetate in hexanes) to give **287** as a colourless oil (528 mg, 100%).

^{1}H NMR (500 MHz, $CDCl_3$) δ 5.37 (1H, d, *J* = 7.0 Hz, CC*H*CHDO), 5.08 – 4.99 (2H, m, 2 x (CH_3)CC*H*), 4.00 (1H, d, *J* = 7.0 Hz, CHC*H*DOH), 2.06 – 2.00 (4H, m, 2 x allylic CH_2), 1.99 – 1.94 (4H, m, 2 x allylic CH_2), 1.68 (3H, s, CH_3), 1.62 (6H, s, 2 x CH_3), 1.54 (3H, s, CH_3). **^{13}C NMR** (75 MHz, $CDCl_3$) δ 140.0 ((CH_3)*C*CHCHDO), 136.2 & 131.7 (2 x (CH_3)*C*CH), 124.5 (C*C*HCHDO), 124.4 & 124.2 (2 x (CH_3)C*C*H), 59.1 – 58.3 (CH*C*HDO), 32.2 & 31.9 & 26.6 & 26.3 (4 x allylic *C*H_2), 25.8 (*C*H_3), 23.5 & 23.4 ((2 x (*C*H_3)CCH), 17.7 (*C*H_3). **^{2}H NMR** (77 MHz, $CDCl_3$) δ 4.06 (1 x ^{2}H, s, CCHCH*D*O). **LRMS** (EI^+): 205.20 (80% [M – H_2O]), 190.17 (50%), 162.14 (95%), 143.08 (65%), 134.11 (70%), 120.09 (100%), 106.08 (80%), 93.07 (95%), 80.06 (47%), 67.05 (30%). **HRMS** (EI^+): calculated for [$C_{15}H_{25}$][M – H_2O]; 205.1955, found 205.1956.

Table 22. 2D proton NMR correlations revealing spatial arrangement in 287

287: NOESY ^{1}H - ^{1}H interactions	
From / ppm	To / ppm
5.37	4.00
5.37	1.68
5.04	2.03
5.04	1.97
5.04	1.62
4.00	2.03

Preparation of (2Z,6Z)-1-deutero-3,7,11-trimethyldodeca-2,6,10-trienal (288):

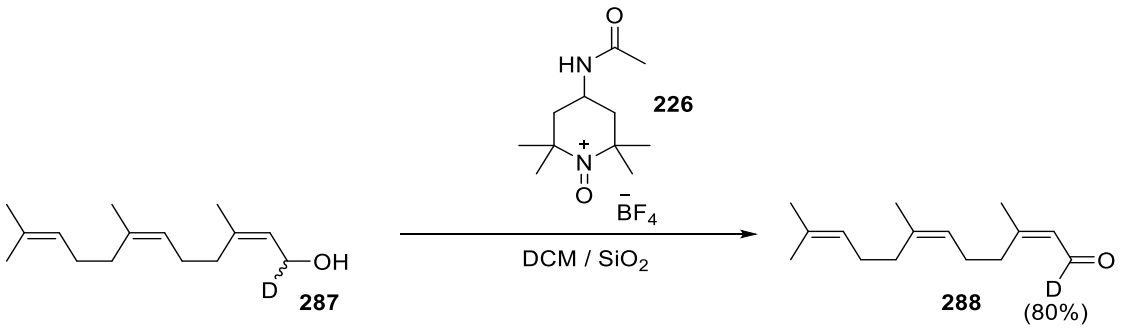

TEMPO salt **226** (781 mg, 2.60 mmol, 1.1 eq.) and silica (20 mg, 0.33 mmol, 0.14 eq.) was suspended in dichloromethane (20 mL). Alcohol **287** was added dropwise to the stirred suspension and the reaction monitored by TLC (20% ethyl acetate in hexanes) until complete consumption of starting material was observed. Reaction mixture was filtered through a silica plug with DCM and the eluent concentrated under reduced pressure to give **288** as a pale yellow oil (507 g, 97%, 80% ^{2}H incorporation) which was used without further purification.

^{1}H NMR (300 MHz, $CDCl_3$) δ 9.91 (0.2H, d, *J* = 7.9 Hz, CHC(O)*H/D*), 5.55 (1H,s, C*H*C(O)H), 5.19 – 5.04 (1H,m, $(CH_3)CCH$), 4.99 – 4.81 (1H, m, $(CH_3)CCH$), 2.20 (2H, t, *J* = 7.3 Hz, allylic CH_2), 2.15 – 2.07 (2H, m, allylic CH_2), 2.07 – 1.98 (4H, m, 2 x allylic CH_2), 1.73 (3H, s, CH_3), 1.69 (3H, s, CH_3), 1.61 (3H, s, CH_3), 1.47 (3H, s, CH_3).

Preparation of (2Z,6Z)-1,1-di deutero-3,7,11-trimethyldodeca-2,6,10-trien-1-ol (289):

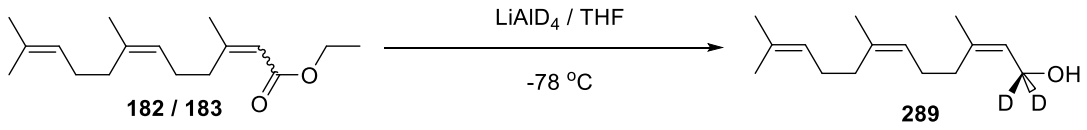

A mixture of ethyl farnesoates **182** and **183** (150 mg, 0.57 mmol, 1 eq.) was added to a stirred suspension of lithium aluminium deuteride (72 mg, 1.7 mmol, 3 eq.) in anhydrous tetrahydrofuran (20 mL). Reaction was stirred for 1 hour at -78 °C and 16 hours at temperature and quenched with hydrochloric acid (1 M). Reaction products were extracted with diethyl ether (3 x 10 mL) and combined organic extracts washed with water (3 x 10 mL), brine (2 x 10 mL), dried over anhydrous sodium sulphate and filtered. Purification by flash chromatography (5% ethyl acetate in hexane) gave **289** as a colourless oil (33 mg, 26%).

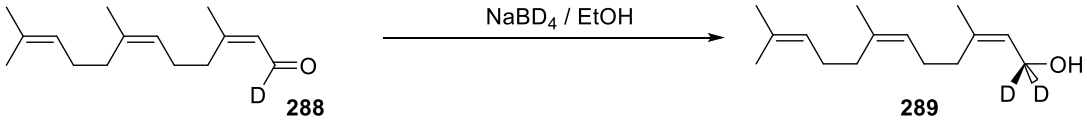

To a suspension of sodium borodeuteride (287 mg, 6.87 mmol, 3 eq.) in ethanol (10 mL) was added crude aldehyde **288** (507 mg, 2.29 mmol, 1 eq.) and the reaction stirred at room temperature. The reaction was quenched with 1 M hydrochloric acid (5 mL) upon complete consumption starting material by TLC (20% ethyl acetate in hexanes). Organic products were extracted with diethyl ether (3 x 10 mL) and washed with water (3 x 10 mL), brine (3 x 10 mL), dried over anhydrous sodium sulphate and filtered. Dried organic extracts were concentrated under reduced pressure and purified *via* flash chromatography (20% ethyl acetate in hexanes) to give **289** as a colourless oil (506 mg, 99%, 91% ^{2}H incorporation).

^{1}H NMR (300 MHz, $CDCl_3$) δ 5.37 (1H, s, CC*H*CD_2O), 5.04 (2H, t, *J* = 6.6 Hz, 2 x $(CH_3)CCH$), 2.04 – 1.89 (8H, m, 4 x allylic CH_2), 1.68 (3H, d, *J* = 1.4 Hz, CH_3), 1.62 (6H, s, 2 x CH_3), 1.54 (3H, s, CH_3). **^{13}C NMR** (75 MHz, $CDCl_3$) δ 140.1 ($(CH_3)CCHCD_2O$), 136.2 & 131.7 (2 x $(CH_3)CCH$), 124.5 ($CCHCD_2O$), 124.3 & 124.8 (2 x $(CH_3)CCH$), 32.2 & 31.9 & 26.6 & 26.3 (4 x allylic CH_2), 25.8 (CH_3), 23.5 & 23.7 ((2 x CH_3)CCH), 17.7 (CH_3). **^{2}H NMR** (77 MHz,) δ 4.05 (2 x ^{2}H, d, *J* = 0.6 Hz, $CCHCD_2O$). **LRMS** (EI^+): 206.20 (75% [M – H_2O]), 191.18 (40%), 163.14 (90%), 135.11 (32%), 121.09 (100%), 107.08 (53%), 95.08 (80%), 71.0 (20%). **HRMS** (EI^+): calculated for [$C_{15}H_{24}$][M –HDO]; 206.2019, found 206.2024.

Preparation of (2Z,6Z)-1-deutero-3,7,11-trimethyldodeca-2,6,10-trienal (290):

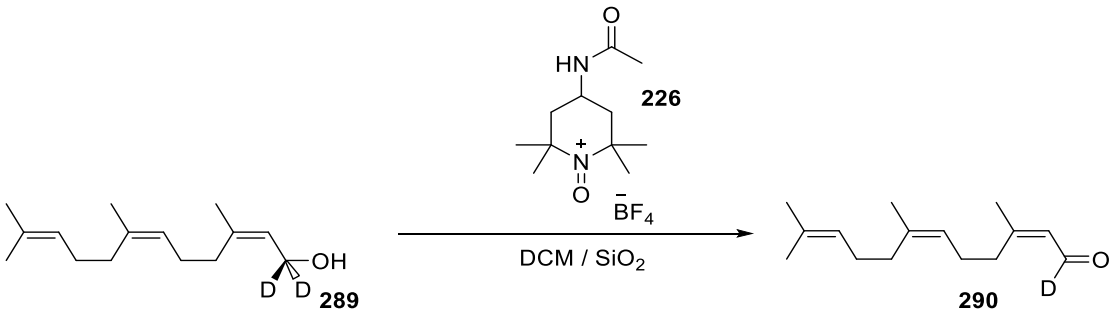

Alcohol **289** (100 mg, 0.45 mmol, 1 eq.) was added to a stirred suspension of TEMPO salt (**226**) (147 mg, 0.49 mmol, 1.1 eq.) and silica (3 mg, 0.044 mmol, 0.14 eq.) in dichloromethane. The reaction mixture was stirred at room temperature until complete consumption of starting material was observed *via* TLC (20% ethyl acetate in hexanes).Reaction mixture was filtered through a silica plug with dichloromethane and the eluent concentrated under reduced pressure to give aldehyde **290** as a crude yellow oil (97 mg, 100%, 100% ^{2}H incorporation). Crude aldehyde **290** was used without further purification.

^{1}H NMR (300 MHz, $CDCl_3$) δ 5.85 (1H, s, , C*H*C(O)H), 5.18 (1H, t, *J* = 5.8 Hz, $(CH_3)CCH$), 5.05 (1H, t, *J* = 6.5 Hz, $(CH_3)CCH$), 2.21 (2H, t, *J* = 7.3 Hz, allylic CH_2), 2.17 – 2.10 (2H, m, allylic CH_2), 2.07 – 1.99 (4H, m, 2 x allylic CH_2), 1.74 (3H, s, CH_3), 1.67 (3H, s, CH_3), 1.61 (3H, s, CH_3), 1.48 (3H, s, CH_3).

Preparation of (S,2Z,6Z)-3,7,11-trimethyldodeca-2,6,10-trien-1-d-1-ol (291):

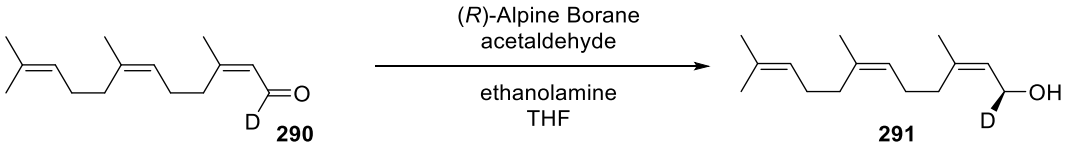

(*R*)-Alpine borane (975 µL, 0.49 mmol, 1.24 eq., 0.5 M in THF) was added to aldehyde **290** (87 mg, 0.39 mmol, 1 eq.) in anhydrous tetrahydrofuran (10 mL). The reaction was quenched with acetaldehyde (11 µL, 0.197 mmol, 0.5 eq.) after stirring at room temperature for 4 hours. Reaction solvent was removed under reduced pressure and subjected to high vacuum for 1 hour to remove pinene. Organic products were dissolved in diethyl ether (5 mL) and cooled to 0 °C. 2-Aminoethanol (26 µL, 0.43 mmol, 1.1 eq.) was added at 0 °C; the resultant precipitate was filtered, washed with cold diethyl ether and the filtrate washed with water (3 x 5 mL). Organic layers were dried over anhydrous magnesium sulphate, filtered and concentrated under *vaccuo*. The crude product was

purified *via* flash chromatography (10:1 toluene / ethyl acetate) to give the desired alcohol **291** as a colourless oil (42 mg, 47%). Enantiomeric analysis was determined by the synthesis of Mosher esters and analysis of the ^{1}H NMR spectrum.

^{1}H NMR (300 MHz, $CDCl_3$) δ 5.38 (1H, d, *J* = 7.2 Hz CC*H*CHDO), 5.07 – 5.01 (2H, m, 2 x (CH_3)CC*H*), 4.00 (1H, d, *J* = 7.2 Hz, CHC*H*DOH), 2.06 – 2.00 (4H, m, 2 x allylic CH_2), 1.99 – 1.91 (4H, m, 2 x allylic CH_2), 1.68 (3H, s, CH_3), 1.62 (6H, s, 2 x CH_3), 1.54 (3H, s, CH_3). **^{13}C NMR** (75 MHz, $CDCl_3$) δ 140.0 ((CH_3)*C*CHCHDO), 136.2 & 131.7 (2 x (CH_3)*C*CH), 124.5 (C*C*HCHDO), 124.4 & 124.2 (2 x (CH_3)C*C*H), 59.4 – 58.2 (CH*C*HDO), 32.2 & 31.9 & 26.6 & 26.3 (4 x allylic *C*H_2), 25.8 (*C*H_3), 23.5 & 23.4 ((2 x (*C*H_3)CCH), 17.7 (*C*H_3). **^{2}H NMR** (77 MHz) δ 3.98 (1 x ^{2}H, s, CCHCH*D*O).). **LRMS** (EI^+): 206.20 (72% [M – H_2O]), 191.18 (40%), 163.14 (90%), 135.11 (32%), 121.09 (100%), 107.08 (53%), 95.08 (77%), 71.0 (18%). **HRMS** (EI^+): calculated for [$C_{15}H_{24}$][M –HDO]; 206.2019, found 206.2018.

Table 23. 2D proton NMR correlations revealing spatial arrangement in 291

291: NOESY ^{1}H - ^{1}H interactions	
From / ppm	To / ppm
5.38	4.00
5.38	1.68
5.04	2.03
5.04	1.95
5.04	1.62
4.00	2.03

Preparation of (S)-[1-^{2}H]-(2Z,6Z) farnesol Mosher esters (297 and 298)

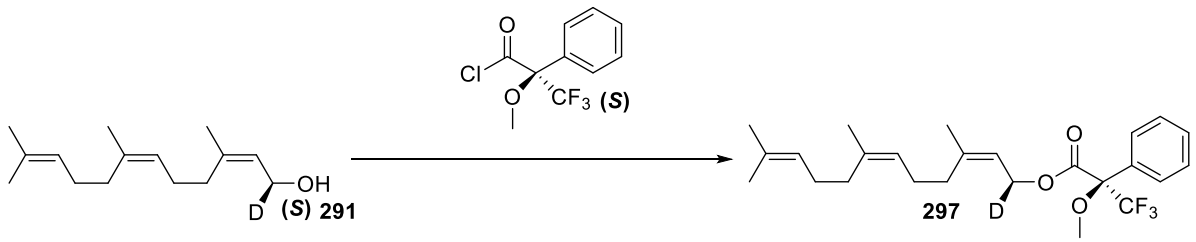

To a stirred solution of (*S*)-[1-^{2}H]-(2*Z*,6*Z*)-farnesol **291** (1 mg, 0.0045 mmol, 1 eq.) and pyridine (1.1 mg, 0.0139, 3.1 eq.) in anhydrous dichloromethane (1 mL) was added (S)-α-methoxy-α-(trifluoromethyl)phenylacetyl chloride (2.4 mg, 0.0094 mmol, 2.1 eq.) and stirred for 6 hours at room temperature. Reaction was quenched with water (500 µL) and the crude product dissolved in diethyl

ether (2 mL). The solution was washed with 0.1 M hydrochloric acid (1 mL), *sat*. sodium bicarbonate solution (1 mL), water (1 mL) and dried over anhydrous magnesium sulphate. Dried organic fraction were purified by preparative TLC (20% ethyl acetate in hexane) and extracted directly into deuterated chloroform for ^{1}H NMR analysis.

^{1}H NMR (600 MHz, $CDCl_3$) δ 7.56 – 7.53 (3H, m, 3 x aromatic *H*), 7.42 – 7.40 (2H, m, 2 x aromatic *H*), 5.40 (1H, d, *J* = 7.1 Hz, CC*H*CHDO), 5.14 – 5.06 (2H, m, 2 x ((CH$_3$)CC*H*), 4.78 (1H, d, *J* = 7.1 Hz, C*H*DO), 3.58 (3H, s, OC*H*$_3$), 2.20 – 1.97 (8H, m, 4 x allylic C*H*$_2$), 1.78 (3H, s, C*H*$_3$), 1.70 (6H, s, 2 x C*H*$_3$), 1.62 (3H, s, C*H*$_3$).

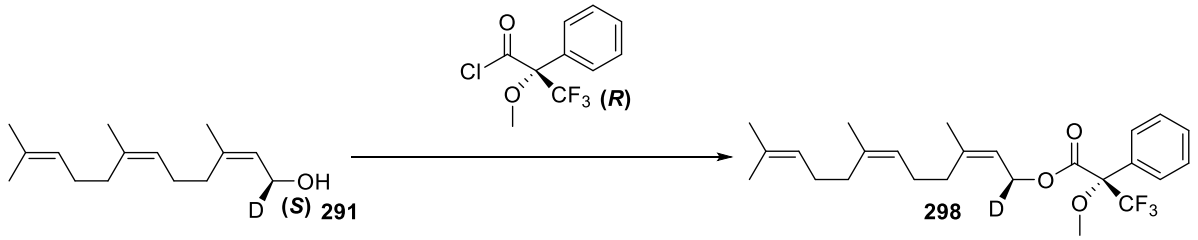

(*S*)-α-Methoxy-α-(trifluoromethyl)phenylacetyl chloride (2.4 mg, 0.0094 mmol, 2.1 eq.) was added to a stirred solution of (*S*)-[1-^{2}H]-(2*Z*,6*Z*) farnesol **291** (1 mg, 0.0045 mmol, 1 eq.) and pyridine (1.1 mg, 0.0139, 3.1 eq.) in anhydrous dichloromethane (1 mL) and stirred for 6 hours at room temperature. Reaction was quenched with water (500 µL) and the crude product dissolved in diethyl ether (2 mL). The solution was washed with 0.1 M hydrochloric acid (1 mL), *sat*. sodium bicarbonate solution (1 mL), water (1 mL) and dried over anhydrous magnesium sulphate. Dried organic fraction were purified by preparative TLC (20% ethyl acetate in hexane) and extracted directly into deuterated chloroform for ^{1}H NMR analysis.

^{1}H NMR (600 MHz, $CDCl_3$) δ 7.56 – 7.53 (3H, m, 3 x aromatic *H*), 7.42 – 7.40 (2H, m, 2 x aromatic *H*), 5.40 (1H, d, *J* = 7.0 Hz, CC*H*CHDO), 5.14 – 5.06 (2H, m, 2 x ((CH$_3$)CC*H*), 4.82 (1H, d, *J* = 7.0 Hz, C*H*DO), 3.58 (3H, s, OC*H*$_3$), 2.21 – 1.97 (8H, m, 4 x allylic C*H*$_2$), 1.79 (3H, s, C*H*$_3$), 1.72 (6H, s, 2 x C*H*$_3$), 1.62 (3H, s, C*H*$_3$).

(R,2Z,6Z)-1-chloro-3,7,11-trimethyldodeca-2,6,10-triene-1-d (292):

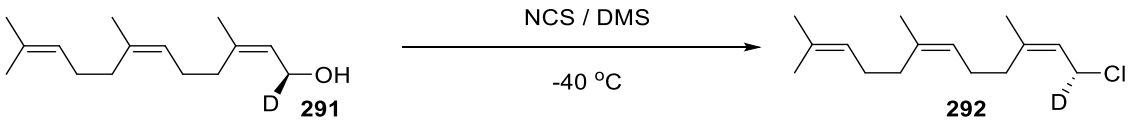

N-Chlorosuccinamide (55 mg, 0.414 mmol, 2.2 eq.) in anhydrous dichloromethane (3 mL) was cooled to -40 °C and dimethyl sulphide (33 µL, 0.451 mmol, 2.4 eq.) added dropwise. The mixture was warmed to 0 °C, cooled to -40 °C and (*S*)-[1-^{2}H]-farnesol **291** (42 mg, 0.188 mmol, 1 eq.) in anhydrous dichloromethane (1 mL) was added to the suspension dropwise. The reaction was allowed to warm to 0 °C over 1 hour, stirred at 0 °C for 1 hour and at room temperature for 15 minutes. The reaction mixture was diluted with dichloromethane (2 mL), washed with cold brine (2 mL) and the aqueous layer washed with cold hexane (3 x 3 mL). Combined organic layers were washed with water (3 x 2 mL), brine (3 x 2 mL), dried over anhydrous sodium sulphate and filtered. Solvent was removed under reduced pressure to give chloride **292** as a pale yellow oil (41 mg, 91%).

^{1}H NMR (500 MHz, $CDCl_3$) δ 5.37 (1H, d, *J* = 7.9 Hz CC*H*CHDCl), 5.08 – 5.00 (2H, m, 2 x (CH_3)CC*H*), 3.99 (1H, d, *J* = 7.9 Hz, CHC*H*DCl), 2.07 – 2.03 (4H, m, 2 x allylic CH_2), 2.01 – 1.95 (4H, m, 2 x allylic CH_2), 1.70 (3H, s, CH_3), 1.62 (6H, s, 2 x CH_3), 1.54 (3H, s, CH_3). **^{2}H NMR** (77 MHz) δ 4.05 (1 x ^{2}H, s, CCHCH*D*Cl).

(S,2Z,6Z) -3,7,11-trimethyldodeca-2,6,10-trien-1-d – yl diphosphate (233):

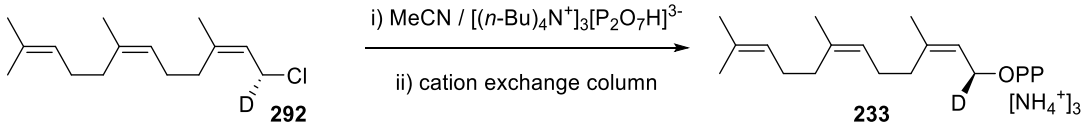

A mixture of crude chloride **292** (41 mg, 0.170 mmol, 1 eq.) and tris tetrabutyl ammonium pyrophosphate (306 mg, 0.339 mmol, 2 eq.) in anhydrous acetonitrile (2 mL) was stirred at room temperature for 16 hours. The reaction mixture was concentrated under reduced pressure and the resultant residue dissolved in buffer solution (25 mM NH_4HCO_3, 2% iPrOH) (5 mL) and the tris tetrabutylammonium salt counter ions were exchanged for ammonium by ion exchange column containing Amberlyst 131 (wet H^+ form) mesh cation exchange resin pre-equilibrated with ion-exchange buffer (25 mM NH_4HCO_3, 2% isopropanol). The appropriate fractions were collected and lyophilized to yield diphosphate **233** as a white powder. The powder was dissolved in buffer solution (25 mM NH_4HCO_3, 2% iPrOH) (5 mL) and purified using HPLC (Solvent A: acetonitrile, solvent B: 2%

iPrOH). The appropriate fractions were collected and lyophilized to give diphosphate **233** as a white powder (1 mg, 1%).

^{1}H NMR (300 MHz, $CDCl_3$) δ 2.01 – 1.76 (4H, m, 2 x allylic CH_2), 1.62 – 1.39 (4H, m, 2 x allylic CH_2), 1.25 (3H, s, CH_3), 1.19 (6H, s, 2 x CH_3), 1.14 (3H, s, CH_3). **HRMS** (ES^-): calculated for $[C_{15}H_{26}DO_7P_2][M]$; 382.1295, found 382.1294.

8.2.13 Synthesis of (2*Z*,6*Z*)-(*R*)-[1-^{2}H]-farnesyl diphosphate (234)

Preparation of (R,2Z,6Z)-3,7,11-trimethyldodeca-2,6,10-trien-1-d-1-ol (300):

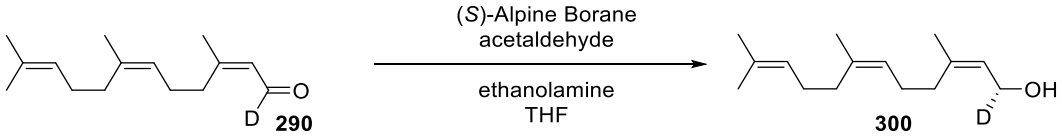

Aldehyde **290** (73 mg, 0.33 mmol, 1 eq.) was dissolved in anhydrous tetrahydrofuran (5 mL). (*S*)-Alpine borane (817 µL, 0.41 mmol, 1.24 eq., 0.5 M in THF) was added and the reaction stirred at room temperature for 4 hours. Acetaldehyde (9.3 µL) was added to the reaction mixture, solvent removed under reduced pressure and the crude product subjected to high vacuum for 1 hour to remove pinene. Concentrated product was dissolved in diethyl ether (5 mL), cooled to 0 °C and 2-aminoethanol (22 µL) added dropwise. The resultant precipitate was washed with diethyl ether (5 mL) and the filtrate washed with water (3 x 5 mL). Organic filtrate was washed with water (3 x 5 mL), dried over anhydrous magnesium sulphate and concentrated under reduced pressure. Crude product was purified *via* flash chromatography (10:1 toluene / ethyl acetate) to afford alcohol **300** and a colourless oil (32 mg, 43%). Enantiomeric analysis was determined by the synthesis of Mosher esters and analysis of the ^{1}H NMR spectrum.

^{1}H NMR (300 MHz, $CDCl_3$) δ 5.37 (1H, d, *J* = 6.9 Hz CC*H*CHDO), 5.08 – 4.98 (2H, m, 2 x (CH_3)CC*H*), 4.00 (1H, d, *J* = 6.9 Hz, CHC*H*DOH), 2.06 – 2.00 (4H, m, 2 x allylic CH_2), 1.99 – 1.91 (4H, m, 2 x allylic CH_2), 1.68 (3H, s, CH_3), 1.62 (6H, s, 2 x CH_3), 1.54 (3H, s, CH_3).**^{13}C NMR** (75 MHz, $CDCl_3$) δ 140.0 ((CH_3)*C*CHCHDO), 136.2 & 131.7 (2 x (CH_3)*C*CH), 124.5 (C*C*HCHDO), 124.4 & 124.2 (2 x (CH_3)C*C*H), 59.1 – 58.3 (CH*C*HDO), 32.2 & 31.9 & 26.6 & 26.3 (4 x allylic *C*H_2), 25.7 (*C*H_3), 23.5 & 23.4 ((2 x (*C*H_3)CCH), 17.7 (*C*H_3).**^{2}H NMR** (77 MHz) δ 3.96 (1 x ^{2}H, s, CCHCH*D*O). **LRMS** (EI^+): 206.20 (78% [M – H_2O]), 191.18 (40%), 163.14 (87%), 135.11 (35%), 121.09 (100%), 107.08 (57%), 95.08 (75%), 71.0 (20%). **HRMS** (EI^+): calculated for $[C_{15}H_{24}][M – HDO]$; 206.2019, found 206.2015.

Table 24. 2D proton NMR correlations revealing spatial arrangement in 300

300: NOESY ^{1}H - ^{1}H interactions	
From / ppm	To / ppm
5.37	4.00
5.37	1.68
5.03	2.03
5.03	1.95
5.03	1.62
4.00	2.03

Preparation of (R)-[1-^{2}H]-(2Z,6Z) farnesol Mosher esters (303 and 304)

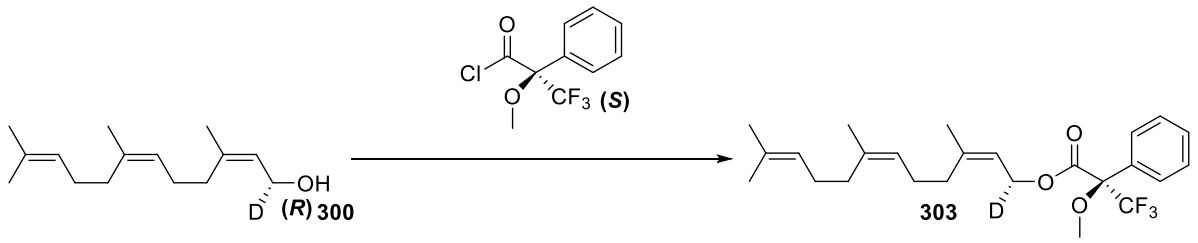

To a stirred solution of (*R*)-[1-^{2}H]-(2*Z*,6*Z*) farnesol **300** (1 mg, 0.0045 mmol, 1 eq.) and pyridine (1.1 mg, 0.0139, 3.1 eq.) in anhydrous dichloromethane (1 mL) was added (S)-α-methoxy-α-(trifluoromethyl)phenylacetyl chloride (2.4 mg, 0.0094 mmol, 2.1 eq.) and stirred for 6 hours at room temperature. Reaction was quenched with water (500 µL) and the crude product dissolved in diethyl ether (2 mL). The solution was washed with 0.1 M hydrochloric acid (1 mL), *sat*. sodium bicarbonate solution (1 mL), water (1 mL) and dried over anhydrous magnesium sulphate. Dried organic fraction were purified by preparative TLC (20% ethyl acetate in hexane) and extracted directly into deuterated chloroform for ^{1}H NMR analysis.

^{1}H NMR (600 MHz, $CDCl_3$) δ 7.56 – 7.52 (3H, m, 3 x aromatic *H*), 7.43 – 7.40 (2H, m, 2 x aromatic *H*), 5.40 (1H, d, *J* = 6.7 Hz, CC*H*CHDO), 5.14 – 5.08 (2H, m, 2 x ((CH$_3$)CC*H*), 4.83 (1H, d, *J* = 6.8 Hz, C*H*DO), 3.57 (3H, s, OCH_3), 2.16 – 2.00 (8H, m, 4 x allylic CH_2), 1.78 (3H, s, CH_3), 1.70 (3H, s, CH_3), 1.69 (3H, s, CH_3), 1.62 (3H, s, CH_3).

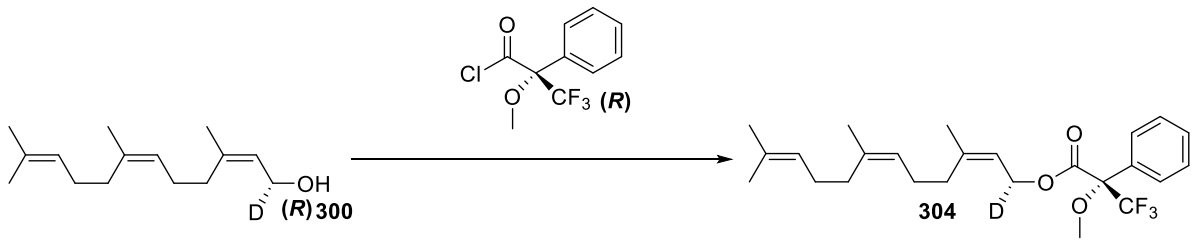

(*S*)-α-Methoxy-α-(trifluoromethyl)phenylacetyl chloride (2.4 mg, 0.0094 mmol, 2.1 eq.) was added to a stirred solution of (*R*)-[1-^{2}H]-(2*Z*,6*Z*) farnesol **300** (1 mg, 0.0045 mmol, 1 eq.) and pyridine (1.1 mg, 0.0139, 3.1 eq.) in anhydrous dichloromethane (1 mL) and stirred for 6 hours at room temperature. Reaction was quenched with water (500 µL) and the crude product dissolved in diethyl ether (2 mL). The solution was washed with 0.1 M hydrochloric acid (1 mL), *sat*. sodium bicarbonate solution (1 mL), water (1 mL) and dried over anhydrous magnesium sulphate. Dried organic fraction were purified by preparative TLC (20% ethyl acetate in hexane) and extracted directly into deuterated chloroform for ^{1}H NMR analysis.

^{1}H NMR (600 MHz, $CDCl_3$) δ 7.56 – 7.51 (3H, m, 3 x aromatic *H*), 7.43 – 7.39 (2H, m, 2 x aromatic *H*), 5.40 (1H, d, *J* = 6.7 Hz, CC*H*CHDO), 5.14 – 5.07 (2H, m, 2 x ((CH$_3$)CC*H*), 4.78 (1H, d, *J* = 6.7 Hz, C*H*DO), 3.58 (3H, s, OCH_3), 2.17 – 1.99 (8H, m, 4 x allylic CH_2), 1.78 (3H, s, CH_3), 1.70 (3H, s, CH_3), 1.69 (3H, s, CH_3), 1.62 (3H, s, CH_3).

(S,2Z,6Z)-1-chloro-3,7,11-trimethyldodeca-2,6,10-triene-1-d (301):

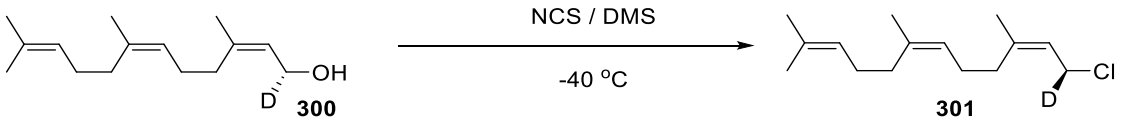

Dimethyl sulphide (57 µL, 0.784 mmol, 2.4 eq.) added dropwise to a suspension of *N*-chlorosuccinamide (96 mg, 0.719 mmol, 2.2 eq.) in anhydrous dichloromethane (4 mL) at -40 °C. The mixture was briefly warmed to 0 °C prior to the suspension being cooled to -40 °C and (*R*)-[1-^{2}H]-farnesol **300** (73 mg, 0.327 mmol, 1 eq.) in anhydrous dichloromethane (1 mL) added dropwise. The reaction was warmed to 0 °C over 1 hour, stirred at 0 °C for 1 hour and then room temperature for 15 minutes. The reaction mixture was diluted with dichloromethane (2 mL), washed with cold brine (2 mL) and the aqueous layer washed with cold hexane (3 x 3 mL). Combined organic layers were washed with water (3 x 3 mL), brine (3 x 3 mL), dried over anhydrous sodium sulphate and filtered. Solvent was removed under reduced pressure to give chloride **301** as a pale yellow oil (70 mg, 89%).

^{1}H NMR (500 MHz, $CDCl_3$) δ 5.37 (1H, d, *J* = 7.9 Hz CC*H*CHDCl), 5.07 – 5.02 (2H, m, 2 x (CH_3)CC*H*), 3.99 (1H, d, *J* = 7.9 Hz, CHC*H*DCl), 2.07 – 2.03 (4H, m, 2 x allylic CH_2), 2.00 – 1.95 (4H, m, 2 x allylic CH_2), 1.70 (3H, s, CH_3), 1.62 (6H, s, 2 x CH_3), 1.54 (3H, s, CH_3). **^{2}H NMR** (77 MHz) δ 4.05 (1 x ^{2}H, s, CCHCH*D*Cl).

(R,2Z,6Z)-3,7,11-trimethyldodeca-2,6,10-trien-1-d – yl diphosphate (234):

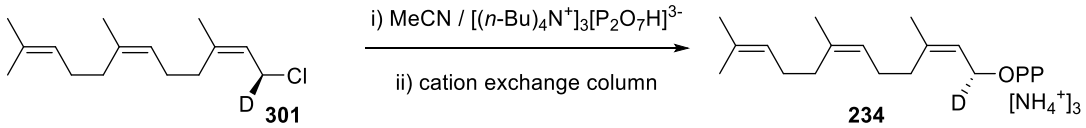

A mixture of **301** (70 mg, 0.289 mmol, 1 eq.) and tris tetrabutyl ammonium pyrophosphate (522 mg, 0.579 mmol, 2 eq.) in anhydrous acetonitrile (4 mL) was stirred at room temperature for 16 hours. The reaction mixture was concentrated under reduced pressure and the resultant residue dissolved in buffer solution (25 mM NH_4HCO_3, 2% iPrOH) (5 mL) and the tris tetrabutylammonium salt counter ions were exchanged for ammonium by ion exchange column containing Amberlyst 131 (wet H^+ form) mesh cation exchange resin pre-equilibrated with ion-exchange buffer (25 mM NH_4HCO_3, 2% isopropanol). The appropriate fractions were collected and lyophilized to yield diphosphate as a white powder. The powder was dissolved in buffer solution (25 mM NH_4HCO_3, 2% iPrOH) (5 mL) and purified using HPLC (Solvent A: acetonitrile, solvent B: 2% iPrOH). The appropriate fractions were collected and lyophilized to give **234** as a white powder (2 mg, 2%).

^{1}H NMR (300 MHz, $CDCl_3$) δ 2.02 – 1.73 (4H, m, 2 x allylic CH_2), 1.61 – 1.40 (4H, m, 2 x allylic CH_2), 1.22 (3H, s, CH_3), 1.18 (6H, s, 2 x CH_3), 1.14 (3H, s, CH_3). **HRMS** (ES^-): calculated for [$C_{15}H_{26}DO_7P_2$][M]; 382.1295, found 382.1299.

8.2.14 Synthesis of (2*Z*,6*Z*)–[1-^{3}H]–farnesyl diphosphate (229)

Preparation of (2Z,6Z)-1- tritio-3,7,11-trimethyldodeca-2,6,10-trien-1-yl diphosphate (229):

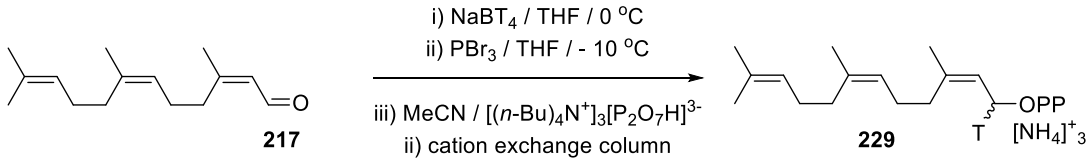

Sodium [^{3}H] borohydride 5 mCi (15 mCi/mmol) in anhydrous tetrahydrofuran (0.5 mL) was cooled to 0 °C. (2*Z*,6*Z*) farnesal (**217**) (20 mg, 0.091 mmol, 1 eq.) in anhydrous tetrahydrofuran (0.3 mL) was added to the reaction mixture and stirred at 0 °C for 4 hours. Sodium borohydride (10 mg, 0.272 mmol, 3 eq.) in anhydrous tetrahydrofuran (0.3 mL) was added to the reaction mixture and stirred at 0 °C for 16 hours. The reaction was quenched with brine (0.5 mL) and the reaction product extracted with diethyl ether (3 x 0.5 mL). Combined organic extracts were washed with water (3 x 1 mL), brine (3 x 0.5 mL), dried by passage through a pipette of sodium sulfate and concentrated under a stream of nitrogen to give (2*Z*,6*Z*)-[1-^{3}H]-farnesol (**227**) as a colourless oil (20 mg, 100%). Analysis *via* TLC (20% ethyl acetate in hexane) showed a single reaction product. A sample from the TLC plate was suspended in Ecoscint A scintillation cocktail (15 mL) and analysed using a liquid scintillation counter confirming tritium incorporation. The reaction product **227** was taken forward without further purification.

Alcohol **227** (20 mg, 0.091 mmol, 1 eq.) was dissolved in anhydrous tetrahydrofuran (2 mL) and cooled to -10 °C. Phosphorus tribromide (5 µL, 0.045 mmol, 0.5 eq.) was added to the reaction mixture an stirred at -10 °C until complete consumption of starting material was observed *via* TLC (20% ethyl acetate in hexane). Saturated sodium bicarbonate solution (1 mL) was added and reaction mixture stirred until effervescence had ceased. The organic layer was removed and the aqueous layers extracted with diethyl ether (3 x 1 mL). Combined organic layers were washed with *sat.* sodium bicarbonate solution (3 x 1 mL), water (3 x 1 mL) and brine (3 x 1 mL). Washed organic layers were dried by passage through a pipette of sodium sulfate and concentrated under a stream of nitrogen to give crude bromide **228** as a pale yellow oil (22 mg, 85%). Crude bromide **228** was analysed *via* TLC (20% ethyl acetate in hexane) and showed a single product. A sample from the product spot was removed from the TLC plate, suspended in Ecoscint A scintillation cocktail (15 mL) and analysed using a liquid scintillation counter confirming tritium incorporation. Crude bromide **228** was taken forward without further purification.

A solution of tris-tetra-n-butyl ammonium hydrogen pyrophosphate (104 mg, 0.115 mmol, 1.5 eq.) in anhydrous acetonitrile (1 mL) was added to a stirred solution of bromide **228** (22 mg, 0.0766, 1 eq.) in anhydrous acetonitrile (0.5 mL) and stirred at room temperature for 16 hours. Solvent was removed under a stream of nitrogen to give crude diphosphate as a pale brown oil. Crude diphosphate was dissolved in 25 mM ammonium bicarbonate, 2% isopropanol buffer (2 mL), applied to a 1 x 6 cm column of Amberlyst 131 (wet H^+ form) mesh cation exchange resin pre-equilibrated with ion-exchange buffer (25 mM NH_4HCO_3, 2% isopropanol) and slowly eluted with the same buffer. Eluent fractions were tested for radioactivity by sample dilution into Ecoscint A scintillation cocktail (15 mL) and radioactive fractions lyophilised to give a white powder. Lyophilised product was dissolved in 25 mM ammonium bicarbonate, 2% isopropanol buffer (2 mL) and applied to a SNAP Ultra C18 Biotage column. Product was eluted with H_2O (2 x column volume), H_2O:MeCN (2:1)(1 x column volume), H_2O:MeCN (1:1)(2 x column volume), H_2O:MeCN (1:2)(1 x column volume) and MeCN (2 x column volume). Fractions eluted by H_2O:MeCN (1:1) exhibited radioactivity when diluted in Ecoscint A scintillation cocktail (15 mL)and analysed *via* liquid scintillation counter. Appropriate fractions were combined and lyophilised to give (2*Z*,6*Z*)–[1-^{3}H]–farnesyl diphosphate (**229**) as a white powder 1.55 mCi (specific activity = 0.028 Ci mmol^{-1}, 18 mg, 46% over 3 steps).

8.2.15 Synthesis of (2*Z*,6*Z*)-10,11-epoxyfarnesyl diphosphate (361)

Preparation of 2-(((2Z,6Z)-3,7,11-trimethyldodeca-2,6,10-trien-1-yl)oxy)tetrahydro-2H-pyran (395):

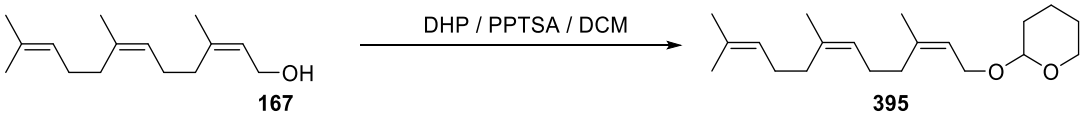

167 **395**

Pyridinium *p*-toluenesulfonate (154 mg, 0.61 mmol, 0.1 eq.) was added to stirred solution of (2*Z*,6*Z*) farnesol **167** (1.35 g, 6.1 mmol, 1 eq.) and 3,4-dihydropyran DHP (1.41 g, 15.3 mmol, 2.5 eq.) in dichloromethane(40 mL). The reaction was stirred at room temperature for 2 hours and water added to the reaction mixture. The aqueous layer was washed with dichloromethane (3 x 20 mL) and combined organic layers washed with brine (30 mL). Washed organic layers were dried over anhydrous sodium sulphate, filtered and solvent removed under reduced pressure. Purification *via* flash chromatography (10% ethyl acetate in hexanes) afforded **395** as a colourless oil (1.86 g, 100%).

^{1}H NMR (300 MHz, $CDCl_3$) δ 5.39 (1H, t, *J* = 6.3 Hz, C*H*CH_2O), 5.18 – 5.05 (2H, m, 2 x(CH_3)CC*H*), 4.68 – 4.61 (1H, m, OC*H*O), 4.11 (2H, ddd, *J* = 19.3, 11.8, 6.3 Hz, CHCH_2O), 3.94 – 3.47 (2H, m, CHOCH_2), 2.07 (8H, m,4 x CH_2), 1.92 – 1.44 (6H, m, CH(CH_2)$_3$CH_2O), 1.76 (3H, s, CH_3), 1.69 (6H, s, 2 x CH_3), 1.62 (3H, s,

C*H*$_3$). **^{13}C NMR** (125 MHz, $CDCl_3$) δ 140.5 & 135.6 & 131.6 (3 x (CH_3)*C*CH), 124.6 & 124.3 (2 x (CH_3)C*C*H), 121.6 ((CH_3)C*C*HCH_2O), 97.9 (O*C*HO), 63.45 (CH*C*H_2O), 62.2 (O*C*H_2(CH_2)$_3$), 32.3 & 31.8 & 26.6 & 26.4 (4 x allylic *C*H_2), 30.5 (OCH_2*C*H_2), 25.6 (*C*H_3), 25.3 (*C*H_2), 23.4 & 23.2 (2 x *C*H_3), 19.6 (*C*H_2), 17.5 (CH_3). **LRMS** (ES^+): 329.25 (100% [M + Na]). **HRMS** (ES^+): calculated for [$C_{20}H_{34}O_3Na$]; 329.2457, found 329.2462.

Preparation of (6Z,10Z)-2-bromo-2,6,10-trimethyl-12-((tetrahydro-2H-pyran-2yl)oxy)dodeca-6,10-dien-3-ol (396):

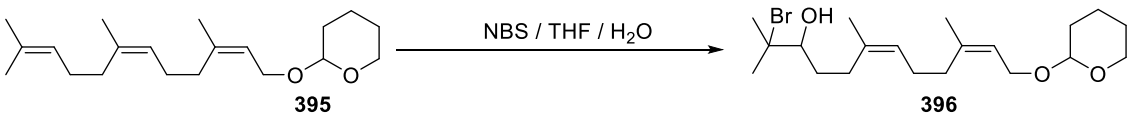

395 (1.83 g, 5.96 mmol, 1 eq.) was dissolved in THF:H_2O (50 mL, 2:1) and cooled to 0 °C. N-bromosuccinimide (1.17 g, 6.56 mmol, 1.1 eq.) was added in portions over 30 minutes at 0 °C and stirred for 2 hours, warmed to room temperature and stirred for a further 2 hours. The reaction was diluted with hexane (30 mL), separated with brine (20 mL) and the aqueous layer extracted washed with hexane (3 x 10 mL). The combined organic extracts were dried over anhydrous sodium sulphate and concentrated under reduced pressure. Purification *via* flash chromatography (20% ethyl acetate in hexane) gave **396** as a pale yellow oil (983 mg, 40%).

^{1}H NMR (300 MHz, $CDCl_3$) δ 5.39 (1H, t, *J* = 6.3 Hz, C*H*CH_2O), 5.25 – 5.16 (1H, m, (CH_3)CC*H*), 4.65 (1H, t, *J* = 3.4 Hz, OC*H*O), 4.29 – 3.98 (2H, m, CHC*H*$_2$O), 3.96 (1H, dd, *J* = 11.3, 1.8 Hz, CBrC(OH)*H*), 3.90 – 3.49 (2H, m, CHOC*H*$_2$), 2.33 – 1.97 (8H, m, 4 x C*H*$_2$), 1.90 – 1.46 (6H, m, CH(C*H*$_2$)$_3$$CH_2$O) 1.78 (3H, s, C*H*$_3$), 1.69 (3H, s, C*H*$_3$), 1.36 (3H, s, C*H*$_3$), 1.35 (3H, s, C*H*$_3$). **^{13}C NMR** (125 MHz, $CDCl_3$) δ 140.2 & 133.9 (2 x (CH_3)*C*CH), 126.3 & 121.7 (2 x (CH_3)C*C*H), 97.9 (O*C*HO), 72.4 (CBr*C*(OH)), 70.8 (*C*BrC(OH)), 63.6 (CH*C*H_2O), 62.1 (O*C*H_2(CH_2)$_3$), 32.5 & 32.3 & 26.4 (3 x allylic *C*H_2), 30.7 & 30.5 (2 x *C*H_2), 26.64 & 26.61 (2 x *C*H_3CBr), 25.5 (*C*H_2), 23.7 & 23.3 (2 x *C*H_3), 19.5 (*C*H_2). **LRMS** (AP^+): 425.17 (100% [M + Na]), 387.25 (20%), 345.24 (30%), 306.09 (15%), 243.08 (10%), 203.18 (12%). **HRMS** (AP^+): calculated for [$C_{20}H_{35}O_3BrNa$]; 425.1667, found 425.1657.

Preparation of 2-(((2Z,6Z)-9-(3,3-dimethyloxiran-2-yl)-3,7-dimethylnona-2,6-dien-1-yl)oxy)tetrahydro-2H-pyran (397):

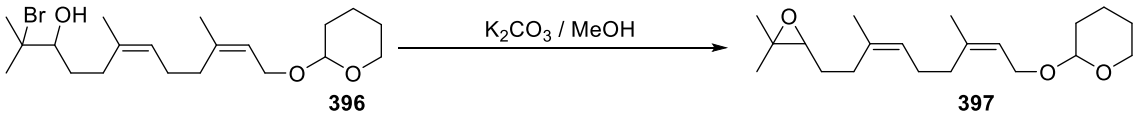

396 **397**

396 (901 mg, 2.25 mmol, 1 eq.) in methanol (50 mL) was stirred at room temperature and potassium carbonate (623 mg, 4.5 mmol, 2 eq.) added. The resultant suspension was stirred for 1 hour and concentrated under reduced pressure prior to dilution with water (50 mL) and brine (20 mL). The aqueous layer was separated, washed with hexane (3 x 30 mL) and combined organic fractions with 1 M hydrochloric acid (20 mL), brine (30 mL) and dried of anhydrous sodium sulphate. Dried organic extracts were filtered, concentrated under *vaccuo* and purified by column chromatography (20% ethyl acetate in hexane) to give **397** as a colourless oil (710 mg, 99%).

^{1}H NMR (300 MHz, $CDCl_3$) δ 5.39 (1H, t, *J* = 6.4 Hz, C*H*CH_2O), 5.22 – 5.10 (1H, m, $(CH_3)CC$*H*), 4.67 – 4.59 (1H, m, OC*H*O), 4.10 (2H, ddd, *J* = 19.1, 11.3, 7.4 Hz, CHCH_2O), 3.93 – 3.44 (2H, m, CHOCH_2), 2.72 (1H, t, *J* = 6.3 Hz, C(O)C*H*), 2.24 – 2.02 (6H, m, 3 x CH_2), 1.90 – 1.45 (8H, m, 3 x CH(CH_2)$_3$CH_2O & C(O)CHCH_2), 1.76 (3H, s, CH_3), 1.70 (3H, s, CH_3), 1.31 & 1.28 (6H, s, 2 x (CH_3)$_2$C(O)C). **^{13}C NMR** (75 MHz, $CDCl_3$) δ 140.3 & 134.6 (2 x (CH_3)*C*CH), 125.2 & 121.7 (2 x (CH_3)C*C*H), 97.9 (O*C*HO), 64.1 (C(O)*C*H), 63.4 (CH*C*H_2O), 62.2 (O*C*H_2(CH_2)$_3$), 58.4 (*C*(O)CH), 32.3 & 28.5 &26.5 (3 x allylic *C*H_2), 30.7 (OCH_2*C*H_2), 27.4 (*C*H_2), 25.5 (*C*H_2), 24.9 (*C*H_3), 23.6 & 23.3 (2 x *C*H_3C(O)C), 19.6 (*C*H_2), 18.7 (*C*H_3). **LRMS** (ES^+): 345.24 (100% [M + Na]), 221.19 (40%), 203 (20%]). **HRMS** (ES^+): calculated for [$C_{20}H_{34}O_3Na$]; 345.2406, found 345.2404.

Preparation of (2Z,6Z)-9-(3,3-dimethyloxiran-2-yl)-3,7-dimethylnona-2,6-dien-1-ol (398):

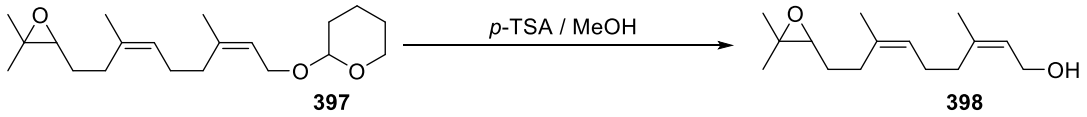

397 **398**

p-Toluenesulfonic acid (5.9 mg, cat.) was added to a stirred solution of **397** (100 mg, 0.31 mmol, 1 eq.) in methanol (10 mL) and stirred at room temperature for 2 hours. The reaction volume was reduced by 80% under *vaccuo* and diluted with *sat*. sodium bicarbonate solution (10 mL) and separated with hexane (10 mL). The aqueous layer was washed with hexane (3 x 10 mL) and combined organic fraction washed with brine (10 mL), dried over anhydrous sodium sulphate and

filtered. Solvent was removed under reduced pressure and purified by flash chromatography (20% ethyl acetate in hexane) to give **398** as a colourless oil (68 mg, 92%).

^{1}H NMR (300 MHz, $CDCl_3$) δ 5.37 (1H, t, *J* = 7.2 Hz, C*H*CH_2OH), 5.09 (1H, t, *J* = 6.5 Hz, $(CH_3)CCH$), 4.02 (2H, d, *J* = 7.2 Hz, $CHCH_2O$), 3.32 (1H, dd, *J* = 10.4, 1.8 Hz, C(O)C*H*) 2.44 – 2.28 (2H, m, $C(O)CCH_2$), 2.12 – 1.93 (6H, m, 3 x allylic CH_2), 1.68 (3H, s, CH_3), 1.62 (3H, s, CH_3), 1.05 & 1.02 (2 x 3H, s, $(CH_3)_2C(O)C$). **^{13}C NMR** (75 MHz, $CDCl_3$) δ 140.1 & 135.9 (2 x $(CH_3)CCH$), 125.2 & 124.4 (2 x $(CH_3)CCH$), 76.3 (C(O)*C*H), 58.8 ($CHCH_2O$), 49.1 (*C*(O)CH), 32.3 & 28.9 & 26.8 (3 x allylic CH_2), 29.6 ($C(O)CHCH_2$), 23.8 & 23.3 (2 x $CH_3C(O)C$), 20.7 (CH_3), 18.9 (CH_3). **LRMS** (ES^+): 221.19 (100% [M – H_2O]), 203.18 (15%). **HRMS** (ES^+): calculated for $[C_{15}H_{25}O]^+$ [M – H_2O]; 221.1905, found 221.1906.

Preparation of 3-((3Z,7Z)-9-bromo-3,7-dimethylnona-3,7-dien-1-yl)-2,2-dimethyloxirane (399):

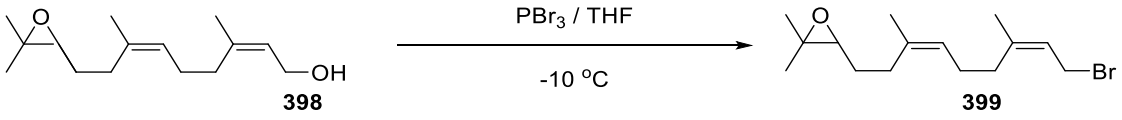

Alcohol **398** (44 mg, 0.18 mmol, 2 eq.) in anhydrous tetrahydrofuran (5 mL) was cooled to -10 °C and phosphorus tribromide (9 µL, 0.09 mmol, 1 eq.) added dropwise. The reaction mixture was stirred at -10 °C until complete consumption of starting material was observed *via* TLC (20% ethyl acetate in hexane) and quenched with *sat*. sodium bicarbonate solution (3 mL). Organic product was extracted with diethyl ether (3 x 5 mL) and combined organic extracts washed with water (3 x 5 mL), brine (3 x 5 mL), dried over anhydrous sodium sulphate and filtered. Solvent was removed under *vaccuo* to give bromide **399** as a pale yellow oil (55 mg, 97%) which was used without further purification.

^{1}H NMR (300 MHz, $CDCl_3$) δ 5.35 (1H, t, *J* = 7.2 Hz, C*H*CH_2Br), 5.09 (1H, t, *J* = 6.5 Hz, $(CH_3)CCH$), 3.97 (2H, d, *J* = 7.2 Hz, $CHCH_2Br$), 3.32 (1H, dd, *J* = 10.4, 1.8 Hz, C(O)C*H*) 2.44 – 2.28 (2H, m, $C(O)CCH_2$), 2.12 – 1.93 (6H, m, 3 x allylic CH_2), 1.68 (3H, s, CH_3), 1.62 (3H, s, CH_3), 1.05 & 1.02 (2 x 3H, s, $(CH_3)_2C(O)C$).

Preparation of 3-((3Z,7Z)-9-bromo-3,7-dimethylnona-3,7-dien-1-yl)-2,2-dimethyloxirane diphosphate (361):

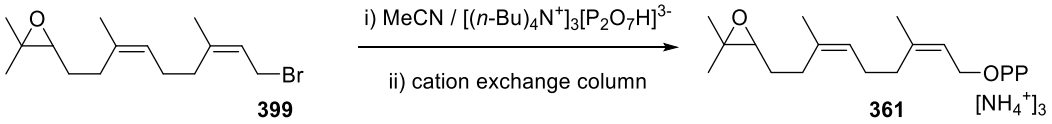

A mixture of **399** (55 mg, 0.18 mmol, 1 eq.) and tris tetrabutyl ammonium pyrophosphate (333 mg, 0.37 mmol, 2 eq.) in anhydrous acetonitrile (3 mL) was stirred at room temperature for 16 hours. The reaction mixture was concentrated under reduced pressure and the resultant residue dissolved in buffer solution (25 mM NH_4HCO_3, 2% iPrOH) (5 mL) and the tris tetrabutylammonium salt counter ions were exchanged for ammonium by ion exchange column containing Amberlyst 131 (wet H^+ form) mesh cation exchange resin pre-equilibrated with ion-exchange buffer (25 mM NH_4HCO_3, 2% isopropanol). The appropriate fractions were collected and lyophilized to yield diphosphate as a white powder. The powder was dissolved in buffer solution (25 mM NH_4HCO_3, 2% iPrOH) (5 mL) and purified using HPLC (Solvent A: acetonitrile, solvent B: 2% iPrOH). The appropriate fractions were collected and lyophilized to give **361** as a white powder (0.7 mg, 1%).

^{1}H NMR (500 MHz, D_2O) δ 5.42 – 5.36 (1H, m, $(CH_3)CCHCH_2O$), 5.15 – 5.09 (1H, m, $(CH_3)CCH$), 4.41 – 4.36 (2H, m, $CCHCH_2O$), 3.57 (1H, dd, *J* = 10.4, 1.8 Hz, C(O)CH), 2.18 – 2.04 (4H, m, 2 x allylic CH_2), 2.02 – 1.88 (4H, m, 2 x allylic CH_2), 1.70 (3H, s, CH_3), 1.64 (3H, s, CH_3), 1.58 (6H, s, 2 x CH_3). **^{31}P NMR** (202 MHz, D_2O) δ -8.71 (d, *J* = 12.0 Hz), -9.95 (d, *J* = 16.3 Hz). **HRMS** (ES^-): calculated for $[C_{15}H_{27}O_8P_2][M]$; 397.1181, found 397.1177.

8.2.16 Synthesis of (2*Z*,6*Z*,10*Z*)-12-methoxyfarnesyl diphosphate(362)

Preparation of (4Z,8Z)-4,8-dimethyl-10-((tetrahydro-2H-pyran-2-yl)oxy)deca-4,8-dienal (401):

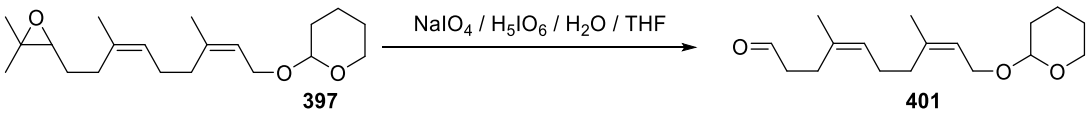

A solution of periodic acid (462 mg, 2.03 mmol, 1.1 eq.) and sodium periodate (197 mg, 0.92 mmol , 0.5 eq.) in dH_2O was added dropwise over 15 minutes to a stirred solution of **397** (594 mg, 1.84 mmol, 1 eq.) in THF:H_2O (16.5 mL, 10:1) at 0 °C. The reaction was stirred for 30 minutes at 0 °C and warmed to room temperature and stirred for a further 2 hours. The reaction was quenched with *sat*.

sodium bicarbonate sol. (10 mL) and separated with hexane (20 mL). The aqueous layer was washed with hexane (3 x 10 mL) and the combined organic extracts washed with 1M hydrochloric acid (10 mL), brine (2 x 10 mL), dried over anhydrous sodium sulphate and filtered. Solvent was removed under reduced pressure and purified by column chromatography (10% ethyl acetate in hexane) to give **401** as a colourless oil (452 mg, 71%).

^{1}H NMR (300 MHz, $CDCl_3$) δ 9.79 (1H, s, (O)C*H*CH_2), 5.40 (1H, t, *J* = 5.6 Hz, C*H*CH_2O), 5.23 – 5.11 (1H, m, C*H*CH_2CH_2), 4.63 (1H, s, OC*H*O), 4.10 (2H, ddd, *J* = 19.3, 11.8, 6.3 Hz, CHC*H*$_2$O), 3.92 – 3.46 (2H, m, CHOC*H*$_2$), 2.57 – 2.47 (2H, m, (O)CHC*H*$_2$), 2.39 – 2.31 (2H, m, (O)CHCH$_2$C*H*$_2$), 2.11 (4H, s, 2 x allylic C*H*$_2$), 1.90 – 1.45 (6H, m, 3 x C*H*$_2$), 1.76 (3H, s, C*H*$_3$), 1.69 (3H, s, C*H*$_3$). **^{13}C NMR** (75 MHz, $CDCl_3$) δ 202.3 ((O)*C*HCH$_2$), 140.2 & 133.4 (2 x (CH_3)*C*CH), 126.0 & 121.8 (2 x (CH_3)C*C*H), 97.9 (O*C*HO), 63.4 (CH*C*H$_2$O), 62.2 (O*C*H$_2$(CH_2)$_3$), 42.4 ((O)CH*C*H$_2$), 32.2 & 26.5 (2 x CH_2*C*H$_2$), 30.7 (OCH$_2$*C*H$_2$), 25.5 (*C*H$_2$), 24.2 (*C*H$_2$), 23.6 & 23.1 (2 x C*H*$_3$), 19.6 (*C*H$_2$). **LRMS** (ES^+): 303.19 (100% [M + Na]), 243.08 (50%), 179.14 (20%), 161.12 (20%). **HRMS** (ES^+): calculated for [$C_{17}H_{28}O_3Na$]; 303.1936, found 303.1933.

Preparation of ethyl (2Z,6Z,10Z)-2,6,10-trimethyl-12-((tetrahydro-2H-pyran-2-yl)oxy)dodeca-2,6,10-trienoate (402):

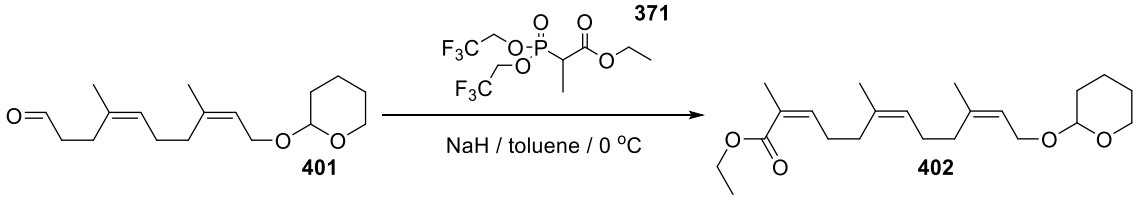

371 (187 mg, 0.54 mmol, 2 eq.) was added to a stirred suspension of sodium hydride (24 mg, 0.6 mmol, 2.2 eq.) in anhydrous toluene (20 mL) at 0 °C. The reaction mixture was warmed to room temperature and stirred for 1 hour. The reaction mixture was cooled to 0 °C and **401** (76 mg, 0.27mmol, 1 eq.) was added dropwise and stirred for 16 hours at room temperature. The reaction was quenched with water (5 mL) and organic products extracted with diethyl ether (3 x 10 mL). Combined organic extracts were washed with water (3 x 10 mL), brine (3 x 10 mL), dried over anhydrous sodium sulphate and filtered. Solvent was removed under reduced pressure and crude product purified *via* flash chromatography (10% ethyl acetate in hexane) to give ester **402** as a colourless oil (94 mg, 95%).

^{1}H NMR (300 MHz, $CDCl_3$) δ 5.91 (1H, td, *J* = 7.4, 1.4 Hz, (EtO(O)CCC*H*)), 5.39 (1H, t, *J* = 7.6 Hz, C*H*CH_2O), 5.19 – 5.11 (1H, m, (CH_3)CC*H*), 4.64 (1H, t, *J* = 3.4 Hz, OC*H*O), 4.21 (3H, q, *J* = 7.1 Hz, CH_3C*H*$_2$O), 4.29 – 3.94 (2H, m, CHC*H*$_2$O), 3.93 – 3.47 (2H, m, CHOC*H*$_2$), 2.55 (2H, q, *J* = 7.4 Hz,

(EtO(O)CCCHCH_2), 2.18 – 2.03 (6H, m, 3 x allylic CH_2), 1.90 (3H, s, CH_3), 1.76 (3H, s, CH_3), 1.69 (3H, s, CH_3), 1.67 – 1.47 (6H, m, 3 x CH_2), 1.31 (3H, t, *J* = 7.1 Hz,CH_3CH$_2$O). **^{13}C NMR** (75 MHz, $CDCl_3$) δ 168.1 (EtOC(O)*C*CH), 142.2 (EtOC(O)C*C*H), 140.4 & 134.9 & 127.4 (3 x (CH$_3$)*C*CH), 125.2 & 121.7 (2 x (CH$_3$)C*C*H), 97.9 (O*C*HO), 63.4 (CH*C*H$_2$O) 62.2 (O*C*H$_2$(CH$_2$)$_3$), 60.1 (CH$_3$*C*H$_2$O), 32.4 & 31.3 & 26.5 (3 x allylic *C*H$_2$), 30.7 (OCH$_2$*C*H$_2$) 27.9 (EtOC(O)CCH*C*H$_2$), 25.5 (*C*H$_2$), 23.61 (*C*H$_2$), 23.2 (*C*H$_3$), 22.7 (*C*H$_3$), 20.7 (*C*H$_3$), 14.3 (*C*H$_3$CH$_2$O). **LRMS** (AP$^+$): 387.25 (100% [M + Na]), 306.09 (10%), 263.20 (35%), 217.16 (10%), 161.12 (20%). **HRMS** (AP$^+$): calculated for [$C_{22}H_{36}O_4Na$]; 387.2511, found 387.2503.

Preparation of (2Z,6Z,10Z)-2,6,10-trimethyl-12-((tetrahydro-2H-pyran-2-yl)oxy)dodeca-2,6,10-trien-1-ol (403):

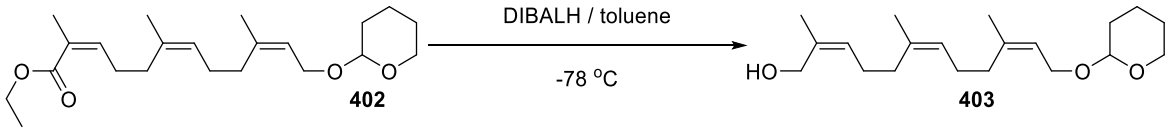

Ester **402** (94 mg, 0.26 mmol, 1 eq.) in anhydrous toluene (10 mL) was cooled to -78 °C and DIBALH (770 µL, 0.77 mmol, 3 eq.) added dropwise. Reaction was stirred at -78 °C until complete consumption of starting material was observed *via* TLC (20% ethyl acetate in hexane), warmed to room temperature and quenched with Rochelle salts (2 mL). Quenched reaction mixture was stirred at room temperature for 16 hours and reaction products extracted with DCM (3 x 5 mL). Combined organic extracts were washed with water (3 x 5 mL), brine (3 x 5 mL), dried over anhydrous sodium sulphate and filtered. Solvent was removed under reduced pressure and crude products purified by column chromatography (10% ethyl acetate in hexane) to give alcohol **403** as a colourless oil (89 mg, 100%).

^{1}H NMR (300 MHz, $CDCl_3$) δ 5.31 (1H, t, *J* = 6.9 Hz, (HOCH$_2$(CH$_3$)CC*H*), 5.21 (1 H, t, *J* = 7.1 Hz, C*H*CH$_2$O), 5.07 (1H, t, *J* = 7.9 Hz, (CH$_3$)CC*H*), 4.56 (1H, t, *J* = 3.6 Hz, OC*H*O), 4.03 (2H, dd, *J* = 11.8, 7.0 Hz, CHC*H*$_2$O), 4.02 (2H, s, C*H*$_2$OH), 3.85 – 3.40 (2H, m, CHOC*H*$_2$), 2.11 – 1.92 (8H, m, 4 x allylic C*H*$_2$), 1.73 (3H, s, C*H*$_3$), 1.68 (3H, s, C*H*$_3$), 1.61 (3H, s, C*H*$_3$), 1.58 – 1.37 (6H, m, 3 x C*H*$_2$). **^{13}C NMR** (75 MHz, $CDCl_3$) δ 140.4 & 135.3 & 134.9 (3 x (CH$_3$)*C*CH), 127.9 (*C*HCH$_2$O), 125.2 ((CH$_3$)C*C*H), 121.6 (HOCH$_2$(CH$_3$)C*C*H), 97.9 (O*C*HO), 63.5 (CH*C*H$_2$O), 62.1 (O*C*H$_2$(CH$_2$)$_3$), 61.4 (*C*H$_2$OH), 32.5 & 32.0 & 26.7 & 26.2 (4 x allylic *C*H$_2$) 30.7 (OCH$_2$*C*H$_2$), 25.5 (*C*H$_2$), 23.7 & 23.5 & 21.4 (3 x *C*H$_3$), 19.5 (*C*H$_2$). **LRMS** (ES$^+$): 345.24 (100% [M + Na]), 305.25 (10%), 287.24 (7%), 265.06 (7%), 243.08 (6%), 221.19 (12%), 203.18 (30%), 163.15 (3%). **HRMS** (ES$^+$): calculated for [$C_{20}H_{34}O_3Na$]; 345.2406, found 345.2421.

Table 25. 2D proton NMR correlations revealing spatial arrangement in 403

403: NOESY ^{1}H - ^{1}H interactions	
From / ppm	To / ppm
5.31	3.62 / 1.68
5.21	2.01 / 1.61
5.07	1.68 / 2.01
4.02	2.01 / 1.68

Preparation of 2-(((2Z,6Z,10Z)-12-methoxy-3,7,11-trimethyldodeca-2,6,10-trien-1-yl)oxy)tetrahydro-2H-pyran (404):

403 **404**

A solution of **403** (168 mg, 0.52 mmol, 1 eq.) in anhydrous tetrahydrofuran (5 mL) was added dropwise to a stirred suspension of sodium hydride (125 mg, 3.13 mmol, 6 eq.) in anhydrous tetrahydrofuran (20 mL) and stirred for 15 minutes. Methyl iodide (2.81 g, 19.83 mmol, 38 eq.) was added dropwise and stirred for 48 hours at room temperature at which complete consumption of starting material was observed *via* TLC (20% ethyl acetate in hexane). The reaction was quenched with 1 M hydrochloric acid (10 mL) and the aqueous layer extracted with diethyl ether (3 x 10 mL). Combined organic layers were washed with *sat*. sodium bicarbonate (3 x 10 mL), water (3 x 10 mL), brine (3 x 10 mL),dried over anhydrous sodium sulphate and filtered. Solvent was removed under reduced pressure and crude product was purified by column chromatography (20% ethyl acetate in hexane) to give **404** as a colourless oil (88 mg, 52%).

^{1}H NMR (300 MHz, $CDCl_3$) δ 5.44 – 5.32 (1H, m, ($CH_3OCH_2(CH_3)CCH$), 5.20 – 5.07 (1 H, m, $CHCH_2O$), 4.64 (1H, s, $OCHO$)), 4.11 (2H, dd, *J* = 11.6, 7.1 Hz, $CHCH_2O$), 3.93 (2H, s, CH_2OCH_3), 3.87 – 3.45 (2H, m, $CHCH_2O$), 3.30 (3H, s, CH_2OCH_3), 2.19 – 2.00 (8H, m, 4 x allylic CH_2), 1.75 (3H, s, CH_3), 1.69 (3H, s, CH_3), 1.91 – 1.49 (6H, m, 3 x CH_2), 1.27 (3H, s, CH_3). **^{13}C NMR** (75 MHz, $CDCl_3$) δ 140.4 & 135.1 & 132.1 (3 x (CH_3)CCH), 129.2 ($CHCH_2O$), 125.0 ((CH_3)CCH), 121.6 ($CH_3OCH_2(CH_3)CCH$), 97.9 ($OCHO$), 70.7 (CH_3OCH_2), 63.4 ($CHCH_2O$), 62.2 ($OCH_2(CH_2)_3$), 57.6 (CH_3OCH_2), 32.4 & 32.1 & 26.6 & 26.2 (4 x allylic CH_2), 30.7 (CH_2), 25.5 (CH_2), 23.6 & 23.4 & 21.5 (3 x CH_3), 19.6 (CH_2). **LRMS** (ES^+): 359.26 (100% [M + Na]), 287.24 (7%), 235.21 (5%), 203.18 (32%), 163.14 (2%). **HRMS** (ES^+): calculated for [$C_{21}H_{36}O_3Na$]; 359.2562, found 359.2567.

Preparation of (2Z,6Z,10Z)-12-methoxy-3,7,11-trimethyldodeca-2,6,10-trien-1-ol (405):

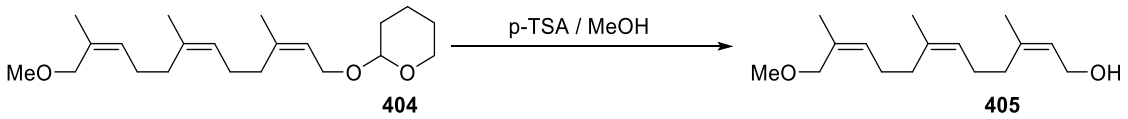

To a stirred solution of **404** (59 mg, 0.17 mmol, 1 eq.) in methanol (5 mL) was added *p*-toluenesulfonic acid (3 mg, cat.) and stirred at room temperature for 2 hours. The reaction volume was reduced by 80% under *vaccuo* and diluted with *sat*. sodium bicarbonate solution (5 mL) and separated with hexane (5 mL). The aqueous layer was washed with hexane (3 x 5 mL) and combined organic fraction washed with brine (10 mL), dried over anhydrous sodium sulphate and filtered. Solvent was removed under reduced pressure and purified by flash chromatography (20% ethyl acetate in hexane) to give **405** as a colourless oil (22 mg, 54%).

^{1}H NMR (300 MHz, $CDCl_3$) δ 5.38 (1H, t, *J* = 6.8 Hz, ($CH_3OCH_2(CH_3)CCH$), 5.30 (1H, t, *J* = 7.0 Hz, $CHCH_2O$), 5.12 – 5.00 (1H, m, $CH_2(CH_3)CCH$), 4.02 (2H, d, *J* = 7.0 Hz, $CHCH_2O$), 3.85 (2H, s, $CH_3OCH_2(CH_3)CCH$), 3.22 (3H, s, $CH_3OCH_2(CH_3)$), 2.13 – 1.92 (8H, m, 4 x CH_2), 1.68 (6H, s, 3 x CH_3), 1.62 (3H, s, CH_3). **^{13}C NMR** (75 MHz, $CDCl_3$) δ 139.8 & 135.6 & 132.2 (3 x (CH_3)*C*CH), 129.1 (*C*HCH_2O), 124.9 & 124.5 (2 x (CH_3)*C*CH), 70.9 (CH_3OCH_2), 59.0 ($CHCH_2O$), 57.7 (CH_3OCH_2), 32.2 & 32.1 & 26.4 & 26.2 (4 x allylic CH_2), 23.5 & 23.3 & 21.6 (3 x CH_3). **LRMS** (ES^+): 252.22 (2% [M]), 235.21 (45%), 203.18 (7%), 189.17 (14%), 163.14 (3%), 147.11 (2%). **HRMS** (EI^+): calculated for [$C_{16}H_{28}O_2$] [M]; 252.2089, found 252.2088.

Preparation of (2Z,6Z,10Z)-12-methoxy-1-bromo-2,6,10-trimethyldodeca-2,6,10-triene (406):

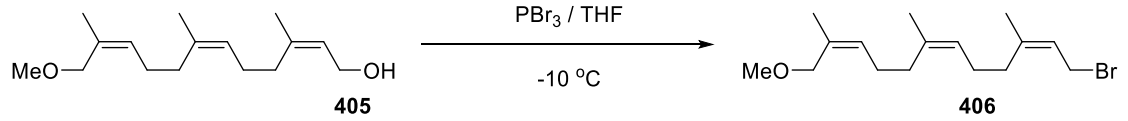

Phosphorus tribromide (9 µL, 0.09 mmol, 1 eq.) was added dropwise to a stirred solution of **405** (45 mg, 0.18 mmol, 2 eq.) in anhydrous THF (10 mL) at -10 °C. the reaction mixture was stirred at -10 °C until complete consumption of starting material was observed *via* TLC (20% ethyl acetate in hexane). Reaction was quenched with *sat*. sodium bicarbonate sol (5 mL) and product extracted with diethyl ether (3 x 5 mL). Combined organic extracts were washed with water (3 x 5 mL), brine (3 x 5 mL),

dried over anhydrous sodium sulphate and filtered. Solvents were removed under reduced pressure to give bromide **406** as a pale yellow oil (56 mg. 100%) that was used without further purification.

^{1}H NMR (300 MHz, $CDCl_3$) δ 5.51 – 5.45 (1H, m, ($CH_3OCH_2(CH_3)CCH$), 5.35 – 5.26 (1H, t, *J* = 7.0 Hz, $CHCH_2Br$), 5.09 – 5.01 (1H, m, $CH_2(CH_3)CCH$), 3.93 (2H, d, *J* = 8.4 Hz, $CHCH_2Br$), 3.85 (2H, s, $CH_3OCH_2(CH_3)CCH$), 3.22 (3H, s, $CH_3OCH_2(CH_3)$), 2.28 – 1.97 (8H, m, 4 x CH_2), 1.67 (3H, s, CH_3), 1.61 (3H, s, CH_3), 1.55 (3H, s, CH_3).

Preparation of (2Z,6Z,10Z)-12-methoxy-3,7,11-trimethyldodeca-2,6,10-trien-1-yl diphosphate (362):

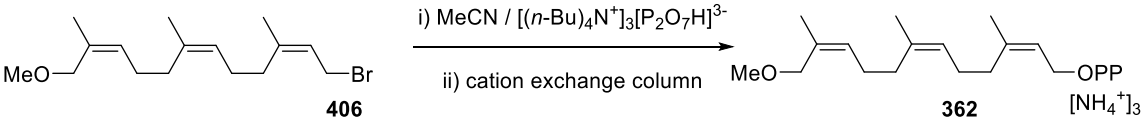

Tris tetra butyl ammonium pyrophosphate (240 mg, 0.266 mmol, 1.5 eq.) in anhydrous acetonitrile (3 mL) was added to crude bromide **406** (56 mg, 0.178 mmol, 1 eq.) under argon. The reaction was stirred for 16 hours at room temperature and volatile solvents removed under reduced pressure to give crude diphosphate as a brown oil. Crude diphosphate was dissolved in buffer solution (25 mM NH_4HCO_3, 2% iPrOH) (5 mL) and the tris tetrabutylammonium salt counter ions were exchanged for ammonium by ion exchange column containing Amberlyst 131 (wet H^+ form) mesh cation exchange resin pre-equilibrated with ion-exchange buffer (25 mM NH_4HCO_3, 2% isopropanol). The appropriate fractions were collected and lyophilized to yield diphosphate **362** as a white powder. The powder was dissolved in buffer solution (25 mM NH_4HCO_3, 2% iPrOH) (5 mL) and purified using HPLC (Solvent A: acetonitrile, solvent B: 2% iPrOH). The appropriate fractions were collected and lyophilized to give **362** as a white powder (2 mg, 2%).

^{1}H NMR (500 MHz, D_2O) δ 5.41 – 5.30 (2H, m, 2 x (CH_3)CC*H*)), 5.14 – 5.06 (1H, m, (CH_3)CC*H*), 4.36 – 4.30 (2H, m, $CHCH_2O$), 3.88 (2H, s, $CH_3OCH_2(CH_3)CCH$), 3.18 (3H, s, $CH_3OCH_2(CH_3)$), 2.10 – 1.94 (8H, m, 4 x CH_2), 1.64 (3H, s, CH_3), 1.59 (3H, s, CH_3), 1.56 (3H, s, CH_3). **^{31}P NMR** (202 MHz, D_2O) δ -5.87 (d, *J* = 19.0 Hz), -9.43 (d, *J* = 17.7 Hz). **HRMS** (ES^-) [$C_{16}H_{29}O_8P_2$][M]; 411.1338, found 411.1338.

8.2.17 Synthesis of (2*Z*,6*Z*,10*E*)-13-methoxyfarnesyl diphosphate(363)

Preparation of ethyl (2E,6Z,10Z)-2,6,10-trimethyl-12-((tetrahydro-2H-pyran-2-yl)oxy)dodeca-2,6,10-trienoate (417):

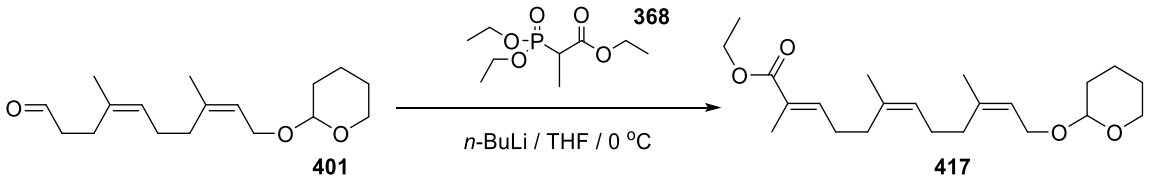

A stirred solution of **368** (440 mg, 1.27 mmol, 2 eq.) in anhydrous tetrahydrofuran (20 mL) was cooled to 0 °C and *n*-butyl lithium (51 µL, 1.27 mmol, 2 eq., 2.5M in hexanes) was added dropwise. The resulting solution was stirred at room temperature for 1 hour, cooled to 0 °C and **401** (178 mg, 0.64 mmol, 1 eq.) added dropwise. The reaction mixture was stirred for 16 hours at room temperature. The reaction was quenched with water (5 mL) and the product was extracted with diethyl ether (3 x 5 mL). The combined organic phases were washed with water (3 x 10 mL) and brine (2 x 10 mL), then dried over sodium sulphate, filtered and the solvent removed under reduced pressure. Purification *via* flash chromatography on silica gel (5% ethyl acetate in hexane) provided ester **417** as a clear oil (210 mg, 91%).

^{1}H NMR (300 MHz, $CDCl_3$) δ 6.75 (1H, td, *J* = 7.3, 1.4 Hz, (EtO(O)CCC*H*)), 5.43 – 5.36 (1H, m, C*H*CH_2O), 5.17 (1H, dt, *J* = 9.2, 2.8 Hz, (CH_3)CC*H*), 4.63 (1H, t, *J* = 3.4 Hz, OC*H*O), 4.19 (3H, q, *J* = 7.1 Hz, CH_3CH_2O), 4.27 – 3.94 (2H, m, $CHCH_2O$), 3.93 – 3.47 (2H, m, $CHOCH_2$), 2.32 – 2.05 (8H, m, 4 x allylic CH_2), 1.85 (3H, s, CH_3), 1.76 (3H, d, *J* = 1.0 Hz, CH_3), 1.71 (3H, s, CH_3), 1.65 – 1.47 (6H, m, 3 x CH_2), 1.30 (3H, t, *J* = 7.1 Hz,CH_3CH_2O). **^{13}C NMR** (75 MHz, $CDCl_3$) δ 168.2 (EtOC(O)*C*CH), 141.6 (EtOC(O)C*C*H), 140.3 & 134.4 & 127.9 (3 x (CH_3)*C*CH), 125.5 & 121.7 (2 x (CH_3)C*C*H), 97.9 (O*C*HO), 63.4 ($CHCH_2O$), 62.2 ($OCH_2(CH_2)_3$), 60.4 (CH_3CH_2O), 32.3 & 30.6 & 27.3 & 26.9 (4 x allylic CH_2), 30.7 (OCH_2CH_2), 25.5 (CH_2), 25.3 (CH_2), 23.6 (CH_3), 23.3 (CH_3), 14.3 (CH_3CH_2O), 12.4 (CH_3). **LRMS** (ES^+): 387.25 (70% [M + Na]), 382.30 (35%), 263.20 (100%), 217.16 (5%), 189.16 (10%). **HRMS** (ES^+): calculated for [$C_{22}H_{36}O_4Na$]; 387.2511, found 387.2517.

Preparation of ethyl (2E,6Z,10Z)-2,6,10-trimethyl-12-((tetrahydro-2H-pyran-2-yl)oxy)dodeca-2,6,10-trien-1-ol (418):

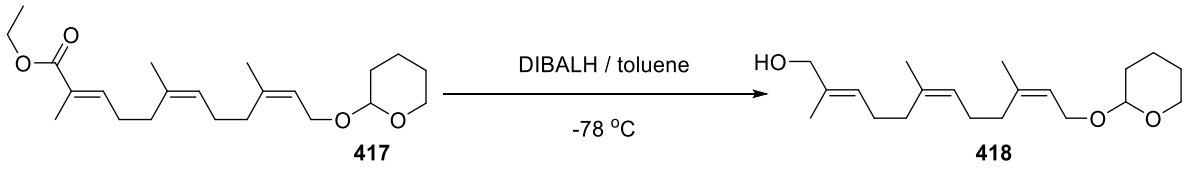

417 **418**

Diisobutylaluminimiun hydride (922 µL, 0.922 mmol, 3 eq.) was added to a stirred solution of **417** (112 mg, 0.307 mmol, 1 eq.) in anhydrous toluene (5 mL) at -78 °C. The reaction was stirred for 3 hours at -78 °C and quenched with saturated potassium sodium tartrate solution (5 mL). Reaction products were extracted with dichloromethane (3 x 5 mL). Combined organic extracts were washed with water (3 x 5 mL), brine (3 x 5 mL), dried over sodium sulphate and concentrated under reduced pressure. Purification *via* flash chromatography on silica gel (20% ethyl acetate in hexane) to yield **418** as a clear oil (97 mg, 98%).

^{1}H NMR (300 MHz, $CDCl_3$) δ 5.37 – 5.27 (2H, m, 2 x $(CH_3)CCH$), 5.12 – 5.00 (1H, m, $(CH_3)CCH$), 4.57 (1H, t, $OCHO$), 4.20 – 3.86 (2H, m, $CHCH_2O$), 3.92 (2H, s, CH_2OH), 3.85 – 3.38 (2H, m, $CHOCH_2$), 2.13 – 1.90 (8H, m, 4 x allylic CH_2), 1.69 (3H, s, CH_3), 1.61 (3H, s, CH_3), 1.60 (3H, s, CH_3), 1.56 – 1.40 (6H, m, 3 x CH_2), 1.18 (3H, s, CH_3). **^{13}C NMR** (75 MHz, $CDCl_3$) δ 140.4 & 135.3 & 135.0 (3 x $(CH_3)CCH$), 125.5 ($CHCH_2O$), 124.9 ($(CH_3)CCH$), 121.6 ($HOCH_2(CH_3)CCH$), 97.8 ($OCHO$), 68.8 (CH_2OH), 63.5 ($CHCH_2O$), 62.1 ($OCH_2(CH_2)_3$), 32.5 & 31.5 & 26.6 & 26.1 (4 x allylic CH_2), 30.7 (OCH_2CH_2) 25.5 (CH_2), 23.6 & 23.3 & 21.3 (3 x CH_3), 19.4 (CH_2). **LRMS** (ES^+): 345.24 (100% [M + Na]), 323.15 (2%), 203.18 (6%). **HRMS** (ES^+): calculated for $[C_{22}H_{36}O_3Na]$; 345.2406, found 345.2409.

Table 26. 2D proton NMR correlations revealing spatial arrangement in 418

418: NOESY ^{1}H - ^{1}H interactions	
From / ppm	To / ppm
5.32	1.61 / 1.48
5.06	1.61
3.92	5.06 / 1.69
2.02	1.69

Preparation of 2-(((2Z,6Z,10Z)-13-methoxy-3,7,11-trimethyldodeca-2,6,10-trien-1-yl)oxy)tetrahydro-2H-pyran (419):

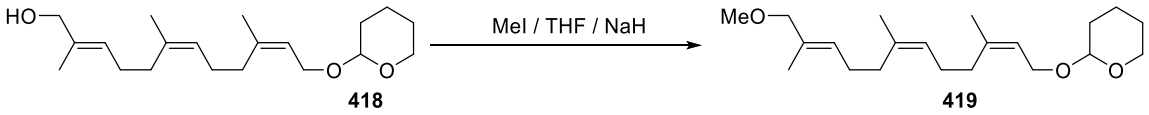

418 **419**

To a stirred suspension of sodium hydride (121 mg, 3.03 mmol, 6 eq.) in anhydrous tetrahydrofuran (20 mL) a solution of **418** (163 mg, 0.51 mmol, 1 eq.) in anhydrous tetrahydrofuran (5 mL) was added dropwise and stirred for 15 minutes. Methyl iodide (2.73 g, 19.2 mmol, 38 eq) was added dropwise and stirred for 48 hours at room temperature at which complete consumption of starting material was observed *via* TLC (20% ethyl acetate in hexane). The reaction was quenched with 1 M hydrochloric acid (5 mL) and the aqueous layer extracted with diethyl ether (3 x 10 mL). Combined organic layers were washed with *sat*. sodium bicarbonate (3 x 10 mL), water (3 x 10 mL), brine (3 x 10 mL),dried over anhydrous sodium sulphate and filtered. Solvent was removed under reduced pressure and crude product was purified by column chromatography (20% ethyl acetate in hexane) to give **419** as a colourless oil (95 mg, 56%).

^{1}H NMR (300 MHz, $CDCl_3$) δ 5.49 – 5.34 (1H, m, ($CH_3OCH_2(CH_3)CCH$), 5.20 – 5.06 (1 H, m, $CHCH_2O$), 4.64 (1H, s, $OCHO$), 3.94 – 3.48 (2H, m, $CHCH_2O$), 3.80 (2H, s, CH_2OCH_3), 3.94 – 3.48 (2H, m, $CHCH_2O$), 3.28 (3H, s, CH_2OCH_3), 2.28 – 1.99 (8H, m, 4 x allylic CH_2), 1.76 (3H, s, CH_3), 1.70 (3H, s, CH_3), 1.90 – 1.47 (6H, m, 3 x CH_2), 1.66 (3H, s, CH_3). **^{13}C NMR** (75 MHz, $CDCl_3$) δ 140.5 & 135.3 & 132.2 (3 x (CH_3)CCH), 128.0 ($CHCH_2O$), 124.8 ((CH_3)CCH), 121.6 ($CH_3OCH_2(CH_3)CCH$), 97.9 ($OCHO$), 72.3 (CH_3OCH_2), 63.4 ($CHCH_2O$), 62.2 ($OCH_2(CH_2)_3$), 57.4 (CH_3OCH_2), 32.4 & 31.6 & 26.5 & 26.3 (4 x allylic CH_2), 30.7 (CH_2), 25.5 (CH_2), 23.6 & 23.4 & 22.7 (3 x CH_3), 19.6 (CH_2). **LRMS** (ES^+): 359.26 (100% [M + Na]), 319.27 (2%), 287.24 (7%), 235.21 (5%), 203.18 (32%), 163.14 (2%), 147.11 (2%). **HRMS** (ES^+): calculated for [$C_{21}H_{36}O_3Na$]; 359.2562, found 359.2565.

Preparation of (2Z,6Z,10E)-12-methoxy-3,7,11-trimethyldodeca-2,6,10-trien-1-ol (420):

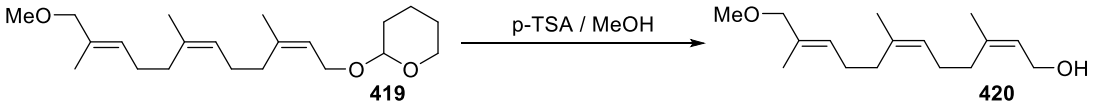

p-Toluenesulfonic acid (5 mg, cat.) was added to a stirred solution of **419** (99 mg, 0.29 mmol, 1 eq.) in methanol (5 mL) and stirred at room temperature for 2 hours. The reaction volume was reduced by 80% under *vaccuo* and diluted with *sat*. sodium bicarbonate solution (5 mL) and separated with hexane (5 mL). The aqueous layer was washed with hexane (3 x 5 mL) and combined organic fraction washed with brine (5 mL), dried over anhydrous sodium sulphate and filtered. Solvent was removed under reduced pressure and purified by flash chromatography (20% ethyl acetate in hexane) to give **420** as a colourless oil (73 mg, 98%).

^{1}H NMR (300 MHz, $CDCl_3$) δ 5.53 – 5.35 (2H, m, 2 x $(CH_3)CCH$), 5.21 – 5.08 (1H, m, $(CH_3)CCH$), 4.10 (2H, d, *J* = 7.0 Hz, $CHCH_2O$), 3.80 (2H, s, $CH_3OCH_2(CH_3)CCH$), 3.29 (3H, s, $CH_3OCH_2(CH_3)$), 2.31 – 2.01 (8H, m, 4 x CH_2), 1.76 (3H, s, CH_3), 1.71 (3H, s, CH_3), 1.66 (3H, s, CH_3). **^{13}C NMR** (75 MHz, $CDCl_3$) δ 139.9 & 135.9 & 132.3 (3 x $(CH_3)CCH$), 127.8 ($CHCH_2O$), 124.8 & 124.5 (2 x $(CH_3)CCH$), 78.7 (CH_3OCH_2), 59.0 ($CHCH_2O$), 57.5 (CH_3OCH_2), 32.2 & 31.5 & 26.4 & 26.3 (4 x allylic CH_2), 23.5 & 23.3 & 13.8 (3 x CH_3). **LRMS** (ES^+): 252.22 (2% [M]), 235.21 (45%), 203.18 (10%), 189.17 (14%), 163.14 (5%), 147.11 (2%). **HRMS** (EI^+): calculated for $[C_{16}H_{28}O_2]$ [M]; 252.2089, found 252.2093.

Preparation of (2E,6Z,10Z)-12-bromo-1-methoxy-2,6,10-trimethyldodeca-2,6,10-triene (421):

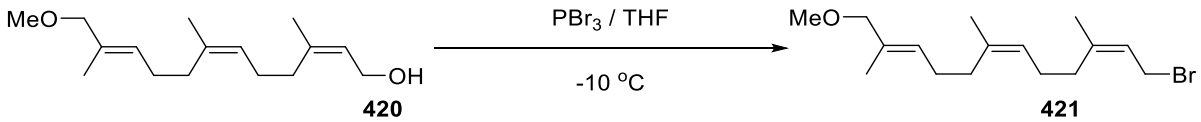

Phosphorus tribromide (11 µL, 0.12 mmol, 1 eq.) was added dropwise to a stirred solution of **420** (60 mg, 0.24 mmol, 2 eq.) in anhydrous THF (10 mL) at -10 °C. Reaction was quenched with sat. sodium bicarbonate sol. (5 mL) upon completion observed *via* TLC (20% ethyl acetate in hexanes). Reaction products were extracted with diethyl ether (3 x 5 mL) and ethereal layers were washed with water (3 x 5 mL) and brine (3 x 5 mL). Products were dried over sodium sulphate, filtered and concentrated under reduced pressure to give **421** as a crude yellow oil (75 mg, 100%) which was used without further purification.

^{1}H NMR (300 MHz, $CDCl_3$) δ 5.39 – 5.27 (2H, m, 2 x $(CH_3)CCH$), 5.09 – 5.01 (1H, m, $(CH_3)CCH$), 4.06 (2H, d, *J* = 8.4 Hz, $CHCH_2Br$), 4.00 (2H, s, $CH_3OCH_2(CH_3)CCH$), 3.29 (3H, s, $CH_3OCH_2(CH_3)$), 2.23 – 1.93 (8H, m, 4 x CH_2), 1.68 (3H, s, CH_3), 1.62 (3H, s, CH_3), 1.58 (3H, s, CH_3).

Preparation of (2E,6Z,10Z)- 1-methoxy-2,6,10-trimethyldodeca-2,6,10-trien-12-yl diphosphate (363):

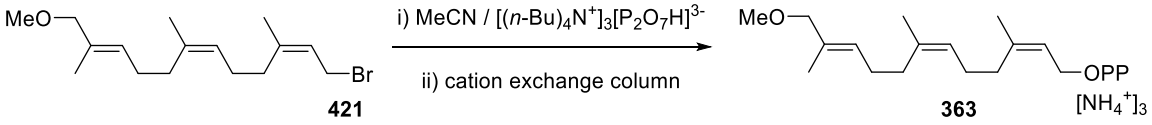

A mixture of crude bromide **421** (75 mg, 0.238 mmol, 1 eq.) and tris tetrabutyl ammonium pyrophosphate (322 mg, 0.357 mmol, 1.5 eq.) in anhydrous acetonitrile (5 mL) was stirred at room temperature for 16 hours. The reaction mixture was concentrated under reduced pressure and the resultant residue dissolved in buffer solution (25 mM NH_4HCO_3, 2% iPrOH) (7 mL) and the tris tetrabutylammonium salt counter ions were exchanged for ammonium by ion exchange column containing Amberlyst 131 (wet H^+ form) mesh cation exchange resin pre-equilibrated with ion-exchange buffer (25 mM NH_4HCO_3, 2% isopropanol). The appropriate fractions were collected and lyophilized to yield diphosphate **363** as a white powder. The powder was dissolved in buffer solution (25 mM NH_4HCO_3, 2% iPrOH) (10 mL) and purified using HPLC (Solvent A: acetonitrile, solvent B: 2% iPrOH). The appropriate fractions were collected and lyophilized to give diphosphate **363** as a white powder (2 mg, 2%).

^{1}H NMR (500 MHz, D_2O) δ 5.47 – 5.35 (2H, m, 2 x $(CH_3)CCH$), 5.19 – 5.08 (1H, m, $(CH_3)CCH$), 4.48 – 4.33 (2H, m, $CHCH_2O$) 3.81 (2H, s, $CH_3OCH_2(CH_3)CCH$), 3.21 (3H, s, $CH_3OCH_2(CH_3)$), 2.17 – 1.96 (8H, m, 4 x CH_2), 1.83 (3H, s, CH_3), 1.62 (3H, s, CH_3), 1.57 (3H, s, CH_3). **^{31}P NMR** (202 MHz, D_2O) δ -5.92 (d, *J* = 19.1 Hz), -9.48 (d, *J* = 17.9 Hz). $[C_{16}H_{29}O_8P_2][M]$; 411.1338, found 411.1333.

8.2.18 Synthesis of ethyl 2-(bis(2,2,2-trifluoroethoxy)phosphoryl)acetate (204)

Preparation of ethyl 2-(bis((trimethylsilyl)oxy)phosphoryl)acetate (205):

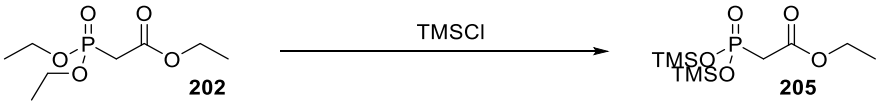

Triethyl phosphono acetate (**202**) (2.26 g, 10.0 mmol, 1 eq.) and trimethyl silyl chloride (5.47 g, 50 mmol, 5 eq.) were placed in a sealed pressurised tube under argon and stirred at 60 °C for 7 days. The mixture was concentrated under a steam of nitrogen and dried under vacuum for 1 hour to give **205** as a light yellow oil (2.64 g, 84%) which was taken forward without further purification.

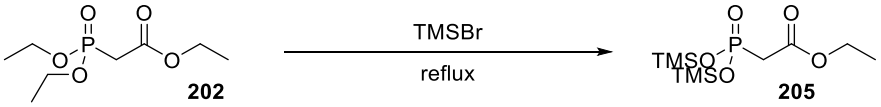

Triethyl phosphono acetate (**202**) (15 g, 59.3 mmol, 1 eq.) was added to trimethyl silyl bromide (39 mL, 296.1 mmol, 5 eq.) and refluxed at 80 °C for 5 hours. The mixture was concentrated under a steam of nitrogen and dried under vacuum for 1 hour to give **205** as an orange oil (20 g, 100%) which was taken forward without further purification.

^{1}H NMR (300 MHz, $CDCl_3$) δ 4.13 (2H, q, *J* = 7.1 Hz, OCH_2CH_3), 2.92 (2H, d, *J*= 22.2 Hz, PCH_2CO), 1.22 (3H, t, *J* = 7.1 Hz, OCH_2CH_3), 0.26 (18H, s, 2 x $(CH_3)_3Si$). **^{31}P NMR** (162 MHz, $CDCl_3$) δ 13.93. **LRMS** (ES^+): 312.10 (10% [M]), 297.08 (40%), 269.04 (70%), 211.00 (100%). **HRMS** (ES^+): calculated for $[C_{10}H_{25}O_5Si_2P]^+$; 312.0974, found 312.0978.

Preparation of ethyl 2-(dichlorophosphoryl)acetate (206):

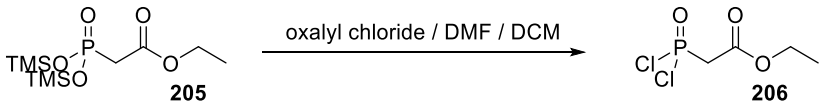

A stirred solution of ethyl 2-(bis((trimethylsilyl)oxy)phosphoryl)acetate (**205**) (20 g, 59.25 mmol, 1 eq.) in dichloromethane (50 mL) was added dropwise oxalyl chloride (21.3 g, 279.25 mmol, 2.5 eq.), dimethyl formamide (0.1 mL, cat.) and stirred for 2 hours. The mixture was concentrated under a

steam of nitrogen and dried under vacuum for 1 hour to give **206** as a light orange oil (13.7 g, 100%) which was taken forward without further purification.

^{1}H NMR (300 MHz, $CDCl_3$) δ 4.31 (2H, q, *J* = 7.1 Hz, OCH_2CH_3), 3.75 (2H, d, *J*= 19.1 Hz, PCH_2CO), 1.34 (3H, t, *J* = 7.1 Hz, OCH_2CH_3). **^{31}P NMR** (162 MHz, $CDCl_3$) δ 33.42.

Preparation of ethyl 2-(bis(2,2,2-trifluoroethoxy)phosphoryl)acetate (204):

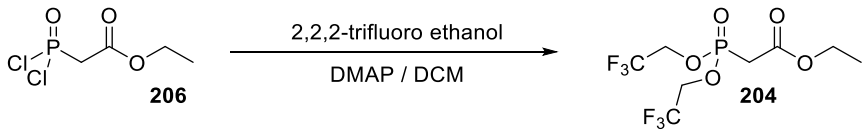

A stirred solution of ethyl 2-(dichlorophosphoryl)acetate (**206**) (13.7 g, 59.25 mmol, 1 eq.) in dichloromethane (50 mL) was cooled to 0 °C. A solution of 2,2,2-tri fluoro ethanol (26.8 g, 268.1 mmol, 4 eq.) and triethylamine (40.7 g, 402.15 mmol, 6 eq.) was cooled to 0 °C and added to the reaction mixture dropwise. 4-dimethylaminopyridine (164 mg, 1.34 mmol, 0.02 eq.) was added and the reaction mixture was stirred for 2 hours at room temperature, diluted with dichloromethane (100 mL) and stirred for 1 hour. Mixture was washed with water (3 x 50 mL) and brine (3 x 50 mL), dried over magnesium sulfate and concentrated under reduced pressure. Purification *via* flash chromatography on silica gel (40% ethyl acetate in hexane) provided phosphono acetate **204** as a brown oil (10.48 g, 47%).

^{1}H NMR (300 MHz, $CDCl_3$) δ 4.40 (2H, quin, *J* = 8.1 Hz, OCH_2CF_3), 4.16 (2H, q, *J* = 7.2 Hz, OCH_2CH_3), 3.10 (2H, d, *J*= 21.1 Hz, PCH_2CO), 1.23 (3H, t, *J* = 7.2 Hz, OCH_2CH_3). **^{13}C NMR** (125 MHz, $CDCl_3$) δ 164.7 ($CH_2C(O)OCH_2$), 124.3 (d, J_{CF} = 8.2 Hz, OCH_2CF_3), 120.6 (d, J_{CF} = 8.6 Hz, OCH_2CF_3), 62.8 (d, $^{3}J_{CF}$ = 5.5 Hz, 2 x CF_3CH_2O), 62.3 (2 x CH_3CH_2O), 34.0 (d, J_{CP} = 144.5 Hz, $P(O)CH_2CO$), 13.9 (OCH_2CH_3). **^{31}P NMR** (202 MHz, $CDCl_3$) δ 23.55. **^{19}F NMR** (471 MHz, $CDCl_3$) δ -77.11. **LRMS** (ES^+): 333.03 (100% [M + H]), 305.00 (15%), 286.99 (10%). **HRMS** (ES^+): calculated for $[C_8H_{12}O_5F_6P]^+$; 333.0327, found 333.0327.

8.2.19 Synthesis of ethyl 2-(diphenoxyphosphoryl)acetate (203)

Preparation of ethyl 2-(diphenoxyphosphoryl)acetate (203):

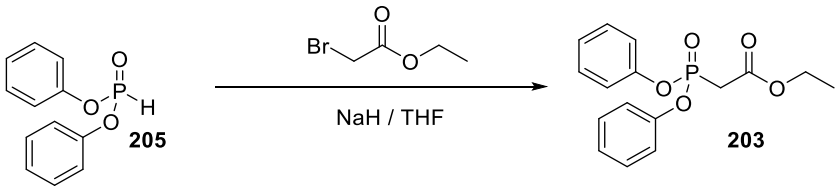

205 (3.51 g,15 mmol, 1 eq.) was added dropwise over 30 minutes to a stirred suspension of sodium hydride (360 mg, 15 mmol, 1 eq.) in anhydrous THF (40 mL) and stirred at room temperature for 1 hour. Ethyl bromoacetate (2.5 g, 15 mmol, 1 eq.) was added to the reaction mixture dropwise over 30 minutes and the reaction mixture stirred at room temperature for 16 hours. The reaction was quenched with water (20 mL) and organic products extracted with DCM (3 x 20 mL). Combined organic layers were washed with brine (3 x 20 mL), dried over anhydrous magnesium sulphate and filtered. Solvent was removed under *vaccuo* and the crude product purified by flash chromatography on silica (50% ethyl acetate in hexane) to give **203** as a colourless oil (3.27 g, 68%).

^{1}H NMR (300 MHz, $CDCl_3$) δ 7.40 – 7.17 (10H, m, 10 x aromatic C*H*), 4.25 (2H, q, *J* = 7.1 Hz, OCH_2CH_3), 3.29 (2H, d, *J* = 21.6 Hz, PCH_2CO), 1.29 (3H, t, *J* = 7.1 Hz, OCH_2CH_3). **^{13}C NMR** (75 MHz, $CDCl_3$) δ 164.82 ($CH_2C(O)OCH_2$), 150.02 and 149.91 (2 x $OC(CH)_5$), 129.89, 125.61, 125.59, 120.70 and 120.64 (aromatic *C*), 62.08 (OCH_2CH_3), 34.09 (d, J_{CP} = 137.2 Hz, $P(O)CH_2CO$), 14.10 (OCH_2CH_3). **LRMS** (ES^+): 321.09 (100% [M + H]), 275.05 (25%). **HRMS** (ES^+): calculated for [$C_{16}H_{18}O_5P$]; 321.0892, found 321.0878.

8.2.20 Synthesis of ethyl 2-(diethoxyphosphoryl)propanoate (368)

Preparation of ethyl 2-(diethoxyphosphoryl)propanoate (368):

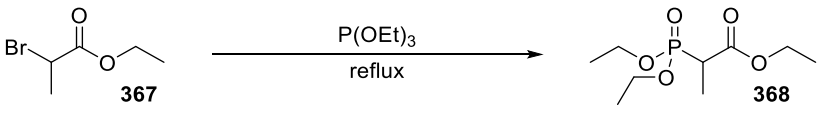

A mixture of ethyl 2-bromopropionate **367** (15.0 g, 82.8 mmol, 1 eq.) and triethyl phosphite (13.75 g, 82.8 mmol, 1 eq.) were heated under reflux at 150 °C for 16 hours. Product was purified *via* vacuum distillation giving **368** as a light brown oil (11.3 g, 57%).

^{1}H NMR (300 MHz, $CDCl_3$) δ 4.31 – 4.01 (6H, m, 3 x OCH_2CH_3), 3.01 (1H, dq, *J* = 23.4, 7.3 Hz, $PCH(CH_3)$), 1.43 (3H, dd, *J* = 18.0, 7.3 Hz), 1.35 (3H, t, *J* = 2.2 Hz, OCH_2CH_3), 1.32 (3H, t, *J* = 2.2 Hz, OCH_2CH_3), 1.29 (3H, t, *J* = 2.2 Hz, OCH_2CH_3). **^{13}C NMR** (125 MHz, $CDCl_3$) δ 169.8 (d, $^{3}J_{CP}$ = 4.58, $CHC(O)OCH_2$), 62.7 & 62.6 (2 x CH_3CH_2OP), 61.4 (CH_3CH_2O), 30.3 (d, $^{2}J_{CP}$ = 133.46, $PCH(CH_3)C(O)$), 16.43 & 16.40 (2 x $P(O)CH_2CH_3$), 11.6 ($C(O)OCH_2CH_3$). **^{31}P NMR** (202 MHz, $CDCl_3$) δ 23.8. **LRMS** (ES^+): 239.10 (100% [M + H]), 211.07 (25%). **HRMS** (ES^+): calculated for $[C_9H_{20}O_5P]^+$; 239.1042, found 239.1048.

8.2.21 Synthesis of ethyl 2-(bis(2,2,2-trifluoroethoxy)phosphoryl)propanoate (371)

Preparation of ethyl 2-(bis((trimethylsilyl)oxy)phosphoryl)proponate (369):

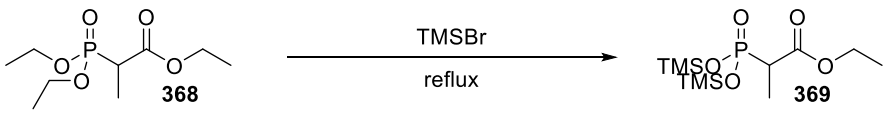

368 **369**

A mixture of trimethyl silyl bromide (32.1 g, 20.9 mmol, 5 eq.) and ethyl 2-(diethoxyphosphoryl)propanoate (**368**) (10 g, 4.19 mmol, 1 eq.) was refluxed at 80 °C for 16 hours. The mixture was concentrated under a steam of nitrogen and dried under vacuum to give **369** as an orange oil (13.1 g, 100%) which was taken forward without further purification.

^{1}H NMR (500 MHz, $CDCl_3$) δ 4.16 – 4.08 (2H, m, CH_2CH_3), 2.87 (1H, dd, *J* = 23.4, 6.6 Hz, $PCH(CH_3)CO$), 1.35 (3H, dd, *J* = 18.7, 7.1 Hz, $PCH(CH_3)$), 1.22 (3H, t, *J* = 7.1 Hz, CH_2CH_3), 0.24 (18H, s, 6 x CH_3Si). **^{31}P NMR** (202 MHz, $CDCl_3$) δ 4.71. **LRMS** (AP^+): 327.12 (100% [M + H]), 242.28 (5%). **HRMS** (AP^+): calculated for $[C_{10}H_{28}O_5Si_2P]^+$; 327.1213, found 327.1205

Preparation of ethyl 2-(dichlorophosphoryl)propanoate (370):

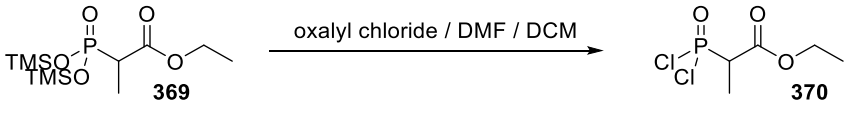

369 **370**

Oxalyl chloride (13.3 g, 10.49 mmol, 2.5 eq.) was added dropwise to a stirred solution of **369** (13.1 g, 4.19 mmol, 1 eq.) in dichloromethane (50 mL), dimethyl formamide (100 µL, cat.) was added and the mixture was stirred for 3 hours. The mixture was concentrated under a steam of nitrogen and

solvent removed under vacuum to give **370** as a light orange oil (9.19 g, 100%) which was taken forward without further purification.

^{1}H NMR (500 MHz, $CDCl_3$) δ 4.27 – 4.12 (2H, m, OCH_3CH_2), 3.58 (1H, dq, *J* = 18.5, 7.2 Hz, $PCH(CH_3)CO$), 1.59 (3H, dd, *J* = 27.3, 7.2 Hz, $PCH(CH_3)CO$), 1.23 (3H, t, *J* = 7.1 Hz, OCH_2CH_3). **^{31}P NMR** (202 MHz, $CDCl_3$) δ 44.24. **LRMS** (ES^+): 218.89 (2% [M]), 190.94 (67%), 172.93 (100%), 145.95 (62%), 117.91 (77%), 82.95 (20%).

Preparation of ethyl 2-(bis(2,2,2-trifluoroethoxy)phosphoryl)propanoate (371):

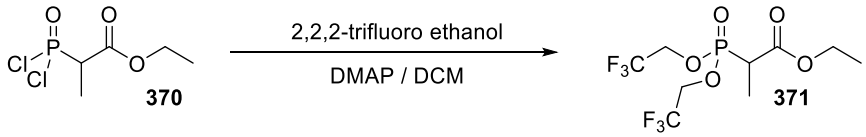

A solution of 2,2,2-tri fluoro ethanol (12 mL, 16.8 mmol, 4 eq.) and triethylamine (35 mL, 251 mmol, 6 eq.) was added dropwise to a stirred solution of **370** (9.19 g, 4.19 mmol, 1 eq.) in dichloromethane (50 mL) at 0 °C. 4-Dimethylaminopyridine (10 mg, 0.094 mmol, 0.02 eq.) was added and the reaction mixture was stirred for 4 hours at room temperature, diluted with dichloromethane (100 mL) and stirred for 16 hours. Mixture was washed with water (3 x 50 mL) and brine (3 x 50 mL), dried over magnesium sulfate and concentrated under reduced pressure. Purification *via* flash chromatography on silica gel (50% ethyl acetate in hexane) provided phosphono acetate **371** as a brown oil (8.72 g, 60%).

^{1}H NMR (500 MHz, $CDCl_3$) δ 4.38 – 4.25 (4H, m, 2 x $CHCF_3$), 4.11 (2H, q, *J* = 7.1, OCH_2CH_3), 3.11 – 3.01 (1H, dq, *J* = 22.5, 7.4 Hz, $PCH(CH_3)$), 1.39 (3H, dd, *J* = 19.4, 7.4 Hz, $PCH(CH_3)$), 1.17 (3H, t, *J* = 7.1 Hz, OCH_2CH_3). **^{13}C NMR** (75 MHz, $CDCl_3$) δ 168.5 ($CH(O)OCH_3$), 124.3 (d, J_{CF} = 8.0 Hz, OCH_2CF_3), 120.6 (d, *J* = 8.3 Hz, OCH_2CF_3), 62.8 (d, $^{3}J_{CF}$ = 6.0 Hz, OCH_2CF_3), 62.2 (2 x OCH_2CH_3), 39.5 (d, J_{CP} = 140.8 Hz, $PCH(CH_3)$),.13.9 (OCH_2CH_3), 11.6 (d, $^{2}J_{CP}$ = 6.6 Hz, $PCH(CH_3)$). **^{31}P NMR** (202 MHz, $CDCl_3$) δ 27.15. **^{19}F NMR** (471 MHz, $CDCl_3$) δ -75.42. **LRMS** (ES^+): 347.05 (100% [M + H]), 319.02 (30%), 273.02 (5%). **HRMS** (ES^+): calculated for [$C_9H_{14}O_5F_6P$]; 347.0483, found 347.0485.

8.2.22 Synthesis of ethyl 2-(bis(2,2,2-trifluoroethoxy)phosphoryl)acetate-d_2 (272)

Preparation of ethyl 2-(bis(2,2,2-trifluoroethoxy)phosphoryl)acetate-d_2 (272):

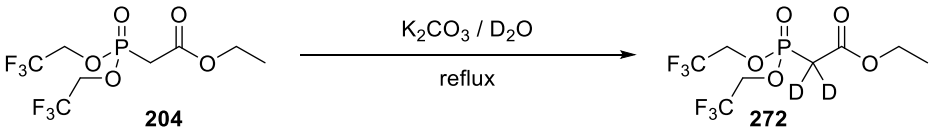

A mixture of **204** (2.0 g, 6.02 mmol, 1 eq.) and potassium carbonate (2.50 g, 18.06 mmol, 3 eq.) in deuterium oxide (40 mL) was refluxed at 100 °C for 16 hours. Reaction mixture was extracted with dichloromethane (3 x 20 mL) to give **272** as a colourless oil (1.91 g, 95%, 100% ^{2}H incorporation).

^{1}H NMR (400 MHz, $CDCl_3$) δ 4.30 – 4.05 (6H, m, 3 x OC*H*$_2$CH$_3$), 1.43 – 1.21 (9H, m, 3 x OCH$_2$C*H*$_3$). **^{31}P NMR** (162 MHz, $CDCl_3$) δ 19.81. **^{2}H NMR** (61 MHz, $CDCl_3$) δ 2.90 (2 x ^{2}H, d, *J* = 3.0 H).

8.2.23 Synthesis of 4-acetamido-2,2,6,6-tetramethyl-1-oxopiperidin-1-ium tetra fluoroborate salt (226)

Preparation of 4-acetamido-2,2,6,6-tetramethyl-1-oxopiperidin-1-ium tetra fluoroborate salt (226):

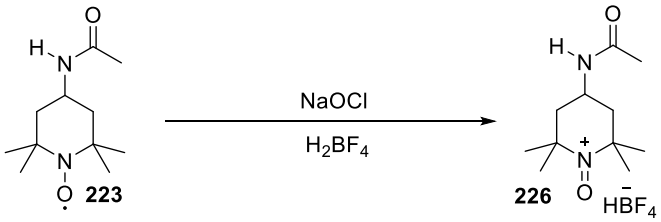

Fluoroboric acid (3.1 mL, 25.1 mmol, 1.16 eq., 50% aqueous solution) was added dropwise over 30 minutes to a stirred suspension of 4-acetylamino-2,2,6,6-tetramethyl-1-piperidinyloxy TEMPO **226** (5.0 g, 25.1 mmol, 1 eq.) in water(20 mL). The reaction was stirred for 30 minutes and sodium hypochlorite (7.23 mL, 10.9 mmol, 0.5 eq., 10-15% available Cl) added dropwise over 1 hour. The slurry was cooled to 0 °C, stirred for 1 hour and diluted with water (20 mL). Aqueous phase was extracted with dichloromethane (3 x 20 mL) and the product isolated from the aqueous phase by lyophilisation to give **226** as a yellow powder (5.47 g, 78%).

LRMS (ES^+): 215.18 (100% [M]), 199.14 (12%), 140.10 (6%)**. HRMS** (ES^+): calculated for $[C_{11}H_{23}O_2N_2][M]$; 215.1760, found 215.1755.

8.2.24 Synthesis of tert-butyl 2-acetoxy-3-oxobutanoate (184)

Preparation of tert-butyl 2-bromo-3-oxobutanoate (183):

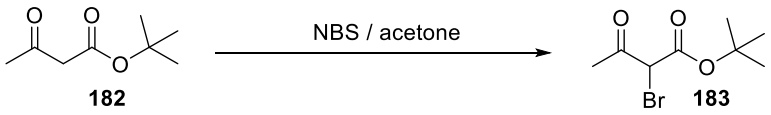

N-Bromosuccinimide (5.87 g, 3.7 mmol, 1.2 eq.) was added portion wise to a stirred solution of *tert*-butyl acetoacetate **182** (4.75 g, 3.0 mmol, 1 eq.) in acetone (20 mL). The suspension was stirred for 16 hours at room temperature, filtered through celite (ethyl acetate eluent) and filtrate concentrated under reduced pressure. Crude product was dissolved in hexane (20 mL) and the organic layer washed with water (3 x 10 mL), brine (3 x 10 mL), dried over anhydrous magnesium sulphate and filtered. Removal of solvent under *vaccuo* gave **183** as a colourless oil (6.00 g, 85%) which was used without further purification.

^{1}H NMR (300 MHz, $CDCl_3$) δ 4.69 (1H, s, C*H*Br), 2.43 (3H, s, C(O)CH_3), 1.50 (9H, s, OC(CH_3)$_3$).

Preparation of tert-butyl 2-acetoxy-3-oxobutanoate (184):

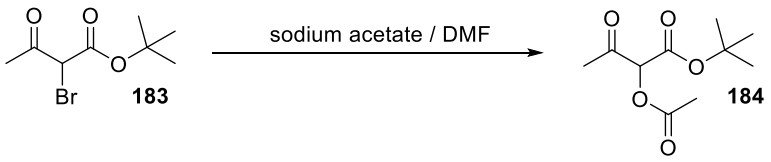

183 (7.06 g, 2.5 mmol, 1 eq.) was added to a stirred suspension of sodium acetate (3.76 g, 3.57 mmol, 1.4 eq.) in dimethylformamide (25 mL). The reaction was stirred at room temperature for 3 hours and water (20 mL) added to the mixture. The aqueous layer was extracted with ethyl acetate (3 x 10 mL) and combined organic layers washed with water (3 X 10 mL), brine (1 x 20 mL), dried over anhydrous sodium sulphate and filtered. Solvent was removed under reduced pressure and crude product purified by flash chromatography on silica (40% ethyl acetate in hexane) to give **184** as a colourless oil (6.12 g, 95%).

^{1}H NMR (300 MHz, $CDCl_3$) δ 5.41 (1H, s, C*H*(OAc)), 2.34 (3H, s, CH(OAc)C(O)CH_3), 2.23 (3H, s, CH_3C(O)OCH), 1.50 (9H, s, OC(CH_3)$_3$).

8.2.25 Synthesis of tris (tetrabutyl ammonium) hydrogendiphosphate

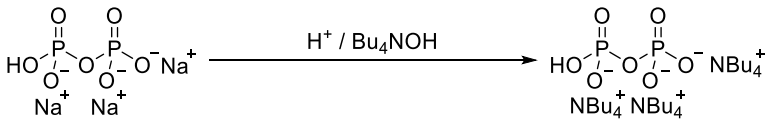

Disodium dihydrogen diphosphate (3.3 g, 15 mmol) in aqueous ammonium hydroxide (15 mL 10% (v/v)) was passed through a cation-exchange column (resin: H^+ form, amberlyst 131 wet, 10 g). Free acid was eluted with deionized water (120 mL) and the resulting solution titrated to pH 7.8 by the addition of tetrabutylammonium hydroxide (40% w/w in aqueous solution). The solution was lyophilised to give the hygroscopic product as white powder. Tris (tetrabutyl ammonium) hydrogendiphosphate was purified by recrystallization. The lyophilised product was partially dried by azeotropic removal of water by the addition of acetonitrile (30 mL) and concentration under reduced pressure to yield a tacky brown solid. The product was suspended in ethyl acetate (50 mL) and warmed to 40 °C before being filtered under vacuum to remove insoluble inorganic side products. The clear colourless filtrate was concentrated to half the volume and cooled to -20 °C to give tris (tetrabutyl ammonium) hydrogendiphosphate as white crystals (5.7 g, 43%).

^{1}H NMR (500 MHz, $CDCl_3$): δ 3.17 - 3.13 (8H, m, 4 x $NCH_2CH_2CH_2CH_3$), 1.62-1.56 (8H, m, 4 x $NCH_2CH_2CH_2CH_3$), 1.36 - 1.27 (8H, m, 4 x $NCH_2CH_2CH_2CH_3$), 0.90 (12H, t, J = 7.5, 4 x $NCH_2CH_2CH_2CH_3$). **^{31}P NMR** (121 MHz, D_2O): δ -8.22 (s). **HRMS** (ES^-): calculated for $(C_{16}H_{39}NO_7P_2 - [H])^-$: 418.2124, found: 418.2119.

References

1 J. A. Aaron and D. W. Christianson, *Pure Appl. Chem.*, 2010, **82**, 1585–1597.

2 P. M. Bleeker, P. J. Diergaarde, K. Ament, S. Schütz, B. Johne, J. Dijkink, H. Hiemstra, R. de Gelder, M. T. J. de Both, M. W. Sabelis, M. A. Haring and R. C. Schuurink, *Phytochemistry*, 2011, **72**, 68–73.

3 P. M. Bleeker, R. Mirabella, P. J. Diergaarde, A. Vandoorn, A. Tissier and M. R. Kant, *PNAS*, 2012, **109**, 20124–20129.

4 T. J. A. Bruce, M. A. Birkett, J. Blande, A. M. Hooper, J. L. Martin, B. Khambay, I. Prosser, L. E. Smart and L. J. Wadhams, *Pest Manag. Sci.*, 2005, **61**, 1115–1121.

5 J. Stökl, J. Brodmann, A. Dafni, M. Ayasse and B. S. Hansson, *Proc. R. Soc. B Biol. Sci.*, 2011, **278**, 1216–1222.

6 H. J. Bouwmeester, J. Gershenzon, M. C. J. M. Konings and R. Croteau, *Plant Physiol.*, 1998, **117**, 901–912.

7 C. N. Tetzlaff, Z. You, D. E. Cane, S. Takamatsu, S. Omura and H. Ikeda, *Biochemistry*, 2006, **45**, 6179–6186.

8 E. M. Coutinho, *Contraception*, 2002, **65**, 259–263.

9 X. Tang, M. Demiray, T. Wirth and R. K. Allemann, *Bioorganic Med. Chem.*, 2018, **26**, 1314–1319.

10 R. Croteau, R. E. B. Ketchum, R. M. Long, R. Kaspera and R. Mark, 2010, **5**, 75–97.

11 R. K. Allemann, *Pure Appl. Chem.*, 2008, **80**, 1791–1798.

12 J. Bohlmann, G. Meyer-Gauen and R. Croteau, *Proc. Natl. Acad. Sci. U. S. A.,* 1998, **95**, 4126–4133.

13 J. S. Dickschat, *Nat. Prod. Rep.*, 2011, **28**, 1917–1936.

14 H. Miziorko, *Arch. Biochem. Biophys.*, 2011, **505**, 131–143.

15 M. Rohmer, M. Knani, P. Simonin, B. Sutter and H. Sahm, *Biochem. J.*, 1993, **295**, 517–524.

16 D. Arigoni, S. Sagner, C. Latzel, W. Eisenreich, A. Bacher and M. H. Zenk, *Proc. Natl. Acad. Sci.*, 1997, **94**, 10600–10605.

17 S. A. Holstein and R. J. Hohl, *Lipids*, 2004, **39**, 293–309.

18 K.-P. Adam, R. Thiel, J. Zapp and H. Becker, *Arch. Biochem. Biophys.*, 1998, **354**, 181–187.

19 L. A. Oh, *J.Biol. Chem.,* 1969, **236**, 326–332.

20 K. Clifford, J. W. Cornforth, R. Mallaby and G. T. Phillips, *J. Chem. Soc. D Chem. Commun.*, 1971, 1599–1600.

21 I. P. Street, D. J. Christensen and C. D. Poulter, *J. Am. Chem. Soc.*, 1990, **112**, 8577–8578.

22 J. Schwender, M. Seemann, H. K. Lichtenthaler and M. Rohmer, *Biochem. J.*, 1996, **316**, 73–80.

23 W. Eisenreich, A. Bacher, D. Arigoni and F. Rohdich, *Cell. Mol. Life Sci.*, 2004, **61**, 1401–1426.

24 V. S. Dubey, R. Bhalla and R. Luthra, *J. Biosci.*, 2003, **28**, 637–646.

25 W. N. Hunter, *J. Biol. Chem.*, 2007, **282**, 21573–21577.

26 T. Gräwert, M. Groll, F. Rohdich, A. Bacher and W. Eisenreich, *Cell. Mol. Life Sci.*, 2011, **68**, 3797–3814.

27 W. Eisenreich, F. Rohdich and A. Bacher, *Trends Plant Sci.*, 2001, **6**, 78–84.

28 N. Hirai, R. Yoshida, Y. Todoroki and H. Ohigashi, *Biosci. Biotechnol. Biochem.*, 2000, **64**, 1448–1458.

29 D. W. Christianson, *Science*, 2007, **316**, 60–61.

30 C. Sallaud, D. Rontein, S. Onillon, F. Jabès, P. Duffé, C. Giacalone, S. Thoraval, C. Escoffier, G. Herbette, N. Leonhardt, M. Causse and A. Tissier, *Plant Cell.*, 2009, **21**, 301–17.

31 F. Chen, D. Tholl, J. Bohlmann and E. Pichersky, *Plant J.*, 2011, **66**, 212–29.

32 D. J. Newman, G. M. Cragg and K. M. Snader, *Nat. Prod. Rep.*, 2000, **17**, 215–234.

33 T. W. Goodwin and R. T. H. Williams, *Biol. Sci.*, 1966, **163**, 515–518.

34 B. L. Archer, D. Barnard, E. G. Cockbain, J. W. Cornforth, R. H. Cornforth and G. Popjak, *Proc. R. Soc. B Biol. Sci.*, 1966, **163**, 519–523.

35 D. V. Banthorpe, C. A. Bunton, O. Cori and M. J.O. Francis, *Phytochemistry*, 1985, **24**, 251–252.

36 E. M. McCarron and R. L. Harlow, *J. Am. Chem. Soc.*, 1983, **105**, 6179–6181.

37 M. J. 0. F. Patourel, D. V. Banthorpe and G. N. J. Le, *Biochem. J.*, 1972, **130**, 1045–1054.

38 A. L. Schilmiller, I. Schauvinhold, M. Larson, R. Xu, A. L. Charbonneau, A. Schmidt, C. Wilkerson, R. L. Last and E. Pichersky, *Proc. Natl. Acad. Sci.*, 2009, **106**, 10865–10870.

39 D. Tholl, *Curr. Opin. Plant Biol.*, 2006, **9**, 297–304.

40 B. P. Moore, *J. Org. Chem.*, 1980, **45**, 1126–1130.

41 L. Verheggen, Francois J. Arnaud, S. Bartram, M. Gohy and E. Haubruge, *J. Chem Ecol*, 2008, **34**, 301 – 307.

42 L. Pazouki and Ü. Niinemets, *Front. Plant Sci.*, 2016, **7**, 1–16.

43 L. Pazouki, H. R. Memari, A. KÃ¤nnaste, R. Bichele and Ã. Niinemets, *Front. Plant Sci.*, 2015, **6**, 1–15.

44 C. G. Jones, J. Moniodis, K. G. Zulak, A. Scaffidi, J. A. Plummer, E. L. Ghisalberti, E. L. Barbour and J. Bohlmann, *J. Biol. Chem.*, 2011, **286**, 17445–17454.

45 J. Bohlmann, J. Crock, R. Jetter and R. Croteau, *Proc. Natl. Acad. Sci. U. S. A.*, 1998, **95**, 6756–61.

46 M. W. Huff and D. E. Telford, *Trends Pharmacol. Sci*, 2005, **26**, 335–340.

47 M. Huang, C. Abel, R. Sohrabi, J. Petri, I. Haupt, J. Cosimano, J. Gershenzon and D. Tholl, *Plant Physiol.*, 2010, **153**, 1293–1310.

48 J. A. Faraldos, D. J. Miller, V. González, Z. Yoosuf-Aly, O. Cascón, A. Li and R. K. Allemann, *J. Am. Chem. Soc.*, 2012, **134**, 5900–5908.

49 R. K. Allemann, N. J. Young, S. Ma, D. G. Truhlar and J. Gao, *J. Am. Chem. Soc.*, 2007, **129**, 13008–13013.

50 L. C. Tarshis, M. Yan, C. D. Poulter and J. C. Sacchettini, *Biochemistry*, 1994, **33**, 10871–10877.

51 M. J. Rynkiewicz, D. E. Cane and D. W. Christianson, *Proc. Natl. Acad. Sci.*, 2001, **98**, 13543–13548.

52 D. W. Christianson, *Chem. Rev.*, 2006, **106**, 3412–3442.

53 V. González, D. J. Grundy, J. A. Faraldos and R. K. Allemann, *Org. Lett.*, 2016, **14**, 7451–7454.

54 C. M. Starks, K. Back, J. Chappell, J. P. Noel, M. E. M. Guedes, J. Kuc, R. Hammerschmidt, R. Bostock, M. A. Morse, A. L. Toburen, D. E. Cane, R. Croteau, J. Chappell, K. Back, S. Yin, J. Chappell, K. Back, J. Chappell, K. Back, J. Chappell, J. Navaza, V. X. Lamzin, K. S. Wilson, A. E. Aleshin, C. Hoffman, L. M. Firsov, R. B. Honzatko, M. Juy, L. C. Tarshis, M. Yan, C. D. Poulter, J. C. Sacchettini, L. C. Tarshis, P. J. Proteau, B. A. Kellogg, J. C. Sacchettini, C. D. Poulter, D. E. Cane, Q. Xue, B. C. Fitzsimons, D. A. Dougherty, M. R. Wildung, R. Croteau, X. Lin, M. Hezari, A. E. Koepp, H. G. Floss, R. Croteau, M. Carson, C. E. Bugg, A. Nicholls, K. A. Sharp, B. Honig, T. A. Jones, J. Y. Zou, S. W. Cowan and M. Kjeldgaard, *Science*, 1997, **277**, 1815–1820.

55 R. P. McAndrew, P. P. Peralta-Yahya, A. DeGiovanni, J. H. Pereira, M. Z. Hadi, J. D. Keasling and P. D. Adams, *Structure.*, 2011, **19**, 1876–84.

56 H. J. Koo, C. R. Vickery, Y. Xu, G. V. Louie, P. E. O'Maille, M. Bowman, C. M. Nartey, M. D. Burkart and J. P. Noel, *J. Antibiot.*, 2016, **69**, 524–533.

57 R. P. McAndrew, P. P. Peralta-Yahya, A. DeGiovanni, J. H. Pereira, M. Z. Hadi, J. D. Keasling and P. D. Adams, *Structure.*, 2011, **19**, 1876–1884.

58 M. J. Mitchell and M. R. King, *J. Am. Chem. Soc.,* 2014, **402**, 1–23.

59 R. K. Allemann, N. J. Young, *J. Am. Chem. Soc.,* 2007, **43**, 366–369.

60 H. A. Gennadios, V. Gonzalez, L. Di Costanzo, A. Li, F. Yu, D. J. Miller, R. K. Allemann and D. W. Christianson, *Biochemistry*, 2009, **48**, 6175–6183.

61 D. A Whittington, M. L. Wise, M. Urbansky, R. M. Coates, R. B. Croteau and D. W. Christianson, *Proc. Natl. Acad. Sci. U. S. A.*, 2002, **99**, 15375–15380.

62 D. W. Christianson, *Chem. Rev.*, 2017, **117**, 11570–11648.

63 S. Prisic, J. Xu, R. M. Coates and R. J. Peters, *ChemBioChem*, 2007, **8**, 869–874.

64 K. Zhou, Y. Gao, J. A. Hoy, F. M. Mann, R. B. Honzatko and R. J. Peters, *J. Biol. Chem.*, 2012, **287**, 6840–6850.

65 M. Köksal, Y. Jin, R. M. Coates, R. Croteau and D. W. Christianson, *Nature*, 2011, **469**, 116–122.

66 M. Köksal, Y. Jin, R. M. Coates, R. J. Peters and D. W. Christianson, *Nat. Chem. Biol.,* 2012, **7**, 431–433.

67 R. J. Peters, J. A. Hoy, Y. Gao, K. Zhou, R. B. Honzatko and F. M. Mann, *J. Biol. Chem.*, 2012, **287**, 6840–6850.

68 D. P. Kloer, R. Welsch, P. Beyer and G. E. Schulz, *Biochemistry*, 2006, **45**, 15197–15204.

69 M. De Rosa, A. Gambacorta, L. Minale and J. D. Bu'Lock, *Phytochemistry*, 1973, **12**, 1117–1123.

70 A. Ruf, F. Müller, B. D'Arcy, M. Stihle, E. Kusznir, C. Handschin, O. H. Morand and R. Thoma, *Biochem. Biophys. Res. Commun.*, 2004, **315**, 247–254.

71 T. Sato, S. Yoshida, H. Hoshino, M. Tanno, M. Nakajima and T. Hoshino, *J. Am. Chem. Soc.*, 2011, **133**, 9734–9737.

72 K. U. Wendt, *Angew. Chemie - Int. Ed.*, 2005, **44**, 3966–3971.

73 M. A. Philips and R. B. Croteau, *Trends Plant Sci.*, 1999, **4**, 184–190.

74 R. Wilderman, M. Determan and R. J. Peters, *J. Am. Chem. Soc.,* 2008, **129**, 15736–15737.

75 R. J. Peters and R. B. Croteau, *Proc. Natl. Acad. Sci.*, 2002, **99**, 580–584.

76 M. M. Ravn, R. M. Coates, J. E. Flory, R. J. Peters and R. Croteau, *Org. Lett.*, 2000, **2**, 573–576.

77 M. M. Ravn, R. J. Peters, R. M. Coates and R. Croteau, *J. Am. Chem. Soc.*, 2002, **124**, 6998–7006.

78 D. E. Cane, *Pure Appl. Chem.*, 1989, **61**, 493–496.

79 D. J. Miller and R. K. Allemann, *Nat. Prod. Rep.*, 2012, **29**, 60–71.

80 S. H. Kim, K. Heo, Y. J. Chang, S. H. Park, S. K. Rhee and S. U. Kim, *J. Nat. Prod.*, 2006, **69**, 758–762.

81 N. J. White, *Science*, 2008, **320**, 330–334.

82 P. J. Westfall, D. J. Pitera, J. R. Lenihan, D. Eng, F. X. Woolard, R. Regentin, T. Horning, H. Tsuruta, D. J. Melis, A. Owens, S. Fickes, D. Diola, K. R. Benjamin, J. D. Keasling, M. D. Leavell, D. J. McPhee, N. S. Renninger, J. D. Newman and C. J. Paddon, *Proc. Natl. Acad. Sci.*, 2012, **109**, E111–E118.

83 D. Lubertozzi and J. D. Keasling, *J. Ind. Microbiol. Biotechnol.*, 2008, **35**, 1191–1198.

84 C. R. Benedict, J. L. Lu, D. W. Pettigrew, J. Liu, R. D. Stipanovic and H. J. Williams, *Plant Physiol.*, 2001, **125**, 1754–1765.

85 T. G. Köllner, C. Schnee, S. Li, A. Svatoš, B. Schneider, J. Gershenzon and J. Degenhardt, *J. Biol. Chem.*, 2008, **283**, 20779–20788.

86 J. A. Faraldos, B. Kariuki and R. K. Allemann, *J. Org. Chem.*, 2010, **75**, 1119–1125.

87 J. A. Faraldos, V. Gonzalez and R. K. Allemann, *Chem. Commun. (Camb).*, 2012, **48**, 3230–2.

88 M. Chen, N. Al-Lami, M. Janvier, E. L. D'Antonio, J. A. Faraldos, D. E. Cane, R. K. Allemann

and D. W. Christianson, *Biochemistry*, 2013, **52**, 5441–5453.

89 Y. Gao, R. B. Honzatko and R. J. Peters, *Nat. Prod. Rep.*, 2012, **29**, 1153–75.

90 J. Y. Chow, B. X. Tian, G. Ramamoorthy, B. S. Hillerich, R. D. Seidel, S. C. Almo, M. P. Jacobson and C. D. Poulter, *Proc. Natl. Acad. Sci.*, 2015, **112**, 5661–5666.

91 D. B. Little and R. B. Croteau, *Arch. Biochem. Biophys.*, 2002, **402**, 120–135.

92 R. K. Allemann, N. J. Young, S. Ma, D. G. Truhlar and J. Gao, *J. Am. Chem. Soc.,* 2013, **6**, 13008–13013.

93 J. A. Faraldos, B. Kariuki and R. K. Allemann, *J. Org. Chem.*, 2010, **75**, 1119–1125.

94 M. Chen, N. Al-Lami, M. Janvier, E. L. D'Antonio, J. A. Faraldos, D. E. Cane, R. K. Allemann and D. W. Christianson, *Biochemistry*, 2013, **52**, 5441–5453.

95 S. Leitner, *J. Eur. Soc. Policy*, 2001, **11**, 99–115.

96 V. Gonzalez, S. Touchet, D. J. Grundy, J. A. Faraldos and R. K. Allemann, *J. Am. Chem. Soc.*, 2014, **136**, 14505–14512.

97 B. T. Greenhagen, P. E. O'Maille, J. P. Noel and J. Chappell, *Proc. Natl. Acad. Sci.*, 2006, **103**, 9826–9831.

98 A. Roy, F. G. Roberts, P. R. Wilderman, K. Zhou, R. J. Peters and R. M. Coates, *J. Am. Chem. Soc.*, 2007, **129**, 12453–12460.

99 F. M. Mann, S. Prisic, H. Hu, M. Xu, R. M. Coates and R. J. Peters, *J. Biol. Chem.*, 2009, **284**, 23574–23579.

100 D. J. Miller, F. Yu, D. W. Knight and R. K. Allemann, *Org. Biomol. Chem.*, 2009, **7**, 962–975.

101 C. Ni and J. Hu, *Chem. Soc. Rev.*, 2016, **45**, 5441–5454.

102 D. J. Miller, F. Yu and R. K. Allemann, *ChemBioChem*, 2007, **8**, 1819–1825.

103 B. Felicetti and D. Cane, *J. Am. Chem. Soc.*, 2004, 7212–7221.

104 D. E. Cane and Y. S. Tsantrizos, *J. Am. Chem. Soc.*, 1996, **118**, 10037–10040.

105 F. Yu, D. J. Miller and R. K. Allemann, *Chem. Commun.*, 2007, 4155–4157.

106 S. Touchet, K. Chamberlain, C. M. Woodcock, D. J. Miller, M. A. Birkett, J. A. Pickett and R. K. Allemann, *Chem. Commun.*, 2015, **51**, 7550–7553.

107 D. E. Cane, H. T. Chiu, P. H. Liang and K. S. Anderson, *Biochemistry*, 1997, **36**, 8332–8339.

108 D. E. Cane, *Chem. Rev.*, 1990, **90**, 1089–1103.

109 J. Faraldos, V. Gonzalez and A. Li, *J. Am. Chem. Soc.*, 2012, **133**, 8–12.

110 T. Yomo, T. Yamano, K. Yamamoto and I. Urabe, *J. Theor. Biol.*, 1997, **188**, 301–312.

111 P. D. Buckley, L. F. Blackwell, M. F. Dunn and J. P. Hill, *Biochem. Educ.*, 1990, **18**, 101–102.

112 D. E. Cane and C. Bryant, *J. Am. Chem. Soc.*, 1994, **116**, 12063–12064.

113 N. Duhamel, D. Martin, R. Larcher, B. Fedrizzi and D. Barker, *Tetrahedron Lett.*, 2016, **57**,

4496–4499.

114 X. Lin, M. Hezari, A. E. Koepp, H. G. Floss and R. Croteau, *Biochemistry*, 1996, **35**, 2968–2977.

115 D. D. E. Cane, P. C. P. Prabhakaran, J. S. Oliver and D. B. McIlwaine, *J. Am. Chem. Soc.*, 1990, **112**, 3209–3210.

116 D. E. Cane, P. C. Prabhakaran, E. J. Salaski, P. H. M. Harrison, H. Noguchi and B. J. Rawlings, *J. Am. Chem. Soc.*, 1989, **111**, 8914–8916.

117 S. Picaud, P. Mercke, X. He, O. Sterner, M. Brodelius, D. E. Cane and P. E. Brodelius, *Arch. Biochem. Biophys.*, 2006, **448**, 150–155.

118 J. K. Weng, R. N. Philippe and J. P. Noel, *Science*, 2012, **336**, 1667–1670.

119 Y. Yoshikuni, T. E. Ferrin and J. D. Keasling, *Nature*, 2006, **440**, 1078–82.

120 A. Bar-Even, E. Noor, Y. Savir, W. Liebermeister, D. Davidi, D. S. Tawfik and R. Milo, *Biochemistry*, 2011, **50**, 4402–4410.

121 J. X. Li, X. Fang, Q. Zhao, J. X. Ruan, C. Q. Yang, L. J. Wang, D. J. Miller, J. a Faraldos, R. K. Allemann, X. Y. Chen and P. Zhang, *Biochem. J.*, 2013, **451**, 417–26.

122 K. U. Wendt and G. E. Schulz, *Structure*, 1998, **6**, 127–133.

123 B. Gust, G. L. Challis, K. Fowler, T. Kieser and K. F. Chater, *Proc. Natl. Acad. Sci.*, 2003, **100**, 1541–1546.

124 N. N. Gerber, *Biotechnol. Bioeng.*, 1967, **9**, 321–327.

125 N. N. Gerber, *Crit. Rev. Microbiol.*, 1979, **7**, 191–214.

126 J. Jiang, X. He and D. E. Cane, *Nat. Chem. Biol.*, 2007, **3**, 711–715.

127 D. E. Cane and R. M. Watt, *Proc. Natl. Acad. Sci. U. S. A.*, 2003, **100**, 1547–51.

128 X. He and D. E. Cane, *J. Am. Chem. Soc.*, 2004, **126**, 2678–2679.

129 J. Jiang and D. E. Cane, *J. Am. Chem. Soc.,* 2008, **130**, 428–429.

130 T. Nawrath, J. S. Dickschat, R. Müller, J. Jiang, D. E. Cane and S. Schulz, *J. Am. Chem. Soc.*, 2008, **130**, 430–431.

131 P. M. Bleeker, P. J. Diergaarde, K. Ament, J. Guerra, M. Weidner, S. Schütz, M. T. J. de Both, M. A. Haring and R. C. Schuurink, *Plant Physiol.*, 2009, **151**, 925–35.

132 C. G. Jones, J. Moniodis, K. G. Zulak, A. Scaffidi, J. A. Plummer, E. L. Ghisalberti, E. L. Barbour and J. Bohlmann, *J. Biol. Chem.*, 2011, **286**, 17445–17454.

133 I. H. Hall, K. H. Lee, C. O. Starenes, Y. Sumida, R. Y. Wu, T. G. Waddell, J. W. Cochran and K. G. Gerhart, *J. Pharm. Sci.*, 1979, **68**, 537–542.

134 P. P. Peralta-Yahya, F. Zhang, S. B. Del Cardayre and J. D. Keasling, *Nature*, 2012, **488**, 320–328.

135 J. P. Bartley and A. L. Jacobs, *J. Sci. Food Agric.*, 2000, **80**, 209–215.

136 N. J. White, *Science*, 2008, **320**, 330–334.

137 Y. Wong, Y. Lous and X. Tang, *Acta Pharm Sin.*, 1979, **14**, 662–666.

138 National Agents Coordinating Group on Male Infertility, *China Med J*, 1978, **4**, 417.

139 J. K. Srivastava, E. Shankar and S. Gupta, *Mol. Med. Rep.*, 2010, **3**, 895–901.

140 J. Ferreira do Nascimento, P. Hein, A. Davide, L. Amaral de Melo and P. Trugilho, *J. Near Infrared Spectrosc.*, 2015, **23**, 33.

141 G. P. P. Kamatou and A. M. Viljoen, *J. Am. Oil Chem. Soc.*, 2010, **87**, 1–7.

142 P. P. Peralta-Yahya, M. Ouellet, R. Chan, A. Mukhopadhyay, J. D. Keasling and T. S. Lee, *Nat. Commun.*, 2011, **2**, 483–488.

143 S. C. Phulara, P. Chaturvedi and P. Gupta, *Appl. Environ. Microbiol.*, 2016, **82**, 5730–5740.

144 F. K. Davies, V. H. Work, A. S. Beliaev and M. C. Posewitz, *Front. Bioeng. Biotechnol.*, 2014, **2**, 1–11.

145 S. C. Wang, T. Y. Tseng, C. M. Huang and T. H. Tsai, *J. Chromatogr. B Anal. Technol. Biomed. Life Sci.*, 2004, **812**, 193–202.

146 J. Šobotník, R. Hanus, B. Kalinová, R. Piskorski, J. Cvačka, T. Bourguignon and Y. Roisin, *J. Chem. Ecol.*, 2008, **34**, 478–486.

147 R. W. Gibson and J. A. Pickett, *Nature*, 1983, 302, 608–609.

148 J. Degenhardt, T. G. Köllner and J. Gershenzon, *Phytochemistry*, 2009, **70**, 1621–37.

149 M. A. Rude and A. Schirmer, *Curr. Opin. Microbiol.*, 2009, **12**, 274–281.

150 D. Markovic, R. Glinwood, U. Olsson and V. Ninkovic, *Arthropod. Plant. Interact.*, 2014, **8**, 171–181.

151 C. I. Keeling and J. Bohlmann, *New Phytol.*, 2006, **170**, 657–675.

152 H. R. Beller, T. S. Lee and L. Katz, *Nat. Prod. Rep.*, 2015, **32**, 1508–1526.

153 P. C. Onyenekwe and S. Hashimoto, *Eur. Food Res. Technol.*, 1999, **209**, 407–410.

154 J. G. Millar, *J. Nat. Prod.*, 1998, **61**, 1025–1026.

155 C. Gherlardhini, N. Galeotti, L. Di Cesare Mannelli, G. Mazzanti, A. Bartolini, *Il Farmaco.,* 2001, **56**, 387-389

156 E. Ormeño, V. Baldy, C. Ballini and C. Fernandez, *J. Chem. Ecol.*, 2008, **34**, 1219–1229.

157 L. Jirovetz, G. Buchbauer, M. B. Ngassoum and M. Geissler, *J. Chromatogr. A*, 2002, **976**, 265–275.

158 C. M. Compadre, R. A. Hussain, R. L. de Compadre Lopez, J. M. Pezzuto and A. D. Kinghorn, *Experientia*, 1988, **44**, 447–449.

159 C. M. Compadre, J. M. Pezzuto, A. D. Kinghorn and S. K. Kamath, *Science*, 1985, **227**, 417–419.

160 P. F. De Oliveira, R. A. F. MacHado, A. Bolzan and D. Barth, *J. Supercrit. Fluids*, 2012, **63**,

161–168.

161 K. Chamberlain, J. A. Pickett and C. M. Woodcock, *Mol. Plant Pathol.*, 2001, **1**.

162 F. J. Verheggen, L. Diez, L. Sablon, C. Fischer, S. Bartram, E. Haubruge and C. Detrain, *PLoS One*, 2012, **7**, 2–7.

163 L. R. Nault, M. E. Montgomery and W. S. Bowers, *Science*, 1976, **192**, 1349–1351.

164 F. J. Verheggen, L. Arnaud, S. Bartram, M. Gohy and E. Haubruge, *J. Chem. Ecol.*, 2008, **34**, 301–307.

165 F. J. Verheggen, Q. Fagel, S. Heuskin, G. Lognay, F. Francis and E. Haubruge, *J. Chem. Ecol.*, 2007, **33**, 2148–2155.

166 R. K. Mensah and C. Moore, *J. Biol. Control*, 2011, **25**, 253–269.

167 A. L. Mauchline, M. R. Hervé and S. M. Cook, *Arthropod. Plant. Interact.*, 2017, **95**, 1–13.

168 L. C. Rodríguez and H. M. Niemeyer, *Crop Prot.*, 2005, **24**, 615–623.

169 R. Kataria and D. Kumar, *Int. J. Pharma Bio Sci.*, 2015, **6**, 553–574.

170 F. J. Verheggen, M. C. Mescher, E. Haubruge, C. M. Moraes and E. G. Schwartzberg, *J. Chem. Ecol.*, 2008, **34**, 1146–1148.

171 B. Fassotte, C. Fischer, D. Durieux, G. Lognay, E. Haubruge, F. Francis and F. J. Verheggen, *PLoS One*, 2014, **9**, 1–16.

172 S. M. Cook, Z. R. Khan and J. A. Pickett, *Annu. Rev. Entomol.*, 2007, **52**, 375–400.

173 G. N. Lanier, R. M. Silverstein and J. W. Peacock, *Perspect. For. Entomol.*, 1976, 149–175.

174 R. S. Detrick, J. D. Mudie, B. P. Luyendyk and K. C. Macdonald, *Nat. Phys. Sci.*, 1973, **243**, 232.

175 C. M. Brasier and S. A. Kirk, *Mycol. Res.*, 2001, **105**, 547–554.

176 T. J. Bruce, M. A. Birkett, J. Blande, A. M. Hooper, J. L. Martin, B. Khambay, I. Prosser, L. E. Smart and L. J. Wadhams, *Pest Manag. Sci.*, 2005, **61**, 1115 – 1121.

177 M. A. Birkett, S. Al Abassi, T. Kröber, K. Chamberlain, A. M. Hooper, P. M. Guerin, J. Pettersson, J. A. Pickett, R. Slade and L. J. Wadhams, *Phytochemistry*, 2008, **69**, 1710–1715.

178 S. Touchet, K. Chamberlain, C. M. Woodcock, D. J. Miller, M. A. Birkett, J. A. Pickett and R. K. Allemann, *Chem. Commun.*, 2015, **51**, 7550–7553.

179 E.-C. Oerke, *J. Agric. Sci.*, 2005, **144**, 31.

180 J. E. Polston and P. K. Anderson, *Plant Dis.*, 1997, **81**, 1358–1369.

181 J. A. Freitas, W. R. Maluf, M. das G. Cardoso, L. A. A. Gomez and E. Bearzotti, *Euphytica*, 2002, **127**, 275–287.

182 J. J. Glas, B. C. J. Schimmel, J. M. Alba, R. Escobar-Bravo, R. C. Schuurink and M. R. Kant, *Int. J. Mol. Sci.*, 2012, **13**, 17077–17103.

183 F. E. Dayan, C. L. Cantrell and S. O. Duke, *Bioorganic Med. Chem.*, 2009, **17**, 4022–4034.

184 C. Sallaud, D. Rontein, S. Onillon, F. Jabès, P. Duffé, C. Giacalone, S. Thoraval, C. Escoffier, G. Herbette, N. Leonhardt, M. Causse and A. Tissier, *Plant Cell*, 2009, **21**, 301–17.

185 A. Brancale, Cardiff University, School of Pharmacy (generation of homology model).

186 C. L. Steele, J. Crock, J. Bohlmann and R. Croteau, *J. Biol. Chem.*, 1998, **273**, 2078–2089.

187 M. Seemann, G. Zhai, J.-W. de Kraker, C. M. Paschall, D. W. Christianson and D. E. Cane, *J. Am. Chem. Soc.*, 2002, **124**, 7681–7689.

188 V. J. Davisson, A. B. Woodside, T. R. Neal, K. E. Stremler, M. Muehlbacher and C. D. Poulter, *J. Org. Chem.*, 1986, **51**, 4768–4779.

189 S. Garneau, L. Qiao, L. Chen, S. Walker and J. C. Vederas, *Bioorg. Med. Chem.*, 2004, **12**, 6473–94.

190 T. Kato, M. Suzuki, T. Kobayashi and B. P. Moore, *J. Org. Chem.*, 1980, **45**, 1126–1130.

191 J. S. Yu, T. S. Kleckley and D. F. Wiemer, *Org. Lett.*, 2005, **7**, 4803–4806.

192 T. Kitahara and A. Horiguchi, *Tetrahedron*, 1988, **44**, 4713–4720.

193 S. S. Syeda, E. J. Carlson, M. R. Miller, R. Francis, D. E. Clapham, P. V. Lishko, J. E. Hawkinson, D. Hook and G. I. Georg, *ACS Chem. Biol.*, 2016, **11**, 452–459.

194 S. O. Simonetti, E. L. Larghi and T. S. Kaufman, *Org. Biomol. Chem.*, 2016, **14**, 2625–2636.

195 D. Basu, M. Chandrasekharam, P. S. Mainkar and S. Chandrasekhar, *Arkivoc*, 2011, **2011**, 355–362.

196 A. Pascariu, G. Ilia, A. Bora, S. Iliescu, A. Popa, G. Dehelean and L. Pacureanu, *Cent. Eur. J. Chem.*, 2003, **1**, 491–534.

197 B. S. Chen, V. Resch, L. G. Otten and U. Hanefeld, *Chem. A. Eur. J.*, 2015, **21**, 3020–3030.

198 G. Scheid, W. Kuit, E. Ruijter, R. V. A. Orru, E. Henke, U. Bornscheuer and L. A. Wessjohann, *European J. Org. Chem.*, 2004, **10**, 1063–1074.

199 M. Anastasia, P. Allevi, P. Ciuffreda, A. Fiecchi, P. Gariboldi and A. Scala, *J. Chem. Soc., Perkin Trans. 1*, 1985, 595–599.

200 J. A. Faraldos, S. Wu, J. Chappell and R. M. Coates, *J. Am. Chem. Soc.*, 2010, **132**, 2998–3008.

201 L. Horner, H. M. R. Hoffman and H. G. Wippel, *Chem. Ber.*, 1958, **91**, 61–63.

202 W. S. Wadsworth and W. D. Emmons, *J. Am. Chem. Soc.*, 1961, **83**, 1733–1738.

203 K. Ando, *J. Org. Chem.*, 1997, **62**, 1934–1939.

204 W. C. Still and C. Gennari, *Tetrahedron Lett.*, 1983, **24**, 4405–4408.

205 F. Messik and M. Oberthür, *Synth.*, 2013, **45**, 167–170.

206 S. K. Thompson and C. H. Heathcock, *J. Org. Chem.*, 1990, **55**, 3386–3388.

207 T. D. Parks, K. K. Leuther, E. D. Howard, S. A. Johnston and W. G. Dougherty, *Anal. Biochem.*, 1994, 216, 413–417.

208 L. Yi, M. C. Gebhard, Q. Li, J. M. Taft, G. Georgiou and B. L. Iverson, *Proc. Natl. Acad. Sci.*,

2013, **110**, 7229–7234.

209 R. B. Kapust, J. Toözseór, T. D. Copeland and D. S. Waugh, *Biochem. Biophys. Res. Commun.*, 2002, **294**, 949–955.

210 M. M. Bradford, *Anal. Biochem.*, 1976, **72**, 248–254.

211 H. Christensen and R. H. Pain, *Eur. Biophys. J.*, 1991, **19**, 221–229.

212 A. Malik, *3 Biotech*, 2016, **6**, 1–7.

213 D. K. Yadav, N. Yadav, S. Yadav, S. Haque and N. Tuteja, *Arch. Biochem. Biophys.*, 2016, **612**, 57–77.

214 S. Costa, A. Almeida, A. Castro and L. Domingues, *Front. Microbiol.*, 2014, **5**, 1–20.

215 C. L. Young, Z. T. Britton and A. S. Robinson, *Biotechnol. J.*, 2012, **7**, 620–634.

216 D. Esposito and D. K. Chatterjee, *Curr. Opin. Biotechnol.*, 2006, **17**, 353–358.

217 P. Zhou and G. Wagner, *J. Biomol. NMR.*, 2010, **46**, 23–31.

218 M. M. Yakimov, L. Giuliano, G. Gentile, E. Crisafi, T. N. Chernikova, W. R. Abraham, H. Lünsdorf, K. N. Timmis and P. N. Golyshin, *Int. J. Syst. Evol. Microbiol.*, 2003, **53**, 779–785.

219 M. Ferrer, T. N. Chernikova, M. M. Yakimov, P. N. Golyshin and K. N. Timmis, *Nat. Biotechnol.*, 2003, **21**, 1266–1267.

220 Agilent Technologies, *Instr. Man.*, 2010.

221 L. Dumon-Seignovert, G. Cariot and L. Vuillard, *Protein Expr. Purif.*, 2004, **37**, 203–206.

222 F. W. Studier, *Protein Expr. Purif.*, 2005, **41**, 207–234.

223 B. Miroux and J. E. Walker, *J. Mol. Biol.*, 1996, **260**, 289–298.

224 G. Sezonov, D. Joseleau-Petit and R. D'Ari, *J. Bacteriol.*, 2007, **189**, 8746–8749.

225 K. E. Kram and S. E. Finkel, *Appl. Environ. Microbiol.*, 2015, **81**, 4442–4450.

226 A. Deligeorgopoulou, S. E. Taylor, S. Forcat and R. K. Allemann, *Chem. Commun. (Camb).*, 2003, **17**, 2162–2163.

227 A. Deligeorgopoulou and R. K. Allemann, *Biochemistry*, 2003, **42**, 7741–7747.

228 K. Ishihara, H. Ishibashi and H. Yamamoto, *J. Am. Chem. Soc.*, 2002, **124**, 3647–3655.

229 N. Tumma, M. Jacolot, M. Jean, S. Chandrasekhar and P. Van De Weghe, *Synlett*, 2012, **23**, 2919–2922.

230 A. J. Mancuso and D. Swern, *Synthesis (Stuttg).*, 1981, **3**, 165–185.

231 D. B. Dess and J. C. Martin, *J. Org. Chem.*, 1983, **48**, 4155–4156.

232 J. M. Bobbitt and N. Merbouh, *Org. Synth.*, 2005, **82**, 80 – 86.

233 M. Vardakou, M. Salmon, J. A. Faraldos and P. E. O'Maille, *MethodsX*, 2014, **1**, 187–196.

234 P. E. O'Maille, J. Chappell and J. P. Noel, *Anal. Biochem.*, 2004, **335**, 210–217.

235 D. C. Ghosh and R. Biswas, *Int. J. Mol. Sci.*, 2002, **3**, 87–113.

236 C. O. Schmidt, H. J. Bouwmeester, S. Franke and W. A. König, *Chirality*, 1999, **11**, 353–362.

237 C. A. Citron, P. Rabe, L. Barra, C. Nakano, T. Hoshino and J. S. Dickschat, *European J. Org. Chem.*, 2014, **2014**, 7684–7691.

238 D. J. Tantillo, *Nat. Prod. Rep.*, 2011, **28**, 1035–1053.

239 T. Yamakawa, M. Masaki and H. Nohira, *Bull. Chem. Soc. Jpn.*, 1991, **64**, 2730–2734.

240 T. R. Hoye, C. S. Jeffrey and F. Shao, *Nat. Protoc.*, 2007, **2**, 2451–2458.

241 J. A. Dale, D. L. Dull and H. S. Mosher, *J. Org. Chem.*, 1969, **34**, 2543–2549.

242 P. Rabe, J. Rinkel, E. Dolja, T. Schmitz, B. Nubbemeyer, T. H. Luu and J. S. Dickschat, *Angew. Chemie - Int. Ed.*, 2017, **56**, 2776–2779.

243 R. L. Edelstein, V. A. Weller, M. D. Distefano and J. S. Tung, *J. Org. Chem.*, 1998, **63**, 5298–5299.

244 R. L. Edelstein, V. A. Weller, M. D. Distefano and J. S. Tung, *J. Org. Chem.*, 1998, **63**, 5298–5299.

245 V. J. Davisson, A. B. Woodside, T. R. Neal, K. E. Stremler, M. Muehlbacher and C. D. Poulter, *J. Org. Chem.*, 1986, **51**, 4768–4779.

246 H. A. Gennadios, V. Gonzalez, L. Di Costanzo, A. Li, F. Yu, D. J. Miller, R. K. Allemann and D. W. Christianson, *Biochemistry*, 2009, **48**, 6175–6183.

247 E. W. Colungton and A. I. Meyers, *J. Org. Chem.*, 1971, **36**, 3044–3045.

248 H. I. Jacobson, M. J. Griffin, S. Preis and E. V. Jensen, *J. Am. Chem. Soc.*, 1957, **79**, 2608–2612.

249 K. Surendra and E. J. Corey, *J. Am. Chem. Soc.*, 2008, **130**, 8865–8869.

250 K. Surendra, W. Qiu and E. J. Corey, *J. Am. Chem. Soc.*, 2011, **133**, 9724–9726.

251 J. Bergueiro, J. Montenegro, C. Saá and S. López, *Chem. A. Eur. J.*, 2012, **18**, 14100–14107.

252 R. D. Walker and J. Erskine Hawkins, *J. Am. Chem. Soc.*, 1952, **74**, 4209–4210.